

**UNIVERSITY OF MINING AND GEOLOGY  
"ST. IVAN RILSKI"**

**JOURNAL  
OF  
MINING AND GEOLOGICAL  
SCIENCES**

**Volume 62**

**Number 2**



**Sofia 2019**

## Editorial Board

Prof. Dr. Pavel Pavlov (Editor-in-Chief), Prof. DSc. Ruslan I. Kostov (Deputy Editor-in-Chief), Assoc. Prof. DSc. Irena Grigorova, Assoc. Prof. Dr. Boris Valchev, Assoc. Prof. Dr. Diana Decheva, Prof. Dr. Valentin Velez, Assis. Prof. Monika Hristova, Kalina Marinova (Secretary)

## Contributing Editors

Prof. Dr. Lyuben Totev, Prof. Dr. Ivaylo Koprev, Prof. Dr. Marinela Panayotova, Prof. DSc. Stoyan Grudev, Prof. Dr. Ivan Nishkov, Prof. Dhc Carsten Drebenstedt (Germany), Prof. DSc. Andrey V. Korchak (Russia), Prof. Dr. Alexander V. Myaskov (Russia), Prof. Dr. Zoran Despodov (North Macedonia)

University of Mining and Geology "St. Ivan Rilski"  
1, Prof. Boyan Kamenov Str., 1700 Sofia, Bulgaria  
<http://www.mgu.bg>

ISSN 2682-9525 (print)  
ISSN 2683-0027 (online)

[www.mgu.bg/new/journal](http://www.mgu.bg/new/journal)

© Publishing House "St. Ivan Rilski", Sofia, 2019

## CONTENTS

<i>Aleksandrova, E., S. Asenovski, D. Georgiev, D. Kaykov, I. Koprev.</i> Methods for determining an optimal technological solution for underwater mining	5
<i>Begnovska, M.</i> Opportunities for the application of different mine surveying mapping technologies in determining volumes in underground mine workings	9
<i>Eftimov, Z., D. Anastasov.</i> New underground infrastructure in "Varba - Batantzi" mine	13
<i>Eftimov, Z., D. Anastasov.</i> Innovation in the mining methods in the "Varba – Batantzi" underground mine	17
<i>Eremeeva, A. M., G. I. Korshunov, N. K. Kondrasheva.</i> Reduction of emissions impact on the environment and health of coal mine workers	21
<i>Georgiev, D., S. Asenovski, D. Kaykov, L. Dimitrov, I. Koprev.</i> Evaluation of the possibilities for sustainable exploitation of a deposit for kaolin and silica sands	25
<i>Gospodinova, V.</i> Research on creating digital photogrammetric model by using different number of control and check points	29
<i>Gospodinova, V., R. Yordanova, A. Kandilarov.</i> Vegetation indices as a means of monitoring of objects in the region of open pit mines	34
<i>Khayrutdinov, A. M.</i> Processing and recycling of resources in outer space: international legal aspects	41
<i>Kolev, N., P. Savov, M. Vatzkitcheva, K. Velichkova, D. Dimitrov, B. Vladkova, S. Toncheva.</i> The impact of outdoor mining activities on atmospheric air quality in nearby settlements	45
<i>Kulikova, E.</i> The requirements for concrete lining of a sewage collector tunnels	50
<i>Kulikova, E., A. Ivannikov.</i> Environmental sustainability in the development of urban underground space	54
<i>Makedonska, D., M. Michaylov.</i> Need for fixed fire fighting systems in road tunnels	60
<i>Mamray, V., V. Korobiichuk, V. Shlapak.</i> Experience of dimension stone extraction by quarry cutting machine in Pokostovsky deposit, Ukraine	66
<i>Mollova, Z.</i> New insights into the impact of blast wave on the human body	70
<i>Mollova, Z.</i> Blast load analysis and effect on building structures	75
<i>Pulev, S.</i> Dynamic ascent of a mining dumper on a road with longitudinal slope	81
<i>Rodionov, A. O.</i> Increasing the economic efficiency of mining complex structural gold deposits	85
<i>Stefanov, D., Ts. Balov, I. Koprev.</i> Developing a measurements plan to study blasting stress waves induced by the explosive breakage of rock in the Chelopech Underground mine	89
<i>Stoycheva, N., P. Shishkov.</i> Innovative formulations for a new generation of low-speed explosive compositions, designed for blasting in tender conditions and for extraction of rock-cladding materials	94
<i>Tamaskovics, N., D. Tondera, P. Pavlov, L. Totev.</i> Computational pothole mine subsidence analysis for multilayer sites	99
<i>Trifonova-Genova, V.</i> On the distorted contour of an elliptical opening passing a rock mass with a horizontal plane of isotropy	103
<i>Tzonkov, A.</i> Mine surveying activities in management of geomechanical processes	107
<i>Ananyev, P., A. Plotnikova.</i> Analysis of selective destruction criteria of iron ores using provisional magnetic pulse treatment	111
<i>Angelov, A., A. Stefanova, K. Nikolova.</i> Regression analysis of factors affecting microbial fuel cell efficiency	115

<b>Angelov, A., E. Kraichev, M. Lecheva, S. Plochev.</b> Volumetric coefficient of oxygen mass transfer analysis in column photobioreactor	<b>119</b>
<b>Grigorova, I., M. Ranchev, I. Nishkov.</b> Crushing circuit optimization in lead-zinc processing plant	<b>124</b>
<b>Ignatovich, A., D. Luckiy, R. Khismatullin.</b> Extraction of rhenium from ammoniacal leaching solutions of copper smelting slag and model solutions	<b>129</b>
<b>Ivanova, M.</b> Mechanical load during shredding of tough-plastic materials with a two-shaft shredder	<b>132</b>
<b>Ivannikov, A., K. S. Cheynesh, A. Khayrutdinov, Y. Tyulyaeva.</b> Modern approach to the technology of the backfilling	<b>135</b>
<b>Ivanov, R., A. Stefanova, A. Angelov.</b> Treatment of water contaminated by petroleum products through constructed wetlands with integrated plant sediment microbial fuel cells	<b>139</b>
<b>Ivanova, Ts., I. Grigorova, M. Ranchev.</b> Possibilities for PNEUFLOT flotation machine application in copper-porphyry ore processing plant	<b>143</b>
<b>Ivanova, Ts., M. Ranchev, I. Grigorova, I. Nishkov.</b> Pre-contact pneumatic flotation of copper porphyry ore from Assarel deposit	<b>148</b>
<b>Manastirli, M., M. Nicolova.</b> Investigation of the possibilities to use recycled construction waste in road construction	<b>153</b>
<b>Nicolova, M., I. Spasova, P. Georgiev, S. Groudev.</b> bioleaching of copper ores by means of different chemolithotrophic bacteria and archaea	<b>159</b>
<b>Panayotova, M., L. Djerahov, G. Gicheva.</b> Investigation of the possibility for extracting ions, possessing a corrosive action on construction materials, by washing solid inclusions in a clayey overburden	<b>162</b>
<b>Spasova, I., M. Nicolova, P. Georgiev, S. Groudev.</b> Microbial extraction of precious metals from a gravity-flotation concentrate	<b>167</b>
<b>Toshev, S., A. Loukanov, S. Nakabayashi.</b> Colorimetric sensor from citrate capped silver nanoparticles for trace detection of arsenic (III) in groundwater	<b>170</b>
<b>Toshev, S., A. Loukanov, S. Nakabayashi.</b> Design of self-propelling Janus nanoimpeller as a nanomachine for targeting and destruction of pathogenic microorganisms	<b>174</b>
<b>Tsvetkov, P., S. Bratkova.</b> Semi-passive treatment of mine waste water in anaerobic conditions	<b>179</b>
<b>Zubkova, O. S., A. I. Alexeev.</b> Complex processing of saponite waste of a diamond-mining enterprise	<b>183</b>

## METHODS FOR DETERMINING AN OPTIMAL TECHNOLOGICAL SOLUTION FOR UNDERWATER MINING

*Evgeniya Aleksandrova, Simeon Asenovski, Daniel Georgiev, Dimitar Kaykov, Ivaylo Koprev*

*University of Mining and Geology "St. Ivan Rilski", 1700 Sofia; orpi\_vr@mgu.bg*

**ABSTRACT.** The key factors which determine the choice of an optimal technical scheme for underwater mining have been analysed. Several methods for multi-criteria analysis have been used in this research, depending on the specific mining conditions. The different methods for establishing an optimal decision have been compared and their pros and cons have been analysed.

**Keywords:** underwater mining, multi-criteria decision analysis

### МЕТОДИ ЗА ОПРЕДЕЛЯНЕ НА ОПТИМАЛНО ТЕХНОЛОГИЧНО РЕШЕНИЕ ПРИ ПОДВОДНИЯ ДОБИВ НА ПОЛЕЗНИ ИЗКОПАЕМИ

*Евгения Александрова, Симеон Асеновски, Даниел Георгиев, Димитър Кайков, Ивайло Копрев*

*Минно-геоложки университет "Св. Иван Рилски", 1700 София*

**РЕЗЮМЕ.** Анализирани са основните фактори, определящи избора на оптимална технологична схема при подводния добив. Използвани са методи на многокритериален анализ, като са взети под внимание специфичните условия на находището. Различните методи за избор на оптимално решение са сравнени по между си и са посочени техните положителни и отрицателни страни.

**Ключови думи:** подводен добив, многокритериален анализ

### Introduction

The choice of a suitable type of equipment and its corresponding extraction technology in the underwater mining of mineral resources has a significant importance about the overall result from the mining activities. On the one hand, this is related to the high responsibility, which comes with the amount of capital required for investment in the mining equipment. On the other hand, the effects on the environment from the mining activities are irreversible and this could lead to a negative outcome with a large scale effect. The increased requirements for the artificial footprint on the environment especially due to the mining activities are a serious limiting factor for underwater mining. Nevertheless, the development of modern-day technologies and mining equipment provides the possibility for extracting minerals in harsh conditions as well as the maintenance of the artificial footprint in certain predetermined boundaries. It is considered that some types of modern mining equipment not only reduce the ecological threat, but also provide good working performance and good revenue. In order to choose the most adequate mining technology and equipment for a certain deposit, the main factors should be considered individually for every type of mining equipment. Although, the individual approach is related

to the consideration of many possibilities due to the great number of factors for every deposit, certain general conclusions and relations could be drawn from researching the decision making process.

### Stages of the decision-making process

Based on an analysis of different sources, related to the underwater mining technologies, several stages of determining the most suitable mining equipment could be pointed out (Koprev, 2017).

**The first stage** includes the consideration of the technological factors of the deposit, determining the possibility of its extraction. These factors are determined by the possible technological schemes for extraction as well as the different types of mining equipment suitable for the conditions. Table 1 represents the most commonly used types of mining equipment and their application for exploiting different types of deposits. The deposits are separated into three main groups (river deposits, lake and sea deposits, deep sea and oceanic deposits). This classification is based on the distance of the deposit from the land and its depth (Koprev, 2017; 2018).

Table 1. Mining equipment utilised in different conditions

Types of utilized mining equipment	River deposits	Lake and sea deposits	Deep sea and oceanic deposits
1. Bed leveller	+	+	-
2. Pontoon dredger	+	+	-
3. Grab pontoon dredger	+	+	~ (experimental stage)
4. Multiple-bucket dredger	+	+	-
5. Suction dredger	+	+	-
6. Specialised vessels with mechanised or hydraulic cutting and suction pipes	-	+	~ (dissatisfactory results)
7. Specialised deep-sea robots	-	-	~ (experimental stage)

(+) – successfully utilised; (-) – unsuccessful utilisation; (~) – utilised in specific conditions

It is necessary to add that the results in the table determine the current level of technical and technological development and it is not definitive as some of the types of equipment are still in experimental period.

The second stage of the decision making process should consider the factors, related to the ecological effect of the mining technology. This stage has a significant importance as it eliminates some of the possibilities considered in the first stage. It is considered that the ecological impact resulting from underwater mining has a large-scale effect, but it has not been fully researched yet. To this moment researches have shown that the utilised technologies for mining from the seabed lead to irreversible changes which could potentially result in the death of the sea microflora and microfauna. Hence, at this stage, these types of mining equipment are not yet applicable for underwater mining in deep-sea conditions. On the other hand, some shallow underwater deposits are exploited because certain extraction technologies have proven that they can prevent the negative effect from an ecological point of view. They reduce the negative impacts of sedimentation and the water muddiness by the use of special curtains which isolate the area impacted by the extraction process. Capsulated excavator buckets also prove to minimise the ecological impact (Bray, 2008). These technological solutions are applied in conditions where the ecological requirements are met. Those modifications of the standard types of mining equipment are the remaining alternatives in the decision-making process.

After determining the acceptable mining technology for exploiting a certain deposit from an ecological and technical point of view, one should consider the factors from the third stage of the decision-making process. This stage of the process involves the economic parameters related to the choice of the mining technology – revenue, costs, ore loss, etc. Thus, out of the remaining variants, the alternative, which is considered to be the most suitable one from an economic point of view, is chosen. This is related to the working performance of the types of mining equipment and several parameters which include the highest cutting precision, leading to minimal ore loss and a higher revenue. Other parameters could be considered as well, which further minimise the negative impact on the environment.

## Parameters determining the decision

In order to establish a grounded decision for the choice of suitable mining equipment for a certain deposit, several key parameters should be considered. In this article 4 main groups of parameters could be established for the decision making process. The four groups represent certain characteristics of the mining equipment and should be considered in a complex manner regarding the full analysis of the most suitable mining technology. The groups are divided into:

- 1) Characteristics of the equipment – mining depth, rock output, cutting force, cutting precision, etc. (H<sub>1</sub>);
- 2) Environmental impact – sedimentation, noise, gas emissions, etc. (H<sub>2</sub>);
- 3) Economic efficiency – total costs, revenue, ore loss, dilution, etc. (H<sub>3</sub>);
- 4) Social factors – safety factors, personnel qualification, etc. (H<sub>4</sub>).

## Methods for decision-making

These groups of parameters provide the establishment of a complex assessment of the types of mining equipment for a certain deposit. A quick way for establishing a complex numeric value for the different characteristics is by applying the proposed method in Table 2.

Table 2. Assessment points for the mining equipment

Assessed mining equipment, A <sub>i</sub>		A <sub>1</sub>	A <sub>2</sub>	A <sub>3</sub>	A <sub>4</sub>
Characteristics	Weight				
H <sub>1</sub>	w <sub>1</sub>	P <sub>11</sub>	P <sub>12</sub>	P <sub>13</sub>	P <sub>14</sub>
H <sub>2</sub>	w <sub>2</sub>	P <sub>21</sub>	P <sub>22</sub>	P <sub>23</sub>	P <sub>24</sub>
H <sub>3</sub>	w <sub>3</sub>	P <sub>31</sub>	P <sub>32</sub>	P <sub>33</sub>	P <sub>34</sub>
H <sub>j</sub>	w <sub>j</sub>	S <sub>1</sub> =∑P <sub>j1</sub> .w <sub>j1</sub>	S <sub>2</sub> =∑P <sub>j2</sub> .w <sub>j2</sub>	S <sub>3</sub> =∑P <sub>j3</sub> .w <sub>j3</sub>	S <sub>4</sub> =∑P <sub>j4</sub> .w <sub>j4</sub>

- H<sub>j</sub> – assessed characteristics for the mining equipment;  
 j – number of assessed characteristics;  
 A<sub>i</sub> – the reviewed alternatives of mining equipment considered for the deposit;  
 i – number of alternatives for mining equipment;  
 w<sub>j</sub> – weight for the characteristics;  
 P<sub>ij</sub> – points for characteristic j of mining equipment i.

The points P<sub>ij</sub> are formed by applying the following relation:  $P_{ij} = \frac{H_i}{H_{i \max}} \cdot 100$ , where H<sub>i max</sub> is the highest value of each characteristic for the group of alternatives. An important condition is that the sum of all the weights should be 100%: ∑w<sub>j</sub> = 100%, as well as that all the characteristics should be unidirectional (the improvement of the characteristic should be related to higher values of its corresponding points). Depending on the end result the sums of all the points for each alternative are arranged in a descending order (Trapov, 2011). The best possible alternative is the one with the higher sum S<sub>i</sub>.

A method which is often used is the one, where a complex value could be established by representing the different alternatives as points in the n-dimensional space  $A(H_1, H_2, H_3, H_4)$ . It is assumed that an ideal point exists, which represents the ideal alternative for the deposit  $I(H_1 \text{ ideal}, H_2 \text{ ideal}, H_3 \text{ ideal}, H_4 \text{ ideal})$ . The alternatives are arranged depending on their distance from the ideal point. The shortest distance represents the alternative which is closest to the ideal solution. The distances ( $R_i$ ) for each alternative could be calculated in the following way:

$$R_i = \sqrt{\left(1 - w_1 \frac{H_{1i}}{H_{1 \text{ ideal}}}\right)^2 + \left(1 - w_2 \frac{H_{2i}}{H_{2 \text{ ideal}}}\right)^2 + \left(1 - w_3 \frac{H_{3i}}{H_{3 \text{ ideal}}}\right)^2} \quad (1)$$

The points which each alternative gets, depending on its distance to the ideal solution, are calculated by using the formula:

$$P_i = \frac{1}{1 - R_i} \cdot 100 \quad (2)$$

An important requirement for using the method is that the considered characteristics of the mining equipment should be independent. A major flaw of the implementation of the method is the considered way for determining the values of the weights for the different characteristics. An easy way is to establish the values by applying the subjective approach. However, this method usually proves to be very inaccurate. In order to establish the correct values for the weights, a factor analysis based on statistical data should be implemented or a sensitivity analysis considering the end-result of the mining process (rock output or revenue) should be applied.

It is advisory that this method is used for arranging the alternatives only when the decision-making process is provided with full information about the specific conditions of the deposit. However, this approach is limited as it does not account for the possible changes that could occur while the exploitation of the deposit takes place. That is why, a stochastic approach is more suitable for considering the best possible alternative in accordance with the limited information which the decision-maker has.

Each characteristic  $H_j$  for every alternative has values which fall into the interval  $[H_{j \text{ min}}, H_{j \text{ max}}]$ . Hence, the grade which each alternative gets should be in the interval  $[P_j \text{ min}, P_j \text{ max}]$ . This leads to the formation of different cases where the mining equipment alternatives are arranged and each case is valid and possible under certain circumstances. This requires that a different approach should be used in order to get a grounded decision, although the information is incomplete. Hence, it is suitable to apply the game theory approach.

In the game model it is assumed that the first player is the decision-making person (the engineer), whose strategies are the choices of the different types of mining equipment ( $A_i$ ). The other player is the "nature", which is represented by its strategies for the different possible scenarios for the conditions of the deposit ( $U_k$ ). Each scenario  $U_k$  is related to a certain combination of characteristics ( $H_1, H_2, H_3, H_4$ ) for each type of equipment  $i$ , and their corresponding points  $P_1, P_2, P_3, P_4$ , which are determined by its work performance under these conditions. Each scenario for the deposit's conditions is related

to an individual grade  $S_i$  for the types of equipment. Table 3 represents an exemplary game matrix:

Table 3. Game matrix for the alternative strategies for choosing the type of equipment according to the conditions

		"Nature's" strategies (deposit's conditions)		
		$U_1$	$U_2$	$U_3$
Alternatives for the types of equipment	$A_1$	$S_{11}$	$S_{12}$	$S_{13}$
	$A_2$	$S_{21}$	$S_{22}$	$S_{23}$
	$A_3$	$S_{31}$	$S_{32}$	$S_{33}$
	$A_4$	$S_{41}$	$S_{42}$	$S_{43}$

For finding out the most suitable decision several criteria could be used: **optimistic criterion:**  $\max_i \max_j (S_{ij})$ ; **Wald's maximin model:**  $\max_i \min_j (S_{ij})$  and **Hurwitz's criterion:**  $\max_i (\lambda \cdot \min_j (S_{ij}) + (1 - \lambda) \cdot \max_j (S_{ij}))$ .

The optimistic criterion is used when the information of the deposit's conditions is full and the established decision is based on the best possible solution. It is not advisory that this criterion is used in the situation when there is not enough information about the deposit. Wald's model is also known as the "rational pessimist" during the decision-making process and it is suitable when the information is limited and no further information can be collected. Hurwitz's criterion is recommended in the scenario where the risk could be assessed with a certain numeric value. A number is considered for the coefficient of pessimism  $\lambda \in [0;1]$ . The optimal solutions for each criterion are the ones which apply to the condition of a saddle point in the matrix as the decision-making process takes place only once and the strategies should be clear. If the solution corresponds to a mixed strategy, a thorough comparison analysis of the different alternatives should be made in order to choose the most suitable one.

## Conclusion

In conclusion, the decision-making process in the conditions of underwater mining is similar to the one in open-pit and underwater mining (Koprev, 2018; Stefanov, 2016).

However, a great importance is put on the ecological aspect of the mining process. That is why, the different stages of considering the possible alternatives for exploiting a certain deposit should be considered in the following order: considering the technologically possible mining technologies, eliminating those alternatives which are related to an unacceptable level of environmental impact, and choosing those alternatives which provide satisfactory working performance and revenue.

The proposed methods could be used as a solution for a real decision-making problem, but certain drawbacks need to be considered when applying the methods. For example, the subjective character of the weights of the different characteristics, as well as the incorrect determination of the work performance, depending on the conditions of the deposit, are key factors which could lead to wrong conclusions, if their values are not properly determined. Furthermore, it is expected that when different criteria are used in the game matrix some

of the optimal solutions may differ from one another. This leads to the following cases: 1) If the different criteria point out the same optimal solution, this solution is considered to be the optimal one; 2) If the different criteria point out different solutions, it is advisory that the criteria should be reconsidered whether they are adequately related to the conditions of the deposit.

Furthermore, the points for each alternative should be recalculated in order to get adequate solutions. It is important to notice that this method is suitable for independent values and if it is applied for dependent values, there is a possibility that the result may not be the desired one. Hence, the results should be considered with a bit of scepticism.

## References

- Bray, R. 2008. *Environmental Aspects of Dredging*. CRC Press, London, 394 p.
- Koprev, I. 2017. Types of underwater mining equipment and their environmental impact. – *Third National Scientific and Technical Conference "Mineral Resources and Sustainable Development"*, Sofia (in Bulgarian).
- Koprev, I. 2018a. *Mathematical Modelling in the Open-pit Mining of Mineral Resources*. Avangard Prima, Sofia, 72 p. (in Bulgarian)
- Koprev, I. 2018b. *Technological aspects of the Underwater Mining of Mineral Resources*. Avangard Prima, Sofia, 208 p. (in Bulgarian)
- Stefanov, D., I. Garkov. 2016. *Underground Mining*. Sofia (in Bulgarian).
- Trapov, G. 2011. *Mathematical Methods in Management*. Sofia (in Bulgarian).

## OPPORTUNITIES FOR THE APPLICATION OF DIFFERENT MINE SURVEYING MAPPING TECHNOLOGIES IN DETERMINING VOLUMES IN UNDERGROUND MINE WORKINGS

**Milena Begnovska**

University of Mining and Geology "St. Ivan Rilski", 1700 Sofia; m\_begnovska@abv.bg

**ABSTRACT.** The main task in the underground mine surveying practice is to determine the volumes of mined out mass. The possibilities for the application of modern equipment during mine surveying mapping in underground mining are evaluated. An analysis of the results obtained for the calculated amounts of mined out mass was carried out. A comparison was made of the relevancy of different technologies for the determination of volumes in mine workings.

**Keywords:** mine surveying mapping, modern mine surveying equipment, volume calculation

### ВЪЗМОЖНОСТИ ЗА ПРИЛОЖЕНИЕ НА РАЗЛИЧНИ ТЕХНОЛОГИИ ЗА ЗАСНЕМАНЕ ПРИ ОПРЕДЕЛЯНЕ НА ОБЕМИ В ПОДЗЕМНИ МИННИ ИЗРАБОТКИ

**Милена Бегновска**

Минно-геоложки университет "Св. Иван Рилски", 1700 София

**РЕЗЮМЕ.** Една от основните задачи, свързани с маркшайдерското обслужване при подземното разработване на находищата, е определяне на обемите добита минна маса. Оценени са възможностите за приложението на съвременна техника и технологии при извършване на маркшайдерско заснемане в подземни минни изработки. Извършени са анализ на получените резултати за изчислените количества отбита и извозена минна маса и сравнение на приложимостта на различни снимачни технологии при определяне на обеми в подземни минни изработки.

**Ключови думи:** маркшайдерско заснемане, съвременни маркшайдерски инструменти, изчисляване на обеми

## Introduction

Successful solving of various mining and technical tasks in the exploitation of the deposits of underground resources largely depends on the quality of mine surveying mapping. Based on the mine surveying mapping, a precise and up-to-date model of mine workings is created and an opportunity is provided to determine their location, size and shape in space. An important aspect of the mine surveying activity is the carrying out of a report on mined out mass and the volume of mining works, carried out periodically for each mine workings (opening, permanent, development, sill cut or extraction working). On the basis of these quantities, implementation of the annual mine development project is taken into account and the remuneration of the staff of the mining company (Tzonkov, 2019) is calculated. According to the calculations, the stability of the roof and the protection of the objects and the surface facilities can be predicted.

Underground mine workings are complicated and irregular in shape, their volume is defined as a function of the areas of the "body" sections.

$$V = f(P), \quad (1)$$

Traditionally, the calculation according to the form of workmanship is done using the method of the vertical or horizontal sections, in the same or variable interval.

Recently, new techniques and technologies have become more and more popular. Methods for calculating the volumes of mining workings also evolve in the direction of multivariate. Most often, each company producing geodetic tools and technologies also offers relevant software for post-processing of measurements, the corresponding calculations, and the construction and maintenance of numerical models (Pflipsen, 2006). There are still many conventional geodetic programs as well as a number of continuously improved CAD applications.

Regardless of the technique used, the determination of the volume of underground mining works consists of two processes (Ivanova, 1991; Mazhdakov, 2007; Tzonkov, 2019):

- ✓ Mapping an object whose volume is to be determined and creating a pattern on the captured surface.
- ✓ Determining the volume by entering (according to established and accepted algorithms) elementary figures in the space limited by this surface and the sum of the volumes, which form the total sought volume.

The total error in determining the volume must be determined by considering the regularities in the accumulation of errors in each of the processes.

## Experimental results

### Mine surveying mapping of a chamber for the extraction of gypsum in "Koshava" deposit

The Koshava Gypsum deposit is located west - southwest of the village of Koshava, Vidin district. The seizure of the stocks is done in an underground way with a chamber-and-pillar system of exploitation. The gypsum removal is carried out by the use of drilling-blasting operations. The report on mined out mass and the determination of the volume of the mining works are currently carried out by the Mine Surveying Department of the mine.

Mine surveying mapping of a gypsum chamber was performed (chamber 56/5 – Figs. 1 and 3) using reflectorless measurement technology. The mine surveying mapping was performed with a total station Trimble S6 (Figs. 3 and 4) by two different methods:

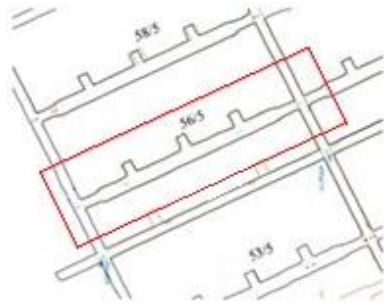


Fig. 1.

- the Surface Scanning application, built into the total station, using the "Rectangular plane" method (<https://apps.trimbleaccess.com/help/en/TrimbleAccess=2017.23>) to define a 3-point plane (Figure 2). Taking into account the shape and dimensions of the mine workings, four surfaces describing the floor, the ceiling and the two walls are selected. In each section of the mine workings three points of the specified surfaces are initially set and then, depending on the spacing between the points specified in the setup, the measurements are performed in automated mode and the results are automatically recorded in the instrument memory. Thus, the captured surfaces, overlapping a certain number of points describing the walls, the floor and the ceiling of the mine workings, provide information about the spatial position of the elements of the gallery. The scanning was performed at distances between points of 0.50 m × 0.50 m.

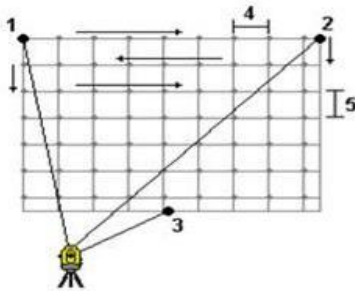


Fig. 2.

- capturing separate points in distinctive locations from the camera's outline, which is the most commonly used method when performing a mine surveying mapping.



Fig. 3.

By the "Rectangular plane" method, a total of 7541 points (for about 8 hours) were captured, while by capturing separate points in distinctive locations from the camera's outline - 666 points (for about less than 2 hours).

The volumes of mined out mass are calculated and the results are presented in Table 1.

Table 1.

Capture method	Number of points	Calculated volume, m <sup>3</sup>
"Rectangular plane"	7541	5336.78
Capture of characteristic points	666	4532.59
Difference		804.19

### Inferences

When analysing the measurement data, the following conclusions can be drawn:

1. When measured by the "Rectangular plane" method, the capture is much more detailed. In turn, the method of capturing only single points in characteristic areas of the camera's contour repeatedly reduces the working time.

2. When performing a mine surveying mapping of mine workings, the method by which the capture will be performed, according to the requirements of the normative base to ensure sufficient accuracy must be carefully assessed, but also the necessary time to capture should be provided for.

3. The resulting difference in calculated volumes by both methods is 804.19 m<sup>3</sup>, which is about 15%. This proves the need for precise planning of mine surveying works. The difference is due to the increased roughness of the walls of the gypsum chamber (Figs. 4 and 5) as well as to the large deviations from the measured reference length found in previous investigations of the author at reflector less measurement of this mineral.



Fig. 4.



Fig. 5.

**Capture of permanent mine working in "Chelopech" mine**

As a good practice for conducting mine surveying mapping in underground mining conditions, the existing "Chelopech" mine operation procedure can be specified. Clear and precise requirements and a standard for unified work on measurement are introduced.

A mine surveying mapping of permanent mine working was performed in the "Chelopech" mine. There is a shotcrete - concrete fastening in the specifically captured area. The capture was done in two ways:

- With a Trimble S6 total station, using the "Rectangular plane" method, by defining a 3-point plane (Fig. 2), at distances between points of 0.50 m × 0.50 m. (<https://apps.trimbleaccess.com/help/en/TrimbleAccess=2017.23>)

- Using the CMS - Cavity Monitoring System (Grunin, 2003), through which the mine workings outlines were scanned. CMS has been developed to research, measure and capture the image of inaccessible or unsafe for staying underground cameras. It ensures that thousands of precisely coordinated points are captured that are used to determine the size, orientation, and volume of the chamber. The capture is done in automated mode. Laser scanning technology is one of the most advanced methods of capturing, providing spatial location data for objects in the form of three-dimensional computer models.

When measured with a Trimble S6 total station (Fig. 6), 3829 points (for about 3.5 hours) were registered using the "Rectangular plane" method, and 153282 points (for about 20 minutes) with CMS scanning (Fig. 7).



Fig. 6.

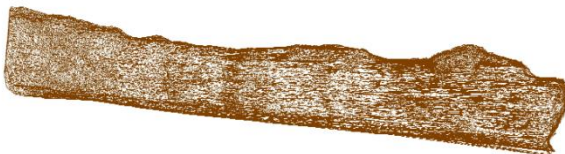


Fig. 7.

From the two surveys done in this way, the volumes of seized rock mass are calculated and presented in Table 2, Fig. 9 and Fig. 10.

Table 2.

Capture method	Number of points	Calculated volume, m <sup>3</sup>
„Rectangular plane” - Trimble S6	3829	1037.62
Scanning - CMS	153282	1023.40
Difference		14.22

In Fig. 8 a combined image of the captured mine workings elements is presented by both methods (Trimble S6 total station and CMS).



Fig. 8.

**Inferences**

A comparison is made between two different technologies.

1. The difference in the calculated volumes by the two methods is 14.22 m<sup>3</sup>, which is about 1.5%. This gives us a reason to conclude that the two technologies are equally applicable in the described conditions.

2. After analysing the results, the following should be noted: each measuring technology has its own positive and negative aspects: different detail, different time for measurements, different number of specialists required to carry out the measurement.

3. When capturing underground mining, account must be taken of the specific conditions in the mines, the purpose of the mine surveying mapping, the tasks to be solved by the results, and the proper assessment of the application of one or the other method of capture.

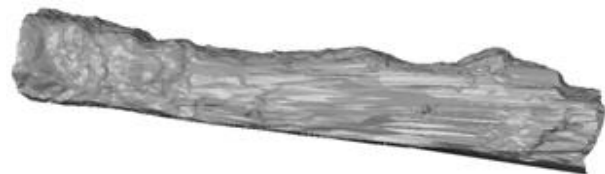


Fig. 9.

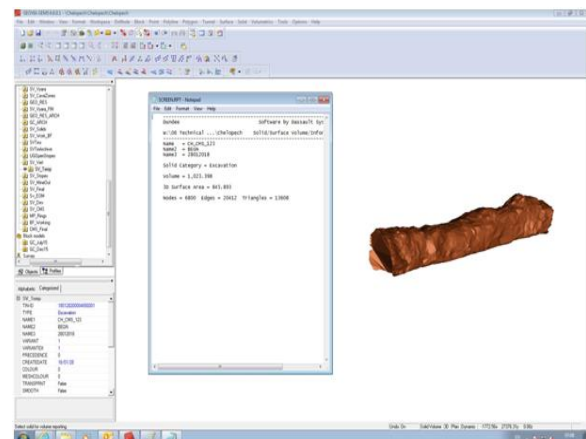


Fig. 10.

## Conclusion

In a previous study of the author, such a mine surveying mapping was made in "Krushevdol" underground mine (Begnovska et al., 2014). A horizontal drift - gallery 1 level 450, was originally measured by a total station SOKKIA SET 5 (total station capabilities allow the measurement of lengths only to a reflective prism) and a Laser Distance Measurer - BOSCH. The same gallery was also captured with a total station Trimble S6. With the capture made in this way, the difference between the determined volumes of mined out mass between both methods is about 75 m<sup>3</sup>, which is about 18%.

The presented methods do not exhaust all possibilities for capturing mine workings. This can also be done in a photogrammetric way (Gospodinova, 2018; Gospodinova et al., 2018). Studies for the creation of a digital photogrammetric model in an underground mine workings and its comparison with mine surveying mapping with a total station have been presented. The volumes by the two methods were calculated and a comparison was made between the two technologies, and it was concluded that the methodology was applicable for the capture of underground mining and the calculation of volumes.

As far as the mine surveying mapping and the calculation of volumes of mined out spaces are concerned, it is difficult to give a concrete answer to the question of what is the best method. Various factors such as: shape (configuration) and size of the space captured, equipment available, required precision, and economic indicators should be taken into account. The use of measurement and computing technology, combining modern hardware solutions and corresponding software, are the key prerequisites for obtaining accurate and fast results, which is valid for every type of mine surveying activity.

Various methods for mine surveying mapping of underground spaces are presented in the development. They are also applicable in studying the stress-strained state of the rock massif (Tzonkov, 2014; 2019). Knowledge of the state of the array or object and the processes in it is based on a high-precision determination of the spatial position change of observed points in time provided by the proposed methods. The need to predict the deformable state of the environment and facilities requires the application of appropriate monitoring methods to identify and track the deformation processes and to implement timely measures for their regulation. Knowledge of them would lead to making adequate decisions on the development system, work order in the space and time of individual jobs, safety measures, and risk prediction in specific situations.

When analysing the results of the author's research carried out so far and published in various scientific publications and proceedings, and the relevant inferences and conclusions formulated, the following questions arise, which determine the intentions for future research:

- Classification of mine workings in relation to the deviation from the draft section and determination of the optimal option for mine surveying mapping (justification of the distances between the detailed points when the capture is taken).

- Calculation of volumes of mined out spaces with different roughness of the walls of mine workings.

- Definition of a method for mine surveying mapping in areas with higher humidity of the rocks and with increased roughness, as well as capturing of underground spaces with a reflective environment formed by minerals with different optical properties.

## References

- Begnovska, M., R. Petkov, D. Atanasova. 2014. Markshayderska snimka na horizontalna izработка v rudnik "Krushevdol" chrezrazlichni tehnologii. – *Chetvarta natsionalna nauchno-tehnicheska konferentsia s mezhdunarodno uchastie "Tehnologii praktiki pri podzemen dobiv i minno stroitelstvo"*, Devin, Bulgaria, 254–261 (in Bulgarian with English abstract).
- Gospodinova, V. 2018. Prilozhenie na tsifrovata fotogrametria za markshaydersko kartografirane na podzemni minni izrabotki. – *Shesta natsionalna nauchno-tehnicheska konferentsia s mezhdunarodno uchastie "Tehnologii praktiki pri podzemen dobiv i minno stroitelstvo"*, Devin, Bulgaria, 171–176 (in Bulgarian with English abstract).
- Gospodinova, V., P. Georgiev, P. Ivanov. 2018. Sazdavane na chislen fotogrametrichen model v podzemen rudnik. – *Shesta natsionalna nauchno-tehnicheska konferentsia s mezhdunarodno uchastie "Tehnologii praktiki pri podzemen dobiv i minno stroitelstvo"*, Devin, Bulgaria, 155–161 (in Bulgarian with English abstract).
- Grunin, A. G. 2003. Primenenie lazernoy skaniruyushtey sistemy CMS dlya markshayderskih rabot. – *Geoprofi*, 2, 30-31 (in Russian).
- Ivanova, I. 1991. Snimka na nedostapni prazni prostranstva v podzemni rudnitsi. – *Geodezia, kartografia, zemeustroystvo*, 3–4 (in Bulgarian).
- Mazhdakov, M. 2007. *Markshayderstvo. Metodika na markshayderskite raboti v otkritite rudnitsi*. Universitetsko izdatelstvo "Sv. Kliment Ohridski", Sofia, 52–67 (in Bulgarian).
- Pflipsen, B. 2006. *Volume computation – a comparison of total station versus laser scanner and different software*. Master's Thesis in Geomatics, University of Gävle, 9–13.
- Tzonkov, A. 2014. Izsledvane na geomehanichni protsesi chrez markshayderski izmervania. – *Chetvarta natsionalna nauchno-tehnicheska konferentsia s mezhdunarodno uchastie "Tehnologii praktiki pri podzemen dobiv i minno stroitelstvo"*, Devin, Bulgaria, 147–155 (in Bulgarian with English abstract).
- Tzonkov A. 2019a. *Geomehanichni izsledvania chrez markshayderski izmervania*. IK "Sv. Ivan Rilski", Sofia (in Bulgarian).
- Tzonkov, A. 2019b. *Markshayderstvo pri podzemno razrabotvane na nahodishta (kratak kurs)*. IK "Sv. Ivan Rilski", Sofia, 108–111 (in Bulgarian).
- <https://apps.trimbleaccess.com/help/en/TrimbleAccess=2017.2>  
3.

## NEW UNDERGROUND INFRASTRUCTURE IN "VARBA – BATANTZI" MINE

**Zdravets Eftimov, Dimitar Anastasov**

University of Mining and Geology "St. Ivan Rilski" 1700 Sofia; Zdravetse@yahoo.com

**ABSTRACT.** In this report the need of building up a new underground infrastructure in "Varba – Batantzi" mine is presented with the aim of reaching the deposits in depth. New capital workings and equipment, such as new underground mobile equipment are reviewed and presented. The changes and improvement of the workings for reaching and preparing the deposits connected with the new underground equipment are described. The report presents the challenges connected with the water drainage and ventilation of the "Varba – Batantzi" mine. The results and conclusions about the need of building a new infrastructure are presented, as well as equipping the mine with a new mobile equipment and the results that should be met.

**Keywords:** underground infrastructure, mine, water drainage, ventilation

### НОВА ПОДЗЕМНА ИНФРАСТРУКТУРА В РУДНИК „ВЪРБА – БАТАНЦИ“

**Здравец Ефтимов, Димитър Анастасов**

Минно-геоложки университет "Св. Иван Рилски", 1700 София

**Резюме.** В статията е представена е необходимостта от изграждане на нова подземна инфраструктура в рудник "Върба – Батанци", с цел разкриване на запасите в находището в дълбочина. Разгледани и представени са нови капитални изработки и съоръжения, както и нова мобилна самоходна механизация. Описани са промените в минно-проходческите работи за подготовка на запасите с оглед на новата механизация. В статията са разгледани и предизвикателствата свързани с водоотлива и вентилацията в рудник "Върба – Батанци". Представени за изводи и заключения относно необходимостта от изграждане на нова подземна инфраструктура, оборудване на рудника с нова мобилна самоходна механизация, както и резултатите, които следва да бъдат постигнати.

**Ключови думи:** подземна инфраструктура, рудник, водоотлив, вентилация

### Need to reach the deposits in the "Varba - Batantzi" mine in depth (Anastasov, Eftimov, 2013, 2018)

With the advancement of mining and the development of the "Varba - Batantzi" underground mine there is a need for reaching the reserves in depth below the 540th horizon. This is dictated by a number of factors, on the one hand, the fact that the currently discovered and prepared for mining reserves in the mine are above the horizon 540, at the same time, in depth the deposit is studied up to level 300. On the other hand, considering the concessionaire's wish to increase the annual production capacity of the mine. These are the two main tasks to be solved in the "Varba - Batantzi" deposit.

To accomplish these tasks, it is necessary to change the technology and the working order of the entire deposit. It is necessary to make adjustments in the mining methods. In order to accomplish this task, it is necessary to build an entirely new underground infrastructure in the underground mine "Varba - Batantzi". This, in itself, is not sufficient for the complete fulfilment of the two main tasks, it is necessary to undergo a modernisation of the mechanisation and equipment

in the underground mine besides the construction of a new infrastructure.

### Capital workings and facilities. Choosing a mobile self-propelled underground equipment

The new capital workings and facilities are related to the changes, which should occur in the "Varba - Batantzi" mine, in order to reveal the reserves in depth as well as to increase the production capacity of the mine 2.5 times.

The new capital inclined ramp "Varba" is designed to reach the deposit in depth, starting from the end of the existing working – from level 733 m. The capital inclined ramp "Varba" is designed to develop in an approximately vertical plane with direction to the northwest and southeast. The inclined shaft is positioned to be as far away from the ore body as possible to avoid areas of influence from the mining operations and possible deformation processes caused by them.

The project route of the capital inclined ramp "Varba" is 3885 m. The initial elevation of the track is 733 m and the final elevation is 194.3 m, which determines the displacement of 538.7 m. The slope of the construction is permanent and is 14%. Curved sections are designed with a minimum radius of 20 m, according to the possibilities of mobile equipment.

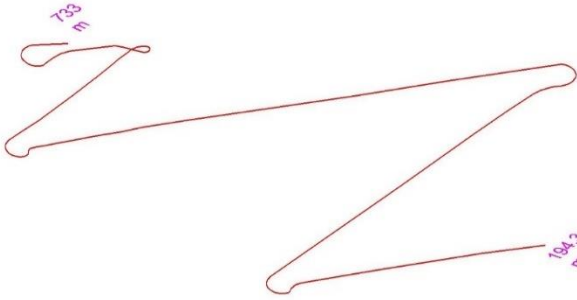


Fig. 1. Project track of the capital inclined ramp "Varba"

From the capital inclined ramp route, mine workings for connection on different levels are planned to be done at 610-600 m, 680 m, 550-540 m and 540 m. There are also two connections with the Varba 2 shaft at 540 m and 300 m. From level 412 m downstream in the southeast inclined shaft for the reserves in the Batantzi deposit is planned to be developed.

In view of the project for development of the mine works of the "Varba - Batantzi" underground mine, the mine is planned to be reequipped with new self-propelled mobile equipment. It consists of three sets of machines of small and medium-class mechanisation. For drifting and mining, combined drill rigs type DD 210 from Sandvik are planned, front-end loaders for transport and delivery of the mined ore and rock fill are planned with a bucket volume of 1.75-1.9 m<sup>3</sup> from Sandvik and underground mine trucks TH 320 with a load capacity of 20 t for extraction of the ore from the mine to the entrance of the flotation plant and transport of rock mass for backfill.

### Mine drifting workings and operations for preparation of the reserves

The mine drifting workings in the "Varba-Batantzi" underground mine are characterised by building new main level workings, new cross entries, creating new ventilation and auxiliary workings, developing new local ramps for the preparation of each individual ore body and the enlarging of the existing workings. When designing the parameters of all of the new underground workings, attention is paid to the dimensions of the new mobile self-propelled mechanisation, the shape and dimensions of the ore bodies, the requirements for increasing the annual mine productivity as well as the specific requirements of the concessionaire. On this basis, the optimal solutions for the number, cross-sections and lengths of workings were taken.

In order to ensure a normal mining production process and preparation of the ore bodies, cross entries from the main inclined shaft to the main level gallery at horizon 435 are done, as well as connections with the existing infrastructure (Varba vertical shaft - 2, local ramps, existing level galleries, etc.). The overall length of the workings is 2546 m with a cross section of 14 m<sup>2</sup>. It is also planned to install vertical ventilation drifts with a section of 4 m<sup>2</sup> and enlarging the gallery at a horizon 590 from 7 m<sup>2</sup> to 14 m<sup>2</sup> with a length of 2039 m. Through the launch of this new underground mining network, the total volume of prepared reserves is about 3.2 million tons.



Fig. 2. Part of the new underground infrastructure in "Varba – Batantzi" mine

For the preparation of each individual ore body in the project local ramps are designed. In their design, the aim is to cover a maximum quantity of ore reserves with a minimal amount of workings, ensuring a normal working environment and maximum execution of production tasks (such as annual ore volumes). Local ramps are designed to be drifted aside from the ore bodies as they are equipped with vertical drifts, overload points and material storage.

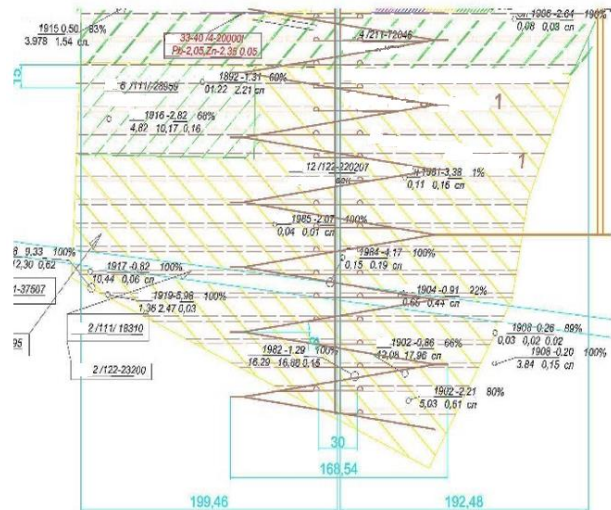


Fig. 3. Mine drifting workings for preparation of the reserves by applying the sublevel caving mining method

Each local ramp is uniquely projected to the particular body to which it relates as well as to the corresponding mining method that is applied in the given area of the underground mine, the sublevel caving mining method and the cut and fill mining method. The local ramps for the preparation of the reserves in the ore bodies are designed with a general slope of 8° and a cross section of 14 m<sup>2</sup> with a total length of 14489 m. Thus, the mining of the whole quantity of the studied reserves at the deposit up to the moment is being prepared.

The mine drifting workings in a deposit, for each applied mining method consists of sublevel drilling galleries for the sublevel caving method in the first mining layer (cut layer) in the cut and fill mining method. In blocks where the cut and fill method is used, the cut layers are developed through 63 m in height in order to increase the number of mine faces and to enable an earlier start of the ore extraction. The cross section of these layers is 7.5 m<sup>2</sup> (2.5x3.0). According to the sublevel

caving method, the sublevel galleries are drifted in 15 m through ore, and the cross section again is 7.5 m<sup>2</sup>. The number and lengths of the galleries are connected with the dimensions of each individual ore block to which they are applied.

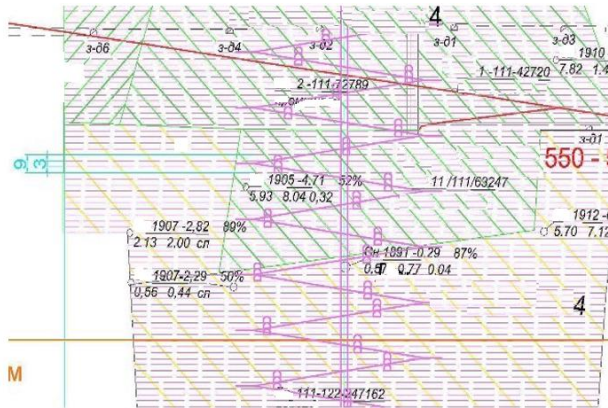


Fig. 4. Mine drifting workings for preparation of the reserves by the applying cut and fill mining method

The total volume of the mine drifting workings for the preparation of the reserves in "Varba-Batantszi" deposit are as follows: (Anastasova, Yanev, 2015; 2013)

- Linear coefficient:

$$\sum l_{n.} = 28\,377\text{ m}; \sum V_{n.} = 318\,745\text{ m}^3;$$

$$\sum l_{h.} = 16\,920\text{ m}; \sum V_{h.} = 124\,770\text{ m}^3;$$

$$K_{n.h.} = \frac{\sum l_{n.h.} \cdot 1000}{Z_{ob.} - Z_{n.h.}} = \frac{45\,297.1\,000}{3\,202\,290 - 376\,805,4} = 16,03\text{ m}/1000\text{ t}$$

- Volume coefficient:

$$K'_{n.h.} = \frac{\sum V_{n.h.} \cdot 1000}{Z_{ob.} - Z_{n.h.}} = \frac{443\,515.1\,000}{3\,202\,290 - 376\,805,4} = 156,97\text{ m}^3/1000\text{ t}$$

In this way, we obtain relative costs of 12.11 BGN/t in the mining works for the preparation for extraction and 3.56 BGN/t during the drifting of the first sublevels and layers.

The mine drifting workings for preparation of the deposits are characterised by completely new parameters of mine drifts (galleries, crosscuts, rises, ramps etc.) and implementation of completely new underground mining equipment for ensuring the mine-production processes and tasks.

### Water intake and ventilation in the "Varba" and "Batantszi" deposits

The project for the Varba - Batantszi deposit envisages vertical and horizontal workings that will be used for ventilation, water intake, transport of ore and materials, auxiliary purposes and emergency exits from the main levels. The ventilation scheme of the Varba - Batantszi mine provides a suction operation of the ventilation system, as the analysis of the

airflow of the individual main levels and workplaces will be carried out by means of ventilation partitions, ventilation doors and fans for local ventilation.

The following air quantity was calculated for the ventilation of the "Varba - Batantszi" underground mine.

- the required amount of air needed – during drifting

Table 1.

Factor	Blasting works	Minimal air seed	Dust
AIR m <sup>3</sup> /s	19.96 m <sup>3</sup> /s	3.5 m <sup>3</sup> /s	16.64 m <sup>3</sup> /s

- the required amount of air needed – during mining

The production programme and the applied mining methods in the mine foresee the simultaneous exploitation of 3 ore blocks, from which follows:

Table 2.

Factor	Drilling	Mobile equipment	Blasting works	Maximum number of persons
AIR m <sup>3</sup> /s	19.5 m <sup>3</sup> /s	61.68 m <sup>3</sup> /s	40.38 m <sup>3</sup> /s	5.5 m <sup>3</sup> /s

According to the requirements of "PBT for the development of ores and non-metallic deposits in the underground mines" and "Instruction for safe application of self-propelled non-rail machines in the underground mines" the required and sufficient air flow for ventilation of the "Varba - Batantszi" mine is taken to be 90 m<sup>3</sup>/s.

For normal mine operation on local ramps and mine faces in the ore bodies, the use of local ventilation fans from Epiroc Atlas Copco AVH 100 is envisaged.

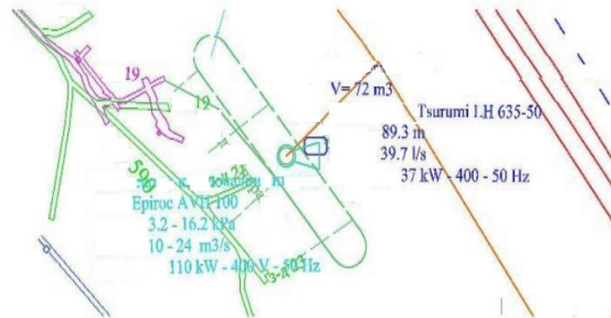


Fig. 5. Water intake and ventilation complex to a local ramp

Ventilation fans for local ramps should be placed at the beginning of each ramp: on level 590 for spirals 1.2 and 3; on level 540 for spirals 5, 6 and 7; on level. 640 for spiral 4. As mining work progresses in depth on each of the local spirals, it is necessary to use additional ventilators for local ventilation in a combined scheme. The aim is to facilitate and optimise the process of ventilation of workplaces by creating normal working conditions.

The water intake scheme provides water drainage to be carried out by 3 main water intake complexes located on level. 300 and level. 435 for the Varba deposit and level. 435 for Batantszi deposit.



Fig. 6. Main water intake complex at level 435 "Batantzi"

The volume of each of the water intake complex must comply with Art. 499 from PBT B-01-02-04 or  $V = 8 \text{ hours} \times 144 \text{ m}^3/\text{h} = 1152 \text{ m}^3$

- For the Varba section of the deposit - the pumping of the water will take place at two levels (two stages) from a main water intake complex at level 300 with a displacement of 105 m to the main water intake complex at level 435, and from there with a displacement of 135 m to an existing water intake complex at level 540 (Vertical Shaft Varba 1) from where, on the existing grid, water will go out of the mine. For the implementation of the water drainage and water intake scheme, it is necessary to build connections (drift mining galleries and rises) between the newly built underground infrastructure and the Vertical Shaft Varba 2.

- For the Batantzi section of the deposit – the water drainage scheme foresees the mine water to be pumped by a main water intake complex at level 435 with a displacement of 155 m through a ventilation stack to a gallery on level 590 from where the water will enter the existing catchment complex and through the existing network the water will go away from the underground mine.

In view of the development of the mining works in depth, a possibility is provided for pumping the water from the water intake complex at level 435 in the direction of the Vertical Shaft Varba 1 through a central inclined ramp.

The water intake of the local ramps and the mining blocks should be carried out by mining pumps type LH 637-50 and the water will be led to the main water intake complexes.

## Conclusions

The new infrastructure in the deposit is designed in line with the need for reaching the reserves in depth, the commissioning of an entirely new self-propelled mobile equipment, the introduction of new mining methods and the overall modernisation of the mine (Siderova, 2016).

The following investment will be needed for the implementation of the project for construction of new infrastructure in the "Varba - Batantzi" underground mine:

Table 3.

No	Type of cost	Total amount, BGN
1.	Purchase of a new self-propelled mobile equipment – 3 full sets	5 420 000
2.	Capital workings	9 401 000
3.	Ventilation	300 762
4.	Water intake	1 695 700
5.	Auxiliary mine workings	375 000
6.	Mine ore and rock mass storages	962 500
7.	Electricity	575 590
	Total	18 730 552

As a result, lower production cost is obtained, the ore production is increased from 101.000 tons to 236.000 tons, i.e. 2.3 times more per year, flexibility and mobility in terms of the overall mining process and the individual production processes are created. There will be a positive final effect of the mining activities.

## References

- Anastasov D., Z. Eftimov et al. 2018. *Working project for reaching opening the reserves in depth and mine preparation works of the Varba-Batantzi deposit under the 590 horizon by drifting a central inclined ramp from horizon 720 to the level of the marbles*. Putting into operation of new mining methods – 2018 (in Bulgarian).
- Anastasov D., Z. Eftimov et al. 2013. *General working project for the extraction and primary processing of metal minerals – lead-zinc ores from "Varba-Batantzi" deposit on the territory of the village of Varba and the town of Madan, municipality of Madan Smolyan region* (in Bulgarian).
- Anastasova, Y., N. Yanev. 2015. Possible application of Internet of Things in the mining industry. – *Proceedings of the 6th Balkan Mining Congress*, Petrosani, 135–140.
- Siderova, G. 2016. Criteria for assessing the competitiveness of mining enterprises. – *Annual of the University of Mining and Geology "St. Ivan. Rilski"*, 59, 4, 43–46 (in Bulgarian).
- Yanev, N., Y. Anastasova. 2013. Means for describing data for application in mining and geology. – *Journal Mining and Geology Magazine*, 7-8, 61–63 (in Bulgarian).

## INNOVATIONS IN THE MINING METHODS IN THE "VARBA – BATANTZI" UNDERGROUND MINE

**Zdravets Eftimov, Dimitar Anastasov**

University of Mining and Geology "St Ivan Rilski" 1700 Sofia; Zdravetse@yahoo.com

**ABSTRACT.** The paper reviews the innovations in the mining methods applied in the "Varba - Batantzi" underground deposit. The mining method applied at the moment in the mine, "sublevel caving", is analysed and attention is paid to the need of creating and designing new mining methods for the "Varba – Batantzi" underground mine. Innovations in the new mining methods are described – "sublevel caving" and "cut and fill" for the specific conditions in the mine. The technological parameters of the new mining methods are presented. Some conclusions are given.

**Keywords:** mine, innovation, technological parameters

### ИНОВАЦИИ ПРИ СИСТЕМИТЕ НА РАЗРАБОТВАНЕ ЗА НАХОДИЩЕ „ВЪРБА – БАТАНЦИ“

**Здравец Ефтимов, Димитър Анастасов**

Минно–геоложки университет "Св. Иван Рилски", 1700 София

**РЕЗЮМЕ.** Статията разглежда иновациите при системите на разработване прилагани в находище "Върба - Батанци". В статията е направен анализ на сега прилаганата система на разработване с подетажно обрушаване в находището и е обърнато сериозно внимание на необходимостта от разработване и конструиране на нови системи на разработване за рудник "Върба - Батанци". Също така са разгледани и иновациите при новите системи на разработване – с подетажно обрушаване и крепене и запълване с прилагане на мобилна механизация. Представени са технологични показатели при системите на разработване и са дадени изводи и заключения.

**Ключови думи:** рудник, иновация, технологични параметри

### Need for changes in the applied mining methods

The development of mining works in the "Varba - Batantzi" underground mine necessitates its modernisation both with the introduction of new machinery and with the introduction of new technology – the introduction of new and innovative mining methods.

It is necessary to apply different mining methods for the different mining areas for the complete mining of the reserves in the deposit. There are no restrictions for protection of objects and facilities in and outside the mine on the flanks of the two sections of Varba and Batants deposits. The project deals with a much more productive and less mine process engaged mining method (sublevel caving mining method). However, a heavy, energy-intensive and resource-intensive mining method with a single-layer of cut and fill mining method is required in the central area of the deposit to guarantee the stability of the existing infrastructure and to ensure the mining of the reserves in the vertical shaft pillar.

The aim of the project is to find optimal parameters of the proposed new mining methods in order to increase the production and to achieve the optimal effect.

### Applied mining method in the "Varba - Batantsi" deposit (Anastasov, Eftimov, 2013)

The preparation of the block in the applied mining method, sublevel caving, is characterised by rock drifts. The block rise is running out of the influence area of rock movement, and it is made with an inclination of 72° according to the ore body. The main level gallery is drifted in the rock mass with cross-section of 7.0 m<sup>2</sup>. Its length is 50 m and it is attached with ¾ wooden frames through 0.75 m, which defines a light cross section of 6.2 - 6.4 m<sup>2</sup>. The rise starts at the 25<sup>th</sup> meter (in the middle of the ore block) and it is with cross section of 6 m<sup>2</sup> (3 m x 2 m). The rise is with two compartments – one is a walk-in ventilator and the other is an ore pass.

From the block rise the cross cuts are drifted to the sub level gallery. The cross section is 7.0 m<sup>2</sup> and is secured with ¾ wooden frames and siding. Their light section is 6.2-6.4 m<sup>2</sup> and is connected with the mechanisation used or mining.

At the mail level gallery, a 10-meter-long cross cut is made with a 7.0 m<sup>2</sup> cross section, which is again secured with ¾ wooden frames. It makes a connection with the first sub level, and the same is used for ventilation and second exit for the next block.

At the bottom of each intersection, a scraper area is formed (5 pieces), with a length of 2.5 m, a section of 7.0 m<sup>2</sup>, in which a scraper is mounted.

At both ends of each of the sub level galleries, it is planned to run initial compensatory spaces with a height of 7.5 m and sections of 6.0 m<sup>2</sup> (3 m x 2 m). They are classically made by sectional blasting of boreholes with a diameter of 51 mm (special passport) and use of the ANFO explosive.

The required time for all mine workings for the preparation of one ore block is 8.01 months.

The drilling and blasting works foresee the drilling of boreholes with a diameter of 51 mm and a heights of 10 m. The drilling gallery has a cross section of 7.0 m<sup>2</sup>.

Borehole loading is mechanised with bulk explosive ANFO and use of AZS-35 or "Kurama" charging machine.

At the same time, one fan is blasted to obtain a 1.8 m thick layer, ensuring normal draining of the ore.

The drain is carried out by a scraper system with a volume of 0.4 m<sup>3</sup> and a scraper with a capacity of 30 kW.

The ore supply under this mining method is done by angular scraping along the undercut work and the intersection to the block rise.

The frames are dismantled before drilling of the boreholes by dismantling 2 frames at the same time spaced 0.75 m apart.

Table 1.

No	Parameter	Dimension	Quantity
1.	Type of block preparation – in the rock mass	-	-
2.	Block parameters		
	- length	m	50
	- main level height	m	50
	- average thickness of the vein	m	3.0
3.	Angle of inclination of the vein	°	80
4.	Drill costs	m <sup>3</sup> /m <sup>3</sup>	0.84
5.	Blasted ore from 1 m of drill hole	m <sup>3</sup> /m'	1.19
6.	Ore density	t/m <sup>3</sup>	3.0
7.	Sublevel height	m	10.0
8.	Mining method losses	%	10
9.	Primary sterile mass intake	%	17
10.	Productivity of miner	m <sup>3</sup> /person per shift	11.98
		t/ person per shift	35.94
11.	Daily block production	t/day	158.5
12.	Monthly block production	t/month	3486.8
13.	Number of blocks in simultaneously works for 120 000 t/year ore production.	number	3
14.	Number of blocks in preparation	number	5

## Innovations in the mining methods in the "Varba - Batantsi" deposit (Anastasov, Eftimov, 2018; Yanev, Anastasova, 2015)

The existing mining method in the underground mine "Varba - Batantsi" is characterised by the use of a large amount of manual labour, using the old equipment which leads to achieving unsatisfactory results. The innovations related to the proposed new mining methods are linked with the use of modern equipment, manual labour reduction and increased production performance. This leads to the design of new mining methods for the deposit and their connecting to the specific conditions in the underground mine.

A sub level caving method for mining the reserves in the flanks of the deposit and a cut and fill method for the reserves in the vertical shaft pillar are introduced.

### Sub level caving mining method

#### - Option I

The preparation of the block with this version of the mining method is done in the rock mass and includes the drifting of a 210-meter-long gallery with a section of 7 m<sup>2</sup>, as well as a 61m-high block rise with a 6 m<sup>2</sup> cross section.

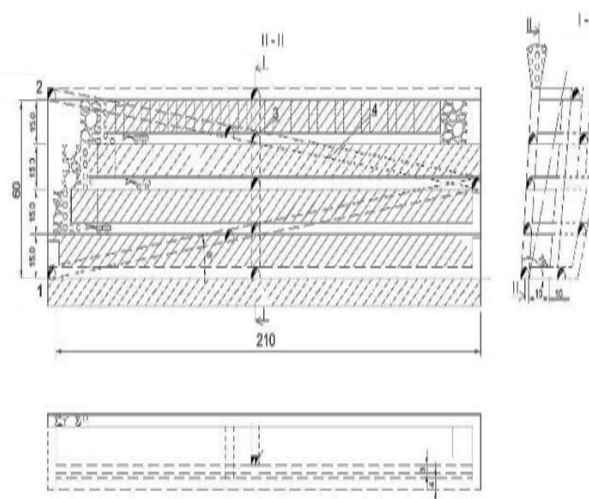


Fig. 1. Sub level caving method

Preparatory mining work includes drifting of cross cuts from the rise with a length of 10 m, a cross section of 12 m<sup>2</sup> and a local inclined ramp 212 m in length and 14 m<sup>2</sup>. Four cross cuts are drifted from the local ramp with a single length of 25 m and a cross section of 14 m<sup>2</sup>, which provide the access of the mobile mechanisation to the extraction mine faces in each block.

In order to enter the block and start with the mining of the ore four sub level galleries are to be done with a cross section of 12 m<sup>2</sup> (4 x 3 m), a total length of 840 m and a compensatory space of 8 pieces with a cross section of 9 m<sup>2</sup> and a total length of 80 m for ensuring the mining activities. The compensatory spaces are driven at the bottom of each sub level gallery.

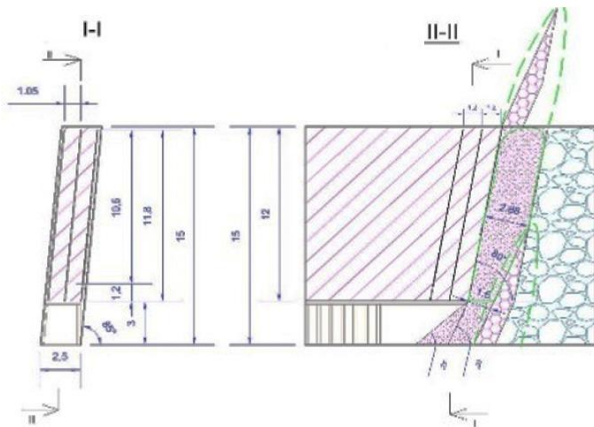


Fig. 2. Drilling and blasting design applied to the sub level caving mining method

- Option II

The mining method design (the block design) applying the sub level mining method Option II includes drifting of sub level galleries through the ore body and in the local inclined ramps, intersections and rises of the rock mass.

The dimensions of the designed blocks in this version of the mining method are different for each block and are limited by the specific dimensions of the ore body in the area. The design of the parameters takes into account the optimal distances for the new mobile equipment which is used. The block sizes of this sub level caving mining method Option II are approximately 200x105x2.5 m.

For the preparation for mining of the reserves at "Varba-North" all of the mine workings include sub level galleries, local ramp N1, cross cuts and rise with a total length of 4165 m, the costs for this task is BGN 5709700. The reserves prepared for mining are 668749 t with relative costs 8.54 BGN/t.

The mining drifts for preparing the reserves of the "Batantsi" mine include sub level galleries, local ramp N 2 and 3, cross cuts and rises with a total length of 4335 m, costs of BGN 4966259. Thus, the total running costs are BGN 6629420 with relative production costs of 7.94 BGN/t.

**Cut and fill mining method**

- Option I

For mining the reserves in the "Varba - Batantsi" underground mine a new innovative cut and fill mining method designed for use of a mobile equipment is offered.

The parameters of the exploitation ore block are: 210 m length; height 60 m; ore body width - 3 m with an angle of 80°.

In order to optimise the mining processes, it is considered to simultaneously work in faces in 3 different dimensions both from bottom to top and from top to bottom.

14m<sup>2</sup> cross cuts are made to provide the drill rig and the front end loader approach. After the cross cut, the first layer is done and the lower part of the inclined local ramp is placed.

The drifting of the main level gallery and the block rises (the movement of each mine face) are combined in order to prepare the reserves in block for mining for not more than 5.6 months.

- Option II

For mining of the reserves in the Varba Central section of the mine a cut and fill mining method with local ramps and usage of new mobile equipment are offered.

The dimensions of the exploitation ore block according to Version II of the cut and fill mining method are different for each block and are limited by the specific size of the ore body in the area. The design of the parameters takes into account the optimal distances for mobile equipment as well as the necessary distance from the ore vein to ensure that mining operations do not enter a zone of motion. The block unit dimensions are approximately 160x105x2.5 m.

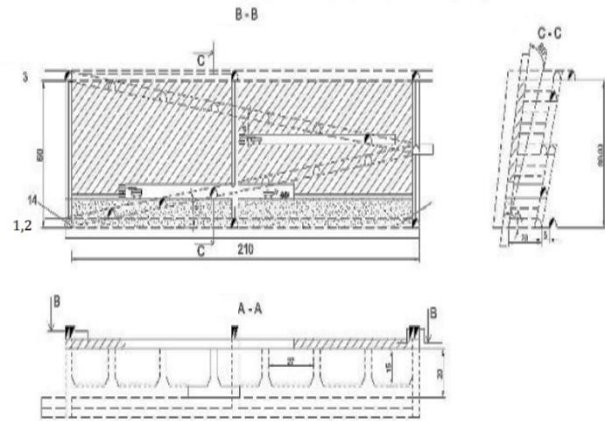


Fig. 3. Cut and fill mining method

The mine workings for this mining method for preparation of the ore body for development are made in the rock mass and include a local ramp, a block rise and triple cross cuts as follows:

- Spiral No 4, triple cross cuts and rise with a total length of 4590 m with a total value of BGN 5434250. The prepared reserves are 693452 t. The relative costs for mining are BGN 7.84 per ton.

- Spiral No 5, cross cuts and rise with a total length of 3437 m and a value of 4776980 BGN. Prepared ore reserves are 372910 t. The relative costs are BGN 12.81 per ton.

- Spiral No 6, cross cuts and rise with a total length of 3401 m, amounting to BGN 4755940 is required, with the prepared reserves being 308251 t. The relative costs are 15.43 BGN/t.

- Spirals No 7, cross cuts and rise with a total length of 3534 m with a value of BGN 4954940. The prepared reserves are 323919 t at a relative cost of 15.30 BGN/t.

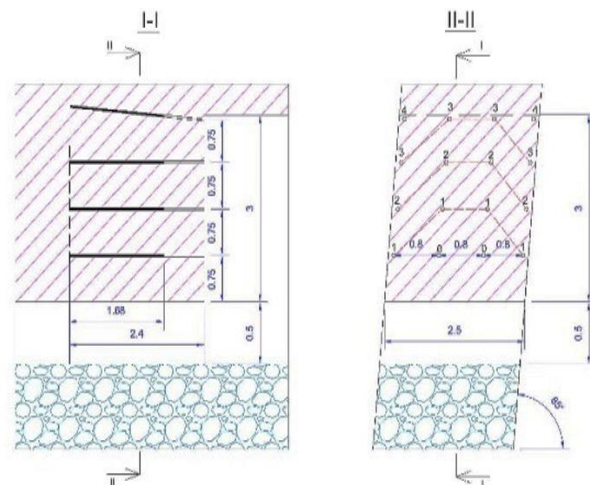


Fig. 4. Drilling and blasting design applied to the cut and fill mining method

## Technical and economic indicators in the new mining methods

Table 2.

Parameters	Measure	MINING METHODS		
		Sub level mining method applied at the moment	Cut and fill mining method Option II	Sub level caving mining method Option II
Length of the ore block	m	50	160	200
Height of the main levels	m	50	105	105
Width of the ore body	m	3.0	2.50	2.50
Inclination of the ore body	°	85°	85°	85°
Extracted ore from 1 m of drill hole	m <sup>3</sup> /m	0.6	0.47	1.02
Height of the layer/sub level	m	7.0	3.0	15.0
Average production of a mine operator	m <sup>3</sup> /miner per shift	5.45	9.04	22.21
Number of the miners up to August 2018	number	229	164	164
Annual mined volumes based on the mining activities	t/year	101 000	130 000	106 524
Average monthly mine production	t/month	8 486	10 805	8 877
Beneficiation costs	BGN/t	25.94	25.94	25.94
Production cost for 1 ton of ore for mining and beneficiation	BGN/t	106.24	84.36	90.13

The economic efficiency of the combined implementation of the sub level caving and cut and fill mining methods Option II shows the following (Anastasova, Yanev, 2017; Siderova, 2018):

- Applying the current mining method, with annual output of 101000 tons of ore and a cost of 106.24 BGN/t an annual loss of approximately BGN 650000 is generated.

- When combining and implementing the new mining methods, sub level caving and cut and fill Option II, the annual output is increased to 236000 tons from both mining methods (130000 tons and 106000 tons, respectively) and an average mine production cost of BGN 87.30 per ton. An annual profit of approximately BGN 3,000,000 before tax and concession fee is realized.

## Conclusions

The proposed new mining methods, sub level caving and cut and fill Option II are uniquely designed and developed for each extraction ore block from the deposit. Optimal results are obtained when the two methods are applied together in the underground mine.

The proposed new mining methods, sub level caving and cut and fill Option II, allow the annual production of the mine to increase from 101000 t/y up to 236000 t/y or 2.3 times.

The average productivity of a mine worker is increased from 5.45 m<sup>3</sup>/miner per shift up to 15.63 m<sup>3</sup>/miner per shift or about 3 times.

The introduction of new mining methods with the usage of mobile equipment allows for the optimisation of the number of workers assigned from 229 to 164, mainly due to the reduction of the staff in extraction, fitters, as well as workers in the field of transport and electric machines.

The implementation of the new mining methods, sub level caving and cut and fill Option II, generates an annual profit of approximately BGN 3000000 before taxes and a concession fee.

## References

- Anastasov, D., Z. Eftimov et al. 2018. *Working project for reaching opening the reserves in depth and mine preparation works of the Varba-Batantzi deposit under the 590 horizon by drifting a central inclined ramp from horizon 720 to the level of the marbles*. Putting into operation of a new mining methods (in Bulgarian).
- Anastasov, D., Z. Eftimov et al. 2013. *General working project for the extraction and primary processing of metal minerals - lead-zinc ores from "Varba-Batantzi" deposit on the territory of the village of Varba and the town of Madan, municipality of Madan Smolyan region* (in Bulgarian).
- Anastasova, Y., N. Yanev, I. Vecherkov. 2017. Possible application of Business Intelligent in the mining industry. – *Proc. of 7th Balkan Mining Congress*, Banja Luka, Bosnia and Herzegovina.
- Siderova, G. 2018. Methodology for the assessment of the competitiveness of a mining company. – *Journal of Mining and Geological Sciences*, 61, 4.
- Yanev, N., Y. Anastasova. 2015. Intelligent Information Technologies, Applicable in the Mining Industry. – *Annual Univ. Mining and Geology "St. Ivan Rilski"*, 58, 4, 95–98 (in Bulgarian with English abstract).

## REDUCTION OF EMISSIONS IMPACT ON THE ENVIRONMENT AND HEALTH OF COAL MINE WORKERS

*Anzhelika M. Ereemeeva, Gennadiy I. Korshunov, Natalia K. Kondrasheva*

*Saint-Petersburg Mining University, 199106 Saint-Petersburg; eremeevaanzhelika@rambler.ru*

**ABSTRACT.** The maximum permissible concentrations of poisonous and harmful gases in the mine atmosphere in existing underground mines during the operation of self-propelled mining equipment with diesel drive used for the transport of people and mined minerals, repair and other types of work were considered. The qualitative composition of pollutants during the operation of a diesel engine has been studied, namely, the main emissions that cause dangerous diseases in workers, such as carbon oxides, oxides and nitrogen dioxide, hydrocarbons, fine particulate matter, sulphur compounds and others, and their concentrations have been determined. The main characteristics of the ZETOR 1404 turbo diesel engine were obtained and studied, and the amount of harmful emissions generated from the use of diesel fuel in this engine was determined. The main methods of reducing emissions of pollutants from diesel vehicles into the atmosphere were also considered, and a method was proposed for reducing harmful substances in exhaust gases by changing the composition of diesel fuel, namely, introducing an environmentally friendly bio-additive into oil fuel, which, when burned, does not form harmful compounds.

**Keywords:** coal mines, diesel engine, MPC, harmful gases

### НАМАЛЯВАНЕ НА ВЪЗДЕЙСТВИЕТО НА ЕМИСИИТЕ ВЪРХУ ОКОЛНАТА СРЕДА И ЗДРАВЕТО НА РАБОТНИЦИТЕ В МИНИ ЗА ДОБИВ НА ВЪГЛИЩА

*Анжелика М. Еремеева, Геннадий И. Коршунов, Наталия К. Кондрашева*

*Санктпетербургски минен университет, 199106 Санкт Петербург*

**РЕЗЮМЕ.** Разгледани са максимално допустимите концентрации на отровни и вредни газове в атмосферата на рудника в съществуващи подземни мини при експлоатацията на самоходно минно оборудване с дизелово задвижване, използвано за транспортиране на хора и добивани минерали, ремонт и други видове работа. Изследван е качественият състав на замърсителите по време на експлоатацията на дизелов двигател, а именно основните емисии, които причиняват опасни заболявания на работниците, като въглеродни оксиди, оксиди и азотен диоксид, въглеводороди, фини прахови частици, серни съединения и др., като техните концентрации са определени. Получени са и изследвани основните характеристики на турбодизеловия двигател ZETOR 1404 и е определено количеството вредни емисии, генерирани от използването на дизелово гориво в този двигател. Разгледани са и основните методи за намаляване на емисиите на замърсители от дизеловите превозни средства в атмосферата и е предложен метод за намаляване на вредните вещества в отработените газове чрез промяна на състава на дизеловото гориво, а именно въвеждане на екологосъобразна биологична добавка. в мазута, който при изгаряне не образува вредни съединения.

**Ключови думи:** въглищни мини, дизелови двигатели, максимално допустима концентрация, вредни газове

### Introduction

The use of self-propelled mining equipment with a diesel drive in coal mines significantly increases labour productivity during such auxiliary work as the transportation of technical fuel and lubricants, repair and rigging works, construction and repair of underground roads, transportation of people, etc. However, the advantages achieved when using self-propelled mining machines and mechanisms with diesel drive in underground conditions can be achieved only under the condition of ensuring safe conditions for their operation (Davies, 2004).

At enterprises using self-propelled mining equipment with a diesel drive, the air of working zones is intensively polluted not only with dust, but also with components of exhaust gases. In addition to increased concentrations of nitrogen oxides, carbon monoxide in the workplace, acrolein and formaldehyde are present in the air (Bagley et al., 2002; Air-Met, 2003). It should be emphasised that in mine air the concentrations of these gases often exceed the permissible values. It should be borne

in mind that the gaseous exhaust products are sorbed on dust and soot particles, increasing the fibrogenicity of dust (Cohen et al., 2002; Davies, 2000). Therefore, the determination of the nature of the combined action of the main components of exhaust gases, the identification of risk factors at these enterprises is of particular importance, as well as the improvement of methodological approaches for the reduction of harmful substances in the specific conditions of mining workings.

One way to improve working conditions in mines is to reduce the harmful effects of emissions on workers' health by changing the composition of the fuel used in self-propelled diesel equipment.

### Analysis of the state of gas pollution in coal mines

Table 1 shows the number of diesel locomotives used in the coal mines of JSC SUEK-Kuzbass.

Table 1. The number of used diesel locomotives in the mines of JSC "SUEK-Kuzbass"

№	Name of mine	Number of diesel locomotives
1	Komsomolets	6
2	Polysaevskaya	6
3	them. S.M.Kirov	12
4	them. A.D.Ruban	3
5	Trunk	8
6	November 7th - new	2
7	im.V.D. Yalovsky "pl. 50	5
8	im.V.D. Yalovsky "pl. 52	7
9	T -West 1	4
10	T -West 2	7
Total:		60

The analysis of the routes of diesel locomotives showed that most of them pass through capital workings with the main incoming and outgoing air jets intended for airing several "consumers", including cleaning and tunnel faces. Due to the high methane content at excavation sites and dead-end preparatory workings in most of the mines of SUEK-Kuzbass, the main criterion determining the amount of air in the ventilation jets is dilution of methane to the maximum allowable concentrations. Thus, the calculated air flow rate required for diluting exhaust gases of diesel engines is almost universally a multiple of the accepted air flow rate for airing the workings. However, in some cases, routes of movement of diesel locomotives pass outside the routes of movement of the main air flow (for example, the ventilation drift of the adjacent prepared or already prepared extraction column, the disassembly chamber, etc.) 5, the Yalovsky mine), which necessitates the conduct of mine research to determine the degree of gas pollution of these mine workings by exhaust gases and the potential for its reduction.

The average quantitative and qualitative characteristics of the pollutants from the work of diesel locomotives in the mine air at the mines of SUEK-Kuzbass, are given in Table 2.

Table 2. The composition of the mine air in the main positions

Sampling point	Gas concentration, %				
	CO <sub>2</sub>	O <sub>2</sub>	CO	CH <sub>4</sub>	NO <sub>x</sub>
In workplace driver	0.04	20.92	0.0005	0.00	0.00004
Baseline	0.03	20.92	0.0006	0.00	0.00002
At the exhaust (min. Load)	2.02	16.06	0.0017	0.00	0.0008
At the exhaust (max. Load)	2.04	16.05	0.0034	0.00	0.0014
20 meters from the diesel locomotive	0.12	20.62	0.0001	0.00	0.00001

As can be seen from the data in Table 2, the largest amount of emissions comes from carbon dioxide and carbon monoxide. Carbon monoxide is tasteless and odourless, but at high concentrations causes dizziness, headache, nausea, and can lead to fainting. A slight increase in the concentration of carbon dioxide, up to 2-4%, in the premises leads to the development of drowsiness and weakness in people.

The current regulatory and technical document for the regulation of exhaust gases when diesel engines operate in coal mines is the Order of the Federal Service for Ecological, Technological and Nuclear Supervision dated January 12, 2016 N7 "On approval of Safety Guidelines" Recommendations for use in coal mines transport vehicles with diesel drive", according to which the maximum permissible concentrations (MPC) of exhaust gases are summarised in Table 3.

Table 3. Recommendations for use in coal mines transport vehicles with a diesel engine

Harmful gases	Maximum permissible concentration of gas in operating mountain conditions	
	%	mg/m <sup>3</sup>
CO	0.00170	20
NO <sub>x</sub>	0.00025	5
Sulphurous anhydride	0.00038	10
H <sub>2</sub> S	0.00070	10

Analysing the data from Tables 2 and 3, we can conclude that the values of emissions of nitrogen oxides and carbon oxides exceed the norm at the exhaust (at maximum and minimum load), but the concentration of carbon dioxide exceeds the norm in all measurement sites.

According to GOST 12.1.005-88 Occupational Safety Standards System (OSS) the general sanitary and hygienic requirements for the air of the working area (with a change in N 1) MACs of harmful gases are listed in Table 4.

Table 4. General sanitary and hygienic requirements for working area air

Harmful gases	MPC mg/m <sup>3</sup>	Hazard Class	human influence
NO <sub>x</sub>	7	III	O
CO	20	IV	O
Sulfurous anhydride	10	III	
H <sub>2</sub> S	10	II	O

Note: O - substances with a highly directional mechanism of action requiring automatic control of their content in the air.

Based on the MPC values in GOST 12.1.005-88, it can be concluded that the concentration of nitrogen oxides and carbon oxides exceed the norm on the exhaust (at maximum and minimum load).

### The way to reduce the concentration of harmful substances in the air of the working area of coal mines

Significant reduction of aerotechnogenic load during the work of diesel locomotives can be achieved through an integrated approach, involving the implementation of several tools in practice. Particular attention should be paid to the development of diesel fuel additives to reduce harmful

emissions. The use of biodiesel in traditional diesel engines significantly reduces the amount of hydrocarbons emitted into the atmosphere, carbon monoxide, sulphates and particulate matter, toxic and carcinogenic substances (Anchita, 2017). Due to the fact that biodiesel does not contain sulphur, sulphur dioxide does not enter the atmosphere when it is burned. The high content of oxygen in biodiesel contributes to a more complete burning of CO<sub>2</sub> (Bezergianni, Dimitriadis, 2013).

In the last decade, the esterification process of fatty acids contained in vegetable oils (for example, sunflower, corn, flax, etc.) and animal fats has become very popular. This technology is based on the interaction of organic acids with alcohols, leading to the formation of esters (Fig. 1), (Bezergianni, Dimitriadis, 2013).

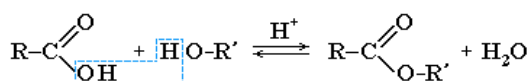


Fig. 1. Scheme of the esterification reaction

For the synthesis of biodiesel according to the esterification method, the authors selected acids contained in sunflower oil and dihydric alcohol (ethylene glycol) as raw materials. After this process, the separation of the phases (organic and aqueous) in the product mixture was carried out by sedimentation, drying and distillation. Table 5 shows the main indicators of the quality of biodiesel fuel obtained by esterifying fatty acids of sunflower oil (FASO) with a dihydric alcohol in comparison with the physicochemical properties of a mixture of fatty acids isolated from sunflower oil (Kondrasheva et al., 2018; Kondrasheva et al., 2019).

Table 5. Physical and chemical properties of a mixture of FASO and biodiesel fuel obtained by the esterification of FASO with ethylene glycol

Indicator	FASO	Biodiesel fuel
Density at 20 °C, kg/m <sup>3</sup>	0.90978	0.91400
Viscosity at 40 °C, mm <sup>2</sup> /s	27.995	23.250
Flash point in closed crucible, °C	115	>110
Sulphur content, mg / kg	13	71
Lubricity (CWSD) * at 60 °C, microns	157	202

Note: \* CWSD - corrected wear spot diameter.

## Calculation of harmful emissions from fuel combustion

At the mining enterprises, the most common is the Zetor 1404 engine in the underground monorail transport. The engine operating parameters are presented in Table 6.

Table 6. The parameters of the diesel engine Zetor 1404

Engine's type	ZETOR 1404 turbo (for mine conditions)
Engine type	with compression ignition, direct fuel injection
Max. power	81 kw – 5 %
Nominal speed	2300 min <sup>-1</sup>
Number of cylinders	4
Fuel consumption	255 g/ kWh
fuel	diesel fuel

The amount of pollutants emitted into the atmosphere during the operation of this engine was determined through the material balance (Fig. 2).

$$S_s / S_c = 0,3746S_c;$$

$$S_c / S_H = 0,0839C/H;$$

$$\alpha S_c / S_o = 0,1678C / (0,3356C + H);$$

$$S_o / S_N = 1,1082(0,21 + O);$$

Fig. 2. Material balance of substances in the exhaust gases

The calculated amount of harmful substances when using petroleum diesel fuel and improved diesel fuel (NPFD) are presented in Table 7.

Table 7. The amount of harmful substances when using petroleum diesel and improved diesel fuel

Harmful gases	NPFD, g/min	DF, g/min
NO <sub>2</sub>	1.976	3.19
NO	0.321	0.518
C	0.41	0.662
Sulfurous anhydride	0.23	0.39
CO	1.57	3.108
Kerosene	0.51	0.9

As can be seen from Table 8, the amount of harmful substances when using diesel fuel with a bio-additive decreases by almost 2 times.

## Conclusion

The most effective way to reduce harmful substances is to improve the quality of the fuel used, the use of additives or alternative fuels. All these methods can be combined using the introduction of bio-additives based on animal and vegetable fats and oils into the composition of the fuel and including the composition of esters (Kondrasheva et al., 2018). Simultaneously with the reduction of harmful emissions when using these additives, the engine life increases by 2-3 times, the diameter of the fuel wear spot decreases, and the calorific value decreases.

## References

- Air-Met, Diesel Particulate Monitoring*. 2003. Spotlight, Customer Information Circular, August/September.
- Anchita, J. 2017. HYDRO-IMP technology for upgrading of heavy petroleum. – *Journal of Mining Institute*, 224, 229–234.
- Bagley, S. T., W. F. Watts, J. P. Johnson, D. B. Kittelson, J. H. Johnson, J. J. Schauer. 2002. *Impact on Low-Emission Diesel Engines on Underground Mine Air Quality*. NIOSH Grant No. R01/CCR515831-01.
- Bezergianni, S., A. Dimitriadis. 2013. Comparison between different types of renewable diesel. – *Renewable and Sustainable Energy Reviews*, 21, 110–116.
- Cohen, H. J., J. Borak, T. Hall, G. Sirianni, S. Chemerynski. 2002. Exposure of miners to diesel exhaust particulates in underground non-metal mines. – *AIHA Journal*, 63, 651–658.
- Davies, B. 2000. *Application of an Elemental Carbon Analyser to the Measurement of Particulate Levels from Diesel Vehicles*. ACARP Report C7014.
- Davies, B. 2004. *The control of diesel particulates in underground coal mines*. PhD Thesis, Victoria University of Technology.
- Kondrasheva, N. K., A. M. Eremeeva, K. S. Nelkenbaum. 2018. Development of domestic technology for producing high-quality environmentally friendly diesel fuel. – *Izv. Universities. Chemistry and Chem. Technology*, 61, 9-10, 76–82.
- Kondrasheva, N. K., A. M. Eremeeva, K. S. Nelkenbaum, O. A. Baulin, O. A. Dubovikov. 2019. Development of environmentally friendly diesel fuel. – *Petroleum Science and Technology*, 37, 12, 1478–1484.

## EVALUATION OF THE POSSIBILITIES FOR SUSTAINABLE EXPLOITATION OF A DEPOSIT FOR KAOLIN AND SILICA SANDS

*Daniel Georgiev, Simeon Asenovski, Dimitar Kaykov, Ljupcho Dimitrov, Ivaylo Koprev*

*University of Mining and Geology "St. Ivan Rilski", 1700 Sofia; orpi\_vr@mgu.bg*

**ABSTRACT.** The article reviews the development of an existing open-pit mine for kaolin and silica sands. The possibilities for the development of the pit have been considered for a period of 10 years. The key parameters for the efficiency of the open-pit mine have been determined according to the specific conditions of the deposit and the location of the pit. A solution for the development of the open-pit mine has been proposed.

**Keywords:** open-pit mining, kaolin-silica sands

### ОЦЕНКА НА ВЪЗМОЖНОСТИТЕ ЗА УСТОЙЧИВО РАЗВИТИЕ НА МИНИТЕ РАБОТИ В НАХОДИЩЕ ЗА КВАРЦ-КАОЛИНОВИ ПЯСЪЦИ

*Даниел Георгиев, Симеон Асеновски, Димитър Кайков, Лючо Димитров, Ивайло Копрев*

*Минно-геоложки университет "Св. Иван Рилски", 1700 София*

**РЕЗЮМЕ.** В настоящия материал е разгледан съществуващ открит рудник за добив на кварц-каолинови пясъци. Разгледани са възможностите за продължаването на неговото разработване за период от 10 години. Формулирани са ключовите показатели, определящи ефективността на открития рудник, съобразени с неговите специфични условия. Предложено е крайно решение за развитие на минните работи.

**Ключови думи:** открит добив, кварц-каолинови пясъци

### Introduction

In order to choose a suitable mining technology for extracting certain mineral resources the key factors which determine the efficiency of the mining process must be considered. In the current paper the possibilities for maintaining a stable mining process in an open-pit mine for kaolin and silica sands for the next 10 years has been researched. The deposit is situated in the northern part of Bulgaria and has certain important limiting conditions which lead to a unique problem and a unique solution which can, however, be considered as typical for a conventional non-metallic open-pit mine.

### Factors which affect the choice of mining technology

The main goal for achieving an optimal mine design is to establish a link between the surface and the layers of kaolin and silica sands while maintaining the volume of excavated overburden as low as possible. In order to achieve the goal, several main factors which affect the choice of the mining technology for extraction have to be pointed out:

- the terrain of the mined area;
- the area which is planned for mining;
- the annual output for the pit;
- the shape of the deposit;

- the mechanical properties of the rocks;
- the height of the benches;
- the climate conditions;
- the annual strip ratio.

First of all, the terrain has a mild slope of around 4° and stretches over 72000 m<sup>2</sup>. Therefore, this does not require any special preliminary preparations for the utilisation of the conventional mining equipment for similar non-metallic deposits (excavator, mining trucks and bulldozer). Furthermore, the shape of the deposit is near-horizontal and stretches all around the boundaries of the deposit. However, the depths of the overburden and the silica sands vary from 9 m to 15 m across the boundaries of the deposit. According to the geological surveying some neighbouring layers of silica sands vary in their depth due to the inclusions of sandstones.

Based on the overall geological report on the deposit, an annual production of 30 000 m<sup>3</sup> kaolin and silica sands has been established for a period of over 30 years. Until this moment the open-pit mine has been in exploitation and will further be exploited. In the current paper a different part of the deposit is considered to be mined in order to open up a new mining surface and to maintain the level of the annual output.

The mechanical properties of the rocks are as follows:

- cohesion –  $C = 35 \cdot 10^5$  Pa;
- angle of internal friction –  $\varphi = 25^\circ$ ;
- density (kaolin and silica sands) –  $\gamma = 1900$  kg/m<sup>3</sup>.

For that purpose, the current height of the benches is 6 m and the slope angle is 55°.

According to the past experience of exploiting the deposit, two more key factors which influence and limit the further development of the pit can be pointed out:

- Slope stability;
- Limited area for overburden storage.

Maintaining a low volume of overburden due to the limited storage also achieves another benefit from the technological solution – lower costs for overburden extraction and storage.

For maintaining the desired level of stability it is recommended that the highest value of the slope angle for the pit should be 55°. Although the stability coefficient is greater than 1.5 this slope angle is based on the experience in similar pits and on past experience. Furthermore, this slope angle guarantees the stability on a longer-term scale, including during the winter season and during snow meltdowns.

For each case the width of the working bench is considered to be 20 m. In addition, the width of the transport ramps is 7 m which ensures the safe passage of one truck as the truck fleet for each shift consists of only up to three trucks.

### Parameters of efficiency

In order to make a grounded decision for the further development of the pit, certain parameters of efficiency have to be established (Bosnev et al., 2018). In order these parameters to be established in an adequate manner, they have to reflect the economic and technological side of the problem. For this reason, the three key parameters of efficiency, which should be considered when choosing the mining technology, are:

- The volume of overburden required for extraction, m<sup>3</sup>;
- The volume of estimated losses of the mineral resource, m<sup>3</sup>;
- Transportation distances for overburden storage, m.

In addition, a secondary parameter of efficiency can be added in order to measure how the mining fleet is utilised for a period of 10 years by applying the variance coefficient for the overburden ration for the different years (Bosnev, Kaykov, 2018). It is important to notice that this parameter gives only a basic information how stable the volumes of overburden are during the open-pit mine development and it has to be used only as a further argument for the decision.

The specific conditions for the deposit have shown that very little can be achieved via interchanging the values of the slope angles for the pit or the overburden storage facility due to the smaller size of the pit. Hence, this requires a different type of solution regarding the choice of a mining technology. For this purpose, three scenarios have been considered for establishing the desired results.

The first scenario utilises the area of the previously used pit for storing the overburden, while the second and third scenario utilise the old pit for removing the overburden and reaching the silica sands.

#### Scenario 1

The first scenario deals with the problem of the limited space for dumping the overburden.

The utilisation of the old open-pit mine ensures an area of about 17 000 m<sup>2</sup> for overburden storage. The entry point to the pit is situated as close as possible to the road leading to the overburden dump. Table 1 shows the four parameters of efficiency.

Table 1. Parameters of efficiency for Scenario 1

Total volume of overburden, m <sup>3</sup>	Volume of estimated loses, m <sup>3</sup>	Average distance to overburden stockpile facility, m	Variation coefficient of the overburden
429 600	13 500 (4.5%)	250	0,285

Furthermore, the direction of development of the pit is situated perpendicularly to the direction of the slope. Table 2 shows the different volumes of extracted silica sands and overburden, as well as the strip ratio.

Table 2. Volumes of overburden for Scenario 1

Year	Volume of overburden, m <sup>3</sup>
1	62 280
2	41 520
3	48 600
4	32 400
5	36 720
6	24 480
7	46 080
8	30 720
9	64 080
10	42 720

Figure 1 is a general representation of the designed position for the 10<sup>th</sup> year of exploitation. The light-coloured lines represent schematically the position of the toe of the bench level 36.

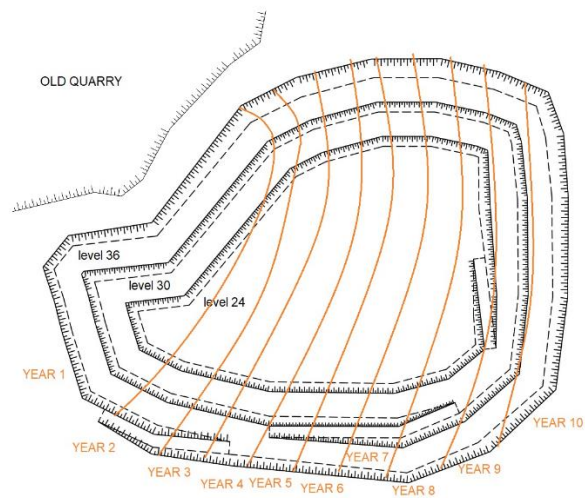


Fig. 1. Approximate annual development of the open-pit mine for reaching the design contour at year 10 in Scenario 1

The most important conclusion of this scenario is that the volume of overburden from the initial stages of the period of 10 years is the biggest as the closest entry point to the overburden dump is situated where the higher parts of the terrain are situated.

The variation coefficient has a low value, which means that the mining fleet will be utilised in an efficient manner during the 10-year period.

#### Scenario 2

The second scenario deals with the problem of reducing the required area for storing the overburden, especially during

the later stages of the development of the pit. Furthermore, the direction of the pit development is parallel to the direction of terrain rising. The old open-pit mine is utilised as an entry point to the new boundaries of the pit. During the initial stages the volumes of overburden are slightly lower than the ones from Scenario 1, leading to a lower required space for the dump. Furthermore, the extracted space in the pit is used for storing a bigger part of the overburden. Table 3 shows the four parameters of efficiency.

Table 3. Parameters of efficiency for Scenario 2

Total volume of overburden, m <sup>3</sup>	Volume of the blocked mineral resource, m <sup>3</sup>	Average distance to overburden stockpile facility, m	Variation coefficient of the overburden
676 500	16 200 (5.4%)	70	0,288

Table 4 shows the volumes of overburden, extracted sands and the strip ratio for the period of 10 years. The variation coefficient is also high in this scenario and slightly differs from scenario 1.

Table 4. Volumes of overburden for Scenario 2

Year	Volume of overburden, m <sup>3</sup>
1	114 135
2	76 090
3	73 900
4	49 265
5	70 615
6	47 075
7	72 805
8	48 535
9	74 450
10	49 630

Figure 2 is a general representation of the designed position for the 10<sup>th</sup> year of exploitation. The light-coloured lines represent schematically the position of the toe of the bench level 36.

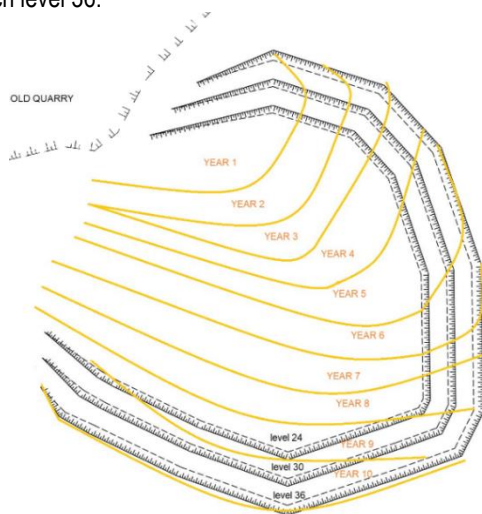


Fig. 2. Approximate annual development of the open-pit mine for reaching the design contour at year 10 in Scenario 2

**Scenario 3**

The third scenario is a modification of Scenario 2, however, they differ in the direction of the pit development. In Scenario 3 it is parallel to the direction of the slope. Table 5 presents the parameters of efficiency for this scenario.

Table 5. Parameters of efficiency for Scenario 3

Total volume of overburden, m <sup>3</sup>	Volume of estimated loses, m <sup>3</sup>	Average distance to overburden stockpile facility, m	Variation coefficient of the overburden
676 500	10 200 (3.4%)	70	0.466

Table 6 presents the volumes of overburden, silica sands and the strip ratio for the 10-year period.

Table 6. Volumes of overburden for Scenario 3

Year	Volume of overburden, m <sup>3</sup>
1	140 580
2	93 720
3	74 520
4	49 680
5	46 260
6	30 840
7	54 000
8	36 000
9	90 540
10	60 360

Figure 3 is a general representation of the designed position for the 10<sup>th</sup> year of exploitation. The light-coloured lines represent the position of the toe of the bench level 36.

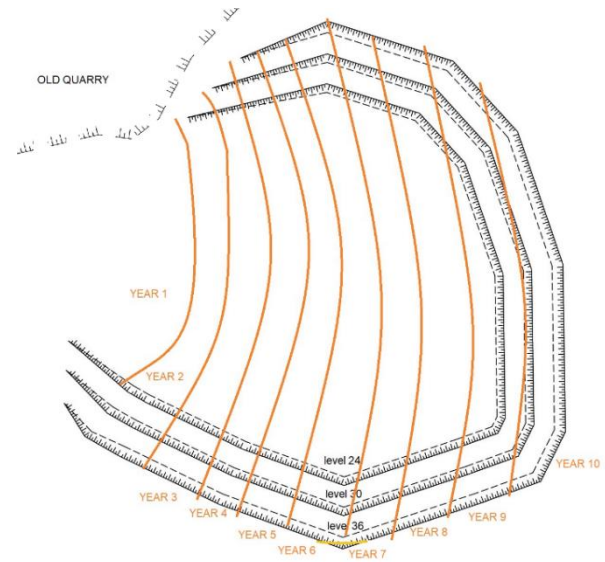


Fig. 3. Approximate annual development of the open-pit mine for reaching the design contour at year 10 in Scenario 3

It is important to notice that the slope of the old quarry ceases to exist after the 10<sup>th</sup> year due to the mining operations starting for the old mining site. The slope of the quarry on figures 2 and 3 is just for illustration.

## Conclusions

From the consideration of the three scenarios, the following conclusions can be made:

- The direction of the pit development leads to the different volumes of overburden during the 10-year period.
- The variation coefficient indicates that in each scenario the utilisation of the mining equipment will be different during the different years. This could be further adjusted in order to maintain a more stable work flow on an annual level.
- The variation coefficient can prove to be an informative parameter for the steadiness of the process on a strategic level as the total volume of overburden will be excavated. The differences that occur apply only to the mining sequence which leads to the bigger variations in the output flows.
- Scenario 1 may not be entirely better than Scenario 3, but it provides a good short-term solution for the development of the pit.
- However, if the open-pit mine is to be exploited during a full 30 to 35-year life span, then it would be wiser to adjust the

output of overburden for Scenario 3 in order to minimise the transportation costs, as well as to limit the volumes of losses.

- The scenarios which utilise the extracted space within the current pit for storing the overburden are related not only to shorter distances for dumping the overburden, but also to the lesser environmental impact.

## References

- Bosnev, S., D. Kaykov. 2018. A comparison of scenarios for optimising the development project of an open-pit mine. – *Mining and Geology*, 1-2, 39-41 (in Bulgarian).
- Bosnev, S., I. Koprev, D. Kaykov. 2018. Analysis of the essential factors, determining the efficiency of the design for the development of an open-pit mine. – *Proc. XXV World Mining Congress, Astana, Kazakhstan*.

## RESEARCH ON CREATING A DIGITAL PHOTOGRAMMETRIC MODEL BY USING DIFFERENT NUMBER OF CONTROL AND CHECK POINTS

**Veselina Gospodinova**

University of Mining and Geology "St. Ivan Rilski", 1700 Sofia; veselina\_gospodinova80@abv.bg

**ABSTRACT.** Improvement of the digital cameras and development of the digital image processing methods have led to the application of digital photogrammetry in underground mining. These days many studies are focused on the creation of digital models, which is one of the most important activities in mining. The reason is that a number of mine surveying and geological problems are solved through the models. A study related to the number of control points used in creating a digital photogrammetric model is presented in the paper. The obtained results are illustrated and analysed.

**Keywords:** close-range photogrammetry, digital photogrammetry, underground mine, control and check points

### СЪЗДАВАНЕ НА ЧИСЛЕН ФОТОГРАМЕТРИЧЕН МОДЕЛ, ИЗПОЛЗВАЙКИ РАЗЛИЧЕН БРОЙ ОПОРНИ И КОНТРОЛНИ ТОЧКИ

**Веселина Господинова**

Минно-геоложки университет "Св. Иван Рилски", 1700 София

**РЕЗЮМЕ.** Усъвършенстването на апаратурата за заснемане и развитието на цифровите методи за обработка на изображения доведе до прилагането на цифровата фотограмметрия в подземния добив. Все повече проучвания са насочени към създаване на числени модели което е една от най-важните дейности в минното дело, тъй като чрез тях се решават маркшайдерски и геоложки задачи. Представено е изследване свързано с броя на използваните опорни точки при създаване на числен фотограметричен модел. Получените резултати са онагледени и анализирани.

**Ключови думи:** блискообхватна фотограмметрия, цифрова фотограмметрия, подземен рудник, опорни и контролни точки

### Introduction

The photogrammetric methods allow three dimensional models in underground mines to be generated. They are used as well to create digital models of galleries or parts of them, to calculate the volume of mined-out mass, to map the progress of mining activities, geological and structural mapping. These methods are applied also while observing walls and pillars. The number of used control points, their locations, as well as the root mean square error of the model and the points in the model itself are very important. The reason is because the solving of certain mine surveying and geological tasks requires accurate determination of coordinates of points, measurement of lengths, angles and other geometric features.

The deformation state of rock mass, galleries and pillars, and also their observation is a very important task for every underground mine. Most often they are followed by visual observations and specialised equipment. Even though, the subjectivity of surveillance techniques may be admitted to vague or incomplete analyses, due to the small amount of measured data. Observing changes with standard tools is costly and time-consuming, and the collected information is limited. An alternative to these methods is the use of digital photogrammetry for the exploration and monitoring of rock mass in underground mines, presented by Benton and colleagues. They have conducted two laboratories and field

studies to prove that photogrammetry is a useful tool, which provides not only high precision but also occupational safety (Benton et al., 2016).

Other studies have evaluated the photogrammetric systems for ground control in underground mines. The research was conducted over a three-year period in Lucky Friday Mine, the United States, for the extraction of ore from rocks, which are susceptible to destruction, at a depth to 2,100 meters. The analysis of the results shows that the photogrammetric system is commensurate with conventional tools for measure of deformations, especially with regard to the interpretation of the potential movement in crossing the geological disturbance across the fault. The advantages of photogrammetry are presented, namely the increase of measurements compared to standard tools as crackmeter and the use of photogrammetric data together with 3D visualisation software for the synthesis and integration of complex information from a variety of sources, such as geology, mining technical conditions, seismicity and geotechnical toolkit (Benton et al., 2017).

Digital photogrammetric models help different specialists in mining companies - managers, engineers, miners, employees who are responsible for logistics, safety and health care. These models give a more comprehensive picture of the situation in the underground mine and they would be a suitable tool for both managers (investors, directors, managers) and employees in mining companies.

One of the main purpose of this research is to make comparison between points, whose coordinates are measured by a total station and the same points whose coordinates are received from the photogrammetric model. Another aim is to analyse both obtained results.

### Experiments

In this study, data from a realized scientific research project at the University of Mining and Geology "St. Ivan Rilski" in 2018 is used. During the project a part of a gallery in the underground mine "Erma Reka", Gorubso Zlatograd Corporation was shot by a photogrammetric method. The capture was executed by a Canon EOS 600D digital camera with a 16Mpix resolution and with the help of two external additional LED lamps. In order to create the model 314 photos were captured. There were 21 fixed points permanently marked on the researched object, which were evenly spaced. Their location is shown in Figure 1. The control points were measured with a total station – "Trimble S6" in a local coordinate system. The Russian software "Agisoft Photo Scan Professional Edition" processed the data, which were images in raw format. The resulting mean square error (absolute precision of the model) after the adjustment is 0.0072m and it is shown in Figure 2. In the same area a survey was conducted with a total station "Trimble S6" with built-in module for scanning of surface. A scanning step was selected - 0.50 m x 0.50 m (Begnovska, 2016). A comparison between the volume of mined-out mass from the model obtained from the photogrammetric shooting and the one from the geodetic survey was made. The difference in the volumes is in the range of 1.02%, which suggests that the proposed photogrammetric method can be used to calculate the volume of mined-out mass in underground mines. The results show that the presented methodology can be applied in real conditions for solving various mine surveying tasks: creation of three-dimensional mining models and graphic documentation, monitoring the progress of the exploitation activities, of volumes' calculations, structural mapping and others (Gospodinova et al., 2018).

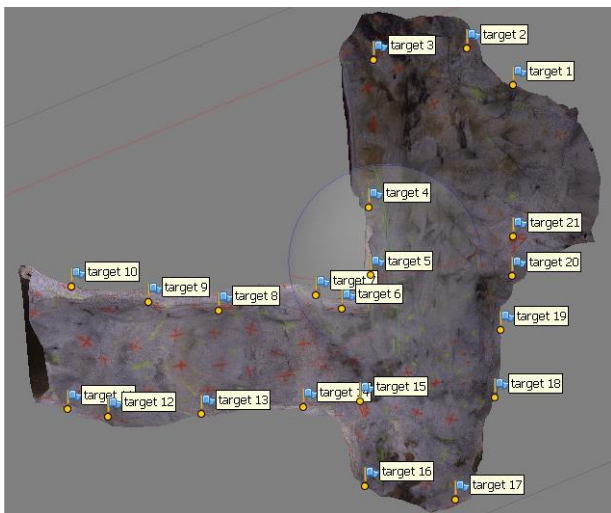


Fig. 1. Visualisation of a generated textured top-view photogrammetric model using 21 control points

Markers	X (m)	Y (m)	Z (m)	Accuracy (m)	Error (m)	Projectio
<input checked="" type="checkbox"/> target 1	1998.082000	1001.688000	501.257000	0.005000	0.007195	39
<input checked="" type="checkbox"/> target 2	1997.088000	1000.774000	501.936000	0.005000	0.003509	43
<input checked="" type="checkbox"/> target 3	1997.070000	998.849000	501.933000	0.005000	0.003742	44
<input checked="" type="checkbox"/> target 4	2000.318000	998.512000	500.553000	0.005000	0.003638	24
<input checked="" type="checkbox"/> target 5	2001.512000	998.293000	501.724000	0.005000	0.003651	63
<input checked="" type="checkbox"/> target 6	2002.147000	997.616000	501.578000	0.005000	0.007792	31
<input checked="" type="checkbox"/> target 7	2001.951000	997.197000	500.695000	0.005000	0.011681	41
<input checked="" type="checkbox"/> target 8	2001.799000	995.080000	501.881000	0.005000	0.010022	71
<input checked="" type="checkbox"/> target 9	2001.505000	993.702000	501.416000	0.005000	0.008574	69
<input checked="" type="checkbox"/> target 10	2001.111000	992.232000	500.645000	0.005000	0.008643	49
<input checked="" type="checkbox"/> target 11	2003.567000	991.836000	500.922000	0.005000	0.003695	51
<input checked="" type="checkbox"/> target 12	2003.620000	992.537000	502.137000	0.005000	0.007770	31
<input checked="" type="checkbox"/> target 13	2004.032000	994.557000	500.913000	0.005000	0.008336	54
<input checked="" type="checkbox"/> target 14	2004.108000	996.633000	501.264000	0.005000	0.012756	74
<input checked="" type="checkbox"/> target 15	2004.022000	997.742000	501.961000	0.005000	0.007754	73
<input checked="" type="checkbox"/> target 16	2005.795000	997.649000	501.896000	0.005000	0.006457	68
<input checked="" type="checkbox"/> target 17	2006.272000	999.433000	502.143000	0.005000	0.008327	62
<input checked="" type="checkbox"/> target 18	2004.450000	1000.554000	501.248000	0.005000	0.001633	54
<input checked="" type="checkbox"/> target 19	2003.035000	1000.802000	501.562000	0.005000	0.006715	69
<input checked="" type="checkbox"/> target 20	2002.031000	1001.218000	501.080000	0.005000	0.004029	45
<input checked="" type="checkbox"/> target 21	2001.009000	1001.223000	502.375000	0.005000	0.003347	75
<b>Total Error</b>						
Control points					0.007247	

Fig. 2. Coordinates of the control points and mean square error of the photogrammetric model's adjustment

The main task of the present study is to identify the differences between geodetic and photogrammetric coordinates of control points located in a part of an underground mine gallery. The control points were obtained once by direct geodetic measurements with a total station "Trimble S6" and the second time they were measured by the created photogrammetric model of the same part.

A minimal number of required control points is used for the creation of the digital photogrammetric model – in this case 4 (3, 10, 17, 21). This will reduce the time to measure the control points and will lead to increasing the efficiency of the workflow. Figure 3 presents the location of control points in the model.

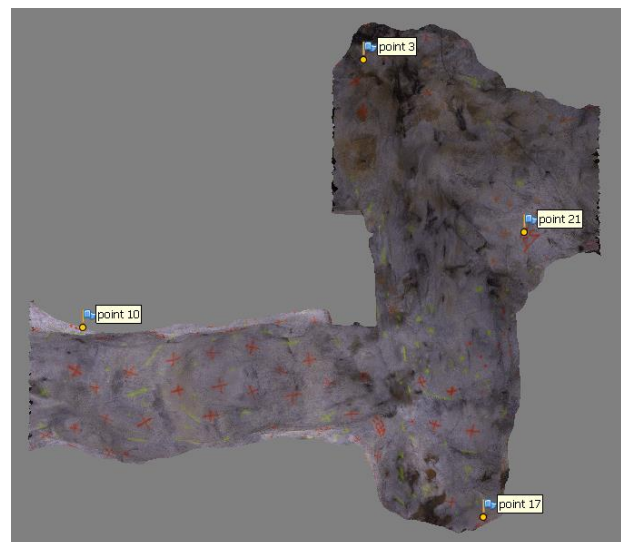


Fig. 3. Visualisation of a generated textured photogrammetric model using 4 reference points

**Determination of the coordinate differences by manual measurement of the coordinates of the control points in the photogrammetric model**

The photogrammetric model was generated by the “Agisoft Photo Scan Professional” software. The coordinates of 17

marked points in the photogrammetric model are measured. For the same point the geodetic coordinates are also measured. They serve as control points. Differences (errors) of x, y and z between the geodetic and photogrammetric coordinates are calculated and presented in Table 1.

Table 1.

№ of point	The values obtained from geodetic measurements			The values measured from the photogrammetric model			Errors		
	X <sub>r</sub> [m]	Y <sub>r</sub> [m]	Z <sub>r</sub> [m]	X <sub>φ</sub> [m]	Y <sub>φ</sub> [m]	Z <sub>φ</sub> [m]	Δx <sub>i</sub> [m]	Δy <sub>i</sub> [m]	Δz <sub>i</sub> [m]
1	1998.082	1001.688	501.257	1998.079	1001.683	501.252	0.003	0.005	0.005
2	1997.088	1000.774	501.936	1997.086	1000.770	501.933	0.002	0.004	0.003
4	2000.318	998.512	500.553	2000.318	998.508	500.551	0.000	0.004	0.002
5	2001.512	998.293	501.724	2001.513	998.291	501.726	-0.001	0.002	-0.002
6	2002.147	997.616	501.578	2002.140	997.620	501.586	0.007	-0.004	-0.008
7	2001.951	997.197	500.695	2001.946	997.192	500.694	0.005	0.005	0.001
8	2001.799	995.080	501.881	2001.791	995.076	501.892	0.008	0.004	-0.011
9	2001.505	993.702	501.416	2001.499	993.701	501.411	0.006	0.001	0.005
11	2003.567	991.836	500.922	2003.569	991.836	500.927	-0.002	0.000	-0.005
12	2003.620	992.537	502.137	2003.618	992.534	502.138	0.002	0.003	-0.001
13	2004.032	994.557	500.913	2004.032	994.556	500.915	0.000	0.001	-0.002
14	2004.108	996.633	501.264	2004.100	996.622	501.254	0.008	0.011	0.010
15	2004.022	997.742	501.961	2004.025	997.735	501.962	-0.003	0.007	-0.001
16	2005.795	997.649	501.896	2005.799	997.641	501.900	-0.004	0.008	-0.004
18	2004.450	1000.554	501.248	2004.442	1000.551	501.249	0.008	0.003	-0.001
19	2003.035	1000.802	501.562	2003.025	1000.802	501.562	0.010	0.000	0.000
20	2002.031	1001.218	501.080	2002.035	1001.221	501.076	-0.004	-0.003	0.004
number of control points							17	17	17
arithmetic mean [m]							0.003	0.003	0.000
standard deviation [m]							0.005	0.004	0.005
root mean square error by x, y and z [m]							0.005	0.005	0.005

In the same table arithmetic mean errors, standard deviation and root mean square errors are calculated. Table 2 and the following figures illustrate the results obtained as percentage ratio.

Table 2.

Differences	to 5 mm	To 10 mm	above 10 mm
Δx	70.59%	29.41%	0%
Δy	82.35%	11.77%	5.88%
Δz	82.35%	11.77%	5.88%

**Determination of Δx, Δy and Δz**

$$\begin{aligned} \Delta x_i &= X_{r_i} - X_{\phi_i}; \\ \Delta y_i &= Y_{r_i} - Y_{\phi_i}; \\ \Delta z_i &= H_{r_i} - H_{\phi_i}; \end{aligned} \quad (1)$$

X<sub>φ</sub>, Y<sub>φ</sub> and H<sub>φ</sub> are values for X, Y and H reported by stereo model, and X<sub>r</sub>, Y<sub>r</sub> and H<sub>r</sub> are values for corresponding points obtained from direct geodetic measurements.

**Calculation of average arithmetic errors**

$$\bar{x} = \frac{1}{n} \sum_{i=1}^n \Delta x_i; \quad \bar{y} = \frac{1}{n} \sum_{i=1}^n \Delta y_i; \quad \bar{z} = \frac{1}{n} \sum_{i=1}^n \Delta z_i; \quad (2)$$

where n - is the number of measurements, and Δx<sub>i</sub>, Δy<sub>i</sub> and Δz<sub>i</sub> are i- errors, where i = from 1 to n.

**Calculation of the standard deviation**

$$\begin{aligned} s_x &= \sqrt{\frac{1}{n-1} \sum_{i=1}^n (\Delta x_i - \bar{x})^2}; \quad s_y = \sqrt{\frac{1}{n-1} \sum_{i=1}^n (\Delta y_i - \bar{y})^2}; \\ s_z &= \sqrt{\frac{1}{n-1} \sum_{i=1}^n (\Delta z_i - \bar{z})^2} \end{aligned} \quad (3)$$

where n - is the number of measurements, and Δx<sub>i</sub>, Δy<sub>i</sub> and Δz<sub>i</sub> are i-errors,  $\bar{x}$ ,  $\bar{y}$  and  $\bar{z}$  are arithmetic mean errors and i = from 1 to n, where n- is the number of measurements.

**Calculation of the root mean square error - m**

$$\begin{aligned} m_x &= \sqrt{\frac{1}{n} \sum_{i=1}^n (x_{i(r)} - x_{i(\phi)})^2}; \quad m_y = \sqrt{\frac{1}{n} \sum_{i=1}^n (y_{i(r)} - y_{i(\phi)})^2}; \\ m_z &= \sqrt{\frac{1}{n} \sum_{i=1}^n (H_{i(r)} - H_{i(\phi)})^2} \end{aligned} \quad (4)$$

The diagram of error's distribution by x

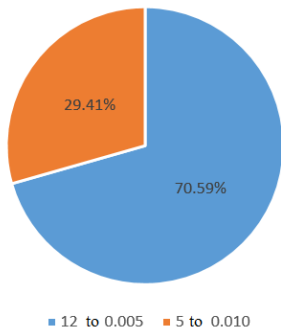


Fig.4. Number of errors' values by x in the respective interval and their percentage ratio of the total number of values.

The diagram of error's distribution by y

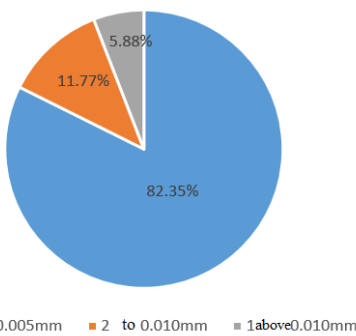


Fig. 5. Number of errors' values by y in the respective interval and their percentage ratio of the total number of values

The diagram of error's distribution by z

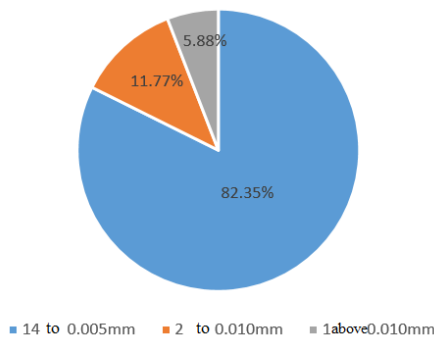


Fig.6. Number of errors' values by z in the respective interval and their percentage ratio of the total number of values.

**Automatic determination of coordinate differences, using the same points as control points**

In order to avoid subjectivity in marking the points' centre and the coordinates' measurement from the photogrammetric model, an automatic determination of the check points' coordinates is realized. For the creation of the photogrammetric model are used only four control points (3, 10, 17 and 21) and other 17 as check points. Figure 7 and Table 3 show the calculated errors by "Agisoft Photo Scan" photogrammetric software at check points' coordinates, arithmetic mean errors, standard deviation and mean square errors.

Label	X error (mm)	Y error (mm)	Z error (mm)	Total (mm)
target 11	-2.10849	-1.10916	10.413	10.6821
target 13	5.6361	0.475569	5.67418	8.01175
target 14	-2.46877	-13.5137	-3.5049	14.1774
target 15	1.59711	-8.74819	1.94044	9.10203
target 12	1.1671	2.44761	11.9427	12.2467
target 9	-6.6656	3.36296	-0.775175	7.50604
target 8	-9.18216	-0.367256	10.076	13.6372
target 7	-6.4127	6.63919	-2.88419	9.67058
target 6	-7.07436	1.90471	5.20107	8.98474
target 19	-8.15203	-2.38079	0.517456	8.50832
target 16	0.041933	-7.99581	2.783	8.46639
target 18	-1.84587	-2.12368	-1.49714	3.18727
target 20	2.00499	-2.66162	-4.04013	5.23707
target 1	1.23688	-10.2517	-2.63051	10.6558
target 2	-0.537735	-5.75093	-2.0317	6.12292
target 5	0.0996442	-5.34294	1.42034	5.5294
target 4	-1.96161	-1.80033	-2.84222	3.89453
<b>Total</b>	<b>4.50941</b>	<b>5.82541</b>	<b>5.33867</b>	<b>9.09789</b>

Fig. 7. Differences (errors) by x, y and z, and mean square error for each of them

Table 3.

number of control points	17	17	17
arithmetic mean [m]	-0.002	-0.003	0.002
standard deviation [m]	0.004	0.005	0.005
root mean square error by x, y and z [m]	0.005	0.006	0.005

**Automatic determination of coordinate differences, using twice as many control points - in this case 8pcs**

A study is conducted where a photogrammetric model is created by using twice more control points - in this case 8 pcs. (1, 3, 6, 10, 12, 15, 17, 21). These points are selected to be evenly distributed in the model. The purpose of the study is to determine the errors' values and to find out whether the increased number of control points has a significant impact on the root mean square error of x, y and z.

After the photogrammetric model with 8 control points and 13 check points is generated, it is found that there is no significant difference in the error's values compared to the model generated using 4 control points, as well as for arithmetic mean, standard deviation and root mean square error by x, y and z. This can be seen in Figure 8 and Table 4.

Label	X error (mm)	Y error (mm)	Z error (mm)	Total (mm)
target 11	-2.04356	-0.756156	3.09871	3.78813
target 13	6.15834	1.66331	0.242815	6.38363
target 14	-1.57844	-11.925	-7.30186	14.0717
target 9	-6.89568	4.19092	-5.85501	9.96972
target 8	-9.0065	0.513783	6.08469	10.8814
target 7	-6.3379	9.08692	-5.71897	12.4679
target 19	-7.03542	0.450182	0.305893	7.05644
target 16	1.80088	-6.74837	-0.595215	7.00985
target 18	-0.403272	0.702709	-2.46122	2.59115
target 20	2.68965	0.781438	-3.77146	4.69774
target 2	-1.21937	-2.52913	-0.203739	2.81512
target 5	0.496096	-3.2716	-0.12725	3.31145
target 4	-2.30994	1.36127	-4.20994	4.99124
<b>Total</b>	<b>4.64621</b>	<b>4.89697</b>	<b>3.97589</b>	<b>7.83424</b>

Fig. 8. Differences (errors) by x, y and z, and mean square error for each of them

Table 4.

number of control points	13	13	13
arithmetic mean [m]	-0.002	-0.000	-0.001
standard deviation [m]	0.004	0.005	0.004
root mean square error by x, y and z [m]	0.005	0.005	0.004

## Conclusion

There is difference between points' coordinates obtained by accurate geodetic measurements and the ones received by the photogrammetric model. This difference is evaluated quantitatively by value of the arithmetic mean and the mean square error. The result of the comparisons shows that with the available image quality and the form of the captured object, the applied method ensures enormous accuracy when different tasks are solved. Moreover, when the conditions are suitable, the method may even claim to detect deformations in the support of mining excavations or mining equipment. Registering the effects of rock pressure on individual elements of excavations requires the determination of appropriate periodicity and the chosen shooting methodology to be followed each time.

## References

- Begnovska, M. 2016. Markshayderska snimka na kapitalna izработка pri razlichna detaylnost na informatsiyata. – *Sbornik s dokladi ot Peta natsionalna nauchno-tehnicheska konferentsia s mezhdunarodno uchastie „Tehnologii i praktiki pri podzemen dobiv i minno stroitelstvo”*, 101–106 (in Bulgarian with English abstract).
- Benton, D., J. Seymour, M. Boltz M. Raffaldi, S. Finley. 2017. Photogrammetry in underground mining ground control – Lucky Friday mine case study. – *Proceedings of Eighth International Conference on Deep and High Stress Mining*, 587–598.
- Benton, D, S. Iverson, L. Martin, J. Johnson, M. Raffaldi. 2016. Volumetric measurement of rock movement using photogrammetry. – *International Journal of Mining Science and Technology*, 26, 123–130.
- Gospodinova, V., P. Georgiev, P. Ivanov. 2018. Sazdavane na chislen fotogrametrichen model v podzemen rudnik. – *Sbornik dokladi ot VI Natsionalna nauchno-tehnicheska konferentsia s mezhdunarodno uchastie „Tehnologii i praktiki pri podzemen dobiv i minno stroitelstvo”*, Bulgaria, 155–161 (in Bulgarian with English abstract).

## VEGETATION INDICES AS A MEANS OF MONITORING OF OBJECTS IN THE REGION OF OPEN PIT MINES

**Veselina Gospodinova<sup>1</sup>, Radostina Yordanova<sup>2</sup>, Aleksandar Kandilarov<sup>3</sup>**

<sup>1</sup> University of Mining and Geology "St. Ivan Rilski", 1700 Sofia; veselina\_gospodinova80@abv.bg

<sup>2</sup> University of Architecture, Civil Engineering and Geology, 1164 Sofia; lex1@mail.bg

<sup>3</sup> Neopteryx LLC, 4003 Plovdiv; akandilarov@neopteryx.org

**ABSTRACT.** The article discusses the essence, characteristics and applications of vegetation indices in analysing and assessing the state of vegetation. Photographs of forest and agricultural areas were taken by an unmanned aerial system equipped with an optical and multi-spectral camera. The advantages and disadvantages of the methods under consideration have been structured and the main applications related to the monitoring of such areas have been listed. The proposed method will help establish the reason/s of for the occurrence of environmental disturbances. They will also help solve various cases associated with ecological problems in mining.

**Keywords:** vegetation indexes, open pit mine, monitoring

## ВЕГЕТАЦИОННИТЕ ИНДЕКСИ КАТО СРЕДСТВО ЗА МОНИТОРИНГ НА ОБЕКТИ В БЛИЗОСТ ДО ОТКРИТИ РУДНИЦИ

**Веселина Господинова<sup>1</sup>, Радостина Йорданова<sup>2</sup>, Александър Кандиларов<sup>3</sup>**

<sup>1</sup> Минно-геоложки университет "Св. Иван Рилски", 1700 София

<sup>2</sup> Университет по архитектура, строителство и геодезия, 1164 София

<sup>3</sup> Неоптерикс ЕОД, 4003 Пловдив

**РЕЗЮМЕ.** Статията представя същността, особеностите и приложението на вегетационните индекси за извършване на анализ и оценка на състоянието на растителността. Извършени са заснемания с безпилотна летателна система с оптична и мултиспектрална камера на горски и селскостопански площи. Структурирани са предимствата и недостатъците на изследваната методика и са изброени основни приложения, свързани с наблюдението на такива площи. Предложената методика ще помогне за откриване на причинателите за възникване на нарушения в околната среда и за решаване на различни казуси обвързани с екологични проблеми в минния добив.

**Ключови думи:** вегетационни индекси, открит рудник, мониторинг

### Introduction

The mineral resources of a country are closely connected to its sustainable development and are the subject of research of various specialists. With the increasing needs of the population, the need for supplying more raw materials increases. This determines the search for new natural sources and their exploitation, which is directly related to the provision of a favorable living environment for all living organisms. Very often, the discussion or the mere mentioning of the mining industry is associated with pollution and/or environmental disruption. Other human and natural factors also affect the natural balance. In order to find out the exact cause of these violations, it is necessary to monitor forestry objects and agricultural sites which usually fall in the vicinity of open pit mines and quarries. The persistent monitoring, exploration and analysis of these territories is a responsible task for both environmentalists and mining professionals.

Various ways exist to perform periodic monitoring of areas occupied by forest and agricultural vegetation. Some are related to field measurements, others to remote analysis. Traditionally, satellite images are used to monitor and analyse vegetation for large areas (on a global and/or regional level). They usually provide low spatial resolution data.

The alternative to the previously mentioned methods for monitoring of objects near open-pit mines for a shorter period and with high spatial resolution are unmanned aerial systems. Equipped with miniature compact cameras not only in the visible but also in the invisible area of the electromagnetic spectrum, they are used for the vegetation analysis (Mahajan et al., 2016). Their appearance broadens the monitoring capabilities and allows to solve tasks of a different nature, like the implementation of precision farming and the monitoring of forest areas. Such equipment can also be used for the analyses of environmental problems and solving cases near mining sites. These uses are predetermined by the advantages and disadvantages of the methods.

## Advantages and disadvantages of the methods

### Advantages:

#### - Flexible

Remote sensing as a whole can be used to distinguish between different crops and to assess areas. Territories with complex farming systems are more difficult to be traced when viewed through satellite images with low spatial resolution and temporal resolution and the occasional presence of clouds in images. This imposes the need of systems for data registering which are faster and cheaper when capturing smaller areas (Greenwood, 2016).

#### - Providing high spatial resolution data

The unmanned aerial systems (UAS) provide a high spatial resolution that allows differentiation of various cultures using optical and multi-spectral cameras. The high resolution allows for detailed monitoring and analysis of forest and agricultural areas. By means of UAS accurate numerical surface models can be generated that can be used to track soil erosion, obtain information related to surface water removal, etc. This information will help identify the causes of stress in plants.

#### - Time saving

Usually, the periodic monitoring of agricultural and/or forest areas is performed by field measurements or by walking across the field itself. Sometimes this is difficult due to the nature of the relief, the total area of the site, or to other factors. In other cases, this is even impossible. The use of UAS allows to capture such territories and to significantly reduce observation time.

#### - Continuity of information

For the purposes of the analysis, it is very important to obtain data not only on the individual parts of a certain territory, but also to maintain the continuity of the information. UAS easily solve this task by providing overall territorial observation (Puri et al., 2017).

#### - Health status tracking, vegetation vigour monitoring and yield increase

The maps of vegetation indices provide quality tracking of the health status and vitality of forest and agricultural vegetation. The 3D models and orthophotomaps produced are also an important tool for establishing the water flow and the irrigation, for visual distinguishing of crops, and so on. Combining these data (optical and multi-spectral) from different capture periods will allow for an in-depth analysis of the state of vegetation near mining plants.

#### - Assessment of the damage to agricultural and forest areas as a result of various disasters

UAS data can be used to evaluate area damage due to various factors and, based on historical data, to compile statistical models related to risk management.

#### - Effective and cheaper method

The capture method is effective and less expensive in comparison to the traditional method that uses high resolution multi-spectral space images. It ensures an increase in data for different periods of time and reduces the cost of periodic monitoring of agricultural and forest areas. This also accounts for the tendency for an increase in the number of consumers who apply these methods.

### Disadvantages:

#### - Capture conditions

Capturing can not be performed under the same environmental conditions (flights take place in different

seasons, under varied climatic and weather conditions, and at different times of the day) and at standard settings during each flight.

#### - Availability of an operator

For performing the capture process, an operator is required to guide the capture itself.

#### - Illiteracy and disinterest

There are specialists in various fields of industry, agriculture, forestry and the environment, and other spheres of life in Bulgaria who are not yet aware or unable to apply these new methods.

This technology is a good tool suitable for application in the mining industry which is invariably related to sustainable development. This concept is subject to various interpretations. Initially, it was regarded as a way of using natural resources that would help meet the demands of today's and future human generations while preserving the natural balance in the environment. Gradually, its content began to expand. Objectively and more readily, this concept has begun to be seen as the focal point for the fundamental issues on which the present and future of mankind depends. Today we can say that, in its essence, it represents a new outlook paradigm for the further development of human society. A series of UN and EU solutions for sustainable development are a good basis for establishing national action programmes in the separate countries. Still, real and targeted actions on a national scale are too few, although a number of associations, scientific and educational structures and other organisations have been involved in fruitful action in this area (Josifov, 2016). Therefore, any new idea that has a positive effect on sustainable development is valuable to the society.

Monitoring of the state of vegetation is significant not only from an ecological point of view, but is also important for the sustainable development. The combination of unmanned aerial systems and multi-spectral cameras is an appropriate tool for the monitoring of vegetation near open pit mines by creating maps of the vegetation indices that determine the status, condition and variation of vegetation.

## Capturing and processing of data NDVI Vegetation Index Applications

The plants absorb light in the visible area and reflect it most strongly in the near infrared range of the electromagnetic spectrum. Dehydration or the influences of other external factors lead to a disruption of their natural state, and they cease to reflect light so strongly. Depending on the channels of the electromagnetic spectrum, a number of vegetation indices exist (NDVI, ENVI, GRRVI, LAI, SAVI, GNDVI, NDRE, EVI, REDDVI) that have different applications. They primarily serve to determine the vitality and health of vegetation. The most common is the NDVI vegetation index. It provides information about the presence of stress caused by various factors. This method converts the reflective characteristics of each pixel in the image that are associated with the particular type of vegetation. The resulting NDVI images provide primary information which is analogous to field observations aimed at determining plant status. These images contain useful information to distinguish areas occupied by different types of vegetation - forest, agricultural, pastures, meadows, etc., i.e.

as a means of visualising spatial variability. They are employed in identifying critical areas affected by pests, diseases, fires, over-saturation, drought, or other factors disturbing their natural balance.

These data serve to carry out in-depth analyses related to the state of vegetation and can be a valuable tool for vegetation monitoring in the vicinity of opencast mines and quarries. The creation of a database over a long period of time will help solve ecological cases that are directly related to the impact which opencast mining does or does not exert on the plant and animal world and on the human living environment. This will be a good basis for the establishment of a national action strategy aimed at preserving the natural balance of the environment as a key objective of sustainable development.

Forest and agricultural areas are often to be found near the opencast mines. This requires the tracing of their life status in order to identify possible disturbances in their condition caused by various factors such as pollution, pests, deforestation, and others. Experimental results are presented, which have been obtained through capturing with the DJI Matrice600 Pro hexacopter-type of unmanned aerial system equipped with optical and multi-spectral camera. The terrain is captured with an optical 16-megapixel camera and a 5-channel multi-spectral camera.

### Applications of the vegetation indexes in the study of forest vegetation

The red and the adjacent infrared channels are two of the most informative channels for detecting the presence of tree stress caused by bark beetle infestation. The NDVI vegetation index has experimentally been shown to be one of the indices that shows the clearest distinction of the main categories of healthy, contaminated and dead forest (Minařik et al., 2016).

The study involves capturing of mixed coniferous and deciduous forests located north-west of the town of Kalofer in two consecutive years. The purpose is to identify and monitor areas with coniferous trees infested and destroyed by bark beetle. Within the period between the two surveys, a new region infested by bark beetle has been observed in the central part (Figure 1). The probable cause of the infestation of the new site is the removal of felled contaminated wood in this area (bottom left), as well as the pest favourable nutrient medium in this area.



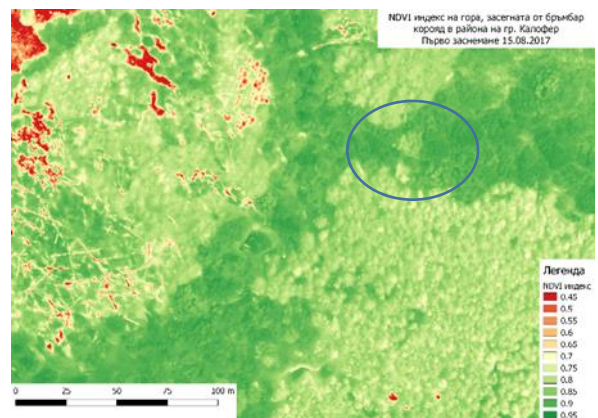
a)



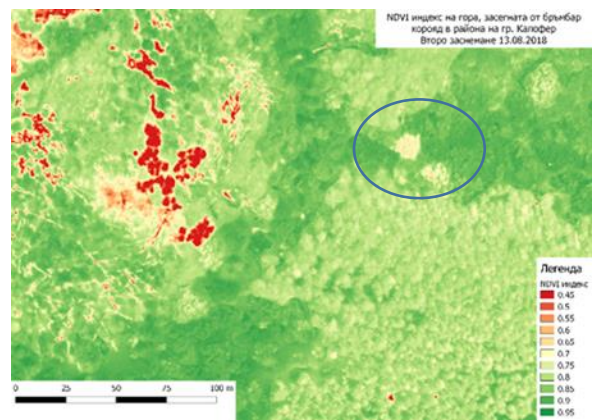
b)

Fig. 1. Orthophoto mosaic of a region affected by bark beetle in the central part of the surveyed territory in mid-August: in 2017 (a) and in 2018 (b), respectively

The area outlined in red on the two pictures shows the appearance of a new area affected by bark beetle in the central part of the surveyed area, which is not visible in the original shot in 2017 – Figure 1(a). The area outlined in blue shows trees that were healthy in 2017 and were infested in 2018 and can not be easily identified on the optical images but they are clearly visible on the NDVI map in Figure 2.



a)



b)

Fig. 2. Maps of the NDVI index in the central part of the surveyed territory in 2017 (a) and in 2018 (b), respectively

The NDVI index map in Figure 2a is derived from the 2017 data, and the one in Figure 2b is from 2018. The NDVI map from 2018 shows infected trees outlined in blue that can not be easily identified as such from the optical images in Figure 1.

The results of the study show that, compared to satellite data, the multi-spectral images obtained from capturing with an unmanned aerial system make a good alternative for remote observation. They can be used for early detection and mapping of small diameter infected areas. This will make it possible to take timely preventive measures to limit and eliminate pest attacks or other external factors (Gospodinova et al., 2018).

Other studies exist that are related to the monitoring and determining of the status of forest vegetation by using various vegetation indices and classification methods (Gospodinova et al., 2018; Dash et al., 2017; Rudolf et al., 2015; Brovkina et al., 2018; Xiao et al., 2005; Minařík et al., 2016). The combination of optical and multi-spectral data broadens the scope for analysis, such as distinguishing coniferous from deciduous tree species in mixed forest surveillance. Performing field measurements, combined with optical data (orthophoto mosaics), along with the classification methods, allow the creation of maps that contain the individual species of forest vegetation and reflect their current state (Brovkina et al., 2018).

The relatively easy, fast and cost-effective generation of NDVI images, their analysis and reliable classification are a promising pest detection tool that will facilitate forest management in the future and save time and finances by more than 50% (the percentage will be significantly higher in the case of almost inaccessible forested areas, even if investment in equipment is taken into account) (Rudolf et al., 2015).

A methodology was presented, which used color compositions, including NIR and SWIR spectral bands to identify areas affected by pests (bark beetle) for two forest sub-regions in Western Bulgaria. A computer-assisted interpretation of the multitemporal satellite and aerial digital images was performed using the methodology, software and images of the CORINE Land Cover 2018 Project. All coniferous forests in the study area (larger than 5 ha), which were damaged in the period 2012-2018, were detected and mapped. The obtained results were compared to ground data. They demonstrated the suitability of the approach in comparison to traditional ground observations, in terms of accuracy, time and money (Tonchev et al., 2018).

To support local GIS users in forestry, the indexed NDVI images can be distributed through an image mapping web service according to the standards of an open geospatial consortium (OGC). Raster data obtained from unmanned aerial systems can be exported in such a format that would ensure the compatibility between the ArcGIS server (ESRI 2014) and the GEO server (OGC 2014). In this way, potential users can easily combine these maps with theirs in order to provide a perspective of the studied areas over a long period of time (Rudolf et al., 2015).

All these studies demonstrate the potential of the vegetation index maps for forest surveying and monitoring. The multispectral data from unmanned aerial systems, especially in the presence of symptoms such as defoliation and altered reflectivity of the foliage, will be increasingly used in the development of forest monitoring strategies. This approach also offers an inexpensive alternative to private owners of forests who aspire to a sustainable management strategy.

Future developments are related to the creation of a three-dimensional NDVI model of forest areas which will further enhance the monitoring and analysis capabilities up to the level of monitoring each individual species of vegetation (<https://www.suasnews.com/2016/12/pix4d-parrot-explore-vegetation-research-3d-ndvi/>).

### Applications of vegetation indices in agricultural crop surveys

NDVI images are widely used in tracking the living status of various crop types – flat-sown, trench, vegetable, orchard, etc. (Kavvadias et al., 2017; Nasir et al., 2017; Duchsherer, 2018; Agüera et al., 2011; Vega et al., 2015; Primicerio et al., 2012; Allah et al., 2015). They demonstrate the applicability of the observation methods for a particular crop during the growing season, as well as their application to precision farming.

Other vegetation indices and algorithms exist that serve to determine the viability of plants and to solve specific tasks in agriculture (Mookherjee, 2016; Papadopoulos et al., 2014; Lelong et al., 2008; Rogers III, 2013; Greenwood, 2016; Wahab et al., 2018; O'Halloran, 2016; Candiago et al., 2015; Shafian et al., 2018).

One of the most important tasks in agriculture is the use of herbicides that can have a negative impact / have side effects on the biotic and abiotic environment and can be hazardous or harmful to human health. Therefore, reducing their quantities in modern agriculture is an important step towards its sustainable development (Lottes et al., 2017).

Establishing the exact cause of a violation committed on agricultural vegetation in open-cast mining areas is of a particular importance for taking the necessary measures to restore it.

A study was carried out to analyse data from a multi-spectral camera, to track the growth of field crops, and to give recommendations for production enhancing. The subject of the survey is a field in the Pleven region of approximately 850 decares sown with rape seed.

From the data obtained, a map of the NDVI index was generated in a georeferenced TIFF format with a resolution of 17 cm per pixel (Fig. 3), and also a digital surface model (Fig. 4).

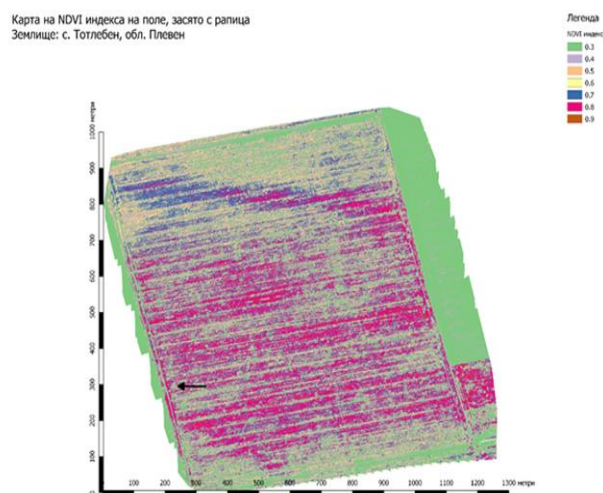
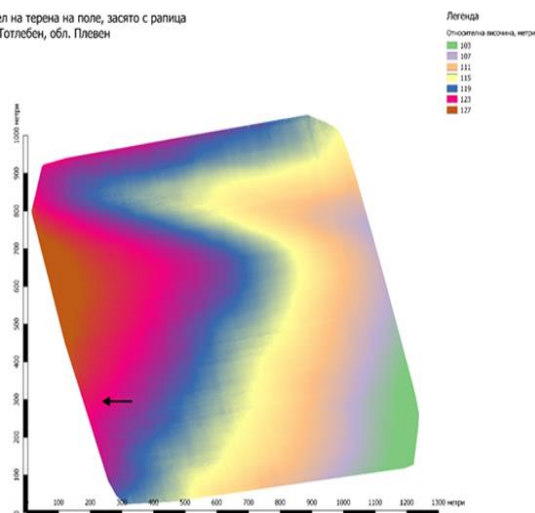


Fig. 3. Map of the NDVI index obtained with the data from the multi-spectral camera. The arrow shows the location of the flight site

Цифров модел на терена на поле, засято с рапица  
Землище: с. Тотлебен, обл. Плевен



**Fig. 4. Digital Surface Model (DSM).** The lowest area of the surveyed region is in the southeast, and the highest is in the northwest

The site under investigation is arable land planted with clearly visible vegetation at the time of capture: rape which is uneven due to poor sowing and pre-sowing preparation. The NDVI culture index is 0.8. The phase is 6-7 sheets. Values with an index lower than 0.7 correspond to poorly developed rape due to retarded germination or to phosphorus deficiency (spots or belts). An NDVI index of 0.5-0.6 corresponds to dried vegetation. The old leaves have a bright pinkish-violet colouration, indicating that they have started to dry. The uneven phosphorus intake, or phosphorus malnutrition, is due to the erosion processes in this field and to the rising of lower soil horizons to the soil surface. Sowing is done on the slope, thus further enhancing terrain erosion and profile flushing.

The results of the laboratory analyses of soil samples show that the soil in the studied plot is a typical black earth. But according to the mapping material, this particular field is predominated by carbonate black earth. Black earth is an alkaline soil, so urea is not used. The analyses show phosphorus deficiency and low nitrogen amounts (therefore, it is good to compensate for the amount of nitrogen in the soil in spring). Ammonium sulphate should have been introduced with the basic fertilisation in autumn. Ammonium nitrate should better be employed in feeding. It is advisable to make a more detailed study of the soils. There are two main species of weeds whose density is 0.5 -1 per square meter and is thus below the harm threshold.

A survey has been carried out of a single array (approximately 500 decares) in the district of Veliko Tarnovo sown with wheat in the stage of intensive growth. The aim is to capture the whole terrain with a multi-spectral camera mounted on an unmanned aerial vehicle. On the basis of the obtained data, a NDVI index map has been drawn and analysed that characterises the agro-ecological state of the terrain, the strength and resistance of the crops. Also, a combined aerial photography has been taken for the purpose of visualisation. After data processing, the following have been obtained: a map of the NDVI index (Fig. 5) in a geo-referenced TIFF format with a resolution of 15 cm per pixel and an orthophoto mosaic (Fig. 6) with a resolution of 3 cm per pixel.

Карта на NDVI индекса на поле, засято с пшеница  
Землище: с. Бутово, обл. Велико Търново

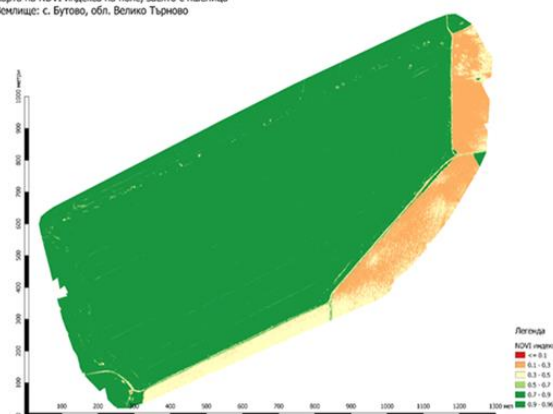


**Fig. 5. Map of the NDVI index obtained with data from the multi-spectral camera**

Фотомозайка на поле, засято с пшеница  
Землище: с. Бутово, обл. Велико Търново

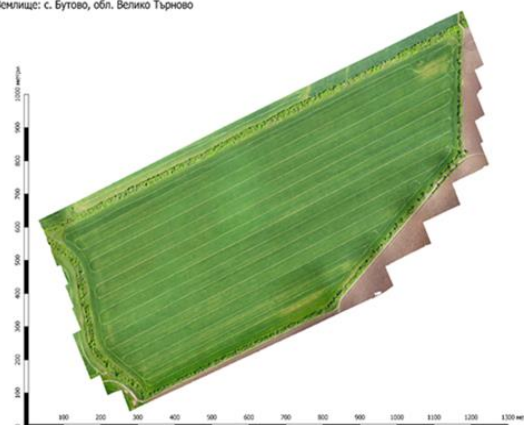


**Fig. 6. Orthophoto mosaic of the terrain obtained with data from the optical camera**

The analysis of the data has shown that the wheat crop is well developed. No morbidity has been observed. There has been no weed vegetation above the harm threshold.

All of these studies show that such technologies raise farm management to a higher, modern level, increasing their profitability and enhancing the healthy crop production.

The storage of information from different vegetation indices over a long period of time will help automate data interpretation and improve the status of vegetation, as well as identify the cause/s of various breaches.

#### **Methods for the monitoring of territories in the vicinity of opencast mines and quarries through a combination of optical and multi-spectral data**

Very often, the effect of mining on the environmental pollution is capitalised on; yet, there are cases where breaches are committed and violations do occur. For this reason, it is essential to carry out periodic monitoring of the areas where there is an opencast mining of minerals. The traditional method of observing the state of the land cover (namely, of the vegetation) is through remote sensing, in particular, through satellite imagery (Suh et al., 2017; Koruyan et al., 2012; WuB et al., 2009; Baodong et al., 2009; Whiteside et al., 2016; Yang et al., 2018). The disadvantage of this method is low spatial resolution that is inappropriate for certain tasks, the lack of

flexibility in data acquisition and processing (e.g. the presence of shadows in some images that are an obstacle in subsequent analyses, etc.). However, with the dynamic development of unmanned aerial systems, these obstacles can be eliminated, especially when performing local capturing.

The modern open-cast mining technologies include mining operations that lead to changes in the land cover (forest biomass, soils, etc.) for a very short period of time, affecting neighboring habitats. A method is available for capturing open pit mines, quarries, and adjacent areas through UAVs using an optical and multi-spectral camera. The combination of images extends the scope for analysis as presented in the above-mentioned studies. Indexed vegetation images can serve not only to track rehabilitation processes (deforestation, afforestation decision making, and actual afforestation), but also to monitor these areas and solve various environmental cases during the expiration period. They will help identify the causes of vegetation disorder in the vicinity of open pit mines and quarries, as well as find such a solution to the problem that will appropriately ensure the yield continuance. Providing timely and valuable information on the impact of mining activities in a particular area will also be beneficial to ecologists and to the mining companies themselves, especially since the latter are often erroneously referred to as environmental pollutants.

The remote sensing systems and the geographic information systems play an increasingly important part in the management of mining. Their joint application provides information and statistical data to assess habitat diversity and land-cover change. This information can be used to formulate policies and guidelines on land management, monitoring, reclamation, and landscape preservation.

## Conclusion

Mining is invariably related to sustainable development and ecology. These issues are discussed at almost every mining conference, whereby various results, analyses, and specific solutions and recommendations are given for expedient mining while maintaining the natural equilibrium.

The accessibility of data and the analyses obtained from the observation of sites in the vicinity of open pits through UAS will allow for better communication and cooperation between mining enterprises, environmental and governmental organisations, and society.

The availability of information in the form of maps with vegetation indexes, orthophoto maps and, if necessary, field measurements and lower resolution data (from satellites) is important for the management of natural resources not only on the regional and national levels, but also on the international one.

## References

- Agüera, F., F. Carvajal, M. Pérez. 2011. Measuring sunflower nitrogen status from an unmanned aerial vehicle-based system and an on the ground device. – *ISPRS Journal of Photogrammetry and Remote Sensing*, 38, 1/C22, 33–37.
- Allah, M., O. Vergara, J. Araus, A. Tarekegne, C. Magorokosho, P. Tejada, A. Hornero, A. Albà, B. Das, P. Craufurd, M. Olsen, B. Prasanna, J. Cairns. 2015. Unmanned aerial platform-based multi-spectral imaging for field phenotyping of maize. – *Plant Methods*, 11–35.
- Baodong, M., C. Shaojie, W. Lixin. 2009. Vegetation monitoring method in mining area based on SPOT-VGT NDVI. – *Geography and Geo-Information Science*, 24, 1, 84–87.
- Brovkina, O., E. Cienciala, P. Surov, P. Janata. 2018. Unmanned aerial vehicles (UAV) for assessment of qualitative classification of Norway spruce in temperate forest stands. – *Geo-spatial Information Science*, 21, 12–20.
- Candiago, S., F. Remondino, M. Giglio, M. Dubbini, M. Gattelli. 2015. Evaluating multispectral images and vegetation indices for precision farming applications from UAV images. – *Remote Sensing*, 7, 4, 4026–4047.
- Dash, J., M. Watt, G. Pearse, M. Heaphy, H. Dungey. 2017. Assessing very high resolution UAV imagery for monitoring forest health during a simulated disease outbreak. – *ISPRS Journal of Photogrammetry and Remote Sensing*, 131, 1–14.
- Duchsherer, C. 2018. *On the profitability of uas-based NDVI imagery for variable rate nitrogen prescriptions in corn and wheat in North Dakota*. A Thesis Submitted to the Graduate Faculty of the North Dakota State University of Agriculture and Applied Science.
- Gospodinova, V., A. Kandilarov. 2018. Remote sensing method for monitoring forest areas. – *XXVIII International Symposium "Modern technologies, education and professional practice in geodesy and related fields"* (in Bulgarian with English abstract).
- Greenwood, F. 2016. Drones on the horizon: new frontier in agricultural innovation. – *Drones for agriculture, ICT UPDATE*, 82, 2–4.
- Josifov, D. 2016. Instead of foreword. – In: *Proceedings of the Second National Scientific and Technical Conference Mineral Resources and Sustainable Development*. Scientific and Technical Union of Mining, Geology and Metallurgy, Sofia, 3–7.
- Kavvadiasa, A., E. Psomiadis, M. Chanotic, A. Sitouras, L. Toulidos, N. Dercas. 2017. Unmanned Aerial Vehicle (UAV) data analysis for fertilization dose assessment. – *Ecosystems and Hydrology*, 4, 1–9.
- Koruyan, K., A. Deliormanli, Z. Karaca, M. Momayez, H. Lu, E. Yalçin. 2012. Remote sensing in management of mining land and proximate habitat. – *The Journal of the Southern African Institute of Mining and Metallurgy*, 112, 667–672.
- Lelong, D., F. Burger, G. Jubelin, B. Roux, S. Labbe, F. Baret. 2008. Assessment of Unmanned Aerial Vehicles imagery for quantitative monitoring of wheat crop in small plots. – *Sensors*, 8, 5, 3557–3585.
- Lottes, P., R. Khanna, J. Pfeifer, R. Siegwart, C. Stachniss. 2017. UAV-based crop and weed classification for smart farming. – *IEEE International Conference on Robotics and Automation (ICRA)*.
- Mahajan, U., B. Bundel. 2016. Drones for Normalized Difference Vegetation Index (NDVI), to estimate crop health for precision agriculture: A cheaper alternative for spatial satellite sensors. – *International Conference on Innovative Research in Agriculture, Food Science, Forestry, Horticulture, Aquaculture, Animal Sciences, Biodiversity, Ecological Sciences and Climate Change*.

- Minařík, R., J. Langhammer. 2016. Use of a multispectral UAV photogrammetry for detection and tracking of forest disturbance dynamics. – *ISPRS Journal of Photogrammetry and Remote Sensing*, XLI-B8, 711–718.
- Mookherjee, A. 2016. *A study to determine yield for crop insurance using precision agriculture on an aerial platform*. Thesis submitted to Symbiosis Institute of Geoinformatics for partial fulfillment of the M.Sc. degree.
- Nasir, A., M. Tharani. 2017. Use of greendrone uas system for maize crop monitoring. – *IAPRSS, International Conference on Unmanned Aerial Vehicles in Geomatics. XLII-2/W6*, 263–268.
- O'Halloran, J. 2016. *Potential applications of Unmanned Aerial Vehicle multispectral imagery in vegetables*. Department of Agriculture and Fisheries and Nathaniel Parker of Airborn Insight. State of Queensland.
- Papadopoulos, A., M. Iatrou, F. Papadopoulos, I. Metaxa, S.Theodoridou, K. Kalogeropoulos, S. Kiparissi. 2014. Preliminary results for standardization of NDVI using soil nitrates in corn growing. – *PSP Fresenius Environmental Bulletin*, 23.
- Primicerio, J., S. Gennaro, E. Fiorillo, L. Genesio, E. Lugato, A. Matese, F. Vaccari. 2012. A flexible unmanned aerial vehicle for precision agriculture. – In: *Precision Agriculture*. Springer.
- Puri, V., A. Nayyar, L. Raja. 2017. Agriculture drones: A modern breakthrough in precision agriculture. – *Journal of Statistics and Management Systems*, 20, 507–518.
- Rogers III, D. 2013. *Unmanned Aerial System for Monitoring Crop Status*. Thesis submitted to the Faculty of the Virginia Polytechnic Institute and State University in partial fulfillment of the requirements for the degree of Master of Science in Mechanical Engineering.
- Rudolf, J., K. Lehmann, F. Nieberding, T. Prinz, C. Knoth. 2015. Analysis of unmanned aerial system-based CIR images in forestry – A new perspective to monitor pest infestation levels. – *Forests*, 6, 594–612.
- Shafian, S., N. Rajan, R. Schnell, M. Bagavathiannan, J. Valasek, Y. Shi, J. Olsenholler. 2018. Unmanned aerial systems-based remote sensing for monitoring sorghum growth and development. – *Plos One*, 13, 5, e0196605.
- Suh, J., S. Kim, H. Yi, Y. Choi. 2017. An Overview of GIS-based modeling and assessment of mining-induced hazards: soil, water and forest. – *Intern. J. Environ. Res. Public Health*, 14, 1463.
- Tonchev, T., R. Koleva, Y. Tepeliev. 2018. Detection and mapping of coniferous forests in western Bulgaria damaged by biotic and abiotic factors in the frame of the 'CORINE Land Cover 2018' project. – *Forestry Ideas*, 24, 2, 131–140.
- Vega, F., F. Ramirez, M. Saiz, F. Rosu. 2015. Multi-temporal imaging using an unmanned aerial vehicle for monitoring a sunflower crop. – *Biosystems Engineering*, 132, 19–27.
- Wahab, I., O. Hall, M. Jirstrom. 2018. Remote Sensing of Yields: Application of UAV Imagery-Derived NDVI for Estimating Maize Vigor and Yields in Complex Farming Systems in Sub-Saharan Africa. – *Drones*, 2, 28.
- Whiteside, T., R. Bartolo. 2016. *Monitoring the vegetation success of a rehabilitated mine site using multispectral UAV imagery*. Publication of Australian Government.
- WuB, L., D. MaS, J. Liu. 2009. Analysis to vegetation coverage change in Shendong mining area with SPOT NDVI data. – *Journal of the China Coal Society*, 34, 9, 1217–1222.
- Xiao, Q., E. Mcpherson. 2005. Tree health mapping with multispectral remote sensing data at UC Davis, California. – *Urban Ecosystems*, 8, 349–361.
- Yang, Y., P. Erskine, A. Lechner, D. Mulligan, S. Zhang, Z. Wang. 2018. Detecting the dynamics of vegetation disturbance and recovery in surface mining area via Landsat imagery and LandTrendr algorithm. – *Journal of Cleaner Production*, 178, 353–362.
- <https://www.suasnews.com/2016/12/pix4d-parrot-explore-vegetation-research-3d-ndvi/>

## PROCESSING AND RECYCLING OF RESOURCES IN OUTER SPACE: INTERNATIONAL LEGAL ASPECTS

**Albert M. Khayrutdinov**

*RUDN University, 117198 Moscow; khayrutdinov.albert99@gmail.com*

**ABSTRACT.** This paper deals with current issues of legal regulation of mining activities on the Moon and other celestial bodies. The Outer Space Treaty 1967 and the Moon Agreement 1979 provisions, relating to these activities, are interpreted in different ways by the outer space participants, which do not contribute to a unified legal approach to the exploration, extraction and utilisation of space resources. To date, one of the most prospective areas of activity in outer space is the exploration of natural resources on celestial bodies. Of course, from an economic point of view, the extraction of natural resources on the Moon and other celestial bodies and their subsequent delivery to the Earth today is not appropriate, since the development of terrestrial resources is much easier, cheaper and more efficient. However, with the advance of technological progress and the decrease in the amount of minerals on Earth, this activity could become beneficial to mankind. In addition, it is also worth noting that the interest in space research is shown not only by the states within its space programmes, but also by private corporations. This paper shows how exploration, extraction and utilisation of space resources is regulated under international space law to date.

**Keywords:** international space law, natural resources, outer space

### ПРЕРАБОТВАНЕ И РЕЦИКЛИРАНЕ НА РЕСУРСИТЕ В КОСМИЧЕСКОТО ПРОСТРАНСТВО: МЕЖДУНАРОДНИ ПРАВНИ АСПЕКТИ

**Алберт М. Хайрутдинов**

*Руски университет на дружбата на народите, 117198 Москва*

**РЕЗЮМЕ:** Този доклад е свързан с актуални въпроси относно правната регулация на минните дейности на Луната и други небесни тела. Разпоредбите на Договора за Космоса от 1967 г. и Лунното споразумение от 1979 г., свързани с тези дейности, се тълкуват по различен начин от участниците в космическото пространство, което не допринася за единен правен подход относно проучването, добива и използването на космическите ресурси. Към днешна дата една от най-перспективните области на дейност в космическото пространство е проучването на природните ресурси в небесните тела. Разбира се, от икономическа гледна точка, извличането на природни ресурси на Луната и други небесни тела и последващото им транспортиране до Земята днес не е подходящо, тъй като разработването на земни ресурси е много по-лесно, по-евтино и по-ефективно. С напредъка на технологичния прогрес и намаляването на количеството на минералите на Земята обаче, тази дейност може да се окаже полезна за човечеството. Освен това, заслужава да се отбележи, че интересът към космическите изследвания проявяват не само държавите в рамките на своите космически програми, но и частните корпорации. Докладът показва как проучването, добивът и използването на космическите ресурси са регулирани според международното космическо законодателство до този момент.

**Ключови думи:** международно космическо право, природни ресурси, космическо пространство

### Introduction

One of the most perspective areas of activity in outer space is the extraction of natural resources on celestial bodies. Of course, from an economic point of view, the extraction of natural resources on the moon and other celestial bodies and their subsequent delivery to the Earth today is not appropriate, because the development of terrestrial resources is much easier, cheaper and more efficient. However, with the advance of technological progress and the decrease in the amount of minerals on Earth, this activity could be beneficial to mankind. Moreover, it is also worth noting that interest in space exploration is shown not only by states in the framework of their space programmes, but also by private corporations.

In addition, this work will address the issues of the legal status of mining and processing plants as a space station on celestial bodies, as it is also a subject of discussion.

The object of this research are the interstate relations arising in the sphere of mining activity on celestial bodies.

The subject of this study are the international conventions, international customs, general principles of law, judicial decisions and doctrines governing inter-state relations arising in the field of mining on celestial bodies.

The purpose of this study is to investigate and analyse the legal status of mining and processing plants in the celestial bodies. To achieve this goal, it is necessary to perform the following scientific tasks:

- ❖ Analyse the right status of natural resources on celestial bodies;
- ❖ Analyse the right status of space stations on celestial bodies.

## The legality of extraction of mineral resources

Of the five outer space treaties, only two (the Outer Space Treaty, 1967 and the Moon Agreement, 1979) address the exploration, exploitation and utilisation of space resources. The legal status of the Moon and other celestial bodies is mentioned only in Article I of the Outer Space Treaty, according to which "The exploration and use of outer space, including the moon and other celestial bodies [...] and shall be the province of all mankind.", and that "Outer space, including the moon and other celestial bodies, shall be free for exploration and use by all States". In accordance with article IV of the Outer Space Treaty, "The moon and other celestial bodies shall be used by all States Parties to the Treaty exclusively for peaceful purposes". But it should be borne in mind that in this Treaty there is no direct reference to the term "natural resources".

Art. 11 of the Moon Agreement deals specifically with the legal status of the moon and its natural resources. It states that the Moon and its natural resources are the common heritage of mankind, the Moon is not subject to national appropriation, and that the surface or subsoil of the moon, as well as neither the surface nor the subsurface of the moon, nor any part thereof or natural resources in place, shall become property of any State, international intergovernmental or non-governmental organisation, national organisation or non-governmental entity or of any natural person. In accordance with art. 11 States undertake to establish an international regime, to govern the exploitation of the natural resources of the moon as such exploitation is about to become feasible. However, such a regime will not be established in the near future due to the fact that no state applying for the extraction of natural resources by virtue of developed technologies is a party to the Treaty. Only 18 States are parties to the Treaty (and 4 States are only signatories), and its legal force does not extend to the space powers.

In addition, the Moon Agreement contains many other points for discussion. There are conflicting views of scientists on the concept of *res communis humanitatis*: for example, some argue that the use of celestial bodies requires the actual purchase of parts of these celestial bodies, in particular, in the implementation of mining, while others argue that all natural resources that have been mined in outer space and delivered to Earth can be used for commercial purposes if they are used for the benefit of the world community. In addition, some scientists hold the view that article 11, paragraph 4, of the Moon Agreement does not imply granting additional rights with respect to natural resources, but only applies to such methods of exploration and use of the moon and other celestial bodies as: landing, take-off, deployment of personnel, the creation of manned and unmanned stations, etc.

International treaties in the field of international space law, existing today, cannot give a clear answer to the question of the legal status of natural resources of the moon and other celestial bodies, and paragraph 5 of article 11 of the Moon Agreement from 1979, which involves the adoption of an international regime, has no legal force for space powers. Thus, this work will consider the prospects for the adoption of an international Treaty by the international community that would regulate the legal status of the resources of the moon and other celestial bodies.

Private corporations that need to regulate their activities at the national level are also becoming increasingly influential in the exploration of outer space. National legislation allowing private companies to mine and appropriate resources without claiming ownership of the celestial body itself, such as an asteroid or the Moon, has been adopted in the United States and Luxembourg. These laws have caused a mixed reaction in the international community. Thus, some scientists say, that such actions violate the principle *nemo dat quod non habet*, according to which, States cannot provide their national organisations, non-governmental entities or citizens' rights that they do not have. However, it is worth noting, that the law makes a direct reference to international treaties under which the United States has obligations. The Law of Luxembourg also makes a reference to its international obligations. For example, Russia proposes to ban the mining activities on the Moon and other celestial bodies through the adoption of an implementation agreement.

Summing up what was said above, we can claim, that States do not have an agreement on space resources exploration, exploitation and utilisation regime. Possible solution to this issue might be the following: Accession of the space powers to the Moon Agreement; Adopting a new convention or a Protocol to Outer Space Treaty; Use the Area, Antarctic or Arctic regime; Waiting for the lawsuit at ICJ, concerning mining activities on celestial bodies.

**Accession of the space powers to the Moon Agreement.** To date, the Moon Agreement has not received proper attention from the space nations, due to the lack of consensus on the international regime of the Moon and other celestial bodies. The cause of the disagreement was para 5 Article 11: The United States wanted to start exploration of natural resources prior to establishing the regime, and the USSR after that. To date, this issue is still controversial.

In addition, the space powers are unlikely to become a party to the Moon Agreement due to the fact that it does not give rise to any rights for them, but only obligations.

**Use of the Area, Antarctic or Arctic regime.** This variant should be only temporary until the States establish an international regime to govern the exploration of natural resources on the Moon and other celestial bodies. Thus, the regime of the Area can be applied, in accordance with which "the Authority", that will be created by an analogy with Part XI, Section 4 of United Nations Convention on the Law of the Sea 1982, will be established and will organise, carry out and control mining activities on the Moon and celestial bodies.

If the States will decide to use the Antarctic regime, any activities related to mineral resources, other than scientific research, will be prohibited in accordance with Article 7 of The Protocol on Environmental Protection to the Antarctic Treaty.

In case of using "the old Arctic regime", each space power will be given a territory (a sector), on which it will have sovereign rights for the purpose of exploring and exploiting, conserving and managing the natural resources.

However, it should be noted that the use of these treaties by analogy will not involve all aspects of the governing the exploitation of natural resources in outer space. Thus, there are still uncertainties with mining activities on asteroids because they are small. And this problem may be the most important in the issue of mining activities in outer space due to the fact, that the value of a single asteroid could be somewhere in the trillions of dollars, or even higher.

Raising the issue of the international regime on asteroids, it can be proposed to recognise them in a future treaty as *res nullius* and to allow States, in accordance with the developed procedure, to explore and exploit natural resources on them.

***Waiting for the lawsuit at International Court of Justice, concerning mining activities on celestial bodies.***

One of the most probable, but at the same time the most controversial way of solving this issue, is to do nothing in the field of making such an agreement among space powers. In this instance we should wait, when one State will start mining activities on celestial bodies and the others will file a lawsuit against it with the International Court of Justice.

In connection with the fact that none of the space nations is a party to the Moon Agreement 1979 the International Court of Justice will proceed from the provisions of the Outer Space Treaty and will interpret articles relevant to this issue.

However, it should be noted that in this case, such a decision may not satisfy any of the parties because the decision of the International Court of Justice will not contain the will of any state.

***Adopting a new Convention or a Protocol to Outer Space Treaty.*** Taking into account the fact that the space powers are unlikely to join the Moon Agreement, this option might be the best solution to this issue.

This Convention or Protocol to the Outer Space Treaty will have to contain provisions on the legal status and regime of mineral resources, rules for their extraction, taking into account the characteristics of the lunar environment, other provisions relating to extraction and provisions on the authority to be established for the purpose of the organisation, carrying out and control of the mining activities on the Moon and celestial bodies.

Thus, it can be concluded that international treaties in the field of international space law existing today cannot give a clear answer to the issues of the legal status and regime of the lunar resources. In any case, space powers should find a solution to this issue due to the fact that mining activities on celestial bodies may already begin in the near future.

**Legal status of a mining entity in the celestial body**

In accordance with international space law, the exploration and use of outer space, including the moon and other celestial bodies, is the province of all mankind. In addition, the Moon and its natural resources are the common heritage of mankind. Thus, all States have equal access to parts of the celestial bodies and their natural resources.

However, this does not exclude the need for state control over such mining and processing plants, in order to ensure the necessary safety and security, as well as the avoidance and resolution of any conflicts and disputes between States. States must be able to lawfully carry out "some form of ownership", different from the rights of ownership of these stations, but that is not "full sovereignty". Thus, such possession must be permissible in the event that the state does not exercise "full sovereignty".

The above is enshrined in article VIII of the Outer Space Treaty, which provides that "A State Party to the Treaty on whose registry an object launched into outer space is carried shall retain jurisdiction and control over such object, and over any personnel thereof, while in outer space or on a celestial body".

The main part of this provision relates to the period preceding space missions and originates in the attribution of law enforcement jurisdiction over a vessel on the high seas to the flag state. In addition, international air law recognises a similar principle for aircraft in international airspace law. Jurisdiction in international law means "law and enforcement of laws and regulations concerning persons and objects ". However, the competence of control is something more than a technical possibility. The state of registry may "adopt technical regulations for the mission of a space mission" and, if necessary, "direct, stop, modify and correct elements of a space object and its mission". The act of registration of a space object is the exclusive source for the exercise of "jurisdiction and control over such object and persons as in the case of ships or aircraft, although the space object has no nationality by registration other than that of ships or aircraft ".

Space activities have a strong impact on the environment. This applies not only to the pollution of the Earth during the production of launch vehicles and their launches into outer space, but also to the negative impact on the environment of celestial bodies and on outer space as a whole. Emissions from a mining and processing plant, arising in the course of its activities, will have an additional negative impact on the environment of the celestial body.

The most negative impact on the environment of outer space has space debris, various kinds of nuclear pollution, space stations with a crew, as well as astrobiological pollution. Abandoned space objects have the potential to pollute outer space with all of the above elements. The threat of space debris is the most likely: according to experts, there are about 100000 space objects of different sizes in the earth's orbit. About 10000 objects are tracked, and less than 1000 of them are operational.

Although there is no single concept of space debris in international space law, some definitions have been developed within the framework of the activities of international organisations: the international Academy of Astronautics, the scientific and technical Subcommittee of the Committee on the Peaceful Uses of Outer Space, and the Inter-Agency Space Debris Coordination Committee. The most general and understandable definition is given by the Inter-Agency Space Debris Coordination Committee, according to which space debris are all artificial objects in earth orbit or in the atmosphere that are not functional.

At the same time, such abandoned enterprises may interfere with the radio communications of operating satellites and other spacecraft and disrupt the receiving frequency bands on which sensitive devices such as ground radio telescopes operate. The damage that such a space object may cause may range from a minor damage to the total loss of the spacecraft. It can also lead to contamination with radioactive and other harmful substances. The potential damage caused by even the smallest particle of space debris circulating in outer space is due to the fact that the impact speeds in orbits are enormous; on average, debris moves several times faster than a bullet.

It is worth noting that the question of classifying an object as space debris is in many cases more complex than it might seem at first glance. Under the 1967 Outer Space Treaty, the state on whose registry a space object is located has the authority to exercise jurisdiction and control over that object. It was suggested that the provision implied that only the state of registration had the right to determine whether its space object

was functional. While other States may perceive a space object as completely useless, in fact it may, for example, be in reserve for future activities, carry valuable classified information or be of any other interest to other States. Therefore, the criterion of "functionality" may not be the most appropriate one to distinguish between space debris and other space objects; even seemingly non-functional space objects may be valuable assets.

However, it should be understood that a state that leaves such an abandoned enterprise would violate the Space Treaty provision, which enshrines the principle of free exploration and use of outer space and free access to all areas of celestial bodies on the basis of equality and non-discrimination.

## References

- Baslar, K. 1998. *The Concept of the Common Heritage of Mankind in International Law*. Martinus Nijhoff Publishers, Hague, 62 p.
- Cheng, B. 1997. *Studies in International Space Law*. DOI:10.1093/acprof:oso/9780198257301.001.0001
- H.R.2262. U.S. Commercial Space Launch Competitiveness Act. <https://www.congress.gov/bill/114th-congress/house-bill/2262/text?overview=closed>
- The Hague Space Resource Governance Working Group. Information provided by the Netherlands. A/AC.105/C.2/2018/CRP.18 April 12, 2018. – Committee on the Peaceful Uses of Outer Space/ Legal Subcommittee. Fifty-seventh Session, Vienna, 9-20.
- Pamborides, G. P. 1999. *International Shipping Law: Legislation and Enforcement*. 41 p.
- Schmidt-Tedd, B., S. Mick. 2009a. Article VIII. – In: *I Cologne Commentary on Space Law* (S. Hobe, B. Schmidt-Tedd, K.-U. Schrogl, Eds.), 156.
- Schmidt-Tedd, B., S. Mick. 2009b. Article VIII. – In: *I Cologne Commentary on Space Law* (S. Hobe, B. Schmidt-Tedd, K.-U. Schrogl, Eds.), 157.
- Setsuko, A. 2010. In Search of the Current Legal Status of the Registration of Space Objects. – *Proceedings of the 61<sup>st</sup> International Astronautical Congress*, 4.
- Tronchetti, F. 2009. *The Exploitation of Natural Resources of the Moon and Other Celestial Bodies. A Proposal for a Legal Regime*. Martinus Nijhoff Publishers, Leiden, Boston, 421 p.

## THE IMPACT OF OUTDOOR MINING ACTIVITIES ON ATMOSPHERIC AIR QUALITY IN NEARBY SETTLEMENTS

**Nikolay Kolev, Plamen Savov, Maya Vatzkitcheva, Kalinka Velichkova, Dimitar Dimitrov, Blagovesta Vladkova, Svetlana Toncheva**

*University of Mining and Geology "St. Ivan Rilski", 1700 Sofia; nic\_k@abv.bg*

**ABSTRACT.** Wind erosion breaks down toxic impurities and enables their transport over long distances, thus polluting air, soils and water over vast areas around mines and in surrounding settlements. The purpose of this study is to investigate and analyse the atmospheric air and the concentrations of fine particulate matter in open pits and quarries, and to analyse different types of pollutants. The studies will take into account the pit geometry and the type of the underlying substrate defined by the mined minerals. Specific weather parameters, such as wind pattern defining the direction of transfer, and the temperature profiles defining the temperature inversions which retain the pollution over the region, will be considered as well. The aim is to track the overall process of emission, transmission and sedimentation of aerosol impurities and fine particulate matter concentration in the mine area and in nearby settlements.

**Keywords:** air pollution, particulate matter, weather conditions, open pit, quarry

## ВЛИЯНИЕТО НА ОТКРИТИ МИННИ РАЗРАБОТКИ ВЪРХУ КАЧЕСТВОТО НА АТМОСФЕРНИЯ ВЪЗДУХ В БЛИЗКО РАЗПОЛОЖЕНИ НАСЕЛЕНИ МЕСТА

**Николай Колев, Пламен Савов, Майя Вацкичева, Калинка Величкова, Димитър Димитров, Благовеста Владкова, Светлана Тончева**

*Минно-геоложки университет "Св. Иван Рилски", 1700 София*

**РЕЗЮМЕ.** Ветровата ерозия води до разпрашаване на токсичните примеси и възможност за пренасянето им на големи разстояния, което причинява замърсяване на въздуха, почвите и водите на обширни райони около минните терени и в населените места до тях. Целта на настоящото изследване е да се проучи и анализира атмосферния въздух и концентрациите на фини прахови частици (ФПЧ) в района на открити рудници и кариери, както и да се анализират различни видове замърсители. При тези изследвания ще бъдат отчетени геометрията на рудника, вида на подложната повърхност в зависимост от полезните изкопаеми, които се добиват. Ще бъдат отчетени и конкретните метеорологични условия, като розата на ветровете определяща направлението на преноса и температурните профили определящи наличието на температурните инверсии задържащи замърсяването над района. Целта е да се проследи цялостния процес на емисия, пренос и утаяване на аерозолните примеси и концентрация на ФПЧ в атмосферата в района на рудника и близките населени места.

**Ключови думи:** замърсяване на въздуха, твърди частици, климатични условия, открит рудник, кариера

## Introduction

Open pit mining and quarrying generate significant amounts of particulate matter (PM) and harmful gasses. Particulate matter of varying sizes is generated by rock and soil fragmentation, with particularly high quantities being emitted by blasting. Machines operating on the sites are the main source of aerosol and gas pollution. Measuring the levels of pollution and determining their dependence on quarry-specific activities is important both in protecting the health of the workers and in ensuring a quality of life in nearby settlements.

Pollution spreading is highly affected not only by in-pit operations, but also by the micro-climate specifics of the site. The main meteorological parameters to be monitored are temperature stratification, the site-specific wind patterns, humidity and solar radiation. A number of studies conducted during the recent decades have researched the relation between aerosol impurity dispersion and the regional meteorological features and orography (2, 6, 7, 8, 9 and 10).

Digital models for simulation and predictions of hazardous events in quarries (3, 4 and 5) are being developed alongside experimental research.

The present study investigates and discusses the concentrations of differently sized fine particulate matter in the atmosphere of the open gravel quarry of the Balsha AD Mine extractive factory. The main weather parameters such as wind direction and velocity, temperature, and solar radiation, have been considered. The stratification of aerosols was outlined better by two types of study - measurements in a nearly-horizontal plane were carried during the first day, and vertically at different heights along the quarry slope - during the second day.

## Experimental site and equipment

The quarry is situated 3 km to the north-west of the Balsha village and is 1 km long from east to west, and 500 m at its widest (eastern) part from north to south. Its slopes are vertical and its west-facing wall has 6 benches, the highest difference

in elevation between them being 160 m. The lowest lying western part of the quarry is at 800 m a.s.l., and its eastern end is at 960 m a.s.l.

Figure 1 presents a map of the region with designated measurement points. These data have been taken over two days, 13<sup>th</sup> and 14<sup>th</sup> of June 2019, with the following arrangement of the measuring devices: June 13<sup>th</sup> - points 1

through 4, June 14<sup>th</sup> - points 5, 6, 3, and 7. The difference in level between the first four points is very little (not more than 20 m). The points of the second day were distributed at height - the lowermost points (5 and 6) were at the quarry bottom, and points 3 and 7 were spaced 30-40 m apart vertically along the eastern slope.

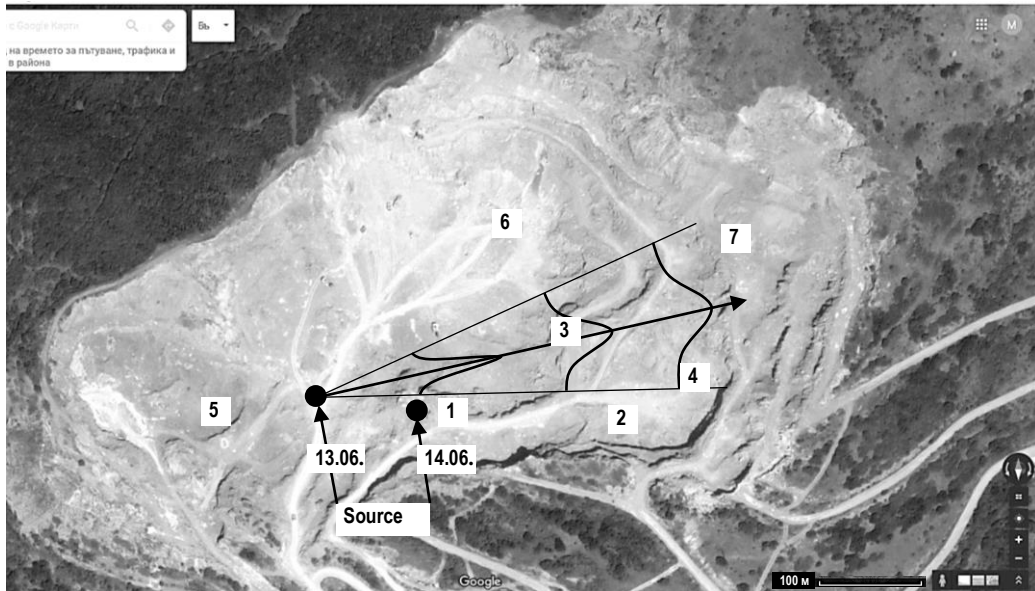


Fig. 1. A map of the quarry with measurement points and pollution sources

### The employed devices

Laser particle counters were used during the experimental campaign – one six-channel HHPC-6 (MetOne, USA) with particle size channels at 0.3  $\mu\text{m}$ , 0.5  $\mu\text{m}$ , 0.7  $\mu\text{m}$ , 1  $\mu\text{m}$ , 2  $\mu\text{m}$ , 5  $\mu\text{m}$  and three two-channel BQ20 (TROTEC, Germany) with particle size channels at 2.5  $\mu\text{m}$  and 10  $\mu\text{m}$  for particle number and mass concentration measurements.

The meteorological data were obtained from the multi-functional weather station with four sensors (temperature, precipitation, relative humidity, air pressure, wind direction and speed).

### Experimental data

#### Meteorological data for 13<sup>th</sup> of July 2019

On this day, meteorological parameters were measured in points 1, 2, and 4. The least change in temperature occurred at point 1, where a slow rise from around 25 degrees to around 26 – 27 degrees was measured at noon. The temperature at point 2, approximately 200 m away from, and 15 m higher than, point 1, rose from 23°C at the beginning of the measurement, to 30°C at lunch. This range was 22-30°C in point 4. A most substantial change in relative humidity occurred at point 4 (at around 30%), and the least change, by less than 10%, was noted at point 1. At noon, the solar radiation reached a high of 850 W/m<sup>2</sup> which is typical of a clear summer day.

### The PM counter data

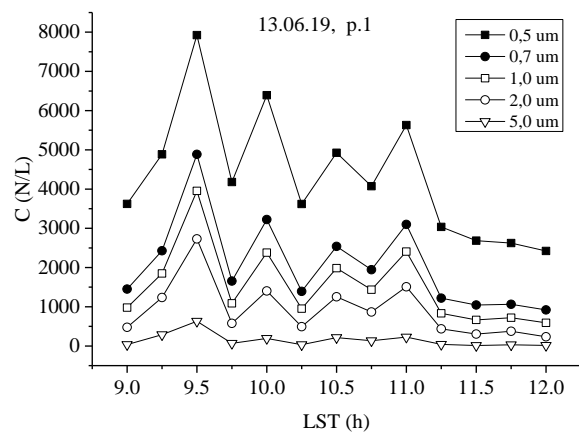


Fig. 2. Numerical concentration of fine particulate matter of varying sizes at point 1 on the 13<sup>th</sup> of June 2019

Figure 2 shows that the number of particles measured at point 1 by all channels was falling as the day advanced. This is especially true of the finer fraction (0.3 and 0.5  $\mu\text{m}$ ) where the number of particles dropped from around 70 000 N/L to around 4 500 N/L. A similar trend was observed at point 2 where the mass concentration for two sizes of fine particulate matter, 2.5 and 10  $\mu\text{m}$ , was measured. No easily discernible trend in the change of mass concentration is present at point 3 (Figure 3).

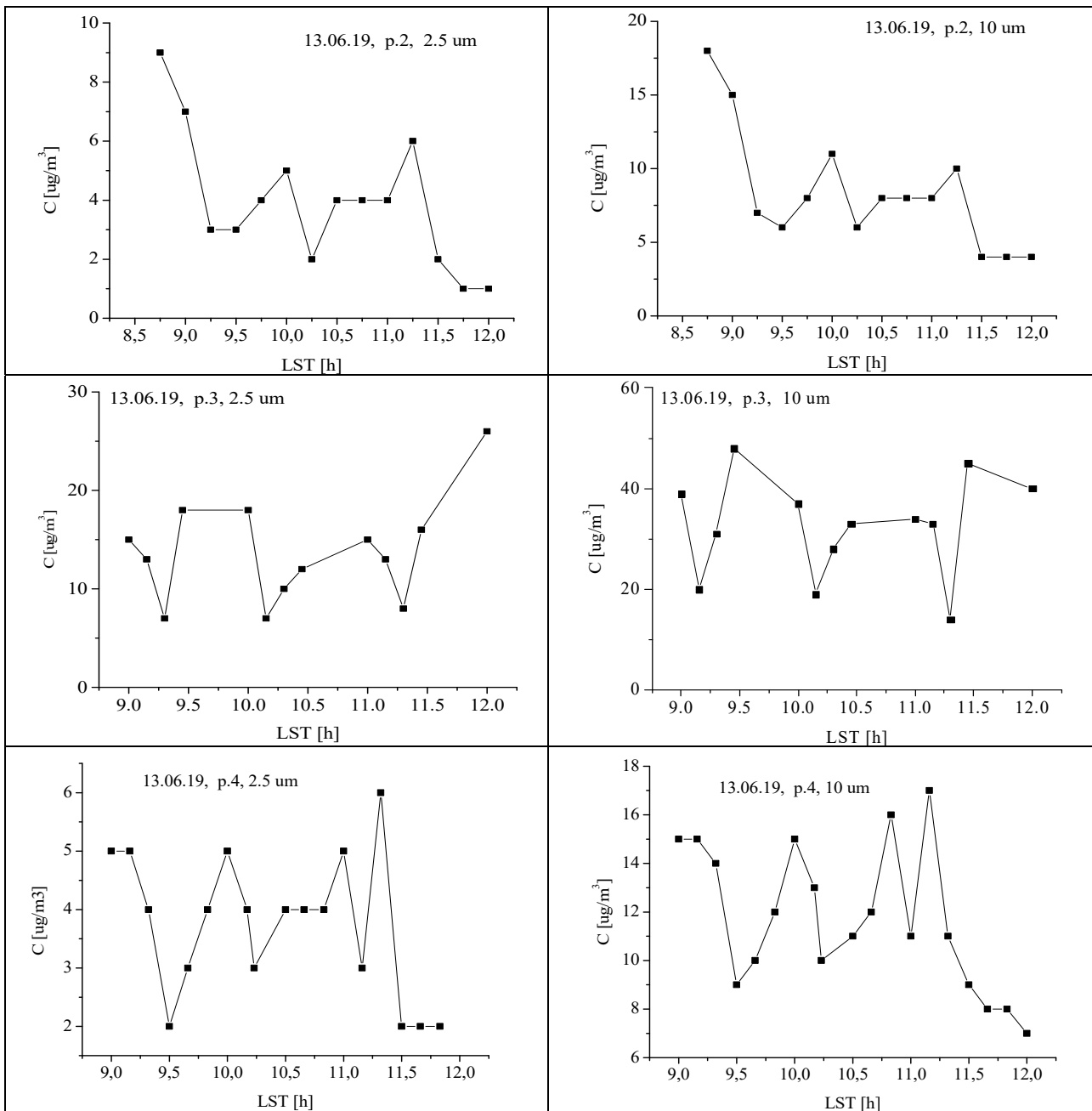


Fig. 3. Mass concentration of 2.5 and 10 µm fine particulate matter at points 2, 3 and 4 on 13<sup>th</sup> of June 2019

**Meteorological data for 14<sup>th</sup> of July 2019**

The second day of the experiment was also clear and sunny, with a monotonous rise in solar radiation up to around 750 W/m<sup>2</sup> at 11 o'clock. On this day, the main meteorological parameters - temperature, relative humidity, wind direction and wind velocity, were measured at each point.

The temperature profile ranged mainly between 25°C and 30°C, with the beginning temperature being lower, at around 22°C, only at point 5. The relative humidity dropped from 65 to 45%.

In all four points the average wind velocity was 1 - 2 m/s, with a slow decrease at experimental point 6 down to around 0 in the afternoon hours. With the exception of point 6 with a predominantly north-north-easterly winds, the wind direction was rather unstable.

**Counter data**

On this day, the number of fine particulate matter at the beginning of the experiment was around 90 000 N/L, while the coarse particles varied from 800 N/L down to several scores at the end of the experiment.

As the day progressed, the mass concentrations decreased in point 6 as well. Almost no decrease was measured in the two remaining points, 3, and 4.

**Discussion**

Orographic forms such as an open quarry predicate changes in the evolution of thermal fields and the characteristic circulation of air flows. If the average background wind velocity is not so high (below 5 m/s), the background wind modification

is mainly a change in the predominant wind direction along the axis (usually the longest) of the quarry. However, this is typical of long and shallow quarries, the circulation being referred to as straight-through, but the flow becomes much more complex in quarries as deep as their horizontal axis is long, where the

so-called recirculation pattern forms, with the flow in the windward part of the quarry running counter to the main wind at height. Such a pattern is referred to as recirculation pattern. In our case the circulation is straight-through.

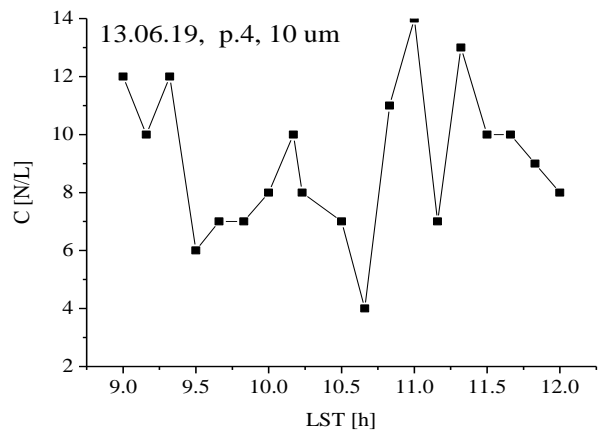
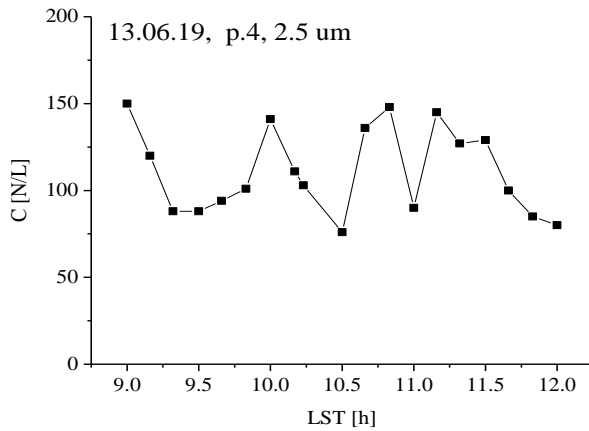


Fig. 4. Numerical concentration of 2.5 and 10 µm fine particulate matter at point 4 on 13<sup>th</sup> of June 2019

On June 13<sup>th</sup>, the wind measured at point 1 was predominantly south-western (Figure 5), with velocities of up to 2 m/s.

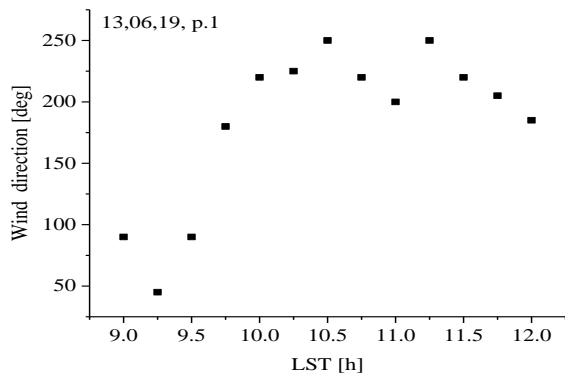


Fig. 5. Wind direction at point 1 on 13<sup>th</sup> of June 2019

This means that the wind was transferring the aerosol impurities to the north-east from the main pollution source - the automotive plant around the excavator and the near-by pneumatic hammer. In a relatively calm atmosphere (no precipitation or storms), the distribution of fine particulate matter is described rather well by the Gauss distribution law. Examples of Gaussian curves consistent with the predominant wind are shown on Figure 1. The maximum pollution levels follow the central axial line along the wind direction. As this line runs closer to point 3 than to points 2 and 4, the pollution levels measured there were higher (by a factor of 3 or 4) than in the two other points. We believe that the absence of a clear downward concentration trend at point 3 was also caused by the wind direction during that day.

Measurements of the number of particles in one litre of air were made at point 1. A comparison was made possible by the fact, that the same measurement was carried out at point 4, Figures 2 and 4 show that the different concentrations of fine particulate matter (2 – 2,5 µm) had dropped from around 700 N/L to around 100 N/L at point 4, which is around 200 m away from point 1.

The machines stopped working at around 11:30 h, meaning that the main source of pollution has disappeared, as can be seen on Figure 2, point 1, and on Figure 3, points 2 and 4 where mass concentration was measured. High pollution levels continued to be observed at point 3 and may have been caused by the specific orography generating local circulation and retaining the impurities in that area.

On the next day, the measurement points were arranged to determine the distribution of aerosol impurities at height. Point 5 was lowermost, around 50 m below the highest point, 7. The two other points, 6 and 3, were at 15 and 30 m respectively, above point 5. The source of pollution was at the same place as on 13<sup>th</sup> of June until 9:30 h, when work was stopped and the machines were relocated to the place marked on Figure 1. Figure 6 presents five measurement channels from the counter at point 5 and shows results with similar values.

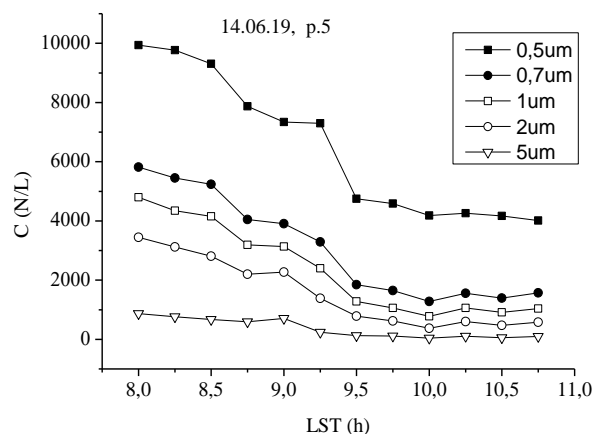


Fig. 6. Numerical concentration of fine particulate matter of varying sizes at point 5 on 14<sup>th</sup> of June 2019

The concentration of the finest particulate matter (0.3 µm) varies between 91,000 N/L and 63,000 N/L. One point of interest is that the number of particles along the entire spectrum in point 5 was 30 – 40% higher than that in the preceding point 1, although the source of pollution was,

initially, at the same place. Subsequently, as the day progressed, the pollution decreased quickly, reaching its levels from the previous day. This means that the temperature inversion had 'caught' the particles and retained them in the bowl on the bottom until the morning. Temperature inversions were registered also by the measurement of the profile at height. A difference of around 2 degrees at the ground level and at a height of 5 m was determined. This is a very strong inversion (4 deg/100 m).

Following the rising of the sun, this inversion, strong but shallow, started to disintegrate and the impurities began to scatter at height, and their ground-level concentration decreased as well.

Preparations for blasting started after 9:30 using other plant, located around point 1 on the previous day. The proximity of the source to points 3 and 4 meant that the level of pollution was 5 to 10 times higher than the level of pollution observed on June 13<sup>th</sup>. Air pollution at point 6 was comparatively low, similar to the levels at point 2 on the previous day. This is explained with the position of this point - 15 m below the level of the operating machines.



Fig. 7. Picture of the open quarry for extraction of ballast materials at Mining Company 'Balsha' AD

The quarry of Balsha AD Mining Company presented in Figures 7 is located 25 km north of Sofia. Open-air quarries are characterised by the generation and typical circulation of airflows. The analysis of the data shows that the concentration of PM in the area of "Balsha" AD Mining Company is within the norm and for similar days of the same month are even lower than the concentrations of PM in the region of Sofia. The study did not detect any contamination and the measured concentrations of PM in the air in the quarry were below the thresholds for human health protection.

## Conclusion

The measurements of fine particulate matter in air in the Balsha quarry lead to the following conclusions:

- Horizontal and height re-distribution of impurities is caused by the specific orography of the region.
- A clear vertical stratification of aerosol impurities is present and, therefore, dispersion is affected more by the vertical positioning of FPM sources within the quarry (the

transferring of particles over the quarry walls being harder) than the horizontal movement of machines.

- Given the particular weather (a clear summer day with a relatively light wind), the concentration of aerosol impurities several hundred meters from the source was not above the admissible air pollution limit values, which, according to the EU directive (1) apply to average daily concentration of particulate matter with a radius of up to 10  $\mu\text{m}$  – 50  $\mu\text{g}/\text{m}^3$  and 2.5  $\mu\text{m}$  – 40  $\mu\text{g}/\text{m}^3$ , although we had asked that the roads over which the trucks hauling waste rock were moving should not be sprayed for the experiment.

**Acknowledgements.** This work is supported by contract No GPF-226/2019 University of Mining and Geology "St. Ivan Rilski". This work has been carried out in the framework of the National Science Programme "Environmental Protection and Reduction of Risks of Adverse Events and Natural Disasters", approved by Resolution of the Council of Ministers № 577/17.08.2018 and supported by the Ministry of Education and Science (MES) of Bulgaria (Agreement № D01-230/06.12.2018). The authors would like to thank the Balsha Quarry management for the kind cooperation during the experiment campaign.

## References

- Dinchev, Z., Y. Gorbunov, N. Kostadinova. 2018. Velocity field visualisation, measured with 3D ultrasonic anemometer. – *Journal of Mining and Geological Sciences*, 61, 39–44.
- EU. 2008. Directive 2008/50/EC of the European Parliament and of the Council of 21 May 2008 on Ambient Air Quality and Cleaner Air for Europe, OJ L 152, 11.6.2008, 1–44.
- Grainger, C., R. N. Meroney. 1992. Dispersion in an open-cut coal mine in stably stratified flow. – *Journal of Boundary Layer Meteorology*.
- Holmes, N.S., L. Morawska. 2006. A review of dispersion modelling and its application to the dispersion of particles: an overview of different dispersion models available. – *Atmospheric Environment*, 40, 5902–5928.
- Mosca, S., G. Graziani, W. Klug, R. Bellasio, R. Bianconi. 1998. A statistical methodology for the evaluation of long-range dispersion models: an application to the ETEX exercise. – *Atmospheric Environment*, 32, 24, 4307–4324.
- Panayotova, M., G. Gicheva, N. Mincheva, L. Dzerahov. 2018. Study on the air quality during the operation of the Mizia quarry. – *Journal of Mining and Geological Sciences*, 61, 92–96.
- Reed, W. R. 2003. *An Improved Model for Prediction of PM10 from Surface Mining Operations*. Dissertation, Virginia Polytechnic Institute and State University, Department of Mining and Minerals Engineering, USA.
- Tayanc, M. 2000. An assessment of spatial and temporal variation of sulphur dioxide levels over Istanbul, Turkey. – *Environmental Pollution*, 107, 61–69.
- Triantafyllou, A. G. 2001. PM10 pollution episodes as a function of synoptic climatology in a mountainous industrial area. – *Environmental Pollution*, 112, 491–500.
- Whiteman, C. D., T. Haiden, B. Pospichal, S. Eisenbach, R. Steinacker. 2004. Minimum temperatures, diurnal temperature ranges, and temperature inversions in limestone sinkholes of different sizes and shapes. – *Journal of Applied Meteorology*, 43, 1224–1236.

## THE REQUIREMENTS FOR CONCRETE LINING OF A SEWAGE COLLECTOR TUNNELS

**Elena Kulikova**

National University of Science and Technology MISiS, 119991 Moscow; [fragrante@mail.ru](mailto:fragrante@mail.ru)

**ABSTRACT.** This article assesses the existing requirements for concrete lining of collectors, identifies weaknesses in each of the studied factors and presents the main directions for increasing the durability of structures. The main emphasis is made on the wear of the lining under the influence of filtration and aggressive media as the main reason for failure and destruction of such tunnels. The basic requirements for concrete lining of collector tunnels are: correct selection of dense waterproof concrete composition (i.e. method of calculation of waterproof concrete composition); choice of additives providing increased density, strength, and water resistance of concrete; investigation of some parameters of concrete mixtures compositions ensuring their resistance to abrasion; the choice of means and methods of protection of concrete lining against water-jet wear and corrosion of concrete caused by the aggressiveness of the media flowing through the tunnels.

**Keywords:** manifold tunnel, wear, concrete lining, fracture, corrosion

### ИЗИСКВАНИЯ КЪМ БЕТОННАТА ОБЛИЦОВКА НА КАНАЛИЗАЦИОННИТЕ КОЛЕКТОРИ

**Елена Куликова**

Национален изследователски технологичен университет МИСиС, 119991 Москва

**РЕЗЮМЕ.** В статията се оценяват съществуващите изисквания за бетонна облицовка на колекторите, посочват се слабостите на всеки от изследваните фактори и се представят основните направления за повишаване на дълготрайността на конструкциите. Основният акцент се поставя върху износването на облицовката под влияние на филтрацията и агресивните среди като основна причина за повреди и разрушаване на такива тунели. Основните изисквания за бетонна облицовка на колекторни тунели са: правилен избор на плътен водоустойчив състав на бетона (т.е. метод за изчисляване на състава на водоустойчивия бетон); избор на добавки, осигуряващи по-голяма плътност, якост и водоустойчивост на бетона; изследване на някои параметри на състава на бетоновите смеси, осигуряващи тяхната устойчивост на износване; избор на средства и методи за защита на бетонната облицовка от износване от водни струи и корозия на бетона, причинени от агресивността на средата, преминаваща през тунелите.

**Ключови думи:** колектор, износване, бетонова облицовка, счупване, корозия

### Introduction

The main requirements for the lining of sewer collector tunnels can be divided into the following:

- waterproofing properties;
- mechanical resistance;
- corrosion resistance;
- resistance to hydro-abrasive wear.

Currently, there is no information about the quantitative parameters of the above-mentioned requirements neither in the literature nor in the practice of underground urban construction. This leads to uncertainty in the creation of new means of protection of concrete lining from external factors and aggressiveness of media flowing through the collector tunnels.

Further research in terms of improving corrosion and water resistance, strength and wear resistance of the lining of the collector tunnels demands the assessment of the above-mentioned requirements.

### Waterproofing properties of lining

Waterproofing properties of lining of sewer collector tunnels should ensure their sufficient water resistance, including by stopping the capillary movement of moisture in the pores of concrete.

Considering the water resistance of the concrete lining, it should be noted that the transfer of moisture in the concrete can be viscous or capillary flows, as well as due to diffusion transfer. In the first two cases, the transfer of the liquid itself with all the substances dissolved in it is carried out. The movement of the liquid through the pores and capillaries caused by its evaporation is determined by the expression:

$$i = X_{\psi} \cdot \Delta\psi, \quad (1)$$

where  $X_{\psi}$  is the coefficient of liquid capillary conductivity;

$$X_{\psi} = \frac{\gamma_g}{8\mu} \int_{r_0}^{2r_x} r^2 f\delta(r) dr, \quad (2)$$

$$\Delta\psi = \frac{\delta}{\gamma_g} \leq \left( \frac{1}{r_1} - \frac{1}{r_2} \right), \quad (3)$$

where  $\gamma_g$  – specific gravity of liquid;  $\mu$  – liquid viscosity;  $r_{1,2}$  – radius of curvature of meniscus.

A number of authors theoretically and experimentally proved that all three types of transport occur at the following

filtration coefficients of materials (table 1). Thus, only  $K_f = (3\div 4) \cdot 10^{-7}$  sm/h can ensure necessary and sufficient quantitative level of waterproofing protection of the collector tunnel.

Table 1. Types of liquid transport

Fluid transfer mechanism	Coefficient of filtration $K_f$ , sm/h
Molecular diffusion	$3.48 \cdot 10^{-7}$
Capillary flow	$3.48 \cdot 10^{-7} \div 3.48 \cdot 10^{-5}$
Viscous flow	$3.48 \cdot 10^{-5} \div 3.48 \cdot 10^{-4}$

### The strength of the concrete lining of sewer tunnels.

The load-bearing capacity of the lining of the collector tunnels is to a certain extent determined by the strength of the material. Since the working conditions of the construction of the collector tunnel lining vary depending on the dynamics of the rock pressure and the nature of the interaction of the rock mass with the support, the strength properties of the lining material should be changed accordingly. In this regard, each material should be considered in terms of its ultimate strength.

Fig. 1 shows the dependence of some indicators characterizing the strength of the collector tunnel lining on the structural parameters of the bearing elements.

As the practice of underground urban construction shows, in the construction of the lining of sewer collector tunnels the most widespread concrete class is "B 40", depending on the geological conditions.

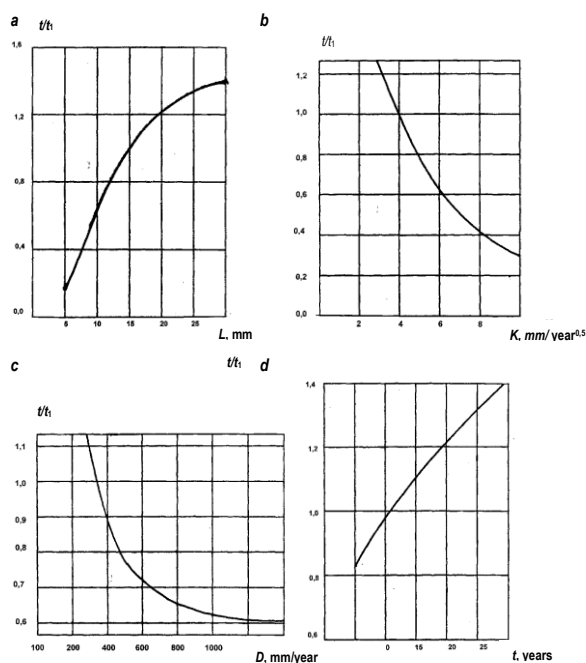


Fig. 1. The dependence of the time of the beginning of cracking ( $t/t_1$ ) in the construction of the tunnel: a – on the thickness of the protective layer of concrete  $L$ ; b – on the coefficient of carbonation  $k$ ; c – on the diffusion coefficient of ions  $D$ ; d – on the time of failure of waterproofing  $t$ ;  $t_1$  – the average time of the beginning of cracking, years;  $t_1$  – the time corresponding to the beginning of the decline in the reliability of the collector lining,  $t_1 = 18.3$  years

An examination of the state of sewer collector tunnels lining in Moscow showed that in some cases the concrete lining of collectors does not satisfy the specified strength. Therefore, to ensure the necessary strength of concrete, it is necessary to overestimate its projected strength by 1.2-1.4 times, and in complex hydrogeological conditions even more.

### Corrosion resistance of collector tunnels concrete lining

Statistics of failures of engineering equipment of cities shows that the frequency of accidents of sewer networks is increasing every year. There are frequent accidents, causing significant material damage associated with the failure of roads, the collapse of buildings, structures, and sometimes the death of people. Often failures of sewage facilities are accompanied by contamination of the soil and groundwater contained in the construction, discharge of domestic sewage into water bodies. Therefore, the fight against violations (failures) of sewer networks is relevant.

One of the aspects of failure control is the task of timely detection of corrosion damage of reinforced concrete structures of collectors.

Direct inspection of concrete structural elements of wells and concrete pipes, the measurement of strength parameters and rate of destruction of reinforced concrete elements under the influence of aggressive gas environment, gives the opportunity to prevent the deterioration of structures, to define the terms of their service and to carry out repair and construction works in proper time.

The corrosion resistance of the lining material has the greatest impact on the durability of the collector tunnels' lining. The calculation of the effect of corrosion weakening of concrete on the bearing capacity of the collector tunnel's lining shows that the loss of the bearing capacity of the lining occurs when the strength of concrete is reduced 2 times compared to the design (under appropriate mining and geological conditions). The thinness of the concrete mostly contributes to the development of the corrosion processes of concrete.

The results of the quantitative assessment of the degree of corrosion resistance of metal and reinforced concrete structures are shown in table 2.

Table 2. The degree of corrosion

The degree of aggressive influence of the environment	Metal construction		Reinforced concrete structure	
	Uniform corrosion rate, mm/year	Average annual loss of bearing capacity during operation, %	Average annual loss of bearing capacity during operation in %	
			Underground construction	Bearing and enclosing structures
Poor	Up to 0.1	5	3	5
Middle	0.1 – 0.5	10	5	10
Strong	More than 0.5	15	8	15

It is assumed, that the structure is subject to major repairs or replacement with a loss of bearing capacity of 40-60 %.

The presence of additives in the concrete affects the degree of corrosion resistance of the reinforcement cage (table 3).

Table 3. Corrosion rate of steel in concrete in humid atmosphere

Concrete	Mass loss, g/m <sup>2</sup> per year	The maximum depth of corrosion of ulcers for the year, mm
Normal, no additives:		
• dense	0	0
• porous	13-210	0.48
With chloride additives	10-660	1.63
Carbonated	30	-

The degree of corrosion of the reinforcement depends on the presence and magnitude of crack opening  $K$  in the body of the concrete lining of the underground structure, which clearly demonstrates Fig. 2 and formula (4):

$$K = \frac{10L^3\delta}{\frac{L}{d}+1} \cdot d^4 \quad (4)$$

where  $L$  – the thickness of the protective layer of concrete, m;  $d$  – diameter of reinforcement, m;  $\delta$  – crack opening, m.

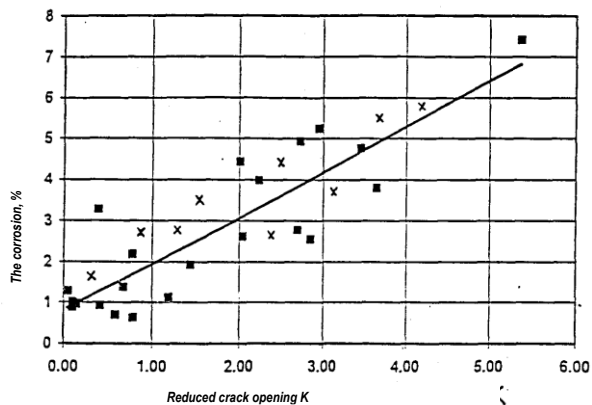


Fig. 2. Dependence of the degree of corrosion of the lining on the reduced crack opening in concrete

The value of corrosion of the reinforcement is a boundary condition for the transition of the structures of an underground building from one technical condition to another. Thus, at the corrosion value  $K(t) = 2\%$  there is a transition of structures from 1<sup>st</sup> to 2<sup>nd</sup> category of technical condition, at  $K(t) = 7\%$  – from 2<sup>nd</sup> to 3<sup>rd</sup> category,  $K(t) = 15\%$  – from 3<sup>rd</sup> to 4<sup>th</sup> category,  $K(t) = 25\%$  – from 4<sup>th</sup> to 5<sup>th</sup> category.

Corrosion of concrete also causes filtration of soft water through the lining of the tunnel. Leaching of 25% CaO from cement leads to a sharp drop in strength and to the complete decomposition of concrete in the future. If we assume that the average consumption of cement per 1 m<sup>3</sup> of concrete is 350 kg and that an average of 1 m<sup>3</sup> of concrete accounts for 210 kg of CaO, we can conclude: leaching 52.5 kg of CaO per 1 m<sup>3</sup> of

concrete lining of the collector tunnel can lead to its destruction.

Studies have found that the process of decomposition of organic compounds in wastewater leads to the appearance of carbon dioxide, ammonia, hydrogen sulfide, methane and other gases in the surface part of gravity reservoirs.

In aerobic decomposition processes (involving oxygen), carbon dioxide is mainly released, and in anaerobic (oxygen-free) processes, hydrogen sulfide and methane are the main decomposition products, with the largest percentage being hydrogen sulfide. The appearance of hydrogen sulfide in the atmosphere of the surface part of the collector is accompanied by the development of thionic bacteria on its walls, under the action of which hydrogen sulfide is oxidised to sulfuric acid and acts as an acid condensate on the arch of the collector.

Chemical analysis of concrete corrosion products shows that they consist mainly of gypsum, silica, aluminum hydroxides and iron compounds. In the water-saturated state, corrosion products have a consistency of liquid dough and easily fall off from the ceiling and vertical surfaces.

The corrosion rate of concrete depends on the concentration of hydrogen sulfide and sometimes reaches up to 20 mm per year. This leads to the fact that such sections of the collector fall off after 5-10 years of operation.

In addition to the leaching aggression, aggression of flowing wastewater also acts on the concrete lining. As a result of the action of the gas condensate and microorganisms, which develop well in the mucous film covering the channel walls, on the concrete lining of sewage, there is a significant decrease in the content of CaO in concrete from 60-64% to 12% and an increase in sulphates from 1.5% to 42%. On average, the corrosion depth of concrete lining of collector tunnels is estimated at 6-13 mm per year.

Therefore, it can be assumed that the service life of the concrete lining according to the corrosion resistance factor varies between 20 to 35 years. However, it is known that the corrosion of concrete can have an avalanche character, which probably could lead to rapid destruction of the lining.

Currently, it is possible to control the characteristics of concrete (to increase its density and reduce porosity) by introducing additives (super-plasticizers to reduce the water-cement ratio, micro-silicates) or covering the concrete surface with materials that promote pore colmatation (Xypex, Squid, Penetron, etc.). This helps to increase the water resistance of concrete tunnel lining, its resistance to aggressive influences. However, this is not enough to prevent the destruction of concrete when exposed to an aggressive environment.

Protection of concrete lining from corrosion damage can be carried out in two directions: either increasing the density of concrete, or protecting the concrete with anti-corrosion coatings.

## Conclusion

The abrasion of the concrete lining is determined by the amount of loss of the initial weight related to the surface of the abrasion area. Due to the impact of abrasive materials in the wastewater at speeds of more than 2 m/s there is an intensive abrasion of the tunnel tray.

As shown by estimations of the influence of the hydro-abrasive wear the tray part of the concrete lining on the bearing capacity of the collector tunnel's lining, when the abrasion is 40-60% of the thickness of the trough part of the

tunnel lining, it loses its bearing capacity. On the basis of statistical data processing it was found that an average of 1.2 cm of the tray is worn out yearly. Consequently, the period of possible operation of the collector tunnel according to the factor of abrasion is within the range of 10-12 years.

Water-abrasive wear of the collector tunnel's lining begins with the washing out of the cement stone and the separation of grains of large and small aggregate, as a result the lining of the tunnel becomes rougher, and this in turn exacerbates wear.

Having considered the basic requirements for concrete lining of collector tunnels, we can assume that the main direction for increasing the durability of concrete lining sewer tunnels is:

- correct selection of dense waterproof concrete composition (i.e. method of calculation of waterproof concrete composition);
- choice of additives providing increased density, strength, and water resistance of concrete;
- investigation of some parameters of concrete mixtures' compositions ensuring their resistance to abrasion;
- the choice of means and methods of protection of concrete lining against water-jet wear and corrosion of concrete caused by the aggressiveness of the media flowing through the tunnels.

## References

- Alekseev, S. N., N. Ye. Rosenthal. 1976. *Corrosion resistance of concrete structures in aggressive industrial environment*. Stroyizdat, Moscow, 396 p. (in Russian)
- Balovnev, S. V., R. V. Shevchuk. 2018. Geomechanical monitoring of mine shafts in difficult mining and geological conditions. – *Mining Information and Analytical Bulletin*, 8, 77–83.
- Causes of destruction of tunnels during their operation*, <http://fecland.ru/tonneli/198>.
- Garber, V. A. 1998. *Durability of tunnel structures in operation and urban construction*. Scientific Center "Tunnels and Subways", JSC "TsNIIS", Moscow, 172 p. (in Russian)
- Ghafar Nima. 2012. Corrosion control in underground concrete structures using double waterproofing shield system. – *Construction and Building Materials*, 36.
- Kirilenko, M. 2013. *Diagnosis of reinforced concrete structures and buildings*. Architecture, Moscow, 365 p. (in Russian)
- Kollektory i tonneli kanalizatsionnyie. Trebovaniya k proektirovaniu, stroitelstvu, kontrolyu kachestva i priemke rabot. (Sewers and sewer tunnels. Designing, construction, quality supervision and acceptance of works)*. 2013. STO NOSTROI 2.17.66-2012, «BST», Moscow, 101 p. (in Russian)
- Kulikova, E. Yu. 2018. Estimation of factors of aggressive influence and corrosion wear of underground structures. – *Materials Science Forum*, 931, 385–390.
- Kulikova, E. Yu. 2004. Influence of biological and electrochemical corrosion processes in sewage tunnels on environmental pollution. – *Mining Information and Analytical Bulletin*, 5, 325–329.
- Kulikova, E. Yu. 2007. *The filtration reliability of the design of urban underground structures*. Publishing House "World of Mining Books", Moscow, 316 p. (in Russian)
- Kuzenkov, E. V. 2004. Problemy obespecheniya nadezhnosti, dolgovechnosti i ekologicheskoy bezopasnosti setey vodosnabzheniya (*Problems of ensuring reliability, durability and ecological safety of water supply networks*). – *STO NOSTROI*, 5-6, 1-8 (in Russian).
- Molev, M. D., S. G. Stradanchenko, S. A. Maslennikov. 2015. *ARPN Journal of Engineering and Applied Sciences*, 10, 16.
- RD 03-422-01*. 2002. *Methodical instructions on carrying out expert examinations of mine lifting installations*. Moscow, 52 p. (in Russian)
- Rusanov, V. E. 2010. To the topic of assess of the effectiveness of the use of fiber concrete in precast tunnel lining. – *Transportnoye stroitelstvo*, 3, 13–16 (in Russian).
- Rybak, J., A. Ivannikov, E. Kulikova. 2018. Deep excavation in urban areas – defects of surrounding buildings at various stages of construction. – *MATEC Web Conference 9th International Scientific Conference Building Defects (Building Defects 2017)*, Section – Mechanical and Materials Engineering, 146, doi.org/10.1051/mateconf/20181460201
- Shilin, A. A. 2017. *Repair of reinforced concrete structures*. Publishing House "Mining book", Moscow, 519 p.
- Shuxue, D., J. Hongwen, C. Kunfu, X. Guo'an, M. Bo. *International Journal of Mining Science and Technology*, 27 p.
- Vasiliev, V., N. Lapšev, Yu. Stolbichin. 2013. Microbiological Corrosion of Underground Sewage Facilities of Saint Petersburg. – *World Applied Sciences Journal 23 (Problems of Architecture and Construction)*, 184–190.
- Vlasov, S. N., A. A. Shilin. 1999. Features of work and anti-corrosion protection of tunnel lining of urban underground structures. – *Durability and corrosion protection of structures. Proceedings of the International Conference, May 25-27 1999*.
- Wenqi Ding, C. Gong, K. M. Mosalem, K. Soga. 2017. Development and application of the integrated sealant test apparatus for sealing gaskets in tunnel segmental joints. – *Tunnelling and Underground Space Technology*, 63, 54–68.
- Yagodkin, F. I., A. Y. Prokopov, M. S. Pleshko, A. N. Pankratenko. 2017. *IOP Conference Series: Earth and Environmental Science Series. "Innovations and Prospects of Development of Mining Machinery and Electrical Engineering – Transportation of Mineral Resources"*, 062014.

## ENVIRONMENTAL SUSTAINABILITY IN THE DEVELOPMENT OF URBAN UNDERGROUND SPACE

*Elena Kulikova, Alexander Ivannikov*

*National University of Science and Technology MISiS, 119991 Moscow; fragrante@mail.ru*

**ABSTRACT.** The application of reliability theory and risk in the field of underground construction permits on the basis of statistical processing of results of laboratory and industrial research to establish the laws of probability distribution of the studied parameters of the rock mass around an underground object. The obtained regularities, in turn, enable the prediction of durability of underground structures in order to introduce rational approaches in their design. This involves the following tasks: identification of ways to ensure ecological and technological reliability of underground objects depending on the applied technology of their construction and possible risks; modelling of construction technology in order to assess the safety and risk of development of underground space; development of ideas about the enforcement mechanism and criteria for eco-technological reliability of urban underground structures; optimisation of structural parameters of underground structures based on the concept of acceptable risk and technological and environmental safety; comprehensive assessment of the reliability of underground structures by using different technologies and methods for their construction.

**Keywords:** geoeological model, rockmass, underground construction

### УСТОЙЧИВОСТ НА ОКОЛНАТА СРЕДА ПРИ РАЗВИТИЕТО НА ГРАДСКИ ПОДЗЕМНИ ПРОСТРАНСТВА

*Елена Куликова, Александър Иванников*

*Национален изследователски технологичен университет "МИСиС", 119991 Москва*

**РЕЗЮМЕ.** Прилагането на теорията за надеждността и риска в областта на подземното строителство позволява на базата на статистическа обработка на резултатите от лабораторни и промишлени изследвания да се установят законите на вероятностното разпределение на изследваните параметри на скалната маса около подземен обект. Получените закономерности от своя страна дават възможност за прогнозиране на издръжливостта на подземните конструкции с цел въвеждане на рационални подходи при тяхното проектиране. Това включва следните задачи: идентифициране на начини за осигуряване на екологична и технологична надеждност на подземни обекти в зависимост от приложената технология на изграждане и възможни рискове; моделиране на строителните технологии с цел оценка на безопасността и риска от развитие на подземно пространство; разработване на идеи за механизма за прилагане и критерии за екологична надеждност на градските подземни структури; оптимизиране на структурните параметри на подземните конструкции въз основа на концепцията за приемлив риск и технологична и екологична безопасност; цялостна оценка на надеждността на подземните конструкции чрез използване на различни технологии и методи за тяхното изграждане.

**Ключови думи:** геоекологичен модел, скална маса, подземно строителство

## Introduction

Sustainable development of society is impossible without ensuring environmental sustainability, which is understood as the ability of the ecosystem to preserve its structure and functional characteristics under the influence of external and internal factors. At present, urban underground construction is becoming much more active in the world. Urban underground structures are the only real means to solve radically planning, transport and communal problems of urban areas. However, large-scale development of underground space of megacities requires substantial financial resources, a significant share of which is spent on combating infiltration of groundwater into underground structures and sanitation. The fight against water flows into the construction and operation of underground facilities in dense urban areas is associated with considerable difficulties and requires the use of special measures.

Materials and design of the lining do not always provide the necessary reliability of underground structures, and, consequently, their normal operation during a given service life period. Thus, up to 5% of the operated sewer tunnels in

Moscow require annual overhaul due to failures of the lining caused by the aggressive impact of external and internal environment and other operating conditions [1]. About 40-45 thousand rubles per 1 m of the tunnel are spent on major repairs of such structures. Up to 30% of the initial cost of construction in the operation of communication tunnels is spent on the elimination of failures that occur much earlier than the estimated period. The consequences of failures are failures of the earth's surface, pollution of groundwater by industrial and domestic sewage, subsidence of buildings and underground structures themselves [3].

It should be taken into account that over the past 5 years, the number of industrial and domestic water discharges has increased significantly (in Moscow, up to 9 million m<sup>3</sup> of wastewater is discharged into sewer tunnels per day). In addition to quantitative changes in wastewater, there was also a qualitative change (the presence of a large percentage of the content of aggressive impurities). The latter is most often manifested in the enhancement of the aggressive properties of the medium [3]. As a result of the development of high-rise construction in large cities, inevitably there are significant loads

on the lining of operated underground structures located in the construction zone.

According to [4], up to 70% of the garages, 60% of the warehouses, up to 50% of the archives and various storage facilities, up to 30% of the cultural institutions, up to 3% of the buildings of research institutes and universities can be located in Moscow below the level of the earth's surface [2], [3]. The city has more than 200 built underground passages and transport tunnels, among which the operated part of municipal tunnels exceeds 160 km. The annual input of such tunnels exceeds 15 km.

It is obvious that environmental sustainability in the development of the underground space of cities, which means the preservation of high operational reliability of underground facilities throughout their service life, is a very urgent task. Therefore, it is necessary to develop a geocological model of underground construction on the basis of criteria of technological reliability and acceptable risk.

## Problem definition

Reliability indicators include quantitative characteristics, which are introduced according to the rules of the statistical theory of reliability. Methods of the statistical theory of reliability at underground construction allow establishing requirements to reliability of components and elements of the underground construction on the basis of requirements to reliability of the natural and technical geosystem "rock massif – technology – underground construction – environment" as a whole.

The statistical theory of reliability is an integral part of a more general approach to the calculation of the reliability of technical objects, in which failures are considered as a result of the interaction of the object as a physical system with other objects and the environment. Thus, in the design of underground structures and their structures, it is necessary to take into account, in explicit or implicit form, the statistical spread of mechanical properties of materials, elements, as well as variability in time and space parameters characterising the external loads and effects on the system "rock mass – technology – design of underground structures – environment". [5].

Most reliability measures are fully meaningful even with a more general approach to the estimated reliability. In the simplest model of calculating the design of an underground structure for strength according to the scheme "load parameter – strength parameter", the probability of failure-free operation coincides with the probability that within a given period of time the value of the load parameter will never exceed the value that takes the strength parameter. Both parameters can be random functions of time.

The development of the underground space of cities is associated with complex physico-chemical and physico-mechanical transformations based on non-deterministic values and phenomena, so the technology of construction of the underground structure can be represented as a stochastic system, as evidenced by the following provisions [6]:

- underground construction is associated with a variety of random variables of prescription, technological, operational nature, factors of interaction of rock mass and the environment and external loads;

- such random factors in their relationship affect the reliability of the structures of the underground facility;
- rock mass around the underground structure is an anisotropic discrete medium, with components representing random variables. Variability of mining and hydrogeological conditions, soil properties, impact on the design of underground structures from the environment are random;
- soil softening in time – the result of interaction with the external environment. Failures occurring during the operation of structures of underground facilities are random events.

Thus, to determine the reliability of underground facilities, it is not enough to know the physical and chemical processes taking place at the same time and to rely on these practices. It is necessary to proceed from the general theory of reliability, applying its laws to calculate the degree of reliability and analytical prediction of changes in the reliability of structures.

For underground facilities of the city, which can be considered as a potential source of danger, an important concept is safety. Although safety is not a general concept of reliability, it is closely related to this concept under certain conditions (for example, when a violation of the working condition of the structures of an underground structure can lead to conditions harmful to people and the environment).

The concept of "risk" is directly related to the concept of safety, as if the reverse side of the latter. The existing methods of substantiation of technological parameters of structures of underground buildings based on deterministic models do not take into account the random nature of the filtering soil massifs and compositions used. Such a deterministic approach does not allow assessing the reliability of calculations of residual water inflows and the risks associated with the creation of the system "rock mass – technology – underground structure – environment". Consequently, there is no possibility to optimise properly the technological parameters of underground construction. However, taking into account the risks and their factors is a very urgent task, especially in the context of optimising the technological parameters of the underground structures.

## Modern approaches to safety and risk problems

Danger in underground construction is considered as a condition inherent in the natural and technical geo-system "rock mass – technology – lining – environment". It is implemented in the form of damaging effects on humans and the environment in the event of its occurrence either in the form of direct or indirect damage in the normal operation of underground facilities.

The simplest optimisation formulation of the problem in the theory of safety and risk can be considered as a probabilistic modification of the usual least cost criterion. This model allows generalisations that take into account the costs associated with the diagnosis, prevention of failures of underground structures, repeated failures, repair and restoration, planned capital costs, etc.

The following factors are the disadvantage of optimisation approaches to safety and risk tasks:

- insufficient development of economic models,

- conditional character of numerical values of cost indicators,
- fundamental difficulties in assessing accidents in underground construction related to environmental and social damage.

To avoid such difficulties, optimisation approaches that do not use economic categories can be used. For example, if the safety of an underground facility can be ensured by purely technical measures that do not lead to high costs, the criterion of optimal safety is exempt from cost restrictions. As a result, we come to the principle of the minimum probability of an accident in underground construction.

In many cases, in urban underground construction, the cheapest solution corresponds to the highest risk and vice versa, the solution with limited risk requires high costs. This inverse relationship of risk and cost can determine the order of technical decision-making when justifying the method of strengthening the rock mass around the underground object.

When designing a particular underground facility with certain technical characteristics, the designer must take into account the issues of reliability. Specific tasks for reliability and evaluation of their implementation at all stages of the creation and operation of underground facilities allow to identify the weakest points and solve a number of tasks for optimal design, reservation, selection of quality of spare parts, establish the frequency and degree of preventive measures. To do this, all the information on the operation of the underground facility must be used.

Any requirement for reliability should be justified not only technologically, but also from an economic point of view. The choice of parameters of underground structures and structures that ensure efficiency, and safety of their operation, determines the need to obtain quantitative estimates of reliability or risk.

## Research task

The application of the theory of reliability and risk in the field of underground construction on the basis of statistical processing of the results of laboratory and industrial research allows to establish the probability distribution laws of the studied parameters of the rock mass around the underground object. The resulting patterns, in turn, make it possible to predict the durability of underground structures and to achieve rational approaches to their design.

In this regard, the following tasks arise:

- identification of ways to ensure environmental and technological reliability of underground facilities, depending on the technologies used for their construction, and possible risks;
- modelling the construction of geotechnology objects for safety and risk assessment of underground space development;
- development of ideas about the mechanism and criteria of ecological and technological reliability of urban underground structures;
- optimisation of design parameters of underground structures based on the concept of acceptable risks and technological and environmental safety;
- comprehensive assessment of the level of reliability of underground structures in the application of various technologies and methods of their construction.

## Comprehensive analysis of geological conditions of construction

The choice and justification of the technology of construction of underground structures should be carried out only on the basis of a comprehensive system analysis of mining conditions of construction according to the main determining factors, including:

1. Technical and technological solutions of underground facilities for the period of operation. This group of factors include:

- functional purpose of the underground structure;
- internal dimensions of the underground structure;
- operational load indicators;
- initial requirements for technical and technological reliability.

2. Engineering-geological and hydrogeological conditions of construction and operation of underground facilities. In this group, the determining criteria for the choice of construction technology include:

- initial requirements for technical and technological reliability;
- geological structure and engineering-geological characteristics of soils containing the object;
- the depth of the structures;
- influence of hydrogeological conditions on the construction and operation of the underground facility.

3. Social and ecological conditions of underground construction placement in the formed urban environment. This group of factors mainly considers the possible harmful effects of the environment and the construction (operated) underground facilities. The most significant features include:

- nature of the earth's surface;
- the presence of underground communications and structures;
- provision of existing transport and pedestrian routes;
- reducing the impact of negative construction processes on the urban environment.

4. The climatic conditions of the construction.

5. Economic conditions of construction. The defining indicators of this group are:

- amount of capital investments;
- preliminary cost of 1 m of the route of the passed underground construction;
- terms of construction, etc.

6. The state of the technical base of the construction organisation.

## Environmentally friendly construction technologies

The main objective of a scientifically based approach to the development of underground space, taking into account all environmental requirements, is the use of high technologies in underground construction.

High technology implies:

- the expansion of mechanised shield driving;
- broader use of the shield method of tunnelling underground structures in combination with advanced methods of strengthening of the array of the host rocks;
- greater use of Novoushitskogo method of tunnelling;

- expansion of the use of railway entries into the underground space to protect the environment of cities;
- application of various methods to prevent possible precipitation of the earth's surface during underground construction;
- creative use of the underground space of cities for the development of underground infrastructure, taking into account environmental requirements.

The up-to-date situation during the underground space development in the world is characterised by a number of features. In particular, the world practice of tunnel construction is focused currently on the placement of public infrastructure at an increasing depth. The need for deeper placement of underground structures is associated with the following main aspects:

- the near-surface levels are already quite saturated with various structures of urban infrastructure;
- the service life of many collectors has expired or is about to expire, making them hazardous in case of overloading with ever-increasing volumes of wastewater;
- the possibility of increasing the capacity of reservoirs;
- the possibility for more "painless" repair and reconstruction of underground structures by placing them at a greater depth;
- the need to eliminate the environmental crisis in a complex system of "rock mass – technology – underground structure – environment".

The upper tier of the underground space of cities is a chaotically branched network of utilities, where sewage and heating systems and other communications are located without taking into account possible emergency releases to nearby water bodies. About 1500 tons of oil products, at least 500 tons of salts of heavy metals and more than 22 000 tons of organic pollutants are discharged into the Moscow reservoirs annually, bypassing the treatment facilities. Thus, despite the ability of the natural ecosystem to ensure self-purification and balance, the Moscow region can become an ecological disaster zone in the coming decades. Therefore, the development of a new approach to the placement of underground structures and new environmentally friendly technologies and methods of their construction is extremely relevant.

## Sustainable construction

From the standpoint of environmental safety, the most acceptable technologies can be justified only with a comprehensive approach to all aspects of the development of the city's underground space, which includes:

1. Improving the quality of engineering-geological surveys of the subsoil for underground construction, followed by taking into account their results in the design and development of solutions to ensure the stability, reliability, durability of underground facilities and water resistance of their supporting structures. It is necessary:

- to substantiate the environmental compatibility of the technologies with the changing nature of the interaction between the elements of PTGS;
- to combine the high technologies and ways of strengthening the rock mass with the aim of increasing the rate of penetration of workings;

- to ensure computer modelling and calculation of parameters of technical and technological solutions based on a comprehensive assessment of the properties of rock mass and their compliance with the properties of the lining;
- to ensure complex consideration of the main factors characterising the current state of the system "rock mass – technology – underground structure – environment"; to identify the optimal combination of the parameters characterising the state of the system as safe;

2. Expansion of underground infrastructure and construction of new generation underground facilities.

3. Increasing the durability of underground structures based on the use of modern knowledge of rock mechanics, geomechanics, environmental aspects of the development of the underground space of the city, construction geotechnology.

4. Risk reduction in underground construction based on the analysis of risk situations in the natural and technical geosystem "rock mass – technology – underground structure – environment" and the forecast of changes in the environmental situation in general when using a particular technology of work.

An integral part of the processes that create conditions for sustainable development is the "sustainable construction", including the underground one. This concept appeared relatively recently, and at the first International conference "Construction and environment" (USA, 1994) it was formulated as follows: "Sustainable construction means the creation and responsible maintenance of a healthy artificial environment based on the effective use of natural resources and environmental principles".

## Geo-ecological modelling

The basic environmental principles and concepts that form the basis of the concept of sustainable, environmentally safe underground construction can be formulated as follows:

- minimisation of negative impacts (pollution, excessive noise, vibration, electromagnetic fields, etc.) on natural ecological systems and natural landscapes at all stages of functioning of the natural and technical geosystem "rock mass – technology – underground structure – environment»;
- restoration and maintenance of biodiversity in construction and urban areas;
- the use of environmentally friendly architectural and planning solutions of underground structures; ecological reconstruction of the urban environment; attention to the aesthetic component of the urban complex;
- application of environmentally friendly building materials and underground construction technologies;
- construction of underground facilities in accordance with "high" technologies;
- making underground structures food-grade, biodegradable properties that allow them to blend and clean up the environment; create a healthy artificial habitat;
- waste reduction in underground construction;

- reclamation of the territories disturbed during the creation of the construction site and conducting works in the open way;
- the use of environmentally friendly man-made raw materials for the manufacture of building materials and products;
- implementation of environmental monitoring systems for underground construction at all stages of the life cycle of the underground facility;
- comprehensive and highly effective environmental control of technological decisions at all stages of the life cycle of the underground facility (environmental support).

In addition, the most important conditions for sustainable underground construction, compatible with the environment, are:

- recognition of the presumption of ecological danger of any planned activity on the development of underground spaces of the city;
- improvement of the regulatory framework to ensure sustainable and environmentally sound underground construction;
- organisation and development of a system of continuous environmental training for decision - makers in the field of underground construction;
- participation of scientific, design, public and other associations in solving problems related to the planned activities for the development of underground space.

A structural geo-ecological model of natural and technical geosystem "underground construction – the environment" is shown in fig. 1.

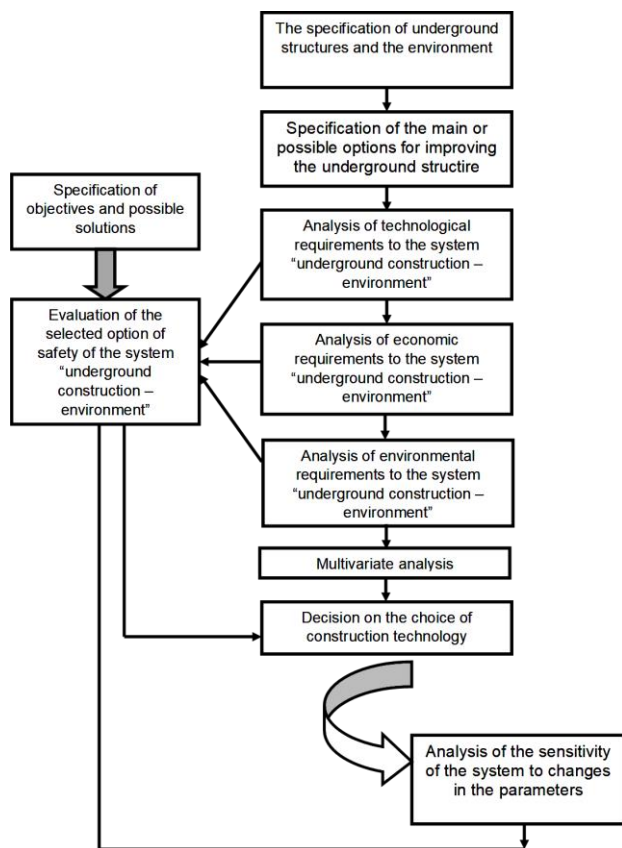


Fig. 1. Structural geo-ecological model

The choice of strategy and tactics for the implementation of sustainable underground construction is a very difficult task, requiring joint creative work of designers and builders, as well as specialists of other services, primarily environmental. All this places high demands on the level of professional training of future mining engineers in the field of environmental knowledge.

## Conclusion

The formation of geo-ecological models of objects of underground construction on the basis of criteria of reliability and technological risk tolerance will allow to obtain the following results:

- Creation of theoretical developments to substantiate the mechanism of environmental and technological reliability of urban underground structures;
- Geo-environmental and geotechnical rationale for the choice of strategic directions for the development of the underground space of cities under the current and future level of development of science, techniques and technologies of underground construction;
- Modelling of parameters of geological and technological reliability on the basis of admissible risks criteria and safety of natural and technical geosystem (Fig. 1).

The results will shed some light on modern approaches related to the design of underground structures in large cities, seek innovative potential of environmentally friendly technologies for the construction of urban underground structures, and ensure environmental sustainability in the development of underground space of megacities.

## References

- Bakhireva, L. V., V. I. Osipov, G. L. Koff, E. E. Rodina. 1990. Geological and geochemical risk as a criterion of ecological regulation of territories. History of interaction between society and nature: facts and concepts. – *Texas. Doc. Part 1*, Moscow, 98–102.
- Bartel, S. M. 1996. Ecological/Environmental risk assessment. – In: *Risk Assessment and Management Handbook*. New York, 10.3–10.59.
- Burkov, V. N., A. V. Schepkin. 2003. *Ecological Safety*. IPU RAN, Moscow, 92 p.
- Bykov, A. A., L. G. Salova, G. M. Zemlyanaya, V. D. Furman. 1999. *Guidelines for the analysis and management of the risk of harmful environmental factors impact on public health*. Moscow, 70 p.
- Chicken, J. C. 1996. *Risk Handbook*. London, 310 p.
- Chicken, J. C., S. A. Harbison. 1990. Differences between Industries in the definition of acceptable risk. – In: *New Risks*. New York, 123–128.
- Cohen, B. L. 1991. Catalog of Risks Extended and Updated. – *Health Physics*, 61, 89–96.
- Dzuray, E. J., A. R. Maranto. 1999. Assessing the status of risk-based approaches for the prioritization of federal environmental spending. – *Federal Facilities Environmental J.*, 5.

- Hallenbeck, W. H. 1993. *Quantitative Risk Assessment for Environmental and Occupational Health*. Boca-Raton, 212 p.
- Kulikova, E. 2016. Basic Directions of Improving the Durability of the Sewage Collector Lining. – *Applied Mechanics and Materials*, 843, 25-32.
- Kulikova E. Yu. 2002. *Environmental Safety in the Development of Underground Space in Large Cities*. Publishing House MGGU, Moscow, 376 p.
- Lihacheva, E., D. Timofeev. 2004. *Ecological Geomorphology Dictionary*. Media-PRESS, Moscow, 240 p.
- Petrenko, I. E. 2002. The organization of underground space development. Accomplishments and hopes. – *TIMR*, 406 p.
- Polovov, B. D., M. V. Cornikov, V. V. Poddubny. 2008. Study engineering solutions for the effective development of underground space largest cities: – Ural State Mining University. Publishing House UGGU, Ekaterinburg, 377 p.
- Postolskaya, O. K., A. V. Man'ko, M. Jarosch. 2001. Information system for large projects in rockengineering. Universitdt Siegen, Institut fur Geotechnik, 234-241.
- Tepman, L. N. 2002. *Risks in the Economy*. Publishing House UNITY-DANA, Moscow, 380 p.
- Vaganov, P. A. 1999. The risk of death and the price of life. – *Jurisprudence*, 3, 67–82.

## NEED FOR FIXED FIRE FIGHTING SYSTEMS IN ROAD TUNNELS

Diana Makedonska, Michael Michaylov

University of Mining and Geology "St. Ivan Rilski", 1700 Sofia

**ABSTRACT.** Road tunnels with heavy traffic are expected to have in place specific emergency measures for prevention and mitigation of effects of road accidents and other critical events associated with fires which might endanger human life, tunnel structure and facilities or cause environmental pollution. It is known that risk management in the event of road tunnel fire cannot be ensured solely by means of emergency ventilation. Fire control systems can save human lives and maintain acceptable environment for evacuation of tunnel users. Fire impact mitigation and reduction of heat release rates are essential also for preservation of tunnel facilities. The purpose of this work is to assess fire dynamics in road tunnels taking into account response time of Fire & Rescue Services and to provide rationale for the use of fixed firefighting systems therein as well as for the need of training of Fire & Rescue personnel involved in suppression and rescue operations in these underground sites.

**Keywords:** tunnels, fire dynamics, FFFS

### НЕОБХОДИМОСТ ОТ СТАЦИОНАРНИ ПОЖАРОГАСИТЕЛНИ СИСТЕМИ В ПЪТНИ ТУНЕЛИ

Диана Македонска, Михаил Михайлов

Минно-геоложки университет "Св. Иван Рилски", 1700 София

**РЕЗЮМЕ.** В пътните тунели с голям трафик се очаква предприемането на конкретни аварийни мерки с цел да се предотвратят и ограничат последиците от пътнотранспортни произшествия и други критични събития, свързани с пожари, които могат да застрашат човешкия живот, конструкцията и съоръженията в тунела или да предизвикат замърсяване на околната среда. Известно е, че управлението на риска при възникване на пожар в пътен тунел не се осигурява в необходимата степен само с използване на аварийна вентилация. Системите за контрол на пожари могат да спасят човешкия живот, като запазят ниско ниво на мощността на пожара и поддържат приемлива среда за евакуация на пътниците в тунела. Ограничаването на размера на пожара и на темпа на нарастване на неговата мощност имат значителна полза и за опазване на техническите системи в тунела. Целта на настоящата работа е да се проследи динамиката на пожарите в пътни тунели, като се отчете времето за реакция на службите за ПБЗН и се обоснове необходимостта от използването на стационарни пожарогасителни системи в тях, както и за провеждането на обучение за поддържане и актуализиране на тактическата подготовка на състава от РСПБЗН, осъществяващ пожарогасителна и аварийно-спасителна дейност в тези подземни обекти.

**Ключови думи:** тунели, динамика на пожари, стационарни пожарогасителни системи

### Fire dynamics in road tunnels

Fire dynamics is essential for the design of emergency ventilation mode, fire alarm and fire suppression in tunnels. It is described by the time of growth  $t_g$ , until reaching of stable burning at maximum rate  $t_{max}$ , and time of decay  $t_d$ , associated with fire load of design fires as detailed in Table 1. Fires where no fuel spills are involved could reach high heat release rates as well. For instance, a fully loaded heavyweight vehicle catching fire may reach a heat release rate of 100 MW, albeit in longer growth time (Fig. 1) until reaching the maximum heat release rate HRRmax (Michaylov, Makedonska, 2017).

Table 1. Fire dynamics scenarios

HRRmax [MW]	Duration of fire stages [min]			Fire load [MJ]
	$t_g$	$t_{max}$	$t_d$	
8	5	25	20	18 000
15	5	60	15	63 000
30	5	0	45	50 000
30	10	50	30	125 000
100	10	60	20	450 000
200	10	60	30	960 000

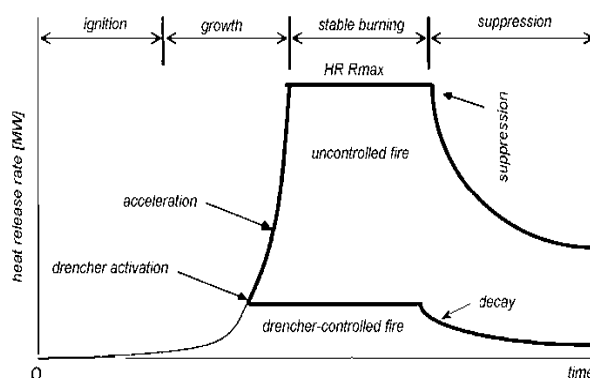


Fig. 1. Fire development stages

There are several methods of calculation of heat release rate of a material. It may be defined by the formula:

$$Q = m'' \Delta H c_{eff} (1 - e^{-k\beta D}) A_{dike} \quad (1)$$

where: Q – heat release rate [kW]

$m''$  – mass fuel burning rate per unit area [kg / m<sup>2</sup>.s]

$\Delta H_{c,eff}$  – effective fuel burning heat [kJ/kg]

$A_f = A_{dike}$  -fire area (area where evaporation occurs) [m<sup>2</sup>]

$k_{\beta}$  – empiric constant [m<sup>-1</sup>]

$D$  – fire diameter (diameter involved in evaporation, assumed to be a circle), [m].

The heat release rate, HRR is a major characteristic of fire dynamics. It predicates generation of undesired effects of the fire and its products which increase as HRR increases. This means that toxic gases, smoke and other fire hazards increase in parallel with heat release rate (table 2).

Comprehensive study of dynamics (HRR in time) of design fires may help prevent human life hazards and property damage.

Table 2. *Burning data of different fuels*

Fuel	$m''$ [kg/m <sup>2</sup> .s]	$\Delta H_{c,eff}$ [kJ/kg]	$k_{\beta}$ [m <sup>-1</sup> ]
Benzene	0.055	43 700	2.1
Kerosene	0.039	43 200	3.5
Diesel	0.045	44 400	2.1
Transformer oil	0.039	46 000	0.7
Crude petroleum	0.0335	42 600	2.8
Lubricant	0.039	46 000	0.7

Tunnel fire risk is evaluated on the basis of representative statistical data about the frequency of road tunnel fires and modelling of consequences of each individual design fire. Design fire development and effects thereof constitute the fire scenario.

It is known that any scenario of design tunnel fire is a unique combination of events and is the result of certain set of circumstances associated with passive and active fire protection measures (Chochev, 2003). Design fire scenario is defined in consideration of the following factors:

- Tunnel geometry (cross sections, gradients, tube connections, evacuation and service workings);
- Type, size, dimensions, and location of ignition source;
- Fuel type in the vehicle;
- Fuel quantity and distribution thereof in vehicle structure;
- Type of combustible material – liquid, solid or gaseous fuel;
- Fire growth rate and time (Fig. 1, Table 1);
- Maximum heat release rate of design fire (HRRmax) – please refer to Table 3 and Fig.1;

Table 3. *Dimensional severity of design fires*

Vehicle type on fire	Maximum fire severity, [MW]	Fire load [GJ]
One car	5	11
2-3 cars	8	18
One van	15	63
One bus or light commercial vehicle	20	50
Heavyweight truck without dangerous load	30	125
Heavyweight truck or cistern with dangerous load	100	450
Cistern with hydrocarbons or trailer	200	960

- Tunnel ventilation system and design fire ventilation mode for the scenario;
- Weather conditions at tunnel inlet and outlet;
- Fire alarm activation – manual and/or automatic;
- Firefighting installations (type, distribution), fire water supply, foamer, and primary extinguishers (Häggkvist, 2009);
- Human intervention for fire suppression and emergency ventilation control.

## Response time of Fire & Rescue Services

Table 4 presents information about tunnels of length > 100 m on the territory of Bulgaria and their specific characteristics: length, distance to the responsible Regional Fire & Rescue Service, and travel time of fire vehicles to each tunnel.

Response time of Fire & Rescue Services is correlated to the time of free fire development which is defined by the equation (Stojanov, 2016):

$$t_{c6} = t_{d,c} + t_{u3} + t_{d6} + t_{\sigma,p} \quad (2)$$

where:

- $t_{d,c}$  – time to fire detection – assumed to be 2-3 [min] for fire alarm installations, and 6 min for manual alarm;
- $t_{u3}$  - departure time of fire vehicle– 1 [min];
- $t_{d6}$  – travel time of fire vehicle to the tunnel (Table 4);
- $t_{\sigma,p}$  – deployment time – from 3 to 5 [min] depending on deployment area, fire location in the tunnel, and type of vehicles and extinguishing agents used.

Fire detection time is essential for the start of evacuation of tunnel users and the response of Fire & Rescue Services. Major characteristics of fire alarm equipment include reliability and accuracy of fire site localisation.

Smoke detectors fail to meet these requirements due to the smoke spreading mode within the tunnel. Smoke spreading may render difficult even for CCTV cameras to detect fire location and follow vehicle travel in dense smoke environment.

In such circumstances, application of thermal cables with semi-conductor maximum-differentiated sensors installed along the entire tunnel length is successful. The distance between addressable sensors may be selected from 7 m to 10 m. Fire detection reliability is achieved by simultaneous reaction of two sensors. The threshold value is set at two alarm levels: maximum- for instance up to 50-600°C, and differential – 30°C/20s. Thus, fire detection time of 120-150 s can be achieved. Thermal-cable- based systems also allow for setting of one pre-alarm level of maximum temperature and of temperature rise rate. Reliability and accuracy of fire localisation render thermal cables particularly suitable for automatic switching of the ventilation system in emergency mode and activation of drencher-type fire suppression system. This is mandatory for tunnels without operative management on site.

In recent years a great deal of research has taken place internationally to ascertain the types of fire which could occur in tunnel and underground spaces. This research has taken

place in real tunnels, in laboratory conditions, and via numerical modelling. As a consequence of the data obtained from these tests, a series of time/temperature curves for the various exposures have been developed as detailed.

**Standard curve** - Standard fire tests to which specimens of constructions are subjected, are based on the use of the

Cellulosic time/temperature curve, as defined in various national standards, e.g. ISO 834, BS 476: part 20, DIN 4102, AS 1530 etc. This curve is based on the burning rate of the materials found in general building materials and contents.

Table 4. Response time of Fire & Rescue

№	REGION	TUNNEL ON ROAD №	Initial kilometer	Tunnel length [m]	Regional F&R Service	Distance b/n Regional FRS and tunnel [km]	Travel time [min]	Time $t_{cb}$ [min]
1	SOFIA	Vitinya RT - Hemus Highway	32+260	1195	Botevgrad	20.50	27.33	33.33
2	SOFIA	Topli Dol RT - Hemus Highway	39+562.30	883	Botevgrad	23.3	31.07	37.07
3	PLOVDIV	RT RELOCATION OF EXISTING ROAD III-868 "DEVIN-MIHALKOVO", tunnel at Lyaskovo Village		880	Devin	16	21.33	27.33
4	SOFIA	Praveshki Hanove RT - Hemus Highway	54+672	834	Pravets	3.4	4.53	10.53
5	SOFIA	Echemishka RT - Hemus Highway	41+904	820	Botevgrad	9	12.00	18.00
6	SOFIA	Trayanovi Vrata RT – Trakia Highway	53+297	685	Ihtman	15.3	20.40	26.40
7	GABROVO	III-5004 "Detour of Gabrovo, Stage Three, Tunnel № 1, size 9/10.5 from km. 12+420 to 13+020	12+420	540	Gabrovo	10	13.33	19.33
8	PERNIK	Golyamo Buchino RT - Lyulin Highway	14+680	490	Pernik	20.5	27.33	33.33
9	SOFIA	Malo Buchino RT - Lyulin Highway	7+712	440	06 Regional FRS	13.3	17.73	23.73
10	SMOLYAN	II-86	97+079	421	Smolyan	5	6.67	12.67
11	LOVECH	II-35 RT at Lovech	43+298	413	Pravets	23	30.67	36.67
12	SOFIA DISTRICT	Kashana RT – Pirdop-Etropole Road		380	Zlatitsa	15	20.00	26.00
13	BLAGOEVGRAD	Zheleznița RT on Road I-1/E-79	370+430	360	Blagoevgrad	13	17.33	23.33
14	KYUSTENDIL	Levski RT - Struma Highway – KocherinovoTown	82+890	350	Rila	15	20.00	26.00
15	PERNIK	Middle RT - Lyulin Highway	10+562	350	Pernik	25.8	34.40	40.40
16	BLAGOEVGRAD	Kresna RT on Road I-1/E-79	388+848	343	Blagoevgrad	30.8	41.07	47.07
17	GABROVO	III-5004 " Detour of Gabrovo, Stage Five, Tunnel № 4, size 9/10.5 28+930 to 29+020 length – 90 m and tunnel № 5, size 9/10.5 from km 29+120 to 29+410	28+930	290	Kazanlak	n.a.		
18	KYUSTENDIL	Struma Highway	56+176	280	Dupnitsa	11	14.67	20.67
19	KYUSTENDIL	RT on Road I-1/E-79 - Dupnitsa	328+100	272	Dupnitsa	4	5.33	11.33
20	GABROVO	III-5004 " Detour of Gabrovo, Stage Five, Tunnel № 3, size 9/10.5 from km. 27+800 to 28+040	27+800	240	Kazanlak	n. a.		
21	PLOVDIV	Konnika RT on Road II-86 Asenovgrad-Bachkovo	32+419	215	Asenovgrad	5.5	7.33	13.33

№	REGION	TUNNEL ON ROAD №	Initial kilometer	Tunnel length [m]	Regional F&R Service	Distance b/n Regional FRS and tunnel [km]	Travel time [min]	Time $t_{cs}$ [min]
22	SMOLYAN	RT on Road III-35 Grohotno – Devin	83+488	178	Devin	10	13.33	19.33
23	VELIKO TARNOVO	RT №1 on Road I-5 Ruse-Veliko Tarnovo, Detour of Valiko Tarnovo	103+524	178	Veliko Tarnovo	3	4.00	10.00
24	PLOVDIV	Martvitsa-4 RT on Road II-86 Asenovgrad-Bachkovo	33+426	165	Asenovgrad	6.5	8.67	14.67
25	GABROVO	III-5004 “ Detour of Gabrovo, Stage Five, Tunnel № 1, size 12/13.5 from km. 22+720	22+720	160	Kazanlak	n. a.		
26	BLAGOEV-GRAD	RT at Ilinden Border Checkpoint on Road II-19 Bulgaria - Greece	106+259	149	Gotse Delchev	20	26.67	32.67
27	VELIKO TARNOVO	RT №2 on Road I-5 Ruse-Veliko Tarnovo, Detour of Valiko Tarnovo	103+814	141	Veliko Tarnovo	3.5	4.67	10.67
28	PLOVDIV	RT on Road III-866 Mihalkovo – Krichim	97+793	132	Stamboliyski	22	29.33	35.33
29	GABROVO	Dyado Nikola RT on Road I-5/E-85 in Gabrovo	150+814	112	Gabrovo	5	6.67	12.67
30	GABROVO	Dryanovski Monastery RT on Road I-5/E-85 between Dryanovo and Gabrovo	133+387	112	Dryanovo	7	9.33	15.33

The temperature development of the Cellulosic fire curve (ISO-834) is described by the following equation:

$$T = 20 + 345 \times \log(8 \times t + 1) \quad (3)$$

**Hydrocarbon curve** - Although the standard curve has been in use for many years, it soon became apparent that the burning rates for certain materials e.g. petrol gas, chemicals etc., were well in excess of the rate at which timber would burn (SOLIT Safety of Life in Tunnels, 2012). As such, there was a need for an alternative exposure for the purpose of carrying out tests on structures and materials used within the petrochemical industry, and thus, the hydrocarbon curve was developed.

The hydrocarbon curve is applicable where small petroleum fires might occur, i.e. car fuel tanks, petrol or oil tankers, certain chemical tankers etc.

The temperature development of the Hydrocarbon (HC) fire curve is described by the following equation:

$$T = 20 + 1080 \times (1 - 0,325 \times e^{-0,167 \times t} - 0,675 \times e^{-2,5 \times t}) \quad (4)$$

**Hydrocarbon Modified curve** - Derived from the above-mentioned Hydrocarbon curve, the French regulation asks for an increased version of that Hydrocarbon curve, the so-called HydroCarbon **Modified** curve (HCM).

The maximum temperature of the HCM curve is 1300°C instead of the 1100°C, standard HC curve.

However, the temperature gradient in the first few minutes of the HCM fire is as severe as all Hydrocarbon based fires (RWS, HCM, HC), possibly causing a temperature shock to the surrounding concrete structure and concrete spalling as a result of it.

The temperature development of the Hydrocarbon Modified (HCM) fire curve is described by the following equation:

$$T = 20 + 1280 \times (1 - 0,325 \times e^{-0,167 \times t} - 0,675 \times e^{-2,5 \times t}) \quad (5)$$

**RABT ZTV curve** (<https://www.promat-tunnel.com>) - The RABT curve was developed in Germany as a result of a series of test programmes such as the Eureka project. In the RABT curve, the temperature rise is very rapid up to 1200°C within 5 minutes. The duration of the 1200°C exposure is shorter than other curves with the temperature drop off starting to occur at 30 minutes for car fires.

**RWS (Rijkswaterstaat) curve** - The RWS curve was developed by the Rijkswaterstaat, Ministry of Transport in the Netherlands. This curve is based on the assumption that in a worst-case scenario, a 50 m<sup>3</sup> fuel, oil or petrol tanker fire with a fire load of 300 MW could occur, lasting up to 120 minutes. The RWS curve was based on the results of testing carried out by TNO in the Netherlands in 1979.

Figure 2 presents comparison of the Standard time/temperature curve ISO 834 and various curves defining tunnel fire development.

The comparison between the response time of Fire & Rescue Services (Table 4) and the fire curves (Figure 2) characterising fire dynamics leads to the conclusion that firefighting in the tunnels under review may only commence after fires have reached maximum heat release rate, i.e. firefighting would proceed at reduced effectiveness and efficacy.

In support of those arguments, results of foreign studies may be pointed out as detailed on Figure 2.

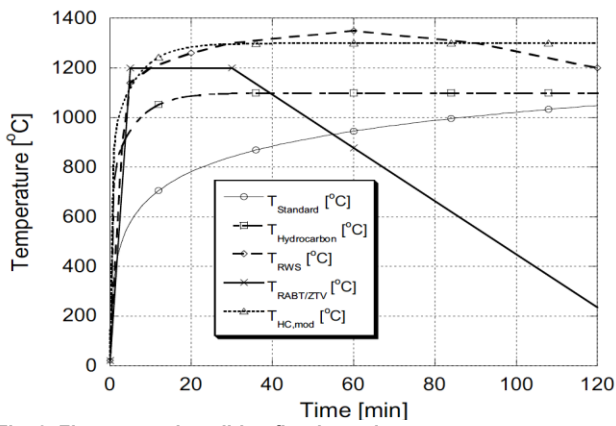


**Fig. 2. Fire curves describing fire dynamics**

$T_{Standard}$  – standard time/temperature (cellulosic) curve;  
 $T_{Hydrocarbon}$  – hydrocarbon curve in North European countries;  
 $T_{RWS}$  – time/temperature curve used in Dutch regulations;  
 $T_{RABT/ZTV}$  – curve according to the German Directive on tunnel equipment and operation;

The issue under review is further aggravated by the fact that, in the event of fire, the tunnel ventilation will be increased to ensure safe evacuation of those present in the tunnel thus increasing fire severity.

Figure 3 provides graphic illustration of the data presented in Table 4 demonstrating that, in 29% of tunnels in Bulgaria, Fire & Rescue teams would start firefighting up to the 15<sup>th</sup> minute after receipt of fire notification. In the remaining 71% tunnels located in the country, firefighting would start after the 15<sup>th</sup> minute from receipt of fire notification when fires would have reached maximum severity.

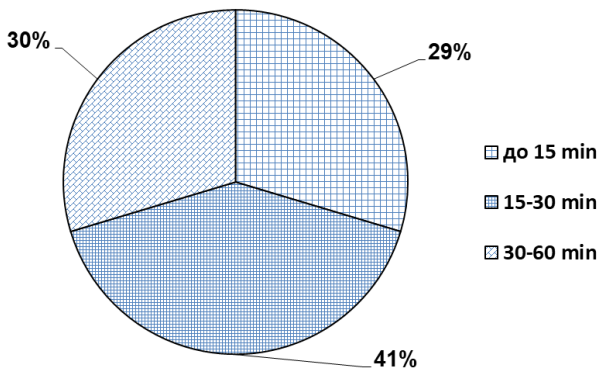


**Fig. 3. Response time of Fire & Rescue Services in the event of tunnel fire**

The aforementioned circumstances call for tunnel protection by a water-based fixed firefighting system or other suitable means for creating a favourable environment for safe evacuation and access to emergency help. Such need is supported by the short time of fire growth (Fig. 2), after which suppression becomes more difficult because it is impossible for firefighting personnel to sufficiently approach the burning area. The situation is further aggravated by the increase of ventilation flowrate to enable safe escape of tunnel users. This impacts fire rate  $m^3$  in (1) and fire severity.

Response and travel times of fire vehicles (Table 4), for almost all tunnels, is much greater than the growth time for most tunnel fires (Fig. 2).

The main hazard is for the fire to spread to adjacent vehicles (Liu et al., 2007). The fixed firefighting system, in the worst-case scenario, will keep the fire at very low energy level (HRR on Fig. 1) and will facilitate evacuation and suppression. After consideration of all impacting factors, at this stage installation of such systems may be recommended in:

- longer tunnels with heavy traffic and long escape routes;
- tunnels with two-directional traffic equipped with longitudinal ventilation systems and long escape routes;
- tunnels associated with too long response time of Fire & Rescue Services.

With reference to the specifics of road tunnel fire occurrence and growth, regular training and upgrade of firefighting skills is necessary for fire and rescue teams operating in underground facilities.

Training should be organised and held in two major directions: theoretical training and practical training.

Theoretical training should include specifics of fire suppression in road tunnels, core principles and methods of training and practical application thereof.

Practical training should aim at acquiring knowledge and skills that are necessary for proper assessment of fire situation, selection of the most appropriate firefighting agents and skilful management of firefighting personnel and means.

Training should employ all possible organisational methods and forms of tactical approach to firefighting.

Response time to beginning of active fire suppression by Fire & Rescue Services should have higher weight in risk assessment.

Emergency ventilation includes two functional and modal stages:

- ⇒ Stage 1 – includes the first 15 min after fire occurrence. During this initial period “self-rescue” and evacuation of tunnel users is of the utmost importance. Evacuees must be protected, by means of ventilation manoeuvres, from smoke exposure – toxic gases, reduced visibility and high temperature. In such cases, ventilation system operation may be controlled automatically to ensure fast response;
- ⇒ Stage 2 – ventilation assists fire suppression via effective suction of smoke from fire area or via unilateral smoke exhaustion from the fire area. At stage 2, ventilation control should be coordinated with rescue personnel involved in fire suppression.

## Conclusion

Given the fire dynamics in road tunnels and response time of Fire & Rescue Services in the Republic of Bulgaria, installation may be recommended of fixed firefighting systems in tunnels to keep low energy level of the fire and facilitate evacuation and fire suppression.

After consideration of all impacting factors, at this stage **installation of such systems** may be recommended in:

- ⇒ unidirectional road tunnels of length exceeding 900 meters;

- ⇒ tunnels with two-directional traffic and length exceeding 600 meters, and
- ⇒ tunnels with lengthy escape routes due to the absence of connection workings therein.

Fixed firefighting systems can control fires, preserve tunnel structure and prevent linear spread of tunnel fire.

## References

- Chochev, V. 2003. *Operativna taktika za gasene na pozhari*. Ognoborec, Sofia, 244 p. (in Bulgarian)
- Dimitrov, V. 2017. *Doklad otnosno sastoyaniето na tunelite po RPM*. Sofia, MRRB (in Bulgarian).
- Directive 2004/54/EC of the European parliament and of the council, EU, 2004.
- Häggkvist, A. 2009. Fixed Fire Fighting Systems in Road Tunnels, 70.
- Liu, Z. G., A. Kashef, G. Lougheed, A. K. Kim. 2007. Challenges for use of fixed fire suppression systems in road tunnel fire protection. – *A Technical Working Conference (SUPDET 2007)*, Orlando, Florida, March 5-8, 2007, 1–10.
- Michaylov, M. 2017. *Sastoyaniето na patnite tuneli v Bulgaria, problemite i perspektivite za tyahnoto osavremenyavane*. Round Table, NTS Sofia (in Bulgarian).
- Michaylov M., D. Makedonska. 2017. Namalyavane na požarniya risk v patni tuneli. – *VIII Nauchna konferentsiya s mejdunarodno uchastie "Grazhdanska besopasnost"*, 168–176 (in Bulgarian).
- Naredba №RD-02-20-2 ot 21.12.2015 za tehniчески pravila i normi za proektirane na patni tuneli, DV, br. 8 ot 29.I.2016 (in Bulgarian)
- Naredba №1 ot 4 April 2007 za minimalnite iziskvaniya za bezopasnost v tuneli po republikanskite patishta, koito savpadat s transevropеyskata patna mrezhа na teritoriyata na Republika Bulgaria, zagl. dop. DV, br. 58 ot 2007, zagl. izm. – DV, br. 102 ot 2008 (in Bulgarian).
- SOLIT Safety of Life in Tunnels. 2012. Engineering guidance for a comprehensive evaluation of tunnels with fixed firefighting systems, 32 p.
- Stoyanov, D. 2016. *Pozharna bezopasnost v tuneli*. Flpus, Sofia, 222 p. (in Bulgarian)
- <https://www.promat-tunnel.com>. Fire curves.

## EXPERIENCE OF DIMENSION STONE EXTRACTION BY QUARRY CUTTING MACHINE IN POKOSTOVSKY DEPOSIT, UKRAINE

**Vasyl Mamray, Valentyn Korobiichuk, Volodymyr Shlapak**

*Zhytomyr State Technological University, 10005 Zhytomyr; mamrayv@ukr.net*

**ABSTRACT.** Modern technology for the extraction of dimension stone in Ukraine involves mining operations with high bench up to 6 m. The separation of a monolith from the massif is carried out mainly by diamond-wire cutting. This technology involves the throwing of the monolith onto a pillow of crushed stone, which causes additional losses and use of special equipment for the dumping of monoliths. Today, diamond-wire cutting machines are replaced by disk saw cutting machines. That is why in this paper the working parameters and technological methods of disk saw cutting machines operations are considered. The analysis of dimension stone extraction technologies has been made showing that the disk saw extraction technology of hard natural stone makes it possible to reduce natural stone waste by 30–40 %. This technology increases the productivity of natural stone blocks extraction up to 1.12 times due to the increased productivity of cutting planes; reduces the cost of blocks extraction by using cheaper diamond disk saws in comparison with diamond wire; improves productivity by reducing time for natural stone blocks sorting and shaping.

**Keywords:** extraction, dimension stone, technological methods

### ОПИТЪТ ПРИ ДОБИВ НА ОБЛИЦОВЪЧНИ КАМЪНИ ЧРЕЗ КАМЕНОРЕЗНИ МАШИНИ В НАХОДИЩЕ "ПОКОСТОВСКИ", УКРАЙНА

**Васил Мамрей, Валентин Коробийчук, Володимир Шлапак**

*Житомирски държавен технологичен университет, 10005 Житомир*

**РЕЗЮМЕ.** Съвременната технология за добиване на облицовъчен камък в Украйна включва добивни работи със стъпала до 6 m. Разделянето на монолитни блокове от масива се извършва главно чрез рязане с диамантено въже. Тази технология включва хвърляне на монолитния блок върху възглавница от натрошен камък, което води до допълнителни загуби и използване на специално оборудване за хвърляне на монолитните блокове. Днес, режещите машини с диамантени въжета са заменени от дисково фрезни каменорезни машини. Ето защо в тази статия са разгледани работните параметри и технологичните методи за работа на циркулярни каменорезни машини. Направен е анализ на технологиите за добив на облицовъчни камъни, който показва, че технологията за добив на твърд естествен камък с циркуляр позволява намаляване на загубите на естествен камък с 30-40%. Тази технология увеличава производителността при добив на блокове от естествен камък до 1,12 пъти поради повишената производителност на режещите повърхнини; намаляване на разходите за добив на блокове чрез използване на по-евтини диамантени циркуляри в сравнение с диамантеното въже; подобряване на производителността чрез намаляване на времето за сортиране и оформяне на блоковете от естествен камък.

**Ключови думи:** добив, облицовъчен камък, технологични методи

### Introduction

The stone industry around the world records significant volumes of stone production (about 35 million tons per year). China is currently occupying the leading position, followed by Italy, Turkey, India, Brazil, Spain and Greece. Ukraine holds the seventh place in the world by the number of granite quarries. Together with other building materials, the extraction of natural stone has a significant impact on the environment. The extraction of raw materials from the earth's surface leads to a change in the landscape, vegetation and fauna, and the relief of the territory. For these reasons, quantitative assessment and management of the relevant environmental impacts is becoming more and more important. Thus, the European Commission, with the support of experts from both academia and industry, is currently implementing a revision of the EU criteria for the environmental label of hard coverings (which include building materials from cement, concrete,

ceramic and clay materials, and also natural and engineering stones), (EU-European Commission, 2010).

The output of blocks after the extraction of natural stone is 25-40% of the rock mass. The main factor that influences the output of natural stone blocks (Sobolevskiy et al., 2016) is natural and man-made fracturing. The second factor is the direction of extraction in relation to the direction of cracks. Quantitative operational losses in the extraction of decorative stone blocks are insignificant, usually up to 10%, and qualitative losses (colour change, development of microcracks) of stone reach considerable volumes. At the beginning of the last century, the extraction of natural stone used a blasting method, which led to significant losses of raw materials, both qualitative and quantitative. In some dimension stone deposits the explosive mining technology reduced the output of blocks to 50%. In recent years, the diamond wire cutting technology has become widespread in granite quarries (Levytskyi, Sobolevskiy, Korobiichuk, 2018; Korobiichuk et al., 2016; Ozcelik, Yilmazkaya, 2011; Yurdakul, Hürriyet, 2012; Ersoy, Atıcı, 2004; Yurdakul, 2015).

The use of mechanical cutting methods has led to reduction of technological losses of natural stone. That is why, the improvement of the mechanical technology of extraction is a substantial scientific and applied problem. Until now, disk saws were used for the extraction of soft rocks - tuffs, limestone and so on. In China, disk machines for the extraction of hard and medium-hard rocks have been developed and manufactured. The technology of natural stone extraction by using disk machines has become widespread in Chinese granite deposits. It should be noted that most of the Chinese granite deposits have rocks with higher porosity and less compressive strength than Ukrainian ones. Due to the difference in physical and mechanical properties of the rocks, it is necessary to adapt this technology to Ukrainian deposits.

### The main exposition

The main technology for natural stone extraction for Ukrainian granite deposits involves the use of diamond wire cutting machines and drilling rigs. Extraction is carried out according to a two-stage separation system of natural stone blocks (Fig. 1).

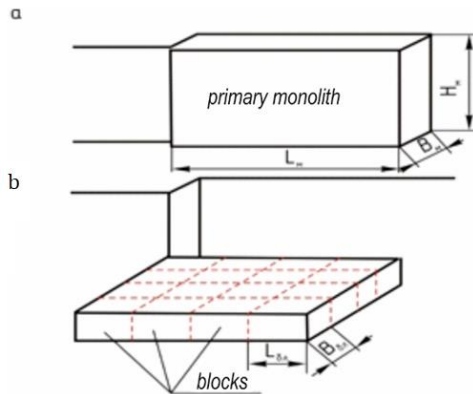


Fig. 1. Two-stage system of separation with fallen down of the primary monolith: a – separation of the primary monolith; b – separation of fallen down primary monolith into blocks

To join together the ends of the diamond wire, two opposite holes are drilled so that they converge at one point (Fig. 2). In this case, drilling can occur in a horizontal and a vertical plane when cutting in a vertical plane or two wells in a horizontal plane when cutting in a horizontal plane.

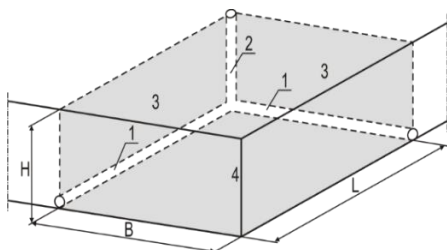


Fig. 2. Scheme of drilling converged holes: L – length of the monolith; B – width of monolith; H – monolith height; 1 – horizontal hole; 2 – vertical hole; 3 – vertical cutting plane; 4 – horizontal cutting plane

In the primary monolith, firstly the horizontal plane is cut and then the vertical one (Fig. 3, a). Secondly, the vertical side of the monolith with the largest area is cut, and in the last

turn the vertical side with the smallest area. After that, the monolith is thrown onto a pillow of crushed stone. At a height of a monolith from 5 to 6 m, there are losses of natural stone during falling of the monolith due to the decomposition of the monolith into smaller pieces.

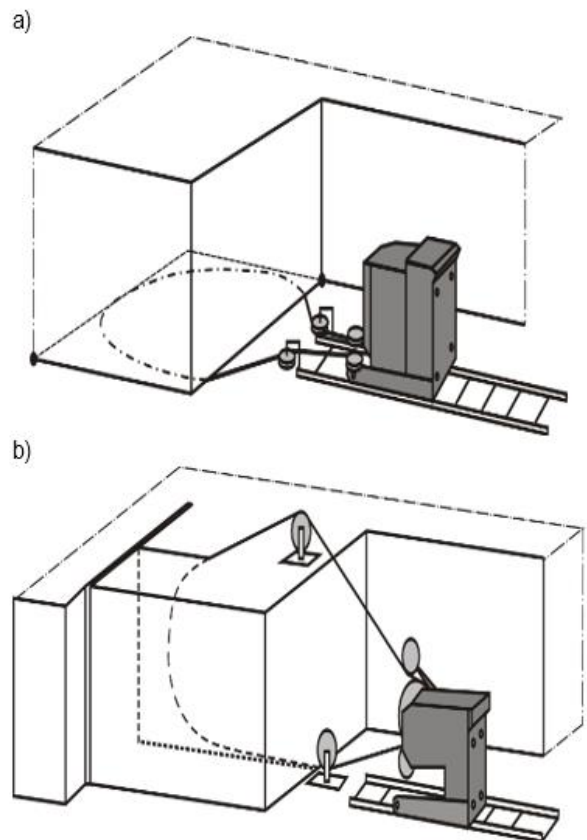


Fig. 3. Scheme of cutting by diamond wire machine: a – horizontal cutting, b – vertical cutting

The use of disk saws involves mining operations with height of the bench of about 1.2 m. The most optimal (minimum) parameters of the monolith for the estimation of technology is a monolith with a length of 10 - 16.0 m and a width of 3 m at its height of 1.2 m. The volume of such a monolith is 36-57.6 m<sup>3</sup>.

The technology for separating monoliths includes the following operations:

- 1) formation of two vertical separating planes (droplet knife) 1.2 m deep along the front of the work - 15.0 m at a distance of 3 m apart with using a saw cutting machine with a disk Ø 2.6 m, followed by cutting with a saw with a diameter of 3.5 m;
- 2) drilling of vertical holes Ø 32.0-50.0 mm along the edge points (corner) of the monolith by a perforator for cutting sharp corners;
- 3) insertion of a diamond wire into a slit along the perimeter of the base of the monolith for cutting the sole;
- 4) wedges hammering in the formed plane, so that the monolith does not catch the diamond wire;
- 5) formation of a horizontal plane in the base of the monolith using the diamond wire cutting machine (cutting the base);
- 5) formation of vertical holes Ø 32.0 mm with a distance between the centres of holes 15.0-20.0 cm to the width of the monolith along the line of planned cutting by a drilling machine.

6) direct separation of the monolith to blocks by means of metal wedges or a hydromachine.



Fig. 4. Implementation of the technology of cutting by disk saw machine at Pokostovsky granite deposit (Ukraine)

The technology of extraction of natural stone blocks by using the disk saw machine in China involves the drilling of horizontal holes for separating the blocks. The application of the bore-wedges technology to create a horizontal plane at Pokostovsky deposit has caused significant loss of natural stone and has complicated the technology for separating the monolith from the massif. Therefore, for the formation of a horizontal plane, a diamond wire has been used (Fig. 5).

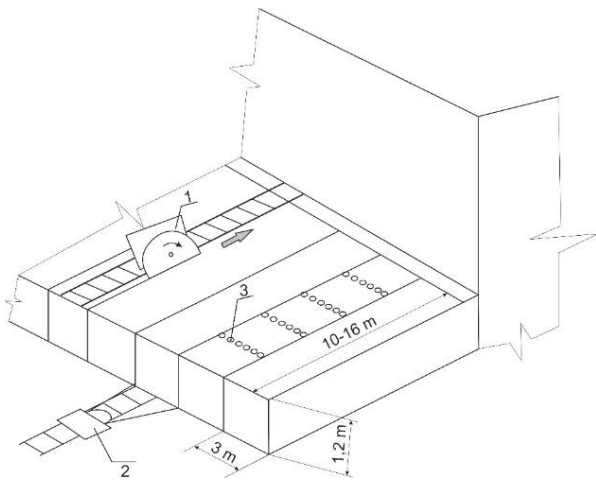


Fig. 5. Scheme of the natural stone block extraction using a disk saw machine: 1 – disk saw machine; 2 – diamond wire machine; 3 – holes

By using a disk saw machine in cracked massif the bottom plane of the monolith is separated by a bore-wedge method. The disk saw machines require a liquid for cooling the diamond saw in a quantity of 140 l/min. It complicates the work of the disk machine when opening a quarry. During this period, there is no debit of natural water in the quarry.

For a disk saw machine, an important factor is the length of the front of the work. The longer the cutting length of the disk saw, the higher the performance of the disk saw machine is. When the front of the work increases from 5 to 60 m, the productivity increases up to 2.8 times (Fig. 6).

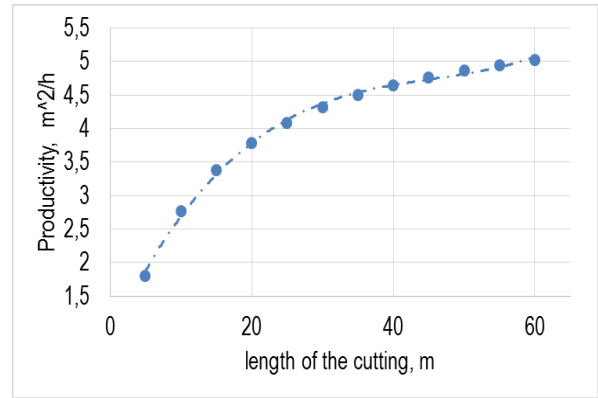


Fig. 6. Dependence of the productivity of the disk saw machine at Pokostovsky deposit on the length of the cutting

Under this technology, the loss of natural stone when cutting the base of monolith with a diamond wire technology is less than 10 times due to the absence of drilling operations (boreholes for wire laying). The absence of drilling works increases the productivity of the diamond wire by 27% compared to the existing technology (Fig. 7).

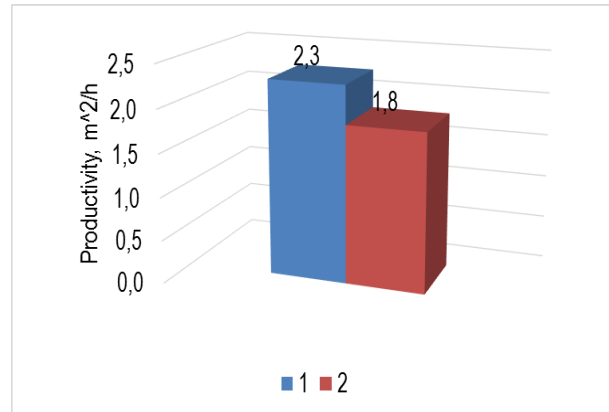


Fig. 7. Productivity of a diamond wire machine at Pokostovsky deposit 1 – technology of natural stone extraction by disk saw machine; 2 – technology of natural stone extraction by diamond wire machine

In general, the disk saw extraction technology (when working on one disk machine) has a higher productivity 12% compared to the existing technology (Fig. 8).

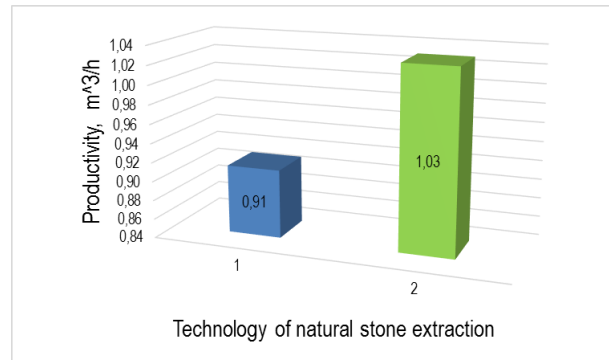
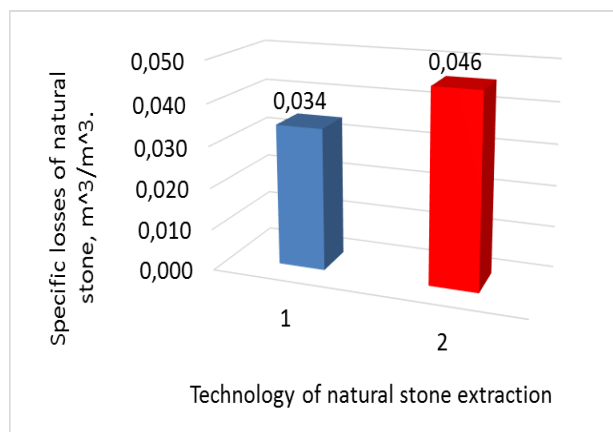


Fig. 8. Productivity of blocks extraction at Pokostovsky deposit 1 – technology of natural stone extraction by diamond wire machine; 2 – technology of natural stone extraction by disk saw machine.

The disk saw technology has quantitative losses of granite of 35% less than with existing technology. This is due to the lack of drilling operations for the diamond wire laying (Fig. 9).



**Fig. 9. Specific losses of natural stone at Pokostovsky deposit: 1 – technology of natural stone extraction by diamond wire machine; 2 – technology of natural stone extraction by disk saw machine**

However, for the effective extraction by disk saw machine, a large area of extraction is required. This extraction technology limits the height of the blocks to 1.2 m. Also, when using disc saw machines it is difficult to take into account the fracture of the massif and inclusions of natural defects. Cracks can reduce the output of blocks from the massif.

## Conclusion

The natural stone extraction technology by using disk saw machines requires a large area of the bench surface. Therefore, the application of this technology in small quarries with height of the bench of 6 m is complicated. This technology limits the height of blocks of natural stone to 1.2 m. However, this technology of extraction has a high productivity and allows the production of blocks with flat surfaces. The natural stone extraction technology with disk saw machines

has higher productivity and lower specific losses of natural stone than the diamond wire technology.

## References

- Ersoy, A., U. Atıcı. 2004. Performance characteristics of circular diamond saws in cutting different types of rocks. – *Diamond and Related Materials*, 13, 1, 22–37.
- EU-European Commission. 2010. *International reference life cycle data system (ILCD) handbook. General guide for life cycle assessment. Detailed guidance*, Institute for Environment and Sustainability.
- Korobiichuk et al. 2016. Peculiarities of natural stone extraction technology with the help of diamond wire machines. – *International Multidisciplinary Scientific GeoConference: Surveying Geology & Mining Ecology Management*, 649–656.
- Levytskyi, V., R. Sobolevskiy, V. Korobiichuk. 2018. The optimisation of technological mining parameters in quarry for dimension stone blocks quality improvement based on photogrammetric techniques of measurement. – *Rudarsko-geološko-naftni zbornik*, 33, 2, 83–89.
- Ozcelik, Y., E. Yilmazkaya. 2011. The effect of the rock anisotropy on the efficiency of diamond wire cutting machines. – *International Journal of Rock Mechanics and Mining Sciences*, 48, 4, 626–636.
- Sobolevskiy, R. et al. 2016. Cluster analysis of fracturing in the deposits of decorative stone for the optimisation of the process of quality control of block raw material. – *Vostochno-Evropeyskiy zhurnal peredovih tehnology*, 5, 3, 21–29.
- Yurdakul, M., A. Hürriyet. 2012. Prediction of specific cutting energy for large diameter circular saws during natural stone cutting. – *International Journal of Rock Mechanics and Mining Sciences*, 53, 38–44.
- Yurdakul, M. 2015. Effect of cutting parameters on consumed power in industrial granite cutting processes performed with the multi-disc block cutter. – *International Journal of Rock Mechanics and Mining Sciences*, 76, 104–111.

## NEW INSIGHTS INTO THE IMPACT OF BLAST WAVES ON THE HUMAN BODY

Zdravka Mollova

University of Mining and Geology "St. Ivan Rilski", 1700 Sofia; mollova.zdravka@gmail.com

**ABSTRACT.** Blast damage is a major problem in both military and civilian practice. For effective protection, we need an assessment of the forces and threats that act on a person exposed to an explosion. In general, the victim can be exposed to rapid changes in pressure (shock wave), fragments and debris (pieces) and bodily displacement, resulting in internal injuries and shear effects. The scale, frequency and clinical significance of the different types of injury depends on the nature of the environment (e.g. open or closed), the type of the explosive device, the protection worn by the victim (which can provide greater protection against one aspect of the threat) and the distance from the explosion. This article presents blast wave effects in predicting blast damage through computer modelling of impact. The results obtained are important for improving the explosion protection.

**Keywords:** shock wave, explosive, blast trauma, detonation

### НОВИ ВИЖДЕНИЯ ЗА ВЛИЯНИЕТО НА ВЗРИВНАТА ВЪЛНА ВЪРХУ ЧОВЕШКИЯ ОРГАНИЗЪМ

Zdravka Mollova

Минно-геоложки университет "Св. Иван Рилски", 1700 София

**РЕЗЮМЕ.** Взривните поражения са все по-голям проблем, както във военната, така и в гражданската практика. За ефективна защита се нуждаем от оценка на силите и заплахите, които действат върху лице, изложено на експлозия. Най-общо, жертвата може да бъде изложена на резки промени в налягането (ударна вълна), фрагменти и отломки (парчета) и изтласкване на тялото, което води до вътрешни наранявания и ефекти на срязване. Машабът, честотата и клиничното значение на различните видове наранявания зависят от околната среда (например отворена или затворена), вида на взривното устройство, защитата, носена от жертвата (която може да осигури по-голяма защита срещу един аспект на заплахата) и разстоянието до взрива. Тази статия представя ефектите от взривната вълна при прогнозиране на щети от взрив чрез компютърно моделиране на въздействието. Получените резултати са важни за подобряване на защитата от експлозия.

**Ключови думи:** ударна вълна, експлозив, взривна травма, детонация

### Introduction

In recent years, explosive devices have become the preferred weapon in the majority of terrorist attacks in war zones and other regions of political conflict worldwide. Relative ease of manufacturing and portability of Improvised Explosive Devices (IEDs) make them the weapon of choice in terrorist and insurgent activities.

Injuries that result from a blast are dependent on many factors, including the type of explosive and explosive charge, height of burst, reflecting boundaries or protective barriers, distance between the victim and the blast, the surrounding environment, and the scattering of fragments or other projectiles. The physical environment in which an explosion occurs plays a significant role in the type and degree of injury that may result. Blasts that occur in an enclosed space (e.g. a closed room, a bus, or a subway car) can intensify the effect of the blast wave, resulting in more severe injury patterns than those that occur in open air (e.g. a square, an open market, a train platform). In addition, explosive events associated with building collapse result in higher mortality and morbidity.

### Blast Wave Dynamics and Forces

An explosion is caused by the rapid exothermic oxidation of a solid or liquid material into gaseous reaction products resulting in a large energy release in the form of increased pressure and temperature within the explosive compound.

Blast waves can be generally classified as simple or complex. The detonation of a typical high explosive in an open space produces a simple, or so-called Friedlander wave, the name comes from the simple equation used to describe the pressure history. The front of the wave, known as the shock front, has a pressure (overpressure) much greater than the region behind it and thus, immediately begins to decay as the shock propagates outward. The pressure may drop to below ambient atmospheric pressure causing suction. A simple blast wave has an overpressure phase called the positive phase and an underpressure phase known as the negative phase with an assumed exponential form as shown in Figure 1.

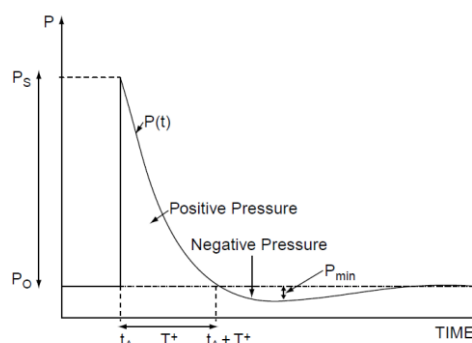


**Fig. 1. Simple blast wave showing peak overpressure and the durations of the positive and negative phases**

Different authors have recommended the use of various functions to represent the pressure-time history  $p(t)$  of the simple blast wave, generally emphasising only the positive phase. A complete function representing the entire positive and negative phase is described by (Dharaneepathy, 1995) by the following:

$$p(t) = p_0 + p_s \left[ 1 - \frac{(t-t_a)}{T_s} \right] \cdot \exp \left[ -b \frac{(t-t_a)}{T_s} \right], \quad (1)$$

where:

- $t$  is the time measured from the instant the shock wave arrives,
- $p_0$  is the ambient atmospheric pressure,
- $p_s$  is the peak overpressure,
- $T_s$  is the duration of the positive phase,
- $t_a$  is the wave arrival time,
- $b$  is a positive constant called the waveform parameter that depends on the peak overpressure.

The most commonly used blast wave scaling is the cube root scaling law, otherwise known as Hopkinson's Law (Baker, 1973). This law states that any pressure generated at a distance  $R_1$  from a reference explosion with weight  $W_1$  will generate the same pressure at a distance  $R_2$  from the same explosive with weight  $W_2$  provided the charges are of similar geometry and in the same atmosphere.

$$\frac{R_2}{R_1} = \left( \frac{W_2}{W_1} \right)^{\frac{1}{3}} = \lambda \quad (2)$$

The parameter  $\lambda$  is referred to as the explosive yield factor. It is customary to use the scaled distance,  $Z$  ( $m/kg^{1/3}$ ), rather than charge distance when dealing with blast waves:

$$Z = \frac{R}{\sqrt[3]{W}} \quad (3)$$

A complex blast wave is typically the result of wave reflections and refractions resulting from interactions with the local environment (e.g. a wall or enclosure). As an explosive charge is detonated the high pressure wave travels outwards from the center of initiation. The high pressure, high speed wave makes contact with everything in its path. The contact between the wave and objects in its path will result in reflections, rarefactions and attenuations of the blast wave. (Katz, 1998). Therefore, the resulting flow field of the blast is not accurately represented by the Friedlander idealised blast wave when an interaction with objects occurs. The exact waveform cannot be determined empirically as it depends on the geometry of the objects in the environment. In order to determine the wave field in a complex environment, a numerical simulation or an experimental simulation is required to obtain the pressure at desired locations.

A charge placed above a flat reflecting surface, such as the ground will produce a complex blast wave. The distance at which the charge is placed above the ground is known as the height of burst (HOB). A diagram of this example is shown in Figure 2.

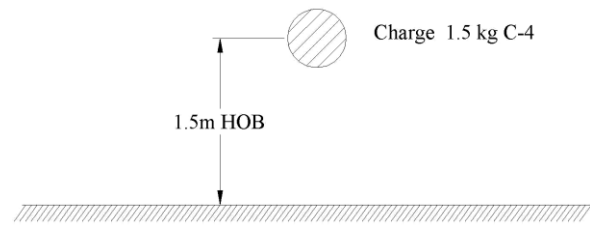


Fig. 2. Bare spherical charge above ground (Cronin, 2004)

In this scenario the explosive is initiated and the blast wave radiates outwards. When the blast wave travels a distance equivalent to the height of burst it makes contact with the ground. As the ground is infinitely rigid, the wave reflects off of the ground and travels back into the initial blast wave. Using a pressure gauge it is possible to measure the interaction between the waves. In this example if a gauge is located directly above the center of the charge, the resulting pressure versus time plot will indicate the initial primary blast wave, followed by the presence of a secondary pressure peak, which represents the reflected blast wave from the ground. The formation of these waves is shown in Figure 3. A characteristic of complex blast wave is the presence of stepped waves, indicating rise and drops in pressure, due to reflections and rarefactions. This is in contrast to the idealised wave, which only includes one peak pressure waveform. The pressure history of the complex waveform shows the initial incident waveform that would be visible in the free field, followed by the waveforms from the reflecting surfaces. In this example there is only one reflecting surface, however, where more reflecting surfaces are present the resulting waveform will depend on the geometry of the reflecting surfaces. The change in geometry will affect both the magnitude and timing of the blast waves.

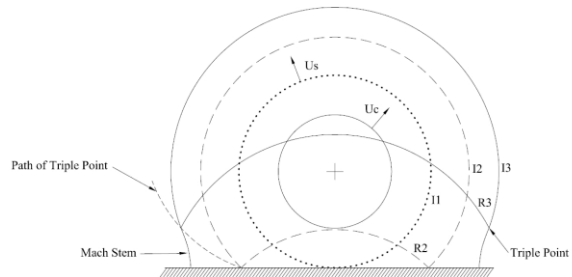


Fig. 3. Complex blast wave formed from ground interaction (Cronin, 2004)

Blast waves can be reflected off a variety of surfaces, including walls, floors and ceilings. As the blast wave impacts the surface the reflected waves' strength is related to the angle of contact with the surface; low angles produce lower strength reflection pressures, whereas perpendicular angles produce very high reflected pressures. The strongest reflected wave occurs when the high pressure wave impacts perpendicular to the surface. At this point the blast wave is further compressed on impact and a reflecting wave begins to travel towards the incident wave. The region where this occurs is known as the reflected region. It contains a very high pressurised zone as compared to a region where no reflection has occurred. The shock wave in this single reflected region can end up being 2 to 20 times greater than the incident shock. (Wightman, 2001) Stronger and more complicated shocks are produced in

enclosed spaces or when the shock makes contact with multiple reflecting surfaces. In enclosed spaces the blast wave may undergo repeated reflections from the interior walls and any objects in the space.

A complex blast wave in an enclosure will lead to a longer pressure-time history as compared to a blast in the free field. The longer pressure time histories enable the gases to heat and expand, filling the enclosure and then eventually venting through any openings. One of the simplest scenarios that produces complex blast waves is the detonation of an explosive in an enclosed room. Even with the simple geometry and a charge placed in the centre of the room the resulting blast waves are complex and require CFD simulations to predict the blast flow field (Stuhmiller, 1997).

Figure 4 displays a plot of three pressure signatures. In Figure 4a, an idealised Friedlander curve is shown. Figure 4b shows the pressure time history record from an actual gauge in an experimental trial. This results show similarity to the Friedlander curve, as can be seen by the near instantaneous rise in pressure, the decay to ambient and the negative duration phase. Noise and other artifacts are clearly visible as the plot is not smooth. These slight variations in the plot can be due to vibrations or the effect of placing a physical gauge in the flow field. Figure 4c shows a plot from an actual complex blast wave. This plot consists of an initial pressure and decay wave followed by a number of secondary peaks and decays. The secondary waves are a result of the interactions between the initial wave and its surroundings. Reflections, rarefactions, coalescing and attenuation of waves are all factors in the pressure signature of the complex wave; the signature shown is from a blast wave inside a military bunker (Josey, 2010).

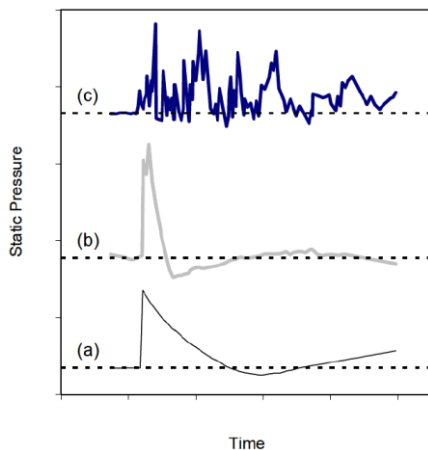


Fig. 4. Blast wave comparisons: (a) idealised blast wave; (b) actual blast wave recorded via a pressure transducer; (c) complex blast wave (Mayorga, 1997)

Enclosed spaces allow the generation of complex blast waves. The reflection of waves from walls, ceilings and floors in enclosed environments enables the development of complex waves with long durations. In terms of blast injury, this allows for a greater transfer of energy to the body. This greater transfer of energy as compared to an idealised blast wave leads to increased bodily injury (Chaloner, 2005).

#### Blast Wave Interaction with Objects and the Human Body

When a blast wave encounters an object of higher density, such as ground or a human body, it will both reflect off the

object and diffract around it. The reflected wave travels back toward the origin and the overpressure of the reflected wave may exceed the overpressure of the incident wave. The magnitude of the reflected pressure is related to both the angle of incidence of the blast wave and to the incident shock strength. The incident wave will also penetrate the object and generate compression and shear stress waves within the object. The exact behaviour depends upon the geometry of the object, the angle of incidence, and the power of the wave. When explosions occur indoors or in street canyons, standing waves and enhanced differences in pressure occur because of the additive effects of reflections from walls and rigid objects (Liang et al., 2002). Figure 5 presents a scheme of an incident shock wave interacting with a body, illustrating the propagating shock wave, shock reflection and diffraction, and stress wave transmitted through the body.

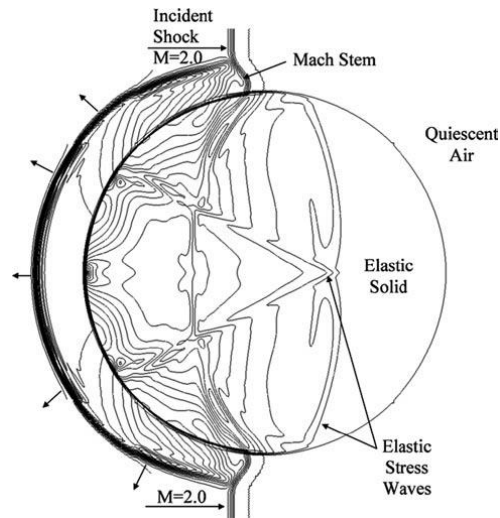


Fig. 5. An example CFD simulations of a planar shock wave diffracting over an elastic cylinder showing pressure contours at a time instant when shock has just passed over the body

In this case, the sound speed in the elastic solid is larger than the shock wave speed in the air and the elastic stress waves inside the body, shown in Figure 5, propagate ahead of the shock wave. The pressure field and the shock wave pattern are shown, including the incident wave, reflected wave, and diffracted waves (Mach stem) around the body, at a time instant when the shock wave passes across the centre of the body.

Shock wave reflections from objects can be either normal, when the wall-shock normal are at a zero angle, or oblique, when the angle of incidence is small, less than about 40° in air. When a blast wave strikes an object it will generate a pressure on the surface of the object that is greater than the peak static pressure of the wave. Intuitively this can be explained by the fact that the forward moving air molecules are stopped at the wall while the molecules behind will still compress the ones on the stopped wave front. Mathematically it can be expressed that, for the normal reflection of an ideal gas from a rigid wall, the total pressure on the object wall (the peak reflected pressure,  $p_r$ ) is the sum of the static pressure,  $p_s$  and the dynamic pressure  $q = \rho v^2 / 2$ :

$$p_r = 2 p_s + (\gamma - 1)q, \quad (4)$$

where  $\gamma$  is the ratio of specific heats ( $\gamma = 1.4$  for ideal gas). Using Rankine-Hugoniot relations (Baker, 1974; Smith, Hetherington, 1994) relating mass, momentum, and energy of the incoming wave before the impact and at the wave reflection instant one can eliminate  $q$  and relate the reflected pressure to the peak overpressure and the ambient pressure:

$$p_r = 2 p_s ((7p_0 + 4p_s) (7p_0 + p_s)) \quad (5)$$

For an object such as a human body, the blast wave reflected pressure ( $p_r$ ) load on the front (proximal) side for a short period of time will be much larger than the peak overpressure,  $p_s$ . The side walls, parallel to the shock propagation direction, will be loaded as the wave passes over them with the  $p_s$ . Therefore, the time for loading can be calculated from the blast wave velocity. The rear side loading begins after the blast wave passes the object and after the diffractive waves meet at the centre back side. In addition to the pressure loading, the object will also experience friction drag forces,  $F_D$ , induced by the blast wind:

$$F_D = C_D \cdot q(t) \cdot A, \quad (6)$$

where  $q(t)$  is the dynamic pressure ( $q = \rho v(t)^2 / 2$ ) of the wind,  $A$  is the friction wall area loaded, and  $C_D$  is the drag coefficient of the object, which depends on its shape. The drag force will appear after the pressure force and its duration will be longer. Therefore, the total transverse force on an object is a sum of the forces caused by the reflected pressure and drag force.

This cursory analysis of shock wave patterns and the reflected pressure levels,  $p_r$ , indicate that blast waves are far more lethal near reflecting surfaces. A person next to a solid wall will be exposed to not only the forward shock wave but also to even stronger reflected waves. Blast injuries in a confined space are particularly severe as the person is exposed to multiple reflected waves coming from various directions. Blast loads on large rigid objects will create strong crushing forces but cause little or no object translocation. Smaller objects, such as explosive casing, debris, and even human beings, will be propelled in the air by pressure and blast wind loading. The translational force will last for a brief time but the drag loading will have a longer duration and can lead to significant body translocation in addition to the overpressure damage.

When a shock wave impacts a living body, a series of instantaneous physical events take place. The body is affected by the primary incident wave, by the wave reflected at the body surface and by the diffracted waves on the side and at the back of the body. From the human injury viewpoint, the most important part of the wave energy is the one that is transmitted into the body in the form of both positive (compression) and negative (tension) stress waves as well as shear stress waves. Normal stress can be defined as the perpendicular force per unit area applied to an object, in a way that compresses (compressive stress) or stretches (tensile stress) the object.

Shear stress, or simply shear, is similar to stress, except that the force applied is such that the material is sheared or twisted. It should be noted that the pressure entering the tissue may be higher than in the primary wave, due to a damming up of pressure against the body surface. In air, high frequency acoustic waves and shock waves are decaying due to viscous dissipation, producing heat. In tissues, the steep gradient pressure waves will also be absorbed by viscoelastic damping and tissue plastic deformation (tearing, breaking), resulting in mechanical injury. When the pressure wave crosses material interfaces with different densities, large perturbations in stress and deformation take place. A wave impacting denser material will compress it, creating larger stress (pressure), and when it emerges from denser to lighter material it will create large deformations. Therefore, in the human body organs and tissues of different densities are accelerated at different relative rates, resulting in displacement, stretching, and shearing forces. For those reasons the most vulnerable parts of the body are the air- and gas-containing organs, such as the ear drums, lungs, and intestines. In spite of the relatively uniform density and protective barriers, including the scalp, skull, meninges, and subarachnoid cerebrospinal fluid, the brain is also susceptible to blast wave injuries. Highly anisotropic material properties in the brain and immense vascular perfusion will result in nonuniform absorption of the wave energy, stretching and breaking neural axons and the capillary blood brain barrier. Other homogeneous solid viscera transmit the pressure wave to the distal side of the body and are much less susceptible to blast wave injury. In general, the risk of injury is related to the blast energy delivered to the body and the absorption by various tissues.

Free-standing objects exposed to the blast wave (shock wave and the blast wind) will also be displaced. The time integral of the total pressure ( $p + \frac{1}{2} \rho v^2$ ) and the viscous drag loads integrated over the entire surface of the object will result in a net force and moment causing object translation and rotation in space. The extent of the movement depends on the object mass (inertia), and the magnitude of the total force and moment according to Newton's law. Typically, solid objects such as shrapnel, debris, and human bodies will experience translational motion after the shock has already passed. The time delay depends on the inertia of the body. Current explosive devices are often loaded with metallic objects, which are accelerated by the detonation and blast waves, to inflict penetrating injuries in addition to the blast wave (Elsayed, Atkins, 2008).

Based on this physical description of the blast wave events, explosions have the potential to inflict three injury types: *primary blast injury (PBI)* due to the shock wave, *secondary* injuries due to blast-propelled debris fragments causing blunt or penetrating ballistic trauma, and *tertiary* injuries due to human body translocation by blast loads and the resulting impact on rigid objects, thus resulting in blunt force trauma. *Quaternary* injury often refers to all other types of injury including burns, environmental wound contamination, among others. For ease of reference, a summary of the possible injuries is given in Figure 6.

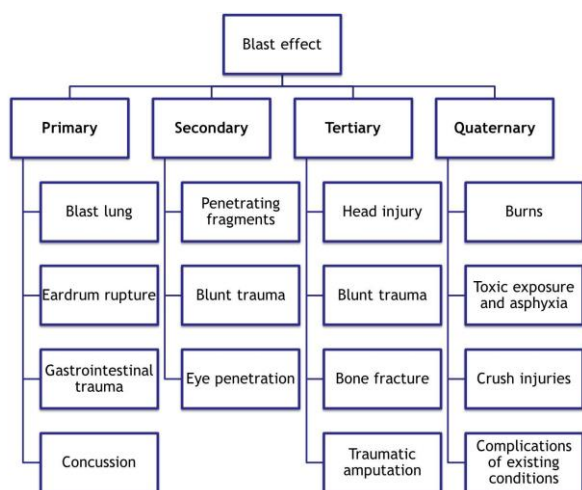


Fig. 6. Blast injury categories (Stewart, 2006)

**Primary blast injuries** are caused when the blast wave compresses the tissues of the internal organs containing air, such as the lung, ear and gastrointestinal tract. Of these three organ systems, the ear is the most easily damaged. Primary injuries are also commonly referred to as the direct effects of the blast on a human being, opposed to the indirect effects where not the blast wave itself but another phenomenon related to the explosion causes harm.

**Secondary blast injuries** are much more common than primary blast injuries. They are caused by flying objects that strike people. These can produce both penetrating and blunt trauma, depending on their size and travelling speed. The penetrating injuries occur most often in the exposed areas, such as the head, neck, and extremities, but thoracic and abdominal injuries may occur as well. As distance from the blast centre increases, the effect of the blast itself is reduced, and the effect of fragments and debris propelled by the explosion becomes more important.

**Tertiary blast injuries** are caused when the victim's body is propelled into another object by the blast winds. This effect is formally known as whole body displacement. If vulnerable body parts such as the skull, the torso or extremities hit a rigid structure, this can obviously cause considerable trauma.

**Quaternary blast injuries** encompass all other injuries caused by the explosion, including burns from fire or radiation, poisoning from carbon monoxide or other toxic products and inhalation of dust. Crush injuries associated with structural collapse also fall under the quaternary or miscellaneous injuries. Although the loss of structural integrity is observed at rather low overpressure, it is often fatal for the occupants. (Debroey, 2015).

## Conclusions

Injuries from explosive materials due to terrorism or other causes are a constant threat that happen worldwide, and they present unique triage, diagnostic, and management challenges. The causes of fatality and injury due to an

explosion may range from impacts of fragments and debris, to thermal effects and blast loading of the human body. Blast related injuries include ear drum rupture, traumatic brain injury, acceleration of the body followed by blunt impact, and injury to the air filled organs like the lungs and the gastrointestinal tract. Understanding the mechanisms behind such blast-induced injuries is of great importance considering the recent trend towards the use of explosives in modern warfare and terrorist-related incidents. This article describes the mechanism of propagation of the blast wave and its interaction with objects and the human body. Understanding these phenomena is essential to define appropriate safety distances and to minimise the risk of handling explosives. The knowledge is also important to design protection measures for civilians and military against deliberate explosive attacks.

## References

- Baker, W. E. 1973. *Explosions in Air*. University of Texas Press, 268 p.
- Chaloner, E. 2005. Blast injury in enclosed spaces. – *BMJ*, 119-120.
- Debroey, J. 2015. *Probit function analysis of blast effects on human beings*. MASc Thesis, KU Leuven, Belgium, 137 p.
- Dharaneepathy, M. V., K. Rao, A. R. Santhakumar. 1995. Critical distance for blast-resistant design. – *Computers and Structures*, 54, 4, 587–595.
- Elsayed, N. M. 1997. Toxicology of blast overpressure. – *Toxicology*, 121, 1–15.
- Elsayed, A., J. Atkins. 2008. *Explosion and Blast-Related Injuries: Effects of Explosion and Blast from Military Operations and Acts of Terrorism*. Academic Press, 397 p.
- Greer, A. D. 2006. *Numerical modeling for the prediction of primary blast injury to the lung*. MSc Thesis, University of Waterloo, Waterloo, Canada, 184 p.
- Josephson, L., P. Tomlinson. 1988. Predicted thoraco-abdominal response to complex blast waves. – *The Journal of Trauma*, 28, 1, S116–S124
- Josey, T. 2010. *Investigation of blast load characteristics on lung injury*. University of Waterloo, 219 p.
- Katz, E., B. Ofek, J. Adler, H. B. Abramowitz, M. M. Krausz. 1989. Primary blast injury after a bomb explosion in a civilian bus. – *Annals of Surgery*, 484–488.
- Liang, S. M., J. S. Wang, H. Chen. 2002. Numerical study of spherical blast-wave propagation and reflection. – *Shock Waves*, 12, 59–68.
- Mayorga, M. A. 1997. The pathology of primary blast overpressure injury. – *Toxicology*, 17–28.
- Smith, P. D., J. G. Hetherington. 1994. *Blast and Ballistic Loading of Structures*. Butterworth-Heinemann, Oxford, 336 p.
- Stuhmiller, J. H. 1997. Biological response to blast overpressure: a summary of modelling. – *Toxicology*, 91–103.
- Wightman, J. M., S. L. Gladish. 2001. Explosions and blast injuries. – *Annals of Emergency Medicine*, 664–678.

## BLAST LOAD ANALYSIS AND EFFECT ON BUILDING STRUCTURES

**Zdravka Mollova**

*University of Mining and Geology "St. Ivan Rilski", 1700 Sofia; mollova.zdravka@gmail.com*

**ABSTRACT.** The increase in the number of terrorist attacks especially in the last few years has shown that the effect of blast loads on buildings is a serious matter that should be taken into consideration in the design process. The analysis and design of structures subjected to blast loads require a detailed understanding of blast phenomena and the dynamic response of various structural elements. This paper presents a comprehensive overview of the effects of explosion on structures. An explanation of the nature of explosions and the mechanism of blast waves in free air is given. Designing the structures to be fully blast resistant is not a realistic and economically viable option, however better understanding of the mechanism of blast load will enable us to make blast resistant building design much more efficient.

**Keywords:** explosion, blast wave, terrorist attacks, shock wave, blast load

### АНАЛИЗ НА ВЗРИВНОТО ВЪЗДЕЙСТВИЕ ВЪРХУ СТРОИТЕЛНИТЕ КОНСТРУКЦИИ

**Здравка Моллова**

*Минно-геоложки университет "Св. Иван Рилски", 1700 София*

**РЕЗЮМЕ.** Увеличаването на броя на терористичните атаки, особено през последните няколко години, показва, че ефектът от взривното въздействие върху сградите е сериозен проблем, който трябва да се вземе под внимание в процеса на проектиране. Анализът при проектирането на конструкции, подложени на взривни натоварвания, изискват обстойно разбиране на взривните явления и динамичната реакция на различните структурни елементи. Тази статия представя преглед на ефектите от взрива върху конструкциите. Дава се обяснение за зависимостта на основните параметри на взрива и механизмите на ударната въздушна вълна. Проектирането на конструкции напълно устойчиви на взрив не е реалистичен и икономически оправдан вариант, но по-доброто познаване на механизма взривното въздействие ще позволи да направим устойчивостта на сградите при взрив много по-ефективна.

**Ключови думи:** експлозия, взривна вълна, терористични атаки, ударна вълна, взривно въздействие

### Introduction

The use of explosives by terrorist groups around the world that target civilian buildings and other structures is becoming a growing problem in modern societies. Bomb explosion near the building can cause such amount of pressure and produces a large amount of heat resulting in a high strain loading on a building and its elements. Such a high strain loading can cause catastrophic damage on building's external and internal structural frame, collapsing of walls, blowing out large expense of windows and shutting down of critical life safety systems.

Due to the threat from such extreme loading conditions, during the past three decades efforts have been made to develop methods of structural analysis and design to resist blast loads. The analysis and design of structures subjected to blast loads require a detailed understanding of blast phenomena and the dynamic response of various structural elements. The aim of this study is to review the work carried out in past few years on blast effects on structures. This article includes introduction and detailed explanation on blast wave phenomenon.

### Explosions and Blast Waves

An explosion can be defined as a very fast chemical reaction involving a solid, dust or gas, during which a rapid release of hot gases and energy takes place. The phenomenon lasts only some milliseconds and it results in the production of very high temperatures and pressures. During detonation the hot gases that are produced expand in order to occupy the available space, leading to wave type propagation through space that is transmitted spherically through an unbounded surrounding medium. Along with the produced gases, the air around the blast (for air blasts) also expands and its molecules pile-up, resulting in what is known as a blast wave and shock front. The blast wave contains a large part of the energy that was released during detonation and moves faster than the speed of sound.

#### Blast wavefront parameters

Of particular importance are the blast wavefront parameters. Analytical solutions for these quantities are first given by Rankine and Hugoniot in 1870 (Rankine, 1870) to describe normal shocks in ideal gases and are available in a number of references such as Liepmann and Roshko (Liepmann & Roshko, 1957). The equations for blast wavefront velocity and maximum dynamic pressure are given below:

$$U_s = \sqrt{\frac{6p_s + 7p_0}{7p_0}} \cdot a_0 \quad (1)$$

$$q_s = \frac{5p_s^2}{2(p_s + 7p_0)} \quad (2)$$

where:

- $p_s$  – peak static wave front overpressure, bar
- $p_0$  – ambient air pressure (atmospheric pressure), bar
- $a_0$  – speed of sound in the air, m/s.

The analysis due to Brode (Brode, 1955) leads to the following results for the peak static overpressure in the near field (when the  $p_s$  is greater than 10 bar) and for medium to far field (when the  $p_s$  is between 0.1 and 10 bar):

$$p_s = \frac{6.7}{Z^3} + 1, \text{ bar; } (p_s > 10 \text{ bar}) \quad (3)$$

$$p_s = \frac{0.975}{Z} + \frac{1.455}{Z^2} + \frac{5.85}{Z^3} - 0.019 \text{ bar} \quad (4)$$

(0.1 <  $p_s$  < 10 bar)

where Z is scaled distance,

$$Z = \frac{R}{\sqrt[3]{W}} \quad (5)$$

- R – distance from the centre of a spherical charge, m
- W – charge mass expressed in kilograms of TNT.

Use of the TNT (Trinitrotoluene) as a reference for determining the scaled distance, Z, is universal. The first step in quantifying the explosive wave from a source other than the TNT, is to convert the charge mass into an equivalent mass of the TNT. The simplest way of achieving this is to multiply the mass of explosive by a conversion factor based on its specific energy and that of TNT. Conversion factors for a number of explosives are shown in Table 1 adapted from Baker (Baker et al., 1983).

Table 1. Conversion factors for explosives

Explosive	Specific energy $Q_x$ / kJ/kg	TNT equivalent $Q_x/Q_{TNT}$
Compound B (60% RDX, 40% TNT)	5190	1.148
RDX (Cyclonite)	5360	1.185
HMX	5680	1.256
Nitroglycerin (liquid)	6700	1.481
TNT	4520	1.000
Blasting Gelatin (91% nitroglycerin, 7.9% nitrocellulose, 0.9% antracid, 0.2% water)	4520	1.000
60% Nitroglycerin dynamite	2710	0.600
Semtex	5660	1.250

An equivalent TNT weight is computed according to Equation (6) that links the weight of the chosen design explosive to the equivalent weight of TNT by utilising the ratio of the heat produced during detonation (Karlos, Solomos, 2013):

$$W_e = W_{exp} \frac{H_{exp}^d}{H_{TNT}^d} \quad (6)$$

where,  $W_e$  is the TNT equivalent weight (kg),  $W_{exp}$  is the weight of the actual explosive (kg),  $H_{exp}^d$  is the heat of detonation of the actual explosive (MJ/kg),  $H_{TNT}^d$  is the heat of detonation of the TNT (MJ/kg).

Table 2 provides estimates of the produced heat of detonation of some common explosives as defined in (TM5-1300). These values can be used for the calculation of the equivalent TNT weight with the use of Equation (6).

Table 2. Indicative values of heat of detonation of common explosives

Name of explosive	Heat of detonation (MJ/Kg)
TNT	4.10-4.55
C4	5.86
RDX	5.13-6.19
PETN	6.69
PENTOLITE 50/50	5.86
NITROGLYSRIN	6.30
NITROMETHANE	6.40
NITROCELLULOSE	10.60
AMON./NIT.(AN)	1.59

### Other important blast wave parameters

Other significant parameters include  $t_0$ , duration of the positive phase (the time when the pressure exceeds the ambient pressure) and  $i_s$  the specific impulse of the wave which is the area beneath the pressure-time curve from the moment of arrival,  $t_A$ , to the end of the positive phase and is given by expression (Mays, Smith, 1995):

$$i_s = \int_{t_A}^{t_A+t_0} p_s(t) dt \quad (7)$$

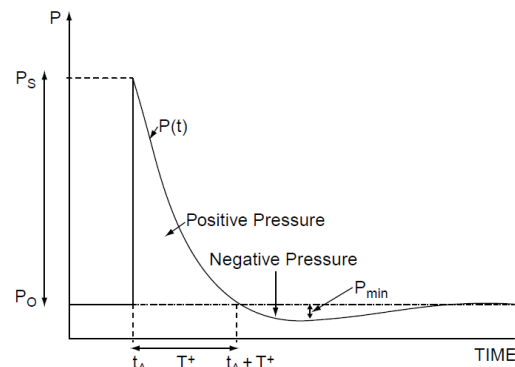


Fig. 1. Pressure-time profile for blast wave in free air

A typical pressure- time profile for a blast wave in free air is shown in Figure 1 where  $p^-$  is the greatest value of underpressure (pressure below ambient) in the negative phase of the blast. This is the rarefaction or underpressure component of the blast wave. Brode's solution for  $p^-$  (bar) is:

$$p^- = \frac{0.35}{Z}, \text{ bar; } Z > 1,6 \quad (8)$$

and the associated specific impulse in this phase  $i_s^-$  is given by:

$$i_s^- \approx i_s \cdot \left(1 - \frac{1}{2Z}\right) \quad (9)$$

**Blast wave scaling laws**

The most commonly used blast wave scaling is the cube root scaling law, otherwise known as Hopkinson's Law (Baker, 1973). This law states that any pressure generated at a distance  $R_1$  from a reference explosion with weight  $W_1$  will generate the same pressure at a distance  $R_2$  from the same explosive with weight  $W_2$  provided the charges are of similar geometry and in the same atmosphere.

$$\frac{R_2}{R_1} = \left(\frac{W_2}{W_1}\right)^{\frac{1}{3}} = \lambda \quad (10)$$

The parameter  $\lambda$  is referred to as the explosive yield factor. Hopkinson's Law approach leads readily to the specification of the scaled distance  $Z$  ( $m/kg^{1/3}$ ), introduced above.

**Hemispherical surface bursts**

The foregoing calculations refer to free- air bursts remote from any reflecting surface and are usually categorised as spherical airbursts. When attempting to quantify overpressures generated by the detonating of high explosives sources in contact with the ground, modification must be made to charge weight. Surface bursts produced blast waves that appear to come from free air bursts are 1-8 times the actual source energy. It should be noted that if the ground was a perfect reflector and no energy was dissipated (in producing a crater and groundshock) the reflection factor would be 2 (Mays, Smith, 1995).

**Blast wave pressure profiles**

The pressure-time history of a blast wave is often described by exponential function such as the Freeland equation (in which the  $b$  is the parameter of the waveform):

$$p(t) = p_s \left(1 - \frac{t}{t_0}\right) \exp\left(-\frac{bt}{t_0}\right) \quad (11)$$

where,  $p_s$  is the peak overpressure,  
 $t_0$  is the positive phase duration,  
 $b$  is a decay coefficient of the waveform and  
 $t$  is the time elapsed, measured from the instant of blast arrival.

For many purposes however, approximations are quite satisfactory. Thus, linear decay is often used in design where the conservative approach would be to present the pressure-time history by a line (Fig. 1).

**Blast wave interactions**

When blast waves encounter a solid surface or an object made of a medium denser than air, they will reflect from it and, depending on its geometry and size, diffract around it. The simplest case is that of an infinitely large rigid wall on which the blast wave impinges at zero angle of incidence. In this case the incident blast wave front travelling at

velocity  $U_s$ , undergoes reflection when the forward moving air molecules are brought to rest and further compressed upon meeting an obstacle. Rankine and Huguenot (Mays & Smith, 1995) derived an equation for refracted overpressure  $p_r$ :

$$p_r = 2p_s + (\gamma + 1) \cdot q_s \quad (12)$$

Substituting (2) into the equation (12):

$$p_r = 2p_s \left(\frac{7p_0 + 4p_s}{7p_0 + p_s}\right) \quad (13)$$

If the rectangular structure is exposed to an explosion, it will be exposed to pressures on all of its surfaces. Each surface suffers two concurrent components of the load. Diffraction of explosion around the structure will enclose a target and cause a normal force to any exposed surfaces (Fig. 2). The structure is pushed to the right if the left side is loaded, while simultaneously pushed slightly to the left as the diffraction ends. Drag force pushes the structure from the left side and that is followed by the suction force on the right when the dynamic pressure crosses (blast wind) over and around the structure. As the shock front expands in the surrounding volume of the air, the peak initial pressure is reduced and the duration of the pressure increases.

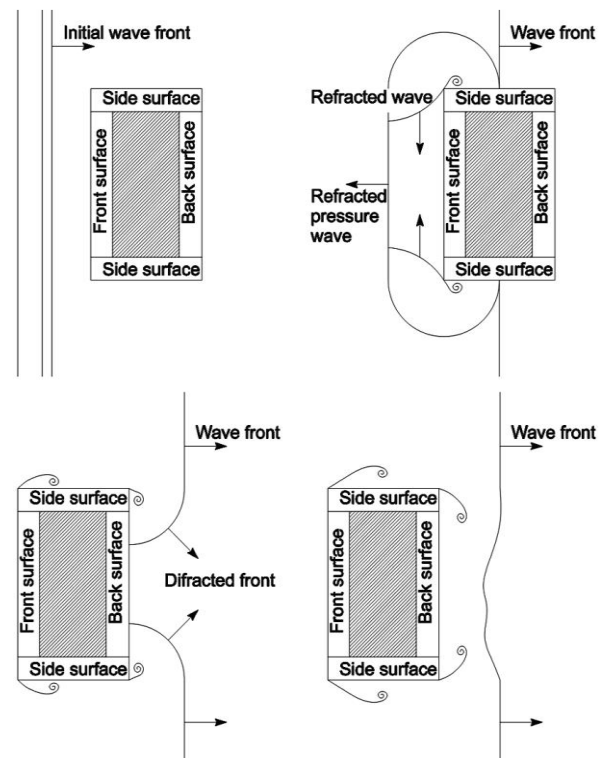


Fig. 2. Behaviour of the wave during its pass around the structure

**Explosion and blast-loading types**

Air blasts phenomena can be separated into three categories: free air burst, ground reflection effects and surface air burst. (Blanc et al., 2005)

**Free Air Burst**

Free air burst occurs when the incident wave reaches the structure before being reinforced. The main wave reinforcement takes place during ground impact.

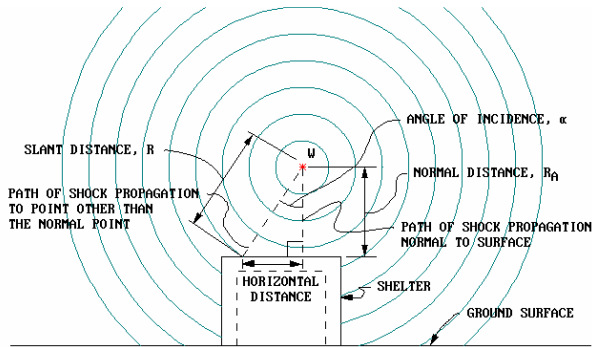


**Fig. 3. Free air burst configuration (TM5-1300)**

**Ground reflection**

It is necessary to take in account the ground effect when the incident wave is reinforced by it. Two phenomena can occur: either a classical reflection (Fig. 4) or a reinforcement reflection (Mach Front, Fig. 5).

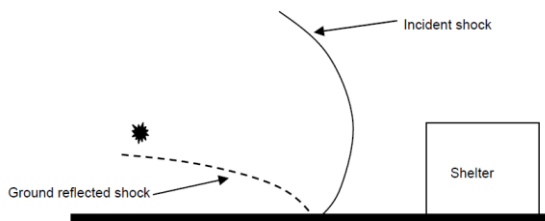


**Fig. 4. Ground reflection configuration – classical**

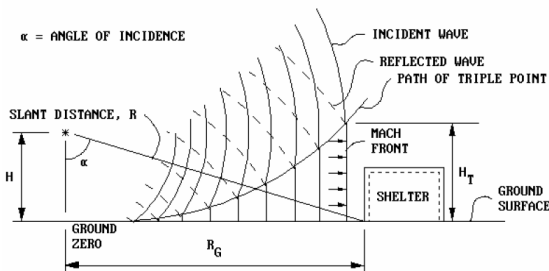


**Fig. 5. Ground reflection configuration – Mach Front (TM5-1300)**

The Mach front is formed by the interaction between incident and reflected pressure waves. This interaction depends on the angle of incidence between ground and incident wave. The critical angle is around  $40^\circ$ . The pressure-time variation of the Mach front is similar to that of the incident wave except that the magnitude is somewhat larger.

**Surface burst**

Surface air burst occurs when the charge detonation takes place close to or on the ground. Unlike what happens in an air burst, the incident and reflected wave are merged near the detonation point to form a single reinforced wave. The created wave is hemispherical.

This wave merging can also take place very far from the detonation point when the height of burst is important (Kinney, Graham, 1985).

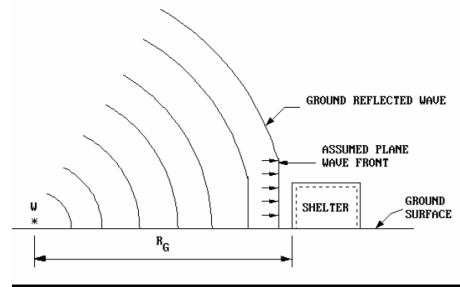


**Fig. 6. Surface burst configuration (TM5-1300)**

**Structural Loading**

The forces acting on a structure associated with a plane shock wave are dependent upon both the peak pressure and the impulse of the incident and dynamic pressures acting in the free-field.

For each pressure range there is a particle or wind velocity associated with the blast wave that causes a dynamic pressure on objects in the path of the wave. In the free field, these dynamic pressures are essentially functions of the air density and particle velocity. For typical conditions, standard relationships have been established between the peak incident pressure, the peak dynamic pressure, the particle velocity, and the air density behind the shock front. The magnitude of the dynamic pressures, particle velocity and air density are solely functions of the peak incident pressure, and, therefore, independent of the explosion size. Of the three parameters, the dynamic pressure is the most important for determining the loads on structures.

For design purposes, it is necessary to establish the variation or decay of both the incident and dynamic pressures with time since the effects on the structure subjected to a blast loading depend upon the intensity-time, history of the loading as well as on the peak intensity. The form of the incident blast wave is characterised by an abrupt rise in pressure to a peak value, a period of decay to ambient pressure and a period in which the pressure drops below, ambient (negative pressure phase).

The rate of decay of the incident and dynamic pressures, after the passage of the shock front, is a function of the peak pressure (both positive and negative phases) and the size of the detonation. For design purposes, the actual decay of the incident pressure may be approximated by the rise of an equivalent triangular pulse. The actual positive duration is replaced by a fictitious duration which is expressed as a function of the total positive impulse and peak pressure:

$$t_{of} = 2i/p .$$

The above relationship for the equivalent triangular pulse is applicable to the incident as well as the reflected pressures; however, in the case of the latter, the value of the pressure and impulse used with Equation 2-6 is equivalent to that associated with the reflected wave. The fictitious duration of the dynamic pressure may be assumed to be

equal to that of the incident pressure.

For determining the pressure-time data for the negative phase, a similar procedure as the one used in the evaluation of the idealised positive phase may be utilised. The equivalent negative pressure-time curve will have a time of rise equal to 0.25, whereas the fictitious duration  $t_{of}^-$  is given by the triangular equivalent pulse equation:

$$t_{of}^- = 2i^- / p^-$$

where  $i^-$  and  $p^-$  are the total impulse and peak pressure of the negative pulse of either the incident or reflected waves. The effects of the dynamic pressure in the magazine phase region may usually be neglected.

For any given set of free-field incident and dynamic pressure pulses, the forces imparted on an above the ground structure can be divided into four general components:

- the force resulting from the incident pressure,
- the force associated with the dynamic pressures,
- the force resulting from the reflection of the incident-pressure impinging upon an interfering surface, and
- the pressures associated with the negative phase of the shock wave. The relative significance of each of these components is dependent upon the geometrical configuration and size of the structure, the orientation of the structure relative to the shock front, and the design purpose of the blast loads (TM5-1300).

**Front Wall Loads**

The blast face (or faces) is described as the area or face on a structure which is directly loaded by the incoming blast wave either from an incident wave or from a wave hitting the structure after undergoing reflection off the ground surface.

A point on the blast face loaded by the incoming blast wave will experience a sudden rise in pressure to the reflected overpressure followed by decay. The time required to relieve the reflected pressure, known as the clearing time can be expressed as:

$$t_c = \frac{4S}{(1+R) \cdot C_r} \tag{14}$$

S – length of the "clearing", is equal to the height of the structure, H or a half-width of the structure, W/2, whichever is less (Fig. 7),

R – ratio S/G, where G is the height of the structure, H or half-width of the structure, W/2, whichever is less,

$C_r$  – speed of sound in refracted area

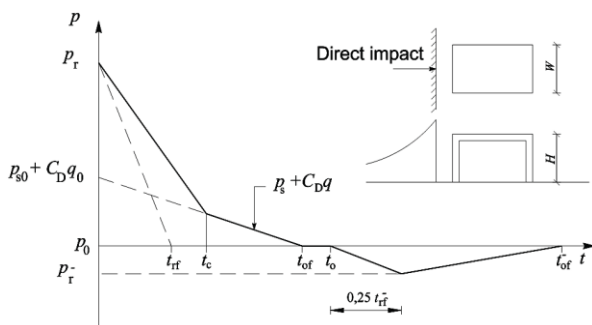


Fig. 7. The load on the front surface of the structure

The pressure that acts on the front surface after the time  $t_c$  is the algebraic sum of the initial pressure  $p_s$  and drag dependent pressure,  $C_D \cdot q$ :

$$p = p_s + C_D \cdot q \tag{15}$$

The drag coefficient  $C_D$  connects the dynamic pressure and the total translational pressure in the direction of the wind-induced dynamic pressure and varies with Mach number (or Reynolds number in the area of low pressure), and depends on the geometry of the structure. It can be taken as  $\geq 1.0$  for the front facade, while for the side, rear and roof surfaces it can be taken  $< 1.0$  (Table 3).

The fictitious length of the refracted wave front,  $t_{rf}$ , is calculated according to the formula:

$$t_{rf} = \frac{2i_r}{p_r} \tag{16}$$

where  $p_r$  is the refracted peak pressure.

Table 3. Drag coefficients

Loaded surface	$C_D$
Front	0.8 ÷ 1.6
Rear	0.25 ÷ 0.5
Side and roof (depending pressure, kN/m <sup>2</sup> )	
0 ÷ 172	-0.4
172 ÷ 345	-0.3
345 ÷ 896	-0.2

**Roof and side walls**

As the wave encloses the structure, the pressure on the top and sides of the structure is equal to the initial pressure and then decreases to a negative pressure due to the drag (Fig. 8). The structural part that is loaded depends on the magnitude of the initial pressure wave front, the location of the wave front and the wavelength of the positive and negative phases.

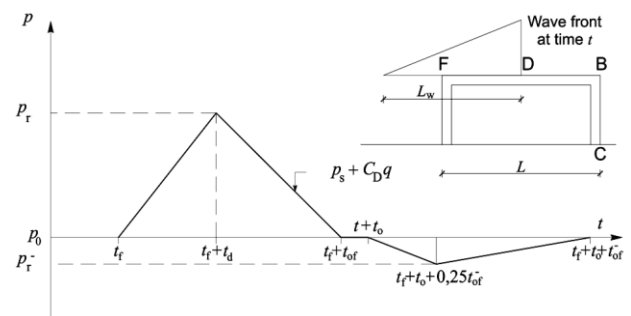


Fig. 8. The load on the roof and side surfaces of the structure

The initial peak pressure on the roof surface is reduced and the wavelength increases when the wave encloses the structure. The equivalent uniform pressure increases linearly from the wave-arrival time  $t_f$  (point F on the element) to the time  $t_d$  when the wave reaches the peak value and gets to the point D. At the point B the equivalent uniform pressure is reduced to zero.

The load coefficient  $C_E$ , increases time and duration of an equivalent uniform. It is a ratio of the wavelength and range,  $Lwf/L$ . The peak pressure that acts on the roof,  $p_R$ , is the sum of the equivalent uniform pressure and the drag pressure:

$$p_R = C_E \cdot p_{Sof} + C_D \cdot q_0 \quad (17)$$

where are:

$p_{Sof}$  – the initial pressure at the point F,

$q_0$  – a dynamic pressure corresponding to  $C_E \cdot p_{Sof}$

### Rear wall

As the wave passes over the ends of the roof and the side surfaces, pressures are spreading, thus creating a secondary wave that continues to spread across the rear surfaces of the structure. The secondary waves that enclose the rear surface, in the case of long structures, are the result of a wave "overflow" from the roof and side surfaces. They are amplified due to the refraction of the structural surfaces. The increase of the waves from the roof is caused by the refraction of the ground at the bottom of the rear surface, and the increase of the waves "overflowed" from the side surface is caused by their mutual collisions in half the length of the surface, or collision with a wave "overflowed" from the roof.

For the loading analysis the procedure equivalent to the procedure for the loading determination on the roof and side surfaces (Fig. 9) can be used. The peak pressure for pressure-time history is determined using the peak pressure on the extreme edge of the roof surface,  $p_{Sob}$ . Dynamic drag pressure corresponds to the pressure  $C_E \cdot p_{Sob}$ , while the preferred drag coefficients are equal to those for the roof and the side surfaces.

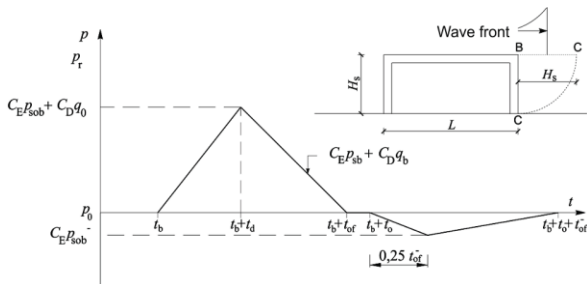


Fig. 9. The load on the rear surface of the structure

## Conclusions

Blast resistant design is an important topic of study and therefore requires careful understanding of the blast phenomena and its effect and impact on various structural elements. Technical information has been collected, adapted and presented in this article for the calculation of the external explosion loads to be considered in the blast protection design of a structure. Empirical methods for the prediction of blast loads have been chosen as this is closer to the traditional engineering design approach. Simple expressions are presented for the calculation of the blast load on building structures. Of course, more complicated cases of blast loading, where obstacles are involved and wave shadowing and channeling phenomena take place, cannot be handled through this approach. The material presented can be used to introduce the subject, and in most cases, it can form a basis for initiating a reliable blast assessment of a structure.

## References

- Baker, W. E., P. A. Cox, J. J. Kulesz, R. A. Strehlow, P. S. Westine. 1983. *Explosion Hazards and Evaluation*. Elsevier, 826 p.
- Baker, W. E. 1973. *Explosions in Air*. University of Texas Press, 268 p.
- Brode, H. L. 1955. Numerical solutions of spherical blast waves. – *Journal of Applied Physics*, 26, 6, 766–775.
- Blanc, G., M. Adoum, V. Lapoujade. 2005. External blast load on structures – Empirical approach. – *5th European LS-DYNA Users Conference*. 5c-39.
- Draganić, H, V. Sigmund. 2012. Blast loading on structures. – *Tehnički vjesnik*, 19, 643–652.
- Karlos, V., G. Solomos. 2013. *Calculation of Blast Loads for Application to Structural Components*. Joint Research Centre. 58 p.
- Kinney, G. F., K. J. Graham. 1985. *Explosive Shocks in Air*. Springer Science+Business Media, 281 p.
- Liepmann, H.W., A. Roshko. 1957. *Elements of Gas Dynamics*. John Wiley, New York, 460 p.
- Mays, G. S., M. Smith. 1995. *Blast Effects on Buildings: Design of Buildings to Optimise Resistance to Blast Loading*. Thomas Telford, 129 p.
- Rankine, W. J. H. 1870. *Philosophical Transactions of the Royal Society*, 160, 277–288.
- U.S. Department of the Army. 1990. *Structures to resist the effects of accidental explosions, Technical Manual 5-1300*.

## DYNAMIC ASCENT OF A MINING DUMPER ON A ROAD WITH LONGITUDINAL SLOPE

Stefan Pulev

University of Mining and Geology "St. Ivan Rilski", 1700 Sofia; st\_pulev@yahoo.com

**ABSTRACT.** The dynamic ascent is achieved via an initial (reached), sufficiently high, velocity. By using the inertial force, the ascent of relatively short sections with a higher slope becomes possible without the risk of flipping over backwards. The ascent of a mining dumper truck travelling with a constant acceleration along an inclined section of a road without bumps is investigated. The truck is described using a one-mass dynamic model with one degree of freedom. The differential equation of the longitudinal angular vibrations is derived and solved analytically. It is assumed that a rear overturn happens when the angle of rotation reaches a maximum and the normal force of the road on the front set of wheels reaches zero. The critical inclination that can cause an overturn is calculated.

**Keywords:** dynamic ascent, mining dumper truck

### ДИНАМИЧНО ИЗКАЧВАНЕ НА РУДНИЧЕН САМОСВАЛ ПО НАКЛОНЕН ПЪТ

Стефан Пулев

Минно-геоложки университет "Св. Иван Рилски", 1700 София

**РЕЗЮМЕ.** Динамичното изкачване се реализира с предварително развита (достигната) достатъчно висока скорост. С помощта на инерционната сила става възможно изкачването на по-стръмни наклонени участъци със сравнително малка дължина без опасност от преобръщане на автомобила назад. Разглежда се изкачване на рудничен самосвал с постоянно ускорение по наклонен участък от пътя без неравности. Той е представен посредством едномасов модел с една степен на свобода, извършващ надлъжни ъглови трептения. Диференциалното уравнение на малките трептения е получено и решено аналитично. Приема се, че преобръщането на самосвала назад настъпва когато ъгълът на завъртане е максимален и реакцията на пътя върху предните колела стане равна на нула. Така се определя критичния наклон на пътя, при който е възможно да настъпи преобръщане.

**Ключови думи:** динамично изкачване, рудничен самосвал

### Introduction

Mining dumpers are used under very harsh conditions. The technological roads in open-pit mines are characterised by extreme unevenness, longitudinal and transverse gradients. The mining dumper truck can climb evenly (at a steady speed) on an inclined road only under the action of the engine thrust. The distance travelled in this case may be unlimited. But overcoming the slope can also be done by pre-accelerating and reaching a high enough speed to enter the slope. The gas supply is then discontinued and the dump truck ascends with the help of inertial forces. Thus, in addition to the thrust of the engine, the accumulated kinetic energy is also used. In this case it is possible to climb steeper sections of the road with a shorter length and it is gaining popularity as a dynamic overcoming of slopes. This increases the capacity of the mining dumper in extreme conditions.

Figure 1 (Vahlamov, 2006) shows the stages of a dynamic ascent. In the first section AB, the driver supplies gas, the dump truck increases its speed, and acceleration is observed. Thus, a sufficiently safe speed is reached in section BC, with which the mining dumper enters section CD that represents the ascent itself. Then the speed starts to decrease (section CD) and deceleration occurs. There is an inertial force whose direction coincides with the direction of movement. It is opposed to a possible roll over of the mining dumper truck. This makes it possible to overcome larger slopes.

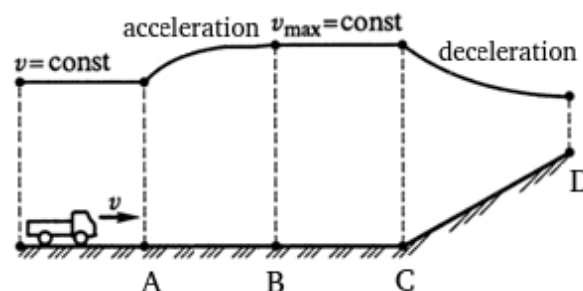


Fig. 1. Stages of a dynamic overturn

### Dynamic model

We consider the climbing of a mining dumper (Fig. 2) along a section of the road with an inclination  $\alpha$  without unevenness (Pulev, 2012). The deceleration  $a$  is constant and the direction of inertial force

$$\Phi = ma$$

coincides with the direction of movement. The following inscriptions have been made:

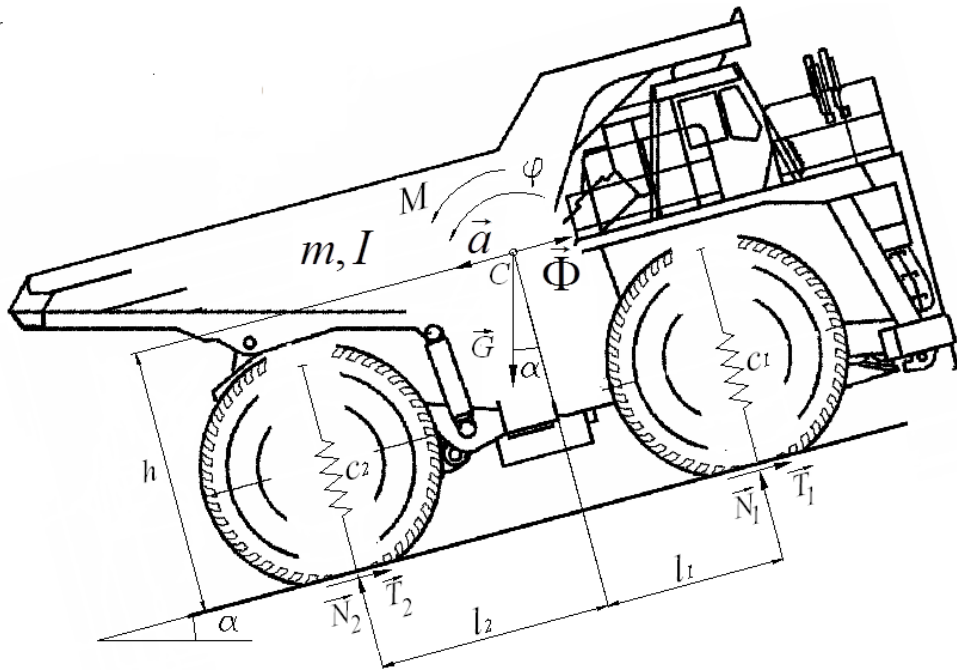


Fig. 2. Dynamic model

$I$  - moment of inertia of the mining dumper truck relative to the transverse axis passing through the centre of gravity;  
 $m$  - aggregate mass of the mining dumper;

$c_1, c_2$  - elasticity of front and rear suspension;

$N_1, N_2$  - normal road reaction to the front and rear wheels respectively;

$T_1, T_2$  - tangential road reaction on the front and rear wheels respectively;

$h$  - height of the centre of gravity of the mining dumper;

$l_1$  - distance from the front suspension to the centre of gravity;

$l_2$  - distance from the rear suspension to the centre of gravity.

As a generalised coordinate, the rotation angle  $\varphi$  of the mining dumper around the transverse axis passing through the centre of gravity is introduced. The vertical oscillations are neglected because there are no vertical external disturbances. It is assumed that the mining dumper is symmetrical, i.e. there is no connection between jumping and galloping.

In the position of static equilibrium, in both springs static deformations  $\delta_{1,0}, \delta_{2,0}$  and elastic forces  $c_1 \cdot \delta_{1,0}, c_2 \cdot \delta_{2,0}$  occur. The equations

$$c_1 \cdot \delta_{1,0} = \frac{l_2 mg \cos \alpha}{L} \text{ and } c_2 \cdot \delta_{2,0} = \frac{l_1 mg \cos \alpha}{L}$$

( $L = l_1 + l_2$ ) are obtained from the equilibrium conditions.

At any moment of the movement, the elastic forces in the two springs are respectively

$$c_1(\delta_{1,0} - l_1 \cdot \varphi) \text{ and } c_2(\delta_{2,0} + l_2 \cdot \varphi).$$

In order to have an equilibrium in the area of contact of the wheels with the road, the normal reactions must be equal to the elastic forces in the springs, i.e.

$$N_1 = c_1(\delta_{1,0} - l_1 \cdot \varphi) = \frac{l_2 mg \cos \alpha}{L} - c_1 \cdot l_1 \cdot \varphi, \quad (1)$$

$$N_2 = c_2(\delta_{2,0} + l_2 \cdot \varphi) = \frac{l_1 mg \cos \alpha}{L} + c_2 \cdot l_2 \cdot \varphi.$$

The tangential reactions  $T_1$  and  $T_2$  act in the opposite direction to the possible slip of the mining dumper on the inclined road. The equation

$$T_1 + T_2 = G \sin \alpha - \Phi.$$

is a condition for the equilibrium of tangential forces. The forces on both sides form a couple with an arm  $h$  and a moment

$$M = h(G \sin \alpha - \Phi) = hm(g \sin \alpha - a).$$

The differential equation of the longitudinal angular oscillations of the mining dumper is obtained using the second order Lagrange equation and has the form

$$\ddot{\varphi} + \frac{c_1 l_1^2 + c_2 l_2^2}{I} \cdot \varphi = \frac{hm(g \sin \alpha - a)}{I}. \quad (2)$$

This is a non-homogeneous second-order differential equation with constant coefficients. Its common solution is the sum of the solution of the homogeneous equation and a particular solution.

The solution of the homogeneous equation is

$$\varphi_0 = C_1 \cos kt + C_2 \sin kt,$$

where  $C_1$  and  $C_2$  are integration constants, and the own frequency of longitudinal angular oscillations is

$$k = \sqrt{\frac{c_1 \cdot l_1^2 + c_2 \cdot l_2^2}{I}}.$$

A particular solution of the following kind is necessary:

$$\eta = A, \quad \dot{\eta} = \ddot{\eta} = 0.$$

After substituting  $\eta$  in the differential equation (2), the following equation is obtained

$$A = \frac{hm(g \sin \alpha - a)}{c_1 \cdot l_1^2 + c_2 \cdot l_2^2}.$$

The general solution of the differential equation (2) is

$$\varphi = \varphi_0 + \eta = C_1 \cos \sqrt{\frac{c_1 \cdot l_1^2 + c_2 \cdot l_2^2}{I}} t + C_2 \sin \sqrt{\frac{c_1 \cdot l_1^2 + c_2 \cdot l_2^2}{I}} t + \frac{hm(g \sin \alpha - a)}{c_1 \cdot l_1^2 + c_2 \cdot l_2^2}$$

Under zero initial conditions for integration constants is found that:

$$C_1 = -\frac{hm(g \sin \alpha - a)}{c_1 \cdot l_1^2 + c_2 \cdot l_2^2} \quad \text{and} \quad C_2 = 0.$$

Therefore, the law on transverse angular oscillations is given by the following expression:

$$\varphi = \frac{hm(g \sin \alpha - a)}{c_1 \cdot l_1^2 + c_2 \cdot l_2^2} \left( 1 - \cos \sqrt{\frac{c_1 \cdot l_1^2 + c_2 \cdot l_2^2}{I}} t \right).$$

It is known that

$$-1 \leq \cos \sqrt{\frac{c_1 \cdot l_1^2 + c_2 \cdot l_2^2}{I}} t \leq 1.$$

Then, the maximum value of the coordinate is obtained when the expression in the brackets of the law for transverse angular oscillations becomes equal to 2. It is

$$\varphi_{\max} = \frac{2hm(g \sin \alpha - a)}{c_1 \cdot l_1^2 + c_2 \cdot l_2^2}. \quad (3)$$

A rear overturn happens when the tipper deviates as much as possible from the static equilibrium and the front wheels lose contact with the road. The following conditions must be met:

$$\varphi = \varphi_{\max} \quad \text{and} \quad N_1 \leq 0. \quad (4)$$

The normal reaction (1) of the road in contact with the front wheels is determined by the expression

$$N_1 = \frac{l_2 mg \cos \alpha}{L} - c_1 \cdot l_1 \cdot \frac{2hm(g \sin \alpha - a)}{c_1 \cdot l_1^2 + c_2 \cdot l_2^2}. \quad (5)$$

The critical inclination  $\alpha_k$  that can cause an overturn is determined by the equality

$$\frac{l_2 mg \cos \alpha_k}{L} - c_1 \cdot l_1 \cdot \frac{2hm(g \sin \alpha_k - a)}{c_1 \cdot l_1^2 + c_2 \cdot l_2^2} = 0. \quad (6)$$

After mathematical transformations, the equation (6) acquires the following form:

$$2hgLc_1 l_1 \sin \alpha_k - l_2 g (c_1 \cdot l_1^2 + c_2 \cdot l_2^2) \cos \alpha_k = 2hLc_1 l_1 a \quad (7)$$

If the substitutions are made

$$\begin{aligned} \sin \psi &= \frac{2hLc_1 l_1}{\sqrt{4h^2 L^2 c_1^2 l_1^2 + l_2^2 (c_1 \cdot l_1^2 + c_2 \cdot l_2^2)^2}}, \\ \cos \psi &= \frac{l_2 (c_1 \cdot l_1^2 + c_2 \cdot l_2^2)}{\sqrt{4h^2 L^2 c_1^2 l_1^2 + l_2^2 (c_1 \cdot l_1^2 + c_2 \cdot l_2^2)^2}}, \\ \sin \varphi &= \frac{2hLc_1 l_1 a}{g \sqrt{4h^2 L^2 c_1^2 l_1^2 + l_2^2 (c_1 \cdot l_1^2 + c_2 \cdot l_2^2)^2}}, \end{aligned}$$

the equation (7) becomes:

$$\sin(\alpha_k - \psi) = \sin \varphi.$$

The solution to this trigonometric equation, which is of practical significance, is

$$\alpha_k = \varphi + \psi. \quad (8)$$

The value of deceleration has the determinant influence on the critical inclination  $\alpha_k$ . The size of the load transported also influences it. The higher the load, the greater the height  $h$  of the centre of gravity and the probability of an overturn increases. The increasing of  $h$  requires a reduction of  $\alpha_k$ . It's also different for the different dump models.

## Numerical experiment and discussion

Using the formula (8) obtained, the critical inclination  $\alpha_k$  value can be calculated for a mining dumper with the following characteristics:

$$L = 5.3 \text{ m}, l_1 = 3.551 \text{ m}, l_2 = 1.749 \text{ m},$$

$$c_1 = 10.93 \times 10^5 \text{ N/m}, c_2 = 22.2 \times 10^5 \text{ N/m},$$

$$h = 5 \text{ m}.$$

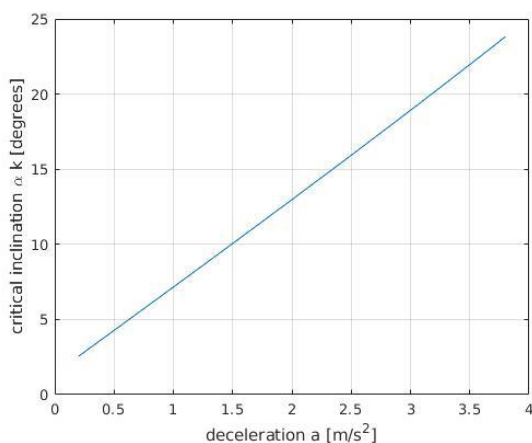


Fig. 3. Influence of deceleration on critical inclination

Figure 3 shows changes of the critical inclination  $\alpha_k$  depending on the deceleration values. Acceleration values of  $1.5 \text{ m/s}^2$  to  $3.5 \text{ m/s}^2$  are recommended.

The dynamic ascent of a mining dumper ensures safe climb of steeper sections of the road with a shorter length. It mostly depends on the driver's abilities, skills, experience, wisdom and quick responses.

## References

- Pulev S. N. 2012. *Treptenia na rudnichen samosval*. Ed. House "Sv. Ivan Rilski", Sofia, 116 p. (in Bulgarian)
- Vahlamov V. K. 2006. *Avtomobili: Ekspluatacionnie svoistva*. Akademia, Moscow, 240 p. (in Russian)

## INCREASING THE ECONOMIC EFFICIENCY OF MINING COMPLEX STRUCTURAL GOLD DEPOSITS

**Aleksandr O. Rodionov**

*Saint-Petersburg Mining University, 199106 Saint-Petersburg; Rodionov.a.o@mail.ru*

**ABSTRACT.** At present the deterioration of geological and engineering conditions of the ore deposits, entails increase of losses of minerals, increasing the mineral production and processing costs. With consideration of the specified limiting conditions, the net present value of deposit mining will be achieved with minimal economic loss resulting from the mineral losses and dilution. According to the results of the research, conclusions were made that the economic loss related to the losses and dilution, increase in direct proportion to the increase of bench heights; the mode of horizon preparation significantly influences the value of losses and dilution and the economic losses related to them; the value of losses and dilution increases with increase of the bench height, and the current stripping ratio reduces. In order to determine the optimal bench height, joint consideration of the losses and dilution with the current stripping ratio, is required. The conducted technical and economic calculations result in recommending the bench height in an ore zone to be 5 m while maintaining the rock bench height of 20 meters.

**Keywords:** Losses, dilution, loss-rationing, separate excavation

### УВЕЛИЧАВАНЕ НА ИКОНОМИЧЕСКАТА ЕФЕКТИВНОСТ ПРИ РАЗРАБОТВАНЕ НА КОМПЛЕКСНИ ЗЛАТОСЪДЪРЖАЩИ НАХОДИЩА

**Александър О. Родионов**

*Санктпетербургски минен университет, 199106, Санкт Петербург*

**РЕЗЮМЕ.** Понастоящем се наблюдава тенденция към влошаване на геоложките и инженерни условия при разработването на рудни находища, което води до увеличаване на загубите и обедняване на полезните изкопаеми, увеличаване на разходите за производство и преработка на минерали. Като се вземат предвид определените ограничителни условия, максималната нетна настояща стойност на добива от дадено находище ще бъде постигната с минимални икономически загуби, произтичащи от загубите и обедняването на рудата. В резултат на изследването може да се заключи, че икономическите загуби, свързани със загубите и обедняването на руда, нарастват пряко пропорционално на увеличаването на височината на стъпалата. Начинът на подготовка на хоризонта значително влияе върху стойността на загубите и обедняването и свързаните с тях икономически загуби; стойността на загубите и обедняването се увеличава с увеличаване на височината на стъпалото, а текущият коефициент на откривка намалява. За да се определи оптималната височина на стъпалото, е необходимо съвместно отчитане на загубите и обедняването със сегашния коефициент на откривка. Проведените технически и икономически изчисления водят до препоръчване височината на стъпалото в рудна зона да бъде 5 m, като се поддържа височината на стъпало на скалата от 20 метра.

**Ключови думи:** загуби, обедняване, съотношение на загубите, отделен добив

### Introduction

One of the most important problems in the rational use of mineral resources is the improvement of existing methods for the complete extraction of minerals from the interior. The effectiveness of monitoring the compliance of the quantity and quality of recoverable reserves determined by the standards depends both on the reliability of the data and on the accounting methodology used. The indicators controlling the quantitative side of the process of mining of mineral resources are the absolute and relative losses of balance reserves, as well as the absolute and relative magnitude of the amount of clogging rocks in the mined ore.

#### Types of losses of mineral resources

The losses of mineral resources are divided into the following types: (i) in redeemed ledges (sides) of the quarry; (ii) in unfinished areas; (iii) in the soil and roof of the deposit; (iv) with separate excavation; (v) in the process of drilling and blasting works; (vi) in the internal dumps during the re-

excavation; (vii) when loaded into transport vessels due to spillage; (viii) in the process of transportation; (ix) when stored in temporary warehouses; (x) at reloading points; (xi) at landslides of sides and ledges.

In a specific production environment, certain types of losses can be absent or new ones added to this list. For example, in coal deposits due to spontaneous combustion of certain coals, in the case of improper mining operations, coal losses from fires occur. In the case of draperies, there are losses in interstep and inter-path ladders, etc.

In addition to quantitative losses, mining often leads to depletion of minerals. The total amount of the diluting mountain mass is determined by the clogging of the conditioned minerals with an empty rock or substandard grades, and by the blending of valuable varieties with less valuable ones during drilling and blasting operations, and also as a result of local caving of the ledges. Insolvency leads not only to a decrease in the content of useful components in mined minerals, but also to a deterioration in recovery rates at concentrating mills and metallurgical plants.

### Production of blasting

The normalization of losses and dilution includes the issues of operational testing, the organisation of drilling and blasting and excavation, the selection of effective blasting schemes with separation of ores and rocks, using schemes for initiating borehole charges, taking into account the position of ore bodies in the space aimed at achieving maximum preservation of the initial, geological structure or minimising the displacement of contacts of ore bodies and rocks during their joint blasting and subsequent excavation shipment.

Floating trench traverses the ore zone with drilling and blasting operations. The width of the split trench is determined by the parameters of the applied technological equipment, as well as by the number and consistency of the contour of ore bodies. In gross blasting, all three sizes of the blast block (width, length and height) or some of them are set regardless of the position of contacts with different types of rock on the basis of technological considerations.

Separate blasting should be used when it is possible to perform a simultaneous or selective blasting of ore bodies and rocks. The multi-row co-rapidly delayed gross blasting of the block can be carried out on a selected face, in a clamped medium and with a retaining wall.

The advantage of multi-row explosion of charges on the open front with a uniform initiation of charges is to ensure the quality of rock crushing. The disadvantage is the material breach of the initial settings lay down deposits of ore bodies.

Multiple explosion in the clamped medium provides a more complete preservation of the parameters of occurrence of ore bodies after the explosion due to the lower rock openness after the explosion ( $K_p = 1.05 \div 1.2$ ), but for the same reason increases the energy intensity of the excavation and the duration of the excavator cycle (Trubetskoi, 2001). Explosion in a jammed environment requires the use of commutation schemes with longitudinal cutting. What is characteristic for the drilling and explosive preparation of rock mass is the thickening of the well grid by 10-15%, which limits the minimum width of the blast block.

In the case of a multiple-row explosion without a retaining wall, the disintegration coefficient of the blasted rocks varies along the width of the blast block: for the first row of wells, it is the largest and reaches 1.6, for the second and third rows the value of  $K_p$  in comparison with its value in single-shot blasting decreases by 8-10%, for the fourth to fifth rows – by 12-15%, for the sixth to eighth series – by 20-30%. The explosion of rocks in a clamped medium (with a retaining wall) leads to a decrease in the opening ratio. The horizontal power of the buffer of the previously infiltrated rock mass should be taken within 10-15 m with a bench height of 10 m.

### Organisation of technological processes

The complex structure of mineralisation sets increased requirements for the organisation of all technological processes of mining. Separate excavation in the form of exploded rocks can be simple or complex. In this case, the extraction of valuable ores is carried out under the following basic conditions:

- the explosion of rock and ore is mainly carried out by the gross method;
- the position of the contact "ore-rock" and grades of ores is determined by the geological service with the

setting of reference points on the collapse of the blasted rock mass;

- the excavation of rock mass in a complex face is always carried out from the hanging side of the ore body to the bed, with the least loss and dilution of ores. The elimination of ore bodies from the recumbent side of the deposit to the hanging one is unadvisable;
- depending on the conditions of the occurrence, the development of a mining ledge should be envisaged in two 5-meter steps and a 5-meter-high damming subdivision. To increase the level of selective excavation in the development of low-power ore bodies, a 5-meter long canopy can be worked up by two layers 5 m;
- in accordance with the accepted technology of gross explosion, all three sizes of the blast block (width, length and height) or some of them are set regardless of the position of the contacts and the number of ore bodies on the basis of the required volume of the finished blown rock mass;
- the part of the camber is initially shipped along the roof of the ledge, with the passage of the first step on the rock from the side of the hanging side of the ore body.

The sorting is carried out only on the width of the face with a complex split notch. In case of a complex separate seizure, the quality of the mined minerals is achieved by the correct choice of the method, the thorough preparation of the face for the explosion, and the installation of the excavator as close as possible.

Losses and dilution of minerals with a simple separate excavation occur when the roof of the mining ledge is scraped, because of the mismatch between the tractor's scooping of the excavator bucket with the contacts of the deposit and the surrounding rocks, and also during loading.

The methods of complex sorting are: separate scooping, managed collapsing and their combination. With the method of complex sorting with separate scooping of ore and rock, it is advisable to separate the face into 4-5 m tall sub-steppes, and each lead should be worked by layers 2-2.5 m high (Arsentiev, 2002).

Combined methods used in the faces with complex intermittency of ore and rock are combinations of separate scooping with controlled caving or one of these methods with simple segregation or simple sorting methods (by isolating subterranean strata in individual sites, trench excavation of individual sections of the collapse), as well as sorting by fractions, the allocation of diverse and diverse grades of minerals and waste rock with temporary segregated storage in cone-shaped stacks in the bottomhole space.

Opening and preparation of production blocks is carried out on the blown up mountain mass, when dividing a ledge 10 m in height into two 5 m steps, depending on the choice of the technological scheme.

To reduce losses and dilution, it is advisable to use a technologic scheme with backhoe type excavators. Figure 1 shows an example of the excavation of two ore bodies using a PC-400 excavator. The technology includes sequential mining of the rocks by the fork of the hanging side, then the ore. Managed collapse is produced by working the bottom of the face in an order that depends on the location of the useful

object in the collapse. In the lower part of the face, in a staggered manner, trough-shaped notches are formed, into which the rock mass from the top of the face is brought down, it is shipped and then the protrusions between the recesses are worked.

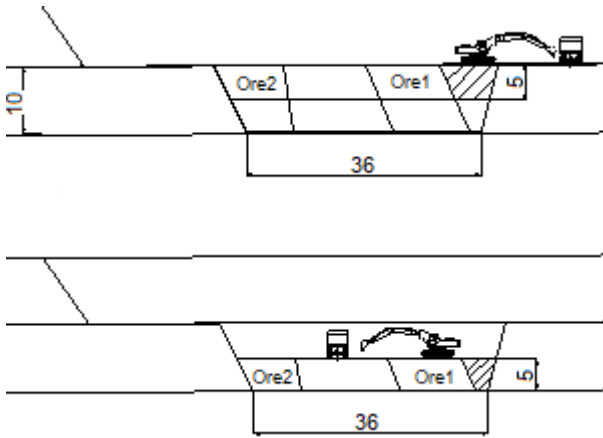


Fig. 1. Scheme of development of the sub-stages excavator PC-400

### Planning of mining operations

At the current planning stage, quality indicators and quantities of extracted ore are determined using operational exploration data and subsequently, after blasting the block, they are specified taking into account the collapse of the blasted rock mass and excavating ditches for its development. The boundary of ore grades is defined as the distance between drilling and blasting wells along the slurry, at which operational exploration is carried out in proportion to the gold content in adjacent wells by the formula.

$$\Delta = L (C_2 - C_b) / (C_2 - C_1), \quad (1)$$

where:

$C_1$  and  $C_2$  are the contents of two adjacent wells, respectively;  $C_b$  is the specified airborne content;  $L$  is the distance between the wells.

Based on the forecast results of the ores' grades for the disintegration of the blown up mass, excavating moves are planned and a passport of the mining excavator is developed. In the excavator passport, in addition to the known parameters and the order of organisation of work, the axis of the excavator stroke, the order of excavation and loading of ores of various qualities should be shown.

To achieve minimum losses and dilution of ores, it is necessary that the excavation of the contact zones of the ore body is carried out with the formation of a slope of the face in accordance with the drop in contact of the ore body. The most unfavourable conditions of excavation with an inconsistent incidence of contact and profile of the slope of the face should be avoided in every way when planning excavating moves.

The angle of the slope of the working face, on which the possibility of qualitative excavation in contact zones depends, is determined by the physical and mechanical properties and the granulometric characteristics of the blasted rock mass. The sequence of constructing the contours of the excavating cavity is as follows: in the plan for the collapse of the blown up block,

the contours of grades of ore are displayed, taking into account the displacement of their boundaries after the explosion; excavation starts are planned for block development; sections are plotted along the characteristic cross-sections of contact zones, on which the rational position of the excavating contour is carried out.

Schemes for constructing excavation contours on sections and determining the amount of removal of the excavation contour from the contour of the ore body to the surface are determined from the height of the upper triangle of losses of the normative variant of the development of the contact zone.

For the normative losses and dilution of the mineral such a level is taken that is technically possible and economically justified with the current state of the technology of mining and processing of ores in the enterprise.

With the high value of minerals, it is necessary to pay close attention to the magnitude of losses and dilution, which decrease with the decreasing height of the ledge. However, a decrease in the height of the ledge leads to a smoothing of the slope of the working bead and, consequently, to an increase in the current stripping ratio.

Thus, the rational height of the ledge can only be found by a joint examination of losses, dilution and the current stripping ratio.

### Conclusions

To achieve the minimum values of loss and dilution of ores, it is necessary the excavation of the contact zones of the ore body to be carried out by: multiple explosion in a clamped medium, which provides a more complete preservation of the parameters of occurrence of ore bodies after the explosion due to a lower rock release rate after explosion ( $K_r = 1.05 \div 1.2$ ); the method of complex sorting with separate scooping of ore and rock, with the division of the face into 4-5 m high, and the development of each approach to be carried out by layers 2-2.5 m high; formation of the slope of the face according to the drop in the contact of the ore body.

### References

- Arsentiev, A. I. 2002. *Open-cast Mine Output*. SPMI, Sankt Petersburg, 85 p.
- Burke, B. 2014. *Improving Mining Efficiency with through Seam Blasting*. 31 p.
- Burke, B. 2015. *Controlling ore blast movement*. 10 p.
- Fomin, S. I. 1999. *Quarry productivity and demand for minerals*. SPGGI (TU), Sankt Petersburg, 167 p.
- Fomin, S. I. 2002. Analiz sprosna na rynke mineral'nogo syr'ja pri opredelenii proizvoditel'nosti kar'erov (The analysis of demand in the market of mineral raw materials at determination of productivity of open-cast mining). – *Gornyj zhurnal*, 4, 48–53.
- Fomin, S. I., D. A. Vedrova. 2013. The mining technology of a thick overburden layer covering a group of flat dipping coal seams. – In: *Mine planning and equipment selection*, Vol.1, Springer, Dresden, 75–81.
- Fomin, S. I., A. O. Rodionov, S. K. Ryzhkov. 2019. Determining height of benches in open mining of

- steeply-dipping deposits with consideration of ore losses and dilution. –*International Journal of Civil Engineering and Technology (IJCIET)*, 10, 5, 312–319.
- Ganickij, V. I. 2013. *Menedzhment gornogo proizvodstva. Terminologicheskij slovar' (Mining management. Specialized dictionary)*. Gornaja kniga, Moscow, 472 p.
- Hustrulid, W. 1998. *Open Pit Mine: Planning & Design* (Eds. Hustrulid, W., M. Kuchta). Balkema, Rotterdam, Brookfield, 735 p.
- Hill, J. H. 1993. *Geological and Economical Estimate of Mining Projects*. London, 85 p. *Reduced Dilution through Ore and Waste Segregation Blasting: Case Study*. 2014. 2 p.
- Roslavtseva, Yu. G., V. P. Fedorko. 2010. Justification of the choice of a rational mode of mining operations. – *Mining Journal, University News*, Ekaterinburg, 20–26.
- Schröder, D. L. 1999. *Large surface miners – applications and cost calculations*. Krupp Fördertechnik GmbH, Essen, 98 p.
- Trubetskoi, K. N. 2001. *Proektirovanie karierov. I*. Moscow, 519 p. (in Russian)

## DEVELOPING A MEASUREMENT PLAN TO STUDY BLASTING STRESS WAVES INDUCED BY THE EXPLOSIVE BREAKAGE OF ROCK IN THE CHELOPECH UNDERGROUND MINE

Dragomir Stefanov<sup>1</sup>, Tsvetan Balov<sup>2</sup>, Ivaylo Koprev<sup>3</sup>

<sup>1,3</sup> University of Mining and Geology "St. Ivan Rilski", 1700 Sofia

<sup>2</sup> Dundee Precious Metals Chelopech EAD, 2087 Chelopech; Tsvetan.Balov@dundeeprecious.com

**ABSTRACT.** Determining the peak particle velocity (PPV) in the near-blast impact zone is a key factor in explosive breakage management. The most reliable way is to obtain actual PPV data through in-situ measurements. Such measurements, however, are difficult to conduct and have features of their own. Therefore, it is necessary to review the current practical experience, select appropriate instruments and create an optimal measurements plan. This study reflects the experience from PPV measurements in the world's leading mining countries such as Australia, Canada and the USA, and in Bulgaria as well, to clarify the mechanism of explosive breakage in the near-blast zone. The objective is to conduct, based on the international experience, successful measurements and obtain real values for the Chelopech mine. From the resulting shape of the stress wave and the PPV values the parameters of the stress waves, the duration of the compression phase, and the blast energy and impulse will be derived. These data will enable management of the blasting effect to improve ore production.

**Keywords:** blasting effect, stress waves, parameters, measurements

### РАЗРАБОТВАНЕ НА ИЗМЕРИТЕЛНА СХЕМА ЗА ИЗСЛЕДВАНЕ ПАРАМЕТРИТЕ НА ВЪЛНИТЕ НА НАПРЕЖЕНИЯ ПРИ ВЗРИВНОТО РАЗРУШАВАНЕ НА МАСИВА ЗА УСЛОВИЯТА НА РУДНИК ЧЕЛОПЕЧ

Драгомир Стефанов<sup>1</sup>, Цветан Балов<sup>2</sup>, Ивайло Копрев<sup>3</sup>

<sup>1,3</sup> Минно-геоложки университет "Св. Иван Рилски", 1700 София

<sup>2</sup> "Дънди Прешъс Металс Чelopeч" ЕАД, 2087 Чelopeч

**РЕЗЮМЕ.** Установяването на пиковата скорост (PPV) на частиците в близката зона на действие на взрива е ключов фактор за управление на взривното разрушаване. Най-сигурният начин да се получат реални данни за PPV е чрез измервания *in situ*. Тези измервания обаче са трудни и имат своите особености. Поради това, е необходимо да се проучи опитът от практиката, да се изберат подходящи измерителни уреди и да се състави оптимална схема на измерване. В настоящото изследване е отразен опитът от измервания на PPV във водещи в минното дело страни в света – Австралия, Канада, САЩ, както и в България, по изясняване на процеса на взривното разрушаване в близката зона. Целта е, въз основа на световния опит да се извършат успешни измервания и се получат реални резултати за условията на рудник Чelopeч. От получената форма на вълната на напрежения и от стойностите на пиковата скорост ще бъдат определени параметрите на вълните на напрежения продължителност на фазата на натиск, енергия и импулс на взрива. С тези данни става възможно действието на взрива да бъде управлявано за постигане на по-добри производствени резултати.

**Ключови думи:** действие на взрива, вълни на напрежения, параметри, измервания

### Introduction

Knowing the peak particle velocity (PPV), especially in the near-blast impact zone – within the line of the least resistance, allows for assessment of the operation of each individual charge in the line or fan-pattern, and of the distribution of energy within the breakage zone. Therefore, measuring it and obtaining its actual values *in situ* are of key significance in explosive-breakage management. Such measurements have their specific features and, therefore, it is necessary to review the current practical experience, select appropriate instruments and create an optimal measurement plan. Furthermore, adequate results require pre-defining of the expected velocity in order to select a suitably sensitive recipient of seismic fluctuations, to determine the method for its fastening onto the rock surface or in a borehole, and to ensure that the direction

of movement coincides with the direction of response of the unit.

While various devices, referred to as geophones, used for measuring of the far-zone blast-seismic fluctuations, are present on the market, no near-zone measurement sensors were available on the market during the studies.

This study reflects the experience from studies in the world's leading mining countries such as Australia, Canada and the USA, and in Bulgaria as well, to clarify the mechanism of explosive breakage in the near-centre blast zone. The aim is to use the global experience in order to obtain *in-situ* results specific to the Chelopech-mine about the stress wave forms and the PPV values which can be used to determine the duration of the compression phase and the blast energy and impulse. These data will enable management of the blasting effect to improve ore production.

### A study of the US Bureau of Mining (USBM) to determine the effect of charge diameter on explosive performance

The US Bureau of Mines carried out a large-scale study (Nicholls, 1966) on the effect of the charge diameter on explosive performance. Three different explosives were detonated in three different charge diameters. Three linear arrays of holes were drilled with 13 holes in each. Each array contained six shot holes, and the remaining were gauge holes with strain gauges suspended in them (Fig. 1). The experiment was used to measure relative deformation (microinch/inch). The shot-to-gauge wave arrival time was measured, as well as the time of entry of the signal into the gauge, the deformation rise and fall times, the compression phase length, and the maximum compression and strain amplitudes. These data were used to infer the pulse types. Three wave types were registered (Fig. 2). It was concluded from the processing of the data that small-diameter charges are much less effective in producing strain waves in rock than larger diameter charges of the same explosive.

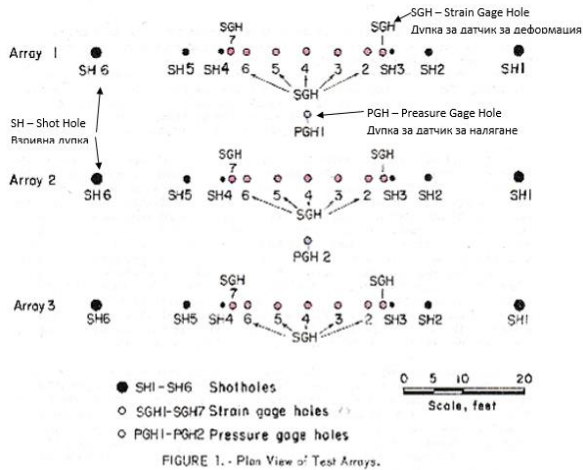


Fig. 1. Test borehole location layout

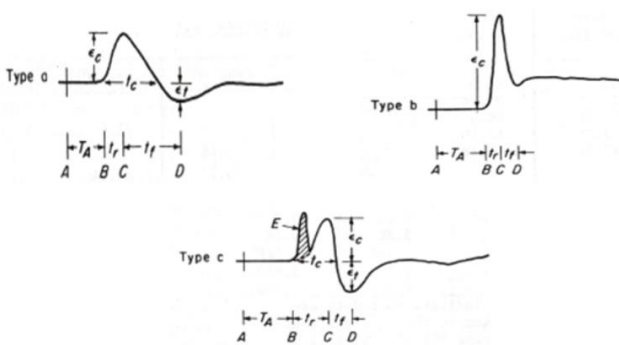


Fig. 2. Strain wave form types

Legend

A	Charge detonation time	$t_r$	Rise time
B	Beginning of strain pulse	$t_c$	Compression time
C	Pressure deformation peak	$t_f$	Fall time
D	End of strain deformation	$\epsilon_c$	Peak compression deformation
E	Part of the booster-explosive pulse	$\epsilon_t$	Strain deformation pulse
T <sub>A</sub>	Initiation time		

### Studying of strain-wave parameters during ore blasting in Bulgaria

In 1990, a study of stress wave parameters was carried out (Stefanov, 1993) in the S. Stefanov shaft mine of the GORUBSO-Zlatograd company. The aim was to determine the stress wave parameters during production blasting *in situ* and to use the study results to optimise the explosion patterns.

The explosive breakage effect in and outside the near-blast zone and, also, the effect of energy dissipation at distance were determined by measuring the peak particle velocity at different distances from the explosion centre. The particle velocity and stress in the near-blast zone are high and the gauges, which were subject to high loads, had to be specially designed.

While various devices (geophones) used for measuring of the far-zone blast-seismic fluctuations, are present on the market, no near-zone measurement sensors were available on the market during the studies. Such a gauge, converting the mechanical motion to electrical signals, can be of an induction type in which case it should ensure that the measured value is proportional to the induced electromotive voltage. Such a gauge was designed for the study (Stefanov, 1993).

When installed, the gauge must be rigidly connected to the rock. As the blast wave reaches the gauge, its body is dragged along with the moving media. Inertia and reduced friction leave the magnet immobile but move the coil, whereby electromotive voltage is generated. The special coil ensures that the resulting electromotive voltage is proportional to the *movement velocity*.

A H117 magneto-electric light-ray oscilloscope (rotating-mirror oscillograph) was used as a measuring instrument. It transformed the electrical signal from the gauge through a reflecting galvanometer (the rotating mirror) into a light ray tracing a photographic film or light-sensitive paper moving at a certain speed.

When studying single fast-flowing processes such as explosions, it is important to synchronise the measuring instrument with the time of explosion. After the oscilloscope is energised, recording the studied signal requires time for the film to reach the required speed, before the explosion pulse is sent. A synchronisation device comprising a time-setting, a power supplying and an implementing unit and with the relevant signalling capabilities was constructed for this purpose.

The schematic diagram of the measuring system is shown on Figure 3.

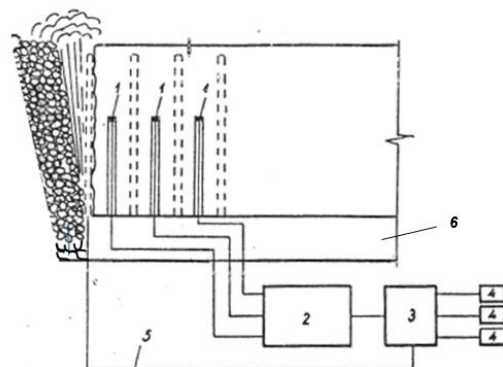


Fig. 3. A system for direct measurement of stress-waves in rocks. 1 – Gauge; 2 – Measuring instrument (rotating-mirror oscillograph); 3 – Synchronisation device; 4 – Power-supply unit; 5 – Explosion circuit; 6 – Sub-level gallery

The studies were conducted during production blasting of boreholes in a fan arrangement with one sequential and one diagonal cut-shots. The gauges were positioned at increasing distances from the blast centre:  $0.5W$ ,  $1W$ ,  $1.5W$  ( $W$  – line of the least resistance), along an axis perpendicular to the fan plane, at the level of the blast centre.

One resulting seismogram is shown on Figure 4. The signal-recording equipment (using film reel, below ground) does not always allow for good recording quality but the resulting record is readable and usable. The film shows the stress wave emitted from the borehole in the centre of the fan and registered by 3 consecutively positioned gauges, as shown on Figure 3. The record allows for measurement of the amplitudes ( $A_1$ ,  $A_2$  and  $A_3$ ) which are the peak particle velocity at three different distances, the duration of the compression phase ( $t_1$ ,  $t_2$  and  $t_3$ ), and, also, the time of entry of the wave into the second and the third gauges ( $T_{1-2}$  and  $T_{2-3}$ ). The stress rising and falling times can also be read.

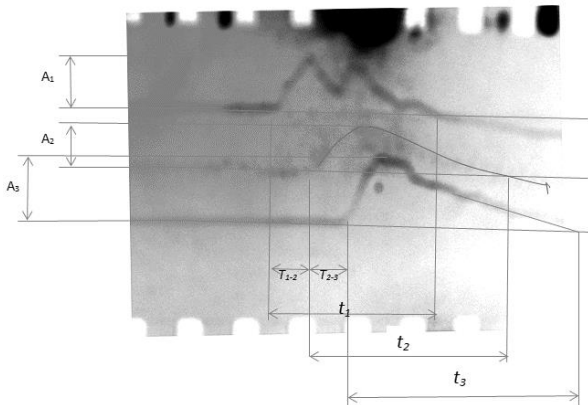


Fig. 4. A record of the stress wave emitted from the central fan borehole

Peak velocities ranging between 0.20 m/s and 4.12 m/s were registered, with a positive phase duration of 1 ms to 4 ms.

These results underlie the dependency between the peak particle velocities and the distance from the blast centre in both blasting patterns used during the study.

### A study by the Australian Centre of Geomechanics of the stress wave parameters to determine their effect on support systems

In 2006, the Australian Centre for Geomechanics published an article (Heal, D., et al. 2004) with results from a study of the performance of underground support systems subjected to rockbursts simulated by explosives. The energy absorbed by the support systems was assessed by a study of the explosion effect.

The rockburst simulation layout is presented on Figure 5. A discontinuous line shows the test wall to which two support systems and measuring instruments are attached.

Three blastholes are drilled parallel to and 5 m from the wall for the rockburst simulation.

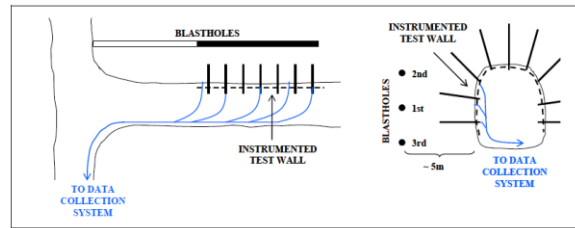


Fig. 5. Rockburst simulation layout

The measurement was conducted using 14 Hz SM6 geophones (25.4 mm in diameter and 35 mm long) connected to a 16 channel monitoring system. Sixteen geophones (2 three-axial and 14 uniaxial) were installed in different places relative to the source of energy. The two triaxial geophones were cemented into 64 mm wide and 2 m deep boreholes drilled perpendicular to the test wall. Six horizontal uniaxial geophones were mounted on the surface of the test wall to measure the stress waves at the rock-air interface. Eight horizontal uniaxial geophones were end-mounted onto 2.4 m long conical rockbolts of one of the support systems. This is a method to assess the dynamic response of the rockbolts and the rock mass.

The highest PPVs, of 2.65 m/s and 3.14 m/s, were produced by exploding of an 8 kg emulsion charge and a 16 kg charge, respectively. Also, the duration of the positive wave phases produced by blast 1 at around 4 ms and blast 2 at 2.5 ms were recorded by the seismographs.

### Measurement of stress wave parameters in rocks and in paste fill stopes at Cannington Mine in Australia

In 2006, a study (van Gool, Bronwyn, 2007) of PPV in ore rocks and in a paste-fill stope was carried out in the Cannington Mine in Western Australia. The study was intended to determine the critical peak velocities at which the artificial massif remains stable and involved two cycles. The first cycle entailed recording of production blasting in adjacent stopes, i.e. blasting in the remote zone. The measuring instruments were positioned so that the geophones could measure the PPV both in the paste fill and in the ore.

The second cycle entailed blasting the holes drilled into a gallery specially made into the paste fill, and the geophones were used to measure peak velocities from explosions in the near-impact zone.

Six three-axial geophones connected to a Blastronics BMX monitor were used. Four geophones were installed into the shot hole. The two remaining geophones were cemented in holes drilled from the side of the gallery, one in the wall adjacent to the blast holes, and the other in the rock, also near the blast holes but at a depth of 1 m.

The resulting data show that the PPVs from the same blast and at the same distances from the blast location vary. In this case this is caused by the reflection and refraction of the wave at the ore/paste-fill interface where two materials with different densities meet.

It is a known fact that waves are partially reflected and refracted at such interfaces. The higher the difference in densities between the two materials, the larger the portion of refracted or reflected wave energy will be. Paste fill is far less dense than the ore and, therefore, much of the wave energy

(up to 90% according to the Cannington Mine study) released from a blast inside it, will reflect and remain in the paste fill and only a small part will enter the rocks. If the blast occurs into the rocks, then much of the wave will reflect back into it and a small part will move into the paste fill.

The PPV results and predicted values at the ore - paste fill interface show that the paste fill is expected to cave from a blast impact with PPV above 2.5 m/s.

### Measuring of fan borehole blast energy in the INCO Mine in Canada

The performance of individual charges in the fan-pattern at the INCO shaft mine in Canada was studied to determine the extent to which charges release their energy (Mohanty B., et al., 2013). Instantel Minimate units, available on the market, were employed to record the blasting fluctuations together with three-component seismographs (geophones) and accelerometers. The recording data were extracted using a data collection analogue system.

The geophones and accelerometers were installed into galleries at certain distances from the blast location which was within the near-impact zone. As required, the units were attached to the rock surface by solid connection.

Summarised results from multiple blasts show that 56% of all shot holes release less than 20% of the expected explosive energy and that only 44% release nearly all of their energy.

### Discussion

Understanding the blast effect and determining the method of its management requires obtaining of *in situ* measurement data of the following blast-induced stress wave parameters: a) Duration of positive phase (compression),  $\tau$ , s; b) Wave length,  $\lambda$  m; c) maximal radial velocity of particle fluctuation behind the wave front (peak velocity)  $v_r$ , m/s; d) maximum radial stress  $\sigma_r$ , Pa; d) displacement of particles  $u$  during the positive wave phase  $\tau$ . e) relative positive phase pulse, Pa.s; f) relative energy,  $J/m^2$ .

The maximum radial velocity of particle fluctuations behind the wave front (peak velocity) and the duration of the positive phase (compression) are determined directly from the seismogram, while the relocation and the relative energy are derived by graphic integration.

The summarised results from the above studies show that peak particle values  $v=(4.12\pm 0.2)$  m/s have been measured in strong rocks at relative distances of  $R/R_0 = (30\div 200)$  (where  $R$  is the distance from the blast centre, and  $R_0$  is the charge radius). The positive phase of the wave varies -  $\tau=(1\div 4)$  ms. The particle movement velocities were measured at 2.65 m/s for an 8 kg of explosive charge and 3.14 m/s for a 16 kg charge. A study of PPV in ore rocks and in paste fill using 69 mm wide production shot holes, each charged with approximately 98 kg of explosive, showed peak values measured at 32 to 55 m from the blast centre of 19.2 mm/s to 32.5 mm/s in rocks and 13.6 mm/s to 78.1 mm/s in paste fill. The higher velocities in the paste fill may be explained with the interference of the stress wave from the first shot hole with those of the subsequently blasted shot holes. PPVs of 80 to 90 mm/s were obtained from other studies, at a distance of approximately 60 m from the blast centre.

Good-quality results during field studies require rigid connection of the gauge to the rock, consistency of the signal-receiving gauges and the measuring equipment with the expected stress-wave parameters, and, also, consideration of the local geological conditions of the locations in which the studies take place.

### A measurement pattern for the Chelopech Mine in Bulgaria

The analysis of such measurements practised worldwide underlies the pattern for the forthcoming measurements in the Chelopech Mine (Fig. 6).

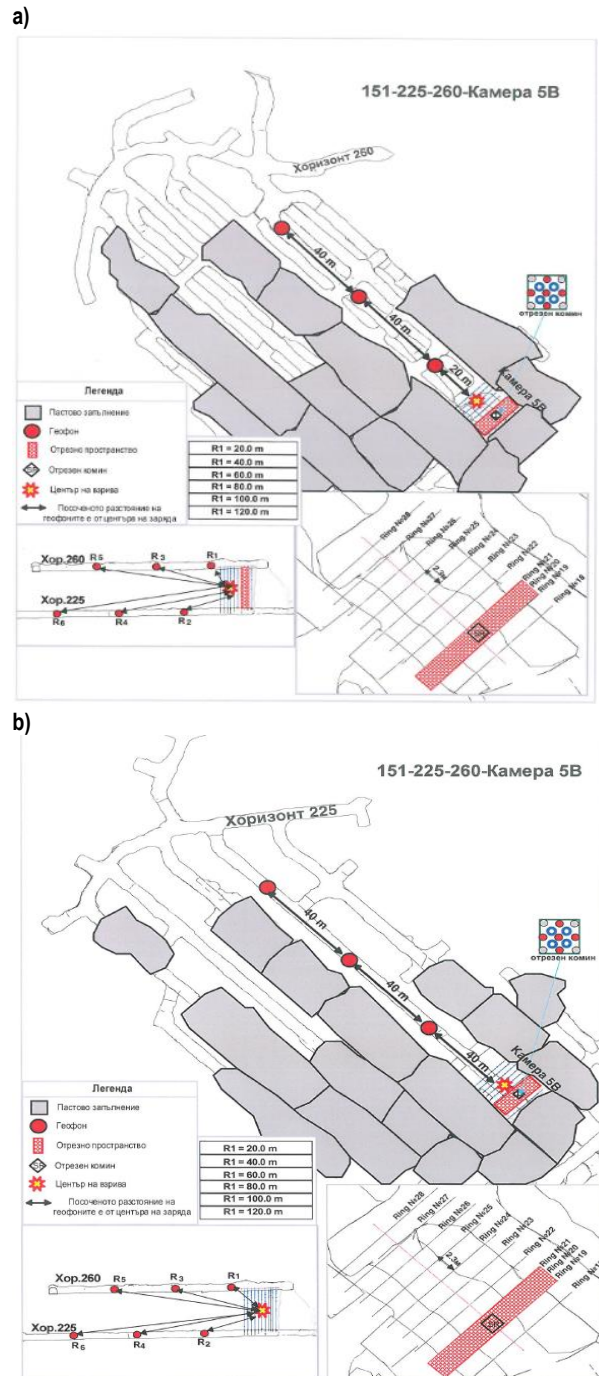


Fig. 6. Location of the geophones at levels 225 a) and 260 b)

This pattern features six geophones, of which three are installed at an upper level and three at a lower level. Each geophone will measure the particle displacement velocity and, being placed at varying distances from the blast centre, the geophones will allow determination of the energy dissipation law. The measurement will be carried out during the end stope forming stage, at which time the highest stress will be transferred through the rocks whose integrity will not have been disrupted by other blasting. The geophones will be positioned at a distance of 20 m from the charge centre. The stope will be positioned between mined and subsequently paste-filled spaces. The fans within the end stope will be positioned 1.3 m apart, and the remaining fans will be 2.3 m apart. This decision was imposed by the need for more rock-fracturing energy when opening up the end stope.

## Conclusion

The PPV study is key for the understanding of the blast effect and for the necessary management measures. According to the global experience of such practices, gauges capable of resisting high acceleration are used in the near blast-impact zone, or breakage zone, and geophones are used at different distances from the near and far zones to measure the seismic effect.

The analysis of such measurements practised worldwide underlies the pattern for the forthcoming measurements in the

Chelopech Mine, where also geophones will be used at different distances from the blast centre. This will enable measuring the particle displacement velocity and determining the energy dissipation law in the Chelopech Mine conditions.

## References

- Nicholls, H. R. 1966. *Effect of charge diameter on explosive performance*. Washington U. S. Dept. of the Interior, Bureau of Mines, 22 p.
- Stefanov, D. A. 1993. *Study of the Blasting and Drawing Processes*. Works of the Mining and Geological University, Sofia, 2. MGU, Sofia, 81 p.
- Heal, D., M. Hudyma, Y. Potvin. 2004. Assessing the in-situ performance of ground support systems subjected to dynamic loading. - In: *Villaescusa E., Y. Potvin (Eds), Ground Support 2004. Proceedings of the 5th International Symposium on Ground Support in Mining & Underground Construction*, Perth, 28-30 September 2004, 319-326.
- Van Gool, B. 2007. *Effects of blasting on the stability of paste fill stopes at Cannington Mine*. PhD thesis, James Cook University, W. Australia, 195 p.
- Mohanty B., D. Zwaan, F. Malek. 2013. Diagnostics of production blasts in a deep underground mine. - As featured in *Womp with E&MJ*, 08, [www.womp-int.com](http://www.womp-int.com).

## INNOVATIVE FORMULATIONS FOR A NEW GENERATION OF LOW-SPEED EXPLOSIVE COMPOSITIONS, DESIGNED FOR BLASTING IN TENDER CONDITIONS AND FOR EXTRACTION OF ROCK-CLADDING MATERIALS

**Nadezhda Stoycheva, Peter Shishkov**

*University of Mining and Geology "St. Ivan Rilski", 1700 Sofia; sfxman86@yahoo.com*

**ABSTRACT.** There are some fields in mining, or construction at industrial and urbanised territories, where application of regular commercial explosives and high explosives is not enough safe for the surrounding objects with regard to the generated fly-rocks, air-blast, toxic fumes, seismic waves and vibrations. The main reasons for these harmful impacts of explosion are the velocity and mechanism of the chemical reaction of explosive mixture's decomposition. The industry redirects its attention from the detonating explosives to the deflagrating pyrotechnic mixtures and propellant compositions. Utilisation of aged military arms is a good source of cheap materials for the explosive industry. The production of low explosive non-detonating mixtures from long term stored single base propellants (SBP), double base propellants (DBP) and ammonium nitrate prills in different configurations, as well as popular flash-powder compositions was studied. The samples of different cartridge casings, filled with non-detonating propellant mixtures, or flash-powder compositions was investigated by two methods for velocity of propagation. The blasting cartridges were made from the investigated materials and were examined via field tests. General information on dimension stones as well as brief information about the explosives involved in their extraction is presented.

**Keywords:** non-detonating blasting cartridges, single base propellants, double base propellants, cautious blasting, dimensional stone extraction

### ИНОВАТИВНИ РЕЦЕПТУРИ ЗА НОВО ПОКОЛЕНИЕ НИСКО-СКОРОСТНИ ВЗРИВНИ СЪСТАВИ, ПРЕДНАЗНАЧЕНИ ЗА РАЗРУШАВАНЕ В УСЛОЖНЕНИ УСЛОВИЯ И ПРИ ДОБИВ НА ДЕКОРАТИВНИ КАМЪНИ

**Надежда Стойчева, Петър Шишков**

*Минно-геоложки университет "Св. Иван Рилски", 1700 София*

**РЕЗЮМЕ.** Съществуват области в минното дело или при строителството в индустриални и урбанизирани територии, където прилагането на обичайните промишлени експлозиви не е достатъчно безопасно за околните обекти, по отношение на разлет на късове, ударно-въздушна вълна, токсични газове, сеизмични вълни и вибрации. Основната причина за вредното въздействие на експлозията са скоростта и механизма на протичане на химичната реакция при разпадане на взривната смес. Промислеността пренасочва вниманието си от детониращите експлозиви към дефлагиращите пиротехнически смеси и барутни състави. Утилизацията на остарели или ненужни боеприпаси е добър източник на евтини материали за взривната промишленост. Беше изследвано производството на ниско-скоростни (недетониращи) взривни смеси от продължително съхранявани едноосновни и двуосновни барути и порьозна амониева селитра в различни съотношения, както и звуково-светлинни пиротехнически състави. Проби от различни корпуси, напълнени с недетониращи барутни смеси, или пиротехнически състави бяха тествани чрез два метода за скорост на взривяване. От изследваните материали са изработени взривни патрони, с които са проведени полеви изпитания. Представена е обща информация за декоративните камъни, както и кратка информация за експлозивите, използвани за техния добив.

**Ключови думи:** недетониращи взривни патрони, едноосновни барути, двуосновни барути, прецизно взривяване, добив на скално-облицовъчни материали

## Introduction

### About explosive chemical decomposition

The velocity of detonation (VOD) is the rate at which the detonation wave moves through the explosive charge. The higher this speed, the greater the "force" or the crushing effect of the explosive. Explosives with high chemical decomposition rates are better suited to working on hard rocks, and those with a slower detonation to work in a soft and cracked rock. In general, "low-speed" explosives tend to release gaseous products for a relatively longer period of time, and therefore, its action is more "heave". The detonation rates of different industrial explosives are between 2500-7500 m/sec. The detonating pressure is the pressure in the reaction zone when the explosive molecules break down. The last is an important

indicator of the explosive's ability to perform a good fragmentation.

Deflagration is a subsonic reaction of the chemical decomposition of the explosives. It is typical of all types of gunpowder and solid rocket fuel. They act on the environment by the pressure generated by gaseous products during a chemical reaction and practically have almost no "shock energy". In practice, such an effect occurs when a charge of blasting gunpowder is ignited in an appropriately tamped blast hole.

### Dimension stone extraction and blasting in tender conditions

Rock cladding materials is a common term for various natural stones used for construction or for decorative purposes in buildings and monuments. The determining characteristic of

a dimension stone is that, unlike other mineral raw materials, which have a value mainly due to their physical properties, the physical properties of the rock are only the minimum qualification to determine its suitability for use as a rock cladding material. Some authors prefer the term "decorative stone", which emphasises the ornamental aspect of its use. In fact, the rock cladding material is defined as "a natural rock material cut, shaped, or selected for use in blocks, slabs, sills or other structural elements with specialised shapes and sizes". Therefore, the decorative stone has a value due to its size and appearance, emphasised by a set of minimal physical properties (among them are various strength parameters, workability, polishing ability and resistance to physical and chemical influences).

The use of explosives in quarries for decorative stones is a rather delicate issue. During the extraction of rock-cladding materials, drilling and blasting operations are carried out, both for removal of poor layers of soil and rocks (stripping) and for the initial separation of large slabs from the rock body and their splitting into smaller blocks suitable for transporting and post-processing of finished products. Across the globe, popular industrial explosives are used to break up unnecessary rock and soil layers, but when approaching high-quality stone deposits, blasting technologies must be more precise and prevent costly material from being destroyed.

In such cases, the high explosives are successfully replaced by low-velocity explosives. There are other areas in the mining industry or in construction in industrial and urban areas, where the use of ordinary industrial explosives is not safe enough for surrounding sites in terms of fly-rocks, shockwave formation, toxic gases, seismic waves and vibration. The main cause of the detrimental effect of the explosion is the speed and mechanism of the chemical reaction of the explosive mixture decomposition. It is exactly the detonation that causes the fragmentation and the formation of cracks in the rock body. The surfaces of the stone blocks must not be deeply damaged by the blast wave with micro-cracks, as this will lead to financial losses due to the high value of the qualitative decorative stones. They should only be affected by the creation of single cleavage cracks in one, two or three planes, depending on the technological needs. Therefore, the use of industrial explosives and high-explosives for dimension stone extraction is not preferred by the owners of such quarries.

The industry is shifting its attention from detonating explosives to deflagrating pyrotechnic mixtures and propellant compositions, which suddenly create a large volume of compressed hot gaseous products with no shock wave and really little solid residue. The charges of these new explosives must be resistant to moisture, shock, heat, friction and electrical discharge. In the past, the usual solution was the black powder. The so called "blasting gun powder" (BGP) was applied orderly for dimensional stone extraction and in other cases - for cautious blasting in tender conditions. But its sensitivity to various influences (flame, heat, moisture, friction, shock) in combination with the lower energy of reaction, the toxic fumes and the solid products induced scientific research for more advanced and safer alternatives. Nowadays, the most important requirement of the industry to the explosive manufacturers is the safety of their products regarding storage, transportation and usage. Another important question is the

price. Utilisation of aged military arms is a good source of cheap materials for the explosive industry.

### Waste smokeless gunpowders

It is well known, that single based propellants (SBP) in general are pelletized or extruded porous grains in different sizes and shapes, which usually contain 93-97% pyroxylin and 3-6% additives like dibutylphtalate or dimethylacrylate or camphor (phlegmatizers), diphenylamine (stabilizer),  $\text{KNO}_3$  or  $\text{K}_2\text{SO}_4$  (pore-forming salt), graphite, remaining alcohol-ether solvent, etc. DBP are mixtures of nitrocellulose (NC), 2-8% additives (similar to these in SBP) and nitro-esters usually nitro-glycerine (NG). The content of NG is about 10-38%. The boiling point of NG is  $50^\circ\text{C}$ . Double base propellants (DBP) may have higher energy content than SBP. Their caloric content varies between 3800 and 5200 kJ/kg depending on their type. The grains of DBP are also with different sizes and shapes. They could be compact or porous. The application of DBP for obtaining an adhesive effect in low-explosive mixtures is a possible approach against the stratification of the ingredients, which are with different sizes and weights. The prices of waste SBP and DBP in Bulgaria are around 0.10 BGN/kg.

### Experiments

The used secondary propellants were produced in 198 at Arsenal EAD, Bulgaria, and were aged in dry atmosphere without any light.



Fig. 1. General image of DBP type NDT-3 18/1 and SBP type 18/1 (down)

The nitro-glycerine gunpowder (DBP) with the brand name NDT-3 18/1 and the 18/1-branded pyroxyline SBP with long tube-shaped bodies should be further processed by grinding after the extraction from the unnecessary army munitions. The size of propellant grains should be similar to the size of the porous prills of ammonium nitrate as protection against stratification of the ingredients. This implies the development of a facility for safe and effective milling of these brands of gunpowder before their further usage.

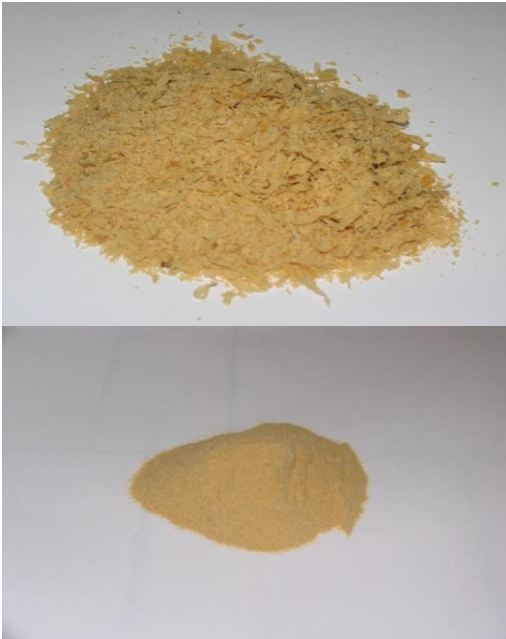


Fig. 2. General image of DBP and SBP type after grinding in the mill

For this purpose, a special facility - a mill has been used. After grinding, the grains pass through a 4 mm, 2 mm, 1 mm, 0.8 mm, 0.4 mm and 0.2 mm clear screen. Figure 2 shows the resulting powdery grains after grinding with a particle size of up to 0.2 mm.



Fig. 3. General appearance of the grinding mill for secondary smokeless gunpowder

Three different low-explosive compositions were prepared and loaded in testing cartridges:

- **Mixture #1:** "flash-powder composition" 65% KClO<sub>4</sub> + 35% Al (dark) with Oxygen Balance = -1.12%;
- **Mixture #2:** 80% gridded DBP + 20% NH<sub>4</sub>NO<sub>3</sub> prills with Oxygen Balance = -7.92%;
- **Mixture #3:** 70% gridded SBP + 25% NH<sub>4</sub>NO<sub>3</sub> + 5% Al (dark) with Oxygen Balance = -5.19%;

The ready compositions were loaded in aluminium testing tubes, plugged from the both sides, with the following dimensions:

- 320 mm /φ10 mm inner diameter/ 1 mm wall thickness;
- 320 mm /φ20 mm inner diameter/ 1 mm wall thickness.

Each pipe has three drill holes: first for electric ignition, second for sensor #1 (located at 3 cm from the first hole) and third for sensor #2 (located at 25 cm from the second hole). The ignition of the samples was made by using regular commercial electric "bridge-wire" igniters with smooth burning fuse-head for fireworks and professional pyrotechnic purposes, manufactured by "META PYRO" s.r.o., Czech Rep.



Fig. 4. Loaded and plugged aluminium pipes with el. igniter - ready for test samples

The deflagration velocity was measured by two different devices:

- the "Trio Chronos" apparatus, manufactured by "TRIO Electronics" Ltd., Republic of Serbia, using optic fibre sensors;



Fig. 5. Apparatus for measurement of VOD optical sensors

- the "CNT-66 Pendulum" apparatus, manufactured by "BRL Test" Inc., USA, using a contact wire impact sensor.



Fig. 6. Apparatus for measurement of VOD with an impact sensor

Sensors and an electric starter were connected to the testing equipment. All laboratory experiments were conducted at the laboratory testing area of "Minproekt", Dragichevo.

After open-air laboratory experiments, a field test at the stone quarry was carried out.

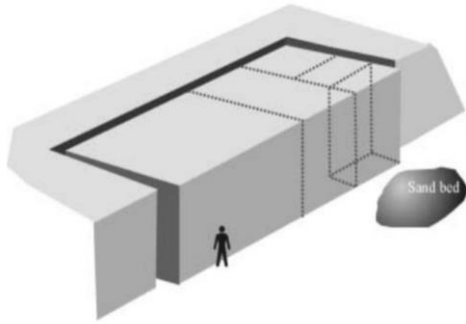


Fig. 7. Principal schedule for extraction of rock-cladding materials – from primary blocks to smaller sized slices, which will be further divided to commercial blocks

## Results and discussion

The results from testing of the deflagration velocity of different samples are given in Table 1.

Table 1. Results from testing of the deflagration velocity of different samples

Sample №	Inner diameter of the testing tube [mm]	Type of mixture	Velocity of reaction [m/sec.]
1	10	#1	224.46
2	10	#1	7.42
3	10	#1	637.59
4	10	#2	182.23
5	10	#2	251.46
6	10	#2	190.12
7	10	#3	208.67
8	10	#3	334.44
9	10	#3	267.16
10	20	#1	531.32
11	20	#1	1847.70
12	20	#1	897.37
13	20	#2	451.45
14	20	#2	390.08
15	20	#2	407.92
16	20	#3	536.88
17	20	#3	467.14
18	20	#3	537.89

It is visible from the results that Mixture #1 (flash-powder) gives higher velocities of explosive decomposition and because of their bigger diameters of the charges it is prone to pass from combustion to detonation, which is not suitable to the industrial requirements for low-explosive charges. Mixture #2 (with SBP) and Mixture #3 (with DBP) are increasing their velocities of deflagration with enlarging the diameter of the charge, but the samples containing DBP and Aluminium are releasing more energy, as expected.

An approach for exploiting the flash powder energy (Mixture #1) without a risk of transition from deflagration to detonation was invented for the field tests at the stone quarry. It is well known, that the main reasons for this transition are the

high temperature, the high pressure and the big volume of the charge. Small amounts of flash powder (4 g.), accommodated in well plugged paper tubes with a tiny hole, were separately used for the preparation of pyrotechnic petards with zero-delay. Ready petards were applied for the creation of decoupled chain charges with different gaps (air-spacing), by fixing them to a wooden stick and connecting them with a quick fuse. Thus, very low concentrations of the explosive charge in the drill-holes (between 0.040 and 0.065 kg/m) were achieved. Hard casing of the petards and air-gaps between adjacent charges, as well as air-gaps between the charges and the walls of the bore-hole do allow the so-called “flash over”, nor increasing of the pressure to dangerous rates for the transition to detonation. Reliable inert stemming from the top charge to the mouth of the blast-hole assured the necessary conditions for enough pressure of gaseous products, which ensures the needed crack in the desired plane.



Fig. 8. Field test with decoupled chain-charges for smooth splitting at stone quarry

These de-concentrated chain-charges become suitable for really smooth blast-splitting of thin stone slabs, preventing the risk of undesirable fractures and micro-cracks in the material. For successful blast-cutting without undesirable losses of expensive stone material, a very important condition for at least four free surfaces should be accomplished. Otherwise, some curvatures in the direction of the planned crevices could be expected.



Fig. 9. Effect after experimental cautious blast-splitting of stone slice with divided chain-charges

For the field tests at the stone quarry, mixtures #2 and #3 were used for the preparation of 100 g charges in thin plastic bags, fitted to the diameter of drilled holes. The length of the blast holes was 1.60 m. For better distribution of the energy of compressed gases, the explosive charge was separated in two

parts with inert stemming between them and simultaneous ignition.



Fig. 10. Ready for loading charges of propellant-based non-detonating compositions

The initial impulse of each charge was provided by fast-speed-deflagrating pyrotechnic booster for better performance of the propellant mixtures. A single petard, containing 4 grams flash composition (Mixture #1) with an electric igniter, was a good solution for that “pyro-booster”. The weight of the bottom charge was 0.200kg. The second charge, located in the middle of the hole’s length contained 0.100 kg mixture. The total explosive quantity in each blast-hole was 0.300kg propellant mixture. Reliable inert stemming between the charges and especially from the second charge to the mouth of the blast-hole assured the necessary conditions for enough pressure of gaseous products. That guarantees the best possible crack formation for splitting. In order to achieve smoother and more even cracks in the necessary cut-planes, the spacing and collaterality between the drill-holes should be very precise.



Fig. 11. Results after the experimental blasting with propellant-based non-detonating compositions (Mixtures #2 and #3)

The price of the applied materials was 0.6 BGN for the production of one testing cartridge.

## Conclusion

The application of waste SBP and DBP after utilisation of old and unnecessary ammunitions is studied for obtaining non-detonating explosive cartridges, suitable in dimension stone mining, as well as for blasting activities in tender and complicated conditions. The velocities of propagation of the reaction of chemical destruction of the tested three different high-energetic compositions were between 180 and 600 m/sec. depending on the diameter of the charges and the ingredients. The propellant based samples did not show any tendency for transition from deflagration to detonation in case of ignition with a soft burning electric fuse-head. The results from the blast-splitting tests in a stone quarry were satisfactory. There were no undesired cracks in the treated rock bodies. No fumes emission, air-blast or fly-rocks were detected after the explosion of propellant-based compositions #2 and #3. The flash-powder (Mixture #1) showed higher velocities of deflagration and because of the bigger diameters of the charges it is prone to pass from combustion to detonation, which makes it useful only for “mini-pyro-boosters” or multi-deck charges from chained small diameter petards.

**Acknowledgements.** Cordial thanks to the management and employees at the laboratory of “MINPROEKT”, Dragichevo and “RIOLIT-B”, Plovdiv for the provided sites, workers and equipment during the laboratory and field experiments of the samples.

## References

- Bozhilov, N. 2018. *Proizvodstvo na vodosadarzhashti promishleni eksplozivi, sensibilizirani s bezdimni baruti, polucheni ot utilizaciyata na nenuzhni boepripasi*. PhD Thesis (in Bulgarian).
- Mitkov, V. 2007. *Proizvodstvo na eksplozivi za grazhdanski tseli* (in Bulgarian).
- Mitkov, V. 2010. *Bezopasnost pri proizvodstvoto i upotrebata na eksplozivi* (in Bulgarian).
- Shishkov, P., N. Stoycheva. 2018. Savremenni vzrivni tehniki za dobiv na skalno-oblicovachni materiali. – *Mining and Geology Magazine*, 10–11, 42–49 (in Bulgarian with English abstract).

## COMPUTATIONAL POTHOLE MINE SUBSIDENCE ANALYSIS FOR MULTILAYER SITES

**Nandor Tamaskovics<sup>1</sup>, Detlev Tondera<sup>1</sup>, Pavel Pavlov<sup>2</sup>, Luben Totev<sup>2</sup>**

<sup>1</sup> Geotechnical Institute, TU Bergakademie Freiberg, 09599 Freiberg; [tamas@tu-freiberg.de](mailto:tamas@tu-freiberg.de)

<sup>2</sup> University of Mining and Geology "St. Ivan Rilski", 1700 Sofia; [srs@mgu.bg](mailto:srs@mgu.bg)

**ABSTRACT.** The use of sites in old or active mining regions or with natural openings in the ground includes an elevated technical risk, as constructions can be constrained due to unplanned deformations of the subsoil. Typical failure modes include pothole subsidence or earth falls, when failing soil masses are displaced and loosened stepwise toward a collapsing opening in the ground. The displacement process continues until a stable static equilibrium is reached and a further propagation of displacements is prevented. In order to determine the failure probability on a given site due to pothole subsidence, an efficient generalised computational prognosis method for the practical estimation of the expected subsidence volume is required and proposed based on simple geotechnical assumptions for multilayer sites and general primary failure volume configurations.

**Keywords:** mine, subsidence, pot-hole, deformation, prognosis

### ИЗЧИСЛИТЕЛЕН АНАЛИЗ НА МУЛДАТА НА СЛЯГАНЕ В МНОГОСЛОЙНИ ОБЕКТИ

**Нандор Тамашкович<sup>1</sup>, Детлев Тондера<sup>1</sup>, Павел Павлов<sup>2</sup>, Любен Тотев<sup>1</sup>**

<sup>1</sup> Геотехнически институт, ТУ Минна академия Фрайберг, 09599 Фрайберг

<sup>2</sup> Минно-геоложки университет "Св. Иван Рилски", 1700 София

**РЕЗЮМЕ.** Експлоатирането на обекти и конструкции в стари или активни минни райони в земята включва повишен технически риск, тъй като конструкциите могат да бъдат ограничени поради непланирани деформации на подпочвените слоеве. Типичните разрушавания включват мулда на слягане или срутища, когато обрушаващите почвени маси се изместват и отслабват стъпаловидно към образувалото се срутище. Процесът на изместване продължава, докато се постигне стабилно статично равновесие и се предотврати по-нататъшното разпространение на пропаданията. За да се определи вероятността за разрушение на даден обект поради мулдата на слягане, е необходим ефективен обобщен изчислителен прогнозен метод за практическото изчисляване на очаквания обем на слягане. Такъв метод е предложен, основан на прости геотехнически предположения за многослойни обекти и общи конфигурации на обема на първични разрушавания.

**Ключови думи:** рудник, слягане, мулда на слягане, деформация, прогноза

### Introduction

The use of sites in old or active mining regions or with natural openings in the ground includes an elevated technical risk, as constructions can be constrained due to unplanned deformations of the subsoil. Typical failure modes include pothole subsidence or earth falls, when failing soil masses are displaced and loosened stepwise toward a collapsing opening in the ground. The displacement process continues until a stable static equilibrium is reached and a further propagation of displacements is prevented.

In order to determine the failure probability on a given site due to pothole subsidence, an efficient generalised computational prognosis method for the practical estimation of the expected subsidence volume is required and proposed based on simple geotechnical assumptions for multilayer sites and general primary failure volume configurations.

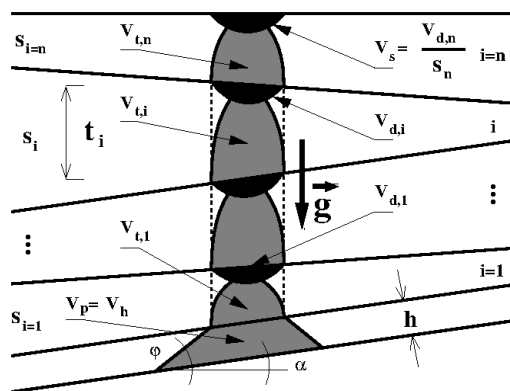


**Fig. 1. The concept of the Generalised Failure Volume Balance Method (GFVBM) in the first layer above the initial volume**

## Generalised Failure Volume Balance Method

The simple and robust concept of the Generalised Failure Volume Balance Method (GFVBM) for computational pothole subsidence analysis on a site with multiple layers can be seen in Figure 1. The method is a straightforward extension of the Failure Volume Balance Method (FVBM) (Meier et al., 2005; Tamaskovics et al., 2017).

In an artificial or natural void space with the height of  $h$  and inclination  $\alpha$ , a local failure with an assumed elliptical cross section takes place in the roof over a length of  $2a_0$  and width of  $2b_0$ . The void space inclined with the angle  $\alpha$  is filled with failing masses, where a primary (initial) volume  $V_p = V_h$  develops with a typical bulk friction angle  $\phi$ . In the subsoil, a failure zone extends vertically in all layers consecutively towards the ground surface.

During the failure process, the material volume is increased with a material specific loosening factor  $s_i$  in each layer "i" that is well known from extensive long term field observations on different types of geogene materials (see Table 1).

If the failure process reaches the ground surface, a secondary (surface) subsidence volume  $V_s$  will result and can be computationally estimated with the simple theoretical framework of the Generalised Failure Volume Balance Method (GFVBM).

Table 1. Typical loosening factor values derived from extensive long term field observations (Sroka et al., 2018)

Author	Value of the loosening factor $s$ [1]
Kuzniecowa (1950)	1.15 - 1.35 (for Russian conditions)
Lisnowski (1959)	1.40 - 1.80
Salustowicz and Galanka (1960)	1.01 - 1.25
Chudek (Borecki, Chudek, 1972)	1.30 - 1.60
Czechowicz, Kuzniecowa, Dawidianic, Kilaczkow (Borecki, Chudek, 1972)	1.40
Znański (1974)	1.08 (shales) - 1.35 (sandstones)
Niemiec (Jarosz 1977)	$1.23 \pm 0.064$
Staroń (1979)	1.35 - 1.40
Peng (1986)	1.10 - 1.50
Whittaker and Reddish (1993)	1.33 - 1.50
Mazurkiewicz, Piotrowski, Tajduś (1997)	1.15 - 1.50 (for Polish conditions)
Das (2000)	1.05
Piechota (2003)	1.35 - 1.45 (shales and other rocks with low strength parameters) 1.40 - 1.60 (hard rocks with medium strength parameters) 1.45 - 1.80 (hard rocks with high strength parameters)
Heasley (2004)	1.05 - 1.35

## Theoretical concept

The theoretical concept of the generalised failure volume balance method (GFVBM) is based on the governing volume conservation equation

$$V_{d,i} = V_p - \sum_{i=1}^n V_{t,i} (s_i - 1), [m^3], \quad (1)$$

where a deficit volume  $V_{d,i}$  is systematically computed at each layer boundary "i" from the failure mass volume  $V_{t,i}$ , the material specific loosening factor  $s_i$  and the layer thickness  $t_i$ .

At each layer boundary, the propagation of the failure process is assumed to continue, if the resulting deficit volume  $V_{d,i}$  in a layer "i" is positive

$$V_{d,i} > 0, [m^3]. \quad (2)$$

In layers with full propagation of the failure process, the form of the failure zone is assumed as a **cylinder** with an elliptical horizontal cross section. The propagation of the failure process is assumed to cease, if the resulting deficit volume  $V_{d,i}$  in a layer "i" is negative or vanishes

$$V_{d,i} \leq 0, [m^3]. \quad (3)$$

In all layers with ceasing propagation of the failure process, the form of the failure zone is assumed as a **half ellipsoid** with elliptic horizontal cross section.

If the pothole failure process propagates up to the ground surface through all "n" layers in the subsoil, a secondary (surface) failure volume  $V_s$  is expected to develop

$$V_s s_n = V_{d,n} > 0, [m^3] \quad (4)$$

that can be estimated with equations (1) and (4) from the primary failure volume  $V_p$ , the consecutive failure volumes  $V_{t,i}$  and loosening factors  $s_i$  in the individual layers

$$V_s = \frac{1}{s_n} \left( V_p - \sum_{i=1}^n V_{t,i} (s_i - 1) \right), [m^3]. \quad (5)$$

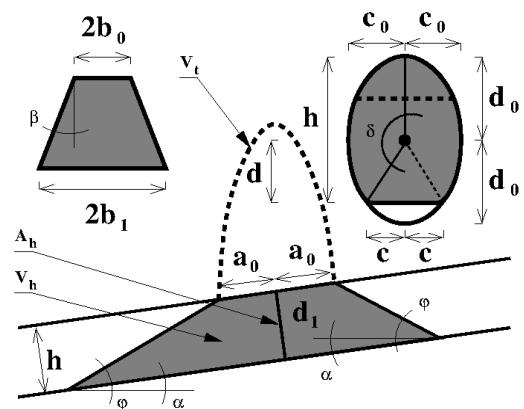


Fig. 2. Initial (primary) failure volume prognosis

### Primary failure volume prognosis

The primary (initial) failure volume in a linear void space, like a mine road or tunnel with a height  $h$ , inclination  $\alpha$ , bulk friction angle of the failing mass  $\varphi$ , elliptic failure aperture with surface area  $A_0$  and void space cross section area  $A_h$  can be easily estimated from the general equation (see Figure 2).

$$V_p = V_h = A_0 h + A_h h \frac{\tan(\varphi - \alpha) + \tan(\varphi + \alpha)}{2 \tan(\varphi - \alpha) \tan(\varphi + \alpha)}, [m^3]. \quad (6)$$

Similar equations can be derived for different volumetric failures in caverns and mine roads or tunnel crossings (Meier et.al., 2005). The accuracy of the primary (initial) failure volume is essential for the quality and reliability of a computational pothole subsidence prognosis.

### Failure aperture surface area

Under assumption of an elliptic form, the surface area  $A_0$  of the failure aperture with a length of  $2a_0$  and width of  $2b_0$  in the roof of the void space can be estimated (see Figure 2).

$$A_0 = a_0 b_0 \pi, [m^2] \quad (7)$$

### Timber securing

In case of a classical timber door securing of failing mine roads with a roof width of  $2b_0$  and a side inclination angle  $\beta$  to the vertical, the cross section area  $A_h$  of the primary (initial) failure volume  $V_p = V_h$  can be derived from (see Fig.2)

$$A_h = b_0 b_1 h, [m^2] \quad (8)$$

where  $b_1$  is the width of the road base

$$b_1 = b_0 + h \tan \beta, [m^3]. \quad (9)$$

### Roads and tunnels with elliptic or circular cross section

The cross section area of a tunnel with elliptic form with a height of  $2d_0$  and a width of  $2c_0$  can be calculated from the equations

$$h \leq d_0 : A_h = 2c_0 d_0 \delta - cd, [m^2] \quad (10)$$

and

$$h > d_0 : A_h = 2c_0 d_0 \delta + cd, [m^2] \quad (11)$$

depending on the height of the void space  $h$ . The height  $d$  and the width  $c$  are obtained from the geometry of the elliptical road cross section of  $d_0$  half height and  $c_0$  half width. In the

preceding equations, the angle  $\delta$  is assumed to be symmetric to the vertical direction and must be inserted in radians.

In case, that the half height  $d_0$  and half width  $c_0$  coincide, the equations (10) and (11) transform to the case of a tunnel with circular cross section and radius  $r=c_0=d_0$ .

Table 2. Computational pothole mine subsidence analysis with the practical application of the Generalised Failure Volume Balance Method for the case of a timber door secured mine road failure in a multi-layer site

Half length of failure aperture	$a_0 =$	1.1 [m]
Half width failure aperture	$b_0 =$	0.9 [m]
Height of failing mine road	$h =$	2.0 [m]
Inclination of failing mine road	$\alpha =$	5.0 [°]
Inclination of timber door	$\beta =$	10.0 [°]
Bulk friction angle	$\varphi =$	30.0 [°]
Primary (initial) failure volume $V_p = V_h = 21.602 [m^3]$		
Layer:	Height:	Loosening factor:
$l$	$t_i$	$s_i$
[1]	[m]	[1]
1	7.0	1.10
2	8.0	1.15
3	9.0	1.20
4	10.0	1.25
Secondary (surface) failure volume $V_s = 3.818 [m^3]$		
Deficit volume:		
$V_{d,i}$		
[m <sup>3</sup> ]		
+19.433		
+15.663		
+10.008		
+4.772		

### Practical application

The practical application of the Generalised Failure Volume Balance Method (GFVBM) is demonstrated in an example calculation for a failing timber door secured mine road in a multi-layer site. The input values and calculation results can be seen in Table 2.

The mine road with a height of  $h=2.0[m]$ , a side inclination of  $\beta=10[^\circ]$  and a base inclination of  $\alpha=5[^\circ]$  is assumed to fail in its roof over an elliptic failure aperture with a half width of  $b_0=0.9[m]$  and a half length of  $a_0=1.1[m]$ , being filled with failing masses depositing with a bulk friction angle of  $\varphi=30[^\circ]$ . In the individual layers in the subsoil with heights  $t_i$  and loosening factors  $s_i$ , consecutively positive deficit volumes  $V_{d,i}$  indicate the propagation of the pothole subsidence failure process up to the ground surface, leading to an expected secondary (surface) failure volume of  $V_s=3.818[m^3]$ .

### Summary and Conclusions

The use of sites in old or active mining regions or with natural openings in the ground includes an elevated technical risk, as constructions can be constrained due to unplanned deformations of the subsoil. Typical failure modes include pothole subsidence or earthfalls, when failing soil masses are displaced and loosened stepwise toward a collapsing opening in the ground. The displacement process continues until a stable static equilibrium is reached and a further propagation of

displacements is prevented. In order to determine the failure probability on a given site due to pothole subsidence, an efficient generalised computational prognosis method for the practical estimation of the expected subsidence volume is required and proposed based on simple geotechnical assumptions for multilayer sites and general primary failure volume configurations.

The simplistic theoretical framework and low number of required input parameters make the practical application of the Generalised Failure Volume Balance Method (GFVBM) very easy and advantageous for inverse analyses, probabilistic studies or risk evaluations with mathematical methods (Tamaskovics, 2019). Based on available long term observations and field studies, the proposed prognosis method can be applied independently from the geogene material in the subsoil (see Table 1).

## References

- Fenk, J. 1981. Eine Theorie zur Entstehung von Tagesbrüchen über Hohlräumen im Lockergebirge. – *Freiberger Forschungshefte, Reihe A, Geotechnik, Ingenieurgeologie, Bergbautechnologie, Verfahrenstechnik, A639b*, Freiberg, 139 S.
- Fenk, J., W. Ast. 2004. Geotechnische Einschätzung von Bruchgefährdeten Baugrunds. – *Geotechnik*, 27, 1, 59–65.
- Kratzsch, H. 1997. *Bergschadenkunde*. Deutscher Markscheiderischer Vereine.V., Herne, 844 S.
- Meier, J., G. Meier. 2005. Modifikation von Tagesbruchprognosen. – *Geotechnik*, 28, 2, 119–125.
- Séchy, K. 1966. *The Art of Tunneling*. Akadémiai Kiadó, Budapest, 891 p.
- Sroka, A., K. Tajduś, R. Misa, M. Clostermann. 2018. The possibility of discontinuity/sinkholes appearance with the determination of their geometry in the case of shallow drifts. – In: *Meier, G. et al. (Eds.). Tagungsband 18. Altbergbau-Kolloquium, Bergwerk Wieliczka, 29*, Freiberg, 173–185.
- Tamaskovics, N. 2018. Unscharfe praktische Tagesbruchprognose. – In: *Meier, G. et al. (Eds.). Tagungsband 18. Altbergbau-Kolloquium, Bergwerk Wieliczka, 16*, Freiberg, 435–457.
- Tamaskovics, N. 2019. Allgemeines unscharfes Verfahren zur rechnerischen Tagesbruchprognose. – In: *Benndorf, J. (Ed.). Tagungsband 20. Geokinematischer Tag, 16*, Freiberg, 435–457.
- Tamaskovics, N., P. Pavlov, L. Totev, D. Tondera. 2017. Computational pothole mining subsidence analysis. – *Journal of Mining and Geological Sciences*, 60, 2, 7–9.

## ON THE DISTORTED CONTOUR OF AN ELLIPTICAL OPENING PASSING A ROCK MASS WITH A HORIZONTAL PLANE OF ISOTROPY

**Violeta Trifonova-Genova**

*University of Mining and Geology "St. Ivan Rilski", 1700 Sofia; violeta.trifonova@yahoo.com*

**ABSTRACT.** The question of determining the displacements in transversal isotropic rock mass is discussed in the article. The plane of isotropy is horizontal. The specified class of tasks is solved by the complex variable theory. According to this method, it is necessary to solve two tasks for determining the displacements in the environment under consideration. In the first task the rock is undistorted, but in the second task it is expressed after advancing the opening. The displacements in the first task are known and those in the second task are expressed by two complex potential functions of stresses. These functions and the displacements themselves in involved form at points of the surrounding rock mass around the opening have been identified in a previous work by the author. Displacements' values on a contour of elliptical opening for a real transverse isotropic rock mass have been obtained. The deformed contour of the opening is depicted through them. The presented solution complements the idea of changing the type of contour.

**Keywords:** elliptical opening, transversal isotropic rock mass, displacements

### ВЪРХУ ДЕФОРМИРАНИЯ КОНТУР НА ЕЛИПТИЧНА ИЗРАБОТКА, ПРЕМИНАВАЩА МАСИВ С ХОРИЗОНТАЛНА РАВНИНА НА ИЗОТРОПИЯ

**Виолета Трифонова-Генова**

*Минно-геоложки университет "Св. Иван Рилски", 1700 София*

**РЕЗЮМЕ.** В статията се разглежда въпросът за определяне на преместванията в трансверзалноизотропен масив около елиптична изработка. Равнината на изотропия е хоризонтална. Указаният клас задачи се решава с теория на функцията на комплексна променлива. Според него е необходимо да се решат две задачи за определяне на преместванията в разглежданата среда. В първата задача скалата е ненарушена, а във втората задача тя се разглежда след прокопаване на отвора. Преместванията в първата задача са известни, а тези от втората задача се изразяват чрез две комплексни потенциални функции на напреженията. Тези функции и самите премествания в явен вид в точки от околната скална маса около отвора са определени в предишна работа на автора. За реален трансверзалноизотропен масив са получени стойностите на преместванията по контура на елиптична изработка. Чрез тях е изобразен деформирания контур на изработката. Представеното решение допълва представата за проявата на вида на контура.

**Ключови думи:** елиптична изработка, трансверзалноизотропен масив, премествания

### Introduction

In order to examine the displacements of the rock mass in underground mining opening it is necessary to periodically determine the mutual position of individual points of its profile and compare with their original location in ground. Study and tracking of displacements is done by organising and conducting instrumental measurements over a fixed period of time according to the observed process of deformation. Special observing stations are used for this purpose. The geodesic and mine surveying methods have an important role in the study (Tzonkov et al., 2018a; 2018b). Specific software packages, software products of a more general nature and separate programmes are used to process measurement data.

In addition to these methods, classical methods of the elasticity theory are known. In these methods the solution depends on an appropriate function of stress. This function in (Nikolaev et al., 2016) is presented in an infinite ascending order. The function in (Muskhelishvili, 1963) is a sum of two functions of a complex variable (England, 1971; Denis, 2011). These functions have been output for a single round hole passing through an isotropic rock mass (Sahoo et al., 2014; Savin,

1961; Minchev, 1960). This solution is also developed for an elliptical opening (Savin, 1961; Minchev, 1960a; 1960b) and for a square opening (Lei et al., 2001; Guangpu et al., 2015).

When the rock mass has the horizontal plane of isotropy and the opening is elliptic, the expressions of stresses are obtained in (Minchev, 1960b). In this work the expressions of the displacements aren't given. This made it necessary to write the analytical expressions of the complex potential functions (Trifonova-Genova, 2018a) and to determine the expressions of the displacements in involved form (Trifonova-Genova, 2018b). Thus, the deformable contour of the hole for real rock mass can be obtained and this is the purpose of the present paper.

### Methods

#### Formulation of the problem

A horizontal opening in the form of an ellipse is drawn in the rock mass at a sufficiently large depth  $H$ . The beginning of the coordinate system is selected to be the centre of the opening. The rock mass is transversally isotropic with a

horizontal plane of isotropy. The vertical stress in undistorted rock mass  $Q$  is obtained after multiplying the volumetric weight  $\gamma$  and the depth  $H$  of the opening (fig.1). The coefficient  $k_1$  of the lateral pressure participates in the expression of horizontal stress in same rock mass.

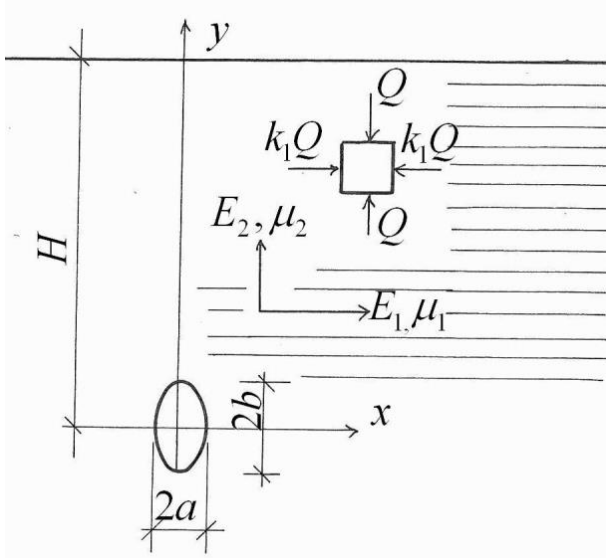


Fig. 1. Horizontal elliptical opening in rock mass with a horizontal plane of isotropy

**Expressions of the displacements**

To solve the problem the plane elastic complex variable function method is used. The displacements are a sum of the displacements in undistorted rock mass and the displacements as a result of work progress (Trifonova-Genova, 2018a; Minchev, 1960a):

$$\begin{aligned} u_x &= u_{x0} + 2 \operatorname{Re}[p_1 \Phi_1(z_1) + p_2 \Phi_2(z_2)]; \\ u_y &= u_{y0} + 2 \operatorname{Re}[q_1 \Phi_1(z_1) + q_2 \Phi_2(z_2)], \end{aligned} \quad (1)$$

where

$$z_l = x + s_l y; \quad l = 1, 2.$$

Here  $x$  and  $y$  are coordinates of a point of rock mass,  $u_x$  is the displacement of the direction  $x$ ,  $u_y$  is the displacement of the direction  $y$ ,  $s_1$  and  $s_2$  are the roots of characteristic equation of the field (Minchev, 1960a).

The components of the displacements in undistorted field which take part in equation (1) are:

$$\begin{aligned} u_{x0} &= (k_1 C_{11} + C_{12}) Q x; \\ u_{y0} &= (k_1 C_{12} + C_{22}) Q y. \end{aligned} \quad (2)$$

Here  $u_{x0}$  is the displacement of the direction  $x$ ,  $u_{y0}$  is the displacement of the direction  $y$ .

In expression (2)  $C_{jl}$  are the reduced coefficients of the deformation, whose expressions can be seen in (Trifonova-Genova, 2012; Minchev, 1960a). They are expressed by the physical and the mechanical characteristics of the rock mass. These characteristics are two types: in the direction parallel to the plane of isotropy and in the direction perpendicular to the plane. The first type includes the Young's modulus  $E_1$  and the Poisson's ratio:  $\mu_1$ . In the second type, the Young's modulus:  $E_2$ , the Poisson's ratio  $\mu_2$  and the shear modulus  $G_2$  participated.

The two functions  $\Phi_j$  of equation (1) are complex potential functions. They are analytical in the region  $S$  occupied by the elastic material (Fig.1). To transform this region into an outer region of a unit circle the transformation given in (Minchev, 1960a) is used. The limit values of complex potential functions and their expressions in the outer region of the unit circle  $\zeta$  are determined. Then they are replaced in the expressions of the displacements. The latter are a function of the polar angle  $\theta$ :

$$u_x = 2u'_x \cos \theta; \quad u_y = (u'_{y0} + 2u'_y) \sin \theta, \quad (3)$$

where

$$\begin{aligned} u'_x &= \operatorname{Re} \bar{\Phi}_{11} + \operatorname{Re} \bar{\Phi}_{21} + \operatorname{Re} \bar{\Phi}_{12} + \operatorname{Re} \bar{\Phi}_{22}; \\ u'_y &= \operatorname{Im} \bar{\Phi}_{32} + \operatorname{Im} \bar{\Phi}_{42} - \operatorname{Im} \bar{\Phi}_{31} - \operatorname{Im} \bar{\Phi}_{41}; \\ u'_{y0} &= (k_1 C_{12} + C_{22}) Q b. \end{aligned} \quad (4)$$

The expressions of  $\bar{\Phi}_{jl}$  ( $j = 1 \div 4; l = 1, 2$ ) are given in (Trifonova-Genova, 2018b). The horizontal displacements in the undistorted rock are small and therefore not included in (3).

**Numerical example**

An opening in the shape of an ellipse has a width of  $2b = 3m$  and a height of:  $2a = 4.8m$ . It draws at a depth of:  $H = 300m$ . The volumetric weight of the material of the rock is:  $\gamma = 0.28 \cdot 10^{-2} MN / m^3$ . The vertical stress in situ is:  $Q = 15MPa$ .

The physical and the mechanical characteristics of the rock mass can be seen in Table 1.

The formulas of the coefficients of deformation can be seen in (Trifonova-Genova, 2018a; Minchev, 1960a). They participate in reduced coefficients  $C_{jl}$  of deformation as well as in the coefficients of the lateral pressure (Trifonova-Genova, 2018a). Their values are given in Table 2.

Table 1. The physical and mechanical characteristics of the rock mass

$E_1$	$\mu_1$	$E_2$	$\mu_2$	$G_2$
$10^3$		$10^3$		$10^3$
MPa		MPa		MPa
14.5	0.105	41.5	0.3	8.24

Table 2. Reduced coefficients of deformation  $C_{jl}$

$C_{11}$	$C_{12}$	$C_{22}$	$C_{66}$	$k_1$
$10^{-5}$	$10^{-5}$	$10^{-5}$	$10^{-5}$	
$cm^2 / kg$	$cm^2 / kg$	$cm^2 / kg$	$cm^2 / kg$	
6.7	-0.94	2.2	12.15	0.34

These coefficients participate in the characteristic equation of the rock mass. The roots of this equation are imaginary numbers:  $s_1 = 0.885i$  and  $s_2 = 1.9708i$ . Here  $i$  is an imaginary unit.

The coefficients:  $\overline{\Phi}_{jl}$ , related to the determination of the complex variable function, can be seen in (Trifonova-Genova, 2018a; 2018b). In the appendix to the first article the expression of real and imaginary parts of the coefficients, used in equation (1), is given. The values for a concrete rock mass are given in Table 3.

Table 3. Coefficients  $p_j$  and  $q_j$

$j$	$Re p_j$	$Im q_j$
	$10^{-5}$	$10^{-5}$
1	-6.193	-3.317
2	-26.963	-2.969

The second appendix in the same article describes the expressions of real and imaginary parts of the coefficients:  $g_{jl}$  and  $G_{jl}$ . They have the following values:

$$Re[g_{jl}] = \begin{bmatrix} 0.115 & 6.848 \\ 1.886 & -0.416 \\ 0.416 & 0.177 \\ 6.848 & -0.540 \\ 1.962 & 1.421 \\ 10.789 & 1.421 \\ 0.115 & -0.177 \\ 1.886 & 0.540 \end{bmatrix};$$

$$Im[g_{jl}] = 0; \quad Im[G_{jl}] = 0; \quad Im[G_{(j+2)l}] = 0;$$

$$Re[G_{jl}] = \begin{bmatrix} -0.709 & -184.638 \\ -11.678 & 11.212 \\ -2.576 & -4.759 \\ -42.412 & 14.562 \\ -12.148 & -38.325 \\ -66.824 & -38.324 \\ -0.709 & 4.759 \\ -11.678 & 14.562 \end{bmatrix}.$$

The real and imaginary parts of the coefficients  $D_j$  and  $\overline{\Phi}_{jl}$  are calculated by an expression, given in the second article. The numerical values of these coefficients can be seen in Table 4.

Table 4. Coefficients  $D_j$

$j$	$D_j$	$j$	$D_j$
	$10^{-5}$		$10^{-5}$
1	2.576	5	1.379
2	42.412	6	22.713
3	-38.325	7	-4.220
4	-38.325	8	-4.220

The numerical values of the complex variable functions  $\overline{\Phi}_{jl}$  ( $j = 1, 2; l = 1, 2$ ) are:

$$Im \begin{bmatrix} \Phi_{11} & \Phi_{12} \\ \Phi_{21} & \Phi_{22} \end{bmatrix} = 0; \quad Re \begin{bmatrix} \Phi_{31} & \Phi_{32} \\ \Phi_{41} & \Phi_{42} \end{bmatrix} = 0;$$

$$Re[\Phi_{jl}] = 10^{-5} \begin{bmatrix} -14.414 & -12.824 \\ -266.007 & -30.538 \end{bmatrix};$$

$$Im[\Phi_{(j+2)l}] = 10^{-5} \begin{bmatrix} 5.457 & -6.868 \\ -29.289 & -3.362 \end{bmatrix}.$$

These functions are involved in expressions for constants:  $u'_x = -647.564 \cdot 10^{-5}$ ,  $u'_y = 27.204 \cdot 10^{-5}$  and  $u'_{yo} = 67.593 \cdot 10^{-5}$  of equation (4). The components of displacements by contour of the opening are obtained by (3). Their values in 7 points have reference to the vertical stress in undistorted rock mass and the results are given in Table 5.

The part of the final contour of a cross section for a shallow elliptic hole (Fig. 2) is drawn using the values in the table. This part is symmetrical to the vertical and horizontal axis of the hole. The final contour is given in a continuous line, but the initial contour is in interrupted line.

Table 5. Results

point	$\theta$	$\frac{u_x}{Q}$	$\frac{u_y}{Q}$
		$10^{-5}$	$10^{-5}$
		$\left[ \frac{m^3}{kN} \right]$	$\left[ \frac{m^3}{kN} \right]$
1	0	-43.17	0
2	15	-41.70	1.64
3	30	-37.39	3.16
4	45	-30.52	4.47
5	60	-21.59	5.47
6	75	-11.17	6.10
7	90	0	6.32

As can be seen in the figure, the contour is moved. The highest point rises, the low point goes down and the horizontal points move inwards in the hole. Thus, the contour of elliptical workmanship takes a curvilinear look.

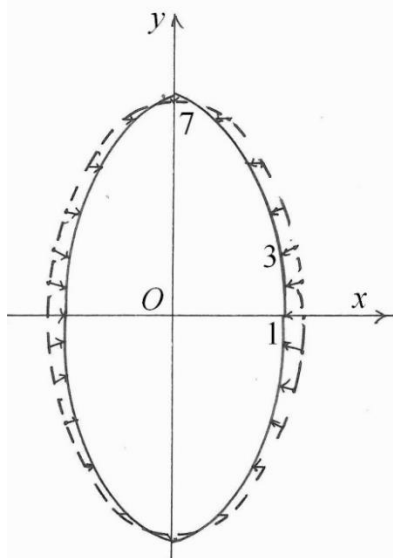


Fig. 2. Initial and final contours of the tunnel cross section for a shallow elliptic tunnel

## Conclusion

The components of the displacements after advancing the opening are expressed by two complex potential functions of stresses. These potential functions are expressed by long formulas. This requires the use of modern means for calculating them (computer, Excel, etc.). These means are affordable and have a low price.

The algorithm implemented in the numerical example can be used in future work to determine the displacements in rock mass with an inclined isotropic plane.

The task under consideration can be solved by the numerical method of finite elements. The area around the hole occupied by a continuous elastic and homogeneous environment divides into triangular elements. The nodes of the elements are recorded equations of mechanics of the continuous environments. These equations are differential. Their numeric solution gives us the displacements in the nodes. This is done by software packages or a separate programme. Such a programme is given in (Mihaylov and al., 2013), applied in the solving of plane and elastoplastic tasks. They measure the body's stability with the failure criteria of Hock-Brown, Mohr Coulomb and the modified stability criterion.

## References

- Denis, R. Y. 2011. *Complex Variable and Integral Transform*. Wisdom Press, New Delhi.
- England, A. H. 1971. *Complex Variable Method in Elasticity*. Wiley, New York.
- Guangpu, Z., S. Yang. 2015. Analytical solutions for rock stress around square tunnels using complex variable theory. – *International Journal of Rock Mechanics & Mining Sciences*, 80, 302–307.

- Hefny, A. M. 1999. Analytical solution for stresses and displacements around tunnels driven in cross-anisotropic rock. – *International Journal of Numerical Analysis Methods in Geomechanics*, 23, 2, 161–177.
- Lehnickii, S. G. 1963. *Theory of Elasticity of an Anisotropic Elastic Body*. Holden-Day, San Francisco.
- Lei, G. H., N. G. CWW, D. B. Rigby. 2001. Stress and displacements around an elastic artificial rectangular hole. *Journal of Engineering Mechanics ASCE*: 127, 9, 880–890.
- Mihaylov, G., G. Trapov, M. Trifonova. 2013. Analysis of state of stress and deformation of body taking into consideration probabilistic nature of mechanical characteristics. – *5<sup>th</sup> Balkan Mining Congress BALKANMINE, Ohrid*.
- Minchev, I. T. 1960. *Mehanika na anizotropnoto tiyalo w minnoto delo*. Tehnika, Sofia, 126 p. (in Bulgarian)
- Minchev, I. T. 1960. Wurhu napregnatoto sostoiyanie na skalniya masiv okolo eliptichen otvor. – *Minno delo i metalurgiya*, 10, 31–35 (in Bulgarian).
- Muskhelishvili, N. I. 1963. *Some Basic Problem of the Mathematical Theory of Elasticity*. Noordhoff, Groningen.
- Nikolaev, N., M. Trifonova. 2016. A method qualifying the generalized tension in rectangular supporting pillars. – *Proceeding of the VII International Geomechanics Conference 2-6 July 2016*, 124–131 (in Bulgarian with English abstract).
- Sahoo, J., P., J. Kumar. 2014. Stability of a circular tunnel in presence of pseudostatic seismic body forces. – *Tunneling and Underground Space Technology*, 42, 264–276.
- Savin, G. N. 1961. *Stress Concentration Around Holes*. Pergamon, New York.
- Trifonova-Genova, V. 2012. *Napregnato sostoiyanie v naplasten masiv okolo krugla izработка*. Ed. House “St. Ivan Rilski”, Sofia, 132 p. (in Bulgarian)
- Trifonova-Genova, V. 2018a. Functions of stresses around of elliptic opening, drawn in transversal isotropic rock. – *Abstract of XVIII Anniversary International Scientific Conference “Construction and Architecture” VSU’2018, 18-20 October, Section 2*, 89 (in Bulgarian with English abstract).
- Trifonova-Genova, V. 2018b. Displacements in points on contour of elliptic opening, passing rock with horizontal plane of isotropy. – *Abstract of XVIII Anniversary International Scientific conference “Construction and Architecture” VSU’2018, 18-20 October, Section 2*, 65 (in Bulgarian with English abstract).
- Tzonkov, A., M. Begnovska. 2018a. Determination by mine surveying measurements the deformation condition of pillars in the extraction of lead-zink ores for the condition of mine “Djurkovo”, “Lucky Invest – Djurkovo” Ltd. – In: *Sixth National Scientific and Technical Conference with International Participation “Technologies and Practices in Underground Mining and Mine Construction”*, Devin, Bulgaria, 147–154 (in Bulgarian with English abstract).
- Tzonkov, A., M. Begnovska. 2018b. Monitoring of rock massive stability by mine surveying measurements in the extraction of lead-zink ore for the conditions of mine “Kruchovdol”. – *Proceeding of the VIII International Geomechanics Conference, 2-6 July 2018*, 313–319 (in Bulgarian with English abstract).

## MINE SURVEYING ACTIVITIES IN MANAGEMENT OF GEOMECHANICAL PROCESSES

**Alexander Tzonkov**

*University of Mining and Geology "St. Ivan Rilski", 1700 Sofia; altzon@abv.bg*

**ABSTRACT.** When investigating and managing geomechanical processes, the activities of the mine surveyor are limited to: receiving primary information; office data processing; creation of intermediate and final documents; preparation of recommendations and instructions for conducting process management events in the massif. To make the work of the mine surveyor efficient, all activities need to be automated, i.e. to create an automated system for managing the geomechanical processes in the array. It should be part of the overall system "RUDNIK". It will contain several modules: 1. "MODEL" - model of natural conditions and model of mining. 2. "TECHNOLOGY" - after taking into account the actual conditions for a particular site, the research technology, the measurement methods, the type and accuracy of the instruments, the intervals between the observations, etc. will be chosen. 3. "MASSIF" - based on the results of the measurements, the data on the physical and mechanical indicators of the rocks, etc. The type of the stress-deformable state of the massif will be determined. The proximity of the array state to a known theoretical model of the environment will be assessed according to set criteria. 4. "PROJECT" - prognosis of the anticipated manifestations of the geomechanical processes will be carried out, zones of influence and dangerous impact of the mining works will be determined, etc.

**Keywords:** geomechanical processes, management, mine surveying works

### МАРКШАЙДЕРСКО ОСИГУРЯВАНЕ В УПРАВЛЕНИЕТО НА ГЕОМЕХАНИЧНИ ПРОЦЕСИ

**Александър Цонков**

*Минно-геоложки университет "Св. Иван Рилски", 1700 София*

**РЕЗЮМЕ.** При изследване и управление на геомеханични процеси дейностите на маркшайдера се свеждат до: получаване на първична информация; канцеларска обработка на данните; създаване на междинни и крайни документи; изготвяне на препоръки и инструкции за провеждане на мероприятия по управление на процесите в масива. За да бъде трудът на маркшайдера ефективен е необходимо всички дейности да бъдат автоматизирани т.е. да се създаде автоматизирана система за управление на геомеханичните процеси в масива. Тя трябва да бъде част от цялостната система „РУДНИК“. Ще съдържа няколко модула: 1. „МОДЕЛ“ – модел на природните условия и модел на минните изработки. 2. „ТЕХНОЛОГИЯ“ – след отчитане на реалните условия за конкретен обект ще се избира технологията на изследванията, методите на измерване, вида и точността на инструментите, интервалите между наблюденията и т.н. 3. „МАСИВ“ – въз основа на резултатите от измервания, данните за физико-механичните показатели на скалите и др. Ще се определя вида на напрегнато-деформируемостта на масива. По критерии ще се оценява близостта на състоянието на масива до познат теоретичен модел на средата. „ПРОЕКТ“ – ще се извършва прогнозиране на очакваните прояви на геомеханичните процеси, ще се определят зоните на влияние и на опасно влияние на минните работи и т.н.

**Ключови думи:** геомеханични процеси, управление, маркшайдерско осигуряване

### Introduction

The development of mining is based on continuous improvement of the scientific knowledge of the extraction environment, the physical and mechanical processes taking place in it, the possibilities for improving the efficiency and safety of the work, for legitimate and reasonable management of the mineral resources reserves.

This implies a very good knowledge of the relationships between the different elements of the complex system of mining. Its management requires constant monitoring of the behaviour of every work place and every process at every stage of underground mining. Analysing the specific situation at a given point in time should lead to a decision on preserving or changing the processes and the links between them to ensure the normal operation of the enterprise.

Regardless of whether the exploitation is conducted in an open or underground way, a number of processes take place in the rock massif, the knowledge of which would lead to

making adequate and realistic decisions about the development system, the order of work in the space and the time of the individual jobs, safety measures, in order to reasonably foresee the risks in specific situations.

The notion of the interaction between the different elements of the environment allows solving the problem of building the most adequate models of the processes in the mining production. Decisions in this regard require experience and knowledge in different areas. To study the reasons for the occurrence and the characteristics of the processes in the array, it is also necessary to accumulate a multitude in terms of quantity and type of data (Valkov, 2011).

The knowledge of mining technology, the laws of rock mechanics, the relationships and dependencies of the processes in the array, as well as the accumulated information from multiple observations on specific objects, allows successful solving of the engineering tasks. Modelling options offer variants that are evaluated according to different criteria. Based on estimates, the best one is chosen. It should characterise the trend of change in time and the extent of the

studied phenomena and processes in view of the management of the open pit or underground mine.

The baseline information needed to provide rational solutions and relevant analyses is mainly gathered from studies and measurements under natural conditions. In addition to methods known to the rock mechanics to determine the physical and mechanical characteristics of the massif and its behaviour, mine surveying's methods are widely used to determine spatial variations of characteristic points from the rock massif and the ground surface by judging changes in rock massif due to natural or technological factors.

The block diagram, shown in Figure 1, shows a basic model for studying the behaviour of the rock massif and the application of the mine surveying's methods for this purpose.

The possibility to use the results of the mine surveying's measurements to assess the state of the rock massif or object is based on observations in the natural environment, which determines the reality of the obtained values for the specific technical, mining-technical and geological conditions.

Mine surveying's measurements define the characteristics of the deformation processes that relate to larger areas in the rock massif due to the easier and quicker acquisition of the required data than other known methods requiring more time, labour, and specialised equipment.

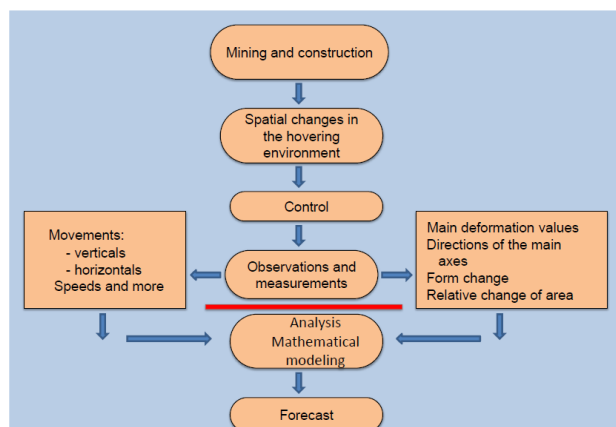


Fig. 1. Principal model for studying the behaviour of the rock massif with mine surveying methods

The main objects of the geomechanical studies in the extraction of underground resources are (Yoffis, 1985):

- the rock massif and the earth's surface;
- mining works;
- mechanical processes induced in the rock massif from natural or artificial impacts;
- the factors affecting the mechanical properties of the rock massif and the mechanical processes in it;
- the means of regulated engineering impact on the rock massif for purpose alteration of its properties and condition.

The rock massif as an environment in which geomechanical phenomena and processes are evoked and manifested is the main object of the research. Its important characteristic is the change in its tense state as a result of the mining works. This tense state is changed from a tri axial - in an unbroken massif, to a two axial or close to it - to the contour of the workings.

An overriding interest in mining geomechanics is "rock pressure". Rock pressure, as a phenomenon, is a collective

concept combining the set of tension states that form in the massif due to a number of natural and technogenic impacts. The determining factor is gravity, as a permanent and ubiquitous natural phenomenon, and the additional ones are the tectonic processes, the human activity in the extraction and the construction of different facilities.

The common methodology for exploring the processes in the rock massif consists in the extensive use and analysis of observations in natural conditions and at the same time also in modelling and analytical methods based on the theoretical aspects of the main sections of modern mechanics and the mathematical and physical analogies.

The geomechanical stability of the "rock massif-underground works" system is determined (Ivanov, 2006; 2007) from the interaction of three main factors:

1. Deformed state of the rock massif;
2. Geological structure, structural features and physical and mechanical properties of rocks;
3. Effects of the technological impacts on the above factors.

Surveying and mechanical methods can be used for their determination.

Surveying methods identify the displacements to fixed points (in absolute coordinates) or to points in the area of influence of mining operations (in relative coordinates). Horizontal and inclined lengths, horizontal and zenith angles, line deviations, angular deviations, exceedances determined by geometric or trigonometric level are measured. It is also possible to apply photogrammetric methods (Ivanova, 1991).

The angular-linear and height measurements applied for studying the deformation state of the rock massif are used to determine (fig.2):

- the linear dimensions of the zones in the rock massif with a different deformation state;
- the boundaries of undermine zones and overmine;
- the parameters of the rock movement process;
- the change in the size and shape of the mining works.

During the various stages of the deformation processes, the following are established:

- absolute and relative displacements;
- moving speeds.

Through the determined displacements in the space of observation points (Tsonkov, 2018) the invariant characteristics of the deformations: can be calculated

- relative change of area – dilation  $\theta$ ;
- form change - maximum displacement  $\gamma_m$
- main deformation values  $E_1$  and  $E_2$  in the  $T_1$  and  $T_2$  directions of the main axes.

In mechanical methods in the rock massif embed in depth repers or repers in the contour of the work section or on their fastening; devices are used to determine the relative displacements of different points from the surrounding rocks. Specialised equipment is used to define elements of the strained-deformed state of the rock massif or to monitor the behaviour of the system "Rock - Support".

General scheme of mine surveying measurements and their results in underground and open groundwater development in connection with studying the geomechanical state of the rock massif and the earth's surface.

Way of mining		Mine surveying	Results
Underground mining	Open mining		
Coal and ore deposits	single mine workings	Landslides	Relative and absolute movements
	mine workings in one layer	Open pit mines	Movement speeds
	undermine	Pit dump	Deformations
	overmine	Quarry	Dimensions of zones
	land surface	Land surface	Border angles
Facilities in the massif and on the land surface		Facilities on the land surface	Angles of movement Tearing angles
		Angular	
		Lengths	
		Height	

**Fig. 2. General scheme of mine surveying measurements and their results in underground and open groundwater development in connection with studying the geomechanical state of the rock massif and the earth's surface**

Based on the results of the studies with the two groups of methods, a mathematical model of the studied geomechanical processes can be created.

The model, though idealised in some ways, due to a number of assumptions and insufficient knowledge of the environment, should serve as a description and as a means for managing the researched object.

The matching of the chosen model with the nature of the research process is done through continuous correction after introducing new elements and results from experimental data.

The adequacy of the model is based on the formation of accurate assessments and their correct use for impact on the real object of the study.

If necessary, according to established methodologies, forecasts of the stress, displacement and deformation values at selected rock massif points are made. Actions for rational deployment of preparatory and extraction works, safe mining, reduction of stresses in the massif, ensuring the safety of facilities and objects on the surface and in the massif are recommended.

## System for mine surveying activities in the management of geomechanical processes

With the introduction of new techniques and technologies in terms of apparatus, tools and methods of mine surveying mapping (Begnovska et al., 2014) and the processing of huge amounts of data, numerical models have already been created in many mines. They are mainly used to visualise the spatial position of the ore bodies and the layers and mining works. Measurements are made only at distances and angles.

In order to make the work of the mining company more efficient, the results more accurate and complete, and in order to achieve the unity of the decisions and the control of their implementation, it is necessary to create a unified automated management system in the mine. It should contain subsystems or separate modules that can provide adequate real-time management. As part of this system called "MINE", for

example, there should be also a mine surveying system for geomechanical processes.

The objectives of the mine surveying system must lead to or be part of the objectives of the "MINE" system.

From a structural point of view, the mine surveying system for geomechanical processes must contain several subsystems.

### MODEL Subsystem

This subsystem has two components:

- "model of natural conditions";
- "model of mine workings".

In order to get effective real solutions, the model needs to meet several conditions:

- to be "adequate" to existing nature mineral deposits;
- to be "technological" - to reflect truly and really the dynamics of technological development processes in mining operations;

- to have the "reversibility" property of numerical type and to be able to pass quickly and accurately in graphic mode and vice versa;

- to be "informative" - to allow only unambiguous answers.

The MODEL subsystem has to create and maintain the mining model by converting the information from the surveying image capture into a numerical model (Begnovska, 2016).

This can be done with specialised or non-specialised software.

The relationship between the geological study and the information on the environment and the numerical model of the mine works is carried out by the model of natural conditions. It binds the numerical spatial arrangement of mining work with that of the underground treasures, its properties, the physical and mechanical state of the massif, the type of rocks, the geological disruptions and all other natural assets. This requires continuous updating of both models.

In general, the model of mining works and the model of natural conditions form the information level - the "database" of the system.

### The MANAGEMENT subsystem

This subsystem must have three modules: "MASSIF", "TECHNOLOGY" and "PROJECT".

#### Module "MASSIF"

Based on the results of the measurements, the data on the physical and mechanical indicators of the rocks, the knowledge of analogous conditions, etc., the type of stress-strained state of the rock massif is determined. The proximity of this state to a certain theoretical model of the environment - elastic, plastic, rheological, model of continuous, layered, block etc. is assessed. Upon confirmation of such proximity, further forecasts, recommendations and events are made on the basis of this theoretical model. If no close theoretical model is found, the medium is considered stochastic as it is.

#### Module "TECHNOLOGY"

With the application of modern scientific achievements and optimisation methods, after taking full account of the actual conditions of the particular site, in accordance with the technical norms for conducting measurements (Ivanova, 2012), it is possible to choose the way of observation, to design an observation station (location, number of observed points, stabilisation, etc.), to define the intervals between the measurements, the measurement accuracy, etc. The module should also choose suitable measuring equipment.

### Module "PROJECT"

After determining the type of strain-strained rock mass condition and after analysing the results of experimental studies and measurements, it is possible to:

- forecast the expected displacements and deformations;
- determine the dimensions of the zones of influence and of dangerous influence;
- determine the degree of undermine of the rock mass and on the Earth's surface;
- assess the state of the sites, facilities and the rock mass as a whole;
- define the parameters of the supports.

The module should offer actions:

- to reduce the harmful impact of mines works;
- to prevent accidents in the mine;
- to ensure normal and safe work;
- for environmental protection;
- rational use of the stocks of underground minerals.

Figure 3 shows a block diagram of the system for mine surveying activities in the management of geomechanical processes.

Since information on the environment of occurrence of geomechanical processes is always insufficient and incomplete, much of the decisions and forecasts will be taken and done by the operator. This will be based on his experience, knowledge and engineering intuition. The "human-machine" dialogue is an important link in the management of geomechanical processes.

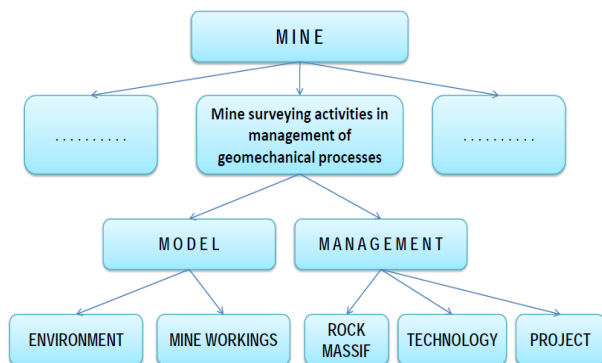


**Fig. 3. Block diagram of the system for mine surveying activities in management of geomechanical processes**

The geomechanical process management system will not exist on its own. As an important unit of the "MINE" system, it participates and will actively support the management and planning of the development of mining operations. The complete and accelerated use of the available information, the application of the most suitable methods for its processing, the avoidance of intermediate processes and the optimal solution (Mazhdrakov, 1983) of the assigned tasks determine the effectiveness of its work.

### Conclusion

In recent years there has been a change in mineral extraction in Bulgaria. With the concession of different types of mineral resources' deposits, investments in the mining industry

have been increasing, the introduction of new high-yielding mining equipment, increased production, and full seizure of stocks have been put in place. Extraction works are carried out at a greater depth, often in very complex mining, technical and geological conditions.

In line with these changes, mine surveying in mining and quarrying companies seeks to assist and technically direct the proper development and maintenance of mining. Together with proven methods and technologies, new instruments and apparatus are based on the achievements of modern science and technology. Their capabilities provide high accuracy, huge data, speed and reliability of the information received.

In order to achieve the desired results in terms of quantity and quality of the mining company's output, it is necessary to have good specialists, reliable and productive modern equipment for all units in the enterprise, high level of safety technique, good organisation and control.

### References

- Begnovska, M., R. Petkov, D. Atanasova. 2014. Markshayderska snimka na horizontalna izработка v rudnik "Krushev dol" chrez razlichni tehnologii. – *Chetvarta natsionalna nauchno-tehnicheska konferentsia s mezhdunarodno uchestie "Tehnologii i praktiki pri podzemem dobiv i minno stroitelstvo"*, Devin, Bulgaria, 254–261 (in Bulgarian with English abstract).
- Begnovska, M. 2016. Markshayderska snimka na kapitalna izработка pri razlichna detaylnost na informatsiyata. – *Peta natsionalna nauchno-tehnicheska konferentsia s mezhdunarodno uchestie "Tehnologii i praktiki pri podzemem dobiv i minno stroitelstvo"*, Devin, Bulgaria, 101–106 (in Bulgarian with English abstract).
- Ivanov, V. 2006. Geomehanichna otsenka na masiva sled zakrivane na rudnik "Rosen", Burgaski medni mini EAD. – *Ann. Univ. Mining and Geology*, 49, 2 (in Bulgarian).
- Ivanov, V. 2007. Geomehanichna otsenka na r-k "Dimov dol", Madansko rudno pole. – *Ann. Univ. Mining and Geology*, 50, 2 (in Bulgarian).
- Ivanova, I. 1991. Fotogrametrichni metodi za opredelyane na deformatsii na mezhdukamerni tselitsi. – *Nat. Simpozium "Fotogrametrichni metodi za izsledvane na deformatsii i svlachishta"*, Geodezia, kartografia, zemeustroystvo, 3-4 (in Bulgarian).
- Ivanova, I. 2012. *Pregled na tehnikeskite normi pri markshayderskoto osiguravane na rudnitsite*. Matteh, Shumen, (in Bulgarian).
- Mazhdrakov, M. 1983. *Markshayderstvo. Metodika na markshayderskite raboti v otkritite rudnitsi*. MNP, Sofia (in Bulgarian).
- Tsonkov, A. 2018. *Opredelyane na invariantnite karakteristiki na deformatsiite chrez markshayderski izmervania*. Doktorska disertatsia, Sofia (in Bulgarian).
- Valkov, M. 2011. *Geomehanichni modeli v minnoto delo*. Ed. House "Sv.Ivan Rilski", Sofia (in Bulgarian).
- Yofis, M. A., A. I. Shmelev. 1985. *Inzhenernaya geomehanika pri podzemnyh razabotkakh*, Nedra, Moscow (in Russian).

## ANALYSIS OF SELECTIVE DESTRUCTION CRITERIA OF IRON ORES USING PROVISIONAL MAGNETIC PULSE TREATMENT

Pavel Ananyev<sup>1</sup>, Anna Plotnikova<sup>2</sup>

<sup>1</sup> Non-Commercial Partnership Scientific Educational Centre "Innovation Main Technologies", 119991 Moscow

<sup>2</sup> National University of Science and Technology "MISiS", 119991 Moscow

**ABSTRACT.** The paper considers the process of selective pre-destruction of interphase boundaries in iron ores by using magnetic pulse treatment. When analysing the stress-strain state and viscous fracture, the relative similarity of the fracture criteria in the main minerals of iron ores due to magnetostrictive deformation of magnetite grains is shown. It has been established that the strength and toughness of the destruction of magnetite exceeds the analogous properties of calcite in the composition of skarn iron ores, the strength and toughness of quartz fracture exceeds the analogous properties of magnetite. A difference in the character of the destruction of skarn ores and ferruginous quartzites is presented. The criterion for estimating the degree of softening of interphase boundaries in iron ores due to the magnetic-impulse action based on the probabilistic approach is formulated. A theoretical estimate is made of the degree of selective softening of iron ores under magnetic pulse treatment, considering the strength and magnetostriction properties of magnetite. The results of experiments on nanoindentation of interphase boundaries before and after magnetic pulse treatment are presented. By analysing the lengths of developing microcracks under the influence of a nanoindenter, the possibility of reducing the fracture toughness after a magnetic pulse treatment of iron ore is shown.

**Keywords:** mineral processing, iron ores, magnetic pulse treatment

### АНАЛИЗ НА ИЗБИРАТЕЛНИ КРИТЕРИИ ЗА РАЗРУШАВАНЕ НА ЖЕЛЕЗНИ РУДИ ЧРЕЗ ИЗПОЛЗВАНЕ НА УСЛОВНО ТРЕТИРАНЕ С МАГНИТЕН ИМПУЛС

Павел Ананьев<sup>1</sup>, Анна Плотникова<sup>2</sup>

<sup>1</sup> Научно-образователен център "Основни иновационни технологии", 119991 Москва

<sup>2</sup> Национален университет за наука и технологии "МИСиС", Русия, 119991 Москва

**РЕЗЮМЕ.** Разгледан е процесът на избирателно предварително разрушаване на междуфазовите граници в желязната руда с помощта на магнитно-импулсна обработка. При анализа на напрегнато-деформираното състояние и вискозното разрушаване се открива относително сходство на критериите за разрушаване в основните минерали на желязната руда, поради магнитостриктивната деформация на зърната магнетит. Установено е, че якостта и издръжливостта на разрушаване на магнетита надвишават сходните свойства на калцита, като якостта на разрушаване на кварца надвишава сходните свойства на магнетита. Представена е разликата в начина на разрушаване на скарновите руди и желязните кварцити. Формулиран е критерий за оценка на степента на омекване на междуфазовите граници в желязната руда, под магнитно-импулсно въздействие. Извършена е теоретична оценка на степента на избирателно омекотяване на желязната руда по време на импулсно-магнитна обработка, като се вземат предвид якостните и магнитни свойства на магнетита. Представени са резултатите от експериментите по наноиндикация на междуфазовите граници преди и след магнитно-импулсно обработване. Чрез анализирани на дължините на образуващите се микропукнатини под въздействието на наноиндентор се демонстрира възможността за намаляване на издръжливостта на пукнатината след магнитно-импулсното обработване на желязната руда.

**Ключови думи:** обработка на минерали, желязна руда, магнитно-импулсна обработка

### Introduction

The whole technological process of ore preparation for enrichment is aimed at the development of conditions that ensure maximum extraction of the useful component and minimise all possible resources (Curry et al., 2014). In order to optimise the extraction of the useful component, it is necessary to perform ore blending properly, then the mixture should be passed through all the necessary crushing and grinding stages to a particle size corresponding to the grain of the useful component and only then it should be extracted by physical or chemical method optimal for this technology (Clout, Manuel, 2015).

When minerals are enriched, the main role of disintegration consists in the complete disclosure of mineral intergrowths with the formation of free grains of components for their subsequent

separation according to physicochemical characteristics (Gutsche, Fuerstenau, 2004; Mwanga et al., 2017). Non-mechanical methods of energy impact are very promising in order to overcome the persistence of ores and intermediate products, the disclosure of finely disseminated mineral complexes (Usov, Tsukerman, 2000).

With a comparable size of grinding, ore and non-metallic minerals of hardly-rich ores are revealed to a lesser extent with respect to averagely and easily enriched ores. A lower amount of free ore grains and an increased amount of phenocrysts should be noted for the hard iron ores (Clout, Manuel, 2015).

The influence of mineralogical and petrographic factors on the enrichment is manifested in the nature of the structural features and correlation relationships of the material composition and ore structure parameters with the enrichment indices (Jankovic, 2015).

## Objects and research methods

The object of research is the process of ore preparation using preliminary magnetic pulse treatment (MPT). Research methods are based on the theoretical comparison of the criteria for the destruction of known power models, including the energy criteria for the destruction of the Balandin theory and the theory of viscous fracture by Irwin. Experimental studies are based on the analysis of cracking process by the method of nanoindentation.

## Results and discussion

It is known that the softening effect of magnetic pulse treatment (MPT) can be determined by a number of physical phenomena, such as the magnetostriction of magnetite grains, the inverse non-metallic phase piezoeffect (for ferruginous quartzites), the movement of charged dislocations, etc. (Golovin et al., 1997; Ananiev et al., 2008; Plotnikova, 2013).

MPT is carried out as an intermediate operation of ore preparation before mechanical grinding. Thus, the development of fracture cracks under the action of mechanical loads, at the stage of crushing and grinding, is largely determined by the elastic-plastic properties of the rock. The selectivity of destruction will be determined by the degree of softening of ore and non-metallic phase fusion boundary. Therefore, the magnitude of the contact stresses generated by the MPT at the boundary of ore and non-metallic phases is of great importance.

The criterion of destruction according to the Balandin theory (Karkachadze, 2004) has the following form:

$$\sigma_1^2 + \sigma_2^2 + \sigma_3^2 - \sigma_1\sigma_2 - \sigma_2\sigma_3 - \sigma_1\sigma_3 - (\sigma_{com.} - \sigma_{ten.})(\sigma_1 + \sigma_2 + \sigma_3) = \sigma_{ten.} \sigma_{com.} \quad (1)$$

where  $\sigma_1, \sigma_2, \sigma_3$  – main stresses;

$\sigma_{ten.}, \sigma_{com.}$  – the limits of tensile and compressive strength.

During magnetostrictive volumetric deformation of magnetite grain at the phase separation boundary, compressive contact stresses arise in the radial direction  $\sigma_{cont.}$  and tangential tensile stresses, the magnitude of which is two times less than the contact stresses. Then the criterion of destruction will take the following form according to Balandin theory:

$$\sigma_{cont} > \frac{2}{3} \sqrt{\sigma_{ten.} \sigma_{com.}} \quad (2)$$

where  $\sigma_{cont}$  is the magnitude of contact stresses at the boundary of the ore and nonmetallic phase caused by magnetostrictive deformation of grain.

If condition (2) is fulfilled, complete destruction will occur at the phase separation boundary. In case of non-fulfilment of the condition (2), partial softening of the boundaries may occur. Table 1 shows the values of critical contact stresses for the main minerals of iron ores.

Table 1. The value of the critical contact stress for various minerals

№	Mineral name	$\sigma_{com.}$ , MPa	$\sigma_{ten.}$ , MPa	The value of critical contact stress
1	Magnetite	52	14	17.99
2	Quartz	120	21	33.47
3	Calcite	16	4	5.33
4	Hematite	30	6	8.94

It should be noted that the strength characteristics of rocks and minerals determine the conditions for the destruction of the massif, but do not fully characterise such technological properties as, for example, grindability. This is due to the fact that when an array is subjected to critical loads, a macrocrack develops, the length of which is many times greater than the characteristic size of the mineral grain (Winiarski, Guz, 2008). During crushing and grinding multiple acts of destruction take place. Thus, the disintegration process is characterised by the energy costs for the newly formed surface. So, for example, the Rittinger criterion is used, which characterises the amount of energy costs for destruction directly proportional to the newly formed surface (Bilenko, 1984; Lojkowski, Fecht, 2000): the energy costs for the newly formed surface are characterised by the value of  $\gamma$  (J/m<sup>2</sup>) – the energy of the newly formed surface unit. The value of  $\gamma$  is related to the fracture toughness (Irwin coefficient) and mechanical properties as follows (Karkachadze, 2004; Winiarski, Guz, 2008; Arutyunyan, Arutyunyan, 2014):

$$\gamma = \frac{(1 - \nu^2) \cdot K^2}{2 \cdot E} \quad (3)$$

where E is the mineral elasticity modulus;

K – the coefficient of fracture toughness by Irwin, N/m<sup>3/2</sup>;

$\nu$  – Poisson coefficient.

Table 2. Calculated values of the specific energy of the newly formed surfaces for various minerals

№	Mineral name	$\nu$	E, MPa	K, 10 <sup>6</sup> N/m <sup>3/2</sup>	$\gamma$ , J/m <sup>2</sup>
1	Magnetite	0.3	215	1.25	3.3
2	Quartz	0.08	96.4	1.6	13.2
3	Calcite (skarn)	0.3	83	0.75	3.1
4	Hematite	0.14	212	1.8	7.5

On the basis of the studies cited in (Goncharov et al., 2006), Table 2 shows the calculated values of the specific energy of the newly formed surface –  $\gamma$  for individual minerals.

Let's compare the fracture criteria for various minerals according to Balandin and Irvine's theories. At that, let's take the properties of magnetite as a standard unit. The comparison results are shown in Table 3.

Table 3. Comparison of the mechanical properties of minerals with respect to magnetite according Balandin and Irvine's criteria

№	Mineral name	Balandin's criterion $\sigma_{cr.}/\sigma_{cr.mag.}$	Irvine's criterion $\gamma./\gamma_{mag.}$
1	Magnetite	1	1
2	Quartz	1.86	3.99
3	Calcite	0.30	0.93
4	Hematite	0.50	2.27

The analysis of the table shows that the difference of the main mineral strength properties according to Balandin and Irvine's criteria have the same character with respect to the properties of magnetite.

As was shown in (Goncharov et al., 2006; Gridin, Goncharov, 2009) the maximum magnitude of the magnetostrictive deformations of magnetite makes  $\lambda = 0.6 \times 10^{-4}$  and is insufficient for the occurrence of critical contact stresses. Therefore, MPT can only provide selective prefracture of ore and non-metallic phase fusion boundary.

Prefracture may begin when plastic deformations occur in the weakest points of mineral fusion zones in a rock (Lojkowski, Fecht, 2000). As a rule, this occurs at the loads of 0.4-0.66 of the critical stress value (Lavrov et al., 2004; Shatemirov, Tilegenov, 2006; Arutyunyan, Arutyunyan, 2014).

Then we assume that the degree of weakening is determined by the following formula:

$$W = \frac{\sigma_{cont.} - k\sigma_{cr.}}{\sigma_{Bal.} - k\sigma_{cr.}} \quad (4)$$

Let's assume that k is in the range of 0.4–0.66 of  $\sigma_{cr}$ , which allows us to estimate the degree of intergranular softening (Goncharov et al., 2006). The calculated values of softening degree of softening lies in the range from 0 to 20%.

Table 4. Results of ferruginous quartzite nanoindentation with MPTs and without MPTs

Sample №	Processing type	Crack length C, mcm	$C_{prod}/C_{cont}$	$\Delta=(Kc_{proc})/(Kc_{cont})$
1	Control (without processing)	29.48 ± 3.0	1.12	1.19
	MPT 1	33.1 ± 4.2		
2	Control (without processing)	32.0 ± 4.6	1.01	1.02
	MPT 2	32.4 ± 2.7		
3	Control (without processing)	36.8 ± 5.5	1.07	1.11
	MPT 3	39.5 ± 6.0		

In (Turin et al., 2013), were shown the results of ferruginous quartzite magnetic pulse treatment influence studies on the fracture toughness coefficient at the magnetite

and quartz fusion boundary. The evaluation of fracture toughness coefficient (Kc) at the phase boundary was carried out by nanoindenter introduction into the region of magnetite and quartz fusion (Turin et al., 2016).

The analysis of Table 4 results shows that the reduction of the fracture toughness coefficient with MPT is from 2% to 19%.

## Conclusions

The difference of basic mineral strength properties according to Balandin and Irvine's criteria, with respect to the properties of magnetite, are of the same nature. So, it is permissible to use the Balandin's force model to analyse the nature of selective destruction.

It was established experimentally that there is a decrease in the fracture toughness coefficient within the range from 2% to 19% with MPT, which corresponds to the calculated estimate according to the formula (4), with the following properties of magnetite: magnetostrictive deformation  $\lambda = 0.6 \times 10^{-4}$ , ultimate compressive strength  $\sigma_{com.} = 52$  MPa, tensile strength  $\sigma_{ten.} = 14$  MPa.

## References

- Ananiev, P. P., O. M. Gridin, A. S. Samerchanova. 2008. Interrelation of properties and electromechanical sensitivity of natural minerals. – *Mining informational and analytical bulletin*, 5, 184-189 (in Russian).
- Arutyunyan, A. R., R. A. Arutyunyan. 2014. Application of the Fracture Mechanics and Reliability Methods to the Fatigue Problem. – *Procedia Materials Science*, 3, 1291–1297.
- Bilenko, L. F. 1984. *Regularities barrel grinding*. Nedra, Moscow, 200 p. (in Russian)
- Clout, J. M. F., J. R. Manuel. 2015. Mineralogical, chemical, and physical characteristics of iron ore. – *Iron Ore*, 45–84.
- Golovin, Yu. I., R. B. Morgunov V. E. Ivanov. 1997. Thermodynamic and kinetic aspects of the softening of ionic crystals by a pulsed magnetic field. – *Solid State Physics*, 39, 11, 2016–2018 (in Russian).
- Goncharov, S. A., P. P. Ananiev, V. Yu. Ivanov. 2006. *Softening of rocks under the action of pulsed electromagnetic fields*. MSMU, Moscow, 91 p. (in Russian)
- Gridin, O. M., S. A. Goncharov. 2009. *Electromagnetic processes*. MSMU, Moscow, 498 p. (in Russian)
- Gutsche, O., D. W. Fuerstenau. 2004. Influence of particle size and shape on the comminution of single particles in a rigidly mounted roll mill. – *Powder Technology*, 143, 186–195.
- James, A. C., M. J. L. Ismay, G. J. Jameson. 2014. Mine operating costs and the potential impacts of energy and grinding. – *Minerals Engineering*, 56, 70–80.
- Jankovic, A. 2015. Developments in iron ore comminution and classification technologies. – *Iron Ore*, 251–282.
- Karkachadze, G. G. 2004. *Mechanical destruction of rocks*. MSMU, Moscow, 222 p. (in Russian)
- Lavrov, A. V., V. L. Shkuratnik, Yu. L. Filimonov. 2004. *Acousto-emission memory effect in rocks*. MSMU, Moscow, 456 p. (in Russian)

- Lojkowski, W., H. J. Fecht. 2000. The structure of intercrystalline interfaces. – *Progress in Materials Science*, 45, 5-6, 339-568.
- Mwanga, A., M. Parian, P. Lamberg, J. Rosenkranz. 2017. Comminution modelling using mineralogical properties of iron ores. – *Minerals Engineering*, 111, 182–197.
- Plotnikova, A. V. 2013. Resource-saving technology for processing refractory ores based on the magnetic-impulse action. – *Bulletin of higher educational institutions. Ferrous metallurgy*, 9, 69–70 (in Russian).
- Shatemirov, D. K., K. T. Tilegenov. 2006. Features of acoustic emission in the relaxation of rocks. – *Bulletin KRSU*, 6, 7, 51–55 (in Russian).
- Turin, A. I., A. M. Kupryashkin, P. P. Ananiev et al. 2013. Softening of interfaces ferruginous quartzite under the influence of magnetic pulse treatment. – *Bulletin of Tambov University. Natural and technical sciences*, 18, 4, 1699–1700 (in Russian).
- Turin, A. I., S. D., Viktotov, A. N. Kochanov et al. 2016. Investigation of the strength properties of individual phases and interphase boundaries of complex multiphase materials on the example of rocks. – *Bulletin of Tambov University. Natural and technical sciences*, 21, 3. 1368–1374 (in Russian).
- Usov, A., V. Tsukerman. 2000. Prospective of electric impulse processes for the study of the structure and processing of mineral raw materials. – *Developments in Mineral Processing*, 13, 8–15.
- Winiarski, B., I. A. Guz. 2008. The effect of cracks interaction for transversely isotropic layered material under compressive loading. – *Finite Elements in Analysis and Design*, 44, 4, 197–213.

## REGRESSION ANALYSIS OF FACTORS AFFECTING MICROBIAL FUEL CELL EFFICIENCY

*Anatoliy Angelov, Ani Stefanova, Katerina Nikolova*

*University of Mining and Geology "St. Ivan Rilski", 1700 Sofia; tonyagev@mgu.bg*

**ABSTRACT.** In a laboratory installation of a Microbial Fuel Cell (MFC), based on the process of microbial sulphate reduction in the anodic chamber of the cell, the factors influencing the efficiency of the fuel element have been investigated. Under the conditions of a planned laboratory experiment, the temperature, pH, H<sub>2</sub>S and sulphate concentration in the anodic chamber, and the dissolved oxygen content in the cathodic chamber of MFC have been varied. Meanwhile, the Open Circuit Voltage (OCV) and the maximum values of power in MFC are measured as possible target functions. A multifactorial regression analysis has been performed with respect to the selected independent parameters and the target function. A mathematical model of the target function has been obtained from the selected independent variables that can be used to optimise the operation of a microbial fuel cell based on the microbial sulphate reduction process.

**Keywords:** Microbial Fuel Cells, microbial sulphate reduction and multifactorial regression analysis

## РЕГРЕСИОНЕН АНАЛИЗ НА ФАКТОРИТЕ ОКАЗВАЩИ ВЛИЯНИЕ ВЪРХУ ЕФЕКТИВНОСТТА НА МИКРОБНА ГОРИВНА КЛЕТКА

*Анатолий Ангелов, Ани Стефанова, Катерина Николова*

*Минно-геоложки университет "Св. Иван Рилски", 1700 София*

**РЕЗЮМЕ.** В лабораторна инсталация на микробна горивна клетка (МГК), базирана в анодната зона на процеса на МСР, са изследвани факторите оказващи влияние върху ефективността на горивния елемент. При условията на планиран лабораторен експеримент са варираны стойностите на температурата, рН, концентрация на H<sub>2</sub>S и сулфати в анодната зона и съдържанието на разтворен кислород в катодната зона на МГК. Паралелно са измервани като възможни целеви функции - напрежението на отворена верига (OCV) и максималната стойност на мощността на микробната горивна клетка. Направен е многофакторен регресионен анализ по отношение на избраните независими параметри и целевата функция. Получен е математически модел на целевата функция от подобрените независими променливи, който може да се използва за оптимизация на работата на микробна горивна клетка, базирана на процеса на микробна сулфатредукция.

**Ключови думи:** микробни горивни клетки, микробна сулфатредукция и многофакторен регресионен анализ

## Introduction

The environmental issues associated with the use of carbon-based fossil fuels and the increasing role of renewable energy sources are becoming more urgent in the development of modern civilization. It has been proven that microbial fuel cells (MFCs) are a promising innovative technology for energy generation and wastewater treatment due to their low costs and sustainability (Chouler et al., 2016). These are systems where electroactive microorganisms using different energy sources (mainly organic compounds, but also some inorganic substrates such as hydrogen, sulphide, iron or ammonium) convert this energy directly into electricity. The efficiency of this type of system for energy generation shows a continuous trend to improvement, but it is still low compared to conventional energy sources.

It has been found that a significant set of factors influences the efficiency of MFCs, such as these related to the constructive features and the choice of suitable materials, as well as those determined by the environmental conditions in the anodic and cathodic chambers of the biological fuel elements (Stefanova et al., 2018).

Some of the studies in recent years have been focused on the application of the microbial sulphate-reduction process in the anodic chamber of MFCs, used for the treatment of sulphate-rich wastewaters (Angelov, et al., 2013). Wastewaters with high sulphate contents (of over 3 g/l) are typical of the mining and the ore processing industries and form a major environmental problem (Johnson and Hallberg, 2005). The microbial fuel cells based on the process of microbial sulphate reduction (MSR) in the anodic zone provide the opportunity to remove sulphates from the incoming water together with the generation of electricity. In this process an oxidation of the hydrogen sulphide on the anode to an elemental sulphur and other final products is performed.

The analysis of the factors affecting the chemical, the electrochemical and the biological processes occurring in MFCs is essential in order to optimise their performance and to demonstrate the applicability of this type of fuel elements in practice.

The main objective of the present study is to perform an analysis of a selected set of technological factors, affecting the operation of a microbial fuel cell, based on the process of microbial sulphate reduction in the anodic chamber of the fuel

element. For this purpose, under the conditions of a planned experiment, the influences of temperature, pH, sulphate and H<sub>2</sub>S concentrations in the anodic zone and oxygen content in the cathodic one, on the open circuit voltage (OCV) and the maximum power values ( $P_{max}$ ) of the MFC are studied.

## Materials and methods

For the conduction of the experiments a laboratory-scaled installation of the microbial fuel cell is used and the scheme is presented in Fig. 1. The microbial fuel cell is constructed in 2 equal in sizes sections, anode and cathode, located in a U-shaped construction, separated by a cation-exchange membrane. The volume of the anodic and cathodic chambers is of 0.48 dm<sup>3</sup> each. For the separation of the anode from the cathode, a cation-exchange membrane type CMI-7000S (Membrane International Inc.) with an area of 0.0012 m<sup>2</sup> is used. Graphite rods with a diameter of 8 mm and a length of 9

cm are used as electrodes. The surface geometric area of one electrode is 0.0028 m<sup>2</sup>. Approximately half of the volume of the buffer tank (the vessel is with a volume of 0.7 dm<sup>3</sup>) is filled with 0.3 kg of modified zeolite(4). The same is a sulphidogenic bioreactor sequentially connected to the anodic chamber of the fuel element. The modified zeolite plays the role of a biofilm carrier from the SRB bacteria and other metabolically related groups of microorganisms.

A modified Postgate nutrient medium with a volume of 1.1 dm<sup>3</sup> is added to fill the anodic chamber volume and the sulphidogenic bioreactor. The inoculation of the microbial cell was performed with 50 ml of a mixed culture of sulphate-reducing bacteria (SRB). After the formation of an active biofilm of SRB, it begins a feeding of the nutrient medium for the continuous cultivation of the bacteria. The medium from the tank (1) feeds into the fuel cell with a regulated flow through the peristaltic pump (2). The homogenisation in the microbial fuel cell is accomplished by means of a recirculating pump (5).

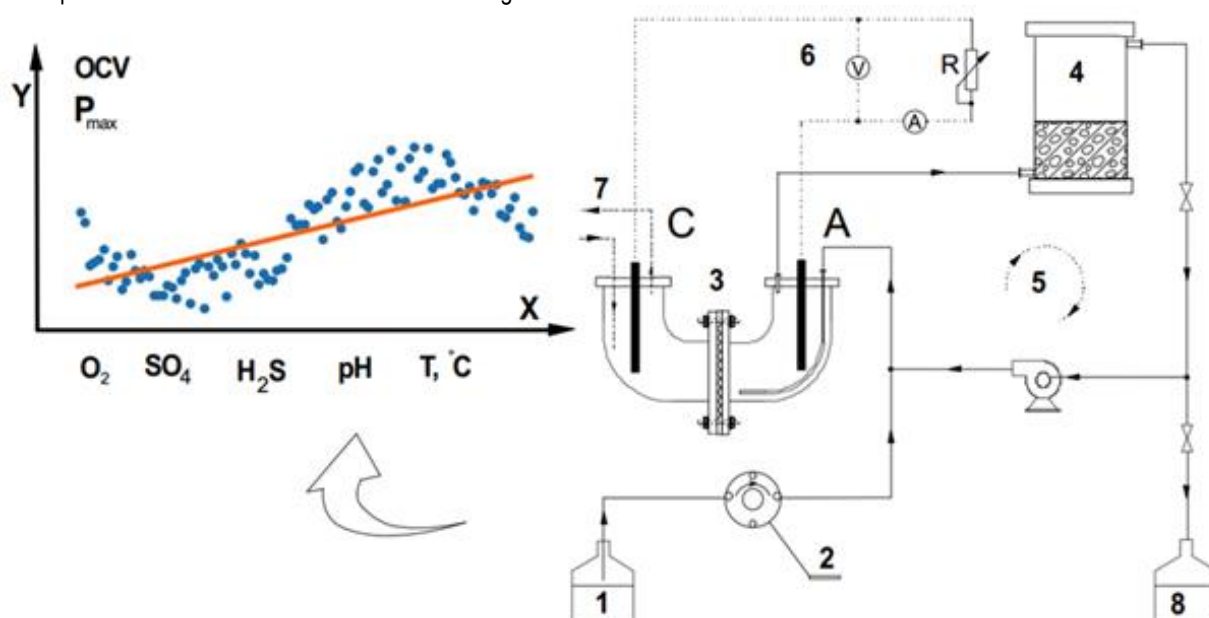


Fig. 1. A scheme of the laboratory-scaled installation of MFC, where experiments are conducted to determine the impact of T, pH, dissolved oxygen, SO<sub>4</sub> and H<sub>2</sub>S contents through the method of the linear regression analysis.

1 - feeding solution in anodic area, 2 - dosing peristaltic pump, 3 - microbial fuel cell, 4 - bioreactor, 5 - recirculation pump, 6 - electricity chain with a consumer, 7 - air flow in cathodic area, 8 - collector tank.

The solutions outgoing from the settler are collected in a collecting tank (8) with a volume of 3 dm<sup>3</sup>. For the achievement of the required temperature in MFC, a thermo-regulated water bath is used. The used nutrient medium has the following composition, in g/l: K<sub>2</sub>HPO<sub>4</sub> - 0.25, NH<sub>4</sub>Cl - 0.5, wt. Na<sub>2</sub>SO<sub>4</sub> - 2.0, CaCl<sub>2</sub> - 0.1, MgSO<sub>4</sub>·7H<sub>2</sub>O - 4.0, Na - lactate - 6.0, yeast extract - 0.25 and has a pH of 6.5.

For the purpose of the linear regression analysis, experiments with the MFC under abiotic conditions are conducted, thus it is possible to maintain the values of the independent parameters (T, pH of the anolyte, dissolved oxygen in the catholyte, SO<sub>4</sub><sup>2-</sup> and H<sub>2</sub>S in the anolyte) constant for the time of the tests. The obtained values of the dependent parameters (OCV and  $P_{max}$ ) under abiotic conditions are compared with those, obtained under biotic MFC operational conditions.

For the purpose of the linear regression analysis with the change in the values of each of the independent parameters, the values of the rest were kept constant. The selected constant values of the independent parameters are T - 24°C, pH 7.5, SO<sub>4</sub><sup>2-</sup> - 3g/l, H<sub>2</sub>S-360 mg/l and dissolved oxygen content in the catholyte - 6.8 mg/l in an open air mode. For the appropriate temperature variation range, the experiments are carried out under thermostated conditions.

The concentration of sulphates in the medium is changed to 4 variants - 0.5, 1.5, 3.0 and 4.5 g/l. Respectively, in order to determine the influence of the H<sub>2</sub>S in the anolyte 4 concentrations are maintained - 150, 250, 350 and 450 mg/l by the addition of an appropriate amount of Na<sub>2</sub>S in the anolyte. The pH value is also changed in 4 variants - 5.5, 6.5, 7.5 and 8.5 by adding 0.1 N HCl solution and/or 0.1 N NaOH solution. A 100 mM solution of K<sub>3</sub> [Fe (CN)<sub>6</sub>] in a 67 mM phosphate buffer solution at pH 7.0 is used as a catholyte in the cathodic

semi-element of the microbial fuel cell. In this case, a final electron acceptor is the oxygen in the air, which in its reduction, together with the protons present in the cathodic space, form water. For this purpose, it is possible to aerate the cathodic chamber, so the experiments are carried out in 4 aeration modes - 0.5, 1.0, 1.5 l/s air and without aeration - in open air mode.

The pH is measured using a pH electrodes (VWR) and a pH meter HANNA HI 9021. The Eh is measured using a WTW Electrode Sen Tix ORP. The electrical conductivity is measured using the Conductivity Electrode WTW LF90.

In some certain points in the laboratory-scaled installation the parameters pH, TDS and Eh are measured. Corresponding to the same sampling points, the concentrations of sulphates by BaCl<sub>2</sub> reagent at 420 nm and hydrogen sulphide using Nanocolor 1-88 / 05.09 at 620 nm are determined spectrophotometrically. The electric parameters of the fuel cell are measured with a Keithley 175 digital multimeter, with a precision potentiometer with a maximum value of 11 kΩ, used for a load resistor (consumer). The maximum power value P<sub>max</sub> is measured by the plotting of polarisation curves for each of the tested variants. Using a NI Sensor DAQ controller (DAQ Board) and a software based on the Virtual Instrumentation LabView<sup>R</sup> (Mironescu et al., 2007), the parameters pH, T, Electrical conductivity, OCV and P<sub>max</sub> are monitored.

## Result and discussion

The purpose of the planned experiment is to achieve an analytical dependence by the appropriate processing of the experimental data, through a multifactor regression analysis- a mathematical model that would allow an assessment of the weight of each of the independent factors on the process. To obtain a correct model in the regression analysis, each one of the independent parameters must be varied, while the remaining ones are kept constant (He et al., 2016).

For the purpose of the regression analysis an experiment is planned, whereas the values of the independent parameters - T - 24°C, pH 7.5, SO<sub>4</sub><sup>2-</sup> - 3g/l, H<sub>2</sub>S - 360 mg/l and dissolved oxygen content in the catholyte - 6.8 mg/l are kept constant at the independent variation of each one of them. At the same time, the values of the dependent parameters - OCV and P<sub>max</sub>, the target functions of this multifactorial linear regression analysis, are monitored. The selected ranges for the variation of the independent parameters correspond to their possible real values, in the MFC operation based on the MSR process in the anodic chamber. The results obtained for the two target functions, OCV and P<sub>max</sub>, and the selected ranges of variation of the independent parameters are presented in Table 1. The measured values of OCV and P<sub>max</sub> are averaged, as from 3 to 5 reiterations are made.

The regression analysis is performed with both programmes - StatPlus<sup>R</sup> and XLStat<sup>R</sup> (Zar et al., 2007) and similar results are obtained. From the various possible variants for the type of resultant regression equation, a multifactorial linear regression of the following type is chosen:

$$Y_{1,2} = a + b.X_1 + c.X_2 + d.X_3 + e.X_4 + f.X_5 \quad (1)$$

Table 1. Data for the target functions OCV and P<sub>max</sub> in the laboratory-scaled installation of MFC for the purpose of the regression analysis

pH- 7.5, SO <sub>4</sub> - 3g/l, H <sub>2</sub> S- 360 mg/l, O <sub>2</sub> - 6.8 mg/l				
T, °C (X <sub>1</sub> )	10	24	32	41
OCV, mV (Y <sub>1</sub> )	650	708	778	820
P <sub>max</sub> , mW (Y <sub>2</sub> )	0.457	0.556	0.613	0.724
T- 24°C, SO <sub>4</sub> - 3g/l, H <sub>2</sub> S- 360 mg/l, O <sub>2</sub> - 6.8 mg/l				
pH, (X <sub>2</sub> )	5.5	6.5	7.5	8.5
OCV, mV (Y <sub>1</sub> )	654	690	749	782
P <sub>max</sub> , mW (Y <sub>2</sub> )	0.385	0.419	0.490	0.529
T- 24°C, pH- 7.5, H <sub>2</sub> S- 360 mg/l, O <sub>2</sub> - 6.8 mg/l				
SO <sub>4</sub> , g/l (X <sub>3</sub> )	0.5	1.5	3.0	4.5
OCV, mV (Y <sub>1</sub> )	516	620	708	781
P <sub>max</sub> , mW (Y <sub>2</sub> )	0.393	0.432	0.568	0.643
T- 24°C, pH- 7.5, SO <sub>4</sub> - 3g/l, O <sub>2</sub> - 6.8 mg/l				
H <sub>2</sub> S, mg/l (X <sub>4</sub> )	113	237	360	561
OCV, mV (Y <sub>1</sub> )	614	661	720	779
P <sub>max</sub> , mW (Y <sub>2</sub> )	0.330	0.418	0.546	0.577
T- 24°C, pH- 7.5, SO <sub>4</sub> - 3g/l, H <sub>2</sub> S- 360 mg/l				
O <sub>2</sub> , mg/l (X <sub>5</sub> )	6,8	7,9	8,8	9,6
OCV, mV (Y <sub>1</sub> )	655	682	736	775
P <sub>max</sub> , mW (Y <sub>2</sub> )	0.452	0.555	0.627	0.762

Accordingly, the accepted indications are as follows: Y<sub>1</sub>- OCV (mV), Y<sub>2</sub>- P<sub>max</sub> (mW), X<sub>1</sub> - temperature (°C), X<sub>2</sub>- pH the anolyte, X<sub>3</sub>-sulphates concentration in the anolyte (g/l), X<sub>4</sub>- H<sub>2</sub>S concentration in the anolyte (mg/l), X<sub>5</sub>-dissolved oxygen content in the catholyte (mg/l). The values of the obtained main regression indicators are presented in Table. 2.

Table 2. Main regression indicators

	Y <sub>1</sub> (OCV)	Y <sub>2</sub> (P <sub>max</sub> )
Correlation coefficient - R	0.9432	0.9304
Determination coefficient - R <sup>2</sup>	0.89	0.87
Uncertainty coefficient	0.15	0.19
Standard error - S, %	28.9162	0.0492
Number of observations	20	20

The final variant of the obtained regression equations is as follows:

$$Y_1 = -127,59 + 5,9114.X_1 + 34,17.X_2 + 68,07.X_3 + 0,38.X_4 + 14,89.X_5 \quad (2)$$

$$Y_2 = -1,063 + 0,0094.X_1 + 0,062.X_2 + 0,058.X_3 + 0,0006.X_4 + 0,073.X_5 \quad (3)$$

The results obtained from the regression analysis confirm the adequacy of the choice of the independent variables and their expected significance for the selected target functions (OCV and  $P_{\max}$ ). The value of the correlation coefficients ( $R_{Y1} = 0.94$ ,  $R_{Y2} = 0.93$  - Table 2) is in the range 0.9-1, which gives reason to believe that the obtained regression equations give functional dependencies between the dependent and the independent variables.

On the basis of the calculated values of the regression coefficients, it can be said that the factors with the greatest influence on the value of the OCV are the pH of the anolyte and the sulphate content therein, followed by the concentration of dissolved oxygen (in the cathodic chamber), the temperature and the concentration of  $H_2S$  in the anode. Regarding the influence on the value of  $P_{\max}$ , it is found that the influence of the dissolved oxygen in the cathodic chamber is the most serious factor, the other independent parameters are arranged in the order mentioned above. This is also confirmed by other studies, in which the influence of oxygen in the catholyte, the conductivity of the anolyte, the influence of pH and temperature are established (Nikolova et al., 2013). It should be kept in mind that for the accurate maintaining of the independent factors values, the OCV and  $P_{\max}$  are measured under abiotic conditions and therefore the influence of the biomass on the electrically active SRBs and other metabolically related microorganisms is not taken into account. The values of the determination coefficients  $R^2$  (89% for OCV and 87% for  $P_{\max}$ ), indicating the percentage of changes in target function values due to the selected independent factors, again leads to a strong dependence between the selected independent and dependent parameters. The resulting regression equations are valid only in the selected ranges of variations of the independent factors.

## Conclusion

The obtained results from the study confirm that a great number of factors influence the efficiency of MFC based on the process MSR in the anodic chamber. In the multifactorial linear regression analysis, are driven models to determine the influence of the temperature, pH, the concentrations of

sulphates and  $H_2S$  in the anode and the oxygen content in the cathodic zone, on the values of OCV and  $P_{\max}$ .

**Acknowledgment.** This study was funded by the Bulgarian National Science Fund, Grant № DN077, 15.12.2016.

## References

- Angelov, A., S. Bratkova, A. Loukanov. 2013. Microbial fuel cell based on electroactive sulphate-reducing biofilm. – *Energy Conversion and Management*, 67, 283–286.
- Chouler, J., G. A. Padgett, P. J. Cameron, K. Preuss, M. M. Titirici, I. Ieropoulos et al. 2016. Towards effective small scale microbial fuel cells for energy generation from urine. *Electrochim. Acta*, 192, 89–98.
- He, Y. J., Z. F. Ma. 2016. A Data-Driven Gaussian Process Regression Model for Two-Chamber Microbial Fuel Cells. – *Fuel Cells*, 16, 3, 365–376.
- Johnson, D. B., K. B. Hallberg. 2005. Acid mine drainage remediation options: a review. – *Science of the Total Environment*, 338, 3–14.
- Lefebvre, O., C. M. Neculita., Y. Xiaodi, N. H. Yong. 2012. Bioelectrochemical treatment of acid mine drainage dominated with iron. – *Journal of Hazardous Materials*, 241–242, 411–417.
- Mironescu, M., C. Posten, K. Kriger, R. Tzoneva. 2007. Control and command of biotechnological processes using a flexible application developed in LabView. – *IFAC Proceedings Volumes*, 40, 18, 801–806.
- Nikolova, K., A. Angelov, S. Bratkova, P. Genova. 2013. Influence of various factors on the efficiency of MFC based on the process of microbial dissimilatory sulfate-reduction. – *Annals of the “Constantin Brancusi”, University of Targu Jiu, Engineering Series*, 3.
- Stefanova, A., A. Angelov, S. Bratkova, P. Genova, K. Nikolova. 2018. Influence of electrical conductivity and temperature in a microbial fuel cell for treatment of mining waste water, *Annals of the “Constantin Brancusi”, University of Targu Jiu, Engineering Series*, 3.
- Zar J. H. 2007. *Biostatistical Analysis*. Prentice-Hall, Englewood Cliffs, 355–390.

## VOLUMETRIC COEFFICIENT OF OXYGEN MASS TRANSFER ANALYSIS IN A COLUMN PHOTOBIOREACTOR

*Anatoliy Angelov, Evgeni Kraichev, Marta Lecheva, Sotir Plochev*

*University of Mining and Geology "St. Ivan Rilski", 1700 Sofia; tonyagev@mgu.bg*

**ABSTRACT.** The oxygen mass transfer speed, as one of the technological factors influencing the growth and development of the phototrophic microorganisms (microalgae), was researched in a column type photobioreactor. A series of experiments under different aeration conditions were performed where the corresponding oxygen mass transfer coefficient values ( $K_La$ ) were measured. The dynamics of basic technological parameters: temperature, pH, electrical conductivity etc. in parallel with the dissolved oxygen concentration were monitored. The oxygen mass transfer coefficient value influence during the different photosynthesis phases, as well as during the various phototrophic microorganisms' cultivation stages, was determined.

**Keywords:** volumetric coefficient of oxygen mass transfer, microalgues, photobioreactor and bioenergy

### АНАЛИЗ НА ОБЕМНИЯ КОЕФИЦИЕНТ НА МАСОПРЕНАСЯНЕ ПО КИСЛОРОД В КОЛОНЕН ФОТОБИОРЕАКТОР

*Анатолій Ангелов, Евгєні Країчев, Марта Лєчева, Сотир Плочєв*

*Минно-геоложки университет "Св. Иван Рилски", 1700 София*

**РЕЗЮМЕ.** В колонен тип фотобиореактор е изследвана скоростта на масопренасяне на кислорода, като един от технологичните фактори оказващи влияние върху растежа и развитието на фототрофните микроорганизми (алги). Направени са серия от експерименти при различни условия на аерация, за които са измерени съответните стойности на коефициента на масопренасяне по кислород ( $K_La$ ). Проследена е динамиката на основни технологични параметри: температура, рН, електропроводимост и др., паралелно с концентрацията на разтворен кислород. Установено е влиянието върху стойността на коефициента на масопредаване по кислород ( $K_La$ ), както през различните фази на фотосинтезата, така и през различните етапи от култивирането на фототрофните микроорганизми.

**Ключови думи:** Обемнен коефициент на масопренасяне по кислород, алги, фотобиореактор и биоенергия

### Introduction

One of the main factors for the successful functioning of gas-liquid reactors is the mass exchange in the gas-liquid system, which in turn depends on the hydrodynamic picture in the reactors, the phase mixing and the physico-chemical properties of the medium. Determination of the volume factor  $K_La$  in gas-liquid bioreactors is essential in order to determine the efficiency of aeration and to evaluate the effect of operating parameters on the oxygen supply to the system (Zedníková et al., 2018).

A major challenge is to develop a model that can well describe the physical nature of mixing in two-phase reactors, taking into account the influence of more parameters, and can be consistent with a wide range of experimental data. The contact between the two phases (liquid and gas) in the bioreactor depends mainly on its type, on the stirring speed and on the formation of gas bubbles.

Typically, the oxygen transfer rate is carried out over the entire contact surface ( $a$ ) and refers to the working volume of the bioreactor. The driving force behind this process is the difference between the equilibrium and the current concentration of oxygen in the liquid phase (1):

$$\frac{dC_L}{dt} = k_L a (C_L^* - C_L) \quad (1)$$

The proportionality factor  $K_La$  is called the volumetric mass transfer coefficient of oxygen and plays an essential role in aerobic processes,  $C_L^*$  and  $C_L$  being the equilibrium and current oxygen concentrations, respectively. It is only measured indirectly, and depending on the environment - model or cultural. A number of authors (Law et al., 2004; Vandu, Krishna, 2004) have referred to the so-called "start-up dynamic method" as one of the most effective for determining  $K_La$  in bubble column reactors.

The use of microalgae for various purposes in biotechnology has attracted considerable scientific interest in recent decades because of its potential for use in wastewater treatment, biofuel production and valuable pharmaceutical products (Poonam & Sharma, 2017). The cultivation of microalgae can be carried out in open (natural and artificial lakes, lagoons, etc.) and in closed systems (photobioreactors - PBRs). Different type of photobioreactors (PBRs) are developed to optimise the various environmental factors and technological parameters (Wang et al., 2012).

Oxygenic photosynthesis (Masojidek et al., 2013) in microalgae includes the so-called. "Light" and "Dark reactions" and photorespiration (Fig. 1 and equation 2). Photosynthesis and respiration are processes that occur simultaneously in microalgae, but nonetheless, the rate of respiration is low compared to the rate of photosynthesis, leading to a net consumption of carbon dioxide and oxygen production. In the absence of light, algae respiration continues until photosynthesis stops, leading to net oxygen consumption and production of carbon dioxide (Masojidek et al., 2013; Malapascua et al., 2014).

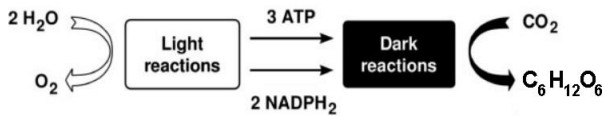
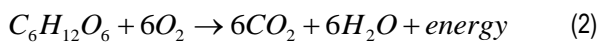


Fig. 1. Light and dark reactions of photosynthesis



One of the important factors in the cultivation of microalgae is the balance between the concentrations of dissolved carbon dioxide and oxygen in the culture medium. Carbon dioxide concentration is vital for the growth and development of microalgae. The source of  $\text{CO}_2$  for microalgae in autophototrophic culture can be a limiting factor if its concentration is low in the supply gas (for example, when only air is used as a source of  $\text{CO}_2$ ). On the other hand, a high concentration of dissolved  $\text{CO}_2$  would lead to a low pH of the culture medium, which may be inhibitory for some microalgae.

With respect to dissolved oxygen, some photobioreactors (eg Tubular and Serpentine PBRs) have been shown to accumulate oxygen and these higher levels of  $\text{O}_2$  in the culture fluid can reduce the productivity of microalgae cultures. On the other hand, at high dissolved oxygen concentrations and high light levels, reactive oxygen species (ROS) can be formed, which can have a toxic effect on microalgae (Weissman et al., 1988).

The main objective of this study is to determine the effect on the value of the mass transfer coefficient for oxygen ( $K_La$ ), both during the different phases of photosynthesis and during the different stages of cultivation of phototrophic microorganisms. At the same time, the dynamics of basic technological parameters are also monitored: temperature, pH and electrical conductivity, in parallel with the dissolved oxygen concentration in the bubble column PBR.

## Materials and methods

To achieve these goals, the experiments were carried out in a laboratory installation (Fig. 2), including a bubble column PBR, representing a Plexiglas tube with an inside diameter of 85 mm, a height of 630 mm and a working volume of  $2.5 \text{ dm}^3$ . For efficient flow of photosynthesis along the PBR, a plexiglas tube with an internal diameter of 36 mm was installed in which a 20W fluorescent lamp - type "SunGlo" was installed in light illumination mode 12h light: 12h dark.

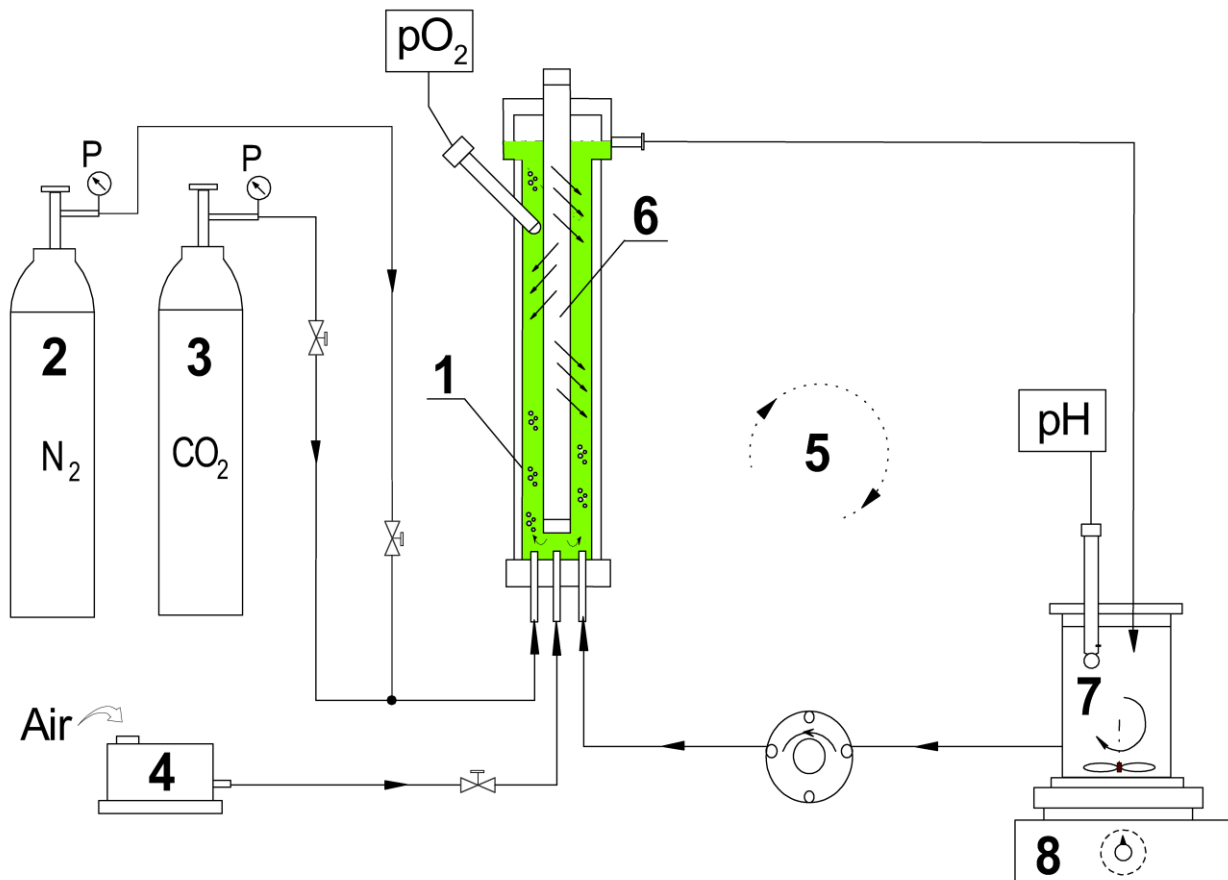


Fig. 2. Scheme of the laboratory installation: 1 - Photobioreactor (PBR), 2 -  $\text{N}_2$  bottle, 3 -  $\text{CO}_2$  bottle, 4 - Air pump, 5 - Recirculation pump, 6 - Fluorescent lamp, 7 - Buffer vessel, 8 - Magnetic stirrer

The culture fluid was recycled at a flow rate of 10 dm<sup>3</sup> / h by a peristaltic pump (5) through a buffer vessel (7) with a volume of 1 dm<sup>3</sup>. From the bottom of the photobioreactor (PBR) through an air pump (4) the aeration was provided and a CO<sub>2</sub> bottle was used (3).

For laboratory testing *Chlorella sp.* algae strain (wild-type) was isolated from local freshwater. For the cultivation of microalgae, the modified medium BG-11 (Adriano et al., 2015) with the following composition was used for 1 L - 1.5 g NaNO<sub>3</sub>, 0.5 g Na<sub>2</sub>CO<sub>3</sub>, 0.04 g K<sub>2</sub>HPO<sub>4</sub>, 0.075 g MgSO<sub>4</sub>.7H<sub>2</sub>O, 0.036 g CaCl<sub>2</sub>.2H<sub>2</sub>O, 0.045 g Citric acid, 0.0015 g, Ferric ammonium Citrate, 0.045 g EDTA (disodium salt), and 1ml trace elements solution consisted of 2.86 g/l H<sub>3</sub>BO<sub>3</sub>; 1.81 g/l MnCl<sub>2</sub>.4H<sub>2</sub>O; 0.222 g/l ZnSO<sub>4</sub>.7H<sub>2</sub>O; 0.39 g/l NaMoO<sub>4</sub>.2H<sub>2</sub>O; 0.079 g/l CuSO<sub>4</sub>.5H<sub>2</sub>O; 0.0494 g/l Co(NO<sub>3</sub>)<sub>2</sub>.6H<sub>2</sub>O.

Algae were inoculated at 10% ( $V_{inoculation}/V_{media}$ ) in a volume of 3.5 dm<sup>3</sup> of PRB together with the buffer vessel (Fig. 2). Microalgae cultivation was carried out at room temperature in the range 23-25°C. The photobioreactor (PBR) was aerated by means of an air pump with a flow rate of 2.5 dm<sup>3</sup>/ h, without further addition of CO<sub>2</sub> to the air.

A variant of the start-up dynamic method based on the liquid phase oxygen balance (Vandu, Krishna, 2004) was used to determine the K<sub>L</sub>a mass transfer coefficient in the photobioreactor. For the purpose of measurement, constant aeration conditions are maintained in the column photobioreactor, whereby the dissolved oxygen concentration reaches a stationary value.

The process is as follows: initially dissolved oxygen dissolved in the liquid phase by purging the culture fluid with N<sub>2</sub> to reach dissolved oxygen content up to 0.1- 0.05 mg/l O<sub>2</sub>. The system is then aerated again by passing purified air through the liquid (with an air flow rate of 2.5 dm<sup>3</sup>/60 s), immediately measuring the dissolved oxygen concentration C<sub>L</sub> over time (t) using an oxygen optic sensor - DO-BTA Vernier<sup>®</sup> and using the LabQuest<sup>®</sup> interface.

The measurements are continued until the equilibrium oxygen concentration is reached. The process is described by equation (1) and after its integration at t = 0, C<sub>L</sub>\* = const and C<sub>L</sub> = C<sub>L,0</sub>, assuming that at the beginning there is no oxygen in the liquid phase C<sub>L,0</sub> = 0, we obtain:

$$\ln \left[ \frac{C_L^*}{C_L^* - C_L} \right] = k_L a t \quad (3)$$

When plotted the graph -  $\ln \left[ \frac{C_L^*}{C_L^* - C_L} \right]$ , as a function of time (t) and the slope of the obtained lines, the volume mass coefficient K<sub>L</sub>a is calculated.

A Burkler counter with optical type microscope (Boeco BM-800) was used to determine the number of microalgae and parallel determination of the optical density (OD) of the cell suspension during microalgae cultivation was measured at 650 nm and a red filter. The laboratory facility provides on-line measurement of dissolved oxygen, pH, electrical conductivity, temperature and illumination by using Vernier<sup>®</sup> BTA sensors and visualisation through the LabQuest<sup>®</sup> interface.

## Result and discussion

PBR work continued in the laboratory and samples from the culture suspension were taken to determine cell count and optical density (OD) during a period of 30 days. The results obtained in Fig. 3 show that the stationary phase was reached up to 20 days, with the exponential (Log) phase continuing between 5 and 20 days from the start of cultivation.

During the various stages of microalgae development, the value of K<sub>L</sub>a was measured (using the start-up dynamic method described above), at days 5, 15, and 25 respectively, during the dark and light phase of photosynthesis.

The dynamics of oxygen concentration for the three cases is shown on Fig.4. From the obtained results for the dynamics of dissolved oxygen, it can be concluded that the higher values of dissolved oxygen (in Light phase) in the medium during the exponential phase (15 days) are probably due to the more intense photosynthesis, respectively the production of photosynthetic oxygen.

At the beginning of the cultivation period (5 day), due to the lower intensity of photosynthesis, no significant differences in DO concentration were observed during the light and dark phases. At the end of the cultivation period (25 days), the equilibrium concentrations of dissolved oxygen C<sub>L</sub>\*, have values between the previous 2 cases (Fig. 4).

The results obtained with respect to the coefficient K<sub>L</sub>a (Table 1) for the 3 periods of cultivation in PBR, cannot be interpreted uniquely, but can serve to more effectively manage the aeration systems in this type of PBRs.

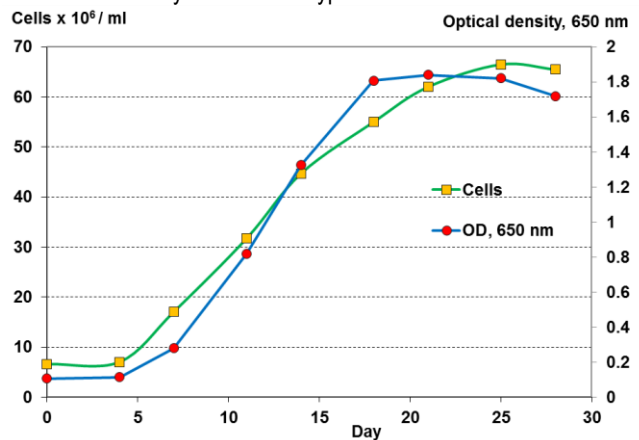


Fig.3. Growth curve and change in optical density (at 650 nm) in PBR

It should be borne in mind that the concentration of dissolved oxygen in the PBR, in addition to temperature, air flow rate and pressure (parameters which are kept constant), are influenced by the respiration rate and photosynthesis of microalgae, as well as the total dissolved solids (TDS), which increased from 1650 μS /cm to 2530 μS /cm (measured as electrical conductivity in the culture fluid) during PBR cultivation (30 days).

The calculated values of K<sub>L</sub>a (Table 1) showed variation in the range 0.0060 - 0.0067 s<sup>-1</sup>, which is confirmed by other studies conducted in bubble column PBR (Kazbar et al., 2019). The relative difference of K<sub>L</sub>a values between the light and dark phases is greatest in the measurements taken on the 15th day from the beginning of the experiment, i.e. during the exponential (Log) phase.

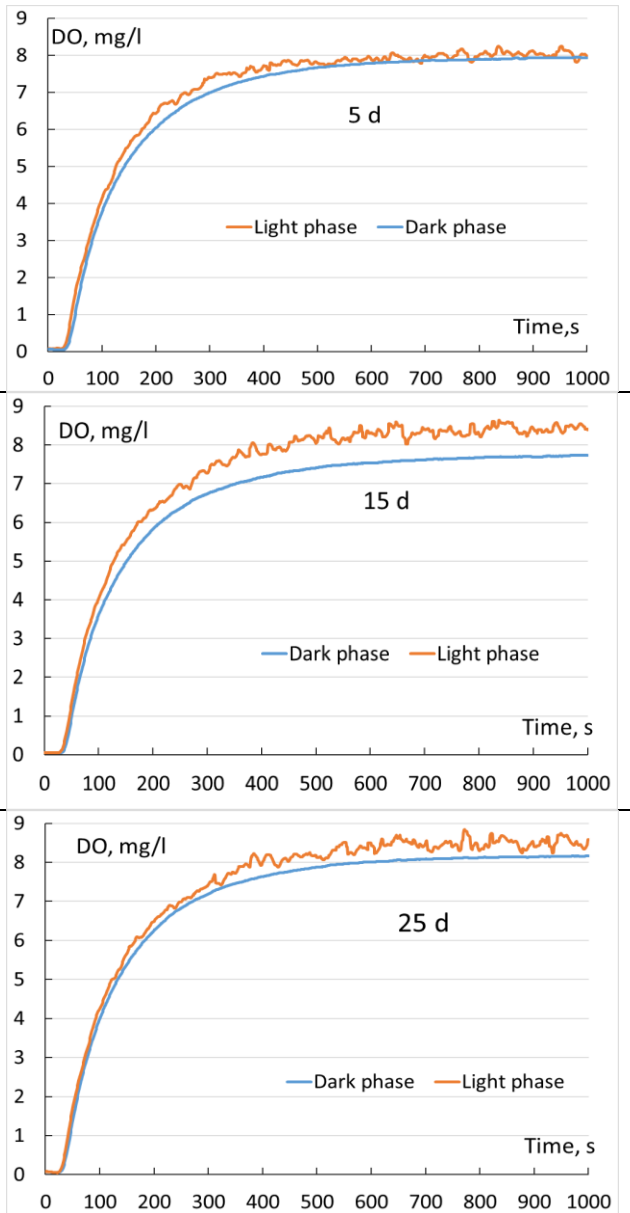


Fig. 4. The dynamics of dissolved oxygen in determining  $K_{La}$  for 5, 15 and 25 days of microalgae cultivation

Table1. Values of  $K_{La}$  at 5<sup>th</sup>, 15<sup>th</sup> and 25<sup>th</sup> days of microalgae cultivation

Day	5	15	25
$K_{La}, s^{-1}$			
Dark phase	0.0060	0.0061	0.0068
Light phase	0.0062	0.0066	0.0071

Table2.  $K_{La}$  values at different air flow rates in the PBR

Q, L/min	1.0	2.5	4.5
$K_{La}, s^{-1}$			
Dark phase	0.0061	0.0063	0.0083
Light phase	0.0062	0.0068	0.0084

In the studies performed to determine the influence of the degree of aeration (for 3 different air flow rates) on the value of  $K_{La}$ , an increase from 0.061 to 0.084  $s^{-1}$  was found during both phases of photosynthesis (Table 2 and Fig. 5). These measurements were performed till the end of the microalgae cultivation in the period (day 30) in PBR.

Undoubtedly, the optimisation of the aeration system and the hydrodynamics of the flow in the bubble column PBR are likely to have a positive effect on the production of microalgae biomass. During the various stages of PBR operation, no accumulation of high oxygen levels in the reactor volume was detected.

For a more detailed study of the photosynthesis and respiration processes of microalgae in PBRs, it is necessary to consider both mass transfer and  $CO_2$  (Kazbar et al., 2019), as well as the ratio of mass transfer rates for  $CO_2$  and  $O_2$  -  $K_{La}(CO_2) / K_{La}(O_2)$ .

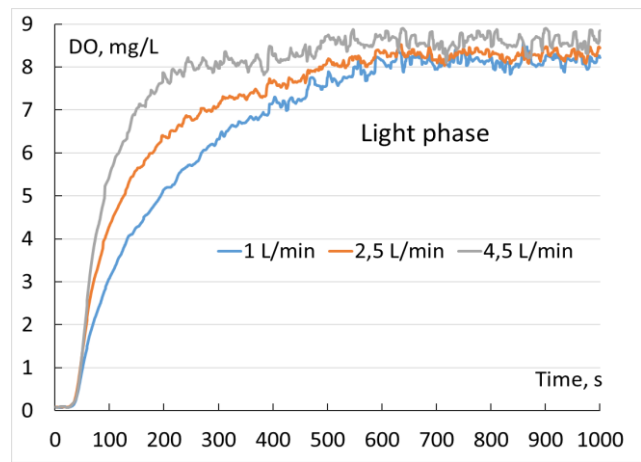
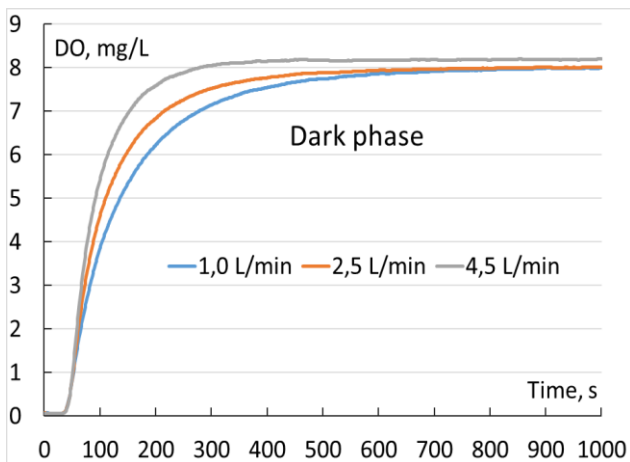


Fig. 5. Dynamics of dissolved oxygen during the determination of  $K_{La}$ , for different flow rates of the supplied air

## Conclusion

In the present bubble column PBR study, the rate of oxygen mass transfer was examined as one of the technological factors affecting the growth and development of microalgae. The values of  $K_La$  in the real culture medium have been established, both during the different phases of photosynthesis and during the different stages of cultivation of phototrophic microorganisms. The results obtained can serve to optimise microalgae cultivation processes and refine PBR design.

**Acknowledgment.** This study was funded by the Bulgarian National Science Fund, Grant № KP\_06\_H27/4, 08.12.2018.

## References

- Adriano, A. H., M. da R. Gabriel, M. Luiza, G. de M. Michele, A. V. C. Jorge. 2015. The cultivation of microalgae *Cyanobium* sp. and *Chlorella* sp. in different culture media and stirring setting. – *African Journal of Microbiology Research*, 9, 21, 1431–1439.
- Kazbar, A., G. Cogne, B. Urbain, H. Marec, B. Le-Gouic, J. Tallec, J. Pruvost. 2019. Effect of dissolved oxygen concentration on microalgal culture in photobioreactors. – *Algal Research*, 39, 101432.
- Lau, R., W. Peng, L. G. Velazquez-Vargas, G. Q. Yang, L. S. Fan. 2004. Gas-Liquid Mass Transfer in High-Pressure Bubble Columns. – *Industrial & Engineering Chemistry Research*, 43, 5, 1302–1311.
- Malapascua, J. R. F., C. G. Jerez, M. Sergejevová, F. L. Figueroa, J. Masojidek. 2014. Photosynthesis monitoring to optimise growth of microalgal mass cultures: application of chlorophyll fluorescence techniques. – *Aquat. Biol.*, 22, 123–140.
- Masojidek, J., Torzillo, G., Koblížek, M. 2013. Photosynthesis in Microalgae. *Handbook of Microalgal Culture*, 21–36.
- Poonam Sharma, Nivedita Sharma. 2017. Industrial and biotechnological applications of algae: A review. – *Journal of Advances in Plant Biology*, 1, 1, 1–25.
- Vandu, C. O., R. Krishna. 2004. Influence of scale on the volumetric mass transfer coefficients in bubble columns. – *Chemical Engineering and Processing: Process Intensification*, 43, 4, 575–579.
- Wang, B., C. Q. Lan, M. Horsman. 2012. Closed photobioreactors for production of microalgal biomasses. – *Biotechnology Advances*, 30, 4, 904–912.
- Weissman, J. C., R. P. Goebel, J. R. Benemann. 1988. Photobioreactor design: Mixing, carbon utilization, and oxygen accumulation. – *Biotechnology and Bioengineering*, 31, 4, 336–344.
- Zedníková, M., S. Orvalho, M. Fialová, M. Ruzicka. 2018. Measurement of volumetric mass transfer coefficient in bubble columns. – *Chem. Engineering*, 2, 2, 19.

## CRUSHING CIRCUIT OPTIMISATION IN A LEAD-ZINC PROCESSING PLANT

*Irena Grigorova, Marin Ranchev, Ivan Nishkov*

*University of Mining and Geology "St. Ivan Rilski", 1700 Sofia; irena\_mt@abv.bg*

**ABSTRACT.** A mineralogical study in order to determine the mineral composition of the ore entering the Rudozem concentrator have been carried out. Polished sections of ore samples from the three hydrothermal Pb-Zn deposits - Petrovitsa, Varba-Batantsi and Kroushev dol have been prepared. The studies were performed using a MEIJI MT 9430 optical microscope equipped with a DK 3000 digital camera. Compared to the ores from the other lead-zinc deposits in the Madan ore field, the ore processed in Rudozem plant contains harder to grind components, resulting in poor plant performance and limited production capacity. Therefore, it was recommended to improve the old crushing and screening circuit (three stage crushing in closed circuit) with new modern equipment comprising of two stage crushing and screening, including – jaw and cone crushers and one high throughput vibrating screen operated in open circuit. This study therefore sets out to assess the benefits of the new equipment for the downstream processes.

**Keywords:** crushing, screening, open circuit, equipment

## ОПТИМИЗИРАНЕ СХЕМАТА НА ТРОШЕНЕ ПРИ ПРЕРАБОТКАТА НА ОЛОВНО-ЦИНКОВИ РУДИ

*Ирена Григорова, Марин Ранчев, Иван Нишков*

*Минно-геоложки университет "Св. Иван Рилски", 1700 София*

**РЕЗЮМЕ.** За определяне минералния състав на рудата, постъпваща на преработка в ОФ „Рудозем“ бяха проведени микроскопски изследвания. Бяха изготвени полирани микроскопски препарати (аншлифи) от три осреднени, квартовани рудни проби от находищата Петровица, Върба-Батанци и Крушев дол. Микроскопските изследвания на препаратите са проведени с помощта на поляризационен микроскоп MEIJI MT 9430, окомплектован с дигитална камера. В сравнение с рудите от другите оловно-цинкови находища в Маданското рудно поле, рудата преработвана в ОФ „Рудозем“, съдържа трудно смлаеми компоненти, което води до ниски технологични показатели и ограничена производителност. Поради това, беше препоръчано старата схема на трошене и пресяване (тристадиална схема на трошене в затворен цикъл) да бъде подменена с ново модерно оборудване, включващо челюстна и конусна трошачка и високо производително вибрационно сито, работещи в отворен цикъл и два стадия на трошене и пресяване. В това изследване се прави оценка на предимствата на новото оборудване върху последващите процеси в технологичната верига на фабриката.

**Ключови думи:** трошене, пресяване, отворен цикъл, оборудване

## Introduction

The largest, economically most important deposits of Pb-Zn ores in Bulgaria are located in the Central Rhodopes, in the Madan ore field. The polymetallic ore mineralisation in Madan ore field is controlled by major six several steep ore fault zones, with length to 10-15 km and more, with NNW- SSE trending (Fig. 1). The Pb-Zn mineralisation has been represented by three morphogenetic types of ore bodies – steep to subvertical ore veins (1 to 3 km wide, up to 7 km long), marble-hosted metasomatic ore bodies and disseminated stockworks. The metasomatic (skarn) ore bodies are developed by hydrothermal replacement at intersections of the ore-controlling faults with the marble horizons.

The main ore minerals in the deposits are represented by galena, sphalerite, pyrite and subordinate amount of chalcopyrite, and non-metallic minerals - mainly of quartz, carbonates, johannsenite-hedenbergite skarns (in metasomatic ores bodies) and others.

The hydrothermal Pb-Zn deposits in Madan ore field are hosted in the Rhodopean metamorphic complex, consisting mainly of high grade metamorphic rocks of the Madan Tectonic Unit (Madan Allochton) and Arda Unit. The Pb-Zn ore deposits

Petrovitsa, Varba-Batantsi and Kroushev dol are hosted in the rocks of the Madan Unit - various gneisses, schists, amphibolites and marbles.

The predominant metamorphic rocks are represented by biotite and amphibole-biotite gneisses, containing amphibolite bodies (metagabbro), irregularly alternating with marbles packages containing graphite and phlogopite. A characteristic feature of the Madan Unit is the abundance of quartz-feldspar veins, located both in parallel and crosscut on the metamorphites. Among the migmatized biotite and amphibole-biotite gneisses, biotite gneiss-schists with and without garnet are established, forming irregular layers.

Comminution processes such as crushing and grinding constitute a significant proportion of capital and operating costs in mineral processing plants (Napier-Munn et al., 2005).

Crushing circuits are an essential part of most mineral processing plants, with various production units such as crushers, screens, bins, conveyors and feeders. There are numerous configuration and number of units in each processing plant, as the main purpose of crushing is to prepare the ore for further processing, i.e. to produce a certain amount of material of a certain size per day so that the grinding circuit has sufficient feed.

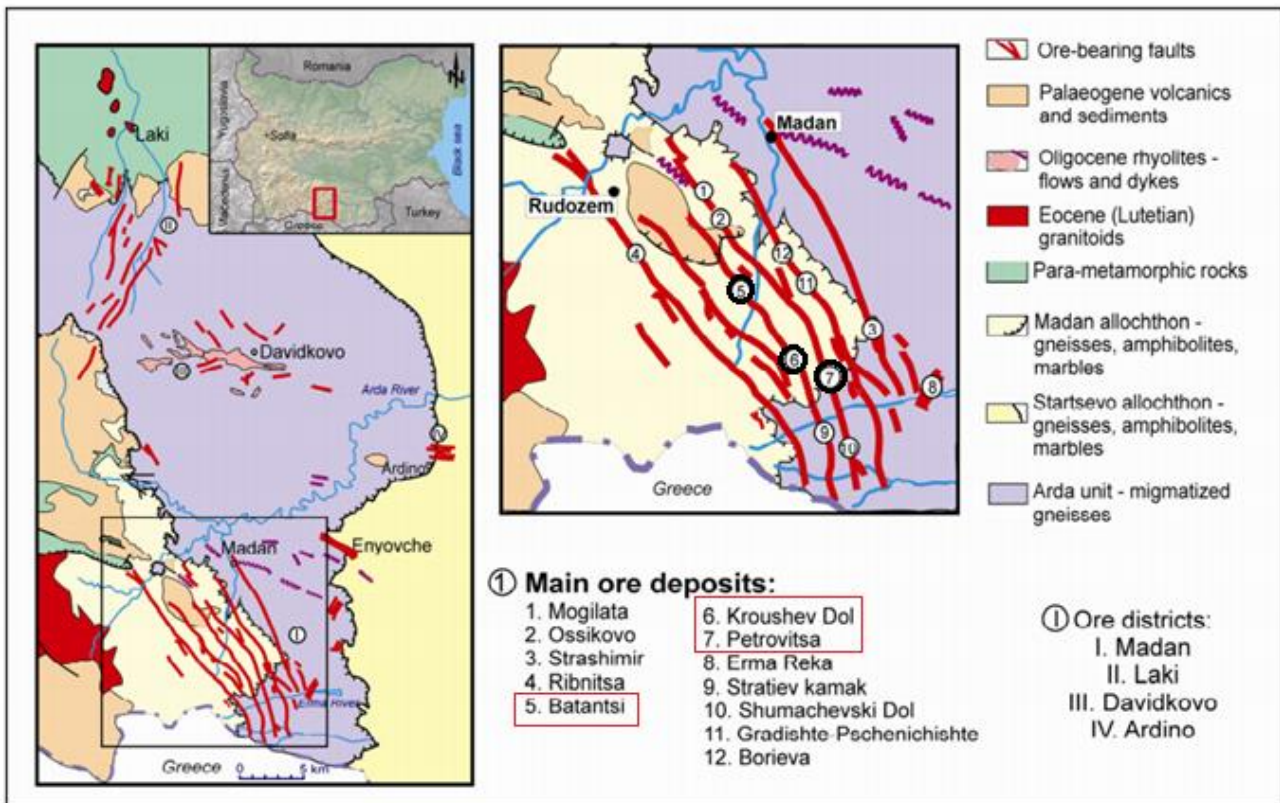


Fig. 1. Simplified geological map of the ore deposits in the Central Rhodopes and location of the main Madan ore deposits (modified from Vassileva et al., 2009, after Ivanov, 2000)

According to Napier-Munn et al. (2005), the criteria for a comminution optimisation campaign are usually determined by the following objectives:

- Maximise throughput and maintain the existing final product size specification;
- Change final product size and maintain the existing throughput;
- Maintain existing throughput and final product size, but minimise working costs.

Following the above mentioned objectives, the optimisation of the old crushing and screening circuit will enable the ball mills to take advantage of the finer feed (change of the final product size) that is produced from the new crushing and screening equipment.

The purpose of this research paper is to assess the benefits of changing the three-stage crushing and screening circuit to two-stage, by replacing the original (old) equipment with new state of the art crushing and screening units.

#### Original three-stage crushing and screening circuit of the Rudozem concentrator

The original crushing and screening circuit includes a primary KKD-500/75, secondary KSD 1750 and tertiary KMDT 2200 cone crushers manufactured in Uralmash, the Ural Heavy Machine Building Plant, Yekaterinburg, Russia, and the vibrating screens type SB-350 manufactured in Monek-Yug (former Komsomolec plant) Kardzhali, Bulgaria, have been in operation for more than 50 years. The flowsheet of the original Rudozem crushing and screening circuit is shown in Figure 2.

## Materials and Methods

### Mineralogical studies

In order to determine the mineral composition of the ore, polished sections of representative ore samples from the three hydrothermal Pb-Zn deposits - Petrovitsa, Varba-Batantsi and Kroushev dol have been prepared. Mineralogical studies of the polished sections were performed using a MEIJI MT 9430 optical microscope equipped with a DK 3000 digital camera.

### Particle size distribution of ball mill feed

Particle size analysis of the ball mill feed have been conducted, in order to assess the performance of the old (original) and the new crushing and screening circuit. The laboratory sieve analysis was carried out with sieve shaker Retsch AS 200 using the following test sieves (200 x 50 mm): 45, 40, 35, 20, 16, 14, 10, 5, 2 and 1 mm. Furthermore, the total reduction ratio for both crushing circuits has been calculated.

### Reduction ratio

The reduction ratio of a crushing stage can be defined as the ratio of maximum particle size entering to maximum particle size leaving the crusher (Wills, Napier-Munn, 2006). All crushers have a limited reduction ratio meaning, that the size reduction will take place in stages (Metso Minerals®, 2002). In order to compare the total reduction ratio for both circuits, data from a plant survey conducted after the installation of the new equipment have been analysed and the results are presented below.

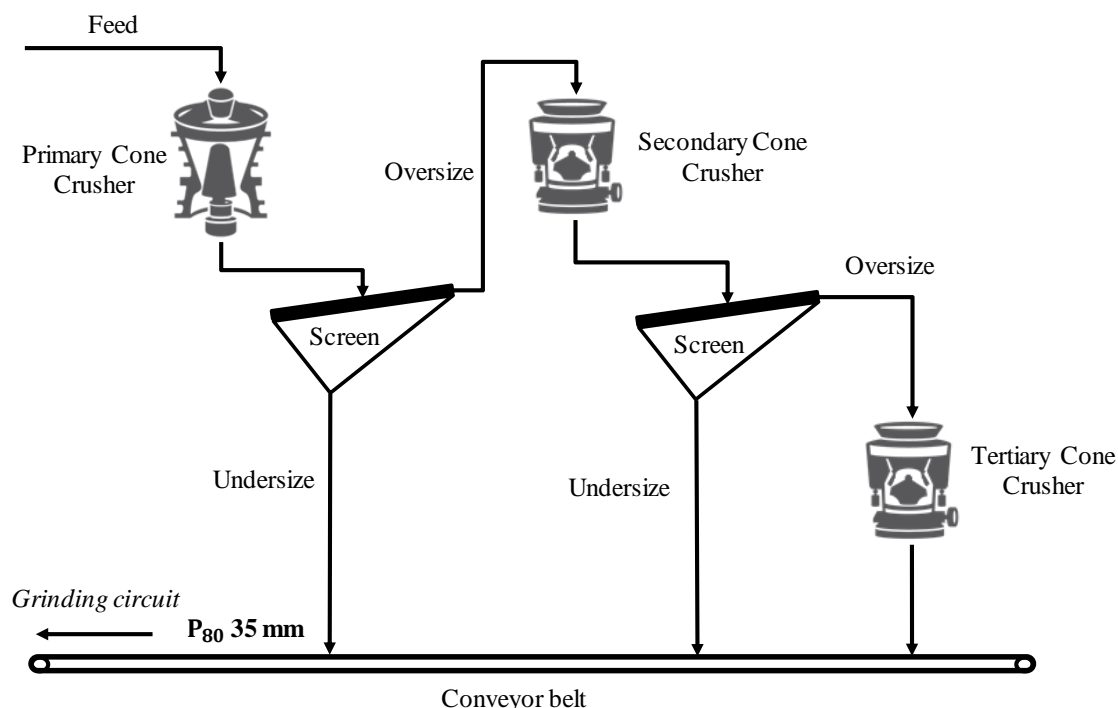


Fig. 2. Original crushing and screening circuit of the Rudozem concentrator

## Results and Discussions

### Mineralogical studies

The data from the conducted studies in polished sections by reflected light microscopy show that in the samples examined there are fragments from both the quartz-sulphide ore veins and the metasomatic ore bodies, formed in the skarns and in the marbles, present among the host metamorphic rocks.

The results obtained show that the main ore minerals in the ores are represented by galena, sphalerite, pyrite and subordinate amount of chalcopyrite and non-metallic minerals - mainly of quartz, carbonates, johannsenite-hedenbergite skarns, flaky phyllosilicate minerals (sericite, chlorite), clayey phases and others (Fig. 3). The presence of pyrrhotite and pyrite-marcasite pseudomorphoses after primary pyrrhotite is also found in the ore from the Varba-Batantsi deposit.

Data on temperature of forming, distribution of main ore minerals within quartz-sulphide mineralization and content of trace elements in separate ore minerals suggest dome-like type of zoning in the Madan ore field (Kolkovski, Dobrev, 2000). In the upper (outer) zone the mineralisation is quartz-sulphide with a sphalerite prevailing over the galena, the galena showing high content of Ag and Sb. In the intermediate zone mineralisation is quartz-sulphide again, but galena prevails over the sphalerite, with the galena being enriched with Bi, as well as with Ag and Sb. At the lowest level of the deposits barren quartz is found.

The host rocks, including the lead-zinc deposits in the Madan ore field, also differ in lithological composition. Some of the deposits such as Varba - Batantsi, Kroushev Dol and Petrovitsa are located in the Madan Unit (Madan allohton), occupying the upper parts of the metamorphic complex in the Central Rhodopes. The Madan Unit is made up of a variety of high grade metamorphic rocks – biotite and amphibole-biotite

gneisses, amphibolites, mica-schists, marble packages containing graphite and phlogopite, etc. A characteristic peculiarity of the Madan Unit is the presence of abundant quartz-feldspar bodies and veins. Skarns and sulphide mineralisation are often developed on the contact of pegmatite bodies with the marbles included among the gneisses.

According to Grigorova et al. (2017), it has become increasingly popular in large scale mineral exploration surveys to use non-invasive geophysical methods for collecting more accurate information about the location and the geological properties of the ore bodies and surrounding area. This information can be particularly important when presence of components such as gneisses and other high grade metamorphic rocks occur in the area of interest.

It is well known that the presence of components, such as gneisses and garnet-containing gneiss-schists, amphibolites (metagabbro), pegmatites, mica, chlorites, graphite etc., will cause difficulties during ball mill grinding, due to the higher bond work index (kWh/t) values, which they possess. Therefore, in order to reduce the size of the ore particles entering the ball mill grinding circuit and to decrease the energy consumption required for ball milling, it was suggested that a replacement of the obsolete crushing and screening machinery should be realized.

### Particle size distribution of ball mill feed

The results from the laboratory particle size analysis clearly demonstrate the higher efficiency of the new crushing and screening equipment, providing a product in the size range of  $-16.00 +0.00$  mm, which will favourably affect the performance of the downstream processes, i.e. the ball mill grinding and flotation. It is important to highlight the fact that despite the contrast in P80 for both products, there is no significant difference in the amount of finer sizes ( $-2.00$  mm) as a result of which the slime production in the circuit will be reduced. The ball mill feed size distribution curve is shown on Figure 4.

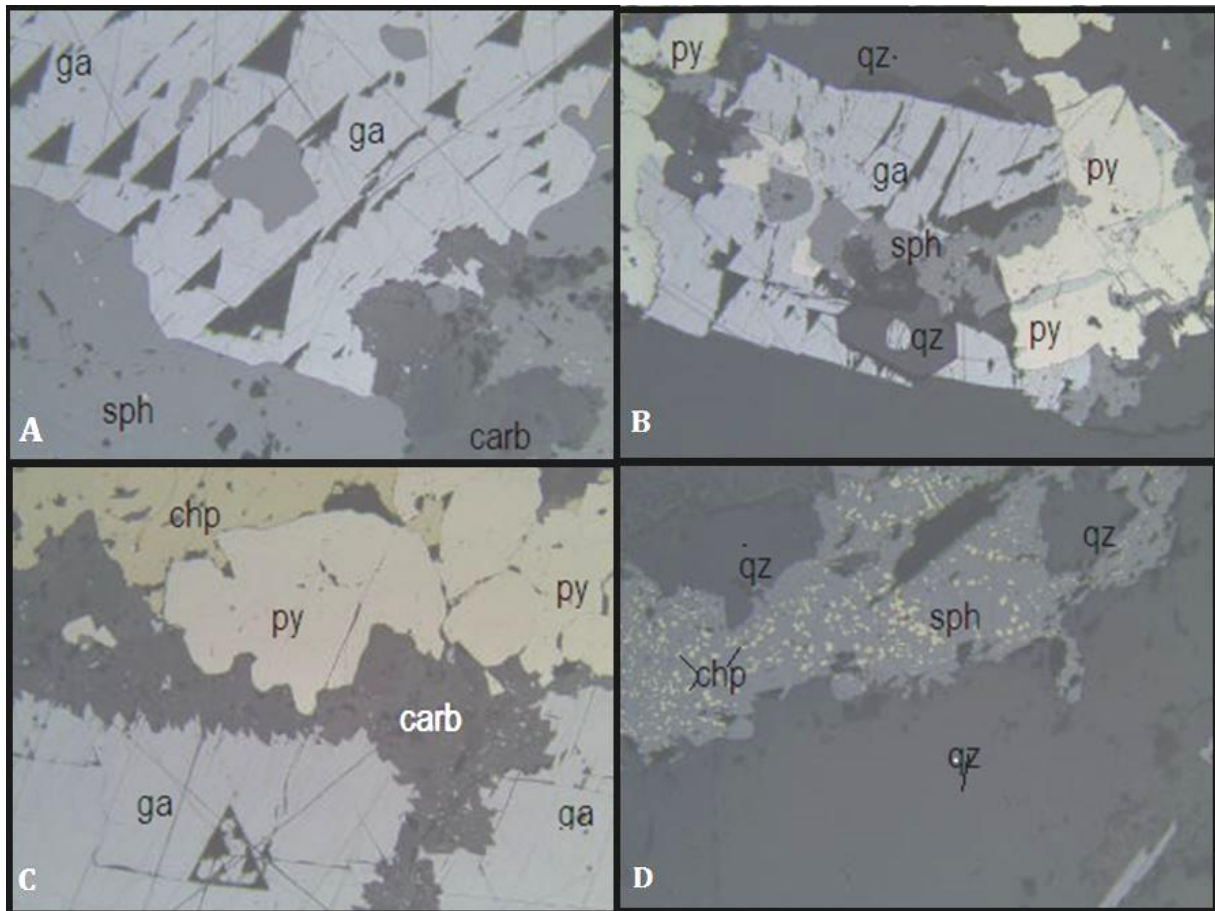


Fig. 3. Photomicrographs of the mineral assemblages from the Pb-Zn ores, processed in the Rudozem concentrator. Reflected light, N II, width of view – 820  $\mu$ m: A) Galena (ga) and sphalerite (sph), corroded by carbonate (carb); B) Galena (ga), pyrite (py), sphalerite (sph) and quartz (qz). C) Galena (ga), pyrite (py) and chalcopyrite (chp), corroded by carbonate (carb) veinlets; D) Sphalerite (sph) with disseminated fine-grained inclusions of chalcopyrite (chp) among quartz (qz)

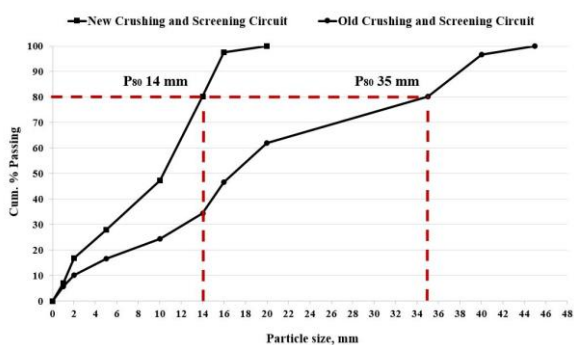


Fig. 4. Comparing the ball mill feed particle size distribution

### Reduction ratio

The results from the sampling campaign, involving a simple size analysis of the crushed products from the original and the new crushing and screening units are presented in Table 1 below:

The estimated total reduction ratio (R) for both circuits is shown below:

- Old crushing and screening circuit: R1 = 2.4; R2=2.1; R3=3.43;

Table 1. Size analysis of the crushed products

Product	Old crushing and screening circuit:	New crushing and screening circuit:
Feed ore, mm	600	600
Primary crushed Product, mm	250	70
Secondary crushed product, mm	120	P <sub>80</sub> 14 mm
Tertiary crushed Product, mm	P <sub>80</sub> 35 mm	-

- Total reduction ratio: R1xR2xR3 = 17.3

- New crushing and screening circuit: R1 = 8.57; R2=5.0

- Total reduction ratio: R1xR2 = 42.85

The results show that a higher reduction ratio with less crushing equipment has been achieved, which is a prerequisite for lower operating costs i.e. saving energy, mechanical reliability, easy and safe maintenance.

### New state of the art crushing and screening circuit

The original crushing and screening circuit includes a vibrating grizzly feeder, providing a continuous feed rate and scalping of the ROM. The primary crushing of the ore is carried out in a jaw crusher with actual feed opening depth of 700 mm and 1060 mm width, with throughput capacity of around 160 – 190 t/h. The size control of the circuit is accomplished by an incline double deck vibrating screen, with 30 mm top deck and

14 mm bottom deck apertures. The screen oversize and mid-size fractions are fed to the cone crusher, the undersize fraction combined with the cone crusher product is conveyed to an intermediate stockpile and then fed to the ball mills. The secondary crushing stage is carried out in a cone crusher with 14 mm closed side setting (stroke setting) and throughput capacity of 110 – 170 t/h. A simplified block flow diagram of the new crushing and screening circuit is shown in Figure 5.

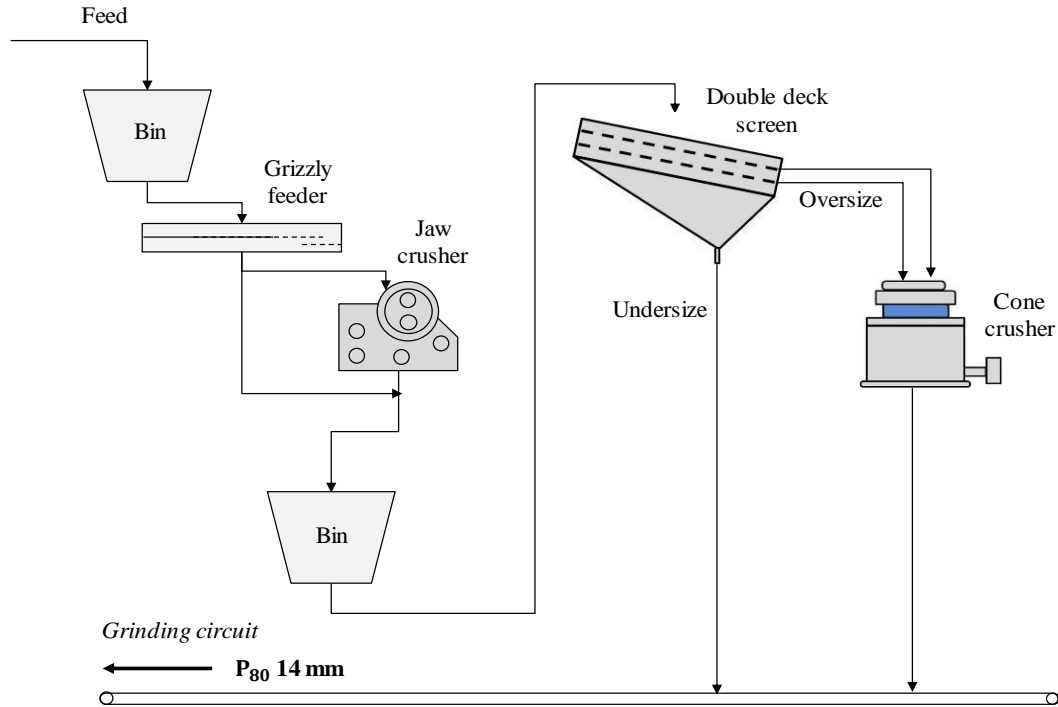


Fig. 5. New crushing and screening circuit of the Rudozem concentrator

### Conclusions

Based on the results from the mineralogical studies, it can be concluded that the improvement of the crushing and screening circuit in the Rudozem concentrator, will provide a finer ball mill feed product, thus boosting the grinding efficiency of the harder to grind ore components and reducing the specific energy consumption. Furthermore, the higher reduction ratio, achieved by fewer machines, ensures an easy maintenance, cost efficiency and safe working environment. Taken together, the findings in this research highlight the benefits of the new crushing and screening equipment installed in the Rudozem concentrator.

**Acknowledgements.** Financial support for this study and permission to publish this paper from MINSTROY HOLDING JSC is gratefully acknowledged.

### References

Grigorova, M., I. Koprev. 2017. 3D model of limestone inclusions in Maritsa Iztok mine based on electrical resistivity tomography. – *Acta Geobalcanica*, 3–2, 51–56.

- Kolkovski, B., S. Dobrev. 2000. Ore mineralization in the Central Rhodopes. Oligocene mineralization. Madan ore field. – In: *Structure, Alpine Evolution and Mineralisations of the Central Rhodopes Area (South Bulgaria)* (Ed. Ivanov, Z.). ABCD-GEODE, Guide to Excursion B, Borovetz, 28–35.
- Metso Minerals®. 2002. *Handbook Basics in Mineral Processing*. 30 p.
- Napier-Munn, T. J., S. Morrell, R. D. Morrison, T. Kojovic. 2005. *Mineral Comminution Circuits – Their Operation and Optimization*. JK/MRC, University of Queensland, Brisbane, 335 p.
- Vassileva, R., R. Atanassova, I. Bonev. 2009. A review of the morphological varieties of ore bodies in the Madan Pb-Zn deposits, Central Rhodopes, Bulgaria. – *Geochemistry, Mineralogy and Petrology*, 47, 31–49.
- Wills, B. A., T. Napier-Munn. 2006. *Mineral Processing Technology: An Introduction to the Practical Aspects of Ore Treatment and Mineral Recovery*. Butterworth-Heinemann, Oxford, 108–109.

## EXTRACTION OF RHENIUM FROM AMMONIACAL LEACHING SOLUTIONS OF COPPER SMELTING SLAG AND MODEL SOLUTIONS

*Aleksandr Ignatovich, Denis Luckiy, Rinat Khismatullin*

*Saint Petersburg Mining University, 199106 Saint Petersburg; asignatovich@yandex.ru*

**ABSTRACT.** It is known that copper ores and waste of copper production often contain rhenium. In some deposits or dumps, its quantity is sufficient to recognize this raw material as profitable for obtaining rhenium in various forms. Rhenium has the status of a strategic raw material; it is used in the creation of refractory alloys and catalysts of the oil refining industry. At the moment rhenium is not produced in the Russian Federation. One of the options for obtaining rhenium is its extraction from leaching solutions of metallurgical slags. The most rational method of extraction is sorption on the ion exchange sorbent perrenate-ion. This process can significantly increase the profitability of copper slag processing. In the course of the work, the effect of various components of the solution on sorption of perrenate-ion on an ion-exchange sorbent AV-17-8 was studied.

**Keywords:** perrenate-ion, sorption, rhenium, hydrometallurgy

## ЕКСТРАКЦИЯ НА РЕНИУМ ОТ АМОНИЯЧНИ ИЗЛУЖВАЩИ РАЗТВОРИ НА РАЗТОПЕНА МЕДНА ШЛАКА И МОДЕЛИ НА РЕШЕНИЯ

*Александър Игнатович, Денис Лъкий, Ринат Кисматулин*

*Санктпетербургски минен университет, 199106 Санкт Петербург*

**РЕЗЮМЕ.** Известно е, че медните руди и отпадъците от производството на мед често съдържат рений. В някои находища или сметища неговото количество е достатъчно, за да се приеме тази суровина като рентабилна за получаване на рений в различни форми. Реният има статут на стратегическа суровина; използва се при създаването на огнеупорни сплави и катализатори в нефтопреработвателната промишленост. В момента рений не се произвежда в Руската федерация. Една от възможностите за получаване на рений е извличането му от разтворите за излужване на металургични шлаки. Най-рационалният метод за екстракция е сорбция на йонообменния сорбент перренат-йон. Този процес може значително да повиши рентабилността на обработката на медната шлака. В хода на работата е изследвано въздействието на различни компоненти на разтвора върху сорбцията на перренат-йон върху йонообменния сорбент AV-17-8.

**Ключови думи:** перренат-йон, сорбция, рений, хидрометалургия

### Introduction

In recent decades, the abundance of natural resources has been significantly depleted. In addition, dumps and "waste" deposits are a long-term source of environmental pollution due to the spontaneous leaching of metals from them. Therefore, to solve these problems, many copper smelters aim at the introduction of technology for processing of copper smelting slurries. The main advanced technology is hydrometallurgical processing, namely the leaching of sludge. In addition to the main component – copper, it can extract by-products such as rhenium, which is found in the composition of copper-molybdenum ores (Luganov, 2004).

Rhenium is a typical dispersed element that does not form independent minerals. Mostly, rhenium is found in molybdenum and copper-molybdenum ores, which are currently its main sources.

The reserves of Russian rhenium are estimated at 310 tons, this is the 3rd place in the reserves worldwide. However, according to some data, there is no mass production of

rhenium at the moment in the Russian Federation. This makes the issue of creating and implementing a cost-effective technology for its production even more acute, since rhenium is a strategic raw material. Rhenium is currently in demand in the industry. A significant step in the production of rhenium is the production of ammonium perrenate by sorption-elution processes with further cleaning. In the future, ammonium perrenate is converted in the form of metallic rhenium. Metal rhenium is a strategically important raw material. 83.3% of the produced rhenium is used to create heat-resistant alloys and super-alloys used in the manufacture of rocket engine nozzles and rotating parts of aircraft engines, as well as in energy. 9.3% of the produced rhenium is used in the production of Pt-Re catalysts for oil refining processes, for example, the production of high-octane gasoline, hydro desulphurisation processes. Rhenium is used in the production of thermocouples, heating elements, electrodes, electrical connectors, electromagnets, as well as in organic synthesis, catalysis and medicine. The main forms of rhenium used are rhenium, rhenium perrenate and rhenic acid.

Due to the fact that rhenium is a concomitant element, methods for obtaining rhenium as a by-product are now in demand since this can significantly increase the profitability of obtaining waste elements such as copper.

The accumulated volumes of copper-containing technogenic mineral resources in Russia practically correspond to the volumes of minerals put on the balance of deposits. Only in the metallurgical industry more than 95 million tons of slag are produced from them annually, more than 10% are in the copper metallurgy. In this situation, it is necessary to find ways to develop the copper raw material base with the involvement of man-made mineral resources, primarily through the improvement of existing technologies for their enrichment.

One of the most accessible resources for copper is slag of copper smelting metallurgical enterprises in the Urals. The Ural region is called the "copper belt" of Russia and it has accumulated a significant number of them over a long period. The predominant factors of the involvement of slag in processing are economic benefits, which are determined by the possible profit of the enterprise and environmental feasibility, which is expressed in terms of environmental performance. In total, the Ural region has accumulated more than 110 million tons of copper slag.

One of the most promising technologies for the associated extraction of rhenium is the ion exchange sorption, as it is effective for the extraction of dispersed components. In addition, sorption processes can have high selectivity, and can be easily integrated into the process cycle. To create the technology and select the sorbent, it is necessary to determine the thermodynamic and kinetic parameters of the ionite.

## **Review and selection of the analysis method**

For the development of technologies related to the recovery of rhenium from the leaching solution a methodology is necessary to determine its content in the samples. It should be noted that the content of rhenium in raw materials is extremely low. What causes the choice of those techniques that are able to provide high accuracy?

Spectrophotometry, gravimetry, kinetic, electrochemical, extraction-fluorimetric methods as well as X-ray fluorescence analysis are used as the main methods for the determination of rhenium.

The main problems of most methods for the determination of rhenium are their lack of sensitivity, reproducibility of the results, and the interfering influence of accompanying elements of the sample. In modern analytical chemistry, methods such as inductively coupled plasma atomic emission spectroscopy (ICP AES), inductively coupled plasma mass spectrometry (ICP MS), as well as a number of electrochemical methods are used to determine rhenium.

However, the main problem that a researcher encounters when using these methods is the influence of incidental sample components. In view of this, the question of concentrating rhenium and separating it from the matrix is extremely important.

Spectrophotometric methods make it possible to determine the content of rhenium in a sample up to  $10^{-2}$ – $10^{-5}$  wt. %. The

advantage of these techniques lies in the simplicity, availability of equipment and relatively high sensitivity. Spectrophotometric techniques are based on the formation of coloured complex compounds of rhenium with appropriate reagents. The distributed methods use rodanide and thiocyanate ions, thiourea. The disadvantage is the need for preliminary separation of rhenium from interfering with the determination of impurities (Mo, W, Cu). This is carried out by concentrating the perrhenate ions by sorption or extraction.

Atomic emission spectroscopy with inductively coupled plasma (AES-ICP) is used to determine rhenium in mineral raw materials and metallurgical products. The advantage of AES-ICP is high stability and reproducibility of results, a wide linear range of concentrations. The method allows to determine up to  $10^{-4}$  wt. % rhenium. However, the correctness of the results of analysis in atomic emission spectrometry with inductively coupled plasma depends on many factors, for example, related to the physical properties of the solutions — their viscosity, surface tension, etc.; with chemical interaction of the sample components; with the superposition of the spectral lines of the sample components and with the negative effect of plasma ionisation. The determination of rhenium by AES-ICP in complex objects, for example, products of metallurgical production, is a difficult task, since the emission lines of rhenium are not very sensitive, moreover, they partially overlap with the lines of accompanying elements.

Nowadays, ICP-MS allows rhenium to be determined at the ng/g level. However, when using ICP-MS, a number of problems arise associated with the influence of various factors on the formation of an analytical signal. The accuracy of the method is affected by the matrix, signal drift, saline background, and isobar overlays.

Over the past decade, the X-ray fluorescence method (XRF) has not lost its relevance for the determination of rhenium. It is fast and often used for mass analysis in industry. However, the method is not without flaws: firstly, the detection limit of rhenium by XRF is low and is only 0.05–0.1 wt.%, Secondly, there is a problem associated with interfering influence from the associated sample components. The use of concentration allows not only to lower the detection limit in the X-ray phase analysis method, but at the same time to reduce the influence of interfering elements on the rhenium signal. For the concentration of rhenium the XRF methods often use sorption of rhenium in the form of perrhenate ions.

A significant place in the analytical chemistry of rhenium is occupied by the electrochemical methods, in particular, inverse voltammetry. This method can determine up to  $10^{-6}$ – $10^{-5}$  wt.% rhenium. The first stage of the inversion voltammetry method is the electrochemical reduction of perrhenate ions on the surface of a graphite electrode, which takes place in two stages, while rhenium is deposited in two forms - in the form of  $\text{ReO}_2$  and  $\text{Re}_0$ . Then, the precipitate concentrated on a graphite electrode is subjected to anodic dissolution, while on the voltammograms there are two anodic oxidation peaks, the peak currents and the areas under the peaks are proportional to the concentration in the analysed solution. In the determination of rhenium by the method of inversion voltammetry, metal ions, which occupy a position higher on the scale of standard potentials than the perrhenate ion, interfere. (Lakernik, 1957; Evdokimova, 2012)

Table 1. The composition of the solution after leaching the slag with an aqueous solution of 3M ammonia

C, g/l			C, mg/l			
Cu	Zn	SO <sub>4</sub> <sup>2-</sup>	Fe	Pb	Re	Ag
17.4	2.3	61.8	<0.1	<0.1	1.0	23.7

Table 1 shows the main components of the leaching solution, as well as their concentration. This composition allows the use of photometric analysis methods for the solution after the extraction of copper extraction. In addition, this method is an affordable and effective option for the analysis of model solutions.

For the selected method, the results were consistent with the ICP MS results.

### Dynamics of perrhenate sorption with the sorbent AV-17-8

At this stage, a study was made of the dynamics of sorption on the AV-17-8 anion exchange resin on model solutions with varying composition of model solutions:

- 1) Model ammonium perrhenate solution.
- 2) Model solution of ammonium perrhenate in the environment of ammonium hydroxide 3M.
- 3) Model solution of ammonium perrhenate in the environment of ammonium hydroxide 1.2 M and ammonium sulphate 0.9 M.

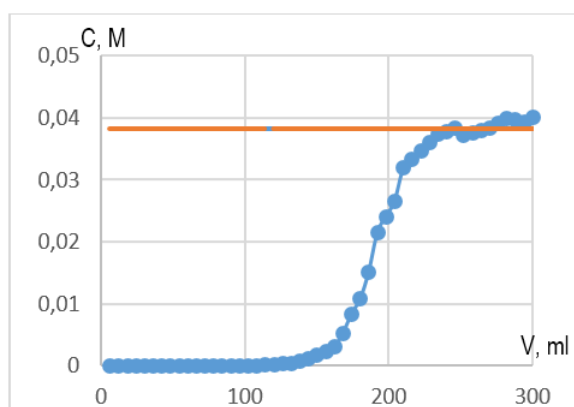


Fig. 1. Output sorption curve of solution N1

Anion exchanger AV-17-8 is a strongly basic ion-exchange resin with gel structure. It is used in the technology for softening and water desalination. AV-17-8 is pre-converted to chloride form. The experiment was carried out in a thermostated unit:  $T = 20^{\circ}\text{C}$  sampling every  $V = 6$  ml. The full exchange capacity according to the regulations is:  $\text{FEC}_{\text{theory}} = 1.15$  mol/l.

As we can see, in the presence of sulphate ions, FDEC remains at the same level. In addition, it was found that for perrhenate ion the capacity of this ion exchange resin exceeds the capacity declared by the manufacturer. This allows to consider this resin for use not only in water treatment, but also for extracting valuable components like rhenium. Also, a series of trial experiments allows us to supplement this conclusion with the fact that the ion exchange technology allows one to selectively extract the perrhenate from the technological leaching solution.

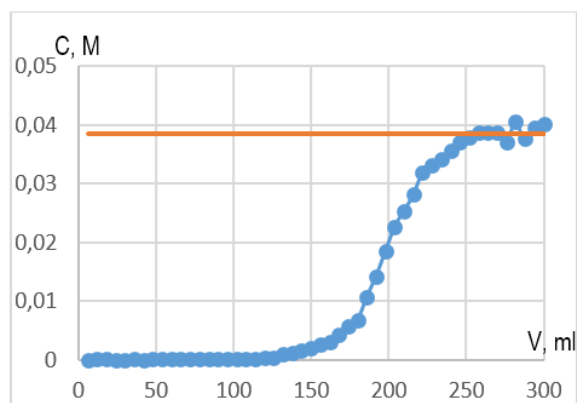


Fig. 2. Output sorption curve of solution N2

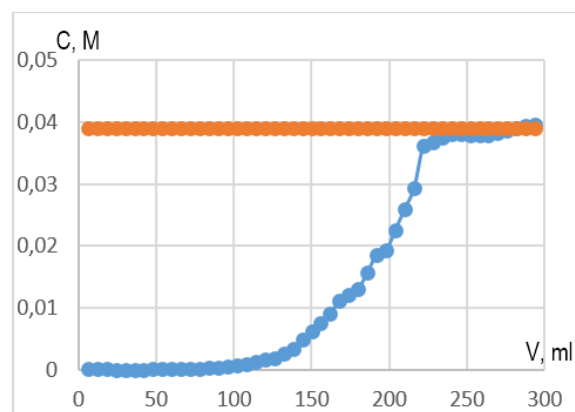


Fig. 3. Output sorption curve of solution N3

Figure 1-3 shows the results of sorption. Based on these data, the values of full dynamic exchange capacity were obtained. These data are presented in table 2.

Table 2. Full dynamic exchange capacity for different compositions of the solution

	ReO <sub>4</sub> <sup>-</sup>	ReO <sub>4</sub> <sup>-</sup> + C(NH <sub>4</sub> OH)=3M	ReO <sub>4</sub> <sup>-</sup> + C(NH <sub>4</sub> OH)=1,2M C((NH <sub>4</sub> ) <sub>2</sub> SO <sub>4</sub> )=0,9M
FDEC, mol/l	1.91	1.78	1.91

The obtained data will allow further comparison with other ion exchange resins and calculate the technological installation for the associated extraction of rhenium.

### References

- Evdokimova, O. V., N. V. Pechischeva. 2012. Sovremennyye metodyi opredeleniya reniya. – *Journal analiticheskoy himii*, 67, 9, 828–841 (in Russian)
- Lakernik, M. M., N. N. Sevryukov. 1957. *Metallurgiya tsvetnykh metallov*. Gosudarstvennoe nauchno-tekhnicheskoe izdatelstvo literatury po chernoy i tsvetnoy metallurgii, 536 p. (in Russian)
- Luganov, V. A., A. O. Baykonurova et al. 2004. *Teoreticheskie osnovy gidrometallurgicheskikh protsessov. Uchebnoe posobie*. VKGTU, Ust-Kamenogorsk, 104 p. (in Russian)

## MECHANICAL LOAD DURING SHREDDING OF TOUGH-PLASTIC MATERIALS WITH A TWO-SHAFT SHREDDER

**Malina Ivanova**

University of Mining and Geology "St. Ivan Rilski", 1700 Sofia; malina\_vatz@abv.bg

**ABSTRACT.** This article is dedicated to the forces and moments that are applied during shredding of tough-plastic materials. A practical task is solved, which determines the magnitudes and directions of the forces and moments necessary for shredding of a particular type of waste, for the purpose of their further use. It includes two directions. In the first direction, sample values of forces and moments are calculated. The equations describing the mechanical processes under operating conditions are solved. In the second direction, the graph of applied forces and moments is analysed.

**Keywords:** forces, moments, tough-plastic materials, two-shaft shredder

### МЕХАНИЧНО НАТОВАРВАНЕ ПРИ РАЗДРОБЯВАНЕ НА ЖИЛАВО-ПЛАСТИЧНИ МАТЕРИАЛИ С ДВУВАЛОВ ШРЕДЕР

**Малина Иванова**

Минно-геоложки университет "Св. Иван Рилски", 1700 София

**РЕЗЮМЕ.** Статията е посветена на силите и моментите, които се прилагат при шредирание на жилаво-пластични материали. Тук е решена практическа задача, с която са определени големините и посоките на силите и моментите, необходими за раздробяване на определен тип отпадъци, с цел понататъшната им употреба. Тя включва две направления. В първото направление се изчисляват примерни стойности на силите и моментите. Решени са уравненията, описващи механичните процеси при работни условия. Във второто направление се анализирани приложените сили и моменти.

**Ключови думи:** сили, моменти, жилаво-пластични материали, двувалов шредер

### Introduction

The use of recycled or waste products of tough-plastic materials, which replace natural mineral forms as a source for making materials with practical applicability, greatly alleviates environmental pollution. This creates more comfortable living conditions for the population and protects it from a number of factors harmful to life and health. A number of productions from the construction, mining and chemical industries adhere to the model of sustainable development.

Waste rubber, plastic, electronic equipment, kevlar, paper, etc. are considered as tough-plastic materials.

European and national waste management policies provide for measures to be taken to increase the recycling and recovery of waste. Thus, it is of particular importance to study and improve the various machines for shredding the different waste streams. In the EU, the requirements for waste management, e.g. of packaging waste, are defined by

Directive 94/62/EU on Packaging and Packaging Waste. The Directive has been transposed into the Bulgarian legislation through the Waste Management Act and the Ordinance on Packaging and Packaging Waste. There is also a National Waste Management Plan for the period 2014-2020 defining the following goals for packaging waste:

- Not less than 60% of the weight of the packaging waste must be recovered;

- Not less than 55% and not more than 80% of the weight of the packaging waste must be recycled.

The fulfilment of these goals can be assisted by the use of shredding machines (shredders).

The process of reducing the size of materials of different origin to the desired size under the action of external forces is called shredding. The technological purpose of shredding depends on the subsequent processes and processing stages or on the purpose of application of the products from shredding. Shredding is the first step in reducing the geometric sizes of the material during recycling.

Shredders have a very wide field of application: from hazardous and medical waste to tires, from plastics, wood, textiles and paper to metals, from construction and household waste to electronic scrap.

The management of waste streams is a challenge because of the high value of the numerous manual operations, high transportation costs and the negative impact on the environment.

### Object of study

The object of study in this work are the necessary forces and moments for shredding of waste products from tough-plastic materials with a two-shaft shredder.

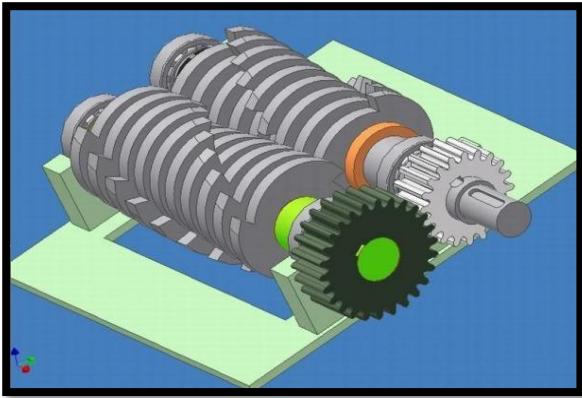


Fig. 1. Diagram of a shredding chamber of a two-shaft shredder

Fig. 1 shows the shredding chamber of the two-shaft shredder for shredding of tough-plastic materials, in which the permissible compressive stress of the destructed elements is  $\sigma_H = 25$  MPa (Borshchev, Dolgunin, Kormilytsin, Plotnikov, 2000), and its productivity is 10 t/h. The granularity of the product obtained after shredding is (0 – 50) mm.

As the material is tough-plastic, shredders working on shear and pressure are used (Sirotyuk, 1999).

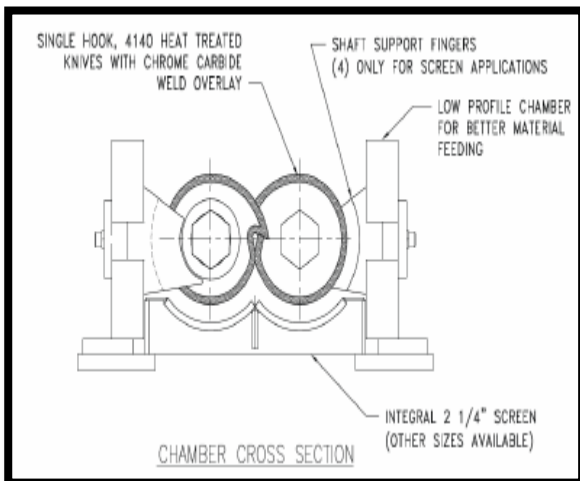


Fig. 2. Diagram of shredding with a two-shaft shredder

Fig.2 presents a diagram of shredding of simultaneously working "destructive" teeth (Tokarskiy, Yankiv, 2008).

The determination and calculation of the necessary forces and moments for shredding of waste products from tough-plastic materials with a two-shaft shredder will be carried out using the following data:

- maximum compressive strength of the destructed elements – 25 MPa;
- approximate dimensions of the area of the chamber - 900 x 700 mm;
- power supply of the shredder – flow, discrete, operator-controlled;
- separation and loading of the shredded material - flow, continuous, automatic;
- machine drive - hydraulic, from a pump / hydraulic motors / cylinders and internal combustion engine / electric motor;
- approximate power of the drive – 100 kW.

### Concept for a model study

The purpose of the study is to determine and calculate the necessary forces and moments for the shredding of waste products from tough-plastic materials with a two-shaft shredder, which is presented on Fig.3.

It was found that the pressure, which each carbide cone on the disc teeth exerts on the destructed material, is 44 MPa. It is nearly 2 times the disruptive tension of 25 MPa (Borshchev, Dolgunin, Kormilytsin, Plotnikov, 2000). The pressure is assumed as applied to an area of the tooth with a diameter of 30 mm. It is transformed into radial forces on the knives, respectively torques (torsion moments) on the shredder shafts (Pisarenko, 1993).

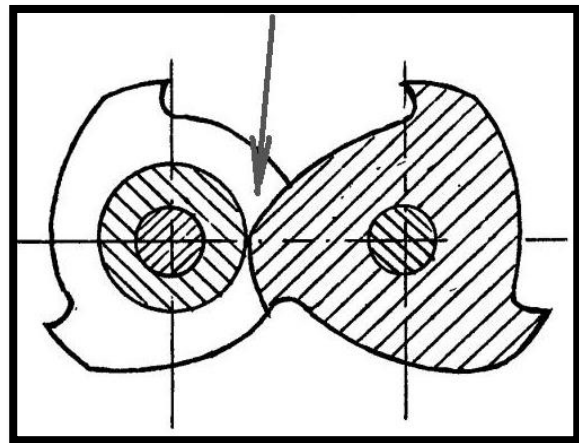


Fig. 3. Force and moments during shredding

Under the accepted condition for 3 simultaneously working "destructive" teeth (Vatskicheva, 2016), the nominal torque of each shaft at 25 rpm - 40 kN.m - is determined. In this case, the appropriate heliocentric -type reducer is PG 3501 with gear ratio  $i = 4.1$ . Accordingly, the drive hydraulic motor is a radial piston one, with constant flow-rate, of type IAM.1600 H, with a maximum speed of 250 min<sup>-1</sup> and a torque equal to 7860 N.m at a pressure of 300 bar.

The end conditions reflecting the mechanical load when operating the steel structure (Borshchev, 2004, Tavakoli et al. 2008) include the following parameters:

- input power:  $P_{inp} = 90$  kW;
- rpm (revolutions) of the working shaft:  $n_v = 25$  min<sup>-1</sup>;
- frequency of rotation of the working shaft:

$$\omega_v = \frac{\pi \cdot n_v}{30} = 2.62 \text{ rad/s};$$

- torque of the working shaft:

$$M_v = \frac{P_{BX}}{\omega_v \cdot \eta} = 35 \text{ kN.m},$$

where  $\eta = 0.98$  is the efficiency of the transmission;

- disruptive tension of the tough-plastic material:

$$\tau_s = 60 \text{ MPa};$$

- shear force by one knife

$$F_s = \frac{M_v}{3.0 \cdot 1.75} = 66.7 \text{ kN.};$$

- moment of resistance of shredding by 1 knife:  $M_{S1} = F_s \cdot l_s = 11.67 \text{ kN.m}.$

The mechanical load during operation of the structure is presented on Fig.4 (Tokarskiy, Yankiv, Siryk, Gochko, Kosenko, 2003).

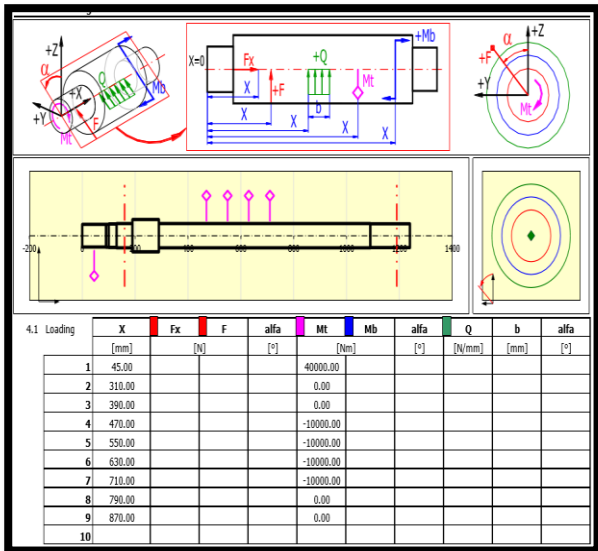


Fig. 4. Mechanical load during shredding of tough-plastic materials

The required power W to drive the shredding shafts is determined by the formula (Vatskicheva, 2017):

$$W = \frac{P_b \cdot \mu \cdot S_t \cdot \frac{D_t}{2} \cdot Z \cdot n_v}{9554} \quad (5)$$

$$W = \frac{25 \cdot 10^6 \cdot 2 \cdot 6 \cdot 10^{-4} \cdot 0,15 \cdot 8 \cdot 25}{9554}$$

$$W = 94.2 \text{ kW},$$

where:

- $P_b$  is the tension for shredding of the tough-plastic material - 25 MPa
- $S_t$  – the maximum contact area of each destructive tooth  $\sim 20 \times 30 \text{ mm}$  or  $6 \cdot 10^{-4} \text{ m}^2$ ;
- $Z$  - number of simultaneously working discs - 8 / 4 from one of the shafts and 4 from the other, with a total length along the axis of the shafts - 320 mm, which is greater than the maximum size of waste materials /
- $D_t$  – diameter of the cutting discs 175 mm / distance of the teeth from the shaft axis ;
- $n_v$  – rpm (revolutions) of the shafts  $25 \text{ min}^{-1}$ ;
- $\mu$  – coefficient of power reserve equal to 2.

### Numerical results

Table 1 summarises the results of the power (force) load during shredding of tough-plastic materials.

Table 1. Change in the power load during shredding

№	$F_y$	$F_z$	Alfa
	[kN]	[kN]	[°]
1	22.81	62.68	20
2	23.90	62.27	21
3	24.99	61.84	22
4	26.06	61.40	23
5	27.13	60.93	24
6	28.19	60.45	25
7	29.24	59.95	26
8	30.28	59.43	27
9	31.31	58.89	28

Table 2 summarises the results of the momentary (instantaneous) load during shredding of tough-plastic materials.

Table 2. Change of the momentary load during shredding

№	x	$M_t$	$M_b$
	[mm]	[kN.m]	[kN.m]
1	45	40	10.97
2	310	0	10.90
3	390	0	10.82
4	470	-10	10.75
5	550	-10	10.66
6	630	-10	10.59
7	710	-10	10.49
8	790	0	10.40
9	870	0	10.31

### Conclusions

The results of the model studies conducted justify the following conclusions:

- the study determined the numerically necessary forces and moments for shredding of waste products from tough-plastic materials with a two-shaft shredder;
- the radial forces on the knives resulting from the disruptive pressure applied to a surface from a tooth surface are included;
- the nominal torque is obtained under a condition for three simultaneously working "destructive" teeth.
- a solution is proposed to a practical problem related to determining the mechanical load during shredding of tough-plastic materials with a two-shaft shredder;
- the magnitudes and directions of forces and moments for shredding of a particular type of waste are determined;
- the problem (task) involves solving the equations describing the mechanical processes under operating conditions and analysing the applied load.

### References

Borshchev, V. Y. 2004. *Equipment for crushing of materials*. State Technical University Tambovsky, Moscow

Borshchev, V. Y., V. N. Dolgunin, G. S. Kormilytsin, A. N. Plotnikov. 2000. *Technique of processing of brittle materials*. State Technical University Tambovski. 40 p.

Pisarenko, G. S. 1993. *Resistance of materials*. Higher School, Kiev

Sirotyuk, S. V. 1999. *Mechanisation of cork and storage of products of plant grower/Course of Lectures*. LDAU, Lviv

Tavakoli, H., S. S. Mohtasebi, A. Jafari. 2008. Comparison of mechanical properties of wheat and barley straw. – *Engineering International: CIGR Journal*. 10. 1–9.

Tokarskiy, Yu. M., V. V. Yankiv. 2008. *The mechanical transmissions, calculation and constructing*. Navsh. Posib., New World. Lviv

Tokarskiy, Yu. M., Yankiv V. V., Siryk Z. M., Gochko M. O., Kosenko I. E., 2003. Calculations of mechanical transmission on computer/Navsh. Posib. Lviv, LDAU.

Vatskicheva, M. 2016. Calculations and verifications of shredding chamber of two-shaft shredder for crushing of concrete, rubber, plastic and wood. – *Proc. International Scientific Conference "High Technologies, Business, Society"*, 4 (190), 49–52.

## MODERN APPROACH TO THE TECHNOLOGY OF THE BACKFILLING

**Alexander Ivannikov<sup>1</sup>, Kongar-Siuriun Cheynesh<sup>1</sup>, Albert Khayrutdinov<sup>2</sup>, Yulia Tyulyaeva<sup>3</sup>**

<sup>1</sup> National University of Science and Technology "MISiS", 119049 Moscow

<sup>2</sup> RUDN University, 117198 Moscow

<sup>3</sup> Florida International University, 33199 Miami

**ABSTRACT.** The article describes a modern approach to the technology of backfilling of working space, taking into account the sustainable development of mining. The aspects of economic efficiency, safety and ecology are considered. A detailed analysis of various backfilling methods that are used in modern enterprises is given. The advantages and disadvantages are given. The article describes in detail the work carried out in this area at the Mining Institute of NUST "MISiS". One of the directions is the study of the possibility of using local natural materials or waste products as backfills. In particular, studies were carried out on the formation of backfill arrays based on sulphide-containing and halite tailings. The influence of the granulometric composition and ratio of coarse and fine aggregates on the quality of the backfill, as well as their quantity per unit of volume, amount of water (water binding ratio), method of preparation, transportation and styling, conditions (temperature) and age of hardening are also considered.

**Keywords:** sustainable mining, backfilling, industrial waste, ecology

### МОДЕРЕН ПОДХОД КЪМ ТЕХНОЛОГИЯТА НА ЗАПЪЛВАНЕ

**Александър Иванников<sup>1</sup>, Конгар-Сюрюн Чейнеш<sup>1</sup>, Альберт Хайрутдинов<sup>2</sup>, Юлия Тюляева<sup>3</sup>**

<sup>1</sup> Национален университет за наука и технологии "МИСиС", 119049 Москва

<sup>2</sup> Руски университет на дружбата на народите, 117198 Москва

<sup>3</sup> Международен университет Флорида, 33199 Маями

**РЕЗЮМЕ.** Статията описва модерен подход към технологията на запълване на отработеното пространство, като се отчита устойчивото развитие на минните работи. Разгледани са аспектите на икономическата ефективност, безопасността и екологията. Даден е подробен анализ на различните методи за запълване, които се използват в съвременните предприятия. Представени са предимствата и недостатъците. Статията описва подробно работата, извършена в тази област в Минния институт на НУИТ "МИСиС". Едно от направленията е проучването на възможността за използване на местни естествени материали или отпадни продукти за запълването. По-специално бяха проведени проучвания за формирането на запълващи масиви на базата на сулфидни и халитови отпадъци. Разгледани са също влиянието на гранулометричния състав и съотношението на груби и фини инертни материали върху качеството на запълване, както и тяхното количество спрямо единица обем, количеството вода (съотношение на свързването с вода), метод на приготвяне, транспортиране и стилизиране, условия (температура) и възраст на втвърдяване.

**Ключови думи:** устойчиво развитие, минни работи, запълване, технологични отпадъци, екология

### Introduction

Man-made disasters during the extraction of minerals occur more frequently. In 2007 there was a collapse of the surface at BKRП-1 Uralkali, in 2014 - water breakthrough at the "Solikamsk-2" mine, in 2017 - a breakthrough of water from a spent pit to an underground mine at the Mir enterprise in Yakutia, etc. (Khayrutdinov, 2007; Khayrutdinov, Ivannikov, 2017). This demonstrates the need for a more thorough development of technology at the mine design stage.

One of the ways to minimise man-made disasters is the use of technology with backfilling of working space (Khayrutdinov, 2009).

An analysis of global experience shows that up to 35% of mines use development systems with backfilling. This is due to the deepening of the mines and the complication of mining and geological conditions. Especially in an environment of constant

struggle for the minerals extraction completeness. Due to the high value of the extracted raw materials, underground mines mainly use systems with hardening backfilling based on the cement binder component (Khayrutdinov, 2009; Khayrutdinov, Ivannikov, 2017). And in coal mines dry or hydraulic backfilling is used. At the same time, coarse-ground rocks from sinking, finely crushed coal waste ore, specially mined sand are used. Hardening backfilling in coal mines is used only in exceptional cases: when extracting powerful, steeply dipping layers or reducing endogenous fire hazard or when mining layers under guard objects (Khayrutdinov, Shaymyrdyanov, 2009; Khayrutdinov, 2008).

The use of backfilling of working space allows the control of mining pressure and increasing the safety of mining operations as well as simultaneous mining of the deposit by underground and open methods. This increases the recovery rate, and also reduces the negative impact of mining on the environment (Khayrutdinov, 2008). In addition, the use of backfilling in the extraction of minerals allows to the extraction

of reserves, previously considered off-balance or left in the pillars. This, in addition to reducing losses and improving the quality of extraction, leads to an increase in the lifetime of the mine that in turn allows to solve the social issue in the regions where the mining enterprise is a city-forming one (Khayrutdinov, Ivannikov, 2017).

Despite the advantages of underground geotechnology with backfilling of working space, at the same time it increases the cost of mining. And therefore, requires the improvement of the relevant processes.

In most cases, the mines "Severny" (Murmansk region), "International" (Yakutia), "Geko" (Canada) and some others use a specially mined aggregate for filling the mines. It is characterised by inconstancy of particle size distribution, humidity, material composition, etc. Therefore, it is associated with relatively high costs (Khayrutdinov, 2008).

Adding to the filling mixture an excessive amount of water in order to increase its transportability leads to the separation of the mixture during transportation. And, as a result, to reduce the strength of the backfill array. For example, at the Outokumpu mine (Finland), with the transition of refining operations to deeper horizons, the side walls of artificial pillars collapsed. In order to eliminate the negative effects of excess water in mixtures, the consumption of the binder was increased that led to an increase in mining costs (Khayrutdinov, Ivannikov, Arad, Huang, 2017). In addition, it should be borne in mind that the use of backfill in mining operations is associated with the construction of backfill complexes. They require significant financial costs as well as complicated technological scheme of the process of mining (Khayrutdinov, 2007; Khayrutdinov, Shaymyardyanov, 2009).

As can be seen, the use of technologies with backfilling is associated with significant costs and is effective in developing more valuable ores.

The use of local natural materials and waste products will significantly reduce the costs not only for backfilling, but also for the maintenance of various types of dumps and tailings. Accordingly, land areas for mining allotments are reduced (Khayrutdinov, 2007; 2009; Khayrutdinov, Votyakov, 2007a; 2007b; Khayrutdinov, Ivannikov, 2017).

The rational use of elements of backfilling with disposal in laying the waste of mining and processing production will allow to effectively develop less valuable mineral deposits.

As it was mentioned above, the use of waste not only affects the technical and economic indicators of the mining enterprise, but also helps to reduce the harmful environmental impact on the environment (Yushina et al., 2019).

The application of the technology of hardening backfill with the utilisation of waste from mining and processing production will significantly reduce the cost of the process and will allow the effective development of mineral deposits (Khayrutdinov, 2007; Khayrutdinov, Ivannikov, 2017).

Work on laying concrete mixes in underground workings was carried out by our scientists before (Kulikova, 1994). But, since 2000 research work has been carried out at the Moscow State Mining University for evaluating the possibility of using mining waste for laying the mined-out space in underground mining of ore deposits. Studies on the formation of backfill arrays on the basis of sulphide-containing and halite tailings of enrichment showed that, if there are appropriate activation methods, they can be successfully used as aggregate. Analysis of the data obtained shows that there are no tailings

that could not be used in the tab as inert aggregate and some can be used as a binder component (Khayrutdinov, Votyakov, 2007a; 2007b; Khayrutdinov, Votyakov, 2007).

If spent mines are not intended to be used in any other capacity, for example, for gas storage (Myaskov, Popov, Popov, Gornyi Zhurnal, 2018), then the use of technology development enterprises with a backfilling on the basis of waste mining production allows to expand the raw material base for the preparation of hardening bookmarks, to free up part of the territory for its more efficient use for sowing or building structures, to reduce the negative impact of tailings and waste dumps on adjacent areas, as well as to reduce irrational transportation, reduce loading and unloading operations and free up part of the rolling stock for the transport of other goods (Khayrutdinov, 2007; 2009; Khayrutdinov, Shaymyardyanov, 2009; Khayrutdinov, Ivannikov, 2017).

Thus, research on the use of mining waste, including those with restrictions, is not only promising, but also solves a number of economic and environmental problems.

The backfill array is characterised by a rather long setting time (curing). This results in poor performance. In the same time the use of various additives that regulate the setting time increases the filling rate that sometimes leads to cases of solidification of the solution in the pipelines (Khayrutdinov, Votyakov, 2007; Khayrutdinov, Ivannikov, Arad, Huang, 2017).

The use of dry or hydraulic backfilling when mining secondary chambers leads to the penetration of backfill material into the ore and, accordingly, to an increase in ore dilution.

Artificial backfill array is a foreign body inside the mountain range. Its quality is determined by several indicators: strength, compression, rheological properties, as well as stability in the outcrop. It is very important to ensure those properties of the backfilling that are acceptable for specific mining conditions (Khayrutdinov, Votyakov, 2007a; 2007b; Khayrutdinov et al., 2017).

The properties of a hardening backfill array are most significantly influenced by: quality, particle size distribution, and the ratio of coarse and fine aggregates as well as their number per unit volume, amount of water (water binding ratio), method of preparation, transportation and installation and also the conditions (temperature) and the age of hardening (Khayrutdinov, Votyakov, 2007).

Studies show that one of the determining factors for the efficiency of a mixture is its water content. The technology of backfilling at the mining enterprises is characterised by the presence of a significant amount of water in mixtures (up to 550 kg/m<sup>3</sup>). This dramatically reduces the strength of the artificial array and impairs the technical and economic indicators of the use of development systems with a backfilling (Khayrutdinov, Votyakov, 2007).

The increase in the mass fraction of the solid constituent in the mixture is a significant reserve for reducing the consumption of the binder.

The type and ratio of aggregates also affect the strength of the filling mixture. The filler in the mixture is 70-90% (mass.). It is significantly cheaper knitting. Therefore, it is economically advantageous that the filling mixture contains as much aggregate as possible and as little binder as possible. However, economic considerations are not the only ones when choosing a placeholder. For the stability of the artificial array the grain composition of the aggregate is also important. It

affects the moistening of the surface of the grains, the relative volume of the aggregate, the good stowability of the filling mixture, and its tendency to delamination (Khayrutdinov, Votyakov, 2007).

An important characteristic of the backfilling is the dynamics of strength in time. The pattern of growth of strength is important in determining the minimum time to start working out of the pillars. This affects the choice of parameters for development systems. Studies have shown that the most intense increase in strength is observed during the first 60 days of hardening. In the subsequent period (up to 3 months), the increase in strength slows down somewhat (an increase of 10-17%). Over the next 3 months there is an even slower increase in strength (by 3-5%). And over the next six months, it increases by another 2-3% (Khayrutdinov, Votyakov, 2007).

Characteristics of the future backfill array largely depend on the properties of the source materials. Therefore, their correct choice is one of the most important factors in the backfill technology. The setting time of the filling mass should not be less than the required time for delivery of the mixture to the space developed. This is especially important for mixtures with coarse aggregate. As in this case, the stratification leads to an uneven distribution of the constituent components in the developed space and also to the heterogeneity of the artificial array and reduced strength. The composition of the filling mixture should be such that high temperatures do not develop in the artificial massif, which have a detrimental effect on its solidity. Theshrinkage of the mixture would be minimal (Khayrutdinov, Votyakov, 2007; Khayrutdinov et al., 2017).

A series of experiments allowed to determine the influence of the content of magnesia cement in the backfill on its strength. For comparison, samples of hydraulic backfill were simultaneously produced.

Halite waste and magnesia cement, taken in the required amount relative to each other, were mixed for 3 minutes. The mixture obtained was sealed with a saturated solution of halite waste with a density of 1.35 g/cm<sup>3</sup> at a temperature of 25°C in an amount that provides the mobility of the mixture along the Suttard taper of 20 cm. The resulting mixture was mixed for 2 minutes until a homogeneous mass was obtained. The results of testing the strength of the uniaxial compression are given in Table 1 and Figure 1.

Table 1. Mixture wastes based on enrichment waste with different binder content

Composition number	The content of components, wt. %		The ratio of saturated solution to solid	Sample Strength under uniaxial compression, MPa			
	Waste	Magnesia cement		Duration of curing, day			
				7	28	60	90
1	99.5	0.5	0.15	-	0.3	0.7	0.8
2	99	1	0.15	0.05	0.65	1	1.25
3	97.5	2.5	0.15	0.10	0.9	1.65	1.8
4	95	5	0.15	0.25	1.7	2.6	2.8
5	100	-	0.15	-	0.1	0.25	0.3

The graph in Fig. 1 shows that the strength of the studied samples increases substantially in proportion to the content of magnesia cement in the filling mixture.

When choosing a technology for extracting minerals from the depths, it is necessary to take into account a combination of many factors: economic, environmental and safety. The use of technology with the backfilling of working space on the basis of man-made waste, allows for more efficient use of natural resources.

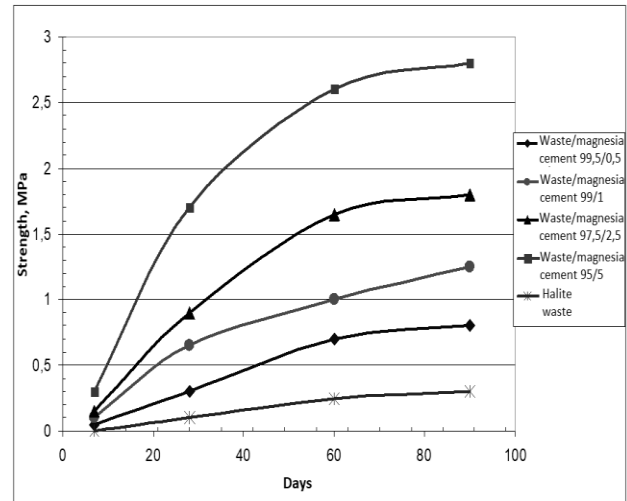


Fig. 1. The kinetics of backfilling strength with different binder content

## References

Kulikova, E. 1994. Novoe sredstvo mehanizatsii i ukladki betonnykh smesey v podzemnykh vyirabotkakh. – In: *Stroitelstvo gornykh vyirabotok*. MGI, Moscow, 68–71 (in Russian).

Khayrutdinov, M. M. 2007. Puti sovershenstvovaniya system razrabotki s zakladkoy vyirabotannogo prostranstva. – *Gornyy Zhurnal*, 11, 40–43 (in Russian).

Khayrutdinov, M. M. 2008. Tehnologiya zakladki vyisokoplotnyimismesyami (na osnove hvostov obogascheniya) pri podzemnoy razrabotke rud. – *Gornyyinformatsionno-analiticheskiybyulleten (nauchno-tehnicheskijurnal)*, 11, 276–278 (in Russian).

Khayrutdinov, M. M. 2009. Primenenie othodov gornogo proizvodstva kachestve zaklad ochnogo materiala dlya snijeniya vrednogo vozdeystviya na okrujayuschuyu sredu. – *Gornyy Zhurnal*, 2, 64–66 (in Russian).

Khayrutdinov, M., A. Ivannikov. 2017. The use of mining waste for backfill as one of sustainable mining activities. – *Proceedings of International Conferences on Geo-spatial Technologies and Earth Resources, Hanoi, Vietnam, 5-6 October 2017*, 715–717.

Khayrutdinov, M. M., I. K. Shaymyrdyanov. 2009. Podzemnaya geotekhnologiya s zakladkoy vyirabotannogo prostranstva: nedostatki, vozmozhnosti sovershenstvovaniya. – *Gornyy informatsionno-analiticheskiy byulleten (nauchno-tehnicheskij jurnal)*, 1, 240–250 (in Russian).

- Khayrutdinov, M. M., M. V. Votyakov. 2007a. Razrabotka sostavov tverde yuschih zakladochny ih smeseyi zotodov pererabotki rud kaliynyih predpriyatiy. – *Gornyy informatsionno-analiticheskiy byulleten (nauchno-tehnicheskiy jurnal)*, 10, 220–222 (in Russian).
- Khayrutdinov, M. M., M. V. Votyakov. 2007b. Gidravlicheskaya zakladka na kaliynyih rudnikah. – *Gornyy informatsionno-analiticheskiy byulleten (nauchno-tehnicheskiy jurnal)*, 6, 214–218 (in Russian).
- Khayrutdinov, M. M., M. V. Votyakov. 2007c. Vozmojnost primeneniya sistem s tverdeyushey zakladkoy priotrabotke kaliynyih mestorojdeniy. – *Gornyy informatsionno-analiticheskiy byulleten (nauchno-tehnicheskiy jurnal)*, 9, 265–286 (in Russian).
- Khayrutdinov, M. M., A. L. Ivannikov, V. Arad, L. V. Huang. 2017. Problemy i transport azakladochnoy smesi k mestu ukladki. – *Sotsialno-ekonomicheskie i ekologicheskie problemi gornoy promyishlennosti, stroitelstva i energetiki. XIII Mejdunarodnaya konferentsiya po problemam gornoy promyishlennosti, stroitelstva i energetiki*, 1, 2, 282–287 (in Russian).
- Myaskov, A. V., E. M. Popov, S. M. Popov. 2018. Prospects for the use of mines in East Donbass as underground gas storage facilities in the integral gas-supply system of Southern Russia. – *Gornyi Zhurnal*, 3, 33–36 (in Russian).
- Yushina, T. I., I. O. Krylov, V. Valavin, K. D'Elia, A. V. Myaskov. 2019. Processing technology of iron-containing industrial waste from the Kamysh-Burun mining complex. – *Proc. 29th International Mineral Processing Congress*, 3103–3112.

## TREATMENT OF WATER CONTAMINATED BY PETROLEUM PRODUCTS THROUGH CONSTRUCTED WETLANDS WITH INTEGRATED PLANT SEDIMENT MICROBIAL FUEL CELLS

Rosen Ivanov, Ani Stefanova, Anatoliy Angelov

University of Mining and Geology "St. Ivan Rilski", 1700 Sofia; rosen\_iv@abv.bg

**ABSTRACT.** Oil exploration and exploitation activities contribute to global economic growth but often lead to pollution of the environment by oil and petroleum products. Constructed wetlands are cheap, environmentally friendly and use biological processes based on photosynthesis process for treatment oil-contaminated waters. Integration of Plant Sediment Microbial Fuel Cells (PSMFC) into them allows the generation of energy in parallel to water treatment. The purpose of this study is to identify the treatment capacity of five variants of PSMFC planted with different vegetation (*Typha latifolia*, *Phragmites*, *Spartina*, mixed marsh vegetation and cell without vegetation). A solution containing crude oil at a concentration of 100 mg/l is delivered to the PSMFC with a horizontal surface flow and a hydraulic retention time of 14 days. From the chemical analyses performed, the highest treatment level was established in PSMFC 4 planted with *Spartina* and inoculated with mixed culture oil-oxidising bacteria. At the end of the experiment the concentration of pollutant dropped to 0.052 mg/l. The same showed the best electrical parameters during the experiment. The power density reached 11.56 mW/m<sup>2</sup> at a current density of 27.16 mA/m<sup>2</sup> and applied resistance of 300 Ω. The open circuit voltage ranged from 900 to 1100 mV. The results obtained show good prospects for application of plant sediment microbial cells in the passive treatment of waters polluted with crude oil and petroleum products.

**Keywords:** constructed wetlands, plant sediment microbial fuel cells, passive wastewater treatment, oil and petroleum products pollution

### ПРЕЧИСТВАНЕ НА ВОДИ ЗАМЪРСЕНИ С НЕФТОПРОДУКТИ ЧРЕЗ КОСТРУИРАНИ ВЛАЖНИ ЗОНИ С ИНТЕГРИРАНИ РАСТИТЕЛНИ СЕДИМЕНТНИ МИКРОБНИ ГОРИВНИ КЛЕТКИ

Росен Иванов, Ани Стефанова, Анатолий Ангелов

Минно-геоложки университет "Св. Иван Рилски", 1700 София

**РЕЗЮМЕ.** Дейностите по проучване и експлоатация на нефтени находища допринасят за икономически растеж в световен мащаб, но често това води и до замърсяване на околната среда с нефт и нефтопродукти. Конструирани влажни зони са евтини, екологично чисти и използват биологични процеси, базирани на процеса фотосинтеза за пречистване на замърсени с нефт води. Интегрирането на растителни седиментни микробни клетки (ПСМГК) в тях позволява генерирането на енергия при паралелно пречистване на водите. Целта на настоящото изследване е да се установи пречиствателната способност на пет варианта ПСМГК, засадени с различна растителност (*Typha latifolia*, *Phragmites*, *Spartina*, смесена блатна растителност и клетка без растителност). Към ПСМГК е подаван разтвор съдържащ нефт в концентрация 100 mg/l, при хоризонтален повърхностен поток и контактно време 14 дни. От направените химични анализи се установи най-висока степен на пречистване при ПСМГК 4 засадена с блатна трева и инокулирана със смесена култура нефт-окисляващи бактерии. В края на експеримента концентрацията на замърсителя спадна до 0,052 mg/l. Същата показа и най-добри електрически параметри по време на експеримента. Плътноста на мощността достигна до 11,56 mW/m<sup>2</sup> при плътност на тока 27,15 mA/m<sup>2</sup> и приложено съпротивление 300 Ω. Напрежението при отворена верига се движеше в границите 900 – 1100 mV. Получените резултати показват добри перспективи за приложение на растителните седиментни микробни клетки при пасивно пречистване на води, замърсени с нефт и нефтопродукти.

**Ключови думи:** конструирани влажни зони, растителни седиментни микробни горивни клетки, пасивно пречистване на води, замърсяване с нефт

### Introduction

Crude oil is the world's largest non-renewable energy resource, accounting for about 33% of the total consumed energy. Drilling and extraction processes for oil and gas generate huge volumes of oil-contaminated water. The worldwide demand for oil is expected to keep rising in the coming years, which will potentially increase the generation of oil-contaminated water.

Worldwide, water contaminated with crude oil is usually stored in evaporation pits before eventual discharge into the environment without any treatment. The remediation of such oil-contaminated water has become a critical problem in oil-producing countries and requires immediate attention. Moreover, the majority of oil and/or gas wells are not highly

productive at the time of their installation and lose their efficiency after some time (Muhammad et al., 2019). Conventional methods of oil-contaminated water treatment based on physical and chemical processes are not feasible to install due to their high capital, operational and maintenance costs (Shubiao et al., 2018).

Using constructed wetlands (CW) with integrated plant sediment microbial fuel cells (PSMFC) is an innovative approach for the remediation of polluted water which requires only aquatic vegetation. They can be applied to any oil-contaminated water stabilisation pit with minimal financial capital (Vymazal, 2014). Recent studies have revealed that the combined use of plants and bacteria in CW with PSMFC can enhance plant growth and pollutant degradation. Plants provide nutrients to rhizospheric microbes through their roots

exudates (Felix et al., 2019). These microorganisms have major roles in the degradation of organic compounds, and their efficiency in degrading hydrocarbons increase in the presence of plants. (Rachnarin et al., 2017) Once the pollutant is taken up by plant, endophytes are actively involved in the *in planta* degradation. However, this combination of plants and associated microorganisms has not yet been evaluated at large scales for remediation of oil-contaminated water (Qing et al., 2017).

Generation of energy from plant sediment microbial fuel cells is additional advantage in using this technology for oil-contaminated water treatment (Rasool et al., 2019). Most PSMFC are open systems with anodes embedded in anoxic sediment and cathodes placed in aerobic water layer. The microorganisms in the sediment consume organic substrates and transfer the electrons to the anode. Dissolved oxygen is utilised as an electron acceptor and combines with protons to form water and generate electricity (Panpan et al., 2014; Boyue et al., 2019).

The aim of this study is to evaluate the treatment efficiency of oil-contaminated water and electricity generation by applying CW with PSMFC.

## Materials and methods

For the purpose of the study five constructed wetlands with integrated plant sediment microbial fuel cells were made (Figure 1). The cells have a volume of 30 dm<sup>3</sup> and are planted with different aquatic vegetation. (Table 1) The cells were filled with 20 dm<sup>3</sup> mixture of sediment and peat in a ratio 20:1. Stainless steel electrodes with an area of 400 cm<sup>2</sup> are placed on the bottom and in the surface layer. The cells are designed to provide a different flow of water in the installation under different operating modes.

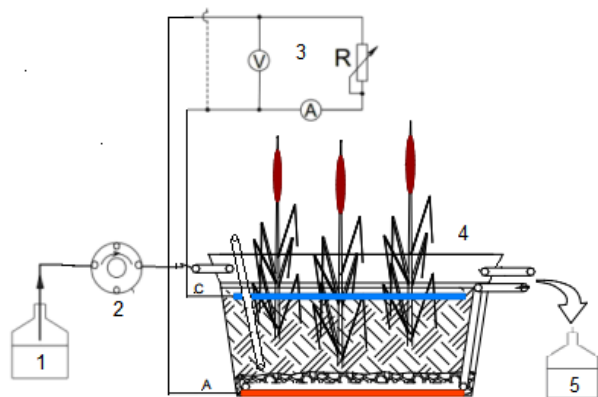


**Fig. 1. Scheme of the laboratory installation**  
1 – Incoming solution; 2 – Peristaltic pump 3 – Digital multimeter, 4 – Constructed wetland with integrated plant sediment microbial fuel cell, 5 – Outgoing solution, A – anode, C – cathode

Before starting the experiment, screening of highly active oil-degrading strains of the laboratory collection, suitable for inoculum in the CW anoxic and aerobic zone, was made.

By peristaltic pump, a solution with a crude oil content of 100 mg/l (total oil content 14 mg/l and COD 39000 mg/l) was delivered to the cells with hydraulic retention time of 14 days. In order to establish the best treatment effect and energy

generation, four modes of operation of the cells were studied. In Mode 1, clean water is flowed into the cells with a horizontal surface flow. In Mode 2, synthetic solution with crude oil is flowed into the cells with a horizontal surface flow. In mode 3, synthetic solution with crude oil is flowed into the cells with a horizontal surface flow. The cells are inoculated with a mixed culture of oil-oxidising bacteria (*Pseudomonas veronii*, *Azoarcus communis*, *Pseudomonas chlororaphis*, *Pseudomonas putida*, *Pseudomonas libanensis*). In mode 4, synthetic solution with crude oil is flowed into the cells with a horizontal subsurface flow. The cells are inoculated with a mixed culture of sulphate-reducing bacteria. After the completion of each of the modes, basic chemical parameters, total oil content and the electrical parameters of the cells were measured.

Table 1. Scheme of the experiment

Cell	Vegetation
Cell 1	Without vegetation
Cell 2	<i>Typha latifolia</i>
Cell 3	<i>Phragmites</i>
Cell 4	<i>Spartina</i>
Cell 5	mixed marsh vegetation

## Results and discussion

Table 2 shows the basic chemical parameters of the constructed wetlands for the four modes of operation

Table 2. Basic chemical parameters of the constructed wetlands

C E L L	Mode 1		Mode 2		Mode 3		Mode 4	
	pH	EC μS/cm	pH	EC μS/cm	pH	EC μS/cm	pH	EC μS/cm
1	7.12	612	6,78	1224	6.83	1105	7.21	1142
2	6.82	825	7.22	1035	7.08	936	7.15	972
3	7.25	890	7.14	997	7.17	952	6.95	1011
4	7.04	734	6.92	894	6.87	789	6.79	846
5	6.97	951	7.31	1012	6.79	960	7.03	999
N e	NH <sub>4</sub> <sup>+</sup> mg/l	PO <sub>4</sub> <sup>3-</sup> mg/l						
	1	3.35	3.28	1.89	3.19	1.14	2.16	1.05
2	2.36	5.24	1.57	0.47	0.86	0.05	0.68	0.05
3	1.4	1.70	1.37	1.51	1.19	0.66	0.89	0.38
4	1.54	3.75	1.46	1.89	1.08	0.01	0.68	0.01
5	1.26	1.69	0.92	1.32	0.67	0.58	0.6	0.28

For all cells, the pH of the water ranges from 6.78 to 7.35, with no significant changes in the individual modes of operation. The same can be said for electrical conductivity. The concentration of nutrients NH<sub>4</sub><sup>+</sup> and PO<sub>4</sub><sup>3-</sup> is low, with a tendency to decrease over time due to their assimilation from plants.

From the measured concentrations of total oil content, the best results are found under mode 3 (Table 3). Cell 4 is characterised by the highest treatment effect – the concentration of petroleum products is dropping to 0.052 mg/l.

Slightly higher concentrations of petroleum products are measured in Mode 4, but again the lowest values are in Cell 4. In Mode 2 the highest values of petroleum products in the outgoing waters from the cells are measured. In the four modes cell 1 is characterised by the lowest treatment effect. Similar results have also been obtained for COD. The lowest COD in all cells is measured in Mode 3, followed by Mode 4 and Mode 2. The COD values can be linked to the residuals of petroleum products in the effluent from the cells in the individual modes.

Table 3. Concentration of total oil content and COD in outgoing water

C E L L	Mode 1		Mode 2		Mode 3		Mode 4	
	COD mg/l	Total oil content mg/l						
1	213	-	363	0.21	188	0.067	133	0.12
2	126	-	186	0.13	143	0.067	158	0.098
3	103	-	188	0.1	163	0.055	176	0.077
4	78	-	148	0.071	108	0.052	126	0.06
5	113	-	153	0.15	138	0.089	156	0.11

Data for the measured electrical parameters are presented in Figures 2-5. There are no significant differences in electrical parameters between modes.

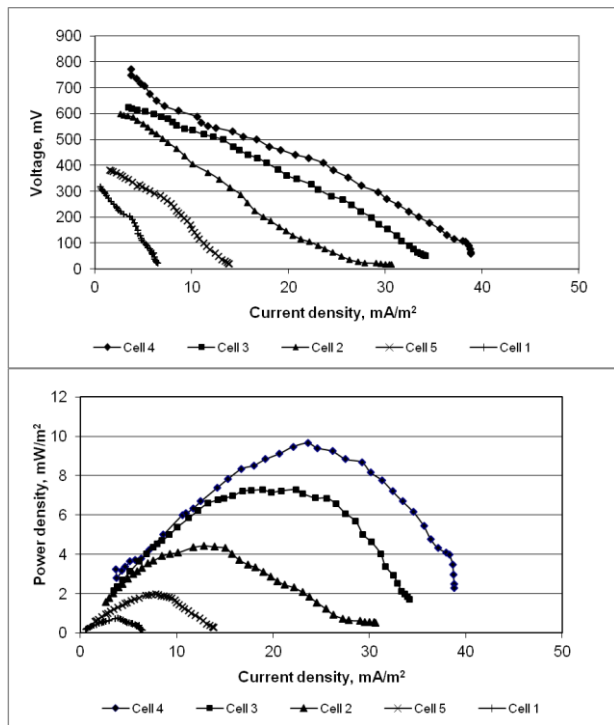


Fig. 2. Polarisation curves in Mode 1

Maximum values of voltage and power density are established in Mode 3. Cell 4 is characterised by the best electrical performance by a power density of 11.56 mW/m<sup>2</sup> at a current density of 27.15 mA/m<sup>2</sup> and applied resistance 300 Ω. The open circuit voltage ranged from 900 to 1100 mV. Approximate values of the electrical parameters are measured

in cell 3 - power density 9.87 mW/m<sup>2</sup> at a current density of 25.46 mA/m<sup>2</sup> and applied resistance of 200 Ω. The lowest values of the electrical parameters are measured in cells 1 and 5.

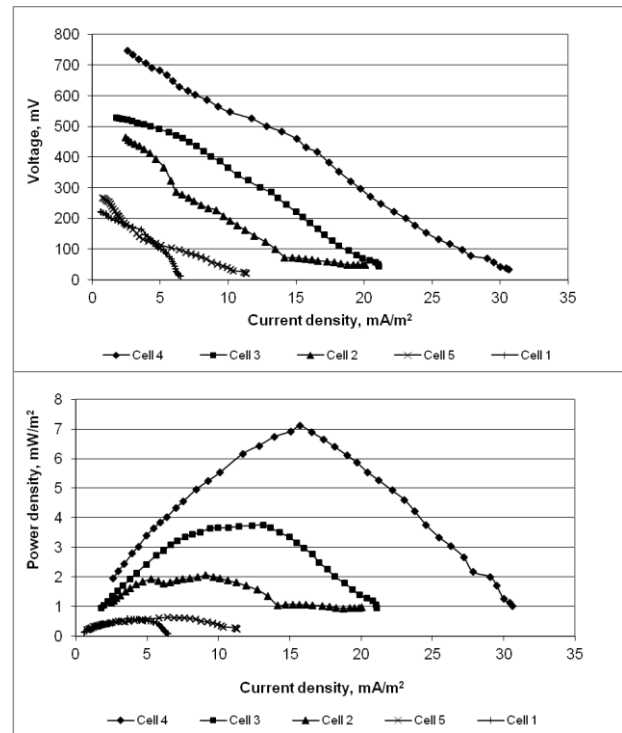


Fig. 3. Polarisation curves in Mode 2

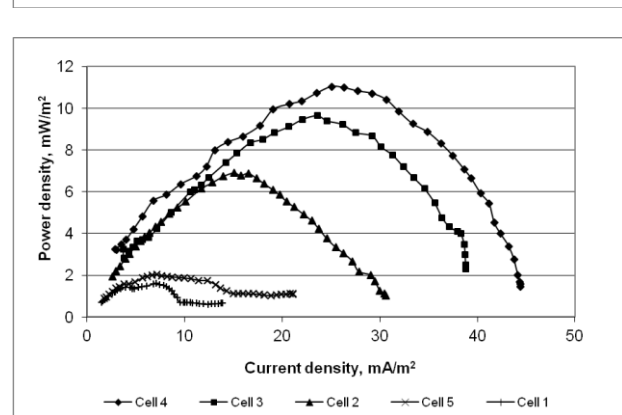
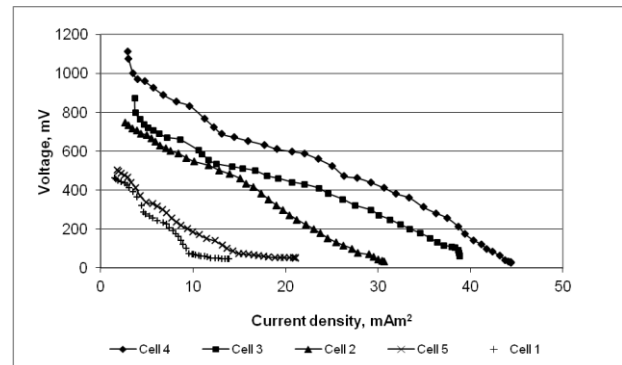


Fig. 4. Polarisation curves in Mode 3

Similar electrical values were measured during Mode 1. Cell 4 again shows the best parameters - a power density of 9.71 mW/m<sup>2</sup>, with a current density of 24.13 mA/m<sup>2</sup> and an applied

resistance of 400  $\Omega$ . In cell 1, the lowest values of the electrical parameters were found.

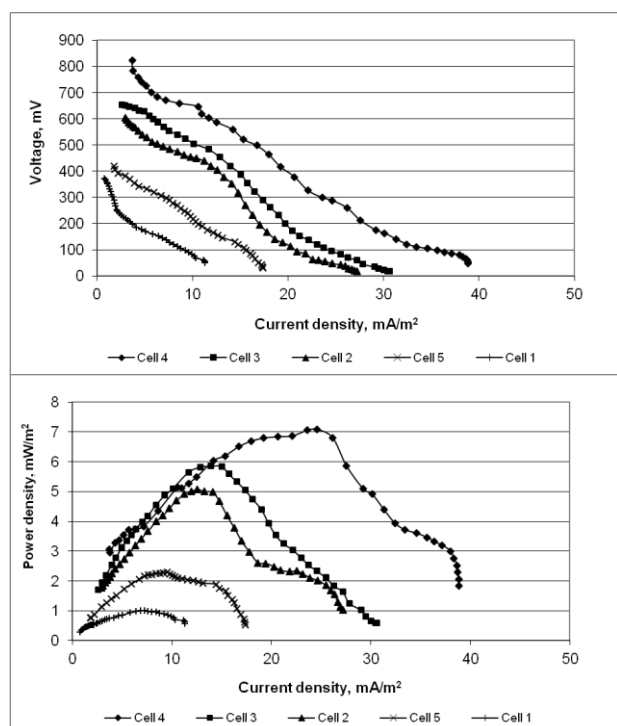


Fig. 5. Polarisation curves in Mode 4

Of the four modes, the lowest electrical characteristics of all cells were measured during mode 2. A maximum power density of 7.16  $\text{mW/m}^2$  at a current density of 17.45  $\text{mA/m}^2$  and a resistance of 200  $\Omega$  was measured in cell 4.

## Conclusions

In order to study the effect of applied high-activity oil-degrading microflora on the purification of water from petroleum products and energy production from constructed wetlands with integrated plant sediment microbial fuel cells, four technological modes of operation were studied. The best treatment effect is achieved in Mode 3, where the cells are inoculated with a mixed culture of aerobic oil-oxidising bacteria. The lowest value of total petroleum product content – 0.055  $\text{mg/l}$  is measured in the outgoing water from cell 4 which is planted with *Spartina*.

From the research and the results obtained, it can be concluded that the added highly active oil-degrading bacteria play a significant role in the water treatment in the constructed wetlands. The vegetation as well as the water flow in the constructed wetlands are also essential.

From the measured electrical parameters of the cells in the individual regimes, it can be seen that the concentration of the

petroleum does not significantly affect the energy generated by plant sediment microbial fuel cells. A more important factor is the species of aquatic vegetation. In all modes, the highest energy is generated in the cell planted with *Spartina*.

The results obtained show good prospects for application of constructed wetlands with integrated plant sediment microbial cells in the passive treatment of waters polluted by crude oil and petroleum products.

**Acknowledgements.** This research was supported by the Bulgarian National Science Fund, Grant No. DM 17/2, 12.12.2017.

## References

- Boyue L., M. Ji, H. Zhai. 2018. Anodic potentials, electricity generation and bacterial community as affected by plant roots in sediment microbial fuel cell: Effects of anode locations. – *Chemosphere*, 209, 739–747.
- Muhammad Afzal, Khadeeja Rehman, Ghulam Shabir, Razia Tahseen, Amna Ijaz, Amer J. Hashmat and Hans Brix. 2019. Large-scale remediation of oil-contaminated water using floating treatment wetlands. – *Clean Water*, 2, 3, 112–119.
- Panpan Meng, Haiyan Pei, Wenrong Hu, Yuanyuan Shao, Zheng Li. 2014. How to increase microbial degradation in constructed wetlands: Influencing factors and improvement measures. – *Bioresource Technology*, 157, 316–326.
- Qing Zhao, Min Ji, Ruying Li, Zhiyong Jason Ren. 2017. Long-term performance of sediment microbial fuel cells with multiple anodes. – *Bioresource Technology*, 237, 178–185.
- Rachnarin Nitisoravut, R. Regmi. 2017. Plant microbial fuel cells: A promising biosystems engineering. – *Renewable and Sustainable Energy Reviews*, 76, 81–89.
- Rasool Alipanahi, M. Rahimnejad, G. Najafpour. 2019. Improvement of sediment microbial fuel cell performances by design and application of power management systems. – *International Journal of Hydrogen Energy*, 125–131.
- Shubiao, W., S. Wallace, H. Brix, P. Kuschik, W. Kipkemoi Kirui, F. Masi, R. Dong. 2018. Treatment of industrial effluents in constructed wetlands: Challenges, operational strategies and overall performance. – *Environmental Pollution*, 201, 107–120.
- Tetteh, F., Kabutey, Q. Zhao, L. Wei, J. Ding, P. Antwi, F. Koblah, Quashie, W. Wang. 2019. An overview of plant microbial fuel cells (PMFCs): Configurations and applications. – *Renewable and Sustainable Energy Reviews*, 110, 402–414.
- Vymazal, J. 2014. Constructed wetlands for treatment of industrial wastewaters: A review. – *Ecological Engineering*, 73, 724–751.

## POSSIBILITIES FOR PNEUFLOT FLOTATION MACHINE APPLICATION IN COPPER-PORPHYRY ORE PROCESSING PLANT

*Tsvetelina Ivanova, Irena Grigorova, Marin Ranchev*

*University of Mining and Geology "St. Ivan Rilski", 1700 Sofia; irena\_mt@abv.bg*

**ABSTRACT.** In the current research work the pre-contact flotation possibilities for recovery of Cu and Mo from copper porphyry ores, have been evaluated. The study was conducted in the form of laboratory flotation experiments with pneumatic flotation machine – PNEUFLOT® (MBE Coal & Minerals Technology). Much attention was paid to the adjustable parameters of the flotation machine such as feed slurry flowrate (l/h); air flowrate (l/h); feed nozzles size (mm) and froth height (mm). Thus, the optimal have been selected for the flotation test programme. Furthermore, in order to evaluate the effect of the reduced froth surface area, using a conical froth crowder (booster cone) on the concentrate mass pull, grade and recovery, a series of flotation experiments with or without central froth crowder have been performed. The obtained results show the possibilities for PNEUFLOT flotation technology implementation in the copper flotation plants.

**Keywords:** Pneufлот, copper-porphyry ore, flotation, parameters

### ВЪЗМОЖНОСТИ ЗА ПРИЛОЖЕНИЕ НА ФЛОТАЦИОННА МАШИНА PNEUFLOT ПРИ ПРЕРАБОТКАТА НА МЕДНО-ПОРФИРНИ РУДИ

*Цветелина Иванова, Ирена Григорова, Марин Ранчев*

*Минно-геоложки университет "Св. Иван Рилски", 1700 София*

**РЕЗЮМЕ.** В представеното изследване бяха анализирани възможностите за флотация с предварителен контакт на Cu и Mo от медно-порфирни руди. Лабораторните изследвания бяха проведени с пневматична флотационна машина PNEUFLOT® (MBE Coal & Minerals Technology). Основно внимание беше обърнато на променливите параметри на флотационната машина, като дебит на пулпа (l/h); дебит на въздуха (l/h); размер на захранващите дюзи (mm) и височината на пенния слой (mm). За флотационните тестове бяха определени и избрани оптималните технически параметри на флотационната машина. Проведени са серия от флотационни тестове с оптимизирани технически параметри на флотационната машина PNEUFLOT, като е контролирана площта на общата повърхност на пенната формация на флотационната машина. Общата повърхност на пенната формация се регулира чрез поставянето на конус в горната част на флотационната клетка, което дава възможност за намаляването ѝ. Проведени са два вида флотационни тестове - със и без конус. Получените резултати от извършените флотационни изследвания, показват възможностите за внедряване на флотационна машина PNEUFLOT в медно преработвателните комплекси.

**Ключови думи:** Pneufлот, медно-порфирна руда, флотация, параметри

### Introduction

Flotation is one of the most important physico-chemical separation processes, used largely in mineral separation operations. In the last three decades the use of pneumatic flotation machines (most common pneumatic flotation columns - "short columns" - refer to other non-mechanical flotation cells, variously referred to as novel columns, pneumatic cells and high intensity cells) became wide-spread throughout the mineral processing industry of metallic, non-metallic ores, coal, etc. (Harbort, Clarke, 2016). Pneumatic flotation has developed very substantially since the 1920's, up to the new designs proposed by Dr. Rainer Imhof in Germany.

The pneumatic pre-contact flotation machines are representatives of a new generation of flotation machines with a number of design features that improve the flotation process. The mixing of the solid and gas phases in an aqueous medium is carried out in advance, outside the volume of the flotation cell, in heterogeneous devices designated by the various manufacturers, such as aeration devices, mixing chambers, and others. The elementary flotation act (attachment of

hydrophilic solid particles to air bubbles) occurs in these devices. Pre-contact flotation machines do not have an impeller system which means there is no wear and tear in the stator-rotor system. Another important feature is the ability to create finer air bubbles and lower air consumption than conventional pneumo-mechanical machines, resulting in flotation of fine products and production of high-quality concentrates.

Since 2009 MBE Coal and Minerals Technology GmbH has been manufacturing and developing the PNEUFLOT flotation machine. A brief description of PNEUFLOT operating principles is presented below.

The flotation pulp is first directed to a single aerating unit arranged in the vertical pipe above the flotation cell. The aerator (self-aerated) is installed in the vertical feed pipe. Following aeration, the pulp flows through the central pipe to the slurry distributor ring located at the bottom of the cell where it is vertically deflected upward through high wear resistant ceramic nozzles. The air bubbles covered with hydrophobic particles ascend to the upper cell area and form a froth layer on the surface which flows off into a froth launder surrounding

the cell like a ring. Particles not clinging to air bubbles are discharged with the pulp from the bottommost point of the cell. The pulp level is kept constant either by a level probe which actuates a valve controlling the discharge or by a device known as a “gooseneck discharge”. The necessary flow rate and pressure are delivered by the appropriate slurry feed pump. The pulp distributor injects the aerated pulp in an upward motion into the flotation vessel. The cell is only responsible for separating the remaining pulp from the froth formed by the loaded bubbles. (Flotation Technology Brochure, PNEUFLOT®, 2011).

The first PNEUFLOT pneumatic flotation plant was put into operation in Pennsylvania in 1987. The installation, owned by Pittstone Coal Co., is for coal flotation, and since then PNEUFLOT has been widely applied in the processing of coal and coal slimes, industrial minerals, iron minerals, and non-ferrous metals such as copper, lead, nickel, and zinc and precious metals - platinum, gold, silver and etc. A schematic view of the PNEUFLOT flotation machine is shown in Figure 1.

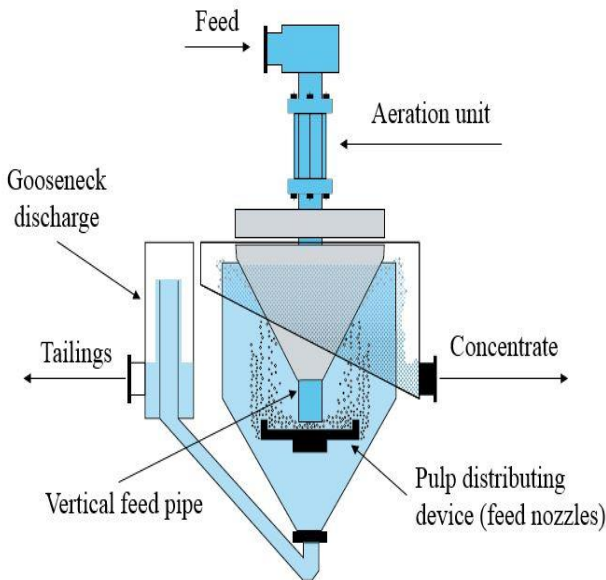


Fig. 1. Schematic view of the PNEUFLOT flotation cell (MBE Coal & Minerals Technology GMBH)

The aim of this study was to evaluate the optimal operating parameters of PNEUFLOT flotation machine and to investigate the influences of these operation variables on the recovery of Cu and Mo during copper-porphyry ore flotation.

## Materials and Methods

A series of flotation tests were conducted on the laboratory PNEUFLOT (Figure 2) flotation machine in order to provide data regarding the following operating parameters:

- Optimal feed slurry flowrate (l/h);
- Optimal air flowrate (l/h);
- Optimal feed nozzles size (mm);
- Optimal froth height (mm).

The feed slurry for the laboratory flotation tests was collected from the hydrocyclone overflow stream, which enters the Cu rougher flotation circuit. The assays for the flotation programme comprised Cu, Mo, SiO<sub>2</sub>, Fe, S.



Fig. 2. Laboratory PNEUFLOT flotation cell

### Investigation of feed slurry flowrate (l/h)

In order to evaluate the optimal feed slurry flowrate (l/h), a series of flotation experiments within the range of 210 to 400 l/h have been conducted. The operating parameters during the flotation experiments are presented in Table 1.

Table 1. Batch laboratory tests operating conditions

Parameters	Value
Feed slurry (l)	50
Solids concentration (%w/w)	30
Residual CaO concentration (mg/l)	650
Flotation time (min.)	9
Air flowrate (l/h)	400
Feed nozzles size (mm)	2.70
Froth height (mm)	60

### Investigation of air flowrate (l/h)

In order to evaluate the optimal air flowrate (l/h), a series of flotation experiments within the range of 150 to 800 l/h have been conducted. The operating parameters during the flotation experiments are presented in Table 2.

Table 2. Batch laboratory tests operating conditions

Parameters	Value
Feed slurry (l)	50
Solids concentration (%w/w)	30
Residual CaO concentration (mg/l)	650
Flotation time (min.)	9
Feed slurry flowrate (l/h)	350
Feed nozzles opening size (mm)	2.70
Froth height (mm)	70

### Investigation of feed nozzles size (mm)

In order to evaluate the optimal opening size of the feed nozzles (mm), a series of flotation experiments with the available nozzle: 2.7, 3.00 and 3.30 mm have been conducted. The operating parameters during the flotation experiments are presented in Table 3.

Table 3. Batch laboratory tests operating conditions

Parameters	Value
Feed slurry (l)	50
Solids concentration (%w/w)	30
Residual CaO concentration (mg/l)	650
Flotation time (min.)	9
Feed slurry flowrate (l/h)	350
Air flowrate (l/h)	300
Froth height (mm)	70

### Investigation of froth height (mm)

In order to evaluate the optimal froth height (mm), a series of flotation experiments within the range of 40 to 100 mm have been conducted. The operating parameters during the flotation experiments are presented in Table 4.

Table 4. Batch laboratory tests operating conditions

Parameters	Value
Feed slurry (l)	50
Solids concentration (%w/w)	30
Residual CaO concentration (mg/l)	650
Flotation time (min.)	9
Feed slurry flowrate (l/h)	350
Air flowrate (l/h)	400
Feed nozzles opening size	2.7

According to Wang et al. (2015) the recovery of gangue particles is greatly influenced by froth heights. As mentioned by Szatkowski (1987) and Wang et al. (2015) a decrease in recovery of gangue minerals occurs when there is an increase in froth height. This is because the increase in froth height extends the froth residence time and promotes drainage of particles per unit mass of water in the froth phase back to the pulp phase.

### Investigation of froth surface area (with/without central froth crowder)

The function of the crowder is to decrease the cross sectional area at the top of the froth to improve the froth removal dynamics in the flotation cell. The walls of a crowder provide a surface to direct froth toward the overflow launder (Cole et al., 2011).

The formation of the froth surface area is regulated by the placement of a cone in the upper part of the flotation cell. In order to evaluate the influence of the reduced froth surface area on the recovery and kinetics efficiencies, a series of flotation experiments with and without central froth crowder have been performed.

The following section of the article will discuss the obtained results from the flotation experiment with the investigated operating parameters - feed slurry flowrate, air flowrate, feed nozzles size, froth height and froth surface area.

## Results and discussions

Based on the results from the flotation experiments, the optimal operating parameters of the PNEUFLOT flotation machine have been determined (Table 5).

Table 5. Selected optimal PNEUFLOT machine operating parameters

Operating parameters	Value
Feed slurry flowrate	350 l/h
Air flowrate	300 l/h
Feed nozzles opening size	2.70 mm
Froth height	80.00 mm

Selected results from the flotation experiments regarding the examination of the optimal operating parameters of the PNEUFLOT flotation machine are presented below.

### Investigation of feed slurry flowrate (l/h)

Throughout the flotation tests, the best Cu & Mo grade and recovery were achieved when the feed slurry flowrate was set to 350 l/h. The flotation test results are presented in Table 6-7.

Table 6. Grade results of flotation test for optimal feed slurry flowrate

Products	Mass pull, %	Grade, %				
		SiO <sub>2</sub>	Cu	Mo, g/t	Fe	S
Conc	40.82	19.91	6.35	329.93	31.75	36.03
Tail	59.18	22.64	1.57	180.91	31.84	37.16
Feed	100.0	21.52	3.52	241.74	31.8	36.7

Table 7. Recovery results of flotation test for optimal feed slurry flowrate

Products	Mass pull, %	Recovery, %				
		SiO <sub>2</sub>	Cu	Mo	Fe	S
Conc	40.82	37.75	73.59	55.71	40.75	40.08
Tail	59.18	62.25	26.41	44.29	59.25	59.92
Feed	100	100	100	100	100	100

### Investigation of air flowrate (l/h)

In the course of the experiments higher Cu & Mo grade and recovery were achieved when the air flowrate was set to 300 l/h. The flotation test results are presented in Table 8-9.

Table 8. Grade results of flotation test for optimal feed slurry flowrate

Products	Mass pull, %	Grade, %				
		SiO <sub>2</sub>	Cu	Mo, g/t	Fe	S
Conc	36.14	16.4	6.87	5108.2	31.40	40.08
Tail	63.86	21.73	1.86	1905	30.50	38.97
Feed	100	19.82	3.67	3062.55	30.83	39.37

Table 9. Recovery results of flotation test for optimal feed slurry flowrate

Products	Mass pull, %	Recovery, %				
		SiO <sub>2</sub>	Cu	Mo	Fe	S
Conc	36.14	29.98	67.69	60.28	36.81	36.79
Tail	63.86	70.02	32.31	39.72	63.19	63.21
Feed	100	100	100	100	100	100

**Investigation of feed nozzles size (mm)**

During the flotation tests with variable feed nozzle the optimum Cu & Mo grade and recovery were achieved with 2.7 mm opening size. The flotation test results are presented in Tables 10-11.

Table 10. Grade results of flotation test for optimal feed slurry flowrate

Products	Mass pull, %	Grade, %				
		SiO <sub>2</sub>	Cu	Mo, g/t	Fe	S
Conc	32.48	15.44	9.15	386.22	31.49	38.30
Tail	67.52	29.48	1.54	215.38	31.76	35.66
Feed	100	24.92	4.01	270.86	31.67	36.52

Table 11. Recovery results of flotation test for optimal feed slurry flowrate

Products	Mass pull, %	Recovery, %				
		SiO <sub>2</sub>	Cu	Mo	Fe	S
Conc	32.48	20.13	74.03	46.31	32.29	34.06
Tail	67.52	79.87	25.97	53.69	67.71	65.94
Feed	100	100	100	100	100	100

**Investigation of froth height (mm)**

Higher values of Cu & Mo grade and recovery while maintaining the froth height around 80 mm were achieved during the flotation experiments. The flotation test results are presented in Table 12-13.

Table 12. Grade results of flotation test for optimal feed slurry flowrate

Products	Mass pull, %	Grade, %				
		SiO <sub>2</sub>	Cu	Mo, g/t	Fe	S
Conc	26.96	12.43	7.46	4230.52	33.38	41.38
Tail	73.04	22.08	2.36	2391	29.95	39.84
Feed	100	19.48	3.73	2887.18	30.87	40.26

Table 13. Recovery results of flotation test for optimal feed slurry flowrate

Products	Mass pull, %	Recovery, %				
		SiO <sub>2</sub>	Cu	Mo	Fe	S
Conc	26.96	17.20	53.83	39.50	29.15	27.71
Tail	73.04	82.80	46.17	60.50	70.85	72.29
Feed	100	100	100	100	100	100

**Investigation of froth surface area (with/without central froth crowder)**

Tables 14, 15, 16 and 17 below, presents the results from the flotation experiments conducted with and without using a conical froth crowder, attached on the top of the flotation cell.

Table 14. Grade results of flotation test with a central froth crowder

Products	Mass pull, %	Grade, %				
		Cu	Mo, g/t	Fe	S	SiO <sub>2</sub>
Ro Conc 1 (2')	10.63	10.46	1939	28.57	36.08	19.43
Ro Conc 2 (5')	9.07	8.29	2907	28.43	33.99	21.16
Ro Conc 3 (7')	7.46	6.68	3784	24.58	3.18	27
Ro Conc 4 (9')	9.47	4.65	4483	24.67	31.86	29.19
Ro Conc	36.64	7.65	3212.04	26.71	27.77	23.92
Scavenger Conc (18')	20.35	4.54	5153	21.63	30.83	31.94
Tail	43.01	0.949	806	29.38	36.9	23.86
Feed	100.0	4.14	2572.37	26.83	32.32	25.53

Table 15. Recovery results of flotation test with a central froth crowder

Products	Mass pull, %	Recovery, %				
		Cu	Mo	Fe	S	SiO <sub>2</sub>
Ro Conc 1 (2')	10.63	26.90	8.02	11.33	11.87	8.09
Ro Conc 2 (5')	9.07	18.19	10.25	9.61	9.54	7.52
Ro Conc 3 (7')	7.46	12.06	10.98	6.84	0.73	7.89
Ro Conc 4 (9')	9.47	10.65	16.50	8.71	9.34	10.83
Ro Conc	36.64	67.79	45.75	36.49	31.48	34.34
Scavenger Conc (18')	20.35	22.34	40.77	16.41	19.42	25.47
Tail	43.01	9.87	13.47	47.10	49.10	40.20
Feed	100	100	100	100	100	100

Table 16. Grade results of flotation test without using a central froth crowder

Products	Mass pull, %	Grade, %				
		Cu	Mo, g/t	Fe	S	SiO <sub>2</sub>
Ro Conc 1 (2')	12.33	10.23	1696	30.67	37.57	15.73
Ro Conc 2 (5')	15.07	6.74	3302	28.06	36.31	21.22
Ro Conc 3 (7')	9.61	4.56	4304	26.31	34.97	26.05
Ro Conc 4 (9')	8.78	3.15	4245	25.85	33.26	23.61
Ro Conc	45.79	6.53	3260.59	27.97	35.78	21.21
Scavenger Conc (18')	17.74	3.289	3060	27.88	36.98	23.49
Tail	36.47	0.979	830	27.87	33.7	27.26
Feed	100.0	3.93	2338.53	27.92	35.24	23.82

Table 17. Recovery results of flotation test without using a central froth crowder

Products	Mass pull, %	Recovery, %				
		Cu	Mo	Fe	S	SiO <sub>2</sub>
Ro Conc 1 (2')	12.33	32.08	8.94	13.55	13.15	8.14
Ro Conc 2 (5')	15.07	25.83	21.28	15.14	15.53	13.42
Ro Conc 3 (7')	9.61	11.14	17.68	9.05	9.54	10.51
Ro Conc 4 (9')	8.78	7.03	15.94	8.13	8.29	8.70
Ro Conc	45.79	76.08	63.84	45.88	46.50	40.77
Scavenger Conc (18')	17.74	14.84	23.21	17.72	18.62	17.49
Tail	36.47	9.08	12.94	36.41	34.88	41.73
Feed	100	100	100	100	100	100

The results show that when using a froth crowder, due to the reduced froth area size, a lower weight pulls (36.64%) was achieved, but with higher Cu grade (7.65%) and nearly the same Mo content (3212 g/t) compared to the experiment conducted without froth crowder. The overall Cu recovery (rougher + cleaner) from both flotation tests reached approximately 90%. Noticeable difference in the Mo grade of the scavenger concentrates from both experiments was found, as in the experiment with central froth crowder the scavenger concentrate assaying 5153 g/t compared to 3060 g/t, without using a central froth crowder. A possible explanation for this might be that during the flotation test with central froth crowder the height of the froth was increased which led to longer froth retention time which in turn contributed to decrease in the recovery of gangue minerals by entrainment. According to Zheng et al. (2006) with an increase in froth retention time, more water and entrained particles (mainly gangue minerals) are expected to drain out of the froth phase, leading to improved concentrate grade.

## Conclusions

The results presented in this paper clearly show the applicability of PNEUFLOT flotation technology for Cu and Mo recovery in the flotation of copper-porphyry ores. The Cu and Mo recoveries in the rougher flotation concentrates during the investigation of optimal parameters were acceptable, ranging from 67 to 76% for Cu and from 39 to 60 % for Mo. Higher molybdenum grades in the scavenger concentrate reaching up to 5153 g/t were accomplished. It seems possible that these results are due to the PNEUFLOT flotation cell hydrodynamic creating a suitable condition for effective separation (higher selectivity) of the sulphide Cu and Mo minerals from gangue

(SiO<sub>2</sub>, clays, etc.) components. Thanks to the very small area where the air injection to slurry is conducted before entering the separation vessel, the flotation process needs less time compared to other flotation technologies. It could be concluded that the PNEUFLOT flotation machine is an effective solution for flotation process plants.

## References

- Cole, K. E., P. R. Brito-Parada, S. J. Neethling, J. J. Cilliers. 2011. *A model of froth motion to test flotation cell crowder designs – experimental validation with overflowing 2D foam*. Rio Tinto Centre for Advanced Mineral Recovery, Froth and Foam Research Group, Department of Earth Science and Engineering, Imperial College London, South ensington Campus, London, United Kingdom, 2 p.
- Harbort, G., D. Clarke. 2006. Fluctuations in the popularity and usage of flotation columns – An overview. – *Mineral Engineering*, 100, 17–30.
- MBE Coal & Minerals Technology GMBH. 2011. *Flotation Technology Brochure*. PNEUFLOT®, Cologne, Germany.
- Szatkowski, M. 1987. *Factors influencing behavior of flotation froth*. – *Ins. Min. Metall. Trans., Sect. C. Miner. Process. Extract. Metall.*, 96, 115–122.
- Wang, L., Y. Peng, K. Runge, D. Bradshaw. 2015. A review of entrainment: Mechanisms, contributing factors and modeling in flotation. – *Minerals Engineering*, 70, 77–91.
- Zheng, X., N. W. Johnson, J. P. Franzidis. 2006. Modelling of entrainment in industrial flotation cells: Water recovery and degree of entrainment. – *Minerals Engineering*, 19, 1191–1203.

## PRE-CONTACT PNEUMATIC FLOTATION OF COPPER PORPHYRY ORE FROM ASSAREL DEPOSIT

*Tsvetelina Ivanova, Marin Ranchev, Irena Grigorova, Ivan Nishkov*

*University of Mining and Geology "St. Ivan Rilski"; 1700 Sofia; irena\_mt@abv.bg*

**ABSTRACT.** The PNEUFLOT flotation machine is a representative of a new generation of pre-contact columns flotation machines combining the principle of pneumatic spraying with the column flotation cell design. The PNEUFLOT flotation machine does not have an impeller system. This means no wear and friction in the system stator - rotor. Another important feature is the ability to create finer air bubbles and lower air consumption than conventional pneumo-mechanical machines, resulting in flotation of fine products and obtaining high-quality concentrates. Porphyry-copper ores in the "Assarel" deposit is characterised by a variable and complex mineral composition and varying physical properties. In order to establish the possibilities for flotation with pre-contact on the ore, processed in the Assarel Flotation Plant, a series of flotation experiments with selected products from the technological circuit of the plant were carried out. The flotation tests were performed at the optimal technical parameters of the flotation machine and the experimental results obtained present the efficient flow of the selectivity of the flotation process, mainly due to the hydrodynamic conditions in the PNEUFLOT flotation machine, which creates a prerequisite for efficient separation of the copper minerals and molybdenite from the gangue.

**Keywords:** flotation, copper ores, Pneufлот, flotation machines

### ФЛОТАЦИЯ С ПРЕДВАРИТЕЛЕН КОНТАКТ НА МЕДНОПОРФИРНА РУДА ОТ НАХОДИЩЕ АСАРЕЛ

*Цветелина Иванова, Марин Ранчев, Ирена Григорова, Иван Нишков*

*Минно-геоложки университет "Св. Иван Рилски", 1700 София*

**РЕЗЮМЕ.** Флотационната машина PNEUFLOT е представител на едно ново поколение колонни флотационни машини с предварителен контакт, комбинираща принципа на пневматичното пулверизиране в съчетание с колонния дизайн на флотационната клетка. Флотационната машина PNEUFLOT не притежава импелерна система, което означава, че няма износване и триене в системата статор - ротор. Друга важна характеристика е възможността да се създават по-фини въздушни мехурчета и по-нисък разход на въздух в сравнение с класическите пневмомеханични машини, което води до флотация на фини продукти и получаване на висококачествени концентрати. Меднопорфирните руди в находище "Асарел" се характеризират с променлив и сложен минерален състав и вариращи физични свойства. С цел установяване възможностите за флотация с предварителен контакт на рудата, преработвана в ОФ „Асарел“, са проведени серии от флотационни експерименти с избрани продукти от технологичната верига на обогатителния комплекс. Флотационните тестове са проведени при оптимални технически параметри на флотационната машина, като получените експериментални резултати ясно показват ефективното протичане на селективността на флотационния процес, дължащо се най-вече на хидродинамичните условия във флотационната машина PNEUFLOT, което създава предпоставка и за добро разделяне на медните минерали и молибденита от скалните примеси.

**Ключови думи:** флотация, медна руда, Pneufлот, флотационни машини

### Introduction

Flotation is an important and versatile mineral processing step used to achieve selective separation of minerals and gangue. It utilises the hydrophobic nature of mineral surfaces and their propensity to attach to rising air bubbles in water-ore pulp as the basis for separation (Biswas, A., Davenport, W., 1994).

Metal sulphide minerals, for which this process was originally developed, are generally weakly polar in nature and consequently, most have a hydrophilic surface (Wills, 1997).

The flotation reagent MINFIT is a unique complex of modified sulphites specifically developed for depressing iron sulphide minerals (pyrite, pyrrhotite, marmatite, etc.).

In the pneumatic pre-contact column flotation machines, such as PNEUFLOT® the contact between the solid phase (feed) and the air flow is performed in a mixing device at the top of a vertical pipe, or in a separate agitating tank (reactor) or

in several aeration devices, disposed along the flotation cell feed slurry pipelines.

The main advantages of these devices are that the total height of the cell is reduced compared to conventional column machines, it can be self-induced with respect to air supply, there are no moving parts and flotation time is relatively fast. All this combined with the appropriate selection of flotation reagents will contribute to higher selectivity and production of high quality concentrates.

The study was conducted in the form of several laboratory flotation experiments in order to assess the effect of the reagent MINFIT®, the optimal concentration of residual CaO (mg/l) and the pros and cons of adding a conical froth crowder on the top of the flotation cell. The flotation tests were conducted in a PNEUFLOT pneumatic flotation machine – PNEUFLOT® (MBE Coal & Minerals Technology).

## Materials and Methods

Table 1 presents the conditions of the flotation experiment performed with PNEUFLOT laboratory machine. The flotation experiment was carried out without using a conical froth crowder.

Table 1. Flotation test conditions

Parameters	Value
Solids concentration (%w/w)	32.00
pH of the pulp	11.76
Feed slurry flowrate (l/h)	350
Air flowrate (l/h)	300
Feed nozzles size (mm)	2.70
Froth height (mm)	70
<b>Without using a conical froth crowder</b>	√
Residual CaO concentration (mg/l)	588.00
MINFIT consumption (g/t)	200
Flotation time (min.)	Rougher flotation 2, 5, 7 and 9 min. Scavenger flotation 18 min.

Table 2 presents the conditions of the second flotation experiment performed with PNEUFLOT laboratory machine, when using a conical froth crowder.

Table 2. Flotation test conditions

Parameters	Value
Solids concentration (% w/w)	32.00
pH of the pulp	12.19
Feed slurry flowrate (l/h)	350
Air flowrate (l/h)	300
Feed nozzles size (mm)	2.70
Froth height (mm)	70
<b>With using a conical froth crowder</b>	√
Residual CaO concentration (mg/l)	590.18
Consumption of MINFIT (g/t)	200
Flotation time (min.)	Rougher flotation 2, 5, 7 and 9 min. Scavenger flotation 18 min.

## Results and discussions

Tables 3-4 present the technological results from the flotation test without using a conical froth crowder.

Table 3. Grade results of flotation test without using a central froth crowder

Products	Mass pull, %	Grade, %					
		Cu	Mo, g/t	Fe	S	Al <sub>2</sub> O <sub>3</sub>	SiO <sub>2</sub>
Ro Conc 1 (2')	13.52	6.036	1121	27.97	31.54	4.97	23.53
Ro Conc 2 (5')	13.18	4.172	1261	28.27	30.25	5.01	23.81
Ro Conc 3 (7')	7.57	3.09	1205	29.07	30.85	4.82	23.34
Ro Conc 4 (9')	5.29	2.376	1097	29.85	33.01	4.78	23.48
Ro Conc	39.55	4.36	1180.50	28.53	31.17	4.93	23.58
Scavenger Conc (18')	7.99	2.151	1299	31.18	32.12	4.79	21.79
Tail	52.45	0.62	232	29.18	33.37	5.48	23.7
Feed	100	2.22	692.45	29.08	32.40	5.21	23.50

Table 4. Recovery results of flotation test without using a central froth crowder

Products	Mass pull, %	Recovery, %					
		Cu	Mo	Fe	S	Al <sub>2</sub> O <sub>3</sub>	SiO <sub>2</sub>
Ro Conc 1 (2')	13.52	36.71	21.88	13.00	13.16	12.90	13.53
Ro Conc 2 (5')	13.18	24.74	24.00	12.81	12.30	12.68	13.35
Ro Conc 3 (7')	7.57	10.52	13.17	7.57	7.21	7.01	7.52
Ro Conc 4 (9')	5.29	5.66	8.38	5.43	5.39	4.86	5.29
Ro Conc	39.55	77.63	67.43	38.80	38.06	37.44	39.69
Scavenger Conc (18')	7.99	7.74	14.99	8.57	7.92	7.35	7.41
Tail	52.45	14.63	17.57	52.63	54.02	55.20	52.90
Feed	100	100	100	100	100	100	100

Figure 1 presents the cumulative (%) recovery of the chemical components versus flotation time (flotation kinetics).

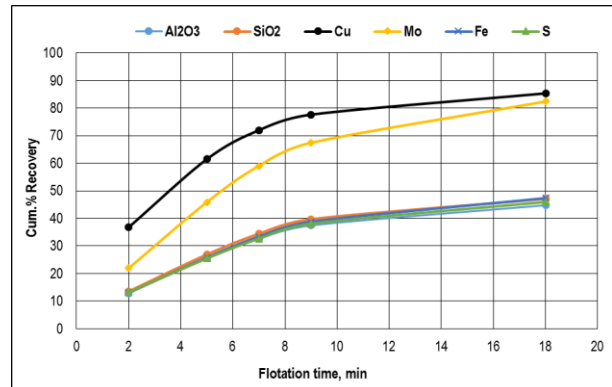


Fig. 1. Flotation time vs cumulative % recovery - flotation test without using a central froth crowder

Figure 2 presents the relation between the cumulative mass pull and the cumulative Cu recovery during the flotation experiment without using a central froth crowder.

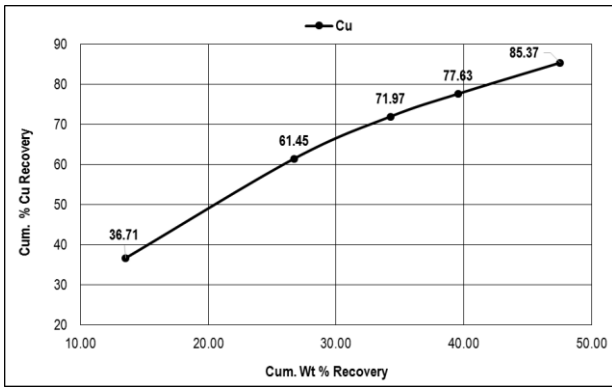


Fig. 2. Cumulative weight recovery vs cumulative Cu recovery - flotation test without using a central froth crowder

The technological results of the flotation test conducted with a conical froth crowder are presented in Tables 5-6.

Table 5. Grade results of the flotation test with a conical froth crowder

Products	Mass pull, %	Grade, %					
		Cu	Mo, g/t	Fe	S	Al <sub>2</sub> O <sub>3</sub>	SiO <sub>2</sub>
Ro Conc 1 (2')	9.98	6.186	1046	30.86	35.47	4.27	19.89
Ro Conc 2 (5')	9.38	4.051	1131	28.87	33.38	4.92	23.62
Ro Conc 3 (7')	5.68	3.452	1173	30.34	35.75	4.56	22.31
Ro Conc 4 (9')	5.82	2.71	1018	29.8	35.5	4.79	23.37
Ro Conc	30.87	4.38	1089.93	29.96	34.89	4.62	22.13
Scavenger Conc (18')	15.12	2.412	1050	30.45	33.28	4.7	22.35
Tail	54.02	0.816	227	30.09	35.42	5.03	22.4
Feed	100	2.16	617.77	30.10	34.93	4.85	22.31

Table 6. Recovery results of the flotation test with a conical froth crowder

Products	Mass pull, %	Recovery, %					
		Cu	Mo	Fe	S	Al <sub>2</sub> O <sub>3</sub>	SiO <sub>2</sub>
Ro Conc 1 (2')	9.98	28.63	16.90	10.23	10.13	8.78	8.90
Ro Conc 2 (5')	9.38	17.62	17.17	9.00	8.96	9.51	9.93
Ro Conc 3 (7')	5.68	9.10	10.79	5.73	5.82	5.34	5.68
Ro Conc 4 (9')	5.82	7.32	9.59	5.76	5.92	5.75	6.10
Ro Conc	30.87	62.66	54.46	30.72	30.83	29.38	30.61
Scavenger Conc (18')	15.12	16.91	25.70	15.29	14.40	14.64	15.15
Tail	54.02	20.44	19.85	53.99	54.77	55.98	54.24
Feed	100	100	100	100	100	100	100

Figures 3 and 4 present the results of rougher copper flotation (9 min) and scavenger copper flotation (9 min) when using a central froth crowder.

Figure 3 presents the cumulative (%) recovery of the chemical components versus flotation time (flotation kinetics).

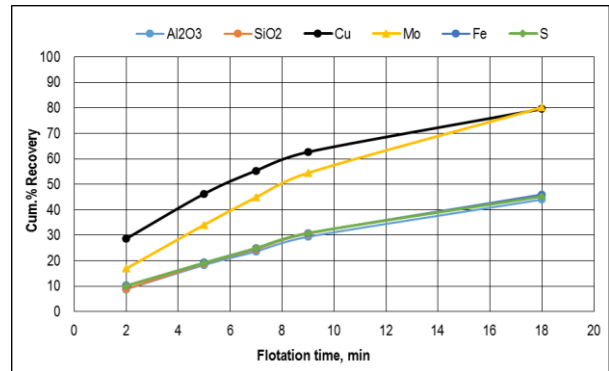


Fig. 3. Flotation time vs cumulative % recovery

Figure 4 presents the relation between the cumulative mass pull and the cumulative Cu recovery during the flotation experiment with a central froth crowder.

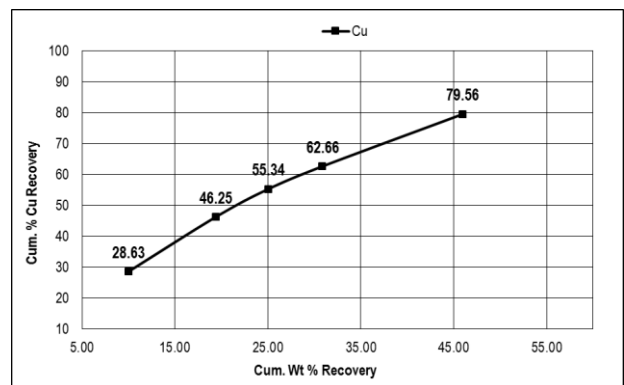


Fig. 4. Cumulative weight recovery vs. cumulative Cu recovery - flotation test with a central froth crowder

Figures 1 and 3 show the effect of MINFIT depressant. The consumption of 200 g/t and hydrodynamic conditions of the PNEUFLOT flotation machine results in higher selectivity against pyrite.

### Investigation of the influence of residual calcium oxide (CaO) concentration on the flotation process efficiency

A series of laboratory flotation experiments were carried out during which the residual calcium oxide (CaO) concentration was maintained and controlled within certain limits, depending on the characteristic of the feed pulp entering the rougher and/or scavenger copper flotation circuit.

The experiments were carried out with a representative slurry sample from the mineral processing plant. The solids' concentration varies between 30-35%, pH of the pulp varies within the range of 12.30-12.66 pH, froth height varies between 60-80 mm and the grain size ranges within certain limits for the individual tests. It was determined that the residual calcium oxide concentration in flotation feed slurry is about 340 mg/l. An appropriate amount of calcium hydroxide [Ca(OH)<sub>2</sub>] was added to the feed pulp, in order to achieve a concentration of residual calcium oxide in the range of 650-700 mg/l.

After rougher copper flotation (9 min), CaO content was around 175 mg/l. In the rougher flotation tail product, calcium hydroxide was added [Ca(OH)<sub>2</sub>] in order to obtain a residual

CaO concentration within the range of 650-700 mg/l. Tables 7-8 present the technological results from the flotation test with residual CaO concentration 700 mg/l.

Table 7. Grade results of the flotation test with residual CaO concentration of 700 mg/l

Products	Mass pull, %	Grade, %					
		Cu	Mo, g/t	Fe	S	Al <sub>2</sub> O <sub>3</sub>	SiO <sub>2</sub>
Ro Conc 1 (2')	7.52	9.47	2867	34.82	41.51	2.38	10.7
Ro Conc 2 (5')	10.14	7.75	4899	33.38	41.1	2.71	12.87
Ro Conc 3 (7')	5.93	6.72	6308	35.05	39.85	2.47	12.74
Ro Conc 4 (9')	5.23	5.55	6343	31.32	38.92	3.26	18.81
Ro Conc	28.82	7.59	4920.24	33.73	40.55	10.31	13.35
Scavenger Conc (18')	19.04	2.96	5560	30.33	40.54	4.1	21.05
Tail	52.15	1.5	1024	29.6	38.77	4.83	23.54
Feed	100	3.53	3010.27	30.93	39.62	6.27	20.13

Table 8. Recovery results of the flotation test with residual CaO concentration of 700 mg/l

Products	Mass pull, %	Recovery, %					
		Cu	Mo	Fe	S	Al <sub>2</sub> O <sub>3</sub>	SiO <sub>2</sub>
Ro Conc 1	7.52	20.17	7.17	8.47	7.88	4.40	4.00
Ro Conc 2	10.14	22.24	16.50	10.94	10.52	6.75	6.48
Ro Conc 3	5.93	11.28	12.42	6.72	5.96	3.60	3.75
Ro Conc 4	5.23	8.21	11.01	5.29	5.13	4.19	4.88
Ro Conc	28.82	61.90	47.10	31.42	29.49	18.93	19.11
Scavenger Conc (18')	19.04	15.95	35.16	18.67	19.48	19.18	19.91
Tail	52.15	22.14	17.74	49.91	51.03	61.89	60.98
Feed	100	100	100	100	100	100	100

Figures 5 and 6 present the results of the flotation test - rougher (9 min.) and scavenger (9 min.) copper flotation with residual CaO concentration of 700 mg/l.

Figure 5 presents the cumulative Cu recovery (%) versus cumulative recovery of other components (Mo, Fe, S, Al<sub>2</sub>O<sub>3</sub>, SiO<sub>2</sub>).

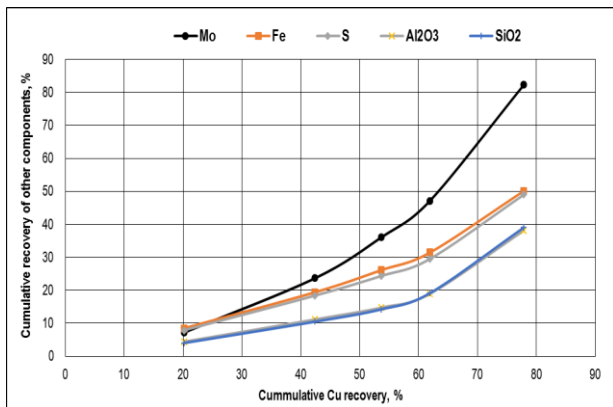


Fig. 5. Cu/Mo, Fe, S, Al<sub>2</sub>O<sub>3</sub>, SiO<sub>2</sub> selectivity as a function of flotation time

Figure 6 presents the Cu and Mo grade of the obtained flotation concentrates.

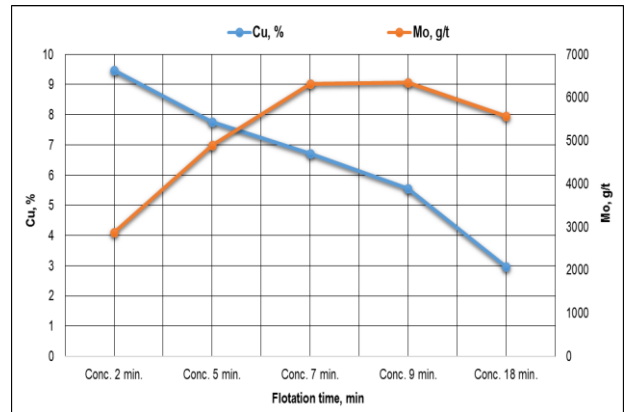


Fig. 6. Cu and Mo grade in the obtained flotation concentrates

It was determined that the residual concentration of calcium oxide in the flotation feed pulp was 436.66 mg/l. In order to increase the concentration, an appropriate amount of calcium hydroxide Ca(OH)<sub>2</sub> was added to the pulp, establishing a concentration of residual calcium oxide within the range of 650-700 mg/l.

After rougher copper flotation (9 min), CaO concentration was 244.24 mg/l. An additional amount of calcium hydroxide Ca(OH)<sub>2</sub> was added to scavenger flotation feed in order to maintain the concentration of residual calcium oxide in the scope of 650-700 mg/l.

Tables 9-10 present the technological results from the flotation test with maintained residual CaO concentration between 650-700 mg/l.

Table 9. Grade results of the flotation test with residual CaO concentration of 677 mg/l

Products	Mass pull, %	Grade, %					
		Cu	Mo, g/t	Fe	S	Al <sub>2</sub> O <sub>3</sub>	SiO <sub>2</sub>
Ro Conc 1 (2')	9.21	9.47	1692	30.78	38.52	3.09	15.23
Ro Conc 2 (5')	11.88	7.98	2893	29.66	37.89	4.23	18.97
Ro Conc 3 (7')	9.11	5.25	4658	29.69	38.65	4.37	20.74
Ro Conc 4 (9')	11.30	3.20	4801	24.57	33.77	5.71	29.42
Ro Conc	41.50	6.41	3533.26	28.53	37.07	4.41	21.37
Scavenger Conc (18')	22.94	2.56	3075	24.07	33.22	5.57	29.56
Tail	35.57	1.04	723	26.76	32.06	6.22	28.87
Feed	100	3.62	2428.61	26.88	34.41	5.32	25.92

Figures 7 and 8 present the results of the flotation test - rougher (9 min.) and scavenger (9 min.) copper flotation with residual CaO concentration of 677 mg/l.

Figure 7 presents the cumulative Cu recovery (%) versus the cumulative recovery of other components (Mo, Fe, S, Al<sub>2</sub>O<sub>3</sub>, SiO<sub>2</sub>).

Table 10. Recovery results of the flotation test with residual CaO concentration of 677 mg/l

Products	Mass pull, %	Recovery, %					
		Cu	Mo	Fe	S	Al <sub>2</sub> O <sub>3</sub>	SiO <sub>2</sub>
Ro Conc 1 (2')	9.21	24.12	6.42	10.55	10.31	5.35	5.41
Ro Conc 2 (5')	11.88	26.19	14.15	13.11	13.08	9.44	8.69
Ro Conc 3 (7')	9.11	13.21	17.47	10.06	10.23	7.48	7.29
Ro Conc 4 (9')	11.30	9.99	22.33	10.33	11.09	12.13	12.82
Ro Conc	41.50	73.50	60.37	44.05	44.71	34.40	34.22
Scavenger Conc (18')	22.94	16.28	29.04	20.54	22.15	24.01	26.16
Tail	35.57	10.22	10.59	35.41	33.14	41.58	39.62
Feed	100	100	100	100	100	100	100

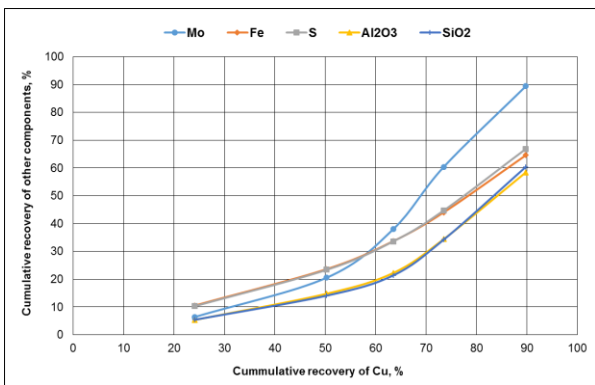


Fig. 7. Cu/Mo, Fe, S, Al<sub>2</sub>O<sub>3</sub>, SiO<sub>2</sub> selectivity as a function of flotation time

Figure 8 presents the Cu and Mo grade of the obtained flotation concentrates.

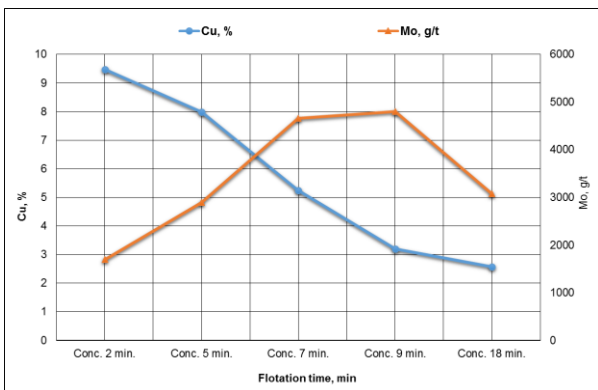


Fig. 8. Cu and Mo grade in the obtained flotation concentrates

### Conclusions

The experimental results obtained during the flotation tests of copper-porphyry ore, showed that when using MINFIT® (200 g/t) depressant in the hydrodynamic conditions of the PNEUFLOT flotation machine, the flotation process proceeds with a higher pyrite selectivity. While, the Cu grade in the gangue is within the range of 0.6 and 0.82% and the Mo grade

is about 230 g/t. The higher content of residual calcium oxide in the flotation pulp, results in low concentrate mass pull, but on the other hand, with an increased Cu grade in the final concentrate.

Maintaining an optimal residual concentration of CaO in the range of 650-700 mg/l in the rougher flotation circuit results in approximately 30% concentrate mass pull with 7.59 Cu grade. Maintaining an optimal residual concentration of calcium oxide in rougher and scavenger copper flotation leads to lower Cu content in the flotation tail and a total recovery of copper and molybdenum within the range of 90%. The selectivity curves clearly show the higher selectivity of the flotation process (depressed pyrite). Apparently, the hydrodynamic conditions in the PNEUFLOT flotation machine create a prerequisite for an effective separation (higher selectivity) of copper minerals and molybdenum from the gangue components (Al<sub>2</sub>O<sub>3</sub> and SiO<sub>2</sub>).

The kinetic curves showed that the copper minerals in rougher flotation circuit floated most rapidly during the first seven minutes, and Mo actively started to float after the fifth minute. It should be noted that the grade of Mo in some of the concentrates reached over 6000 g/t. Apparently, the hydrodynamic conditions in the PNEUFLOT flotation machine enable the flotation of fine molybdenum particles. It should be noted that the efficient flotation of Mo and the higher Mo grade (over 6000 g/t) in the obtained concentrates was possible due to the optimal hydrodynamic conditions created by the flotation cell. The laboratory flotation experiments were performed without using any molybdenum activating reagents, i.e. no suitable physicochemical conditions for Mo flotation were set up.

### References

Biswas, A. K., W. G. Davenport (Eds.). 1994. *Extractive Metallurgy of Copper*. 3rd Ed. Pergamon, Oxford.

Cole, K. E., P. R. Brito-Parada, S. J. Neethling, J. J. Cilliers, 2011. *A model of froth motion to test flotation cell crowder designs – experimental validation with overflowing 2D foam*. Rio Tinto Centre for Advanced Mineral Recovery, Froth and Foam Research Group, Department of Earth Science and Engineering, Imperial College London, London, United Kingdom, 2 p.

Harbort, G., Clarke, D. 2006. *Fluctuations in the popularity and usage of flotation columns – An overview. – Mineral Engineering*, 100, 17–30.

MBE Coal & Minerals Technology GMBH. 2011. *Flotation Technology Brochure. PNEUFLOT®*. Cologne, Germany.

Szatkowski, M. 1987. *Factors influencing behavior of flotation froth. – Ins. Min. Metall. Trans., Sect. C. Miner. Process. Extract. Metall.*, 96, 115–122.

Wang, L., Y. Peng, K. Runge, D. Bradshaw. 2015. *A review of entrainment: Mechanisms, contributing factors and modeling in flotation. – Minerals Engineering*, 70, 77–91.

Wills, B. A., T. Napier-Munn. 2006. *Mineral Processing Technology: An Introduction to the Practical Aspects of Ore Treatment and Mineral Recovery*. Butterworth-Heinemann, Oxford.

Zheng, X., N. W. Johnson, J.-P. Franzidis. 2006. *Modelling of entrainment in industrial flotation cells: Water recovery and degree of entrainment. – Minerals Engineering*, 19, 1191–1203.

## INVESTIGATION OF THE POSSIBILITIES TO USE RECYCLED CONSTRUCTION WASTE IN ROAD CONSTRUCTION

**Maria Manastirli, Marina Nicolova**

University of Mining and Geology "St. Ivan Rilski", 1700 Sofia; manastyrl\_mariy@mail.ru

**ABSTRACT.** The environmental protection and the sustainable development are directly dependent on the proper management of waste. Huge amounts of waste are generated in the process of construction, reconstruction and rehabilitation. The road sector is one of the largest generators of construction waste but it is also a sector that offers the opportunity to use such waste in the construction of new roads and in the reconstruction and rehabilitation of roads. The study of the possibilities to use recycled construction waste in the construction of new roads is an important step towards the environmental protection by reducing the amount of landfilled waste and the volume of natural resources that have been used.

**Keywords:** road construction, recycled material, utilisation

### ИЗСЛЕДВАНЕ НА ВЪЗМОЖНОСТИТЕ ЗА ИЗПОЛЗВАНЕ НА РЕЦИКЛИРАНИ СТРОИТЕЛНИ ОТПАДЪЦИ В ПЪТНОТО СТРОИТЕЛСТВО

**Мария Манастирли, Марина Николова**

Минно-геоложки университет "Св. Иван Рилски", 1700 София

**РЕЗЮМЕ.** Опазването на околната среда и устойчивото развитие са в пряка зависимост от правилното управление на отпадъците. В процеса на строителство и изграждане на инфраструктура се генерират огромни количества строителни отпадъци, голяма част от които може да се използват повторно в ново строителство, реконструкция и рехабилитация. Пътният сектор е сред най-големите генератори на строителни отпадъци, но е и отрасъл, който предоставя възможности за използване на рециклирани строителни отпадъци, както в строителството на нови трасета, така и при реконструкция и рехабилитация на пътища. Изследване на възможностите за използване на рециклирани строителни отпадъци в пътното строителство е важна стъпка за опазването на околната среда посредством намаляването на количествата депонирани отпадъци и обема на използваните природни ресурси.

**Ключови думи:** пътно строителство, рециклирани материали, оползотворяване

### Introduction

With the development of modern infrastructure, the amount of construction waste generated which is one of the worst and most massive waste streams in the European Union (EU) is increasing. Construction waste is among the priority waste streams and accounts for 25-30% of the total waste generated in the EU. The potential for re-use is high because of the high recyclability of construction waste and the availability of a market for recycled building materials used in the road sector. Despite the high potential and affordable technologies for separating and recovering construction waste, the degree of recycling and input of construction waste materials in the EU varies widely.

In the Republic of Bulgaria, despite the increasing number of persons holding permits (Waste Management Act (WMA), Art. 35, State Gazette (SG), No. 53, 2012, and suppl. SG, No. 1, 2019) and carrying out recycling and recovery activities for construction waste, for 2017 only 26% of the generated waste from the Construction sector was handed over for recovery, while the deposited waste was 46%.

Figure 1 shows quantitative data on construction waste generated, handed over for recovery and disposal.

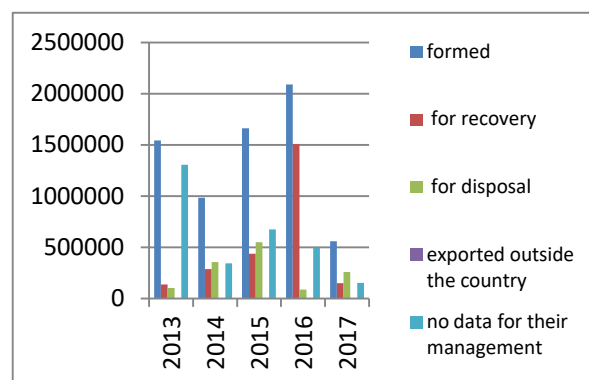


**Fig. 1. Construction waste management for the period 2013-2016 (source: NSI)**

As shown in the chart, only in 2013 and 2016 the waste handed over for recovery is more than the landfilled, and the difference is more significant in 2016 and consists of 1422339 tonnes. During the remaining years the waste handed over for recovery is significantly less than the disposed.

The exploring of the possibilities of using more recycled construction waste in road construction will increase their demand, which will lead to an increase in the amount of waste

utilised. This is an important step in solving the problems of landfilling and waste of mineral resources.

This paper reviews the possibilities of using recycled construction waste in road construction, the specific requirements for their incorporation in building materials and the technologies used for their recovery. The possibilities for increasing the % content of recycled materials in asphalt mixtures, for the construction of new roads with high and medium loads are considered.

## Characteristics of recycled construction waste that can be used in road construction

### Rock materials

The main sources of this waste are road and railway construction, as well as the processes of construction and rehabilitation of the technical infrastructure. Theoretically, over 90% of construction waste generated by road and railway construction can be recycled and/or recovered without further processing. The recycling of the rock materials is accomplished only by sieving and, optionally, by further crushing, i.e. by a very simple technology that allows for a high rate of recyclability and utilisation. The percentage of recyclability is directly related to the extent to which waste rock material is homogeneous and clean (unpolluted with soil, petroleum products, etc.).

Rock materials formed by repairs and demolition of buildings may be used as fractional material provided that their physical and chemical properties meet the requirements. However, this is rarely happening, because in most cases, waste is mixed with other materials detrimental to their qualitative performance.

### Concrete

The predominant process by which concrete waste is generated is the reconstruction and demolition of buildings and facilities. Very few of them can be reused, i.e. have a limited shelf life but, on the other hand, have a very high recycling potential. They contain rock and cement stone that are inert. The final product of the recycling of concrete waste is fractions of crushed material, similar to crushed stone of natural rock materials (Fig. 2).



Fig. 2. Recycled waste from concrete and reinforced concrete

These recycled fractions can be used for the same purposes as natural materials - from mound materials to asphalt aggregates.

Depending on the treatment processes of construction waste, recycled materials very often meet the requirements as well as the primary materials, i.e. their use in construction should not be restricted. They can be used mainly as filler for

drainage works, foundation for road construction (road bed and bottom base layer, soil stabilisation, temporary roads, etc.), car parks, garages, etc.

### Asphalt concrete

Asphalt-concrete waste is generated mainly in road construction, repair, rehabilitation and exploitation, as well as in the repair and reconstruction of streets, car parks, storage areas and the like. In the *Guidance for Construction Waste Management on the territory of the Republic of Bulgaria*, asphalt concrete is defined as a material consisting of aggregates (crushed stone and sand) and bituminous binder, with or without mineral and chemical additives. This is a material with a very high potential for recycling and re-use (Fig. 3). With rehabilitation only partially or completely replacing the top layers of the pavement (wear layer and binder), depending on the technology available, it is possible to recycle the old pavement on site using hot or cold recycling. The milling asphalt concrete material can also serve to stabilise the verges by treating it with polymeric materials. In all three cases, the type and quantity of the secondary materials should be complied with the technology. Laboratory tests are conducted on a case-by-case basis to determine the optimal percentage of the milling material in the preparation of the mixtures and determining the optimal quantity of stabilising additives.



Fig. 3. Recycled wastes from asphalt concrete

## Requirements for used recycled building materials in road construction

The use of recycled building materials is regulated by Regulation No 305 of the European Parliament and of the Council (EU No 305/2011, 2011). In the Republic of Bulgaria this Directive was introduced by the Ordinance on the Essential Requirements for Construction and Conformity Assessment of Construction Products (OERCCACP, SG, No. 106, 2006, amended SG No. 60, 2014).

Recycled construction waste may be used for stabilising verges, execution of sub-basic, basic and asphalt layers, if they meet the relevant physical and chemical indicators (Technical Specification of the Road Infrastructure Agency (TSRIA, 2014).

### Stabilised verges

The implementation of the stabilised verges may be carried out by milling asphalt concrete material and quarry waste or recycled crushed concrete 0.4mm, complying with the physical and chemical characteristics of the requirements set out in Table 1.

Table 1. Characteristics of unfractionated rock material used for the lower layer in the implementation of stabilised verges

№	Parameters	Normative test documents	Value based on traffic category (%)	
			Very light, light, medium	Heavy and very heavy
1.	Coefficient of Sundry grains	BSS EN 13242 + A1/NA	≥ 10	≥ 10
2.	Freeze-thaw resistance after 5 cycles of treatment with MgSO <sub>4</sub> , permissible mass loss of material, %	BSS EN 1367-2	declared value	≥ 35
3.	Resistance of degradation by Los Angeles coefficient, %	BSS EN 1097-2	≤ 50	≤ 40
4.	Content of fine fraction (particles < 0,063 mm), %	BSS EN 933-1	≤ 12	≤ 7
5.	Flat grains coefficient, %	BSS EN 933-3	≤ 50	≤ 40
6.	Shape factor, %	BSS EN 933-4	≤ 55	≤ 40
7.	Content of crushed or broken grains, %	BSS EN 933-5	-	≥ 50
8.	Content of fully rounded grains, %	BSS EN 933-5	≤ 50	≤ 30
9.	Sand equivalent, %	BSS EN 933-8	≥ 25	≥ 30
10.	Indicator of plasticity Plasticity indicator, %	Annex 17 <sup>1</sup>	≤ 6	≤ 4
11.	California Bearing Ratio (CBR)	BSS EN 13286-47	≥ 50	≥ 80
12.	Content of total sulphur aggregates different than air-cooled blast furnace slag, %	BSS EN 1744-1	≤ 1	≤ 1

When performing the stabilisation in each particular case, laboratory tests are held to determine the optimal percentage ratio of the milling material and the new rock material and to determine the optimal amount of stabilising additives.

### Underlay layer

An underlying layer is performed when the earth bed of the pavement consists of associated soils (mixtures of soils and grain materials), fine sand. Sand, gravel, ballast, crushed stone and inert materials from recycled waste conforming to BSS EN 13242 + A1/NA, which have strong and frost-resistant grains and meet the requirements set out in Table 2, are used for its construction. The grain size of the material should be less than or equal to one second of the thickness of the applied layer.

### Base layers of rock materials, unprocessed with binders

Recycled rock materials used to build base layers unprocessed with binders must comply with the requirements of BSS EN 13242 + A1/NA. The basic requirement is that the material is clean and free from organic impurities, clay, binding particles and other inappropriate materials. According to the *Technical Specification*, the use of recycled rock materials in the construction of highway and 1<sup>st</sup> class roads is prohibited. For the construction of the remaining second class, third class and temporary roads, recycled rock materials are used that meet the requirements set out in Table 3.

Table 2. Characteristics of building materials used for the underlying layer

№	Parameters	Normative test documents	Value based on traffic category (%)	
			Very light, light, medium	Heavy and very heavy
1.	Maximum grain size (mm)	BSS EN 933-1	≤ 80	≤ 80
2.	Content of fine fraction (particles < 0,063 mm), %	BSS EN 933-1	declared value	≤ 12
3.	Plasticity indicator, %	"Road design standards", Annex № 17	≤ 6	≤ 6
4.	Freeze-thaw resistance after 5 cycles of treatment with MgSO <sub>4</sub> Permissible mass loss of material, %	BSS EN 1367-2	declared value	≤ 35
5.	Content of fully rounded grains, %	BSS EN 933-5	≤ 70	≤ 50
6.	California Bearing Ratio (CBR)	BSS EN 13286-47	≥ 20	≥ 30
7.	Content of total sulphur aggregates different than air-cooled blast furnace slag, %	BSS EN 1744-1	≤ 1	≤ 1
	- Air-cooled blast-furnace slag, %		≤ 2	≤ 2
8.	Content of water-soluble sulphates in recycled rock materials%	BSS EN 1744-1	-	≤ 1.3
9.	Coefficient of filtration for compacted material, for a drainage layer m/h	BSS 8497	≥ 2 m/ 24 h	≥ 2 m/ 24 h

### Asphalt layers

Nowadays, asphalt is the main building material in road construction. The asphalt mixture consists of sand, rock materials and binder.

For asphalt mixtures intended for a wearing layer for heavy and very heavy traffic, the use of recycled asphalt is not allowed.

For asphalt mixtures intended for a wearing layer for medium, light and very light traffic, it is allowed to include recycled asphalt in their composition, but not more than 10%.

For asphalt mixtures intended for the lower layer of the pavement and the base layer it is allowed to include in their composition recycled asphalt, but not more than 20%.

Recycled asphalt must comply with the requirements of BSS EN 13108-8-1:2006 and all materials must be tested in laboratory conditions and approved prior to their use for the production of asphalt mixtures.

For preparing an asphalt mixture, depending on its purpose, a working recipe is developed, which specifies the physical and chemical characteristics of the mineral materials and the binder, as well as their ratio. The recipe contains the particle size curve showing the single percentage of each sieve, the percentage of each material used in the mixture, and the mixing and compaction temperature.

<sup>1</sup> Annex 17 of Ordinance No RD-02-20-2, 2018. Roads Design

Table 3. Characteristics of recycled rock materials not treated with binders used for base layers

№	Parameters	Normative test documents	Value based on traffic category (%)	
			Very light, light, medium	Very light, light, medium
1.	Freeze-thaw resistance after 5 cycles of treatment with MgSO <sub>4</sub> , permissible mass loss of material, %	BSS EN 1367-2	≤ 35	≤ 25
2.	Resistance of Degradation by Los Angelis coefficient, %	BSS EN 1097-2	≤ 50	≤ 45
3.	Content of fine fraction (particles < 0,063 mm), %	BSS EN 933-1	≤ 16	≤ 10
4.	Flat grains coefficient, %	BSS EN 933-3	≤ 50	≤ 40
5.	Shape factor, %	BSS EN 933-4	≤ 55	≤ 40
6.	Content of crushed or broken grains, %	BSS EN 933-5	-	≥ 50
7.	Content of fully rounded grains, %	BSS EN 933-5	≤ 50	≤ 30
8.	Sand equivalent, %	BSS EN 933-8	≥ 25	≥ 30
9.	Plasticity indicator, %	Annex 17 <sup>2</sup>	≤ 6	≤ 6
10.	California Bearing Ratio (CBR)	BSS EN 13286-47	≥ 50	≥ 80
11.	Content of total sulphur aggregates different than air-cooled blast furnace slag, %	BSS EN 1744-1	≤ 1	≤ 1
	Air-cooled blast-furnace slag		≤ 2	≤ 2
12.	Content of water-soluble sulphates in recycled rock materials, %	BSS EN 1744-1	-	≤ 1.3

## Cold and hot asphalt recycling technologies

Traditional methods of rehabilitation of roads are costly and their implementation time is prolonged and to a great extent dependent on weather conditions. They most often include complete milling of the damaged pavement or intersections thereof, and the milling material must then be removed and transported to waste recycling sites for construction waste landfill. The delivery and installation of new materials for the restoration of the roadway is the next stage.

The alternative solution is the use of cold and hot recycling technologies that allow the removed asphalt layer to be recycled and placed on-site.

### Cold on-site recycling

Cold recycling is a road rehabilitation method that allows 100% use of the layers of existing damaged road pavement, making it a major building material. With appropriate mechanisation, the unsuitable asphalt concrete layer is involved in the construction of a reliable high-strength base for the new pavement without further heat processing.

This type of repair technology is appropriate and economically feasible to extend the service life of the road construction.

Specialised machines (recyclers) designed to process structural layers of certain thicknesses are used. For one

working cycle, only a part of the road is closed, which is a great advantage for the transport traffic.

Depending on the type and thickness of the processed layer, cold recycling can be divided into three types: deep, thin and recycling of roads with surface layers not processed with binders.

To improve the grain size of the mixture, new materials (within 2-10%) and stabilisers (hydraulic binders /3-6%, bitumen emulsion / 3-6% / or penobitumen 2-5%) are added.

Before the cold recycling is done, an analysis of the state of the existing pavement is carried out, which requires preliminary research to determine the depth at which the recycling will take place, the type of material to be added to improve the grain size as well as the type of stabilisers and their quantity.

*Activities related to cold recycling on-site technology include:*

1) milling of the material from the layers of the existing road surface that are to be recycled;

2) changing the grain size of the recycled material by adding a new mineral material (sand or quarry waste sterile, most often 0.5 or 0.10 mm);

3) mixing the milled material with the required amount of water and stabilisers until complete homogenisation;

4) profiling and compaction of the mixture until a new layer of pavement is obtained.

The technology can be applied for rehabilitation of all roads, including highways. Any material that complies with the technical specification can be used as a building material for the relevant layer.

### Hot on-site recycling

If recycling of the asphalt concrete surface layers is required, hot recycling technology can be used as an alternative to the cold recycling. The principle is similar to cold recycling, but it is important to note some specifications. In the case of hot recycling of asphalt pavements, the bituminous properties of the bitumen are largely preserved in the asphalt concrete composition, even though in the operation of the roads it is in solid state. This allows re-heating of the existing asphalt concrete pavement and with small additional quantities of new bitumen, to achieve indicators of recycled asphalt concrete similar to newly produced one.

Prior to performing hot recycling, an analysis of the condition of the existing asphalt pavement is done, which requires preliminary research.

The results of this research determine the depth at which the hot recycling will take place, the type of mineral material to be added to improve the grain size and physical and mechanical characteristics of the mixture, as well as the quantity of binder and/or the fresh asphalt mixture.

The particle size composition of the hot-recycled mixture must comply with the requirements of BSS EN 13108-1/NA for the type of asphalt mixture with which the old layer is implemented.

*The hot on-site recycling process consists of four steps:*

- 1) Softening the road surface by heating;
- 2) Mechanical loosening of the material in the upper layer;
- 3) Mixing the material with a binder and/or a mineral substance and/or a fresh asphalt mixture;
- 4) Laying the recycled mixture as a new road pavement.

<sup>2</sup> Annex 17 of Ordinance No RD-02-20-2, 2018, Roads Design

Road bitumen category B 50-70 or polymer modified bitumen category PmB 45-85/65 is used as a binder in the process of hot on-site recycling.

The technology allows restoration of the surface characteristics of the road pavement and improvement of the physical and mechanical properties of the material from the upper asphalt layer.

Traditional hot asphalt mixes are produced at a temperature of about 170°C, whereas hot asphalt mix technologies allow the production temperature to be around 100°C. This reduces to some extent the energy and transport costs.

Also, with the use of the material from the existing damaged top asphalt layer, savings in building material and savings in transport costs are achieved.

### Opportunities to increase % content of recycled material in asphalt mixtures

According to recent information there are numerous examples on the use of recycled construction materials in road construction in different countries in Europe and the USA (Abukhettala, 2016; Freire et al., 2013; Schimmoller et al., 2000). There are restrictions on the use of recycled materials in the construction of the main, lower and wearable road layers for the high-load roads in Bulgaria.

To increase the percentage of recycled content in the preparation of asphalt mixtures, an investigation and evaluation of the economic resources and the costs required for the construction of 1 km of the main surface and bottom layer of the pavement was carried out. Table 4 calculates the average amount of asphalt mixtures needed for the construction of 1 km of pavement on a highway, first-class and second-class roads. Quantitative accounts for determining the amount of asphalt mixtures for each layer and type of roads are made in accordance with the requirements and specifications for road design (Ordinance RD-02-20-2, 2018).

Table 4. Resource and economic costs needed for the construction of 1 km of pavement of main and bottom layer of the coating (bender)

№	Parameters	Construction of 1 km highway		Construction of 1 km first-class road		Construction of 1 km second-class road	
		Main layer 8 cm	Bottom layer 6 cm	Main layer 6 cm	Bottom layer 6 cm	Main layer 5 cm	Bottom layer 5 cm
1	Average amount of asphalt mixes (t)	3870	2967	2025	2070	1102	1127
2	Conventional asphalt mixtures, average price (BGN)	390870	344172	204525	240120	111302	130732
3	Asphalt mixtures with 20% content of recycled materials, average price (BGN)	367650	281865	192375	196650	104690	107065
4	Difference (3 - 4) in BGN	23220	62307	12150	43470	6612	23667

The average quantity of asphalt mixtures (A) needed for 1 km of pavement is determined using the formula:

$$A = V * P \quad (1)$$

where P is the volume weight of the asphalt mixture intended for the respective layer. For asphalt mixtures intended for the lower layer it is 2.3 g/cm<sup>3</sup>, while for the main layer it consists of 2.25 g/cm<sup>3</sup>. V is the volume of the mixture to be determined by the formula:

$$V = a * b * h \quad (2)$$

where a - the length of the intersection, b - the width of the lane, h - the thickness of the layer.

Average prices of conventional asphalt mixes for building the respective layers are calculated using the formula:

$$C_k = A * c_1 \text{ and } C_p = A * c_2 \quad (3)$$

where A is the average quantity of asphalt mixtures,

c<sub>1</sub> – the average price of conventional asphalt mixes for building a base layer is BGN 101/ ton;

c<sub>2</sub> – the average price of conventional asphalt mixes for building a lower layer of coating (bender) is BGN 116/ton;

Average prices when using asphalt mixtures with 20% content of recycled materials are calculated using the formula:

$$C_p = A * c_3 \quad (4)$$

where A is the average amount of asphalt mixtures, and c<sub>3</sub> – the average price asphalt mixes with 20% recycled materials for the main and bottom layer of the coating is BGN 95/ton.

As a source for the prices of asphalt mixtures, price quotes from inquiries sent to companies, which recycle and produce building materials that wished to remain anonymous, were used.

Cost analysis has shown that the use of 20% recycled materials in asphalt mixtures for the construction of main and lower layers saves more than BGN 85000 for highways, BGN 55000 for first class roads and BGN 30000 for second class roads.

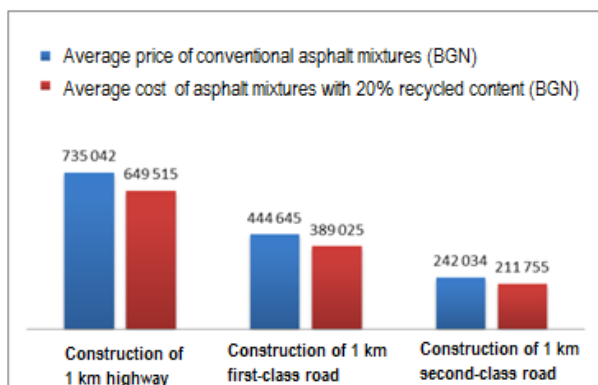


**Fig. 4. Comparative analysis of material costs for construction of 1 km main and bottom layer using conventional asphalt mixtures and mixtures with 20% content of recycled materials**

Restriction of used recycled materials in the construction of new road pavements is dictated by their physical and chemical properties, influencing the quality indicators of the materials. One of the factors restricting their use is their contamination with other substances. Pollutants reduce quality indicators, may react with some of the impurities, or alter the grain size of the materials. This in turn affects the potential of their re-use.

To solve this problem, it is important to apply selective demolition /deconstruction/ and separate collection and storage of the construction waste. This is the first and most important requirement for obtaining high quality of the waste fractions and for increasing the percentage content of recycled construction materials incorporated in asphalt mixtures for the construction of new roads. This increase will positively affect the financial factors by reducing the cost of materials and environmental factors, by reducing the amounts of landfilled waste and the amount of natural resources used.

## Conclusions

In summary, reuse, recycling and recovery of construction waste is an ideal opportunity to reduce the mineral and energy resources used in the conditions of developing road infrastructure on the territory of the Republic of Bulgaria.

Road construction offers great opportunities for re-use and utilisation of recycled construction waste, both in the construction of new routes and in the reconstruction and rehabilitation of existing ones. Applying the technologies discussed in the article allows for reduced transport, energy

and resource costs. Trends in temperature reduction in the production of asphalt mixes for road rehabilitation have shown new possibilities for its use and an increase in the number of technological solutions for the production of asphalt mixtures from recycled construction materials available on the market.

In conclusion, it is important to note that selective demolition and separate collection of construction waste can lead to an increase in the % content of recycled construction materials in the production of asphalt mixtures for building of new road pavements. This in turn will have a positive impact on both the financial side, reducing the cost of building materials and waste disposal, as well as the environment by reducing the amount of landfilled waste and natural resources used.

## References

- Abukhettala, M. 2016. Use of Recycled Materials in Road Construction. – *2<sup>nd</sup> International Conference on Civil, Structural and Transportation Engineering (ICCSTE'16)*, Ottawa, Canada, May 5–6, 2016, Paper No. 138.
- Freire, A. C., J. Neves, A. J. Roque et al. 2013. Use of construction and demolition recycled materials (C&Drm) in road pavements validated on experimental test sections. – *2<sup>nd</sup> International Conference – WASTES 2013: Solutions, Treatments and Opportunities*, 11–13 September 2013, Braga, Portugal, 91–96.
- National Statistical Institute (NSI).
- Ordinance on the Essential Requirements for Construction and Conformity Assessment of Construction Products (OERCCACP), (Prom. SG, No. 106 of 27 December 2006, amd. SG No. 60 of 22 July 2014).
- Ordinance No. RD-02-20-2 of 28 August 2018 For road design (Prom. SG, No. 79 of 25 September 2019, corr. SG. No. 90 of 30 October 2018).
- Regulation (EU) No 305/2011 of the European Parliament and of the Council of 9 March 2011 laying down harmonised conditions for the marketing of construction products.
- Schimmoller, V. E., K. Holtz, T. T. Eighmy et al. 2000. *Recycled Materials in European Highway Environments Uses, Technologies, and Policies*. – Federal Highway Administration, U.S. Department of Transportation.
- Technical Specification of the Road Infrastructure Agency (TSRIA) 2014.
- Waste Management Act (WMA) (Prom. SG, No. 53 of 13 July 2012, amd. and suppl. SG, No. 1 of 3 January 2019).

## BIOLEACHING OF COPPER ORES BY MEANS OF DIFFERENT CHEMOLITHOTROPHIC BACTERIA AND ARCHAEA

**Marina Nicolova, Irena Spasova, Plamen Georgiev, Stoyan Groudev**

*University of Mining and Geology "St. Ivan Rilski", 1700 Sofia; mnikola@mgu.bg*

**ABSTRACT.** Samples of copper ores from some essential Bulgarian deposits were subjected to bioleaching by means of different microorganisms (bacteria and archaea) isolated from these deposits. It was found that the isolated microorganisms were able to leach efficiently copper from the copper ores present in the deposits. High copper extractions (over 80 and in some cases over 90%) were achieved from all copper ores tested in these investigations by means of the mesophilic and moderate thermophilic bacteria at their optimum temperatures (about 35 and 50°C, respectively) as well as by the extreme thermophilic archaea at temperatures higher than 75°C.

**Keywords:** copper ores, leaching, chemolithotrophs, archaea

### БИОЛОГИЧНО ИЗВЛИЧАНЕ НА МЕДНИ РУДИ ПОСРЕДСТВОМ РАЗЛИЧНИ ХЕМОЛИТОТРОФНИ БАКТЕРИИ И АРХЕИ

**Марина Николова, Ирена Спасова, Пламен Георгиев, Стоян Грудев**

*Минно геоложки университет "Св. Иван Рилски", 1700 София*

**РЕЗЮМЕ.** Проби от медни руди от някои основни български находища бяха подложени на биологично излугване с помощта на различни микроорганизми (бактерии и археи), изолирани от тези находища. Установено бе, че изолираните микроорганизми са способни ефективно да извличат мед от медните руди, присъстващи в находищата. При всички медни руди, използвани в това изследване с помощта на мезофилни и умерени термофилни бактерии, (при оптималните им температури съответно около 35 и 50°C), както и с крайни термофилни археи (при температури над 75°C) е постигнато високо извличане на медта (над 80 и в някои случаи над 90%).

**Ключови думи:** медни руди, излугване, хемолитотрофи, археи

### Introduction

The ability of some chemolithotrophic bacteria and archaea to extract valuable metals from different mineral substrates (mainly sulphidic and mixed ores, concentrates and mineral wastes) is largely applied in several countries rich in such natural resources and/or industrial products. The first studies in this area in South Europe started in 1967 and within a relatively short period of time covered a large number of problems: the data about microflora of the different mineral deposits (such as ores of non-ferrous metals, uranium and gold; the investigations of the biochemistry and genetics of the microorganisms participating in the transformations of different mineral substrates such as coal, kaolin, oil, quartz sands, etc.; bioleaching of copper, other non-ferrous metals and uranium by means of heap, dump and in situ techniques; pre-treatment of gold and silver-bearing sulphide concentrates and ores by means of chemolithotrophic bacteria and archaea to expose these precious metals; combined microbial and chemical leaching of the precious metals from the above-mentioned pretreated ores and concentrates, as well as from oxide ores; microbial removal of iron from quartz and kaolin, of sulphur from coal. Silicon from low-grade bauxites, and of phosphorus from iron ores; improvement of the ceramic properties of kaolin; microbial enhanced oil recovery; electricity production by means of microbial fuel cells.

The processing mentioned above is connected with the participation of a large number of microorganisms, mainly of chemolithotrophic bacteria and archaea. It is essential to mention that even the well-studied bioleaching of copper from low-grade ores is connected with the participation of several microorganisms related to different taxonomic species. At the same time, it must be noted that even microbial strains related to one and the same taxonomic species can differ considerably from each other with respect to the level of their leaching ability and the optimum conditions for manifesting their ability.

The present paper contains some data about the microflora participation in the bioleaching of copper from the low-grade ores in some of the Bulgarian deposits subjected to such treatment.

### Materials and Methods

Samples from some of the Bulgarian copper deposits connected with the application of bioleaching of the relevant ores were used in this investigation (Table 1). Some of these samples were inhabited by the local representatives of the microflora participating in the spontaneous and/or industrial bioleaching of the relevant ores.

Table 1. Ore samples used in this investigation

Ore sample	Source of the ore sample
№ 1	Low grade copper ore from the Vlaikovvrah deposit, with 0.53% Cu, 6.2% S, 7.3% Fe; the chalcopyrite was the main copper-bearing mineral, but the pyrite was the main sulphidic mineral in this ore
№ 2	Mixed oxide-sulphidic copper ore also from the Vlaikovvrah deposit, with 0.32% Cu, 3.0% S, 4.8% Fe; several copper-bearing oxides (cuprite, tenorite, chalcocite) and sulphides (mainly covellite and chalcopyrite) were present
№ 3	Sulphidic copper ore from the Elshitzza deposit, with 0.55% Cu, 7.3% S, 6.4% Fe; the chalcopyrite, chalcocite and covellite were the main copper-bearing minerals
№ 4	Copper-pyrite ore from the Chelopetsh deposit, with 0.62% Cu, 9.6% S, 8.2% Fe; the tenantite, chalcopyrite and lusonite were the main copper-bearing minerals in the ore which contained about 21% pyrite
№ 5	Copper-molibdenic ore from Elatzite deposit, with 0.36% Cu, 0.55% S, 1.95% Fe, 0.005% molibdenite; the chalcopyrite, was the main copper-bearing mineral
№ 6	Mixed copper ore from the Tsar Assen deposit, with 0.29% Cu, 1.16% S, 3.2% Fe; the chalcopyrite and malachite were the main copper-bearing minerals

Samples from these ores were subjected to bioleaching experiments performed by the shake-flask technique and by leaching in percolation columns. The bioleaching in flasks was performed by using from 5 to 20 g of ore with a particle size of minus 200 microns and 100 ml of the 9K nutrient medium used as a leach solution in Erlenmeyer flasks of 350 ml each. The duration of leaching was up to 14 days (336 hours) at different temperatures (from 10 to 50°C).

The bioleaching of the ore samples was performed also in plastic cylindrical columns. Each of the columns was 220 cm high, with a diameter of 105 mm and contained 30 kg of the ore, with a particle size of minus 10 mm. The duration of leaching was 300 days at temperatures varying from 10-14 to 18-28°C.

Elemental analysis was done by atomic adsorption spectrometry and inductively coupled plasma spectrometry. The isolation, identification and enumeration of microorganisms were carried out by means of the classical physiological and biochemical tests (Karavaiko et al., 1988) and by the molecular PCR methods (Sanz and Köchling, 2007; Escobar et al., 2008).

## Results and Discussion

The microflora of the six copper ores deposits used in this study was dominated by acidophilic chemolithotrophic bacteria related to the species *Acidithiobacillus ferrooxidans*, *At. thiooxidans*, *At. acidophilus* and *Leptospirillum ferrooxidans*. The bacteria from the species *At. ferrooxidans* possessed both

iron and sulphuroxidising abilities and were the prevalent microorganisms in most copper deposits studied in this investigation. Their numbers in some rich-in-pyrite zones extended  $10^8$  cells/g ore. Regardless of the ability of these bacteria to oxidise the ferrous iron and the different forms of sulphur (the sulphidic, elemental and sulphitic) to sulphate, the mixed cultures of these bacteria with some strains of the typical sulphur-oxidiser *At. thiooxidans* were the most efficient during the leaching of sulphide minerals.

Data about the microbial leaching of copper from the ores used in this study are shown in Tables 2-5.

Table 2. Bioleaching of the copper ores by the shake-flasks technique using mesophilic bacteria

Ore samples	Number of the strains	Cu extraction, %
№ 1	6	68.0 – 81.5
№ 2	4	73.5 – 92.3
№ 3	5	64.4 – 79.0
№ 4	4	61.7 – 77.0
№ 5	6	60.8 – 84.2
№ 6	5	77.0 – 93.2

Leaching conditions: 20 g from each ore with a particle size minus 200 microns were leached in 100 ml 9K nutrient medium in flasks of 300 volume for 10 days (240 hours) at 35°C.

It was found that the different chemolithotrophs even such related to one and the same taxonomic species, can differ considerably from each other with respect to this ability. The most efficient oxidisers were some strains of extreme thermophilic archaea of the species *Sulfolobus metallicus* and *Thermoplasma acidophilum* at 86°C but at relatively low pulp densities (up to 6-8%). Other strains from these species and of the *Metallosphaera sedula* were the most efficient at relatively higher pulp densities (10-15%) at 75°C.

Table 3. Bioleaching of the ore samples in plastic columns

Ore samples	Source of the ore	Cu extraction, %
№ 1	Vlaikovvrah	77.4
№ 2	Vlaikovvrah	84.2
№ 3	Elshitzza	80.6
№ 4	Chelopetch	79.0
№ 5	Elatzite	82.8
№ 6	Tsar Assen	86.4

Each column was 220 cm high, with an internal diameter of 105 mm, containing 30 kg of ore each, with a particle size of minus 10 mm; duration of leaching 300 days at 21-23°C.

Table 4. Bioleaching of the copper ores by the shake flasks technique using moderate thermophilic bacteria

Ore samples	Number of the strains	Cu extraction, %
№ 1	4	77.4 – 86.4
№ 2	5	93.6 – 95.0
№ 3	5	75.2 – 84.0
№ 4	4	73.0 – 81.5
№ 5	6	92.5 – 96.1
№ 6	4	93.0 – 97.0

*Leaching conditions:* The same as these mentioned in Table 2 but at 50°C.

Table 5. *Bioleaching of the copper ores by the shake flasks technique using extreme thermophilic archaea*

Ore samples	Number of the strains	Cu extraction, %
№ 1	5	73.0 – 84.6
№ 2	3	82.4 – 91.8
№ 3	4	70.9 – 82.8
№ 4	3	68.0 – 79.0
№ 5	5	84.0 – 86.4
№ 6	4	77.6 – 84.0

*Leaching conditions:* The same as these mentioned in Table 2 but at 75°C and 10% pulp density.

The study of the different oxidative abilities of strains related to one and the same taxonomic species is essential for the efficient selection of microorganisms suitable for the biotechnological treatment of the relevant mineral substrates. At the same time, it is also essential to evaluate correctly the economical values of the real technological processes connected with the microbial participation.

**Acknowledgements:** The authors express their gratitude to the University of Mining and Geology for the financial support provided for this study (Project GPF 223/2019).

## References

- Dopson, M., D. B. Johnson. 2012. Biodiversity metabolism and application of acidophilic sulphur-metabolising microorganisms. – *Environ. Microbiol.*, 12, 2620–2631.
- Escobar, B., K. Bustos, G. Morales, O. Salazar. 2008. Rapid and specific detection of *Acidithiobacillusferrooxidans* and *Leptospirillumferrooxidans* by PCR. – *Hydrometallurgy*, 92, 102–106.
- Georgiev, P., M. Nicolova, I. Spasova, A. Lazarova, S. Groudev. 2017. Leaching of valuable metals from copper slag by means of chemolithotrophic archaea and bacteria, L. – *Mining and Geological Sciences*, 60, 2, 127–130.
- Hallberg, K. B., D. B. Johnson. 2001. Biodiversity of acidophilic microorganisms. – *Advances of Applied Microbiology*, 49, 37–84.
- Karavaiko, G. I., G. Rossi, A. D. Agate, S. N. Groudev, Z. A. Avakyan (Eds.). 1988. *Biogeochemistry of Metals. Manual*. GKNT Centre for International Projects, Moscow.
- Sanz, J. L., T. Köchling. 2007. Molecular biology techniques used in wastewater treatment: An overview. – *Process Biochem.*, 42, 119–133.

## INVESTIGATION OF THE POSSIBILITY FOR EXTRACTING IONS POSSESSING A CORROSIVE ACTION ON CONSTRUCTION MATERIALS BY WASHING SOLID INCLUSIONS IN A CLAYEY OVERBURDEN

*Marinela Panayotova, Lubomir Djerahov, Gospodinka Gicheva*

*University of Mining and Geology "St. Ivan Rilski", 1700 Sofia; marichim@mgu.bg*

**ABSTRACT.** Considerable amounts of solid phase material of different composition and physical and -mechanical properties are disposed of during the coal extraction. In fulfilling the tasks of the circular economy, some of this material, after proper washing, could be utilised in road construction. This paper presents the results from measurement of integral parameters and from chemical composition analysis of the waters, formed as a result of laboratory experiments by simulated rain leaching and by washing of solid inclusions in clayey overburden from mining activities in Maritsa East Mines Ltd. Based on the results obtained, the following issues are discussed: the possible impact on the environment in case of the material leaching by normal and acid rain; the possibility of extraction in the liquid phase of ions, possessing a corrosive action towards construction materials, at contact of raw and washed materials with water; the possibility for washing water re-use.

**Keywords:** solid inclusions in coal mine overburden, acid rain impact, washing water recycling, carbonates' leaching

### ИЗСЛЕДВАНЕ НА ВЪЗМОЖНОСТТА ЗА ИЗВЛИЧАНЕ НА ЙОНИ, ПРИТЕЖАВАЩИ КОРОЗИОННО-АГРЕСИВНО ДЕЙСТВИЕ СПРЯМО СТРОИТЕЛНИ МАТЕРИАЛИ, ПРИ ПРОМИВАНЕ НА ТВЪРДИ ВКЛЮЧЕНИЯ В ГЛИНЕСТА ОТКРИВКА

*Маринела Панайотова, Любомир Джерахов, Господинка Гичева*

*Минно-геоложки университет "Св. Иван Рилски", 1700 София*

**РЕЗЮМЕ.** При добива на въглища по открит способ се депонират значителни количества твърдофазен материал с различен състав и физико-механични свойства. В изпълнение на задачите на кръговата икономика, част от този материал, след съответно промиване, би могла да се оползотвори в пътното строителство. Настоящата работа представя данни от определяне на интегрални показатели и на химичен състав на водите, формирани в резултат на лабораторни експерименти за моделно излужване от валежи и по промиване на различни твърди включения в глинеста откритка от въгледобива в мини "Марица-изток" ЕАД. На базата на получените резултати са дискутирани: възможното въздействие върху околната среда при евентуално излужване на материала от нормални и кисели валежи; възможността за извличане във водата на йони, притежаващи корозионно-агресивно действие спрямо строителни материали, от непромити и промити твърди включения при контакта им с вода; възможността за обратно използване на промивната вода.

**Ключови думи:** твърди включения в откритка на въглищни мини, въздействие на киселинен дъжд, рециклиране на промивни води, излужване на карбонати

### Introduction

Opencast mining releases huge amount of mining wastes to the land surface as overburden dump materials. Coal mining wastes are one of the major global bulk waste streams. Sometimes the removed overburden occupies large areas of fertile land and leads to soil quality degradation. When they are not properly reclaimed, the dump materials can be a source of fine particulates highly prone to blowing by wind. They can spread over the surrounding fertile land and flora, disturbing their quality and abstaining the growth of fresh leaves. Occurrence of sulphides and/or other geochemically instable materials in the waste rock could result in acid or neutral rock drainage that could make this material an environmental issue. Due to its high acidity the acid rock drainage mobilises heavy metals and thus, it can contaminate the nearby water bodies. The neutral or alkaline rock drainage may also have high pollution potential due to the elevated salinity (Szczerpańska-

Plewa et al., 2010). In addition, some heavy metals can become mobile in neutral pH conditions.

Increase in production capacity of opencast coal mines is achieved by deployment of increasingly larger capacity haul trucks that require appropriately designed and well maintained haul roads. Use of the material representing solid inclusions (after its washing) in the overburden in haul roads or as partial replacement for fine aggregates in other roads will enhance the waste utilisation and minimisation and will also reduce environmental problems. Recently different attempts have been made in this direction (Mary et al., 2016; Mallick et al., 2017).

The objectives of the present study can be summarised as follows: (a) monitoring in laboratory of the possibility for harmful substances leaching from the deposited material as a result of precipitation; (b) identification of chemical indicators related to the possibility of using this material in road construction; (c) exploring the practicability of recycling of the washing water.

## Materials and Methods

Samples of materials representing solid inclusions in the coal mine overburden were collected and kindly supplied by the colleagues from the "Department of Opencast Mining of Mineral Deposits and Blasting Activities" (DOMMDBA). Material milling and separation of the needed size fractions was carried out with the help of colleagues from the "Department of Processing and Recycling of Mineral Resources".

Column leaching tests, aimed at monitoring the possibility of leaching harmful substances from the deposited material as a result of rainfall, were carried out in plastic columns (40 x 280 mm) with perforated bottom. One kg of the tested material was placed in each of the two columns. The material in the first column was periodically sprinkled with distilled water imitating pure rain. The material in the second column was periodically sprinkled with acidified distilled water (pH 2, achieved by addition of HNO<sub>3</sub> – p.a.) imitating extreme acid rain. The lower pH compared to the most common acid rain was chosen to speed up the processes. The volume of water/acidified water used was 1600 cm<sup>3</sup>. Each test was run to provide leaching under unsaturated conditions. The material in the columns was flushed two times per day with portions of 200 cm<sup>3</sup>. The leachates permeated through the columns were collected and analysed. Electrical conductivity (EC), the pH, and oxidation reduction potential (Eh) were measured by using WTW Multi 3400i measuring instrument and corresponding electrodes. Studies on the Maritza East region have shown higher content of many different heavy metals in the coal, coaly clay and coal ash than the Clarke values (Kostova, 2005). Among them are lead, cadmium, copper, zinc, and iron, chosen by us as indicators of eventual leaching and pollution, since the first four usually do not form precipitates of hydroxides and are mobile under the measured pH values and iron presence can be an indication for the sulphides' leaching. The heavy metals were determined by ICP-OES analysis (method CNILG BM-1:2014, point II). The column leaching test was conducted in eight cycles. The number of cycles was based on measurements of physicochemical parameters of leachate and thus it was obtained that practically the steady state is reached in five cycles. In addition, this number of cycles is in accordance with the usually needed minimum number (Kusuma et al., 2012).

Chemical indicators that have been investigated in relation to evaluating the possibility of using this material in road construction are total iron and total sulphur, water soluble chlorides, water soluble sulphates and material's water solubility. Total iron and total sulphur were determined by the Central laboratory "Geochemistry" at the University of Mining and Geology, Sofia by using the laboratory method CNILG BM-1:2014, point III. The other chemical indicators were determined by following the procedures described by the BDS EN 1744-1:2009+A1:2012. Briefly, for determining the water soluble chloride salts clause 9 of the standard was applied – the use of Mohr's method. The aggregate test portion was extracted at room temperature for 60 min by stirring at solid to water ratio = 1:1. The chloride in the supernatant after settling was titrated with silver nitrate using potassium chromate as an indicator. For determining the water soluble sulphate salts clause 10.1 was used, modified by us. The aggregate test portion was extracted at room temperature for 24 hours by stirring at solid to water ratio = 1:2. The modification consisted

in applying the turbidimetry for determining the sulphate concentration in the supernatant after settling, since the expected sulphate concentration (based on the data about the total sulphur content of the material) was too low to apply correctly the BaSO<sub>4</sub> precipitation method. To determine the water solubility of the material clause 16 of the standard was used. Briefly, 500 g of the material was dried at 110°C, weighted and placed in a contact with distilled water at room temperature for 24 hours by stirring and solid to water ratio = 1 : 2. Then, after solids' settling, the clear water was separated from the solid. The latter was dried at 110°C till constant weigh. The difference between the first and the second weight divided by the first weight and multiplied by 100 gives the water solubility of the material in %.

To explore the possibility of the washing water recycling, a portion of the studied material was placed in contact with tap water at solid to water ratio = 1 : 8 and stirred mechanically for 4 hours. The mixture was left for solids' settling and clarified water was collected for analysis and further use as recycled water. The procedure was repeated totally 10 times, each time with new portion of material and using the recycled clarified water. Conductivity, pH and Eh values were determined each time in the clarified water. Some water macro-components were determined after 1<sup>st</sup>, 3<sup>rd</sup>, 6<sup>th</sup>, and 10<sup>th</sup> cycle of washing, as well as for the used tap water. Concentrations of lead, cadmium, copper, zinc, and iron were measured in the clarified water after the 10<sup>th</sup> use. In the Deval washing experiments the studied material was placed in the machine at solid to tap water ratio = 1 : 5, solid to abrasive spheres ratio = 1 : 9, mixed for 3 hours at totally 12000 revolutions and then left till 24<sup>th</sup> hour. Samples from the clarified water (referred to as Deval washing) were supplied by the colleagues from the DOMMDBA for different analyses, as well as samples from the 1<sup>st</sup> washing of the material after it was taken out from the Deval machine.

The mineralogical composition of the raw unwashed material, 10-times washed material, fine material removed by Deval washing and of material subjected to spraying with acidic water was determined by XRD (BRUKER D2 Phaser, Cu/Ni radiation,  $\lambda=1.54184$  Å, 30 kV, 10 mA, 2 theta – 5-70, time 1720 s). The analysis was done by the laboratory "X-Ray diffraction" at the University of Mining and Geology.

## Results and discussion

### Analysis of solid samples

The analysis of the raw solid sample showed total iron (Fe) content of 0.450 wt.% and total sulphur (S) content of 0.047 wt.%. These values are considerably lower compared to the pyrite FeS<sub>2</sub> contents of 1-5% capable to form an acid mine drainage (Tiwary, 2001). The data from the mineralogical characterisation of the samples are presented in Figure 1. The material consists mainly of calcite, dolomite, quartz, illite and kaolinite, as it can be seen in Figure 1. Calcite is the dominant mineral in the raw unwashed sample, 10 times washed, and the fine material removed by washing in Deval machine. Dolomite is the main material in the sample that was subjected to "acid rain".

**Column leaching experiments**

Data on the conductivity, pH and Eh values measured for samples from these experiments are presented in Figs. 2-4 and data for the concentrations of some heavy metals are given in Table 1. Data presented in Figure 2 show that practically a steady state is achieved relatively fast.

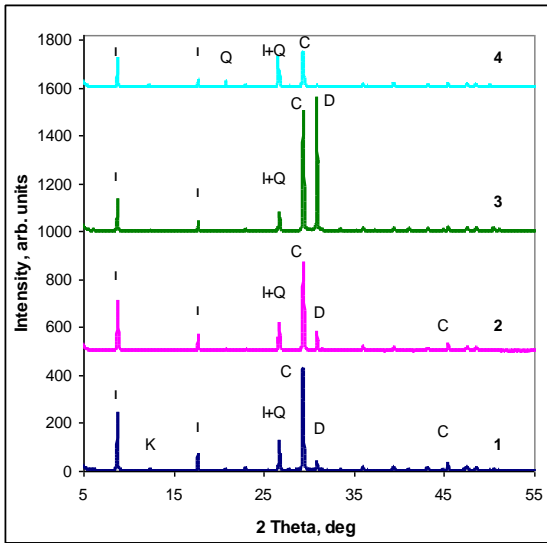


Fig. 1. X-Ray data: 1 – raw unwashed material, 2 – 10-times washed material, 3 – material subjected to spraying with acidic water, 4 – fine material removed by Deval washing; I – illite, K – kaolinite, Q – quartz, C – calcite, D – dolomite

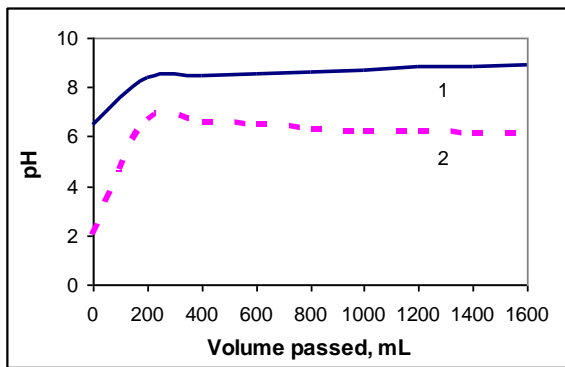


Fig. 2. Change in the pH value of the leachates permeated through the columns: 1 – “clean rain”, 2 – “acid rain”; pH values at 0 mL are for distilled and acidified water

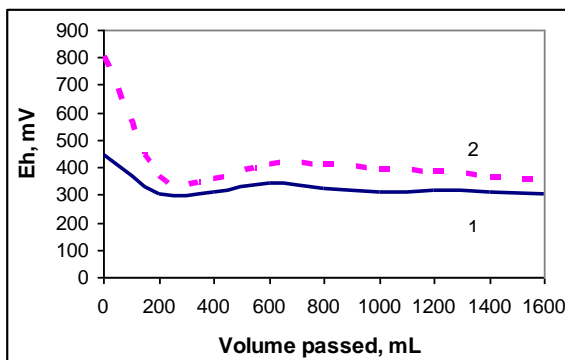


Fig. 3. Change in the Eh value of the leachates permeated through the columns: 1 – “clean rain”, 2 – “acid rain”; Eh values at 0 mL are for distilled and acidified water

Furthermore, the studied material possesses a high neutralising capacity. This finding is not surprising, having in mind the high carbonate content of the material (Fig. 1). Carbonate minerals, such as calcite  $\text{CaCO}_3$  and dolomite

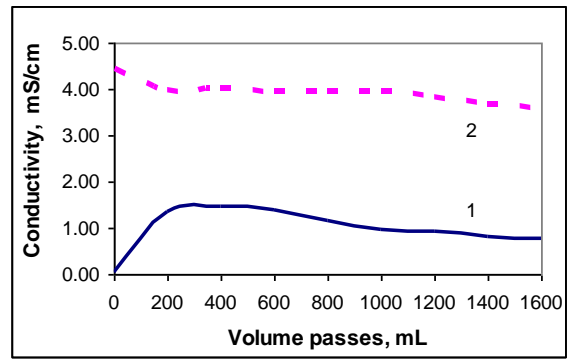


Fig. 4. Change in the conductivity of the leachates permeated through the columns: 1 – conductivity of “clean rain” drainage x 10, 2 – conductivity of “acid rain” drainage; conductivity values at 0 mL are for distilled and acidified water

Table 1. Leached heavy metals

Sample No	1	2	3	4	5
Pollutant					
Fe <sub>tot</sub> , mg/kg	<0.03	<0.04	0.07	0.16	0.09
Pb, mg/kg	<0.01	<0.01	<0.01	<0.01	<0.01
Cd, mg/kg	<0.005	<0.006	<0.005	<0.005	<0.005
Cu, mg/kg	<0.005	<0.006	<0.005	0.033	<0.005
Zn, mg/kg	<0.005	<0.006	0.033	0.222	<0.005

- 1 – leachate – “clean rain” precipitation – passed 400 mL/kg
- 2 – leachate – “clean rain” precipitation – passed 1200 mL/kg
- 3 – leachate – “acid rain” precipitation – passed 200 mL/kg
- 4 – leachate – “acid rain” precipitation – passed 1000 mL/kg
- 5 – recycled water – after 10<sup>th</sup> use

$\text{CaMg}(\text{CO}_3)_2$  that are the main constituents of the studied material can neutralise the acid rain and most probably the neutralisation is mainly due to  $\text{CaCO}_3$  dissolution following the reaction:



This is confirmed by the relative increase in dolomite main peak (Fig. 1 – curve 3) and the 3-fold decrease in the ratio of calcite to dolomite in the solid sample taken from the upper part of the column sprayed with “acid rain”. At the same time the ratio “dissolved magnesium to dissolved calcium” found in the leachate decreased, pointing also at predominant calcite dissolution (Fig. 5). Dolomite dissolution produces waters with a molar  $[\text{Mg}^{2+}] / [\text{Ca}^{2+}]$  ratio of 1. Dissolution of equal moles of dolomite and calcite contributes 0.5 mole of  $\text{Mg}^{2+}$  and 1.5 moles of  $\text{Ca}^{2+}$ , producing waters with a  $[\text{Mg}^{2+}] / [\text{Ca}^{2+}]$  ratio of 0.33. The  $[\text{Mg}^{2+}] / [\text{Ca}^{2+}]$  ratio less than 0.11 points that more than 75% of the carbonate mineral dissolved is calcite (Szramek et al., 2007). Silicate minerals can also participate in the neutralisation process but the reaction is slower (Kusuma et al., 2012). When the amount of carbonate and silicate minerals in the material is sufficient, an acid drainage due to acid rain will not be formed, as it can be seen in Fig. 2 – curve 2. This results also in conditions where the most toxic Pb and

Cd do not leach and the leached amounts of Fe<sub>tot</sub>, Cu and Zn are very low – Table 1, samples 3 and 4. The concentrations of all studied heavy metals in leachates obtained with “clean rain” precipitation are below the detection limit – Table 1, samples 1 and 2. Most probably, in this case dolomite dissolution predominates – Fig. 5. The solubility of dolomite increases compared to that of calcite at temperatures below 25°C as a result of the temperature-dependent relative solubility of these minerals (Szramek et al., 2007).

As it can be seen in Figure 3, after an initial decrease in the Eh value, pointing at a certain reduction process, whose identification needs further studies, the Eh value practically reaches a steady-state.

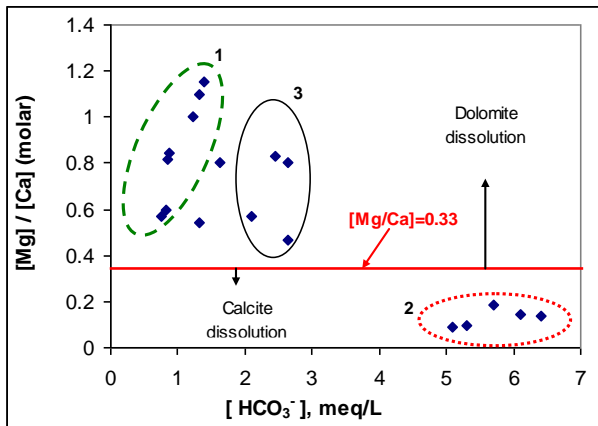


Fig. 5. Mg<sup>2+</sup> / Ca<sup>2+</sup> ratios versus HCO<sub>3</sub><sup>-</sup> values: 1 – leachate from “clean rain”, 2 – leachate from “acid rain”, 3 – water from 1<sup>st</sup>, 3<sup>rd</sup>, 6<sup>th</sup> and 10<sup>th</sup> washing; points outside the cycles – water from Deval washing

The electric conductivity reflects the total amount of dissolved ions in the leachate. For leachate obtained with “clean rain” initially the conductivity increased pointing at fast dissolution of more easily soluble compounds in the material and then practically reached a steady-state (Fig. 4 – 1). The considerably higher conductivity measured in “acid rain” leachates (Fig. 4 – 2) can be attributed to the presence of hydrogen ions in the system and their specific conductivity mechanism resulting in high measured EC values.

**Chemical indicators related to the material use in road construction**

The measured concentration of water soluble chlorides was 0.010 wt.%. The concentration of water soluble sulphates was 0.015 wt.%. These values are well below the threshold values of 4 wt.% water soluble sulphates and 8 wt.% water soluble chlorides required by the Bulgarian legal documents for aggregates for unbound and hydraulically bound materials for use in civil engineering work and road construction (BDS EN 13242:2002 +A1:2007) and for materials for embankments, underlying layers, stabilised banquetts with a top layer of crushed stone (Ministry of Regional Development and Public Works, 2014). The same documents place a legal requirement of less than 1 wt.% total sulphur. The material's water solubility was 0.028 wt.%. The figure is much less than the threshold value of 2 wt.% for coarse aggregates from crushed limestone, re-crystallised limestone, marble and marl (Rostovski et al., 2010).

**Possibility of washing water recycling**

The possibility for multiple use of clarified washing water in closed cycle depends on its physicochemical parameters, such as pH and Eh values related to precipitation of low soluble compounds and EC values that are indicative for the dissolved salts. In addition, information about the concentrations of chloride and sulphate ions that are corrosion – aggressive both to steel and concrete could be useful from a practical point of view. Data on the conductivity, pH and Eh values measured in recycled water samples are presented in Fig. 6.

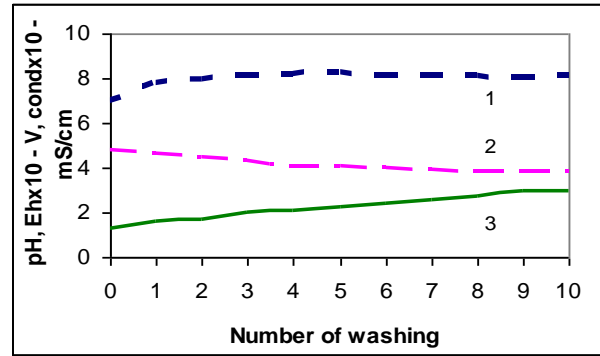


Fig. 6. Change in the pH, Eh values and conductivity of the recycled washing water: 1 – pH; 2 – Eh x 10, V; 3 – conductivity x 10, mS/cm; the values at 0<sup>th</sup> washing are for the used tap water

Initially an increase in the pH and decrease in the Eh values were observed (Fig. 6) that most probably are due to the dissolution of some carbonaceous material. Further, these parameters practically reach a steady state that could be related to the carbonates' equilibriums (of dissolution and precipitation). Conductivity values, measured by us, are within the same range (0.049-0.480 mS/cm) that have been measured in water samples prepared by contacting overburden dump materials from coal mines at similar solid to water ratios and times (Dutta et al., 2018). As it can be seen in Fig. 6, increasing the number of cycles of water use leads to an increase in the EC. This is indicative for the accumulation of salts in the water – mainly chlorides and sulphates (Table 2). However, the accumulated salts and especially the corrosion aggressive ions are in relatively low concentrations which cannot cause corrosion problems of steel or concrete (Panayotova, 2007).

Table 2. Leached corrosion aggressive ions

Pollutant, sample	Cl <sup>-</sup> , wt. %	SO <sub>4</sub> <sup>2-</sup> , wt. %
Water for washing	0.001	0.001
Lab, 1 <sup>st</sup> washing	0.004	0.003
Lab, 3 <sup>rd</sup> washing	0.009	0.009
Lab, 6 <sup>th</sup> washing	0.011	0.012
Lab, 10 <sup>th</sup> washing	0.014	0.024

It is worth noting that the water used by us (from the drinking water supply network in Sofia) is generally with low mineralisation and conductivity. Such type of flushing water can be used in a closed cycle multiple times. However, the accumulation of salts in recycled water will be much faster and more noticeable when the water used for flushing has a higher initial mineralisation and conductivity, as for example is the case with the tap water in many villages in Yambol region, Southeast Bulgaria (Panayotova et al., 2010).

### Characteristics of Deval washing water

Data on some physicochemical parameters, macro-components and some micro-components of washing water from Deval washing tests are presented in Table 3.

Table 3. *Physicochemical parameters, macro-components and some micro-component of washing water from Deval washing*

Parameter	Deval washing	1 <sup>st</sup> washing
pH	8.10	8.21
Eh, mV	245	414
Conductivity, $\mu\text{S/cm}$	240	134
Na <sup>+</sup> , mg/L	10.9	4.0
K <sup>+</sup> , mg/L	6.1	3.2
Ca <sup>2+</sup> , mg/L	20.2	18.1
Mg <sup>2+</sup> , mg/L	9.8	4.9
HCO <sub>3</sub> <sup>-</sup> , mg/L	93.7	68.4
Cl <sup>-</sup> , mg/L	17.6	11.2
SO <sub>4</sub> <sup>2-</sup> , mg/L	21.4	12.2
Pb <sup>2+</sup> , mg/L	<0.01	<0.01
Cd <sup>2+</sup> , mg/L	<0.005	<0.005

By comparing data presented in Table 3 and Figure 6, it can be seen that physicochemical parameters of water samples obtained in experiments aimed at studying the washing water recyclability and Deval washing experiments are in the same range. Since in the 1<sup>st</sup> washing of samples in the Deval machine fresh tap water was used, the conductivity decreased and the Eh value increased. The molar  $[\text{Mg}^{2+}] / [\text{Ca}^{2+}]$  ratios of Deval washing and 1<sup>st</sup> washing are indicative for predominant dolomite dissolution (Fig. 5). The fine material removed from the solid sample by Deval washing, which material practically represents the total suspended particles in the water sample, practically does not contain dolomite (Fig. 1 – 4), thus supporting the idea of dolomite dissolution. The concentrations of corrosion aggressive chlorides and sulphates were 0.009 wt.% and 0.005 wt.% respectively, showing that corrosion problems are not to be expected if the clarified water from this washing is re-used.

### Conclusions

Based on the studies carried out, the following conclusions can be drawn:

1) Normal rain and snow water contacting with the material representing solid inclusions in the overburden from opencast coal mining in Maritsa East Mines Ltd will not generate acid rock drainage and will not leach heavy metals from the material. Moreover, the material is capable to neutralise acid rain, thus contributing to the protection of the surrounding land and water bodies by heavy metal ions pollution.

2) Dolomite is the main leached carbonate mineral in neutral water contacting with the studied material at ambient temperature. At acidic water contacting with the studied material, calcite is the main leached carbonate mineral.

3) From the chemistry point of view, the material is suitable for use in civil engineering work and road construction. It contains acid drainage forming minerals and minerals releasing corrosive-aggressive ions in amounts much less than permitted by the relevant legislation.

4) Tap water used for the materials' washing can be re-used multiple times after its clarification, subjected to the condition that initially used water is not highly mineralised.

**Acknowledgements.** The authors are thankful to the project MTF-172/11.03.2019 for the financial support.

### References

- BDS EN 13242:2002+A1:2007. *Aggregates for unbound and hydraulically bound materials for use in civil engineering work and road construction*, CEN, Brussels.
- BDS EN 1744-1:2009+A1:2012. *Tests for chemical properties of aggregates – Part 1: Chemical analysis*, CEN, Brussels.
- Dutta, M., P. Khare, S. Chakravarty, D. Saikia, B. K. Saikia. 2018. Physico-chemical and elemental investigation of aqueous leaching of high sulfur coal and mine overburden from Ledo coalfield of Northeast India. – *International Journal of Coal Science & Technology*, 5, 3, 265–281.
- Kostova, I. 2005. Geochemical characteristics of coal from Maritsa East, Pernik and Balkan Basins and relation of the elements with pyrite sulphur. – *Review of the Bulgarian Geological Society*, 66, 1-3, 43–60.
- Kusuma, G. J., H. Shimada, T. Sasaoka, K. Matsui, C. Nugraha, R. S. Gautama, B. Sulistianto. 2012. An Evaluation on the Physical and Chemical Composition of Coal Combustion Ash and Its Co-Placement with Coal-Mine Waste Rock. – *Journal of Environmental Protection*, 3, 589–596.
- Kusuma, G. J., H. Shimada, T. Sasaoka, K. Matsui, C. Nugraha, R. S. Gautama, B. Sulistianto. 2012. Physical and geochemical characteristics of coal mine overburden dump related to acid mine drainage generation. – *Memoirs of the Faculty of Engineering, Kyushu University*, 72, 23–38.
- Mallick, S. R., M. K. Mishra. 2017. Evaluation of Clinker Stabilized Fly Ash-Mine Overburden Mix as Sub-base Construction Material for Mine Haul Roads. – *Geotechnical and Geological Engineering*, 35, 4, 1629–1644.
- Mary, O. L., V. R. Krishnan. 2016. Experimental Investigations on the Use of Coal Mine Overburden as Partial Replacement for Fine Aggregate. – *International Journal of Innovative Research in Science, Engineering and Technology*, 5, 12, 20414–20418.
- Agentsia "Patna infrastruktura". 2014. *Tehnicheska spetsifikatsiya*, Ministerstvo na regionalnoto razvitiie, Sofia, 296 s.
- Panayotova, M. 2007. *Korozia i zashtita ot korozia v stroitelstvoto*. IK "Sv. Ivan Rilski", Sofia, 198 p. (in Bulgarian)
- Panayotova, M., V. Hristov, I. Ivanov, K. Gesheva. 2010. Sezonen monitoring na podzemni vodi v Yambolsko-Elhovskia region. – *Godishnik na MGU "Sv. Ivan Rilski"*, 53, 1, 153–158 (in Bulgarian).
- Rostovski, I. A., N. D. Barovski. 2010. *Vzemane na probi i izpitvane na beton i dobavachni materialy po natsionalnite prilozhenia kam BDS EN 206-1/NA:2008 i BDS EN 12620/NA:2008*. TsLFHM – BAN i Evrobul Holding, Sofia, 96 p.
- Szczepańska-Plewa, J., S. Stefaniak, I. Twardowska. 2010. Coal mining waste management and its impact on the groundwater chemical status exemplified in the Upper Silesia coal basin (Poland). – *Biuletyn Państwowego Instytutu Geologicznego*, 441, 157–166.
- Szramek, K., J. C. McIntosh, E. L. Williams, T. Kanduc, N. Ogrinc, L. M. Walter. 2007. Relative weathering intensity of calcite versus dolomite in carbonate-bearing temperate zone watersheds: Carbonate geochemistry and fluxes from catchments within the St. Lawrence and Danube river basins. – *Geochemistry, Geophysics, Geosystems*, 8, 4.
- Tiwary, R. K. 2001. Environmental Impact of Coal Mining on Water Regime and Its Management. – *Water, Air and Soil Pollution*, 132, 185–199.

## MICROBIAL EXTRACTION OF PRECIOUS METALS FROM A GRAVITY-FLOTATION CONCENTRATE

*Irena Spasova, Marina Nicolova, Plamen Georgiev, Stoyan Groudev*

*University of Mining and Geology "St. Ivan Rilski", 1700 Sofia; spasova@mgu.bg*

**ABSTRACT.** The possibility for microbial extraction of precious metals from mineral and metal bearing raw materials and wastes is of special interest in the area of the mineral biotechnologies. Various processes of this type are known and the most important among them are the following: the preliminary oxidation of gold-bearing sulphide ores and concentrates by means of chemolithotrophic bacteria and archaea to liberate and expose the fine gold particles from the sulphide crystal structures; the direct extraction of gold from oxide mineral raw materials by leaching with solutions containing amino acids of microbial origin and suitable chemical oxidisers of the native gold; the leaching of gold by means of heterotrophic bacteria growing on suitable organic sources of carbon and energy in the presence of the mineral gold-bearing mineral raw materials being leached; selective change of the flotation properties of the gold-bearing sulphide minerals by short treatment with chemolithotrophic bacteria to facilitate the subsequent flotation and produce very clean gold-bearing concentrate.

**Keywords:** chemolithotrophs, leaching, valuable metals

### МИКРОБИОЛОГИЧНО ИЗВЛИЧАНЕ НА БЛАГОРОДНИ МЕТАЛИ ОТ ФЛОТАЦИОННО-ГРАВИТАЦИОНЕН КОНЦЕНТРАТ

*Ирена Спасова, Марина Николова, Пламен Георгиев, Стоян Грудев*

*Минно геоложки университет "Св. Иван Рилски", 1700 София*

**РЕЗЮМЕ.** Специален интерес в областта на минералните биотехнологии е възможността за микробно извличане на благородни метали от минерални и метал съдържащи суровини и отпадъци. Известни са различни процеси от този тип и най-важни сред тях са: предварителното окисление на златосъдържащите сулфидни руди и концентрати чрез хемолитотрофни бактерии и археи за освобождаване и излагане на фините златни частици от сулфидните кристални структури; директно извличане на злато от окисни минерални суровини чрез извличане с разтвори, съдържащи аминокиселини от микробен произход и подходящи химически окислителни; извличане на злато с помощта на хетеротрофни бактерии, които растат върху подходящи органични източници на въглерод и енергия в присъствието на излугваните злато-съдържащи суровини; селективна промяна на флотационните свойства на златосъдържащите сулфидни минерали чрез краткотрайно третиране посредством хемолитотрофни бактерии за улесняване на последващата флотация за получаване на много чист злато-съдържащ концентрат.

**Ключови думи:** хемолитотрофи, излугване, ценни метали

### Introduction

The ability of different microorganisms, mainly chemolithotrophic bacteria and archaea to leach precious metals from mineral substrates (ores, concentrates and wastes) is largely applied under real industrial conditions. The role of the microorganisms in these processes can be of different types:

- A preliminary oxidation of the gold-bearing sulphide ores and concentrates to reveal and liberate the fine gold particles from the sulphide crystal structures. In some cases the microbial oxidation of sulphides is performed together with the leaching of the precious metals by means of reagents which are non-toxic for microorganisms (such as thiourea and acidic medium);
- A direct extraction of gold from mineral oxides containing the precious metals by means of solutions of aminoacids of microbial origin and suitable chemical oxidants of the native gold (such as peroxides);

- Bioleaching by means of heterotrophic bacteria grown on suitable organic sources of carbon and energy in the presence of the leached gold-bearing substrate;
- A selective change of the flotation properties of the sulphide minerals present in the complex gold-bearing concentrates by means of a short treatment by chemolithotrophic bacteria and archaea. This treatment results in a change of the flotation properties of the gold-bearing concentrates.

This paper contains data about investigations on the microbial extraction of the precious metals from a sulphidic gold-bearing ore in the western part of Bulgaria.

### Materials and Methods

The initial sample contained 7.1 g/t Au and 14.5 g/t Ag, 2.8% sulphur (from which 2.4% were sulphidic), 7.3% iron and 0.35% copper as the main components. The phase analysis of the gold in the ore was:

- Free Au 0.5%;
- Au in oxides and hydroxides 12.5%;

- Au finely disseminated in sulphides (mainly pyrite) 85.1%;
- Au finely disseminated in silicates 1.9%.

Most of the gold was finely disseminated in pyrite and a relatively small part – in chalcopyrite. The gold was present mainly as small (less than 1 micron) particles. The chalcopyrite was the main copper mineral in the ore but part of the copper was present in secondary sulphidic minerals, mainly in covellite and bornite. The quartz was the main mineral in the ore rock.

A gravity-flotation concentrate was obtained by processing of the initial ore sample. The pyrite was the main gold-bearing mineral in the concentrate. The gold was present in the pyrite as a fine isomorphic impurity. The galena was the main silver-bearing mineral and the silver was present also as isomorphic impurities. A portion of the silver was present in the pyrite.

Data about the concentrate are shown in Tables 1 and 2.

The bioleaching of concentrate was performed in agitated Erlenmeyer flasks of 300 ml volume each containing 100 ml leach solution with the composition of the 9K nutrient medium and different quantities of the mineral substrates used in this study with a particle size of minus 100 microns added in quantities to form the desired pulp density.

Table 1. Data about the gravity-flotation concentrate

Element	Content
S total	6.80 %
S sulphidic	6.17 %
Fe	8.04 %
Cu	1.64%
Zn	0.15 %
Pb	6.35 %
Au	28.4 g/t
Ag	1270 g/t

Table 2. The phase composition of the precious metals in the concentrate

Phase composition	Distribution, %	
	Au	Ag
Free exposed	12.5	-
Capsulated in iron oxides	31.4	20.3
Finely dispersed in sulphides	53.0	71.3
Finely injected in silicate	3.1	8.4
Total	100.0	100.0

Elemental analysis of the liquid samples from the leach systems was performed by atomic absorption spectrometry (AAS) and inductively coupled plasma spectrometry (ICP). The isolation, identification and enumeration of microorganisms were carried out by the classical physiological and biochemical tests and by the molecular PCR methods (Karavaiko et al., 1988; Attia, El-Zeky, 1989; Spasova et al., 1994; Groudev et al., 1996; Sanz, Köchling, 2007; Escobar et al., 2008; Dopson, Johnson, 2012).

## Results and discussion

The direct chemical leaching of the precious metals from the sulphide concentrate used in this study was not efficient (Table 3) due to the fine dissemination of these metals in the

sulphide minerals. The thiosulphate was the main attractive leach agent due to its relatively low toxicity and efficient leaching ability which was very close to that of the very toxic cyanide. The combination of thiosulphate with a protein hydrolysate was even more efficient than the leaching ability of the cyanide. The combination of thiosulphate with a protein hydrolysate was even more efficient than the leaching ability of the cyanide. However, all these reagents were not able to penetrate through the sulphide matrix and to establish a direct contact with the precious metals finely disseminated in the sulphide minerals (mainly in the pyrite) of the concentrate. The addition of some chemical oxidisers (mainly of  $\text{KMnO}_4$ ) to the leach solutions increased considerably the level of extraction of these metals. However, the most efficient extraction of the precious metals was achieved by means of the preliminary sulphide oxidation on the relevant concentrate by chemolithotrophic bacteria and archaea able to expose the precious metals and to make them accessible to the reagents suitable for their solubilisation.

Table 3. Leaching of precious metals from the flotation concentrate by different reagents before and after its pre-treatment by means of microbial oxidation

Leach solutions	The initial concentrate		The pretreated concentrate	
	Au	Ag	Au	Ag
	Extraction, %			
Protein hydrolysate	8.6	4.1	14.5	7.3
Protein hydrolysate + $\text{KMnO}_4$	32.7	14.5	89.4	72.1
Protein hydrolysate + thiosulphate	40.4	21.2	91.8	75.6
Thiosulphate	35.8	17.8	90.1	72.5
NaCN	38.7	20.3	90.5	72.1

A large number of chemolithotrophic microorganisms able to oxidise sulphide minerals (including the most stable pyrite and chalcopyrite) were tested for their ability to oxidise these sulphide minerals (Table 4). It was found that the different chemolithotrophs, even such related to one and the same taxonomic species, can differ considerably from each other with respect to this ability. The most efficient oxidisers were some strains of the extreme thermophilic archaea of the species *Sulfolobus metallicus* and *Thermoplasma acidophilum* at 86°C but at relatively low pulp densities (up to 10-20%). Other strains of these species and some strains of the species *Metallosphaera sedula* were the most efficient at relatively higher pulp densities (14-20%) at 75°C. Some mixed cultures of extreme thermophilic archaea were also very active at these temperatures.

The moderate thermophilic bacteria, mainly such of the species *Sulfobacillus thermosulphidooxidans* and *Alicyclobacillus tolerans*, were also very active at lower temperatures (50-59°C) and pulp densities of 15-20%.

The comparative experiments during this study revealed that the most efficient oxidisers of the sulphide ore and the sulphide concentrate were the chemolithotrophs possessing only the ability to oxidise the ferrous iron but not the elemental sulphur ( $\text{S}^0$ ). The most efficient in this respect were the members of the genus *Leptospirillum*, such as the mesophilic *L. ferrooxidans* and the moderate thermophilic *L. ferriphilum*.

These microorganisms acted according to the well-known indirect oxidative mechanism and their role consisted in the oxidation of the ferrous iron to the ferric state. The ferrous ions were generated in the leach system as a result of the oxidation of the sulphides by the ferric ions.

Table 4. Extraction of precious metals from the flotation concentrate pre-treatment by means of chemolithotrophic microorganisms related to different taxonomic species and different strains from each taxonomic species

Pretreated by means of different microorganisms	Extraction of precious metals after pre-treatment, %		Number of strains tested
	Au	Ag	
<b>Mesophilic bacteria</b>			
<i>Acidithiobacillus ferrooxidans</i>	82 – 93	68 – 77	12
<i>Leptospirillum ferrooxidans</i>	78 – 91	64 – 71	8
<i>Acidithiobacillus ferrivorans</i>	75 – 88	57 – 68	4
<b>Moderate thermophilic bacteria</b>			
<i>Sulfobacillus thermosulfidooxidans</i>	80 – 95	65 – 79	8
<i>Alycyclobacillus tolerans</i>	77 – 90	62 – 71	4
<i>Leptospirillum ferriphilum</i>	75 – 86	57 – 71	4
<b>Extreme thermophilic archaea</b>			
<i>Sulfolobus metallicus</i>	84 – 95	68 – 82	8
<i>Metalosphaera sedula</i>	77 – 91	64 – 78	6
<i>Acidianus infernus</i>	73 – 84	60 – 80	6
<i>Thermoplasma acidophilum</i>	71 – 80	59 – 74	4

Note: The duration of the pre-treatment was up to 168 hours at the relevant temperature: 37 and 55°C for the mesophilic and moderate thermophilic bacteria, respectively, and at 75 and 86°C for the extreme thermophilic archaea, at 20 % pulp density.

On the other side, some microbial species possessing only sulphur-oxidising ability but not able to oxidise the ferrous iron (such as the mesophilic *At. thiooxidans* and the extreme thermophilic *Sulfolobus acidocaldarius* and *S. solfatarium*) were able to leach the sulphides but usually at relatively lower rates.

It must be noted also that at higher temperatures (over 60 – 65°C) there was some chemical oxidation of the ferrous iron to the ferric state by means of the oxygen dissolved in the leach solutions. The ferric ions generated in this way were also involved in the oxidation of sulphides. However, the role of the chemolithotrophic microorganisms mentioned above was considerably more essential than the chemical oxidation of the sulphidic concentrate used in this study.

## References

- Attia, Y. A., M. El-Zeky. 1989. Bioleaching of gold pyrite tailings with adapted bacteria. – *Hydrometallurgy*, 22, 291–300.
- Dopson, M., D. Johnson. 2012. Biodiversity, metabolism and application of acidophilic Sulphur-metabolising microorganisms. – *Environ. Microbiol.*, 12, 2620–2631.
- Escobar, B., K. Bustos, G. Morales, O. Salazar. 2008. Rapid and specific detection of *Acidithiobacillus ferrooxidans* and *Leptospirillum ferrooxidans* by PCR. – *Hydrometallurgy*, 92, 102–106.
- Groudev, S. N., I. I. Spasova, I. M. Ivanov. 1996. Two stage microbial leaching of refractory gold-bearing pyrite ore. – *Minerals Engineering*, 9, 7, 707–713.
- Karavaiko, G. I., G. Rossi, A. D. Agate, S. N. Groudev, Z. A. Avakyan (Eds.). 1988. *Biogeotechnology of Metals. Manual*. GKNT Centre for International Projects, Moscow.
- Sanz, J. L., T. Köchling. 2007. Molecular biology techniques used in wastewater treatment: An overview. – *Process Biochem.*, 42, 119–133.
- Spasova, I. I., S. N. Groudev, I. M. Ivanov. 1994. Extraction of precious metals from low-grade ore from Zlata deposit by means of prior bacterial oxidation and combined chemico-biological leaching. – *Annual of the University of Mining and Geology*, 40, 253–256.

## COLORIMETRIC SENSOR FROM CITRATE CAPPED SILVER NANOPARTICLES FOR TRACE DETECTION OF ARSENIC (III) IN GROUNDWATER

Svetlin Toshev<sup>1</sup>, Alexandre Loukanov<sup>1,2</sup>, Seiichiro Nakabayashi<sup>2</sup>

<sup>1</sup> University of Mining and Geology "St. Ivan Rilski", 1700 Sofia; svetlio\_13@abv.bg; loukanov@mail.saitama-u.ac.jp

<sup>2</sup> Saitama University, Sakura-Ku, 338-8570 Saitama; sei@chem.saitama-u.ac.jp

**ABSTRACT.** The arsenic (III) contamination in groundwater and some surface waters is a high-profile ecological problem due to the causing of acute toxicity. At neutral pH As (III) is usually present in the environment as an uncharged weak arsenious acid ( $H_3AsO_3$ ). In this report a simple and effective colorimetric approach for trace detection of  $H_3AsO_3$  is presented based on the localised change of surface plasmon resonance of silver nanoparticles. The nanoparticles were prepared by chemical reduction method from silver nitrate with trisodium citrate. They were tested for detection of various metal ions and anions, which usually occur in the chemical contents of the natural groundwater. In case of presence of low arsenic (III) concentrations (traces) perceptible shifts of the surface plasmon resonance of the silver nanoparticles have been observed, which were accompanied by colour change of the analytical sample due to the nanoparticle aggregation process.

**Keywords:** Silver nanoparticles, colorimetric sensor, arsenic detection

### КОЛОРИМЕТРИЧЕН СЕНЗОР ОТ ЦИТРАТНО ПОКРИТИ СРЕБЪРНИ НАНОЧАСТИЦИ ЗА ОТКРИВАНЕ НА СЛЕДИ ОТ АРСЕН В ПОДПОЧВЕНИ ВОДИ

Светлин Тошев<sup>1</sup>, Александър Луканов<sup>1,2</sup>, Сейчиро Накабаяши<sup>2</sup>

<sup>1</sup> Минно-геоложки университет "Св. Иван Рилски", 1700 София

<sup>2</sup> Университет Сайтама, Сакура-ку, 338-8570 Сайтама

**РЕЗЮМЕ.** Замърсяването на подпочвените и някои повърхностни води с арсен (III) е сериозен екологичен проблем, поради причиняването на остра токсичност. При неутрално рН арсен (III) се среща обикновено в околната среда, като слаба арсениста киселина ( $H_3AsO_3$ ). В настоящия доклад е представен лесен и ефективен колориметричен подход за откриване на следи от арсен (III), на базата на локализираната на промяна на повърхностния плазмонен резонанс на сребърни наночастици. Наночастиците бяха получени чрез химична редукция на сребърен нитрат с тринатриев цитрат. Те бяха тествани за детекцията на различни метални йони и аниони, които обикновено се срещат в химичния състав на естествените подпочвени води. При наличие на ниски концентрации на  $H_3AsO_3$  (следи) се регистрираха осезаеми промени в повърхностния плазмонен резонанс на сребърните наночастици, които бяха съпроводени с промяна на цвета на аналитичната проба, дължаща се на процеси свързани с агрегиране на наночастиците.

**Ключови думи:** сребърни наночастици, колориметричен сензор, откриване на арсен

## Introduction

The contamination of groundwater and some surface waters with arsenic (III) has been a major problem in various countries mainly in Asia, Africa and South America due to the causing of acute toxicity (Smedley, Kinniburgh, 2002; Bhattacharya et al., 2002). In general, the soluble inorganic form of trivalent As is more prevalent and toxic than its organic form (Brinkel et al., 2009). The permissible level of arsenic in groundwater is 10 ppb (Shankar et al., 2014). This circumstance necessitates the development of a cheap and easy for performance monitoring system to save the ecosystem by restricting the As(III) concentration within the allowable range. The established analytical techniques for measuring the arsenic levels below 10  $\mu\text{g/L}$ , such as hydride generation atomic absorption spectroscopy, atomic fluorescence spectroscopy, inductively coupled plasma mass spectroscopy, etc., are highly sensitive but expensive and require highly trained personnel in the laboratory (Yogarajah, Tsai, 2015). The developing nations do not have an appropriate infrastructure to perform complicated

analytical procedures with high reliability and throughput. In the light of these issues portable tests kits for simple but effective arsenic analysis are needed. Among the numerous analytical methods, the colorimetric detection seems the most popular among the users as a saviour in the context of saving time and expenditure as well. Recently, the nanostructured materials have attracted much attention for analysis of trace metal ions because of their novel optical properties, which could offer significant additional advantages over the commercial detection kits (Moghimi et al., 2015). Nanoparticle aggregation occurrence due to the interaction with the targeted heavy metal ions might change the original colour of nanoparticle suspension. This colour change is the basic principle of metal ions colorimetric detection by nanoparticles (Priyadarshini, Pradhan, 2017; Wang et al., 2013). The functionalised metal nanoparticles of gold and silver have attracted the interest of researchers for effective analysis of some toxic heavy metals due to their high extinction coefficients and unique optical properties (Rosi, Mirkin, 2005). The properties are attributed to the collective dipole oscillation, known as Surface Plasmon Resonance or SPR (Talopin et al., 2010). This phenomenon

makes the silver nanoparticles very desirable for colorimetric sensing of various heavy metal ions because of the interaction between the Ag nanoparticles and the analyte cause changes in the intensity and position of the absorption band in the visible spectrum. This process might be observed even with a naked eye (Hung et al., 2010).

In this report, a new colorimetric detection for As(III) with high sensitivity using citrate stabilised silver nanoparticles (Ag NPs) is presented. The colour change in the absorbance spectra is expected as a result of the interaction between Ag NPs and arsenic ions. In such a way, analysis of low trace of As(III) in the environment is possible. These simple and fast analytical methods for determination of soluble arsenic have potential application for As(III) analysis in drinking water and groundwater.

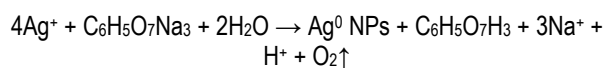
## Experimental Procedures

### Materials

All chemicals used were of analytical-reagent grade and all aqueous solutions were prepared with ultra-pure deionised water (Millipore Corp.). Silver nitrate (AgNO<sub>3</sub>, 99.9 %) trisodium citrate (Na<sub>3</sub>C<sub>6</sub>H<sub>5</sub>O<sub>7</sub>), sodium hydroxide (NaOH, 99 %), hydrochloric acid (HCl) and salts of different cations (KCl, NaCl, CaCl<sub>2</sub>, MgCl<sub>2</sub>, FeCl<sub>3</sub>, ZnCl<sub>2</sub>, NiCl<sub>2</sub>) were purchased from Wako, Japan (Wako Pure Chemical Corporation). Standard arsenic (III) solution of H<sub>3</sub>AsO<sub>3</sub> was purchased from Merck (USA). Chromic acid (mixture made by adding of concentrated sulphuric acid and dichromate) was used for cleaning the glassware. After cleaning, the glassware was kept in an oven to dry for an overnight at 80 °C.

### Synthesis of silver nanoparticles

The silver nanoparticles were prepared by the chemical reduction method with trisodium citrate as a reducing agent. For that purpose, silver nitrate and tri sodium citrate were dissolved in ultra-pure MilliQ water to prepare stock solutions of the precursors. In typical experiment 50 ml of 0.001 M AgNO<sub>3</sub> was heated to boil. 5 ml of 1 % trisodium citrate was added drop by drop to this solution. During this process, the reaction solution was mixed vigorously and heated until change of colour was evident (pale yellow). Then it was removed from the hot plate and stirred until cooled to room temperature. The reaction equation could be expressed as follows:



The colloidal solution of silver nanoparticles was characterised by using UV-VIS absorption spectroscopy and transmission electron microscope.

### Selective colorimetric detection of arsenic (III)

To determine the selectivity of citrate functionalised Ag NPs as a nanosensor for As (III), some metal cations such as K<sup>+</sup>, Na<sup>+</sup>, Ca<sup>2+</sup>, Mg<sup>2+</sup>, Fe<sup>3+</sup>, Zn<sup>2+</sup> and Ni<sup>2+</sup> were taken for the test. In centrifuge Eppendorf, 1.0 ml of citrate capped Ag NPs were kept and mixed with 0.5 ml of the respective metal ion solution. The colour change is an evidence for the occurring of sensor reaction. It was observed by naked eye that only colour change

occurred (from yellow to blue) when Ag NPs were mixed with As (III) solution.

### Analytical instrumentation

The absorbance spectra were measured in a quartz cuvette by UV-VIS Jasco analytical spectrophotometer (model No V-570). pH of all solutions was measured by conventional pH meter (EcoTestr pH1, Euttech Instruments). The zeta potential of the nanoparticles was measured by a ZetaPALS Zeta Potential Analyzed (Brookhaven Instrument Corporation). Transmission electron microscopy (TEM) images were obtained by FEI tecnai G2 20 at 120 kV accelerating voltage. The sample preparation of the nanoparticles observation in TEM was prepared as follows: an aqueous drop (1 μl) contained functionalised nanoparticles before and after sensing reaction (control and detection experiment) were injected by a micropipette on the support graphite film (15 nm in thickness) on a copper grid. The film must be strong, clean and must remain attached on the grid during this preparation step. After that the adsorbed nanoparticles on the support film were simply dried under vacuum and observed without any additional chemical staining.

## Results and discussion

### Optical characterisation of silver nanoparticles in aqueous suspension

The presence of silver nanoparticles in aqueous suspension after reduction of AgNO<sub>3</sub> salt was proved by the exhibition of an intense peak in the visible region due to the surface plasmon excitation as shown on Figure 1A (solid red line). Ag nanoparticles have free electrons, which give an optical effect known as the so-called surface plasmon resonance absorption band. This effect of nanoparticles in aqueous suspension occurred due to the combined vibration of the electrons of the nanoparticles in resonance with the light wave. The obtained local surface plasmon resonance (SPR) is a characteristic phenomenon of metal nanoparticles (particularly of Ag NPs) that depends on dielectric constant of its surrounding environment. The absorption band between 350 nm to 500 nm in the visible range of the light is typical for the silver nanoparticles. With increasing of Ag NPs diameter, the plasmon absorption shifts toward lower energy wavelength, i.e. red shifting. The prepared Ag NPs demonstrated stability in the colloidal solution one week after preparation. However, a week later the absorbance spectrum showed a little red shift (within 10-15 nm) with the decrease in absorbance intensity value. At the same time the absorption peak becomes broader which is an indication for suspension growth and occurring of aggregation. As the dielectric constant changes due to the presence of target analyte in the sample solution, we have observed red shift in localised SPR peak.

### Colorimetric detection of As (III)

Citrate functionalised Ag NPs have negative surface charges. When As (III) ions are introduced with these functionalised nanoparticles, then a specific reaction between heavy metal ions and nanoparticle organic shell occurred in the analytical solution. After the proceeding of the detection reaction, alteration of the authentic SPR spectra was observed.

As shown on the figure, the UV-VIS absorption spectra revealed that arsenic containing Ag NPs have two absorption peaks – one at 420 nm and another around 585 nm (blue dashed line). Thus, as the surrounding environment was changed with the presence of As (III), a red shift in nanoparticles SPR and consequent colour change from yellowish to bluish was measured. Such red-shifted secondary absorption peak was not observed in the test experiments with other metal ions. This result implies that the achieved sensing unit has arsenic selective capability in a complex solution obtained from contaminated groundwater. The limit of detection was obtained in linear range as shown on Figure 1 B. The detection limit of citrate capped Ag NPs was found to be around 6 ppm. Lineal correlation ( $R^2$ ) ~ 0.995 was observed between absorbance  $A_{585}$  and concentration of As (III) ranging from 6 to 14 ppm. The sensor reaction of the functionalised Ag

NPs toward As(III) detection is due to the specific reaction with hydroxyl (-OH) and carboxylic groups (-COOH) on the nanoparticles surface (Ag NPs are functionalised with citric acid ligands), which act as binding sites with the soluble arsenic ions in the media. Because of this specific interaction aggregation of the Ag NPs takes place as shown on Figure 1 C and D.

To determine the selectivity of citric capped Ag NPs toward other metal ions, 1.5 ml test tubes with pH = 7.5 contained chlorides of  $\text{Na}^+$ ,  $\text{Ca}^{2+}$ ,  $\text{Mg}^{2+}$ ,  $\text{Fe}^{3+}$ ,  $\text{Zn}^{2+}$ , and  $\text{Ni}^{2+}$  were prepared. Functionalised Ag NPs were added to the tubes, mixed and observed for colour change. It was proved that only the arsenic containing sample showed prominent colour change of the test from yellow to bluish. In the other test no colour changes were observed in the visible range of the light spectrum.

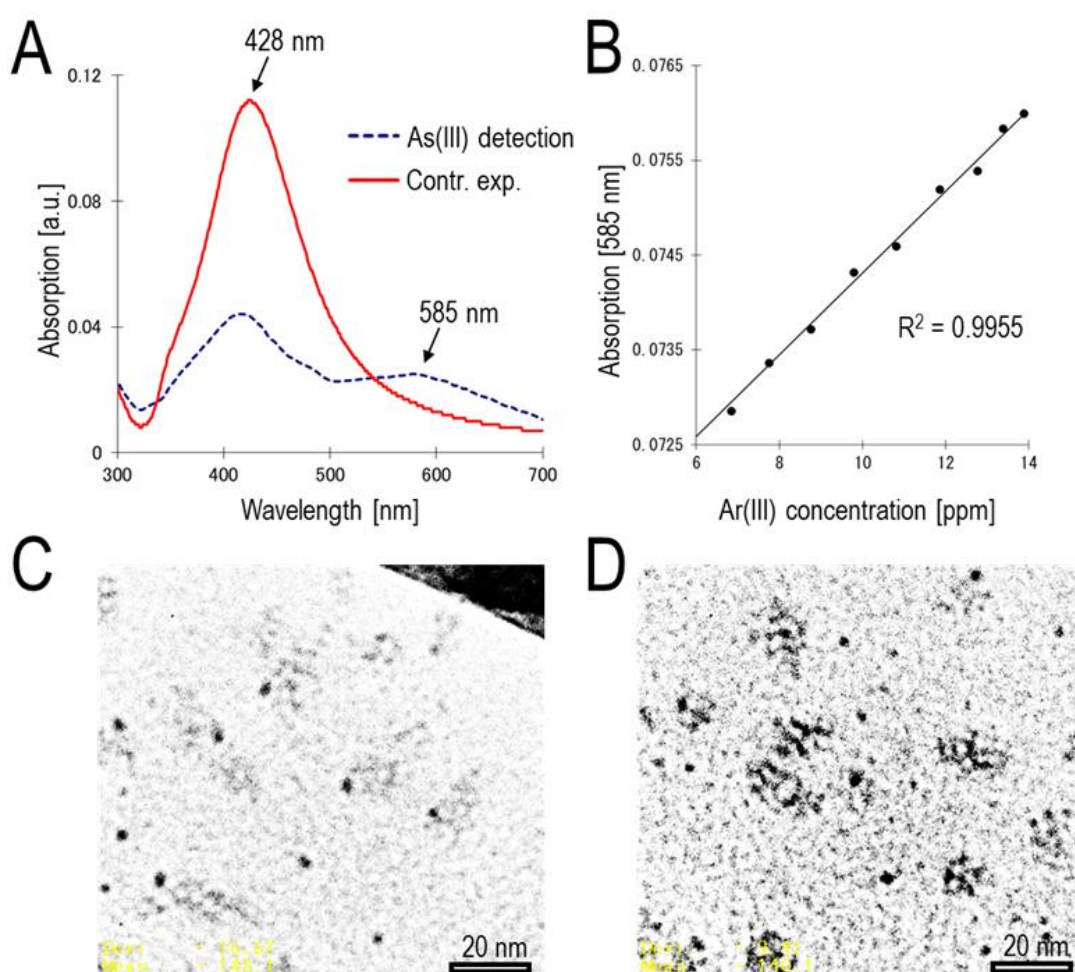


Fig. 1. Silver nanoparticles as colorimetric nanosensor for trace detection of arsenic (III) at pH = 7.5. (A) Absorbance spectra of citrate capped Ag NPs (red solid line) and nanoparticles reacted with As (III) ions (blue dashed line). (B) Detection limit of citrate capped Ag NPs for analysis of arsenic. Transmission electron microscope image of (C) monodispersed bare citrate capped Ag NPs and (D) nanoparticle aggregations formed due to sensor reaction with As (III); scale bar for C and D = 20 nm

#### Electron microscopic analysis of the nanoparticles

The diameter and size distribution of Ag NPs and Ag NPs adsorbed with As(III) were determined using 120 kV transmission electron microscope (TEM). The nanoparticle size histogram (Fig. 2) was obtained by measuring at least 350 NPs. Nanoparticles with different sizes and homogenous spherical shapes (as shown on Fig. 1 C) were obtained by the synthesis described above using sodium citrate reduction. However, the

use of a single reagent as sodium citrate for Ag NPs synthesis results in nanoparticles with a broad range of sizes between 1.5 nm to 8 nm. Surprisingly, bigger nanoparticles with a diameter bigger than 10 nm were not found in the sample during TEM observation. Even the change of reaction conditions, for example increasing the temperature, does not produce uniform in size Ag NPs. After interacting with arsenic the aggregations of Ag NPs were obtained. As shown on TEM

photo (Figure 1 D) the formed aggregations were also heterogeneous but with various sizes. The aggregations are

not stable in the suspension and there is precipitation on the tube bottom after keeping for a few days.

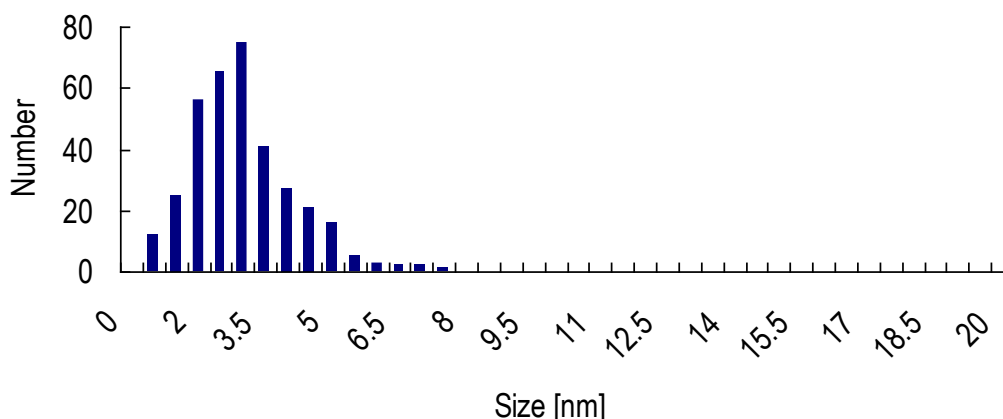


Fig. 2. Size distribution of silver nanoparticles capped with citric acid by number

### Effect of pH on the detection reaction

The pH of analysed sample solution influenced both the solubility of metal ions and the stability of citrate capped Ag NPs. In acid conditions ( $\text{pH} < 4$ ) neutralisation of nanoparticle surface occurred, which results in the change of SPR absorption band. This process happened in the absence of analytes. The experiments have proved that the optimum pH for effective colorimetric sensing was in the range between 5 and 9. Based on the obtained results a pH at 7.5 (using HEPES buffer) was selected for all experiments in order to obtain reproducible analyses. At this pH value the citrate ligands on the nanoparticle surface exhibit negative charges.

### Conclusion

We have developed a colorimetric detection of arsenic (III) in aqueous medium by detection with citrate functionalised silver nanoparticles. The limit of detection was found to be around 6 ppm. It was measured in a linear range with a linear correlation ( $R^2$ ) of 0.99. The proposed colorimetric approach is very simple, sensitive and cost effective. In addition, it required a small amount of reagents and cheap equipment to perform.

**Acknowledgment.** This study was accomplished thanks to the bilateral agreement between the Saitama University, Japan and the University of Mining and Geology "St. Ivan Rilski", Sofia, Bulgaria. The authors would like to express their gratitude to Saitama University for the financial support of the reported investigations.

### References

Bhattacharya, P., G. Jacks, K. M. Ahmed, J. Routh, A. A. Khan. 2002. Arsenic in groundwater of the Bengal Delta

Plain aquifers in Bangladesh. – *Bulletin of Environmental Contamination and Toxicology*, 69, 538–545.

Brinkel, J., M. H. Khan, A. Kraemer. 2009. A systematic review of arsenic exposure and its social and mental health effects with special reference to Bangladesh. – *International Journal of Environmental Research and Public Health*, 6, 1609–1619.

Hung, Y. L., T. M. Hsiung, Y. Y. Chen, Y. F. Huang, C. C. Huang. 2010. Colorimetric detection of heavy metal ions using label-free gold nanoparticles and alkanethiols. – *The Journal of Physical Chemistry C* 114, 16329–16334.

Shankar, S., Shanker, U., Shikha. 2014. Arsenic contamination of groundwater: a review of sources, prevalence, health risks, and strategies for mitigation. – *Scientific World Journal*, 304524.

Moghimi, N., M. Mohapatra, K. T. Leung. 2015. Bimetallic nanoparticles for arsenic detection. – *Anal. Chem.*, 87, 5546–5552.

Priyadarshini, E., N. Pradhan. 2017. Gold nanoparticles as efficient sensors in colorimetric detection of toxic metal ions: a review. – *Sensors and Actuators B* 238, 888–902.

Rosi, N. L., C. A. Mirkin. 2005. Nanostructures in biodiagnostics. – *Chem. Rev.*, 105, 1547–1562.

Smedley, P. L., D. G. Kinniburgh. 2002. A review of the source, behaviour and distribution of arsenic in natural waters. – *Applied Geochemistry*, 17, 517–568.

Talapin, D. V., J.-S. Lee, M. V. Kovalenko, E. V. Shevchenko. 2010. Prospects of colloidal nanocrystals for electronic and optoelectronic applications. – *Chem. Rev.*, 110, 389–458.

Wang, C. C., H. T. Yau, C. C. Wang. 2013. Chaotic and subharmonic motion analysis of floating ring gas bearing system by hybrid numerical method. – *Mathematical Problems in Engineering*, 145716.

Yogarajah, N., S. S. H. Tsai. 2015. Detection of trace arsenic in drinking water: challenges and opportunities for microfluidics. – *Environ. Sci. Water Res. Technol.*, 1, 426.

## DESIGN OF SELF-PROPELLING JANUS NANOIMPELLER AS A NANOMACHINE FOR TARGETING AND DESTRUCTION OF PATHOGENIC MICROORGANISMS

Svetlin Toshev<sup>1</sup>, Alexandre Loukanov<sup>1,2</sup>, Seiichiro Nakabayashi<sup>2</sup>

<sup>1</sup> University of Mining and Geology "St. Ivan Rilski", 1700 Sofia; svetlio\_13@abv.bg; loukanov@mail.saitama-u.ac.jp

<sup>2</sup> Saitama University, Sakura-Ku, 338-8570 Saitama; sei@chem.saitama-u.ac.jp

**ABSTRACT.** The design and ability of a self-propelled Janus nanoimpeller is presented as a nanomachine for targeting and destroying pathogen microorganisms as gram negative *Escherichia coli* 0157:H7 in natural aqueous media. The nanomachine was fabricated from mesoporous silica nanoparticles with an average diameter of about 90 nm as a platform for coating one of the hemisphere sides with a thin nano-gold layer. The mesoporous silica was chosen as a transparent material for photo-control and spectroscopic monitoring with appropriate pore sizes. Its core structure allowed transport and release of some organic compounds (Rhodamine 6G). On the other hand, the gold nano-layer enabled to conjugate chemically with cysteine amino acid. Thus, the nanomachine could readily target and specifically identify the pathogenic *E. coli* through biological recognition due to the occurrence of electrostatic interaction with the bacterial membrane proteins.

**Keywords:** Janus nanoimpeller, light-activation, pathogenic bacteria targeting

### ПРОЕКТИРАНЕ НА САМОХОДЕН ЯНУС НАНОИМПЕЛЕР КАТО НАНОМАШИНА ЗА НАСОЧВАНЕ И УНИЩОЖАВАНЕ НА ПАТОГЕННИ МИКРООРГАНИЗМИ

Светлин Тошев<sup>1</sup>, Александър Луканов<sup>1,2</sup>, Сейчиро Накабаяши<sup>2</sup>

<sup>1</sup> Минно-геоложки университет "Св.Иван Рилски", 1700 София

<sup>2</sup> Университет Сайтама, Сакура-ку, 338-8570 Сайтама

**РЕЗЮМЕ.** В този доклад е представен дизайна и способността на самоходен Янус наноимпелер, като наномашина за насочване и унищожаване на патогенни микроорганизми, като грам отрицателната *Escherichia coli* 0157:H7 в природни водни среди. Наномашината беше изработена от мезопорести силициеви наночастици със среден диаметър около 90 нм, като платформа за покриване на едната полусфера с тънък нано-слой от злато. Мезопорестия силициев диоксид беше избран, като прозрачен материал за фотоконтрол и спектроскопски мониторинг с подходящи размери на порите. Неговата ядрена структура позволява транспортиране и освобождаване на някои органични съединения (Rhodamine 6G). От друга страна, нанослоят от златно покритие дава възможност да се конюгира химически с аминокиселината цистеин. По този начин наномашината лесно може да се насочи и да идентифицира специфично патогенната *E. coli*, чрез биологично разпознаване, поради възникващото електростатично взаимодействие с бактериалните мембранни протеини.

**Ключови думи:** Янус наноимпелер, светлинно-активиране, насочване към патогенни бактерии

### Introduction

A widely known approach for preparation of self-propelling nanomachines involves asymmetrically coated catalytic nanoparticles (Yi et al., 2016). Such two-faced nanoparticles (NPs) are named Janus (in honour of the two-faced Roman god Janus) and they typically consist of two hemispheres with different elemental composition and surface chemistries on the opposite sides (Lattuada, Hatton, 2011). The Janus design allows diverse chemical and physical functionality of NPs, especially the induction of catalytic propulsion in liquid media (Yang, Loos, 2017). Thus, the nanomachines designed for self-propulsion motion on Janus principle must comprised also of asymmetric catalytic and non-catalytic faces on their surface. The decomposition of fuel molecules (for example  $H_2O_2$  to  $H_2O$  and molecular oxygen) on the catalytic face generate a propulsive force that drives the nanomachine motion (Ke et al., 2010). The first active movement of Janus particles was invented by using asymmetric Pt-coated polystyrene (Howse et al., 2007) and Pt-coated silica microspheres (Gibbs, Zhao,

2009). It was proved that the coating of one hemisphere of mesoporous silica nanoparticle with elemental Pt is sufficient to achieve a self-propulsion force of the fabricated nanocomposite in dilute hydrogen peroxide fuel solution. As mentioned above, the reason for movement is due to the catalytic decomposition of the peroxide molecule (used as fuel) into oxygen molecules and water. In all experiments the obtained propulsion velocity increased with raising the peroxide fuel concentration. However, if magnetic nanoparticle is coated on the one side by platinum (named as magnetic Janus nanomachine) the motion can be guided by use of external magnetic field in biological media instead of the toxic peroxide. In this case, the magnetic field might influence not only the direction of the Janus nanomachine but also on its speed (Baraban et al., 2013), which allowed reverse direction of the movement too. The bimetallic Janus spheres with Pt and Au coating on the opposite sides can move in aqueous solution at speeds comparable to bimetallic nanowire motors (Wheat et al., 2010). Further miniaturisation of their spherical diameter, along with biocompatibility open new fields of biotechnological

applications. In addition, higher efficient propulsion can be achieved by opening of a stomatocyte ("nozzle") that serves as an outlet for the generated molecular oxygen. The self-propelling motion of such stomatocyte nanomotor is controlled by both bubbles propulsion and self-diffusiophoresis, which can operate even at very low fuel concentrations (Wilson et al., 2013). The ability for trajectory navigation of these nanomachines and for regulation of their speed is of high importance with respect to the biotechnological application and bacterial targeting. The guiding of Janus nanomachines motion to their target destinations without the use of externally applied fields is essential for the research progress of modern nanomotor science. Another alternative approach is to achieve an autonomous movement through following the concentration gradient of different signalling chemicals (Ebbens et al., 2012). Nevertheless, such external stimuli as temperature, light and/or electric potential can be also used for motion triggering and speed regulation. For example, the temperature control is an attractive method for NPs speed regulation (Balasubramanian et al., 2009). As an example, the thermally induced acceleration or deceleration might reflect on the primarily heat-induced changes of the NPs solution viscosity. By this approach a wide range of NPs speeds can be generated through simply tuning the applied temperature. The speed of artificial nanomachines can be modulated as well as accelerated also via local heating by laser irradiation (Liu et al., 2013). Upon the laser power the propulsion speed displayed a clear linear dependence, the process is reversible and it can be repeated continuously with high reproducibility. Another promising biotechnological application of the Janus nanomachines based on the properties explained above is targeting and drug delivery to single cells, imaging probe or molecular biosensing of the internal cell components. By this approach, a single Janus nanoparticle with incorporated multiple compartments can be exploited to detect and destroy various types of pathogenic cells. The purpose of this report is to develop Janus nanoimpeller for detection and inhibition of *Escherichia coli*. In our study mesoporous silica nanoparticles were coated on the one hemisphere side with a thin nano-gold layer in order to obtain a Janus like nanoimpeller, which was capable to target and destroy *E. coli*. For this purpose, template silica nanoparticles can be used as a convenient platform for coating with gold and attaching of biomolecules that might undergo large amplitude motions. The mesoporous silica NPs are easy to synthesise and such mesostructured particles are transparent materials (for photo-control and spectroscopic monitoring). They can be fabricated into nanoimpellers with useful morphological properties with respect to the designed pore sizes and structures. The cargo transport and release inside the mesoporous silica NPs can be controlled by photoinduced cis-trans isomerisation of diazo bonds (-N=N-) of various azobenzene derivatives which are tethered to the interiors of the mesopores (Angelos et al., 2007). In this report, upon the continuous excitation with blue light (475 nm) the nanoimpeller enabled the cis- and trans-isomers of diazo bonds to be in constant isomerisation reaction at the mesoporous interior. This caused a dynamic wagging of the untethered terminus and impelled the cargo molecules through the pores of mesoporous silica. In addition, it was proven that the transport control can be made to occur in a dynamic manner in the nanomachines with size less than 100 nm containing 2-3 nm diameter pores. The obtained

mesoporous structure enabled also a high drug loading capacity as well as time and light irradiation-depending drug release. The pores might be sealed by a gatekeeper system which could be also used for additional functionalisation with ligands and improvement of the whole specific characteristics.

## Experimental Procedures

### Materials and analytical instrumentation

All chemicals used in the protocols below were of analytical-reagent grade. UV-VIS spectroscopy was performed on UV-VIS Jasco analytical spectrophotometer (model No V-570) using 1 cm quartz cuvette. The zeta potential of NPs was measured using a ZetaPALS Zeta Potential Analyzer (Brookhaven Instrument Corporation). Nanoparticle size distribution was determined using dynamic light scattering (DLS, Zetasizer Nano ZS) and transmission electron microscope (TEM). TEM micrographs of nanoimpellers and *E. coli* 0157:H7 bacteria were taken by JEOL JEM-3100FFC TEM at 300 kV accelerating voltage equipped with Hilbert differential contrast (HDC) phase plate. The collected labelled bacteria cells were dropped on a copper micro-grid coated with amorphous carbon film (20 nm in thickness). The liquid suspension was removed by a filter paper and *E. coli* cells were rapidly frozen in liquid ethane by rapid freezing device (Leica Microsystems, Germany). The frozen cells were kept in a liquid nitrogen for a while. Finally, the frozen labelled *E. coli* were transferred and observed in the transmission electron microscope by cryo-transfer system.

### Synthesis of mesoporous silica nanoparticles (MSN)

MSN were synthesised based on a modified synthesis by using tetraethyl orthosilicate (TEOS) as a precursor reagent for condensation of silica, and of different other template additives, such as cetyltrimethylammonium bromide (CTAB) surfactant, polymers, micelle forming agents or dopants. In brief, the surfactants were stirred in a mixture of ultrapure MilliQ water and ethyl alcohol under basic conditions, and TEOS or other silicates were added under agitation of the reaction suspension. The silica sources concentrations and compositions, as well as the template-agents and stirring conditions determined the nanoparticle size, pore diameter and shape. When the surfactant precursor concentration was above the critical micelle concentration, CTAB is self-aggregating into micelles and the silica reagents condensate at the surface. Thus the silica structure was formed around the surface of obtained micelles. Then, the surfactants were completely removed through centrifugation to obtain biocompatible mesoporous silica nanoparticles which were further coated with gold and modified with diazobenzene derivatives and conjugated cysteine amino acid (as capping ligands). The obtained common pore diameter distribution of MSN ranges between 2 and 5 nm. The nanoimpeller pores were saturated with the organic dye Rhodamine 6G.

### Deposition of gold nanolayer on MSN

The used electroless metal plating technique for Au deposition on MSN spheres includes three steps (Kobayashi et al., 2005). The first step is surface sensitisation of the silica spheres. The second step is surface activation and the final third step is gold plating. The obtained Janus nanoparticles

were washed and kept in a refrigerator in order to be used in next experiments.

**Surface functionalisation of the Janus nanoimpeller with cysteine capping on the gold hemisphere and detection of *E. coli***

Stock solution of cysteine was prepared in CH<sub>3</sub>COONa buffer (0.01 M sodium acetate, pH 10). The immobilisation of cysteine amino acid on the surface of gold coated hemisphere was done by mixing the biomolecule solution with NPs in a 1: 1

ratio and leaving the solution to react for 24 hours at ambient temperature. During the reaction there was a visible colour change of the mixed solution. After that the suspension was subjected to ultracentrifugation in order to separate the nanoparticles with the unreacted cysteine in the suspension. The culture of *E. coli* 0157:H7 was prepared as follows: 50 µl of the antibiotic bacterial suspension was inoculated into 5 ml M9 medium at 37°C for 4h to reach the exponential growth phase.

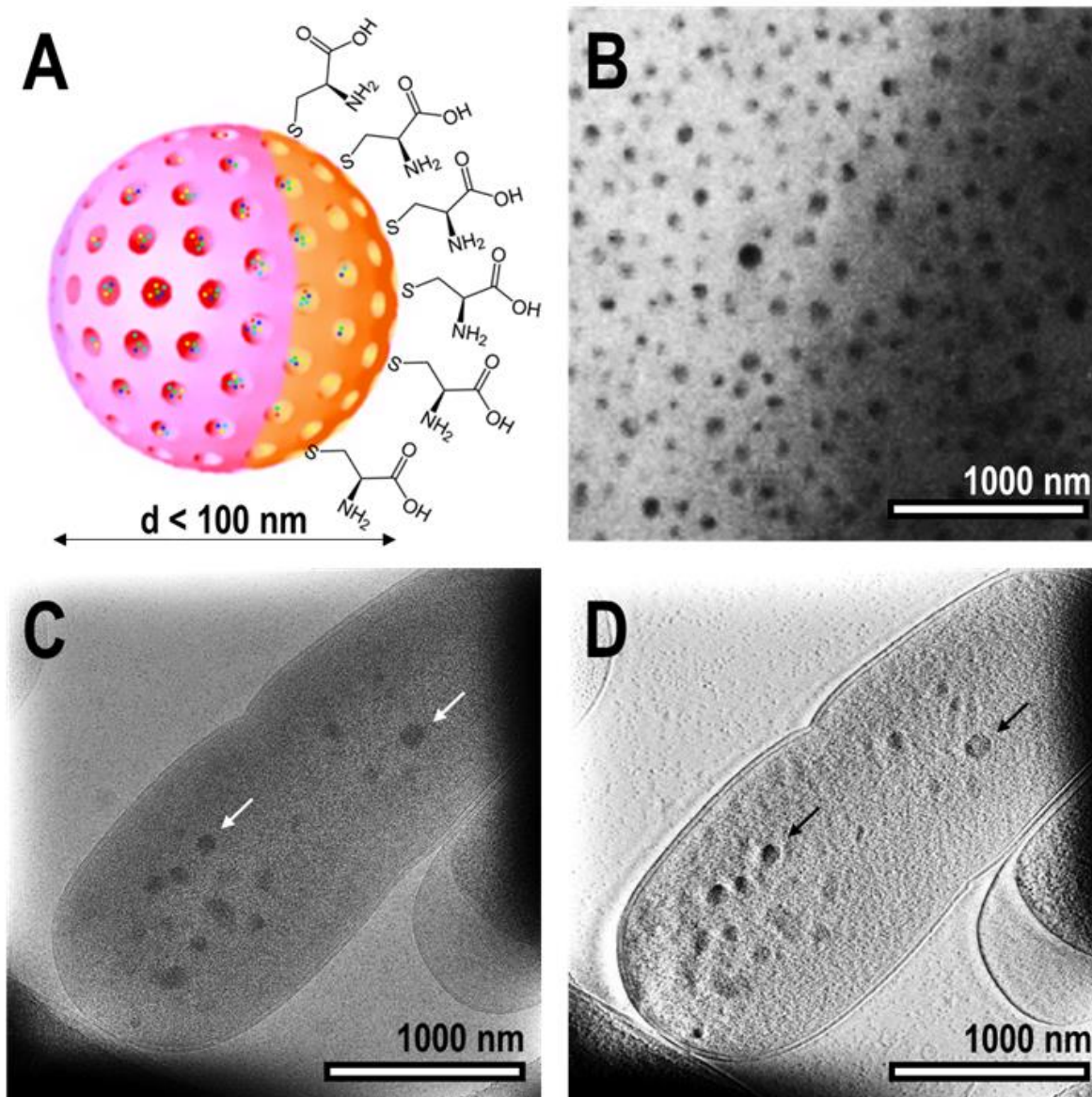


Fig. 1. Self propelling Janus nanoimpeller. (A) Schematic illustration of the nanomachine design. (B) TEM micrograph of Janus nanoimpellers on graphite carbon film with 20 nm thickness. (C) TEM micrograph of cryo-embedded *E. coli* labelled with Janus nanoimpellers (as shown with the arrows). (D) Same object observed with phase-plate Hilbert-differential contrast TEM in order to obtain higher contrast image; scale bar for B, C and D = 1000 nm (1 µm)

**Results and discussion**

**Characterisation of the design of Janus nanoimpeller as a functionalised nanomachine for self-propulsion and drug delivery system**

The design of fabricated two-faced Janus nanoimpeller is shown on Fig. 1A. This self-propelling nanomachine was

functionalised with amino acid cysteine on the gold hemisphere for targeting pathogenic microorganisms. The obtained bonds between the nanoimpeller surface coated with a gold nanolayer and the cysteine ligands shell were covalent through the thiol groups from the amino acid residue. The photo transparent mesoporous core of silica can be loaded with various payload materials (in our experiment with Rhodamine

6G) and capped with the so-called gatekeeper (azobenzene derivatives). The fabricated nanoimpeller particles possess spherical geometric shapes (Fig. 1B) with an average diameter of about  $90 \pm 8$  nm as confirmed with TEM observation and the measurement with dynamic light scattering. The pores inside the nanoparticle core have much smaller diameter with average distribution range between 2 and 5 nm, which enabled to be saturated as a drug delivery system with various organics (in the current experiment as mentioned above with the photosensitizer Rhodamine 6G). The surface plasmon resonance (SPR) peak maximum of the gold coated hemisphere was red-shifted due to the conjugation with cysteine amino acid residues. Under excitation with blue laser diode (InGaN) at 475 nm (for about 10 min) and 9 mW energy dose the azobenzene motion was excited. The organic dye Rhodamine 6G was released in the analysed solution and its amount was measured as a plot function of absorbance maximum and concentration. As a control experiment the nanoimpeller particles were irradiated with equal power but at wavelength of 650 nm at which there was not any absorption of the azobenzene group. In the control experiment there was no releasing of organic dye. These data proved unambiguously that the Janus nanoimpeller responds only to the wavelength that drives the photo-induced cis-trans isomerisation and motion of the azobenzene group, which was tethered to the interiors of the nanomachine mesopores. The releasing of dye molecules inside the nanomachine mesopores upon continuous excitation was in irradiation-depending manner, which demonstrates an "impeller" mechanism of operation of the designed Janus nanoimpeller. The reason is because the excitation of the azobenzene on the nanoparticle surface caused the Rhodamine 6G dyes molecules to wag back and forth and thus effectively imparted the motion of trapped organic compounds in the drug delivery system. This physicochemical process allows them to traverse the pore interior until they escape in the bacterial suspension solution. These data proved the drug-releasing ability of the nanomachine to be controlled by the laser irradiation dose and wavelength.

#### **Bio-detection ability of the nanomachine for targeting and destruction of gram negative pathogenic microorganisms**

To demonstrate the bio-detection ability of the Janus nanoimpeller as a functionalised nanomachine it was determined whether the capping amino acid cysteine ligands on the gold hemisphere surface facilitate targeting and anchoring of the nanomachine onto bacterial cell membrane surface. When the functionalised Janus impeller is added in a bacterial suspension of *E. coli* 0157:H7 shifting of the plasmon absorption peak to longer wavelength region (so called red-shifting effect) can be measured. The reason for the occurred SPR optical effect is that the nanomachine can readily target and specifically identify *E. coli* through biological recognition due to the electrostatic interaction between amino acid charges and bacterial membrane proteins. It was also found that the degree of resulted aggregation onto the cell membrane is completely dependent on the nanoparticle concentration. Analytical cryo- TEM analysis was performed in order to prove the hypothesis of biological recognition occurrence and anchoring of functionalised Janus nanoimpeller on the gram negative *E. coli* bacteria (as shown on Fig. 1C). As shown on the TEM micrographs the nanomachines have come closer to

one another on the cell membrane, which is a clear indication of the occurred electrostatic forces of bio-recognition interactions. To obtain higher contrast imaging of the objects the same, ice-embedded cells were observed and analysed also with 300 kV phase-plate Hilbert-differential contrast TEM (Fig. 1D). On this highly-contrasted image the discrete ultrastructure of bacteria without any preliminary chemical preparation could be observed. The microscopic analysis demonstrated that the nanomachines are attached to the cell membrane but they have not entered inside the cell cytoplasm. Under photo-controlled conditions with laser irradiation the nanomachines can release their payload and generate reactive oxygen species, which have a lethal effect on the pathogenic bacteria.

## **Conclusion**

We have designed and fabricated a functionalised Janus nanoimpeller as a self-propelling nanomachine for targeting and destruction of gram negative pathogenic microorganisms. For that purpose, the optically transparent mesoporous silica nanoparticles were loaded with the photosensitizer Rhodamine 6G and their hemispheres were coated with a gold nano-layer. The release of the organic dye can be controlled by photoinduced isomerisation of the azobenzene molecules, which were tethered to the interiors of the mesoporous silica. The process can be controlled by excitation with blue light. The proposed design opens a new field for development of multifunctional nanomachines for inhibition of pathogenic microorganisms. The reported Janus impeller might find numerous applications in the field of biosensors technology, mineral biotechnology and environmental protection.

**Acknowledgment.** This study was accomplished thanks to the bilateral agreement between Saitama University, Japan and the University of Mining and Geology "St. Ivan Rilski", Sofia, Bulgaria. The authors would like to express their gratitude to Saitama University for the financial support of the reported investigations.

## **References**

- Angelos, S., E. Choi, F. Vögtle, L. De Cola, J. Zink. 2007. Photo-driven expulsion of molecules from mesostructured silica nanoparticles. – *J. Phys. Chem. C* 111, 6589–6592.
- Balasubramanian, S., D. Kagan, C. M. Hu, S. Campuzano, M. J. Lobo-Castanon, N. Lim, D. Y. Kang, M. Zimmerman, L. Zhang, J. Wang. 2011. Micromachine enables capture and isolation of cancer cells in complex media. – *Angew. Chem. Int. Ed.*, 50, 4161–4164.
- Baraban, L., D. Makarov, O. G. Schmidt, G. Cuniberti, P. Leiderer, A. Erbe. 2013. Control over Janus micromotors by the strength of a magnetic field. – *Nanoscale*, 5, 1332–1336.
- Ebbens, S. J., G. A. Buxton, A. Alexeev, A. Sadeghi, J. R. Howse. 2012. Synthetic running and tumbling: an autonomous navigation strategy for catalytic nanoswimmers. – *Soft Matter*, 8, 3077–3082.
- Gibbs, J. G., Y. P. Zhao. 2009. Autonomously motile catalytic nanomotors by bubble propulsion. – *Appl. Phys. Lett.*, 94, 163104–163107.

- Howse, J. R., R. A. L. Jones, A. J. Ryan, T. Gough, R. Vafabakhsh, R. Golestanian. 2007. Self-motile colloidal particles: from directed propulsion to random walk. – *Phys. Rev. Lett.*, 99, 048102.
- Ke, H., Y. Shengrong, R. L. Carroll, K. Showalter. 2010. Motion analysis of self-propelled Pt-silica particles in hydrogen peroxide solutions. – *J. Phys. Chem. A* 114, 5462–5467.
- Kobayashi, Y., Y. Tadaki, D. Nagao, M. Konno. 2005. Deposition of gold nanoparticles on silica spheres by electroless metal plating technique. – *J. Colloid and Interface Sci.*, 283, 601–604.
- Lattuada, M., T. A. Hatton. 2011. Synthesis, properties and application of Janus nanoparticles. – *Nano Today*, 6, 286–308.
- Liu, Z., J. Li, J. Wang, G. Huang, R. Liu, Y. Mei, 2013. Small-scale heat detection using catalytic microengines irradiated by laser. – *Nanoscale*, 5, 1345–1352.
- Wheat, P. M., N. A. Marine, J. L. Moran, J. D. Posner. 2010. Rapid fabrication of bimetallic spherical motors. – *Langmuir* 26, 13052–13055.
- Wilson, D. A., B. van Nijs, A. van Blaaderen, R. J. M. Nolte, J. C. M. van Hest. 2013. Fuel concentration dependent movement of supramolecular catalytic nanomotors. – *Nanoscale*, 5, 1315–1318.
- Yang, Q., K. Loos. 2017. Janus nanoparticles inside polymeric materials: interfacial arrangement toward functional hybrid materials. – *Polym. Chem.*, 8, 641–654.
- Yi, Y., L. Sanchez, Y. Gao, Y. Yu. 2016. Janus particles for biological imaging and sensing. – *Analyst*, 141, 3526–3539.

## SEMI-PASSIVE TREATMENT OF MINE WASTE WATER IN ANAEROBIC CONDITIONS

*Plamen Tsvetkov, Svetlana Bratkova*

*University of Mining and Geology "St. Ivan Rilski", Sofia 1700; s\_bratkova@yahoo.com*

**ABSTRACT.** In this study synthetic acid mine waters, similar to the naturally generated ones in mines, were treated by a passive system under anaerobic conditions. The constructed laboratory-scaled system consisted of three anaerobic chambers connected sequentially, each one with a volume of 15 l. Each chamber was filled with a mixture of 4.5 kg of solid organic substrate (cattle manure, sawdust and hay in a ratio 4:1:1) and 2 kg of limestone with particles size distribution of 5÷10 mm. The model solution contained  $\text{SO}_4^{2-}$  (3000 mg/l),  $\text{Cu}^{2+}$  (10 mg/l),  $\text{Zn}^{2+}$  (25 mg/l),  $\text{Cd}^{2+}$  (5 mg/l),  $\text{As}^{5+}$  (5 mg/l),  $\text{Fe}^{2+}$  (100 mg/l) and  $\text{Mn}^{2+}$  (20 mg/l). Passive and semi-passive treatment was conducted at a hydraulic retention time of 6 days. During the stage of semi-passive treatment, lactate was added as an additional carbon and energy source. The results demonstrated that the sulphate-removal efficiency from mine waste water by passive treatment was insignificant (approx. 9 %), while the addition of lactate at concentrations of 1, 2, 3 and 4 ml/l increased the removal rate for sulphates as follows: 35.7 %, 67.1 %, 82.3 % and 98.3 %. In all studied regimes the ions of copper, iron, zinc, cadmium and arsenic were effectively removed (97 %-99.9 %). The rate of manganese removal was low (30 %). The results could serve as a basis for the establishment of pilot-scaled installations for semi-passive treatment of acid mine water in the studied manner.

**Keywords:** acid mine water, sulphate-reduction, semi-passive treatment

### ПОЛУПАСИВНО ТРЕТИРАНЕ НА МИННИ ОТПАДЪЧНИ ВОДИ В АНАЕРОБНИ УСЛОВИЯ

*Пламен Цветков, Светлана Браткова*

*Минно-геоложки университет "Св. Иван Рилски", 1700 София*

**РЕЗЮМЕ.** Проследено е пречистването на синтетични кисели руднични води, имитиращи генерираните в миннодобивната дейност в лабораторна инсталация за анаеробно пасивно третиране. Лабораторната инсталация е изградена от три последователно свързани анаеробни камери, всяка с обем 15 l. Всеки съд е запълнен със смес от 4.5 kg твърд органичен субстрат (говежда тор, дървени стърготини и сено в съотношение 4:1:1) и 2 kg варовик с размер на частиците 5÷10 mm. Третираният моделен разтвор съдържа  $\text{SO}_4^{2-}$  (3000 mg/l),  $\text{Cu}^{2+}$  (10 mg/l),  $\text{Zn}^{2+}$  (25 mg/l),  $\text{Cd}^{2+}$  (5 mg/l),  $\text{As}^{5+}$  (5 mg/l),  $\text{Fe}^{2+}$  (100 mg/l) и  $\text{Mn}^{2+}$  (20 mg/l). Проведено е пасивно и полупасивно третиране при осигурено контактно време от шест денонощия, като по време на стадия за полупасивно третиране в системата е добавен лактат като допълнителен източник на въглерод и енергия. Установено е, че ефективността на отстраняване на сулфати от водите при пасивно третиране е приблизително 9 %, а при добавяне на лактат в концентрации 1, 2, 3 и 4 ml/l сулфатите на изхода на инсталацията намаляват съответно с 35.7 %, 67.1 %, 82.3 % и 98.3 %. При всички изследвани режими ефективно се отстраняват йоните на тежките метали – мед, желязо, цинк, кадмий и арсен (97 % – 99.9 %). Степента на отстраняване на мангана е ниска – около 30 %. Получените резултати и направените от нас констатации, биха могли да послужат като основа за изграждане на пилотни инсталации, базирани на полупасивно третиране по установен начин.

**Ключови думи:** кисели руднични води, сулфат-редукция, полупасивно третиране

### Introduction

The formation of acid mine water is a natural result of the exploitation of sulphide minerals, ores and coal deposits, abandoned mine sites and mining waste dumps. The negative environmental impact of acid mine drainage (AMD) water is due to its high content of heavy metals, toxic and radioactive elements. Discontinuance and mobility of mine wastewater generation is often difficult and even impossible task, and requires additional treatment of these waters. A passive treatment technology has typically been applied to the treatment of seeps from waste rock piles, acid mine drainage and tailings impoundments at abandoned mine sites. This technology can be also suitable at active mining operations as a means of effluent remediation from tailings ponds for off-site discharge. The systems of this type use completely natural and biological mechanisms to remove sulphate and heavy metals from mine wastewater. For acid mine waters that have a net acidity greater than zero, the treatment design needs to involve systems that add alkalinity. The most common inorganic

source of alkalinity for passive AMD treatment is limestone ( $\text{CaCO}_3$ ).

After the neutralisation of wastewater, depending on the flow rate and type of pollutants, the passive system may include aerobic or anaerobic treatment facilities (Skousen et al., 2019; Naidu et al., 2019).

Treatment of metal-containing wastewaters with sulphate-reducing bacteria (SRB) is quite promising as an alternative to chemical methods. The microbial sulphate reduction in passive treatment of mine water is carried out in anaerobic cells, anaerobic constructed wetlands, sometimes called 'bioreactors' and alkalinity producing system (RAPS), which is also referred to as a successive alkalinity producing system (SAPS) (Taylor et al., 2005). Under anaerobic conditions SRB use sulphate as a terminal electron acceptor for the organic compounds oxidation and produce hydrogen sulphide. Heavy metals are precipitated in the form of sulphides or carbonates. The systems can be suitable for acidic medium and can also function at sub-zero temperatures (Martínez et al., 2019). A few metals (Fe, Cu, Pb, Zn, Cd, Ni e.d.) are successfully

removed by anaerobic constructed wetlands, but manganese, arsenic and cyanides are better removed under aerobic passive systems than anaerobic ones (Fernandez-Rojo et al., 2019; Muhammad et al., 2015).

Although passive systems for improving water quality have certain advantages over natural processes, they are highly complex and susceptible to many factors such as flow rates, hydraulic retention time, rainfall, temperature variations and e.d. (Alsaiani, Tang, 2018). Solid substrates have a limited lifetime and have to be replaced or supplemented with liquid or gaseous substrates once the original substrate has been depleted. Many passive treatment installations require some periodic operation, such as carbon source addition or temperature control to sustain the desired processes and conditions. Under these conditions, they are referred to as semi-passive (Nielsen et al., 2018).

The main objective of the present study is to determine the influence of the amount of added lactate on the removal of sulphate, heavy metals and arsenic in the conditions of semi-passive treatment of mine wastewater.

## Materials and methods

### Design of laboratory installation

The anaerobic wetland consists of three cascade connected anaerobic cells - cuboidal containers with length 190 mm, width 150 mm and an altitude of 560 mm (Fig. 1). Each container is filled with a mixture of 4.5 kg solid organic matter (cow manure, hay and sawdust in the ratio 4:1:1) and 2 kg limestone (particles size 5-10 mm). Water enters in the first anaerobic cell by a PVC tube (50 mm diameter) reaching the bottom of the container. Thus, upstream of the treated water is provided and the volume of the substrate is optimally utilised. The outlet water from the first cell proceeds in the same way in the second cell. The effluent water from the second cell passes through a perforated PVC pipe (50 mm diameter) reaching the bottom of the third container.

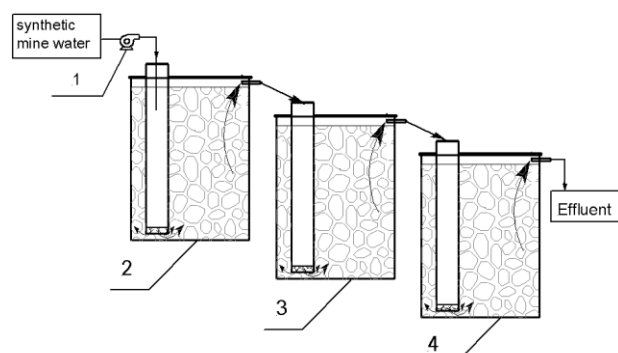


Fig. 1. Design of the laboratory installation: (1) peristaltic (roller) pump, (2, 3 and 4) anaerobic cell

The anaerobic cells were inoculated with mixed cultures of sulphate-reducing bacteria. The inoculum contains genera, belonging to the species *Desulfotomaculum*, *Desulfovibrium*, *Desulfomicrobium* and *Desulfobacterium*.

### Process operation

Synthetic mine water containing iron and copper was treated through the so-constructed laboratory installation

during the period 2013-2017. Within this period, more easily degradable biopolymers were depleted and wastewater purification efficiency decreased to 10% of the initial results.

New research was carried out in 2018. The synthetic mine waters contain  $\text{SO}_4^{2-}$  (3000 mg/l),  $\text{Fe}^{2+}$  (100 mg/l),  $\text{Zn}^{2+}$  (25 mg/l),  $\text{Mn}^{2+}$  (20 mg/l),  $\text{Cu}^{2+}$  (10 mg/l),  $\text{Cd}^{2+}$  (5 mg/l) and  $\text{As}^{5+}$  (5 mg/l). The heavy metals and arsenic were imported in the form of  $\text{FeSO}_4 \cdot 7\text{H}_2\text{O}$ ,  $\text{ZnSO}_4 \cdot 7\text{H}_2\text{O}$ ,  $\text{MnCl}_2 \cdot 4\text{H}_2\text{O}$ ,  $\text{CuSO}_4 \cdot 5\text{H}_2\text{O}$ ,  $\text{CdCl}_2 \cdot 2.5\text{H}_2\text{O}$  and  $\text{K}_2\text{HAsO}_4$ . The concentration of sulphates was adjusted to 3.0 g/l by the addition of  $\text{Na}_2\text{SO}_4$  and  $\text{MgSO}_4 \cdot 7\text{H}_2\text{O}$ . The pH of the synthetic mining water was adjusted to 4.6 by sulphuric acid. Passive and semi-passive treatment was performed by maintaining hydraulic retention time of 6 days. Lactate at concentrations of 1, 2, 3 and 4 ml/l was added as an additional source of carbon and energy during the semi-passive treatment stage.

### Analytical methods

The pH and Eh were measured in key points of the laboratory installation. The sulphate concentration was determined using spectrophotometric method by  $\text{BaCl}_2$ . The total sulphide concentration was measured immediately after sampling using Nanocolor test 1-88/05.09. The organic substrate concentration was estimated by measuring the chemical oxygen demand (COD). The dissolved metal and arsenic concentrations were determined by ICP spectrophotometry.

## Results and discussion

During the first three months, passive treatment of synthetic mine water was carried out. At this mode the pH of treated waste waters increased from 4.6 to 6.75, which is due to the chemical neutralisation with limestone and bicarbonate alkalinity production by sulphate-reducing bacteria (Fig. 2).

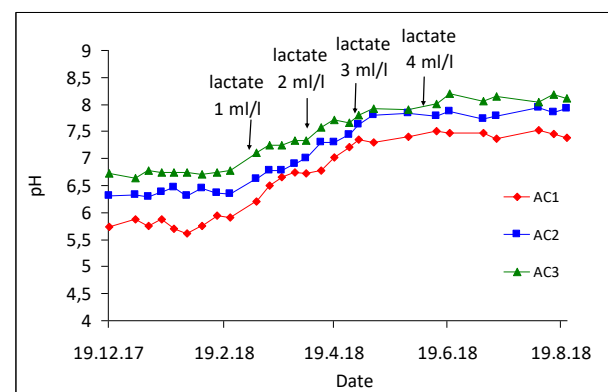


Fig. 2. Dynamics of pH during treatment of wastewater by laboratory installation

The concentration of sulphate at the outlet of the laboratory installation was very high – around 2715 mg/l, and the degree of sulphate removal was only 9% (Fig. 3).

The rate of microbial sulphate reduction under conditions of limitation of SRB with a source of carbon and energy was around 47.5 mg  $\text{SO}_4^{2-}$ /l/day. During this period the hydrogen sulphide was now detected in the effluent from the three anaerobic cells. However, the ions of copper, iron, zinc, cadmium and arsenic were effectively removed (93-99%). Most

of the pollutants were precipitated in the form of sulphides, but part of the iron was also precipitated in the form of ferric hydroxides at condition of increased pH in the anaerobic cells.

The COD values at the effluent were in the range of 78 to 105 mg/l. This shows that due to hydrolysis of the hardly degradable organic polymers in the solid organic substrate, low molecular weight organic compounds, which are used as electron donors for sulphate-reducing bacteria, still entered into the solution.

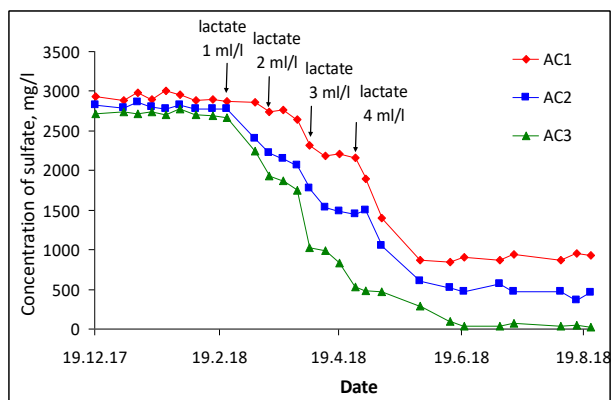


Fig. 3. Dynamics of concentration of sulphate during treatment of wastewater by laboratory installation

Semi-passive treatment of waste water was carried out over a period of 6 months. Sulphate-reducing bacteria oxidise simple organic compounds (such as lactate, acetate, butirate,

ethanol, glycerol, H<sub>2</sub> and other products of fermentations) with sulphate at anaerobic conditions. Lactate is one of the most preferred sources of carbon and energy for sulphate-reducing bacteria, performing incomplete oxidation of organic matter. For this purpose, lactate was added to the synthetic mine water in increasing concentration from 1 to 4 ml/l.

Data for basic chemical parameters of the effluents from anaerobic cells are presented in Table 1. The pH values of the effluent from the laboratory installation were higher than 7 for all tested regimes, due to the higher concentration of microbial produced HCO<sub>3</sub><sup>-</sup> ions by the sulphate reduction (Table 1). There is a correlation between the increase in lactic acid concentration and the increase in pH in the effluents from anaerobic cells (Fig. 2). At the same time, with the increase in the concentration of the organic compound, strong reduction conditions were established due to the increased amounts of microbial produced hydrogen sulphide. The lowest values of Eh (-445 - -497 mV) were measured by adding lactate to the treated wastewater at a concentration of 4 ml/l.

The addition of lactate to the treated water resulted in an increase in the rate of microbial sulphate reduction (Fig. 3). The rate of the process was respectively 178, 336, 412 and 492 mg SO<sub>4</sub><sup>2-</sup>/l.d at lactate concentrations of 1, 2, 3 and 4 ml/l.

We observed that the increase of concentration of lactate from 1 to 4 g/l led to an increase of the rate of the sulphate-reduction in a linear relation (Equation 1).

Table 1. Values of basic parameters in the effluents from anaerobic cells

Parameter	Effluents from anaerobic cells											
	Lactate – 1 ml/l			Lactate – 2 ml/l			Lactate – 3 ml/l			Lactate – 4 ml/l		
	AC1	AC2	AC3	AC1	AC2	AC3	AC1	AC2	AC3	AC1	AC2	AC3
pH	5.8±0.2	6.5±0.1	7.2±0.1	6.4±0.3	7.0±0.3	7.7±0.3	7.14±0.2	7.7±0.1	7.8±0.1	7.4±0.2	7.8±0.05	8.1±0.1
Eh, mV	-160 ±15	-250 ±18	-310 ±21	-320 ±19	-360 ±22	-410 ±19	-420 ±15	-447 ±21	-457 ±19	-454 ±21	-475 ±20	-479 ±18
SO <sub>4</sub> <sup>2-</sup> , mg/l	2864 ±25	2223 ±17	1930 ±30	2639 ±12	1485 ±25	986 ±27	2460 ±31	1324 ±25	531 ±32	910 ±27	360 ±26	50 ±15
H <sub>2</sub> S, mg/l	4 ± 4	8 ± 5	11 ± 4	17 ± 9	78 ± 11	133 ± 5	337 ± 21	548 ± 9	690 ± 16	488 ± 9	571 ± 11	716 ± 21
Fe <sup>2+</sup> , mg/l	21.45	0.341	0.114	5.74	1.31	0.091	2.56	1.08	0.10	1.33	0.08	0.07
Zn <sup>2+</sup> , mg/l	0.278	0.123	0.076	0.198	0.031	0.02	0.125	0.025	0.006	0.110	0.017	0.005
Mn <sup>2+</sup> , mg/l	10.23	7.43	4.67	11.09	8.54	5.96	11.54	9.43	5.78	10.99	8.97	6.06
Cu <sup>2+</sup> , mg/l	0.021	0.019	0.013	0.018	0.015	0.012	0.009	0.007	0.005	<0.005	<0.005	<0.005
Cd <sup>2+</sup> , mg/l	0.024	0.014	0.006	0.011	0.007	0.005	0.006	0.005	<0.005	<0.005	<0.005	<0.005
As <sup>5+</sup> , mg/l	2.54	0.014	0.006	0.011	0.007	0.005	0.006	0.005	0.005	<0.005	<0.005	<0.005
COD, mg/l	500 ±18	115 ±25	87 ±20	1246 ±25	766 ±10	136 ±20	2253 ±5	1683 ±25	693 ±20	3723 ±15	2253 ±25	2073 ±20

$$\text{Rate of sulphate-reduction, (mg/l.d)} = 101.8 \times \text{Concentration of lactate, (g/l)} + 100 \quad (R^2 = 0.9648) \quad (1)$$

The sulphate-reduction rates in natural and constructed wetlands reported in literature, range from 0.3 to 675 mg SO<sub>4</sub><sup>2-</sup>/l/day. Most of the reported values are between 30 and 150 mg SO<sub>4</sub><sup>2-</sup>/l/day. The results obtained show that the COD/SO<sub>4</sub><sup>2-</sup> ratio significantly influenced the sulphate reduction, and the COD/SO<sub>4</sub><sup>2-</sup> ratio can successfully control the rate of microbial sulphate reduction. In the present study the COD/SO<sub>4</sub><sup>2-</sup> ratio was 0.33, 0.67, 1 and 1.33 with the addition of lactate at concentrations of 1, 2, 3 and 4 g/l, respectively. The results are

also a proof of the formation of a stable microbial community in each anaerobic cell within the whole period of operation.

As the rate of microbial sulphate reduction increases, higher concentrations of excess hydrogen sulphide are observed (Table 1). This favours the efficient precipitation of heavy metals and arsenic as insoluble sulphides. In all studied regimes the ions of copper, iron, zinc, cadmium and arsenic were effectively removed (97-99.9%). The removal of manganese in anaerobic conditions was low – around 30%, as the main mechanism of Mn removal was the sorption of this heavy metal from the solid organic matter.

The effluent from the third anaerobic cell contained low concentration of sulphates. However, excess amounts of H<sub>2</sub>S, high value of COD, as well as Mn were determined in the effluent. The measured COD values of the outflow for laboratory installation were high because of the incomplete oxidation of lactate usually with acetate as an end product. This result shows that it is necessary to perform additional treatment of the wastewater. In the passive treatment, the removal of COD, excess hydrogen sulphide and manganese is done in aerobic wetlands. This oxidation step is necessary to remove COD and the excess of H<sub>2</sub>S as elemental sulphur. Under oxidising conditions, the divalent manganese is oxidised to a tetravalent and precipitated in the form of MnO<sub>2</sub>. At present, there are several types of constructed wetlands used for wastewater treatment (Vymazal, 2008). Free water surface systems are used in many countries. The vertical flow systems which are intermittently fed allow higher oxygenation of the bed.

## Conclusions

The following conclusions can be drawn from this study:

Passive systems are attractive in the treatment of mine waste water, but over time, due to the depletion of organic material, the efficiency of water purification decreases. One solution to this problem is the application of semi-passive treatment with the use of lactate as a source of carbon and energy.

The addition of lactate to the treated water resulted in an increase in the rate of microbial sulphate reduction, and the highest rate 492 mg SO<sub>4</sub><sup>2-</sup>/l.d being achieved was with the addition of 4 g/l of lactate.

The reduction of sulphates from 3000 mg/l to below 250 mg/l requires the addition of lactate at concentrations of 4 g/l.

The COD/SO<sub>4</sub><sup>2-</sup> ratio significantly influenced the sulphate-reduction. It was also found that the COD/SO<sub>4</sub><sup>2-</sup> ratio can successfully control the rate of microbial sulphate reduction.

Under anaerobic conditions of semi-passive treatment, the ions of copper, iron, zinc, cadmium and arsenic were effectively removed (97-99.9%), but the rate of manganese removal was low (30%).

The excess amounts of H<sub>2</sub>S, high value of COD, as well as Mn, are determined in the effluent from anaerobic cells, which requires further treatment of the waters in oxidising conditions.

**Acknowledgements.** This research was supported by the National Science Fund, Bulgaria under Grant No. ДН 07/7, 16.12.2016.

## References

- Alsaiani, A., H. L. Tang. 2018. Field investigations of passive and active processes for acid mine drainage Treatment: Are anions a concern? – *Ecological Engineering*, 122, 100–106.
- Fernandez-Rojo, L., C. Casiot, E. Laroche, V. Tardy, O. Bruneel, S. Delpoux, A. Desoeuvre, G. Grapin, J. Savignac, J. Boisson, G. Morin, F. Battaglia-Brunet, C. Joulain, M. Héry. 2019. A field-pilot for passive bioremediation of As-rich acid mine drainage. – *Journal of Environmental Management*, 232, 910–918.
- Martínez, N. M., M. D. Basallote, A. Meyer, C. R. Canovas, F. Macías, P. Schneider. 2019. Life cycle assessment of a passive remediation system for acid mine drainage: Towards more sustainable mining activity - *Journal of Cleaner Production*, 211, 1100–1111.
- Muhammad, S. N., F. M. Kusin, M. S. Md Zahar, N. Halimoon, F. M. Yusuf. 2015. Passive treatment of acid mine drainage using mixed substrates: batch experiments. – *Procedia Environmental Sciences*, 30, 157–161.
- Naidu, G., S. Ryu, R. Thiruvenkatachari, Y. Choi, S. Jeong, S. Vigneswaran. 2019. A critical review on remediation, reuse, and resource recovery from acid mine drainage. – *Environmental Pollution*, 247, 1110–1124.
- Nielsen, G., I. Hatam, K. A. Abuan, A. Janin, L. Coudert, J. F. Blais, G. Mercier, S. A. Baldwin. 2018. Semi-passive in-situ pilot scale bioreactor successfully removed sulphate and metals from mine impacted water under subarctic climatic conditions. – *Water Research*, 140, 268–279.
- Skousen, J. G., P. F. Ziemkiewicz, L. M. McDonald. 2019. Acid mine drainage formation, control and treatment: Approaches and Strategies. – *The Extractive Industries and Society*, 6, 241–249.
- Taylor, J., S. Pape, N. Murphy. 2005. A Summary of Passive and Active Treatment Technologies for Acid and Metalliferous Drainage (AMD). – *Fifth Australian Workshop on Acid Drainage*, 29-31 August 2005.
- Vymazal, J. 2008. Constructed wetlands for wastewater treatment: a review. – *Proceedings of Taal 2007: The 12<sup>th</sup> World Lake Conference*, 965–980

## COMPLEX PROCESSING OF SAPONITE WASTE OF A DIAMOND-MINING ENTERPRISE

*Olga S. Zubkova, Alexey I. Alexeev*

*St. Petersburg Mining University, 199106 St. Petersburg; zubkova-phd@mail.ru*

**ABSTRACT.** The article is devoted to the problem of enrichment of saponite diamond-bearing ore and the problem of utilisation of the enrichment waste. The characteristics of the deposit and the shortcomings of the existing diamond mining method are given, a review of the literature on this issue is made. The material balance of production is shown in the article, the mineralogical composition of the saponite effluent is given and the main tasks for creating a closed water circulation system are put forward on the basis of material balance. The proposed scheme is constructed as follows: extraction of ore → ore enrichment → production of concentrate → waste while enrichment of ore → pure water produced by diluting and thickening the waste with calcium aluminosilicate reagent → obtaining calcium aluminosilicate reagent from condensed waste. The article describes the mineral composition of saponite pulp after the process of enrichment of diamond-bearing ore investigated by X-ray fluorescent method. Research is presented on the deposition of saponite pulp with different reagents (aluminium sulphate, oxychloride, polyacrylamide flocculant) compared with calcium aluminosilicate. The scheme of the closed water circulation of the processing plant and utilisation of the condensed product is presented taking into account the chemical composition.

**Keywords:** diamond ore, saponite, closed cycle of water circulation

### КОМПЛЕКСНА ОБРАБОТКА НА САПОНИТНИ ОТПАДЪЦИ В ПРЕДПРИЯТИЕ ЗА ДОБИВ НА ДИАМАНТИ

*Олга С. Зубкова, Алексей И. Алексеев*

*Санктпетербургски минен университет, 199106 Санкт Петербург*

**РЕЗЮМЕ.** Статията е посветена на проблема за обогатяването на сапонитната диамантоносна руда и проблема с оползотворяването на отпадъците от обогатяването. Дадени са характеристиките на находището и недостатъците на съществуващия метод за добив на диаманти, направен е преглед на литературата по този въпрос. В статията е показан материалният баланс на производството, даден е минералният състав на сапонитните отпадъчни води и са изведени основните задачи за създаване на затворена циркулационна система въз основа на материалния баланс. Предложената схема е изградена по следния начин: извличане на руда → обогатяване на руда → производство на концентрат → отпадъци при обогатяване на руда → чиста вода, получена чрез разреждане и съгъстяване на отпадъците с калциев алумосиликатен реагент → получаване на калциев алумосиликатен реагент от кондензирани отпадъци. В статията се описва минералният състав на сапонитната пулпа след обогатяването на диамантоносна руда, изследван чрез рентгенов флуоресцентен метод. Представени са изследвания за отлагането на сапонитна пулпа с различни реагенти (алуминиев сулфат, оксихлорид, полиакриламиден флокулант) в сравнение с калциевия алумосиликат. Представена е схемата на затворената циркулация на водата в преработвателното предприятие и използването на кондензирания продукт, като се взема предвид химичният състав.

**Ключови думи:** диамантена руда, сапонит, затворен цикъл на циркулация на водата

### Introduction

The assessment of the ecological status and well-being of natural systems and their effective protection and appropriate use are among the major problems of social and economic importance.

The diamond deposit named after M. V. Lomonosov is the main object in the development of the diamond mining industry in the European North of Russia. Its development will be accompanied by a violation of the lithological base of the landscape, changes in the hydrological characteristics of the watercourses in the area of the deposit, and impacts on groundwater. In general, the main factors affecting the components of the environment are as follows (Groshev, 2003):

- Dust emissions from open mine workings that pollute the atmospheric air and form anthropogenic anomalies that are contrasting and really significant (Groshev V.A. 2003.);
- Deflation and erosion of tailing dumps of concentrating factories, which form intensive scattering streams in water

systems and relatively local technogenic areas in soils (Groshev, 2003);

- Drainage from underground mine workings and quarries, which form intensive and extended scattering streams in water systems (Groshev, 2003);
- Effluents from processing plants after treatment facilities, polluting water systems (Groshev, 2003).

It is very important to note here that, in view of the existing problems in the environment, most countries in the world are moving to a completely different principle of handling resources and generated waste, including from mining.

This is the 3R principle:

- reduce is the reduction of waste generation;
- reuse is reutilisation;
- recycle is processing.

Due to increased attention to the scarcity of natural resources and the problem of waste pollution over the past few years, interest in the cyclical economy has grown significantly.

The Russian enterprise PJSC "Severalmaz" has one of the main important unresolved environmental problems and this is

the absence of highly efficient closed water that reduces the efficiency of diamond-bearing ore enrichment process.

## Literature review

At the deposit named after M. V. Lomonosov, the kimberlites are mainly with a predominance of saponite in their composition (more than 70%), the deposit is located in the central part of the White Sea-Kuloi plateau in the bend of the Zolotitsa River, which flows into the White Sea.

The deposit is represented by six kimberlite pipes: "Pomorskaya", "Arkhangelskaya", "Karpinsky-1", "Karpinsky-2", "Pionerskaya" and "Lomonosov".

The technology of ore dressing created by Russian specialists at enrichment plants is at the level of world standards, and exceeds the world level by individual technical processes and equipment.

At the same time, the main lack of enrichment in diamond mining in the Arkhangelsk diamond province (ADP) is the lack of understanding of the material costs to eliminate the shortcomings of the existing method of enrichment and disposal of waste at PJSC "Severalmaz". According to the material balance, in order to obtain 0.42 g of diamonds from the pipes Arkhangelsk and Karpinsky-1, 4 tons of ore need to be processed and this drawback is the rationale for the need for environmental thoroughness of this issue.

In 2002, Vaganov, Golubev and Minorin created a methodical guide to assess the forecast resources of diamonds, precious, and non-ferrous metals. The manual examines the methodological basis and techniques for identifying promising areas and estimating the forecasted diamond resources. The classifications of the main types of diamond deposits are performed and given in the paper. In addition, geological and industrial quantitative models of diamond deposits are described, the characteristics of which can be used to calculate the material balance of industrial facilities (Vaganov et al., 2002).

According to their data, to date, 97% of the mined diamonds in Russia come from the indigenous deposits, and they account for the bulk of the balance reserves (94.7%).

Increase in production at the diamond deposit named after M.V. Lomonosov entails a number of problems, one of which is the utilisation of a large volume of tailings of clay rock. The fact is that a distinctive feature of this diamond deposit is the high content of di- and trioctahedral clay minerals of the smectite group in the kimberlite rock, which is characteristic of the rocks of the alkaline-ultrabasic composition of the Arkhangelsk diamondiferous province. This phenomenon is called claying of kimberlites (Oblitsov, Rogalyov, 2012).

In the course of technological processes using water at the concentrator, waste (sludge) with a large concentration of clay particles (mainly saponite mineral) is formed.

A significant increase in tailing volumes, associated with increased water content of smectites, leads to an increase in the size of the tailing dump, which manifests itself both in the dam's build-up and in the occupation of new areas. During the first two years of operation (from 2005 to 2007) impounding was carried out in the tailings pond of the first stage with a mark of the pier of the pioneer dam of 116 m. In December 2007, the second stage of the dam with a mark of the crest of 120 m was put into operation, providing the work of the tailing

dump in 2011. The annual volume of ore processing in 2009 amounted to 1050 thousand tons. The design density of the particles for calculating the volume of stacked tailings is assumed to be 2.7 g/cm<sup>3</sup>. In parallel to the development of the field, the volume of tailings to be stored increases, and the required capacity for filling the tailing pond accordingly grows. It seems natural that at such volumes of tailings it is necessary to search for ways of utilising their most interesting part, the smectite-containing rock (Oblitsov, Rogalyov, 2012).

According to the material balance, the main drawback of the existing method of dressing saponite ores in the Arkhangelsk region is that practically the entire volume of crushed ore must be passed through the separation aquatic tailing system when processing large volumes of the rock mass.

The further development of deposits will lead to a significant increase in the volume of pulp (water + saponite) in sludge reservoirs. Due to the high dispersity and the developed diffuse layer, the saponite particles are highly resistant to water.

In addition, the presence of microaggregates of clay minerals along with sand grains, which determine their physical and mechanical properties, and the presence of saponite in the sediment deposits, negatively affect the stability of tailing dams (Oblitsov, Rogalyov, 2012).

The disadvantages of thickening saponite-containing suspension by means of high-compression thickeners are: high capital costs, high consumption of reagents, high power consumption and a number of other shortcomings. The use of domestic and foreign coagulants and flocculants to precipitate suspensions has not yet yielded an effective result because of their high ion exchange capacity, and the facts about re-stabilisation of the suspension after addition of coagulants have been revealed.

Alekseev was engaged in the processing of aluminosilicate raw materials, ion exchange in a clay suspension, and complex processing of apatite-nepheline ores on the basis of closed technological schemes.

Dmitrenko investigated the effect of saponite treatment with hydrochloric acid on its acid-base and sorption properties.

Pashkevich developed a method for sludge processing - a method for increasing tailing dumps.

Tutygin studied the influence of the nature of the electrolyte on the process of coagulation of subunit-containing clay minerals.

Sizyakov was engaged in the modernisation of the technology of complex processing of Kola nepheline concentrates at the Pikalevo alumina refinery plant.

Nevezorov investigated the properties of tail sediments in the enrichment of kimberlite ore.

However, the work of the above-mentioned authors does not touch upon the calculation of the effective rate of deposition of saponite and its compaction in the sludge accumulator of the diamond mining concentrator.

In order to achieve the set goals, it is necessary to develop and implement a set of measures in the full processing of saponite-bearing diamond wastes, as well as to encourage buyers to purchase building materials and other products made from man-made raw materials, including from waste (utilisation) or reclamation of disturbed lands in quarries.

## Methods and materials

### Lomonosov Processing Plant material balance calculation

The Lomonosov Ore Mining and Processing Plant is the No. 1 processing plant with a processing capacity of 4 million tons of ore per year, which provides annual production of about 2.2 million carats of diamonds.

1 carat of diamond weighs 0.2 grams  $2,200,000 \cdot 0.2 = 440.000$  g diamonds = 440 kg of diamonds.

Processing 1 million tons of ore per year, 440 kg of diamonds can be obtained.

1. In 2016, 2012.7 thousand carats we reproduced, 402,540 grams = 402.54 kg.

2. The content of diamonds in the ores and sands in the Arkhangelsk and Karpinsky tubes is 2.1 car/ton or  $0.2 \cdot 2.1 = 0.42$  g/t.

3. Calculation of processed ore for 2016 402,540 g:  $0.42$  g/ton of ore = 958428.57 t/year.

4. Calculation of the percentage of diamonds in the parent ore

5. 1 ton of ore contains 0.42 g of diamonds, that is 1,000,000 g of ore contain 0.42 g of diamonds, which is:

$$(0.42 \cdot 100) : 1000000 = 42 : 1000000 = 0.000042\%$$

Thus, 99.000058% is the saponite mineral 0.000042% is the diamond mineral.

According to the data of the material balance, the main drawback of the existing method of saponite ore dressing is that when processing large volumes of rock mass, practically the entire volume of crushed ore (from 1 ton of ore 0.42-1.2 grams of diamond is extracted) is stored in tailing dumps consisting mainly of saponite mineral.

The mineralogical and crystal chemical characteristics of saponite create large technological obstacles for solving the problem of organising a closed water scheme at the processing enterprise of PJSC "Severalmaz".

It is known that water can be in three different states in nature: gaseous, liquid or solid.

As an example in Figure 1, the simplest state diagram of water dioxide describes the properties that determine the performance of the water-saponite diamond ore (crystalline solid) process cycle.

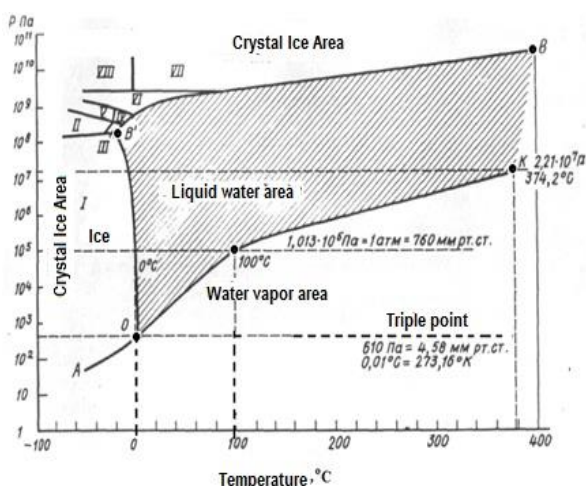


Fig. 1. Single component system - water

The combination of substances or bodies is meant by the physico-chemical system of water (Figure 1) used in the technology of processing diamond ores that are in interaction and separated from the external environment by real or imaginary boundaries.

In this case, water is used as the main technological reagent, which is repeatedly used in the water circulation system in the circulating system. The chemical-technological process of grinding the diamond-saponite ore is carried out in aqueous solutions; therefore, it is advisable to start the study of the equilibrium processes with an analysis of the water state diagram (Fig. 1).

The operating time of the processing plant is presented in Figure 2 by months in 2017. The graph was built depending on the time of four different climatic conditions: winter – spring – summer – autumn with the use of a one-component water chart presented in Figure 1 and the temperature climate conditions corresponding to the Arkhangelsk region for the entire period of 2017. The graph shows that from April to October, for the concentrator, the plant is in a liquid state and with a lower content of suspended substances, and from November to April, everything below the zero line is the formation of ice on the tailings and the natural thickening of liquid water, slurry, into the pulp with a high content of suspended substances.

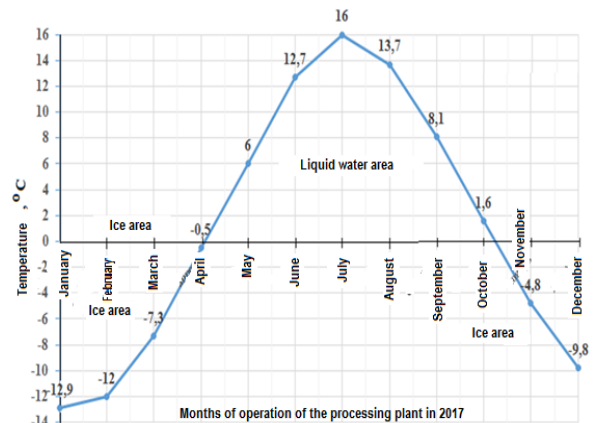


Fig. 2. Influence of climatic parameters on the implementation of the technological process of the concentration plant

These shortcomings can lead to a decrease in the extraction of diamonds in technological processes of heavy medium and X-ray luminescent operations, and to the need of searching of clean water consumption and improvement of the environmental safety of the enterprise.

Research is needed on the mineral and granulometric composition of the pulp after the enrichment of ore at the tailings and the water after the tailings when the water enters the enrichment (circulating water).

### Study of the mineral composition of the pulp after the enrichment process

The clay mineral saponite forms a finely dispersed clay suspension with a concentration of saponite in the circulating water of 5 ... 200 g/d<sup>3</sup>, colloidal particles with a particle size of 1...3 microns. The deposition of the clay mineral saponite ends

after 1.5 years without treatment with coagulants and flocculants.

Because of the properties of the saponite mineral, which has the characteristic not only to «swell», but also to disperse and stabilise, forming a non-precipitating fine-grained gel-like structure bonded with Ca and Mg ions (~20%), the tailings sites allocated by the project increase (Feklichev, 1989).

The pure mineral saponite-stevensite has the mineralogical structural formula  $Na_xMg_3(Al_xSi_{4-x}O_{10})(OH)_2 \cdot 4H_2O$ , a monoclinic syngony, density of 2 g/cm<sup>3</sup>, Mohs hardness 2 (refined data: density 2,3-2,5 g/cm<sup>3</sup>, Mohs hardness 2.5) (Churkina, Lopatin, 2017).

The physical and chemical characteristics of the liquid phase of the samples under study are almost identical and characterised by slightly alkaline pH values, low oxidation-reduction potential, and a small amount of mineralisation.

According to the “Severalmaz” company, it is not difficult to obtain the required quality discharge (500 mg/l), but it is impossible to obtain a thickened product with a density of 70% by weight on thickeners.

The increased content of clay particles in the circulating water to enrich the ore leads to scaling the scheme or attracting additional water from other circulating water for pro sources.

The soil composition is heterogeneous and varies in the depth of occurrence. In the upper layers of its composition there is a mixture of sandy loam (up to 30%), saponite (up to 60%), and vermiculite (up to 10%). With the development in depth in the ground, the content of saponite increases (up to 90%) and, accordingly, the content of sand loam (up to 5%) and vermiculite (up to 5%) decreases.

The mineral composition is shown in Figure 3 and Table 1.

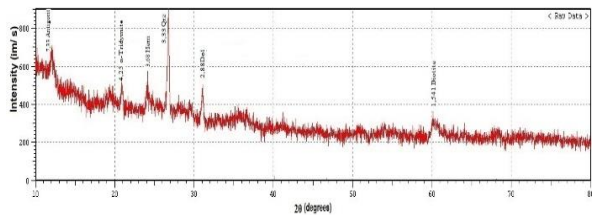


Fig. 3. The mineral composition of the pulp after the enrichment process

The mineral composition is mainly represented by heavy minerals (the density of the mineral is higher than the density of quartz and is considered a heavy fraction) such as hematite, dolomite, biotite, quartz, antigorite, and tridymite (Feklichev, 1989).

Table 1. Oxide composition

Number	Oxide	Content, mass%
1	SiO <sub>2</sub>	55.9
2	Al <sub>2</sub> O <sub>3</sub>	4.01
3	MgO	17.45
4	Fe <sub>2</sub> O <sub>3</sub>	13.12
5	CaO	4.42
6	K <sub>2</sub> O	2.09
7	TiO <sub>2</sub>	0.92
8	MnO	0.23
9	Na <sub>2</sub> O	0.54
10	P <sub>2</sub> O <sub>5</sub>	0.63

The chemical composition of the sample shows that quartz-containing, iron-containing and magnesium-containing substances, which are distributed over the entire surface of the tailing pond, are the ones that mainly enter the environment.

### Investigation of granulometry of saponite suspension

According to the technological scheme, the system of recycled water supply is organised as follows: concentrating plant - tailing dump - concentrating mill. Reserved water after the tailings is fed to the grinding mill, then fed to the classifiers. An express universal laser particle size distribution analyser Horiba LA-950 was used to study the granulometric composition of suspensions, which makes it possible to determine the granulometric composition of the discharge from the classifiers after the saponite ore dressing process (Fig. 4).

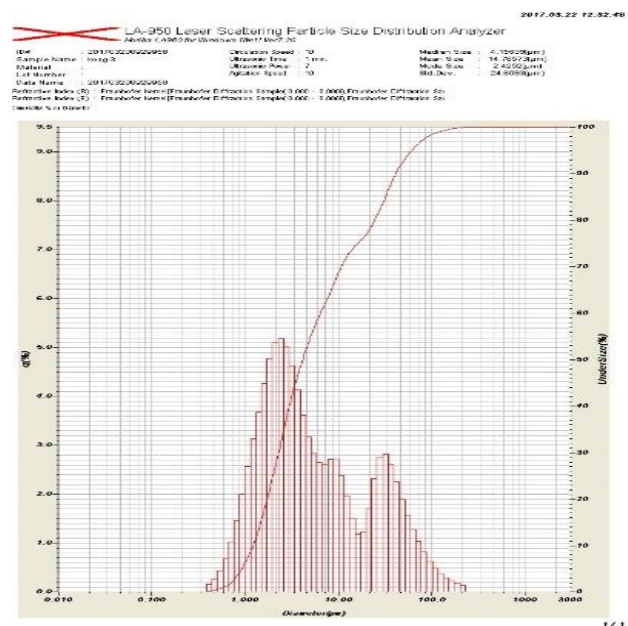


Fig. 4. Granulometric composition of the discharge from the classifier

According to the results of the study, it was found out that the minimum particle size of saponite ore is 0.011 µm in this case, the deposition rate decreases sharply and the Brownian displacement increases. Saponite ore particles are highly dispersed and practically do not precipitate, but due to the Brownian motion they move in any direction.

Let's calculate the deposition rate for a given particle size by the formula:

$$w_{pr} = \frac{d^2(\rho - \rho_d) \cdot g}{18\mu d} (1)$$

The deposition rate for such a particle size is  $1.02 \cdot 10^{-14}$ , this suggests that the saponite pulp is also a colloidal solution and the particles do not settle under the action of gravity. In laboratory conditions, the precipitation of saponite ore without the addition of coagulants and flocculants is about 1 mm per day or about 0.4 m per year.

### Synthesis of inorganic precipitant

To effectively deposit with the St. Petersburg Mining University, a calcium aluminosilicate (CAS) reagent was developed.

The synthesis of the calcium aluminosilicate reagent is carried out in accordance with the diagram of CaO-Al<sub>2</sub>O<sub>3</sub>-SiO<sub>2</sub>(Figure 5) and temperature fields of crystallisation of tricalcium silicate and tricalcium aluminate (Alekseev, Alekseev, 2007).

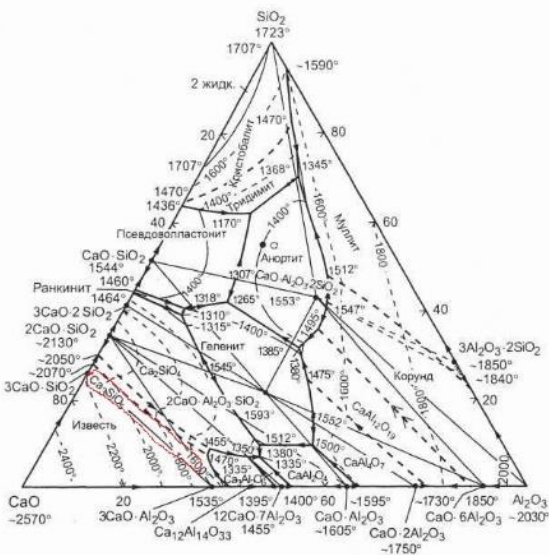
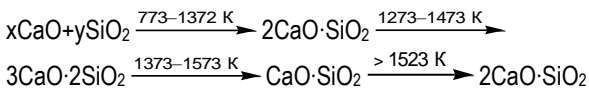


Fig. 5. Diagram of the system state

Taking into account this circumstance, a method of obtaining an active sorbent in the process of wastewater treatment by the decomposition of the initial silicate reagent is proposed.

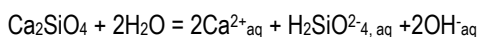
This property of calcium silicates is associated with the structural features of crystalline compounds. Synthesis of calcium silicates of a given composition depending on the initial ratio of CaO: SiO<sub>2</sub> in the charge is recommended in the following temperature ranges:



This composition of the obtained calcium aluminium silicate inorganic coagulant is determined by the initial chemical composition of the raw mix, which varies with different contents of the main minerals of tricalcium silicate, dicalcium silicate, tricalcium aluminate, and quaternary aluminoferrite (Alekseev, 1982).

The composition of the composite coagulant is a granulated mixture of self-separating slag based on calcium and magnesium silicates and hydroaluminosilicates from a number of clays and hydromica mica, and is thermally treated in the 850-900 °C temperature range.

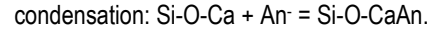
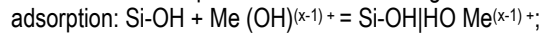
The process of purification of recycled water with the content of clay saponite material is as follows:



When contacting calcium silicates with water, the primary act is its chemical interaction with the formation of ions in the solution.

Calcium hydrosilicate has in its structure hydroxyl groups, capable of cationic and anionic ion exchange (Alekseev, 1985).

The substitution reaction OH- group into cations in an alkaline medium is composed of successive stages:



Since charged particles of the dispersed phase are present in the saponite suspension, the addition of calcium aluminium silicate inorganic coagulant is effective. The use of coagulants with increased basicity will help ensure the production of large aggregates with a high deposition rate and large flakes.

The destruction of the double electron layer of the colloidal saponite particle is achieved due to the chemical activity of the inorganic coagulant.

Experiments were carried out on the deposition of suspended solids in the circulating water with a content of 30-40 g/litre with aluminium sulphate, oxychloride, polyacrylamide flocculant and developed coagulant (Fig. 6).

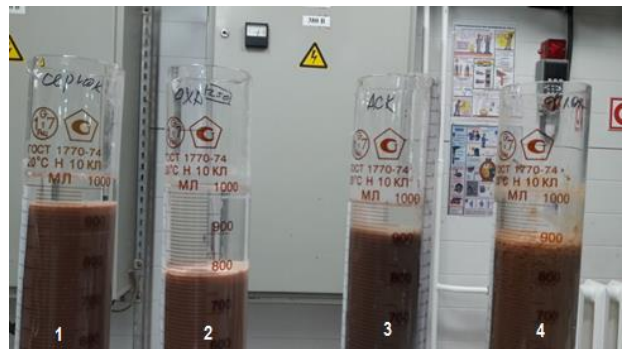


Fig. 6. The results on the deposition of saponite pulp, solid content 25-30 g/l after 60 minutes

Experiments show that compared to traditional coagulants, calcium aluminosilicate reagent thickens saponite pulp and purifies water to enrich the ore.

The results on the removal of suspended solids are presented in Table 2.

Table 2. The results of experiments on the thickening and purification of recycled water

Number	Coagulant	Clean water level, cm
1	7% solution of aluminium sulphate	3
2	9% aluminium oxychloride solution	11
3	Calcium Aluminosilicate Reagent	3
4	Flocculant	7

The chemical composition of the condensed part allows the creation of waste-free production according to the diagram CaO-Al<sub>2</sub>O<sub>3</sub>-SiO<sub>2</sub> and obtaining a coagulant for sedimentation and thickening in the territory of the mining and processing plant. (Table 3).

Table 3. The chemical composition of the condensed product

Number	Oxide	Content, mass%
1	SiO <sub>2</sub>	28.86
2	Al <sub>2</sub> O <sub>3</sub>	6.47
3	MgO	3.83
4	Fe <sub>2</sub> O <sub>3</sub>	5.8
5	CaO	52.89
6	K <sub>2</sub> O	0.44
7	TiO <sub>2</sub>	0.44
8	Na <sub>2</sub> O	0.26
9	P <sub>2</sub> O <sub>5</sub>	0.07

The hazard class of sediment is 4 after the thickening process with aluminum sulphate, oxychloride, polyacrylamide flocculant. Substances in the sediment after coagulation lead to certain violations of the ecological system, but it is able to recover in about 3 years.

## Conclusion

Based on there search, the following conclusions can be drawn:

1. Deposition of the saponite suspension due to its density is impossible without prior dilution.

2. Prior to using traditional coagulants for precipitation (aluminum sulphate), the chemical composition of saponite ore has been studied throughout the process cycle, and their size is taken into account when depositing suspended particles.

3. Based on the granulometric and chemical composition of the ore, and the suspension, a coagulant with specified physical and chemical properties was synthesised.

4. Due to the astringent properties of the synthesised inorganic mineral precipitator, the load on the walls of the dam

reduces, which prevents it from further destruction and leads to a decrease in the areas occupied by the tailing dump.

## References

- Alekseev, A. I. 1982. Method for obtaining a reagent for purification of fluorine-containing wastewater. – *B.I.19852, No. 35 A.s. No. 960129. USSR* (in Russian).
- Alekseev, A. I. 1985. *Calcium Hydroaluminates and Hydrogarnets (Synthesis, Properties, Applications)*. LSU, Leningrad, 184 p. (in Russian)
- Alekseev, A. I., A. A. Alekseev. 2007. *Water Chemistry: Textbook, Handbook. Book II*. Khimizdat, St. Petersburg, 456 p. (in Russian)
- Churkina, O. S., A. V. Lopatin. 2017. Development of cost-effective water purification technology based on complex processing of saponite ore with the use of oxychloride coagulant. – *International Scientific Journal Innovative Development*, 5, Perm, 20–26.
- Feklichev, V. G. 1989. *Diagnostic Spectra of Minerals*. Nedra, Moscow, 479 p.
- Groshev, V. A. 2003. Ecological situation in the Arkhangelsk Region. Abstract. <https://referatbank.ru/referat/preview/12897/referat-ekologicheskaya-obstanovka-arhangelskoy-oblasti.html>.
- Oblitsov, A. Yu., V. A. Rogalyov. 2012. Prospective directions of utilization of waste from the enrichment of the diamondiferous rock of the deposit named after M.V. Lomonosov. – *Zapiski Gornogo Instituta*, 195, 163–167.
- Vaganov, V. I., Yu. K. Golubev, V. E. Minorin. 2002. Methodical guidelines for estimating the forecast resources of diamonds, precious and non-ferrous metals. – In: *The «Diamonds» Issue (Ed. Yu. K. Golubev)*. TsNIGRI, Moscow, 106 p. (in Russian)